

Uniwersytet Łódzki
Wydział Nauk Geograficznych
Rozprawa doktorska
**Rozwój paleogeograficzny Wielkiego
Sertejskiego Basenu Pojeziornego na Pojezierzu
Witebskim w świetle badań paleoekologicznych**

Palaeogeographic development of the Great Serteya Paleolake Basin
in the Vitebsk Lakeland
in the light of palaeoecological research

Agnieszka Mroczkowska

Praca doktorska wykonana pod kierunkiem
prof. dr. hab. Piotra Kittela
Katedra Geologii i Geomorfologii, UŁ
oraz
dr. Mateusza Płociennika
Katedra Zoologii Bezkęgów i Hydrobiologii, UŁ

Łódź 2023

Podziękowania

Serdecznie dziękuję promotorowi prof. dr. hab. Piotrowi Kittelowi oraz dr. Mateuszowi Płociennikowi za wsparcie merytoryczne, wszystkie uwagi oraz cały poświęcony czas. Również dziękuję dr. hab. Michałowi Słowińskiemu za pomoc w jasnym formułowaniu celów naukowych i wsparcie merytoryczne.

Dziękuję także doktorantom i pracownikom Katedry Geologii i Geomorfologii UŁ za stworzenie wspaniałej atmosfery dla rozwoju badań paleogeograficznych na biologicznym gruncie i za codzienną serdeczność.

Dziękuję mojej Rodzinie i Przyjaciołom za wsparcie w realizacji moich celów.

Spis treści

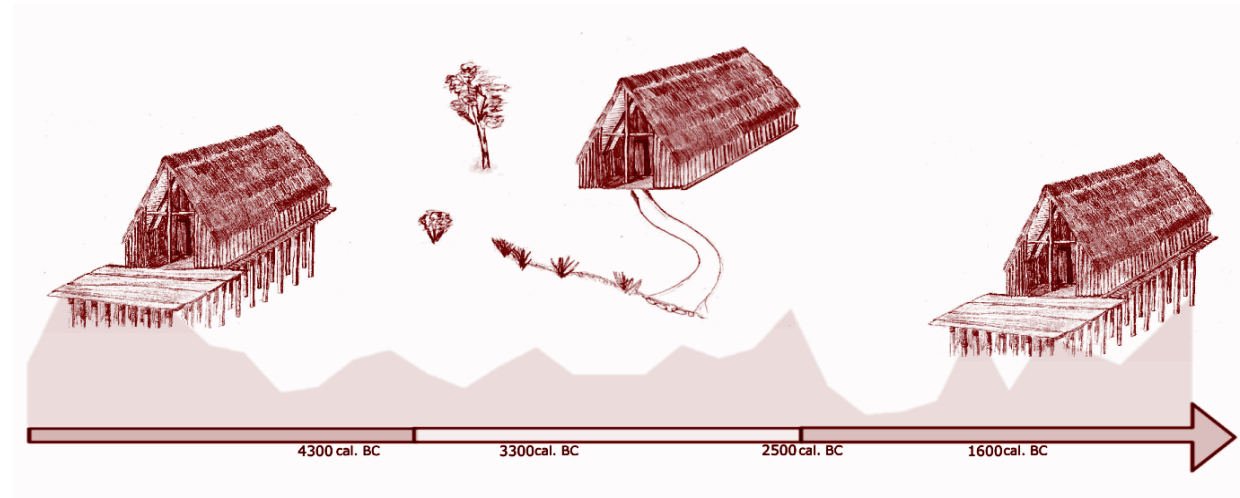
Abstrakt	7
1. Wprowadzenie.....	11
2. Obszar badań	14
2.1 Cechy fizycznogeograficzne regionu	14
2.2 Archeologia regionu.....	19
3. Cel badań	28
3.1 Cel badań i hipoteza badawcza.....	28
4. Metody badań	30
4.1 Materiał badawczy	30
4.2 Analiza Chironomidae jako narzędzie rekonstrukcji środowiska Wielkiego Sertejskiego Basenu Pojeziornego	40
4.3 Analiza jakościowa i ilościowa subfosylnych Cladocera.....	41
4.4 Analiza szczątków Coleoptera.....	42
5. Wyniki	44
5.1. Problem badawczy 1 Zmiany średnich paleotemperatur lipca jako czynnik warunkujący zmiany ekosystemu jeziornego	44
5. 2 Problem badawczy nr 2 Zmiany poziomu wody w WSBP jako czynniki silnie oddziałujące na rozwój biocenozy zbiornika.....	50
5.3 Problem badawczy nr 3 Zmiany siedliskowe na stanowisku Serteya jako obraz naturalnej sukcesji jeziornej.....	60
5.4 Problem badawczy nr 4 Wzajemne relacje człowiek-środowisko.....	66
6. Wnioski.....	73
Spis rycin i zdjęć.....	77
Spis tabeli i rycin.....	79
Bibliografia.....	80
Opis wkładu autorki w artykuł włączone do rozprawy.....	100
Załączniki:	103
Artykuł 1: PŁOCIENNIK, M., MROCKOWSKA, A., PAWŁOWSKI, D., WIECKOWSKA-LÜTH, M., KURZAWSKA, A., RZODKIEWICZ, M., OKUPNY, D., SZMANDA, J., MAZURKEVICH, A. & DOLBUNOVA, E. 2022. <i>Summer temperature drives the lake</i>	

ecosystem during the Late Weichselian and Holocene in Eastern Europe: A case study from East European Plain. Catena, 214, 106206.

Artykuł 2: KITTEL, P., MAZURKEVICH, A., WIECKOWSKA-LÜTH, M., PAWŁOWSKI, D., DOLBUNOVA, E., PŁOCIENNIK, M., GAUTHIER, E., KRĄPIEC, M., MAIGROT, Y. & DANGER, M. 2021. *On the border between land and water: the environmental conditions of the Neolithic occupation from 4.3 until 1.6 ka BC at Serteya, Western Russia.* Geoarchaeology, 36, 173-202.

Artykuł 3: 117. MROCKOWSKA, A., PAWŁOWSKI, D., GAUTHIER, E., MAZURKEVICH, A., LUOTO, T. P., PEYRON, O., KOTRYS, B., BROOKS, S. J., NAZAROVA, L. B., SYRYKH, L., DOLBUNOVA, E. V., THIEBAUT, E., PŁOCIENNIK, M., ANTCAZAK-ORLEWSKA, O. & KITTEL, P. 2021. *Middle Holocene Climate Oscillations Recorded in the Western Dvina Lakeland.* Water, 13, 1611.

Artykuł nr 4: 65. KITTEL, P., MAZURKEVICH, A., ALEXANDROVSKIY, A., DOLBUNOVA, E., KRUPSKI, M., SZMANDA, J., STACHOWICZ-RYBKA, R., CYWA, K., MROCKOWSKA, A. & OKUPNY, D. 2020. *Lacustrine, fluvial and slope deposits in the wetland shore area in Serteya, Western Russia.* Acta Geographica Lodzienia, 110, 103-124.



Wyk. Marlena Mroczkowska

Słowa kluczowe: paleoekologia, Chironomidae, Cladocera, Coleoptera, paleoklimat, relacje człowiek-środowisko

Abstrakt

Tytuł pracy: **Rozwój paleogeograficzny Wielkiego Sertejskiego Basenu Pojeziornego na Pojezierzu Witebskim w świetle badań paleoekologicznych**

Analizy paleoekologiczne z wykorzystaniem subfosylnych szczątków bezkręgowców stanowią interesujące źródło wiedzy na temat zmian paleośrodowiskowych, w tym zwłaszcza paleohydrologicznych i paleoklimatycznych. Na podstawie analiz jakościowych i ilościowych subkopalnych zgrupowań bezkręgowców jesteśmy w stanie zrekonstruować tempo i kierunek zmian zachodzących w środowisku w przeszłości. Analizy paleoekologiczne zostały wykorzystane do odtworzenia tła środowiskowego w regionie Serteji. Jest to obszar położony na Pojezierzu Witebskim w zachodniej części Niziny Wschodnioeuropejskiej, który od końca późnego paleolitu był atrakcyjny dla osadnictwa ludzkiego, zwłaszcza opartego o gospodarkę przyswajalną.

Liczne stanowiska archeologiczne w regionie Serteji stanowią zapis penetrowania obszaru przez człowieka od schyłku paleolitu do czasów współczesnych, dlatego wyniki analiz badań paleoekologicznych są istotnym uzupełnieniem wyników studiów archeologicznych i stanowią nieodzowną część badań z zakresu archeologii środowiskowej (Mazurkevich i in., 2012b, Mazurkevich i in., 2017, Mazurkevich iand Dolbunova, 2015, Kulkova i in., 2015, Mazurkevich i in., 2009c, Mazurkevich i in., 2020a; Kittel i in., 2022). Umożliwiają one ukazanie warunków funkcjonowania dawnych społeczności ludzkich na tle środowiskowym. Szeroki i kompleksowy zestaw badań archeologicznych dla regionu Serteji nie został wcześniej wsparty wieloaspektowymi badaniami paleoekologicznymi o wysokiej rozdzielcości. Społeczności epoki kamienia, w tym neolityczne, prowadziły na interesującym nas obszarze gospodarkę przyswajalną (Mazurkevich i in., 2017), a więc silnie zależną od dostępnych zasobów środowiska. Różnorodność i produktywność środowiska zależy z kolei w znacznej mierze od warunków klimatycznych występujących na danym obszarze, w tym przede wszystkim zmienności sum opadów i przebiegu temperatur (Bolte i in., 2010, Fei i in., 2018, Ammer i in., 2018) oraz warunków hydrologicznych, w tym przede wszystkim wahania poziomu wody w istniejących zbiornikach jeziornych. Proces neolityzacji pośrednio był powiązany zatem z warunkami klimatycznymi (Bendrey i in., 2015, Glais i in., 2016). Pociąga to za sobą

konieczność szczegółowego odtworzenia warunków klimatycznych, między innymi rekonstrukcji ilościowej średniej paleotemperatury powietrza lipca, jak również innych czynników paleoklimatycznych oraz paleohydrologicznych, w tym stosunków wodnych i ich wpływu na rozwój osadnictwa ludzkiego.

Znajomość tła środowiskowego na badanym obszarze pozwoliła na odniesienie danych archeologicznych do informacji paleośrodowiskowych i szczegółowego rozpoznania relacji człowiek–środowisko u schyłku vistulianu i w holocenie. Na podstawie wyników szczegółowych analiz paleośrodowiskowych możemy poznać czynniki, które mogły być decydujące dla prehistorycznych osadników. Istotne jest ustalenie, który z czynników ekosystemu jeziora czy siedlisk lądowych był kluczowy dla rozwoju osadnictwa i gospodarki neolitycznej w rejonie Wielkiego Sertejskiego Basenu Pojeziornego (WSBP - w jęz. rosyjskim: Большая Сертейская Озерная Котловина). W dalszym ciągu brakuje zaawansowanych studiów dotyczących relacji człowiek–środowisko w Europie Wschodniej w epoce kamienia opartych o szczegółowe rekonstrukcje paleoklimatyczne, dlatego tak ważne było podjęcie takich badań w rejonie Sertej.

W ramach rozprawy doktorskiej przeprowadzono badania ośmiu rdzeni osadów biogenicznych, w tym: pięciu rdzeni ze stanowiska archeologicznego Serteya II. W pracy wykonano analizę zgrupowań Chironomidae (rdzenie ST IIa i STII M25, STII L29), analizy Chironomidae i Cladocera (KH, STP I i STP II) oraz Coleoptera ze strefy brzegowej (STII N24 i STII L22). W sumie zostały wykonane analizy dla około 520 próbek z 14 metrów bieżących rdzeni osadów biogenicznych. Analizy wykonywane były z wysoką rozdzielcością od 1 cm do 5 cm. Uzyskane wyniki pozwoliły na dokładne odtworzenie zmian paleoekologicznych zachodzących w regionie Sertej u schyłku ostatniego zlodowacenia i w ciągu całego holocenu. Na podstawie spektrum tolerancji poszczególnych gatunków Chironomidae na warunki środowiskowe wykonano rekonstrukcje zmian warunków klimatycznych w przeszłości. Drugą analizą wykorzystaną głównie do rekonstrukcji zmian poziomu wody i trofii zbiorników była analiza szczątków Cladocera wykonana przez Dominika Pawłowskiego (rdzenie ST IIa, STII M25) oraz przez autorkę (STP I, STP II, STII L29, KH).

Uzyskane dane zostały odniesione i uzupełnione o wyniki analiz paleobotanicznych i paleozoologicznych wykonanych przez innych członków zespołu, takich jak: analiza pyłkowa, analiza makroskopowych szczątków roślinnych, analiza szczątków ryb, analiza malakologiczna, analiza ditomologiczna, analiza antrakologiczna. Ponadto wykorzystane zostały wyniki analiz geochemicznych i sedimentologicznych badanych osadów. Modele

wiekowe rdzeni bazują na analizach geochronometrycznych opartych o datowania radiowęglowe metodą AMS wyselekcjonowanych makroskopowych szczątków roślin. Wyniki badań stanowią część szerzej zakrojonych rekonstrukcji paleogeograficznych regionalnych dla obszaru Serteji położonego na Nizinie Wschodnioeuropejskiej. Wykonane analizy paleozoologiczne i paleobotaniczne pozwoliły na: odtworzenie z dużą rozdzielcością warunków paleośrodowiskowych (w tym m.in.: średnich temperatur powietrza lata, trofii i dynamiki zbiornika jeziornego), w których funkcjonowały dawne społeczności, jak też na odtworzenie antropopresji w kolejnych okresach rozwoju osadnictwa. Znajomość tła środowiskowego, pozwoliła z kolei na odniesienie danych archeologicznych do informacji paleośrodowiskowych i szczegółowego rozpoznania relacji człowiek–środowisko. Głównym celem rozprawy doktorskiej było poznanie rozwoju paleogeograficznego Wielkiego Sertejskiego Basenu Pojeziornego na Pojezierzu Witebskim w późnym vistulianie i holocenie w oparciu o uzyskane wyniki szczegółowych badań paleoekologicznych wykonanych dla pobranych rdzeni osadów biogenicznych.

Prace wchodzące w skład rozprawy doktorskiej – punktacja na podstawie komunikatu Ministra Edukacji i Nauki z dnia 31 grudnia 2021 r. w sprawie wykazu czasopism naukowych i recenzowanych materiałów z konferencji międzynarodowych (art. 267 ust. 3 ustawy z dnia 20 lipca 2018 r. – Prawo o szkolnictwie wyższym i nauce (Dz. U. z 2021 r. poz. 478, 619, 1630 i 2141):

1. Płociennik M., Mroczkowska A., Pawłowski D., Więckowska-Lüth M., Kurzawska A., Rzodkiewicz M., Okupny D., Szmańda J., Mazurkevich A., Dolbunova E., Luoto T.P., Kotrys B., Nazarova L., Syrykh L., Krąpiec M., Kittel P. 2022. *Summer temperature drives the lake ecosystem during the Late Weichselian and Holocene in Eastern Europe: A case study from East European Plain*. Catena, 214, 106206. (140 pkt)
2. Mroczkowska A., Pawłowski D., Gauthier E., Mazurkevich A., Luoto T., Peyron O., Kotrys B., Brooks S., Nazarova L., Syrykh L., Dolbunova E., Thiebaut E., Płociennik M., Antczak-Orlewska O., Kittel P., 2021, *Middle Holocene climate oscillations recorded in the Western Dvina Lakeland*, Water, 13, 1124. (100 pkt)
3. Kittel P., Mazurkevich A., Wieckowska-Lüth M., Pawłowski D., Dolbunova E., Płociennik M., Gauthier E., Krąpiec M., Maigrot Y., Danger M., Mroczkowska A., Okupny D., Szmańda J., Thiebaut E., Słowiński M., 2021, *On the border between land and water: The*

environmental conditions of the Neolithic occupation from 4.3 until 1.6 ka BC at Serteya, Western Russia, Geoarchaeology, 36, 2, s. 173-202. (140 pkt)

4. Kittel P., Mazurkevich A., Alexandrovskiy A., Dolbunova E., Krupski M., Szmańda J., Stachowicz-Rybka R., Cywa K., Mroczkowska A., Okupny D., 2020, *Lacustrine, fluvial and slope deposits in the wetland shore area in Serteya, Western Russia*, Acta Geographica Lodziensia, 110, s. 103-124. (70 pkt)

W rozprawie wykorzystano również dane pochodzące z dwóch artykułów przygotowywanych do druku:

1. Mroczkowska A., Wanat M., Przewoźny M., Ruta R., Stachowiak M., Mazurkevich A., Płociennik M., Jałoszyński P., Kittel P., Karbowiak G., Okupny D., Whitehouse N. J., Kruk A., Słowiński M. *Coleoptera as ecological indicators of Neolithic human impact: Western Russia (Serteya II site - case study)*
2. Piech W., Hrynowiecka A., Stachowicz-Rybka R., Cywa K., Mroczkowska A., Słowiński M., Okupny D., Krąpiec M., Ginter A., Mazurkevich A., Kittel P. *Natural and anthropogenic factors of the intense slope processes in Eastern Europe in the Modern Period; case study in Serteyka River valley*

Prace terenowe realizowane były w ramach współpracy z Północno-zachodnią Ekspedycją Archeologiczną Państwowego Muzeum Ermitaż w Sankt Petersburgu. Analizy specjalistyczne były finansowane w ramach projektu Narodowego Centrum Nauki (NCN) “Środowiskowe warunki funkcjonowania osady palafitowej Serteya II na Wyżynie Smoleńskiej w kontekście globalnych i lokalnych zmian klimatycznych około 4200 lat temu” (grant numer 2017/25/B/HS3/00274). Staż naukowy przygotowujący do analizy subfosylnych Coleoptera został zrealizowany w ramach programu Erasmus plus oraz wyjazdu zagranicznego w ramach programu „PROM”. Dodatkowe dofinansowania na realizację badań: Dotacja celowa Wydziału Nauk Geograficznych na prowadzenie w 2018 r. badań naukowych przez młodych naukowców i uczestników studiów doktoranckich projekt pt. Rozwój paleogeograficzny Wielkiego Sertejskiego Basenu Pojeziernego na Wysoczyźnie Smoleńskiej w świetle badań paleoekologicznych (kod projektu MPK:2172121000 i B1811700001973.02) oraz dotacja celowa Wydziału Nauk Geograficznych na prowadzenie badań w 2019 roku projekt pt. Analiza subfosylnych chrząszczy (Coleoptera) jako narzędzie rekonstrukcji warunków środowiska i biowskaźniki zmian powodowanych obecnością i działalnością człowieka na stanowisku Serteya II (kod projektu MPK: 2172121000 iB1911700002109.02).

1. Wprowadzenie

Zapis paleoekologiczny w rdzeniach osadów biogenicznych stanowi podstawę dla rekonstrukcji historii warunków klimatycznych, hydrologicznych, rozwoju flory i ewolucji innych elementów dawnego środowiska. Szczególną rolę we współczesnych badaniach odgrywają szczątki roślin czy zwierząt znajdowanych w tych osadach. Dzięki badaniom paleoekologicznym mamy możliwość prześledzenia m.in. przebiegu zmian środowiskowych i ich dynamiki. Historia zapisana w osadach pozwala na poznanie warunków środowiskowych, z jakimi mierzyli się nasi przodkowie. Ponadto umożliwia określenie skali i kierunków presji, jaką człowiek wywierał przez lata na środowisko czy ustalenie jakie surowce naturalne wykorzystywał. Poznanie zmian paleośrodowiskowych możliwe jest dzięki narzędziom, do których zalicza się analizy paleobotaniczne i paleozoologiczne. Analizy palinologiczna, makroskopowych szczątków roślinnych, ameb skorupkowych, subkopalnych okrzemek, Chironomidae czy Cladocera to podstawowe metody paleoekologiczne, które pozwalają na poznanie przeszłości środowiska geograficznego.

Stan wiedzy: Region Serteki leży w strefie klimatu umiarkowanego z dużą dynamiką sezonową zmian pogody. Poziom wód jezior i rzek na obszarze Europy Wschodniej charakteryzuje się znacznymi fluktuacjami sezonowymi. Jednocześnie słabo zaznacza się na tym obszarze wpływ NAO (Oscylacji Północnoatlantyckiej) na warunki meteorologiczne, w przeciwieństwie do obszarów Europy zachodniej i północno-zachodniej (Matero i in., 2017).

W 2021 roku powstała baza danych z Niziny Wschodnioeuropejskiej, która uwaglednia 50 stanowisk z przebadanymi szczegółowo pod względem paleoekologicznym osadami jeziornymi i torfowiskowymi obejmującymi holocen (Syrykh i in., 2021). Dla większości z tych stanowisk wykonano analizę pyłkową, a dla niektórych rekonstrukcje paleoklimatyczne - m.in. stanowiska regionu Tallina (Estonia) (Heinsalu i Veski, 2007), Jeziora Myshetskoe-Dolgoe w Moskwie (Kremenetski i in., 2000), Jeziora Kenozero (obwód archangielski) (Sapelko i in., 2006, Zernitskaya i in., 2019), Salpausselkä II (Kalevala) (Shelekhova i Lavrova, 2020), Michurinskoe i Uzorne (Karelia) (Davydova i Servant-Vildary, 1996), torfowiska Nikokolsko-Lutinskoye (obwód nowogrodzki) Shirinsky Mokh i torfowiska Lammin-Suo (obwód leningradzki), jeziora Wiszniewskoje (obwód grodzieński) i torfowiska Sakkała (Karelia) (Arslanov i in., 1999), jeziora Lembolovskoye w Przesmyku Karelskim oraz torfowiska Mshinskoye w obwodzie leningradzkim (Arslanov i in., 2001). Analizy pyłkowe bez rekonstrukcji paleotemperatur uzyskano m.in. dla stanowisk: krateru Kaali (wyspa Sarema)

(Veski i in., 2004), Jeziora Onega (Karelia) (Shelekhova i in., 2005), Dorzecza Donu (Spiridonova, 1991), Lozoviki i Krivoe na Pojezierze Białoruskim; Mezhuzhol i Sudoble (Środkowa Białoruś); Bobrovichskoe i Oltushskoe (Polesie Białoruskie) (Novik, 2014), jezior termokrasowych (obwód jarosławski) (Wohlfarth i in., 2006). Ilościowe oraz jakościowe rekonstrukcje średnich paleotemperatur lata przeprowadzono w oparciu o wyniki analiz pyłkowych dla jezior Babrovickaje (obwód brzeski) i Głębokie (Pojezierze Białoruskie), jezior Mezhuzhol i Nikolay w regionie arktycznym (Andreev i in., 2004), torfowiska Krivetskiy Mokh na Wyżynie Wałdaj (Mazei i in., 2020). Miejsca, które zostały przetestowane za pomocą analiz paleozoologicznych, wykorzystujących szczątki Cladocera lub Chironomidae, obejmują m.in. Jezioro Medvedevskoye (obwód leningradzki) (Syrykh i in., 2015), a stanowiska z wykonaną rekonstrukcją średniej paleotemperatury powietrza lipca to jezioro Glubokoye (obwód moskiewski) (Nazarova i in., 2015) i jezioro Medvedevskoye (Karelia) (Nazarova i in., 2019). Wyniki analiz subkopalnych Cladocera lub Chironomidae zostały opublikowane m.in. przez Andronikova i in. (2014) i Subetto i in. (2017) dla jeziora Medvedevskoye (Karelia) (Nazarova i in., 2020) oraz torfowiska Koz'ye (obwód kaliningradzki) przez Kubitsky i in. (2016).

Z powyższego przeglądu wynika, że badania paleoklimatyczne są słabiej rozwinięte w Europie Wschodniej w porównaniu z zachodnią częścią kontynentu (Berntsson i in., 2014, Feurdean i in., 2014, Kulkova i in., 2015, Moreno i in., 2014). Dla wschodniego wybrzeża Bałtyku najbardziej kompleksowe ilościowe rekonstrukcje paleoklimatyczne zostały oparte o wyniki analizy pyłkowej wykonanej przez Seppä i Poska (2004) oraz Heikkilae i Seppä (2010), a także analizy pyłkowej i analizy Chironomidae (Veski i in., 2015).

Rekonstrukcję wahań poziomu wody w jeziorach i torfowiskach przeprowadzono jedynie dla północnej Polski (Lamentowicz i in., 2010, Gałka i in., 2015, Marcisz i in., 2017) oraz krajów bałtyckich (Šeirienė i in., 2009, Sillasoo i in., 2007, Sohar i Kalm, 2008, Heikkilae i Seppä, 2010, Stivrins i in., 2014, Terasmaa i in., 2013). Dlatego wyniki badań w Sertej w znacznej mierze pozwalają na uzupełnienie luki w stanie wiedzy paleośrodowiskowej dla obszaru Niziny Wschodnioeuropejskiej.

W poprzednich latach w regionie Sertej wykonane zostały badania paleoekologiczne dwu rdzeni osadów biogenicznych obejmujących schyłek vistulianu i holocen. W ramach tych opracowań zostały wykonane analizy: palinologiczna, okrzemkowa i geochemiczna, jednak o małej rozdzielnosci (Dolukhanov i in., 1989, Kulkova i in., 2001, Mazurkevich, 2003, Mazurkevich i in., 2009a, 2009b, 2012a, Tarasov i in., 2019). Pobrane w regionie Sertej w latach 90-tych XX wieku rdzenie osadów biogenicznych nie spełniają współczesnych

standardów wysokorozdzielczych badań paleoekologicznych. Ponadto duże wątpliwości budzi ich wiek ustalony w oparciu o datowania radiowęglowe wykonane z niewielką precyzją i dla różnych materiałów organicznych, w związku z czym występują liczne inwersje uzyskiwanych oznaczeń wieku i w efekcie niepewne są rekonstrukcje czasu i tempa akumulacji osadów.

Zapis 600-letniej historii środowiska lokalnego dla Serteji obrazują z kolei wyniki uzyskane z oddalonego o 8 km od WSBP torfowiska kotłowego z rdzenia KH. Dla tego rdzenia koordynowałam opracowanie rekonstrukcji zmienności warunków klimatycznych w oparciu o wyniki analiz: pyłkowej, makroskopowych szczątków roślinnych, Chironomidae, Cladocera i ameb skorupkowych (Mroczkowska i in., 2021a). Historię paleoekologiczną ostatnich 300 lat w mikroregionie odtworzono szczegółowo na podstawie analizy osadów torfowiska ombrotroficznego Gorodzetsky Moch. Wykonano dla nich szczegółową rekonstrukcję zmian warunków klimatycznych i wahania poziomu wody w torfowisku na podstawie analiz: ameb skorupkowych, pyłkowej, makroskopowych szczątków roślinnych (Łuców i in., 2020).

Nasze badania opierają się zatem o analizy paleoekologiczne wykonane z wysoką rozdzielcością dla osadów o wiarygodnej chronologii opartej o modelowania wiek/gębokość. W podjętych studiach niezbędne było opracowanie analiz multi-proxy o wysokiej rozdzielcości, by udokumentować nawet krótkie oscylacje klimatyczne czy wahania sezonowe. Dodatkowo wyniki badań uzupełniają dane paleoklimatyczne i paleohydrologiczne dla obszaru Zachodniej Rosji. Obszar Nizin Wschodnioeuropejskiej nie posiada jeszcze rekonstrukcji tego typu, dlatego informacje te wpisują się bardzo dobrze w bazy danych o globalnych zmianach klimatu w przeszłości.

W ostatnich latach w dolinie dolnego odcinka Sertejki i w jej otoczeniu wykonano kartowanie geologiczne ręcznym świdrem, głównie w celu określenia zasięgu i miąższości osadów organicznych, a także zalegania osadów rzecznych oraz rozpoznania budowy form polodowcowych. Również wykonano szczegółowe rozpoznanie stożków akumulacyjnych w dnie doliny Sertejki. Zaawansowane badania paleogeograficzne prowadzone były na obszarze stanowiska Serteya II i w jego bezpośrednim otoczeniu (Mazurkevich i in. 2020, Kittel i in., 2018, Piech, 2021).

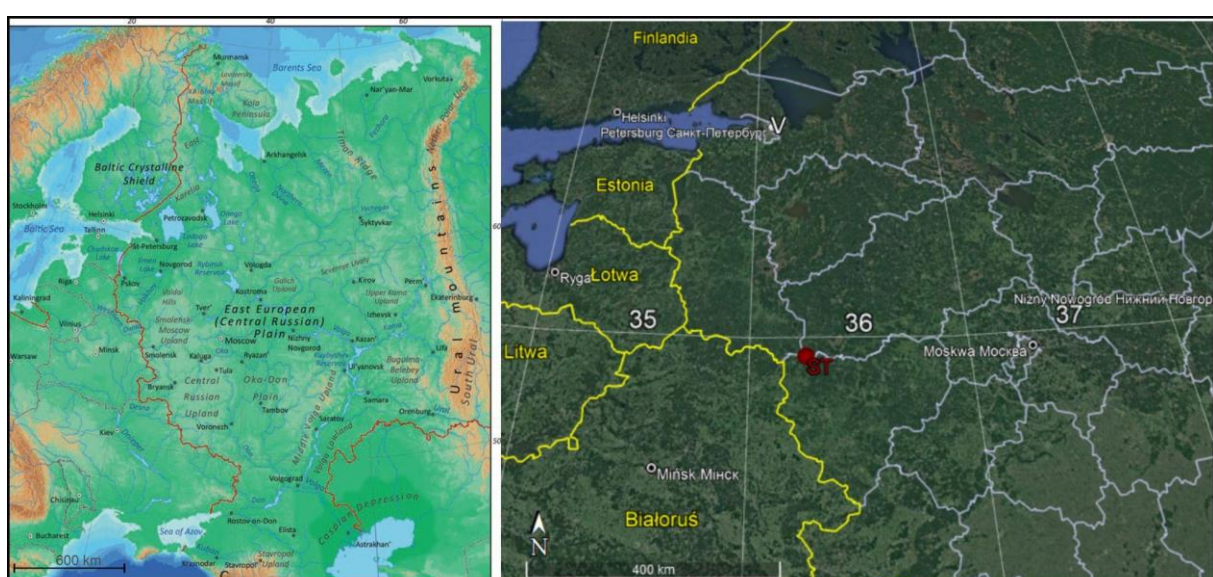
2. Obszar badań

2.1. Cechy fizycznogeograficzne regionu

Obszar badań znajduje się współcześnie w Zachodniej Rosji (rycina 1) w Obwodzie Smoleńskim w regionie Serteki (rycina 2, 3). Region ten położony jest około 20 km na wschód od miasta Wieliz i 100 km na północny zachód od Smoleńska. Jest to szczególnie miejsce pod względem warunków hydrologicznych, ponieważ znajduje się w sąsiedztwie europejskiego działu wodnego. Obszar badań położony jest w zlewnisku Morza Bałtyckiego i odwadniany jest za pośrednictwem Serteki, cieku o długości około 40 km, dopływu Dźwiny. Główne stanowisko badawcze położone jest we współczesnej dolinie rzeki Sertejka, której dolny odcinek ma przebieg południkowy (rycina 3). Według podziałów fizycznogeograficznych, obszar badań należy do mezoregionu Pojezierze Witebskie wg Kondrackiego (1992) lub do Pojezierza Zachodnidźwińskiego według Abramova (1972).

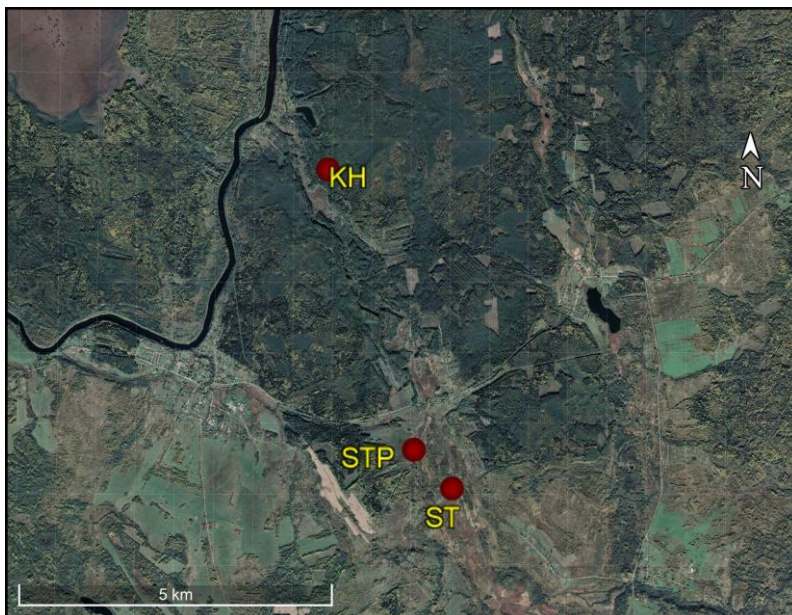


Rycina 1. Lokalizacja terenu badań A) na mapie świata, B) na mapie Federacji Rosyjskiej



Rycina 2. Lokalizacja terenu badań na tle śródkowej Europy i Obwodu Smoleńskiego

Zasadniczy obszar badawczy stanowi WSBP (rycina 4). Otoczenie zbiornika cechuje się zróżnicowaną budową geologiczną. W dnie WSBP rozwinięte są: pojeziorne równiny akumulacji biogenicznej i niskie terasy kemowe oraz kemy. W otoczeniu występują gliniaste wysoczyzny morenowe i piaszczyste równiny wodnolodowcowej (Kittel i in., 2018). Obszar cechuje się zatem znaczną geo- i bioróżnorodnością, które sprzyjały funkcjonowaniu gospodarki przyswajalnej i zapewniały dostęp do różnorodnych zasobów i surowców naturalnych (Mazurkevich i in., 2017).



Rycina 3. Lokalizacja terenu badań stanowiska Serteya II (STII), profili STP i torfowiska Serteya (KH)



Rycina 4. Lokalizacja stanowisk wchodzących w zespół stanowisk Serteya II

Budowa geologiczna. Obszar badań zlokalizowany jest na Platformie Wschodnioeuropejskiej na styku trzech segmentów: Fennoskandzkiego na północy, Wołgo-Uralskiego na wschodzie i Sarmatii na południu. Położony jest w pasie Ostnisk-Mikaszewiczi-Moskwa, stanowiącym powierzchnię paleoproterozoiczną powstałą około 2,0-1,9 mld lat temu (Bogdanova i in., 2005). Około 1,5-1,4 mld lat temu powstał tam uskok marginalny skorupy prekambryjskiej i kratonu wschodnioeuropejskiego. Miąższość osadów paleozoicznych nakrywających platformę prekambryjską wynosi około 5 km i składają się na nią przede wszystkim wapienie dewońskie (Pinneker, 1983, Zektser, 2004). Wyżej zalegają skały karbonu - głównie wapienie. Natomiast osady górnej kredy tworzą głównie margele i kredy (Zektser, 2004).

Powierzchniowa budowa geologiczna i rzeźba obszaru zostały ukształtowane głównie w górnym plejstocenie w trakcie ostatniego zlodowacenia (tj. Weichselianu, zl. Valdai) oraz w holocenie. Ostatnie zlodowacenie objęło swoim zasięgiem północno-zachodnią część Niziny Wschodnioeuropejskiej (Velichko i in., 2011). Działalność ostatniego lądolodu zdeterminowała w rejonie Serteji powstanie wysoczyzn morenowych i równin wodnolodowcowych, wzgórz i pagórków morenowych, kemów, rynien subglacialnych i ozów. W obrębie wklęsłych form polodowcowych rozwinęły się w holocenie liczne zbiorniki jeziorno-torfowiskowe. Powierzchnie piaszczyste urozmaicone są niewielkimi formami wydmowymi. Istotne urozmaicenie rzeźby terenu stanowią młode doliny rzeczne, w tym zwłaszcza dobrze rozwinięta dolina Dźwiny oraz niewielkie doliny jej dopływów, m.in. dolina rzeki Sertejki. Doliny rzeczne najczęściej wykorzystują rynny subglacialne (Kittel i in., 2018).

W obrębie rynny subglacialnej wykorzystywanej współcześnie przez dolinę Sertejki, doszło w trakcie recesji lądolodu, do rozwoju jezior pierwszej generacji pomiędzy zalegającymi bryłami martwego lodu (Płociennik i in., 2022). Reliktem tego zbiornika we współczesnej rzeźbie terenu są kemy i terasy kemowe w dnie rynny. W późnym vistulianie, po wytopieniu brył martwego lodu, powstały jeziora drugiej generacji (Kittel i in., 2018; Płociennik i in., 2022). Na podstawie analizy materiałów kartograficznych oraz w oparciu o wyniki sondowań geologicznych udokumentowano istnienie w obrębie dolnego odcinka współczesnej doliny rzeki Sertejki, czterech rozległych basenów pojeziornych - są to: Nivnikovskay Ozernaya Kotlovina, Rudnyanskaya Ozernaya Kotlovina, WSBP oraz Banya Kotlovina, które rozwinięte zostały w dnie rynny subglacialnej. Ich wymiary dochodzą do 600 m długości i 200 m szerokości (Kalicki i in., 2015, Kittel i in., 2016, 2018). Zbiorniki te zostały w holocenie stopniowo zdrenowane w wyniku erozji wstecznej koryta rzecznego, poczynając od basenu

Nivnikowskiego, położonego w najniższej części biegu Serteki, który funkcjonował najpóźniej do około 4 tys. lat temu. W świetle nowszych danych zbiornik w obrębie WSBP mógł być odnawiany jeszcze w okresie nowożytnym (Kittel i in., 2021, Więckowska-Lüth, 2021, Płociennik i in., 2022).

Zmiany klimatyczne i hydrologiczne prowadziły do okresowego wypłycania jezior i ich zabagniania podczas holocenu. W trakcie faz regresji system jeziorny mógł być okresowo zastępowany przez system fluwialny w obrębie rozległych płytowych basenów (Kulkova i in., 2001; Mazurkevich i in., 2012a; Kalicki i in., 2015; Kittel i in., 2016, 2018). Obecnie WSBP jest największym basenem pojeziornym w dolinie, o długości około 1,2 km i szerokości ponad 0,5 km (Kittel i in., 2018). Zagłębienie wypełnione jest osadami organicznymi (głównie gytią) o miąższości 7,5 metra (Tarasov i in., 2019). W późnym holocenie stoki rynny subglacialnej zostały pocięte wąwozami (Kittel i in., 2018).

Pokrywa glebowa: Na badanym obszarze dominują gleby darniowo-bielicowe oraz bielicowe. Gleby te mają najczęściej odczyn kwaśny, a akumulacja biotyczna jest w nich słaba, w związku z czym zawartość materii organicznej niska (2-4%), warstwa próchnicy glebowej o niskiej zawartości kwasów fulwowych. Gleby te wytworzone są z ilów i piasków gliniastych oraz piasków z przewarstwieniami glin (Stolbovoi, 2002). Ponadto występują histozole składające się głównie z materiału organicznego budującego poziomy o miąższości co najmniej 10 cm, formujące gleby bagienne czy torfowiskowe (WRB 2016). Użytkowanie gruntów obejmuje głównie leśnictwo i obróbkę drewna oraz rolnictwo (głównie w rejonie Wielicha) (Terskii i in., 2019).

Warunki klimatyczne: Region Serteki położony jest w strefie klimatu umiarkowanego kontynentalnego z dużą dynamiką zmian warunków klimatycznych, co silnie kształtuje środowisko przyrodnicze terenu (Kobyshevoy, 2001). Dane ze stacji meteorologicznej z Wielicha wskazują, że średnia temperatura w lipcu może wachać się od 13 do 23°C, a w styczniu od -5 do -8°C. Średnie roczne sumy opadów w wielolecie 1990-2020 osiągają od 400 do 1100 mm, z najwyższymi notowanymi sumami w czerwcu (88 mm) oraz najniższymi w kwietniu (35 mm). W okresie tym często mają miejsce gwałtowne ulewy, które mogą powodować krótkotrwałe wezbrania (Panin i in., 2014). Okres wegetacyjny trwa od 170 do 190 dni. Okres letni trwa 129–143 dni, a pokrywa śnieżna utrzymuje się przez 125–148 dni. Cyrkulacja powietrza zmienia się znacząco w ciągu roku, co ma wpływ na sumy opadów i przebieg temperatur powietrza. Główne kierunki wiatru to: zachodni, południowo-zachodni i południowy (www.tutiempo.net, www.meteoblue.com/en). Około 70% opadów występuje

w postaci deszczu w ciepłych porach roku. Śnieg gromadzi się zimą, a maksymalna grubość pokrywy śnieżnej występuje pod koniec lutego (Danilovich i in., 2019).

Stosunki wodne: Główną arterią wodną obszaru jest Dźwina (Zapadnaya Dvina, Daugava), do której uchodzią liczne dopływy, w tym lewobrzeżna Sertejka. Układ sieci rzecznej ma zasadniczo układ dendrytyczny. Na badanym obszarze licznie występują jeziora o genezie polodowcowej oraz bagna i torfowiska o genezie pojeziornej. Wiele ze zbiorników jeziornych zanika bowiem w wyniku naturalnej eutrofizacji.

Dźwina to typowa rzeka nizinna. Zasilana jest głównie przez roztopy pokrywy śnieżnej nagromadzone w okresie zimy. Roztopy powodują znaczne wiosenne wezbrania. Sezon wezbraniowy zwykle trwa dwa miesiące: najczęściej zaczyna się pod koniec marca (na głównej rzece i w połowie marca na dopływach) i kończy się na początku czerwca, gdy poziom wody opada. Dochodzi często do gwałtownego podniesienia poziomu wody w rzece w wyniku spiętrzania kry (Danilovich i in., 2019).

Reżim hydrologiczny Dźwiny charakteryzuje się okresami odpływów przypadających na okresy zimowe i ciepłą porę roku (od lata do jesieni). Zasilanie w okresie niżów pochodzi z wód podziemnych. Okres niżów zimowych rozpoczyna się zimą hydrologiczną od listopada do grudnia/stycznia, a kończy się, gdy na przełomie marca i kwietnia rozpoczynają się wiosenne wezbrania roztopowe. W okresie niżów letnich często dochodzi do intensywnych i gwałtownych wzrostów poziomu rzeki, spowodowanych intensywnymi opadami konwekcyjnymi. Wartości trendów miesięcznych odpływów są dodatnie w miesiącach zimowych i marcu, a ujemne w kwietniu. Pozytywne tendencje w okresie od grudnia do marca (w okresie zimy hydrologicznej) związane są z ogólnym wzrostem temperatury powietrza w badanym rejonie, częstymi roztopami, brakiem pokrywy lodowej oraz dopływem wód roztopowych do rzek. Negatywne tendencje w kwietniu można wyjaśnić wyczerpaniem zapasów śniegu po ciepłych zimach, które dostarczają rzekom wody roztopowe. Maksymalne przepływy obserwuje się zazwyczaj podczas wiosennych wezbrań. Wzrost temperatury powietrza zimą i częste roztopy w zachodniej części dorzecza Dźwiny powodują natychmiastowe topnienie śniegu, dodatkowe dostawy wody do rzek i powstania zimowych wezbrań. Stany wody według danych z wodowskazu Wielisz wahają się wokół wieloletniej wartości średniej, odchylenia dodatnie i ujemne sięgają nawet 60% od średniej (Terskii i in., 2019).

Wody podziemne obszaru należą do moskiewskiego basenu artezyjskiego (Pinneker, 1983). Większość z nich jest zanieczyszczona w średnim i małym stopniu. W obwodzie

smoleńskim zasoby wód podziemnych wynoszą 6356 tys. m³/dobę, nie wliczane są do nich wody o dużym i wysokim stopniu zanieczyszczeń (<http://www.geomonitoring.ru>. Center of state monitoring of natural resources, 2007).

Szata roślinna: Region Serteki jest współcześnie porośnięty lasami mieszanymi, głównie ze zbiorowiskami świerkowo-brzozowymi, rzadziej osiką, dębem, lipą, jesionem (Podbielkowski, 1995). Według stref potencjalnej roślinności jest to obszar dogodny dla rozwoju boru mieszanego iglastego z przewagą *Picea*, *Betula* i *Pinus* (Bohn i in., 2000). W rejonie wieliskim lesistość wynosi współcześnie około 49,5%. Na łąkach występują takie taksony jak: kostrzewa (*Festuca sp.*), gniszczek błotny (*Pedicularis palustris*). Na torfowiskach rosną: turzyca (*Carex*), trzcina pospolita (*Phragmites australis*), skrzyp (*Equisetum*), mchy (*Bryophyta*). Wśród zbóż uprawia się głównie: żyto (*Secale cereale*), len (*Linum*) i pszenicę (*Triticum*) (Mazurkevich i in., 2009a). Na terenie rejonu wieliskiego utworzono rezerwat Wielisz, w którym rosną gatunki: przetacznik leśny (*Veronica officinalis*), kozłek lekarski (*Valeriana officinalis*), żurawina błotna (*Oxycoccus palustris*), przylaszczka pospolita (*Hepatica nobilis*), zawciąg pospolity (*Armeria vulgaris*), rosiczka okrągłolistna (*Drosera rotundifolia*), wełnianka pochwowata (*Eriophorum vaginatum*), borówka bagienna (*Vaccinium uliginosum*), widlicz spłaszczony (*Diphasiastrum complanatum*) (Shkalikov i in., 2005).

Świat zwierząt: W rejonie smoleńskim pospolitymi ssakami są: dzik (*Sus strofa*), sarna (*Capreolus*), bóbr (*Castor*), zajęc szarak (*Lepus europaeus*), łoś (*Alces*), wilk (*Canis lupus*), lis (*Vulpes vulpes*), kuna (*Martes*). Wśród ptaków występują: dzięcioł duży (*Dendrocopos major*), gil (*Pyrrhula pyrrhula*), drozd śpiewak (*Turdus philomelos*), cietrzew (*Lyrurus tetrix*), bocian biały (*Ciconia ciconia*), batalion (*Calidris pugnax*), czapla siwa (*Ardea cinerea*). Z gatunków ryb obecne są głównie: karaś (*Carassius carassius*), karp (*Cyprinus carpio*), leszcz (*Aramis brama*), okoń (*Perca fluviatilis*), płoć (*Rutilus rutilus*), trawianka (*Percottus glenii*), szczupak (*Esox lucius*), sum (*Silurus glanis*), węgorz europejski (*Anguilla anguilla*) (Shkalikov i in., 2005).

2.2. Archeologia regionu

Początek osadnictwa w zachodniej Rosji miał miejsce w środkowym paleolicie w trakcie interglacjału mikulińskiego (interglacjał eemski). Niewielkie społeczności zamieszkiwały obszary w rejonie Jeziora Usvyatskoje, a także w Jeziora Sennitsa (rejon newelski), nad Jeziorem Żyzyckim (rejon kuniński) oraz we współczesnej dolinie rzeki

Sertejki. Narzędzia kamienne z tego okresu znaleziono wzdłuż brzegów dawnych basenów jezior funkcjonujących w obrębie współczesnej doliny Dźwiny. Miejsca te znajdują się w pobliżu wsi Jastreb i Klimowo (Miklyaev i in., 1995). Teren był porośnięty wówczas lasami brzozowo-sosnowymi i jodłowymi (San'ko, 1987). Z tego okresu licznie znajdują się artefakty i narzędzia kamienne przemysłu aszelkso-mustierskiego. Społeczności podstawy swojego bytowania opierały na gospodarce łowiecko-zbierackiej.

Następną fazą rozwoju kultury człowieka jest okres epipaleolitu, około 16000-15000 cal BP. Region Serteji jest bogaty w stanowiska archeologiczne datowane na schyłkowy paleolit oraz na mezolit. Pierwszymi odkrytymi były stanowiska Serteya i Dubokray (Miklyaev, 1995, 1969). W okolicach Uświat oraz Seretji udokumentowane zostały nieliczne stanowiska i znaleziska z końca paleolitu, m.in. stanowiska Ivantsov Bor i Serteya I. Obozowiska schyłkowopaleolityczne były posadowione wśród lasów sosnowo-brzozowych na piaszczystych wydmach w pobliżu jezior późnoglacialnych. Kilka artefaktów z okresu schyłkowego paleolitu odkryto w pobliżu wsi Łukaszenki, na stanowisku Dubokrai V oraz, na stanowiskach sertejskiego mikroregionu archeologicznego (Kittel i in., 2022). Główne źródła pożywienia stanowiły wówczas zbieractwo, łowiectwo i rybołówstwo (Mazurkevich i in., 2020a).

Kolejnym etapem rozwoju kulturowego społeczności górnej Dźwiny była epoka mezolitu trwająca około 11450-7450 cal BP. Wtedy też odnotowano istotną zmianę szaty roślinnej - młodszodryasowa rośliność tundrowo-stepowa zastępowana jest najpierw borami mieszanyimi brzozowo-sosnowymi, a od okresu borealnego również lasami z wiązem i lipą (Tarasov i in., 2019). Na podstawie zwiększającej się ilości stanowisk z tego okresu oraz wyraźniejszego sygnału wpływu człowieka na środowisko przypuszcza się, że doszło do znacznego wzrostu populacji w trakcie okresu borealnego (10950-10450 cal BP) (Mazurkevich i in., 2012b). Gospodarka tego okresu charakteryzowała się przewagą łowiectwa i zbieractwa. Opierała się głównie na wykorzystaniu zasobów naturalnych dolin rzecznych i basenów jeziornych. Zmniejszyła się populacja koni, żubrów i jeleni, zaś wzrosła populacja łośi, kaczek, cierzwów czy ryb. Na tych terenach żyły plemiona wywodzące się z tradycji kultur epipaleolitycznych (tradycja świdarska). Z tego okresu pochodzą narzędzia kultury kunda odkryte na stanowiskach Dubokray VI oraz Serteya 1, Serteya X, Serteya XIV. Stanowiska były posadowione na wydmach oraz na brzegach jezior i wyspach (Kulkova i in., 2001).

Stanowiska wczesnego neolitu znajdują się w północnej i południowej części mikroregionu sertejskiego i były oddzielone obszarem niezasiedlonym. Położone one są na

południowych brzegach paleojezior (Rudnya Sertejska, Serteya nr 3 i Serteya XII), lub na kemach stanowiących wyspy w obrębie dawnych jezior (Serteya X) oraz na powierzchni równin wodnolodowcowych porośniętych lasami mieszanymi z istotną rolą brzozy. Stanowiska te mogły być miejscami letniego osadnictwa z rozwiniętym rybołówstwem, z osadą centralną na stanowisku Serteya X, gdzie znaleziono ślady stałych konstrukcji. Także relikty obozowisk w północnej części mikroregionu sertejskiego, w otoczeniu paleojeziora Niwniki, położone były na równinach wodnolodowcowych oraz na brzegu wzdłuż dawnych basenów jeziornych. Miejsca te były niedogodne dla stałego zamieszkania, ale mogły być wykorzystywane przy prowadzeniu rybołówstwa lub jako punkty obserwacyjne. Stanowiska na równinach polodowcowych wzdłuż basenów jezior zostały odsunięte od źródeł wody, można je uznać za punkty związane z terenami łowieckimi lub za obozowiska zimowe (Serteya 3-3).

Wczesny neolit to okres dalszego rozwoju gospodarki przyswajalnej. Plemiona łowców-zbieraczy zaczęły produkować i wykorzystywać w tym czasie ceramikę (Mazurkevich i in., 2012a). Najstarszy zespół narzędzi wczesneolitycznych przypisywany jest kulturze Serteya (stanowiska Serteya XIV) datowanej na około 7900-7200 cal BP (Kittel i in., 2018). Stanowiska tej kultury zostały udokumentowane od regionu Serteji po Wałdaj (Mikljaev, 1995). Później (około 7000-6700 cal BP) pojawiają się ślady przedstawicieli kultury Rudnya, odkryte na stanowiskach Rudnya-Serteya i Serteya X, XIV. Kultura ta cechowała się bogatym przemysłem kostnym (Mazurkevich i in., 2018). Okreseneolitu charakteryzuje intensywny rozwój kultury materialnej człowieka. Najstarsze znaleziska to wytwory kultury Khvalynskaya (około 7000-6000 cal BP) (Kittel i in., 2022). W okolice Serteji przenikały grupyeneolitycznej tradycji stepowej (około 6000-5000 cal BP). Ostatnia fala „stepowa”, która była związana z kulturą Średniego Stogu, mogła przyczynić się do powstania kultury Usviaty (Mazurkevich i in., 2020).

Aktywność ludzka w środkowym neolicie w rejonie WSBP była słabsza niż w otoczeniu jeziora Niwniki (w części północnej mikroregionu sertejskiego) (Mazurkevich, 2003). Społeczności tego okresu najprawdopodobniej korzystały z kilku wyspecjalizowanych typów obozowisk: obozów zimowych i letnich oraz obozowisk łowieckich położonych wzdłuż szlaku wędrówek zwierząt, łowisk oraz ewentualnych punktów obserwacyjnych. W środkowym neolicie osady na palach zakładane były tylko w obszarze WSBP (stanowiska Serteya I, II, X, XI, 5). Różnorodność krajobrazu przyrodniczego umożliwiła wydajną gospodarkę łowiecko-zbieracką i silnie wpłynęła na system osadniczy w tym czasie (Dolukhanov i Miklyayev, 1986). Gospodarka ta była oparta na polowaniu z przewagą nad rybołówstwem i zbieractwem.

Na stanowisku Uswiaty IV datowanym na koniec III tys. p.n.e. znaleziono kości udomowanej świni oraz kości krowy i psa (Sablin i Siromyatnikova, 2009). Zęby konia znalezione na stanowisku Serteya XI z początku III tys. p.n.e. Ich niewielkie rozmiary i cienkie, słabe szkliwo wskazują, że zęby te należały do starego udomowanego konia (*Equus caballus*) (Kuz'mina, 2003). Ludność kultury usviackiej używała także sieci rybackie (Sablin i Siromyatnikova, 2009).



Fotografia 1. Badania archeologiczne prowadzone metodą archeologii podwodnej na stanowisku archeologicznym Serteya II (fot. A. Mroczkowska 2017)



Fotografia 2. Pozostałości pali konstrukcji budynków osady palafitowej Serteya II-1 sub. (fot. A. Mroczkowska 2017)

W okresie 4800-3800 cal BP osadnictwo palafitowe rozwija się na obszarze stanowiska Serteya II (fotografia 1, 2) (Mazurkevich i in., 2020b). Osady palafitowe były zamieszkiwane przez cały rok, a wraz z rozwojem osadnictwa ludność zaczęła gromadzić więcej zapasów żywności. Bogata seria datowań radiowęglowych i dendrochronologicznych pozwoliła na dokładne określenie czasu funkcjonowania osadnictwa palafitowego na tym stanowisku. Najstarsza konstrukcja powstała około 5700 cal BP, a najmłodsze budowle funkcjonowały do 3800 cal BP (Mazurkevich i in., 2012b). Osada palafitowa w świetle aktualnych wyników badań składała się z kilku budynków posadowionych na prostokątnych platformach o wymiarach około $7 \times 4,5$ metra. Ustawione one były na licznych słupach o średnicy kilku-kilkunastu centymetrów, na których opierano kłody w układzie poprzecznym. Na nich znajdowała się warstwa mchu, zasypana gruboziarnistym piaskiem. Na piaszczystym podłożu zakładano paleniska obudowane dużymi kamieniami ułożonymi w okrąg. Ściany budowli mogły być wykonane z wąskich dranic. Słupy o dużej średnicy sytuowane były głównie w narożnikach platformy, a między nimi umieszczone słupy o mniejszej średnicy (Mazurkevich, 2011b).



Fotografia 3. Wykop archeologiczny w obrębie osadów jeziornych na stanowisku STII-2 (fot. A. Mroczkowska 2017)

Ślady działalności człowieka mogą wskazywać, że strefa brzegowa paleojeziora WSBP (fotografia 3) w rejonie stanowiska Serteya II służyła czynnościom gospodarczym (przyrządzań posiłków, miejsce składowania odpadów, podział tuszy upolowanych zwierząt). Na podstawie wyników analiz makroskopowych szczątków roślin (odkrycia m.in. orzechów i malin, krzewów i lili wodnych) mamy informacje o intensywnej działalności osadniczej w strefie brzegowej, gdzie odkryto również pozostałości konstrukcji rybackich, łodzi, fragmenty wioseł, czy też ślady uboju zwierząt, świadczących o intensywnych połowach (fotografia 4,5). Odkryto także pozostałości koszy. Przerwa w funkcjonowaniu osady czy zmiana lokalizacji osadnictwa miała miejsce w rejonie stanowiska Sertaya II w okresie od 4100 do 3800 cal BP. Na stanowisku Serteya II zostały odkryte liczne artefakty ze środkowego neolitu zaliczone do kultury Khvalynskaya, kultury usviackiej czy kultury zyżyckiej oraz kultur stepowych.

Dalszym etapem rozwoju kultury materialnej człowieka była kultura Uzmen datowana na około 4150-3750 cal BP. Klimat w tym okresie był cieplejszy i suchszy, wzrosła także produktywność jezior. Mieszkańcy zaczęli osiedlać się na brzegach i wyspach ówczesnych jezior tworząc obozy z wielosezonowymi budowlami naziemnymi (stanowiska Serteya X, II) (Khrustaleva 2016).

Ludność kultury ceramiki kreskowanej (około 3450-2950 cal BP) zajmowała obszar dorzecza Dniepru, Berezyny, Dźwiny oraz obszar nad górnym i środkowym Dnieprem. Działalność społeczności tej kultury mogła doprowadzić do intensyfikacji procesów stokowych udokumentowanych na obszarze stanowiska Serteya II i datowanych na około 3800-3550 cal BP (Kittel i in., 2020). Ludność prowadziła osiadły tryb życia, zamieszkiwała drewniane domy o konstrukcji zrębowej, a podstawę gospodarki stanowiła uprawa roślin i hodowla zwierząt oraz wspierające je łowiectwo i rybołówstwo (Oshibkina, 1987).

Kolejnym etapem rozwoju społeczności interesującego nas obszaru jest kultura dniepródźwińska (około 2800 cal BP - 300 AD). Osady środkowego etapu rozwoju kultury dnieprsko-dźwińskiej znajdują się na brzegach jezior. Okres ten to czas zwiększonego wpływu człowieka na przyrodę, związanego z rozwojem wypasu bydła i trzebieżą lasów z przeznaczeniem pod grunty rolne (Schmidt, 1992).

Na północ wzdłuż Dźwiny i Toropy oraz na zachód do dorzecza Łowaci przez Usiaty i górne partie Kuny, rozprzestrzeniło się osadnictwo ludności kultury Tuszemla (około 300-700 AD) (Shmidt, 2003, Tret'yakov, 1966). W dorzeczu Toropa osady ludności kultury Tuszemla zajmowały niższe terasy ponad terenami zalewowymi wzdłuż brzegów małych jezior lub rzek.

Ceramika dobrze wyprofilowana z domieszką średniego i drobnego tłucznia lub piasku różni się od ceramiki produkowanej przez społeczność kultury leśnej z poprzedniego okresu (Dolukhanov i in., 2009).



Fotografia 4. Grot kościenny ze stanowiska Serteya II-2 z epoki mezolitu (fot. A. Mroczkowska 2017)



Fotografia 5. Kręg jelenia odkryty przez archeologów ze stanowiska Serteya II (fot. A. Mroczkowska 2017)

Kolejnym etapem rozwoju kultury materialnej człowieka jest kultura długich kurhanów (około 700-900 AD). Główne zabytki znajdują się w dolinach dużych rzek, na terenach zalewowych i niskich terasach nad równiną zalewową, na zboczach dolin rzecznych i brzegach jezior o ciepłej wystawie (Kuz'min, 1988).

Dalszym etapem rozwoju kultury materialnej terenu zachodniej Rosji jest okres rozwoju księstw staroruskich 1000-1300 AD. Nad Dźwiną rozwinięło się Księstwo Połockie. Państwo to funkcjonowało od drugiej połowy X do początku XIV wieku i jego terytorium obejmowało północną i centralną część współczesnej Białorusi oraz dolną Dźwinę w granicach współczesnej Łotwy. Głównym źródłem utrzymania był handel produktami rolnymi.

Drugim ważnym ośrodkiem w historii regionu Serteki było Księstwo Smoleńskie, zajmujące tereny w górnym biegu rzek Dniepru, Wołgi i Dźwiny w XII-XIV wieku. Terytorium księstwa było mocno zalesione. Handel Księstwa Smoleńskiego z Zachodem w XIII-XIV wieku odbywał się głównie wzdłuż Dźwiny. Głównym towarem eksportowym był wosk, a także miód i futra (Natanson-Leski, 1922, Alekseev, 1980).

W średniowieczu niewielkie terytorium w dolinie rzeki Serteki należało do powiatu wieliskiego. Od 1318 r. powiat wieliski wchodził w skład Księstwa Witebskiego, które było częścią Wielkiego Księstwa Litewskiego. W wyniku wojny między Wielkim Księstwem Moskiewskim a Wielkim Księstwem Litewskim w latach 1500–1503, Wielisz wraz z przyległymi ziemiami w ramach Księstwa Toropiec stał się częścią państwa moskiewskiego. Po zakończeniu wojny inflanckiej w 1582 r., Wielisz i ziemie tej parafii stały się przedmiotem sporu między państwem moskiewskim a Rzeczypospolitą Obojga Narodów. Ostatecznie do Rzeczypospolitej Obojgu Narodów przynależało tylko miasto Wielisz, natomiast powiat Wielisz i wołosta jako część ziem Toropiec nie zostały podporządkowane państwu polsko-litewskiemu. Strona polsko-litewska nie zgodziła się na to, a spór graniczny ciągnął się przez wiele lat. Na początku 1582 r. wojewoda witebski Stanisław Patz najechał na ziemie wieliske i u zbiegu rzek Mezha i Dźwina zbudował twierdzę. W 1583 r. granicę przesunięto na północ i północny wschód. W rezultacie okolice Serteki znajdowały się w znacznej odległości od granic dwóch walczących państw (Shelomanova, 1967). Od 1654 do 1678 roku tereny te były przyłączone do państwa moskiewskiego, a następnie do Rzeczypospolitej Obojga Narodów i były częścią tego państwa do 1772 roku. Był to zupełnie nowy, stosunkowo pokojowy okres, w którym na tych terenach szybko rozwijało się rolnictwo. W 1714 r. król August II Mocny nadał Wieliszowi przywileje na produkcję nitów, masztów okrętowych, belek, co spowodowało masową eksploatację drewna. Doprowadziło to do prawie całkowitego wycięcia lasów obszaru do roku

1773. W późniejszym okresie lasy nie były eksploatowane aż do początku XX wieku. Przez cały XVII i pierwszą połowę XVIII wieku terytorium to w wyniku konfliktów zbrojnych znajdowało się albo pod jurysdykcją cesarstwa rosyjskiego, albo pod kontrolą Rzeczypospolitej.

Ostatecznie tereny te w 1772 r. weszły w wyniku I rozbioru w skład Imperium Rosyjskiego. Od tego czasu rozpoczął się pokojowy okres w dziejach tych ziem, który odzwierciedlał nowe kierunki i specyfikę rozwoju gospodarczego carskiej Rosji. Na przełomie XVIII/XIX wieku hrabia N.S. Mawrodon w swoim majątku we wsi Selezni, który przylegał od zachodu do doliny rzeki Serteki aktywnie rozwijał rolnictwo, hodowlę bydła i rzemiosło, rybołówstwo. W latach 1906-1917 reforma rolna P. Stołypina wprowadziła nowy system użytkowania ziemi. Rozpoczął się „odpływ” ludności aktywnej do dużych miast (Makotinskaya, 1980). W 1910 r. w Selezny spławiano drewno i powstała fabryka drewna. Do 1917 r. był to jeden z najbogatszych i najlepiej prosperujących gospodarczo folwarków regionu wieliskiego. Od 1919 r. region wieliski przynależał do Białoruskiej Socjalistycznej Republiki Radzieckiej, ale jeszcze w tym samym roku przyłączony został do Rosyjskiej Federacyjnej Socjalistycznej Republiki Radzieckiej, a od 1922 przynależał do ZSRR. W 1932 r. w regionie rozwinęła się uprawa lnu. W czerwcu 1941 r. rozpoczęto meliorację terenu, jednak wojna przerwała te prace. W latach 1941–1943 teren ten znajdował się pod okupacją niemiecką.

Po 1945 r. z powodu ciężkich strat wojennych nie wszystkie wsie zostały odbudowane, ale 2/3 wsi istniało. Dokończono prace melioracyjne w latach 1971-72. Następnie w latach 1984-85 przeprowadzono remont systemu melioracyjnego. Jest to okres również dużej dynamiki demografii regionu. Spadek liczebności ludności wiejskiej rozpoczął się w drugiej połowie lat 80.

Szczególnie osadnictwo neolityczne jak i sam procesy neolityzacji były silnie uzależnione od zmian paleośrodowiskowych, w tym od długości sezonu wegetacyjnego (Kulkova i in., 2015). Osady na palach udokumentowane na stanowisku Serteya II funkcjonowały bezpośrednio na odsłoniętej powierzchni osadów jeziornych (gytia grubodetrytusowa) na okresowo zalewanym brzegu (Mazurkevich i in., 2017, Kittel i in., 2021). Osadnictwo tego typu formowało się najprawdopodobniej podczas faz regresji poziomu wody w jeziorze, kiedy dno zbiornika było odsłonięte lub podczas sezonowych spadków poziomu wody. Konstrukcje mogły przetrwać kilka sezonów przed ponowną transgresją (Mazurkevich, 2011a, Kulkova i in., 2015b). Przejście do gospodarki produkcyjnej jako element procesu neolityzacji mogło być silnie związane nie tylko z warunkami środowiskowymi, ale także

zdeterminowane wyborem społeczno-kulturowym. Zmiana gospodarki i metod wytwarzania narzędzi mogła zmniejszyć wpływ środowiska na człowieka (Burger i Fristoe, 2018). O ile społeczności w południowych rejonach Niziny Wschodnioeuropejskiej przeszły już do rolnictwa, o tyle na północy, jak w przypadku regionu Sertesi, styl życia myśliwych-rybaków-zbieraczy w dużej mierze został utrzymany, a wraz z nim utrzymywał się specyficzny leśny neolit. Jednym z wyjaśnień tego zjawiska mogą być korzystne lokalne warunki środowiskowe - dostępność różnorodnych zasobów środowiska, stabilny i produktywny ekosystem, wysoka geo- i bioróżnorodność. Bogate lokalne zasoby środowiska, które dały możliwość długotrwałego stosowania gospodarki przyswajalnej i opóźniły wprowadzanie rolnictwa. Możemy założyć różne strategie myśliwskie i zbierackie stosowane w różnym czasie, zdeterminowane zarówno czynnikami środowiskowymi, jak i wyborami społeczno-kulturowymi. W tym kontekście wyniki badań paleoekologicznych stanowią cenne źródło informacji, natomiast stanowisko Serteya II, jako miejsce poboru głównych rdzeni organicznych umożliwia szczegółową i kompleksową rekonstrukcję warunków panujących podczas całego holocenu.

3. Cel badań

3.1 Cel badań i hipoteza badawcza

Główym celem badań było poznanie rozwoju paleogeograficznego Wielkiego Serteskiego Basenu Pojeziornego (WSBP - Большая Сертейская Озерная Котловина) na Pojezierzu Witebskim w późnym vistulianie i holocenie w oparciu o uzyskane wyniki szczegółowych badań paleoekologicznych rdzeni osadów biogenicznych. Współcześnie WSBP stanowi największe rozszerzenie doliny dolnej Serteki, o długości około 1,2 i szerokości ponad 0,5 km (Kittel i in., 2016, 2018). Zbiornik jeziorny w obrębie WSBP funkcjonował z przerwami od późnego vistulianu co najmniej do XVII wieku (Kittel i in., 2018, Wieckowska-Lüth, 2021, Ginter i in., 2023, Płociennik i in., 2022). Początkowo był to zbiornik o zasilaniu proglacialnym (Płociennik i in., 2022). Głównym celem podjętych badań było określenie jak zmieniały się warunki środowiskowe w zbiorniku (poziom wody i trofia) wpływające na osadnictwo w tym rejonie: neolityczne społeczności myśliwych, rybaków i zbieraczy pomiędzy 8300 a 1600 cal BP. Celami szczegółowymi badań były:

1. Rekonstrukcje ilościowe warunków paleoklimatycznych u schyłku vistulianu i w holocenie (w tym rekonstrukcja średnich temperatur najcieplejszego i najchłodniejszego

miesiąca, rocznych amplitud temperatur, średnich rocznych sum opadów), w oparciu o analizę subfosylnych szczątków Chironomidae i Coleoptera oraz zestawienie wyników analizy pyłkowej (wyk. Emilie Gauther) w rdzeniach ST IIa, STII M25,

2. Rekonstrukcja jakościowa zmian poziomu wody w dawnym jeziorze, a więc okresów regresji i transgresji zbiornika oraz okresów wkraczania systemu fluwialnego, na podstawie analiz subfosylnych ochotek z rdzenia STII M25 oraz subfosylnych chrząszczy z profili STII L22 i STII N24. Wykorzystane zostały również rekonstrukcje oparte o wyniki badań geochemicznych i sedymentologicznych (wyk. Daniel Okupny, Jacek Szmańda) a także ilościowe rekonstrukcje oparte o Cladocera (wyk. Dominik Pawłowski) dla rdzeni STII M25, ST IIa oraz dla rdzeni STP I, STP II oparte na Cladocera i Chironomidae oraz Coleoptera z rdzeni STII L22, STII N24.

3. Rekonstrukcja jakościowa ewolucji stanu troficznego paleojeziora w oparciu o wyniki badań subfosylnych ochotek i chrząszczy, a także zbiorowisk roślinnych - głównie na podstawie analizy subfosylnych Coleoptera w porównaniu z wynikami analiz makroskopowych szczątków roślinnych (wyk. Magdalena Wieckowska-Lüth), diatomologicznej (wyk. Monika Rzodkiewicz) i analizy palinologicznej (wyk. Emilie Gauthier) w rdzeniach STII M25, ST IIa, STII L22 i STII N24, STP I, STP II.

4. Szczegółowa jakościowa rekonstrukcja warunków paleoekologicznych paleojeziora (w tym: pH, zanieczyszczenie, trofia, zróżnicowanie siedlisk) z wykorzystaniem wyników analizy Chironomidae. Również wykorzystano do porównania wyniki analiz Cladocera (wyk. Dominik Pawłowski), a także wyniki analizy diatomologicznej (wyk. Monika Rzodkiewicz) w rdzeniach STII M25 i ST IIa.

5. Zbadanie małoskalowych i krótkotrwałych zmian środowiskowych w strefie brzegowej WSBP, w oparciu o zgrupowania Coleoptera w profilach STII L22 i STII N24, co wzbogaci dane peleogeograficzne o dane na temat zdarzeń lokalnych.

6. Określenie wpływu czynników paleośrodowiskowych, zwłaszcza klimatycznych, hydrologicznych i siedliskowych, na funkcjonowanie osadnictwa pradziejowego, w tym pozyskiwanie surowców i pożywienia, strategie gospodarcze czy osadnicze w obszarze WSBP i jego otoczeniu oraz na określenie wpływu działalności dawnych społeczności na rozwój paleoekologiczny zbiornika, w oparciu o wyniki analiz Chironomidae, Cladocera oraz Coleoptera dla rdzeni: STII M25, ST IIa, STII N24, STII L22, STII L29, STP I, STP II i KH.

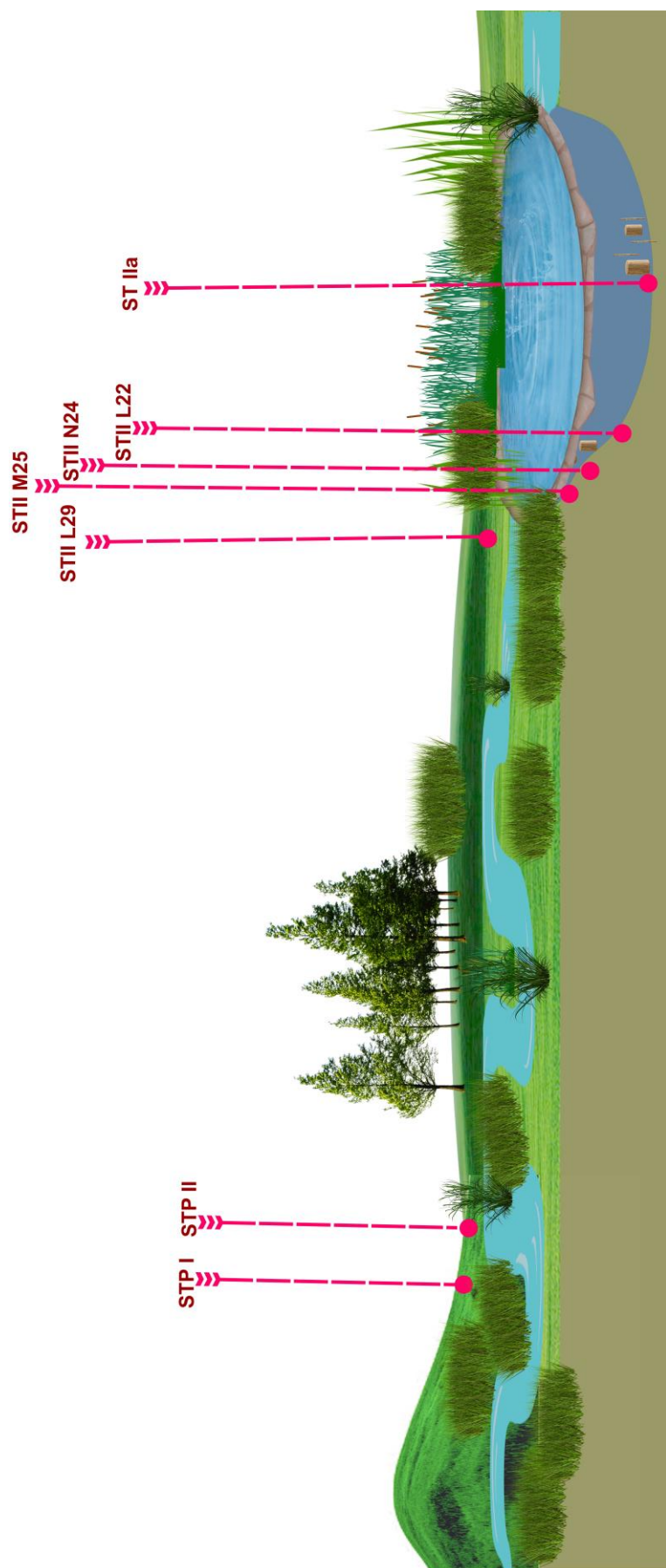
Testowane hipotezy szczegółowe:

- 1) Spadek średnich temperatur lata w rejonie Serteki związany z chłodnymi oscylacjami klimatycznymi 8,2, 5,9 i 4,2 ka cal BP jest większy niż na stanowiskach obszaru Bałtyckiego
- 2) W holocenie dochodziło do I. zmian warunków hydrologicznych zbiornika jeziornego w obrębie WSBP i II. rosnących wpływów systemu rzecznego
- 3) I/Bioarchiwum uzyskane ze strefy głębokowodnej stanowi lepszy zapis zmian paleoklimatycznych, natomiast II/ bioarchiwum ze strefy płytkowodnej zbiornika - lepszy zapis zmiany trofii i wahania poziomu wody
- 4) Stosując analizy wielowymiarowe i system sieci neuronowych w celu przetwarzania wyników, przy użyciu danych z różnych stref zbiornika, możemy oszacować wpływ zaburzeń spowodowanych czynnikami niezwiązanymi z klimatem (np. wpływy antropogeniczne) na uzyskiwane wyniki, w tym rekonstrukcje paleośrodowiskowe
- 5) W okresie atlantyckim i subborealnym wahania lustra wody były na tyle częste, że konstrukcje palafitowe zakładane w III tys. p.n.e. były lokowane prawdopodobnie na obszarach podmokłych wzdłuż brzegów jeziora lub na równinach pojeziornych w okresach regresji
- 6) Zmiany I. klimatyczne i II. hydrologiczne w środkowym holocenie były na tyle niewielkie że nie decydowały w sposób istotny o dostępie do źródeł pożywienia i surowców wykorzystywanych przez społeczności neolityczne w rejonie WSBP
- 7) I. Osadnictwo i gospodarka społeczności neolitycznych w rejonie WSBP były silniej związane z okolicznymi siedliskami lądowymi niż ekosystemem jeziora i II. uzyskiwały szczególnie korzystne środowiskowe warunki funkcjonowania w okresach regresji jeziora
- 8) Funkcjonowanie jeziora w WSBP było silnie uzależnione od reżimu hydrologicznego rzeki Serteki, charakterystycznego dla warunków klimatu kontynentalnego.

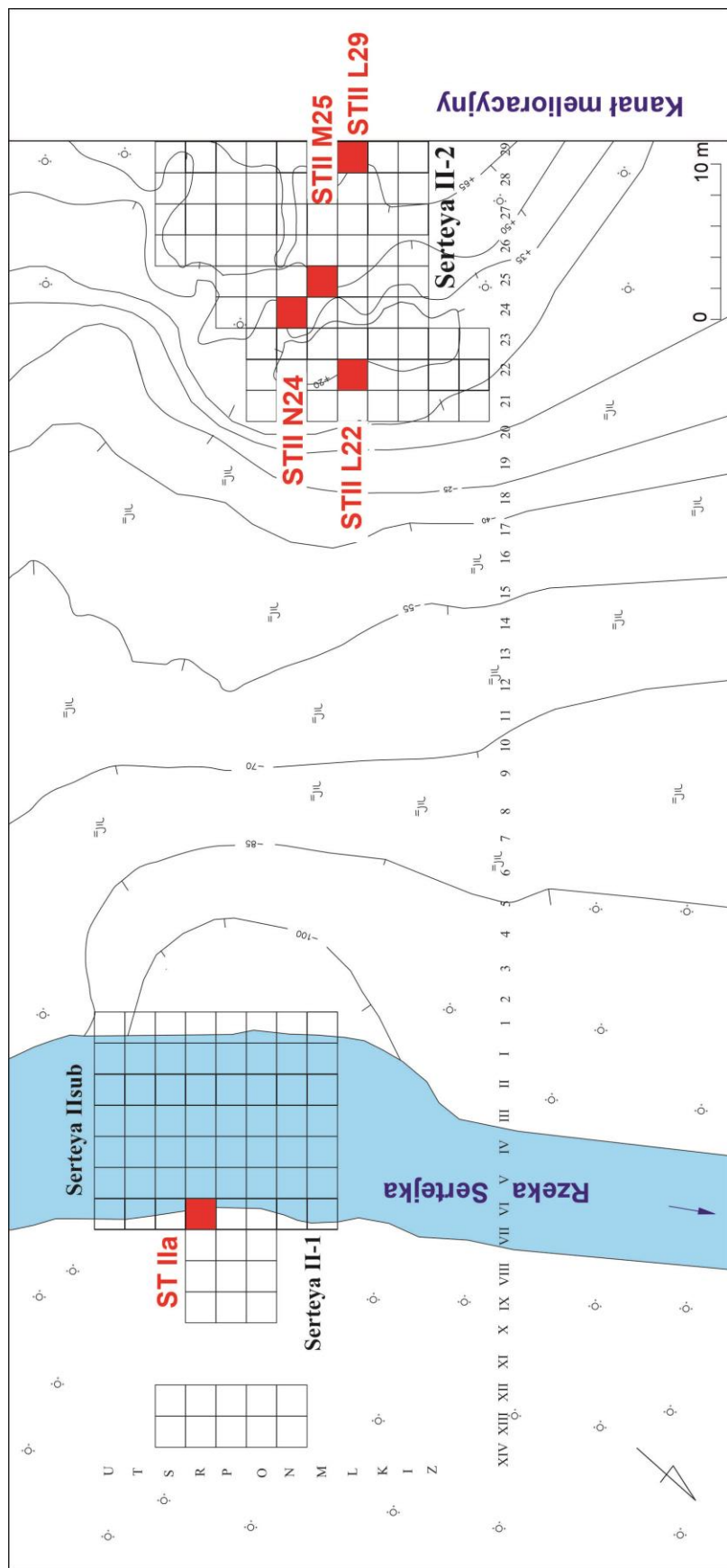
4. Metody badań

4.1 Materiał badawczy

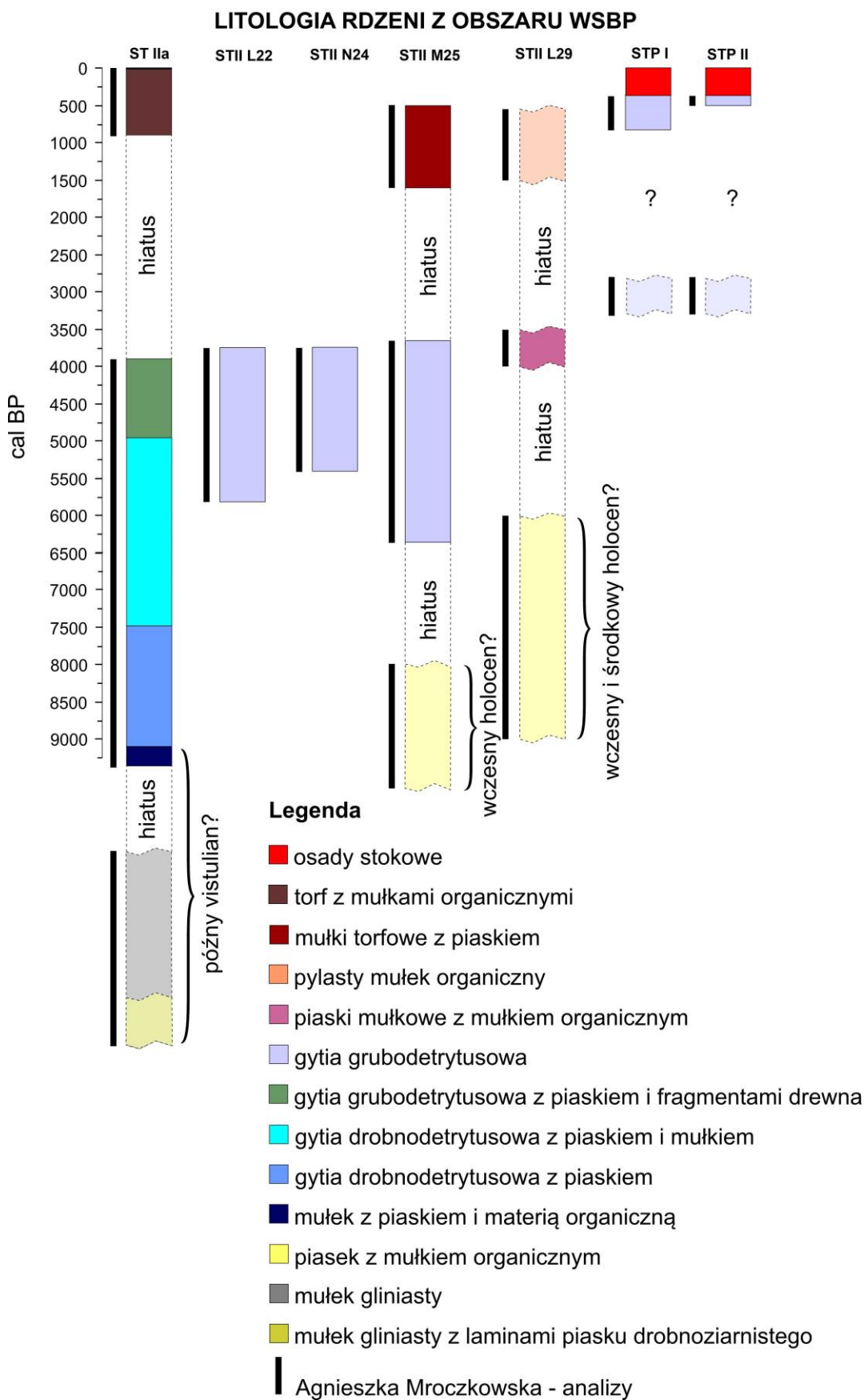
Rekonstrukcja rozwoju paleogeograficznego WSBP została wykonana na podstawie szczegółowych badań 8 rdzeni osadów biogenicznych (tabela 1) pobranych z obszaru i bezpośredniego otoczenia stanowiska archeologicznego Serteya II oraz z obszaru torfowiska Serteya (rycina 5, 6, 7).



Rycina 5. Położenie stanowisk poboru rdzeni na tle rzeźby terenu regionu Sertesi



Rycina 6. Plan rozmieszczenia badanych rdzeni na stanowisku archeologicznym Serteya II
(za Kittel i in., 2021)



Rycina 7. Litologia badanych rdzeni z regionu Sertesi

Tabela 1. Rdzenie i wykonane z nich analiz wraz z opisującymi je publikacjami.

Rdzeń Współrzędne, wysokość	Analiza wykonana w ramach doktoratu	Inne analizy	Bibliografia
ST IIa 55°37'51.69"N 31°32'30.58"E 152.5 m n.p.m.	Chironomidae	geochemiczna i sedimentologiczna, palinologiczna i NPP, makroskopowych szczątków roślin, antrakologiczna, diatomologiczna, malakologiczna, Cladocera, szczątków ryb	Wieckowska- Lüth i in. (2021), Płociennik i in. (2022)
STII 55°37'51.71"N L29 31°32'26.89"E 154 m n.p.m.	Chironomidae, Cladocera	geochemiczna, sedimentologiczna, makroskopowych szczątków roślin, mikromorfologiczna	Kittel i in. (2020)
STII 55°37'51.87"N M25 31°32'27.39"E 153 m n.p.m.	Chironomidae	geochemiczna i sedimentologiczna, palinologiczna i NPP, makroskopowych szczątków roślin, antrakologiczna, szczątków ryb, Cladocera	Mroczkowska i in. (2021b), Kittel i in. (2021)
STII 55°37'51.53"N N24 31°32'27.76"E 152,5 m n.p.m.	Coleoptera	geochemiczna	Mroczkowska i in., w przyg.
STII 55°37'51.78"N L22 31°32'28.35"E 152 m n.p.m.	Coleoptera	geochemiczna	Mroczkowska i in., w przyg.
STP I 55°38'10.45"N 31°31'51.94"E 162 m n.p.m.	Chironomidae, Cladocera	sedimentologiczna, geochemiczna, palinologiczna, makroskopowych szczątków roślin	Kittel i in. (2020), Ginter i in. (2023), Piech i in., w przyg.

STP	55°38'10.42"N	Chironomidae, sedymentologiczna,	Kittel i in.
II	31°31'51.60"E	Cladocera geochemiczna, palinologiczna,	(2020), Ginter i
	156,5 m n.p.m.	makroskopowych szczątków	in. (2023), Piech
		roślin	i in., w przyg.
KH	55°40'33.66"N	Chironomidae, palinologiczna, makroskopowych	Mroczkowska i
	31°30'32.03"E	Cladocera szczątków roślin, ameb	in. (2021a)
	174 m n.p.m.	skorupkowych	

Rdzeń ST IIa (fotografia 6,7) o łącznej długości 795 cm pobrano w 2016 roku próbnikiem Instorf o długości 78 cm.

Tabela 2. Litologia rdzenia ST IIa

Głębokość (cm ppt)	Osady:
0-15	organiczne osady aluwialne
15-95	brunatny torf z osadami organicznymi
95-149	brunatna gytia grubodetrytusowa, z fragmentami drewna i wkładkami piasku
149-314	oliwkowoszara i oliwkowa gytta drobnodetrytusowa z domieszką piasku i mułku
314-444	oliwkowobrunatna gytia drobnodetrytusowa z domieszką drobnego piasku
444-474	jasnobrunatny mułek z drobnoziarnistym piaskiem, z materią organiczną
474-780	beżowy gliniasty mułek
780-795	mułek gliniasty beżowy z laminami piasku drobnoziarnistego

W warunkach laboratoryjnych, z rdzenia pobrane zostały 1 cm plastry w odstępach 2 cm lub 4 cm, z których wypreparowane zostały następnie próbki do analiz paleoekologicznych: pyłkowej i mikrofosyliów pozapyłkowych (NPP), makroskopowych szczątków roślinnych, antrakologicznej, diatomologicznej, malakologicznej, Cladocera, Chironomidae oraz geochemicznej i sedymentologicznej. Ponadto analizie poddano również szczątki ryb wyselekcjonowane w trakcie wykonywania analizy makroskopowych szczątków roślinnych.

Do ustalenia chronologii osadów wykonano serię datowań radiowęglowych metodą AMS wyselekcjonowanych szczątków roślin lądowych. Podstawowa chronologia została opisana przez Więckowska-Lüth i in. (2021).

Rdzeń sekwencji osadów zawiera dwa okresy przerw w sedymentacji (hiatusy) 1/ we wczesnym holocenie oraz 2/ około 4000 do 1300 cal BP, pomiędzy późnym neolitem i wczesną epoką nowożytną (Więckowska-Luth i in., 2021).



Fotografia 6. Wykop archeologiczny na stanowisku archeologicznym STII-1 (fot. A. Mroczkowska 2017)



Fotografia 7. Pobór rdzenia ST IIa (fot. P. Kittel 2016)

W 2016 roku z południowej ściany wykopu archeologicznego na obszarze stanowiska archeologicznego Serteya II-2 pobrany został rdzeń osadów mineralno-organicznych oznaczony symbolem **STII M25** (rycina 8) Miejsce poboru zlokalizowane było w części południowej brzegowej części paleojeziora w obrębie WSBP. Głównym celem analizy tego rdzenia było rozpoznanie sytuacji paleoekologicznej strefy peryferyjnej osady palafitowej oraz w miejscu złożenia neolitycznych szczątków ludzkich (Mazurkevich i in., 2017, Kittel i in., 2021). W miejscu wykopu, około 50 m na WSW od rdzenia ST IIa (fotografia 8 i 9), odkryte zostały kości dwu osobników płci żeńskiej datowane na połowę III tys. p.n.e. oraz towarzyszące im liczne zabytki kultury Usviaty i Zhizhitsa (Kittel i in., 2021). Kości zalegały w stropie gytii grubodetrytusowej na głębokości około 80-110 cm p.p.t. Nad i pod szczątkami ułożone były fragmenty gałęzi drzew. Poniżej miejsca pochówku odkryto dekorowane płytki kostne, drewniane łopatki, płynaki czy fragmenty łuku. Rdzeń pobrany został jako monolity do trzech metalowych pojemników o wymiarach $50 \times 10 \times 10$ cm, obejmując osady z głębokości między 23 a 160 cm p.p.t. (Mazurkevich i in., 2020).



Rycina 8. Szczegółowa lokalizacja rdzeni STII M25 i ST IIa

Chronologię rdzenia określono na podstawie serii datowań radiowęglowych AMS i szczegółowo opisano w Kittel i in. (2021). Pod względem litologicznym profil rdzenia zbudowany jest z: piasku i żwiru z osadami organicznymi i detrytusem roślinnym (160–148,5 cm p.p.t.), gytii gruboziarnistej (148,5-75/80 cm p.p.t.). Dla osadów rdzenia STII M25 wykonano analiz multi-proxy z wysoką rozdzielczością (2 cm) takie jak: analiza subfosylnych Chironomidae, Cladocera, analiza makroszczątków roślinnych, analiza pyłku, analiza geochemiczna i sedymentologiczna, analiza antrakologiczna oraz analiza szczątków ryb (Mroczkowska i in., 2021b, Kittel i in., 2021). Model wiek-głębokość wskazał na ciągłą akumulację jeziorną od około 6300 cal BP do około 3370 cal BP (Kittel i in., 2021).

Monolit STII L29 został pobrany ze ściany wykopu archeologicznego do metalowego pojemnika o wymiarach 50×10×10 cm i obejmuje osady od 65 do 115 cm p.p.t. W profilu litologicznym wydzielono: mułki organiczne (110–109 cm), piasek z mułkiem organicznym (109–100/96 cm), piasek z mułkiem organicznym i detrytusem roślinnym (100/96–80 cm), mułki organiczne rzeczne (80-70 cm), zatorfione mułki organiczne rzeczne (głębokość 70-40 cm p.p.t.). Chronologia rdzenia została uzyskana w oparciu o korelację osadów z rdzenia STII M25 oraz dodatkowe datowanie radiowęglowe (Kittel i in., 2020). Materiał został podzielony na 1 cm plastry z rozdzielczością 2 cm do analizy geochemicznej, sedymentologicznej, analizy subfosylnych Cladocera i Chironomidae oraz analizy makroskopowych szczątków roślinnych. Z pozostałego osadu wykonano cienkie szlify do analizy mikromorfologicznej. Badanie rdzenia skierowane było na poznanie zmian procesów depozycji w strefie brzegowej paleojeziora z uwzględnieniem roli procesów stokowych i rzecznych.

STII L22 i STII N24

Podczas ekspedycji 2018 r. pobrano na stanowisku Serteya II-2 (fot. 8,9) dwa kolejne profile osadów organicznych (o symbolach **STII L22 i STII N24**), przeznaczonych głównie do analizy szczątków subfosylnych chrząszczy. Próbki 1-litrowe pobrane zostały z rozdzielczością 2 lub 4 cm w profilu STII N24 (32 próbki) i 5 cm w profilu STII L22 (21 próbek). Rdzenie datowane zostały na podstawie datowania radiowęglowego metodą AMS makroskopowych szczątków roślin jednorocznych. Dodatkowo, dla uszczegółowienia chronologii, warstwy zsynchronizowano ze stratygrafią uzyskaną dla rdzenia STII M25 (Kittel i in., 2021). Dla warstwy kulturowej przyjęto również jedną datę OSL uzyskaną dla fragmentu ceramiki neolitycznej. Wykorzystano również chronologię archeologiczną warstw kulturowych. W rdzeniach wydzielono następujące poziomy litologiczne: STII L22: poniżej 99 cm - gytia grubodtrytusowa oliwkowa, 99-64 cm - gytia grubodtrytusowa brunatna, 64-50 cm - gytia

grubodtrytusowa jasnobrunatna, 50-0 cm p.p.t. - mułek organiczny, oraz w rdzeniu STII N24: 146-124 cm - gytia grubodtrytusowa oliwkowobrunatna zapiaszczona z fragmentami drewna, 126-108 cm - gytia grubodetrytusowa oliwkowobrunatna z fragmentami drewna i węglami drzewnymi, 108-88 cm - gytia grubodetrytusowa czarnobrunatna z fragmentami drewna i węglami drzewnymi, 88-78 cm - gytia grubodetrytusowa brunatna z fragmentami drewna, 78-70 cm – iły z mułkami organicznymi szare, 70-0 cm p.p.t. – mułki organiczne oliwkowe.



Fotografia 8, 9. Stanowisko STII-2-prace archeologiczne (fot. B. Kotrys 2016)

Rdzenie **STP I** i **STP II** (zostały pobrane z wykopów wykonanych w obrębie stożka akumulacyjnego (Piech, 2021). Wykop STP II miał wymiary $5 \times 2 \times 2$ m i położony był w centralnej części stożka. Natomiast wykop STP I o wymiarach $5 \times 2 \times 1,5$ m położony był w strefie dystalnej stożka. Ze ścian wykopu STP I został pobrany monolit osadów do puszki o wymiarach $50 \times 10 \times 10$ cm z głębokości 138-88 cm p.p.t. Zaś ze ściany wykopu STP II podobny monolit osadów został pobrany z głębokości od 168 cm do 218 cm p.p.t.. W osadach mineralnych budujących stożek wykonano między innymi analizy cech teksturalnych, geochemiczne i paleobotaniczne. Wiek osadu w profilach STP I i STP II określono za pomocą metody stabilnych izotopów ^{210}Pb , oraz metodą OSL i przede wszystkim metodą radiowęglową (Ginter i in., 2023). Dla osadów biogenicznych w rdzeniach STP I i STP II została wykonana analiza subfosylnych Chironomidae i Cladocera w 18 i 21 próbach z rozdzielcością 2,5 cm. Równolegle wykonano analizy geochemiczną, makroskopowych szczątków roślinnych, analizę palinologiczną oraz antrakologiczną.

4.2 Analiza Chironomidae jako narzędzie rekonstrukcji środowiska Wielkiego Sertejskiego Basenu Pojeziornego

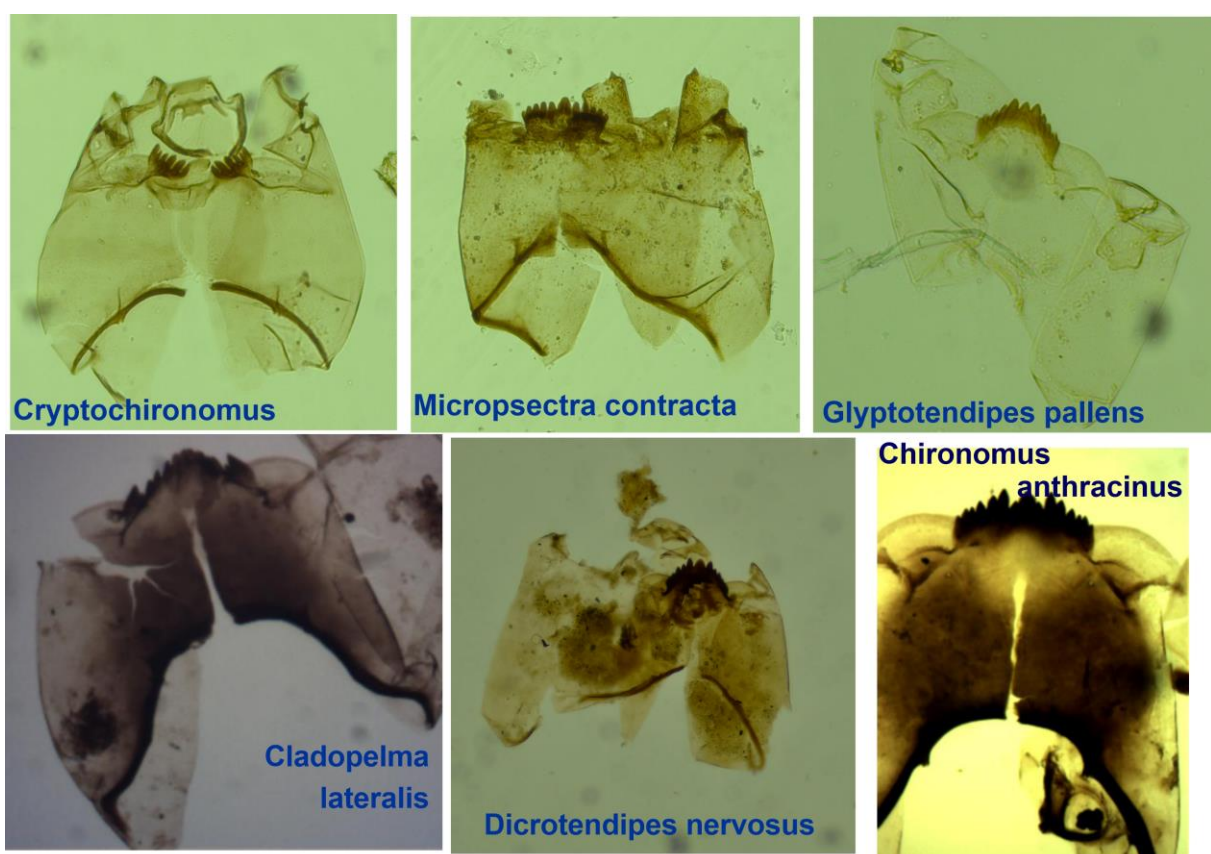
W dysertacji jako podstawową metodę badawczą zastosowano analizę subfosylnych szczątków ochotek (Chironomidae) (rycina 9). Funkcjonowanie larw i poczwarek ochotek jest związane ze środowiskiem wodnym. Rozwój stadium jaja i larwy przebiega na dnie zbiorników wodnych. Chironomidae są bardzo wrażliwe na zmiany środowiska oraz mają krótki cykl życiowy, dzięki czemu świetnie nadają się jako bioindykatory, które pozwalają na dokładne rekonstrukcje paleoekologiczne. Ich szerokie rozprzestrzenienie oraz wąskie optima warunków ekologicznych, w których osobniki rozwijają się i żyją, umożliwiają szczegółowe odtworzenie warunków środowiska na podstawie składu gatunkowego, określonego w oparciu o oznaczanie zachowanych w osadzie puszek głowowych larw (Brooks i in., 2007). Analiza dominacji szczątków poszczególnych gatunków zachowanych licznie w osadzie pozwoliła na zrekonstruowanie zmian paleosrodowiskowych: ilościowo średnich paleotemperatury powietrza w lipcu oraz jakościowo trofii zbiornika, stałości czy reżimu przepływów zbiornika, pH wody zbiornika.

W ramach badań laboratoryjnych oznaczano minimum 50 puszek głowowych Chironomidae w każdej próbce osadów pobranych z profili badawczych z rozdzielcością od 2 cm do 4 cm. Szczegółowo opracowano 3 rdzenie osadów biogenicznych:

- 1/ ST IIa – rozdzielcość 2 i 4 cm, 205 próbek,
- 2/ STII M25 – rozdzielcość 2 cm, 42 próbki,
- 3/ STII L29 - rozdzielcość 2 cm, 21 próbek,
- 4/ STP I - rozdzielcość 2,5 cm, 18 próbek,
- 5/ STP II - rozdzielcość 2,5 cm, 21 próbek.

Próbki przeznaczone do analizy szczątków Chironomidae opracowano laboratoryjnie zgodnie z metodyką opisana przez Brooksa i in. (2007). Następnie uzyskane wyniki dominacji poszczególnych taksonów wykorzystano do analiz statystycznych. Strefowanie zgrupowań wykonano: 1) metodą optimal sum-of-squares partitioning (Bennett, 1996) i liczbę istotnych stref przetestowano z wykorzystaniem modelu broken-stick (MacArthur, 1957) dla profilu STII M25, 2) samouczących się sieci neuronowych Kohonena (SOM) dla profilu ST IIa (Kohonen, 1982, Kohonen, 2001), z wykorzystaniem metody CONISS (Line i Birks, 1996) dla pozostałych profili. Do graficznej prezentacji uzyskanych wyników wykorzystano oprogramowania C2 (Juggins, 2007) lub Tilia (Grimm, 1991) i rioja 1.0-5 (<https://github.com/nsj3/rioja>). W oparciu

o wyniki analizy subfosylnych Chironomidae wykonano także rekonstrukcję średniej paleotemperatury powietrza lipca na podstawie rosyjskiego zbioru testowego (Nazarova i in., 2015), szwajcarsko-norwesko-polskiego zbioru testowego (Kotrys i in., 2020) i fińskiego zbioru testowego (Luoto i Nevalainen, 2017). By móc określić, które czynniki środowiskowe były kluczowe w danym okresie dla zgrupowań Chironomidae wykonano analizę DCA (Detrended Correspondence Analysis - nietendencyjna analiza zgodności) oraz wykorzystano SOM (Self Organizing Maps – samoorganizujące się sieci neuronowe) zgodnie z procedurą przedstawioną przez Płociennika i in. (2015). Część laboratoryjna została wykonana na Wydziale Biologii i Ochrony Środowiska i Wydziale Nauk Geograficznych UŁ, pod opieką merytoryczną dr. Mateusza Płociennika - promotora pomocniczego.



Rycina 9. Przykładowe szczątki Chironomidae z rdzeni osadów biogenicznych (fot. A. Mroczkowska 2019)

4.3 Analiza jakościowa i ilościowa subfosylnych Cladocera

Wioślarki (Cladocera) (rycina 10) są to drobne zwierzęta wodne, należące do podtypu skorupiaków. Szczątki zachowujące się w osadzie umożliwiają identyfikacje do poziomu gatunku. Na podstawie składu i dominacji osobników możliwe jest odtworzenie warunków

środowiska, między innymi: trofii zbiornika, wahań poziomu wody, pH oraz pośrednio zmian klimatu (Szeroczyńska, 1998, Birks i Birks, 1980).

Próbki do analizy Cladocera są przygotowywane według metodyki Frey (1986). Szczątki były oznaczone w próbkach osadu o objętości 1 cm³. W każdej próbce identyfikowano minimum 70 osobników, z analizy wyłączono zaś próbki o małej liczebności (<70 os./ 1 cm³). Do graficznego opracowania wyników użyto programu C2 (Walanus i Nalepka, 1999) strefy wyznaczono metodą CONISS. Identyfikacja i analiza wyników zostały wykonano pod opieką dr Martą Wojewódką-Przybył z ING PAN. W ramach rozprawy doktorskiej wykonano analizę rdzeni:

- 1/ STII L29 - rozdzielcość 2 cm - około 21 próbek,
- 2/STP I - rozdzielcość 2,5 cm, 18 próbek,
- 3/STP II - rozdzielcość 2,5 cm, 21 próbek



Rycina 10. Przykładowe szczątki Cladocera z rdzenia KH (fot. A. Mroczkowska, 2022)

4.4 Analiza szczątków Coleoptera

Subkopalne szczątki chrząszczy (rycina 11) wykorzystywane są często jako indykatory paleośrodowiska zwłaszcza w badaniach osadów pochodzących ze stanowisk archeologicznych. Ich atutem jest występowanie szczątków osobników żyjących zarówno w środowiskach lądowym jak i wodnym (Coope, 1986, Elias, 1994). Dodatkowymi zaletami badań paleoekologicznych szczątków tej grupy są: duża wrażliwość na bodźce środowiska,

ogromna różnorodność gatunkowa, mobilność (szybka migracja), dobre zachowanie szczątków w osadzie oraz identyfikowalność. Znajomość siedlisk poszczególnych gatunków umożliwia odtworzenie wielu cech dawnego środowiska, między innymi: cech paleoklimatu (średnich temperatur najcieplejszego i najchłodniejszego miesiąca, średnich rocznych amplitud temperatury), warunków glebowych, jakości wód zbiorników powierzchniowych, roślinności (rodzaju zbiorowisk roślinnych, ich kondycji, fazy rozwoju roślin, obecności rozkładających się roślin i związanych z nimi grzybów), cech środowisk wodnych (temperatury, trofii, dostępności pożywienia, wielkości zbiornika, prędkości i wielkości przepływu, stopnia przejrzystości wody, warunków hydrologicznych koryt rzecznych, wahania poziomu wody w tym też zaburzeń w zlewniach) (Osborne, 1988, Buckland i Buckland, 2006, Smith i Howard, 2004, Davis i in., 2007, Atkinson i in., 1986).

Próbki przygotowano w oparciu o metodę flotacji kerozynowej (Coope, 1986). Z pojedynczej próbki zidentyfikowano wszystkie występujące szczątki chrząszczy. Identyfikacja została wykonana pod opieką koleopterologów prof. Marka Wanata, dr. hab. Pawła Jałoszyńskiego, dr. Rafała Rutego, dr. Mieczysława Stachowiaka, dr. Marka Przewoźnego w Muzeum Przyrodniczym Uniwersytetu Wrocławskiego oraz prof. Nicole Whitehouse w muzeum The Box: Plymouth, podczas programu Erasmus+.

Na podstawie frekwencji chrząszczy wykonano analizę wzajemnego przedziału klimatycznego (mutual climate range - MCR) (Atkinson i in., 1987, Bray i in., 2006), pozwalającą na rekonstrukcję rocznej amplitudy temperatur dla badanego terenu. Tak jak dla innych analiz w profilu ST IIa, tak dla frekwencji chrząszczy wykonano strefowanie rdzeni STII L22 i STII-N24 za pomocą map Kohonena (SOM, Self-Organizing Map), czyli samouczących się sztucznych sieci neuronowych (Kohonen, 1995).

Uzyskane wyniki umożliwiły dokładne zrekonstruowanie zmian paleoekologicznych zachodzących w WSBP i w okresie 5500-3600 cal BP. Wyniki badań paleoekologicznych dają wiedzę do szerszej rekonstrukcji paleogeograficznej ewolucji systemu jeziornego funkcjonującego w tej części współczesnej doliny rzeki Serteki oraz rekonstrukcji regionalnych dla obszaru położonego w obrębie Niziny Wschodnioeuropejskiej.

Materiał opracowany został z rozdzielcością 2 i 4 cm lub 5 cm z dwóch rdzeni o oznaczeniach:

- 1/STII L22 - 21 próbek (rozdzielcość 5 cm);
- 2/STII-H24 - 32 próbki (rozdzielcość 2 i 4 cm)



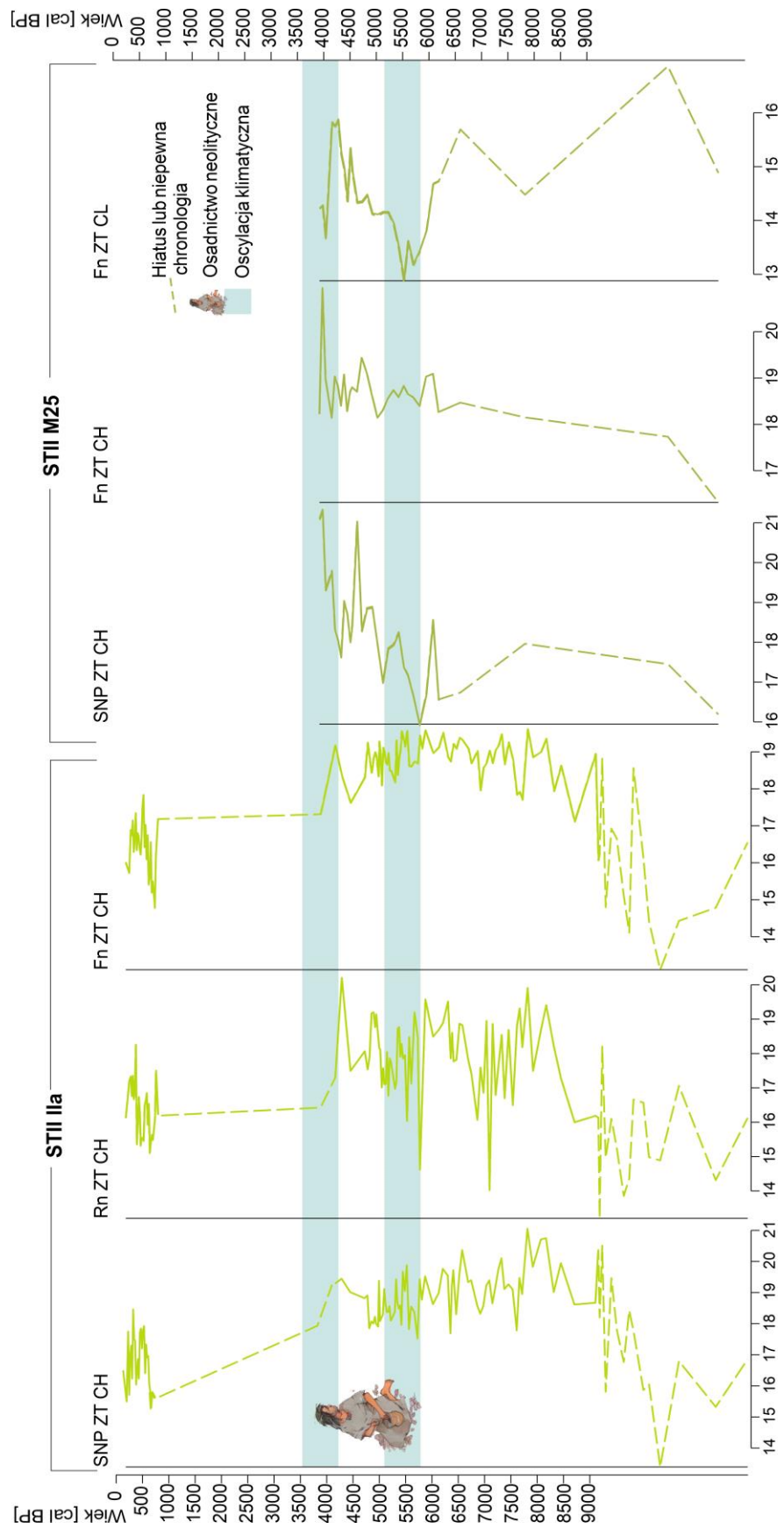
Rycina 11. Kolekcja szczątków subfosylnych chrząszczy użytych do identyfikacji i analizy

5. Wyniki

5.1. Problem badawczy 1

Zmiany średnich paleotemperatur lipca jako czynnik warunkujący zmiany ekosystemu jeziornego

Średnia temperatura lipca była czynnikiem determinującym różnorodność gatunkową w przypadku zgrupowań Chironomidae. Rekonstrukcje paleotemperatur lipca (rycina 12) zostały wykonane dla rdzeni osadów pobranych ze stanowiska Serteya II, w oparciu o wyniki analiz profili ze strefy głębokowodnej (ST IIa) i ze strefy brzegowej (STII M25) paleojeziora. Wykonano je na podstawie jakościowego składu zgrupowań Chironomidae bazując na trzech zbiorach testowych: rosyjskim zbiorze testowym (Rn ZT) (Nazarova i in., 2015), szwajcarsko-norwesko-polskim zbiorze testowym (SNP ZT) (Kotrys i in., 2020) i fińskim zbiorze testowym (Fn ZT) (Luoto i Nevalainen, 2017). Wartości temperatur lata uzyskano także ze zgrupowań Cladocera na podstawie fińskiego zbioru testowego (Fn ZT) (Nevalainen i Luoto, 2017) oraz lata i zimy na podstawie Coleoptera z profili STII N24 i STII L22 (Atkinson i in., 1986). Dodatkowo informacje o temperaturze najchłodniejszego miesiąca, rocznych sumach opadów otrzymano na podstawie zbiorów pyłkowych zrekonstruowanych za pomocą europejskiego ZT (Peyron i in., 2013, Martin i in., 2020).

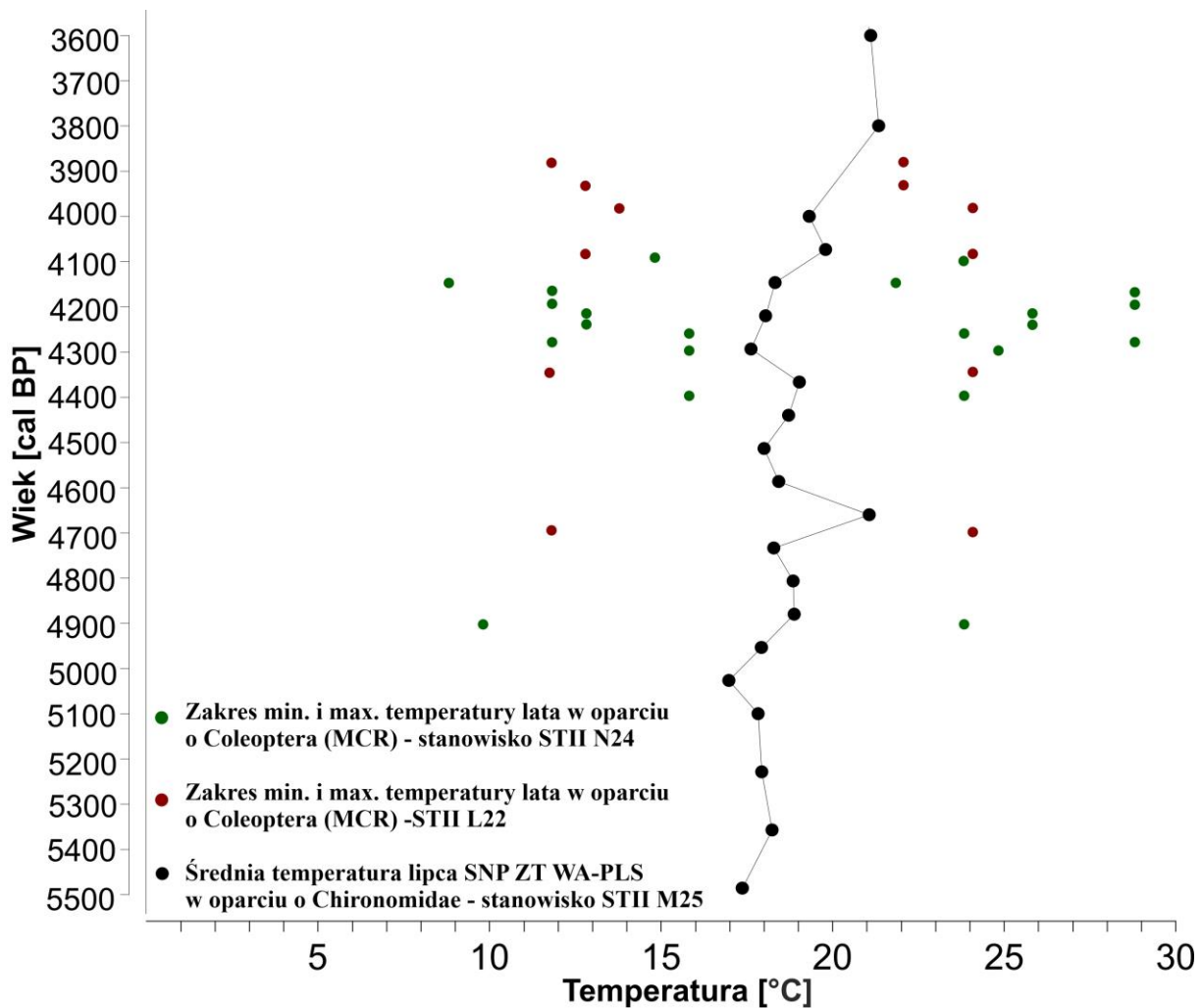


Rycina 12. Zestawienie średnich paleotemperatur lipca odtworzonych w oparciu o szczątki Chironomidae i Cladocera ze stanowisk ST IIa i STII M25

Wyniki DCA wskazują że zarówno w przypadku sekwencji ST IIa jak i STII M25, uzyskane na podstawie Chironomidae ilościowe rekonstrukcje temperatury, są zbieżne z głównymi trendami zachodzącymi w strukturze ich zgrupowań, w przeciwieństwie do Cladocera które bardziej reagowały na zmiany poziomu wody. Zgrupowania Chironomidae znacznie częściej także posiadają dobre współczesne analogi, niż zgrupowania Cladocera które mają same słabe współczesne analogi, w wykonanych rekonstrukcjach (Mroczkowska i in., 2021b, Płociennik i in., 2022).

Wartości rekonstrukcji opartych o Chironomidae dla rdzenia ze strefy brzegowej (STII M25) na podstawie Fn ZT wahały się od 16,3°C (158 cm) do 20,9°C (96 cm), rekonstrukcja SNP ZT WA-PLS od 15,9°C (142 cm) do 21,3°C (96 cm) i rekonstrukcja Rn ZT z 16,8°C (158 cm) do 21,6°C (146 cm). Generalnie rekonstrukcje Fn ZT i SNP ZT wykazały podobny, rosnący trend temperatury lata od spągu do stropu, jednak rekonstrukcja SNP ZT wykazała wyższą amplitudę i zmienność temperatury. Rekonstrukcja w oparciu Rn ZT wykazała odwrotny, lekko spadkowy trend temperatury od spągu do stropu, chociaż wartości pozostają zbliżone do rekonstruowanych w oparciu o SNP ZT i Fn ZT.

Średnie wartości temperatury powietrza w lipcu zrekonstruowane w oparciu o Chironomidae z profilu ze strefy głębokowodnej (ST IIa) na podstawie SNP ZT, wahały się w przedziale od 11,2-13,4°C do 19,1-21,1°C. Wartości rekonstrukcji temperatury z tego profilu na podstawie Rn ZT miały zakres od 13,2°C do 20,2°C. Wartość temperatury rekonstruowanej w oparciu o Fn ZT mieściły się w zakresie od 13,1°C do 19,6°C. Wszystkie rekonstrukcje wykazują podobny trend, od niskich temperatur lata w późnym vistulianie, najwyższych we wczesnej fazie środkowego holocenu (8400-7800 cal BP), po wyraźnie widoczną (SNP WA-PLS (weighted averaging partial least squares regression - regresja metodą cząstkowych najmniejszych kwadratów), Rn ZT) lub słabo zdefiniowaną (SNP ANN (artificial neural network - sztuczne sieci neuronowe), Fn ZT) tendencję spadkową w późnym holocene, oraz ochłodzenie podczas małej epoki lodowej. W okresie od późnego vistulianu do środkowej fazy późnego holocenu amplituda wahań temperatur jest najsłabiej zaznaczona w rekonstrukcji opartej o SNP ANN, a najsilniej zaznacza się w rekonstrukcjach Rn ZT. Zarówno rekonstrukcje SNP WA-PLS, jak i Rn ZT wykazują słabe ochłodzenie do 18,9-14,0°C (Rn ZT) – 19,5-18,7°C (SNP ZT) około 7000 cal BP. Dodatkowo, Rn ZT pokazał bardzo niskie wartości temperatury w okresie około 5850-5800 cal BP, co zbiega się z wydarzeniem Bonda 4 (5900 cal BP) (Bond i in., 2001).



Rycina 13. Zakres temperatur letnich (wzajemny zakres klimatyczny - ang. MCR (Mutual Climate Range) w oparciu o zgrupowania subfosylnych Coleoptera dla rdzeni STII N24, STII L22 zestawione z wykresem paleotemperatury lipca SNP ZT dla rdzenia STII M25

Średnie wartości paleotemperatury powietrza lipca na podstawie wyników uzyskanych dla rdzenia ze strefy głębokowodnej (ST IIa) wg rekonstrukcji Fn ZT bazującej na Cladocera, wahały się od 12,2°C do 17,6°C. Rekonstrukcje oparte o zgrupowania subkopalnych wioślarek wskazywały na wyższe temperatury w okresie od późnego vistulianu do wczesnego holocenu ze stałą tendencją spadkową, jest to sprzeczne z powszechnie znymi trendami klimatycznymi dla tego okresu (Kaufman i in., 2020). Niskie do bardzo niskich, wysoce zmienne wartości zaobserwowano w śródkowym holocenie (8200–5000 cal BP), następnie temperatura wzrosła około 280 cal BP, czyli podczas małej epoki lodowej. Trend na pierwszej osi nietendencyjnej analizy zgodności (DCA Ax1) dla zgrupowań Cladocera jest zbieżny z wynikami rekonstrukcji poziomu wody i nakazuje ostrożność względem interpretacji wyników rekonstrukcji temperatury w oparciu o dane wioślarkowe dla strefy głębokowodnej (ST IIa). Trend dla

pierwszej osi nietendencyjnej analizy zgodności (DCA Ax1) dla makroszczątków roślinnych koreluje z trendem średniej temperatury lipca rekonstruowanej w oparciu o Chironomidae, co sugeruje, że na zbiorowiska roślinne w paleojeziorze i na jego brzegu miały również wpływ warunki klimatyczne, szczególnie w okresie wegetacyjnym (Płociennik i in., 2022).

Wymienione zakresy temperatur z rdzenia ze strefy brzegowej (STII M25) i strefy głębokowodnej (ST IIa) mieszczą się w przedziałach opracowanych w MCR (Mutual Climate Range - Zakres Klimatyczny Temperatur) dla Coleoptera (rycina 13) z rdzeni ze strefy brzegowej (STII N24 i STII L22) (Płociennik i in., 2022, Mroczkowska i in., 2021b, Mroczkowska i in., w przyg.). Przedziały paleotemperatur letnich opracowane na podstawie zgrupowań subkopalnych chrząszczy pokazują zakres od 9°C około 4000 cal BP do 29°C około 4200 cal BP. Wartości temperatur zimowych tolerancji występujących gatunków sięgają do nawet -47°C około 4200 cal BP do 18°C z tego samego okresu. Wynika to jednak z niewielkiej liczebności szczątków w próbach, niewystarczającej do uzyskania wartościowej rekonstrukcji zakresów temperatur (Mroczkowska i in., w przyg.).

Na podstawie badań rdzenia strefy głębokowodnej (ST IIa) udokumentowano, że przed 10500 cal BP w osadzie mineralno-organicznym występowały taksony zimnolubne (*Micropsectra typ contracta*), eurytopowe (*Procladius*, *Polypedilum typ nubeculosum*) oraz słabiej reprezentowane ciepłolubne (*Paratanytarsus typ penicillatus*). Dolny odcinek rdzenia z części głębokowodnej (ST IIa) charakteryzuje się niską liczebnością szczątków Cladocera i Chironomidae oraz nielicznymi makroskopowymi szczątkami roślinnymi. Analiza Cladocera wykonana przez D. Pawłowskiego wskazuje na to, że liczebność wioślarek w tej fazie funkcjonowania strefy głębokowodnej (ST IIa) była stosunkowo niska i charakteryzowała się dominacją taksonów odpornych na zimno, takich jak gatunki planktonowe z rodziny Bosminidae, m.in. *Bosmina (E.) coregoni*, *Bosmina (E.) longispina*, *Bosmina (E.) longirostris* i rodziny Daphniidae, np. *Daphnia longispina* (Korhola, 1999, Sarmaja-Korjonen i in., 2006). Gatunki z rodziny Bosminidae i takson *Chydorus sphaericus* są uznawane za wczesnych kolonizatorów zbiorników powstały po ustąpieniu lądolodu (Hofmann, 2000, Pawłowski, 2011, Płociennik i in., 2022).

HTM (Holocene Thermal Maximum - holocene optimum klimatyczne) na stanowiskach Serteji zbiega się z okresem podanym przez Renssen i in. (2012), natomiast w północnej Eurazji HTM przypada na 7500–7000 cal BP z odchyleniem temperatury w lecie o 2,5–5,0°C w stosunku do czasów przedindustrialnych (Renssen i in., 2012). Zapis średnich paleotemperatur lipca w rdzeniu strefy głębokowodnej (ST IIa) wskazał na odchylenie wartości

temperatur o 3,5–5,5°C w stosunku do czasów współczesnych, w zależności od zastosowanego modelu. Żadna z rekonstrukcji strefy głębokowodnej (ST IIa) nie dostarcza obrazu wyraźnego spadku temperatury, który można powiązać z ochłodzeniem 8200 cal BP. Dla Chironomidae tylko dwa punkty temperaturowe przypadają na okres 8250–7750 cal BP i jest to spowodowane koniecznością zsumowania wyników sąsiednich próbek ze względu na niską koncentrację puszek głowowych. Li i in. (2019) wyraźnie wskazują na słabą reakcję zbiorowisk roślinnych na ochłodzenie 8200 cal BP w Europie Wschodniej w porównaniu ze Skandynawią. Analiza rekonstrukcji średniej paleotemperatury lipca w rdzeniu ze strefy głębokowodnej (ST IIa) rejestruje chłodną oscylację około 7000–6800 cal BP, co może korelować z wilgotnym zdarzeniem klimatycznym 7400–6800 cal BP widocznym też około 7400–6800 cal BP, które zaobserwowano w naciekach w jaskiniach Wyżyny Małopolskiej (Starkel i in., 2006, Starkel i in., 2013) oraz na wyżynach wschodniej Europy (Mazei i in., 2020).

Rekonstrukcja średniej paleotemperatury lata na podstawie Chironomidae w oparciu o Rn ZT z rdzenia strefy głębokowodnej (ST IIa) wskazała na słabo zaznaczoną chłodną oscylację około 5800 cal BP, ale pozostałe rekonstrukcje Chironomidae sugerują wyraźnie niższe temperatury latem, w trakcie 5800 cal BP. Ochłodzenie to zostało również zidentyfikowane w rdzeniu ze strefy brzegowej (STII M25) położonym w płytce strefie litoralnej WSBP (Mroczkowska i in., 2021b). Podczas wydarzeń 6200–5000 cal BP i małej epoki lodowej w północno-wschodniej Europie wystąpiły silne przesunięcia mas powietrza syberyjskiego, sięgające aż na południe Ukrainy i po Bałkany (Weninger i Harper, 2015). Wszystkie trzy rekonstrukcje wykonane na podstawie rdzenia ze strefy brzegowej (STII M25) wykazały chłodne oscylacje korelowane ze zdarzeniami 5.9 i 4.2 cal BP i związany z nimi spadek średnich temperatur lipca o około 1–2°C. W rekonstrukcjach tych wyraźnie widać, że w okresie northgrippianu temperatura powietrza latem była wysoka, najczęściej w przedziale 17–20°C. Porównanie z innymi stanowiskami w Europie Wschodniej wskazuje, że wartości rekonstrukcji średniej paleotemperatury lata opartych o Chironomidae były w regionie Serteki zwykle o 2°C wyższe niż w obszarze bałtyckim, podczas gdy na Nizinie Środkowopolskiej i Wyżynie Środkoworusyjskiej wartości były zbliżone. Wskazuje to, że w regionach bardziej kontynentalnych, odległych od wpływów Bałtyku, temperatury latem były wyższe. Rekonstrukcje Fn ZT i SNP ZT z sekwencji STII M25 wskazują też tendencję wzrostową średnich paleotemperatur lipca od 5900 do 4200 cal BP. Według rekonstrukcji Rn ZT przebieg średnich paleotemperatur lipca wykazywał jedynie słabą tendencję spadkową. Tak samo w zapisach ze stanowisk kontynentalnych położonych pomiędzy 30° do 60° szerokości

geograficznej N oraz w profilu głębokowodnym (ST IIa) widać trend spadkowy temperatury po 6000 cal BP (Nosova i in., 2019, Koff, 2010, Płociennik i in., 2022). Na trendy rekonstrukcji SNP ZT i Fn ZT STII M25 sugerujące rosnący trend wartości w okresie od środkowego do późnego northgrippianu mogą częściowo wpływać lokalne czynniki, jak np. transgresja wód jeziora. Z drugiej strony odtworzenie wyższych temperatur po 5000 cal BP może być związane z eutrofizacją na stanowisku ze strefy brzegowej spowodowaną działalnością społeczności neolitycznych (patrz Problem 4) (Kittel i in., 2018). Taksony ciepłolubne ochockowatych zwykle preferują wyższą trofię (Płociennik i in., 2020). Eutrofizacja wywołana przez działalność ludzką mogła spowodować pośrednio zawyżone wyniki wartości rekonstruowanych temperatur z płytowodnego rdzenia ze strefy brzegowej (STII M25) położonego w obrębie obszaru podlegającego bezpośredniemu oddziaływaniu społeczności neolitycznych (Kittel i in., 2018, 2021).

Zdarzenie 4200 cal BP jest słabo zaznaczone w rekonstrukcjach części głębokowodnej (ST IIa) (Płociennik i in., 2022), pomimo widocznego sygnału w pobliskim rdzeniu ze strefy brzegowej (STII M25) (Mroczkowska i in., 2021b). Może to być spowodowane częściowym przemieszaniem warstw osadów i wpływem człowieka na ich formowanie w przypadku rdzenia ze strefy głębokowodnej (ST IIa) w okresie funkcjonowania budowli palafitowych (Płociennik i in., 2022). Oscylacja 4200 cal BP zapisała się również w osadach zbiorników w Hirvijaervi (jako chłodna), Jeziorze Kurjanovas (dwa etapy: ciepły i chłodny), Zalozhtsy (wilgotne, chłodne lato i łagodna zima) oraz w Stążkach i Rąbieniu (suche i chłodne lato) (Artyushenko i in., 1982, Luoto i in., 2010, Heikkilae i Seppä, 2010, Gałka i in., 2013, Płociennik i Brooks, dane niepublikowane). Wszystkie pozostałe rekonstrukcje z terenu Europy Środkowoschodniej dla tego okresu mają na ogół niską rozdzielcość.

Wyniki rekonstrukcji opartych o zgrupowania Chironomidae z rdzenia ze strefy brzegowej (STII M25) wskazujące, że w northgrippianie oscylacje klimatyczne wystąpiły około 5900, 5000–4700 i 4200 cal BP oraz są bardziej widoczne na podstawie rekonstrukcji paleoklimatycznych z pyłku (Mroczkowska i in., 2021b). Zbiorowiska pyłkowe wskazują na zwiększyony kontynentalizm w trakcie tych epizodów.

Rekonstrukcje paleoklimatyczne oparte na różnych zbiorach testowych nie dostarczają jednego trendu wyników dla ostatniego tysiąclecia z rdzenia ze strefy głębokowodnej (ST IIa). Część wyników rekonstrukcji opartych na SNP ZT i Fn ZT sugeruje, że późne średniowiecze (około 750–600 cal BP) i ostatnie dwa stulecia były zimniejsze niż wczesne czasy nowożytnie

(600–200 cal BP), podczas gdy inne, oparte na Rn ZT rejestrują ochłodzenie około 650–550 cal BP i 450–350 cal BP (Płociennik i in., 2022).

5. 2 Problem badawczy nr 2

Zmiany poziomu wody w WSBP jako czynniki silnie oddziałujące na rozwój biocenozy zbiornika

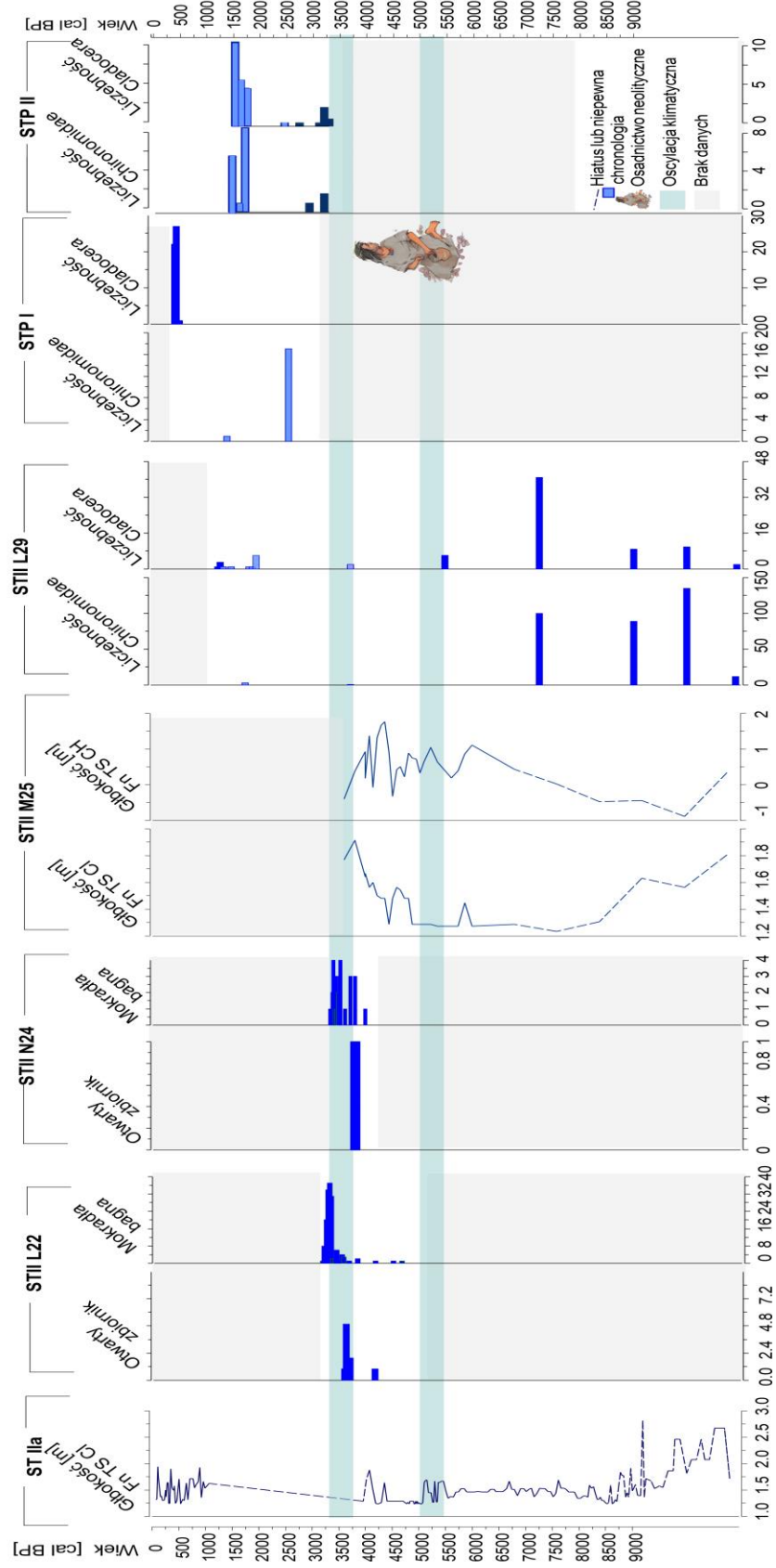
Zmiany poziomu wody były rekonstruowane ilościowo (rycina 14) w oparciu o zgrupowania Chironomidae i Cladocera z profilu głębokowodnego (ST IIa) i ze strefy brzegowej (STII M25) oraz jakościowo z profilu ze strefy okresowo zalewanej - STII L29 i ze strefy brzegowej w rejonie stożka akumulacyjnego (STP I - rycina 15 i STP II - rycina 16), a także jakościowo w oparciu o zgrupowania chrząszczy z profili ze strefy brzegowej (STII N24 i STII L22). Rekonstrukcje z rdzeni strefy głębokowodnej (ST IIa) i ze strefy brzegowej (STII M25) oparto na fińskich zbiorach testowych dla Cladocera oraz dla Chironomidae (Luoto i in., 2010). W przypadku rdzenia ze strefy brzegowej (STII M25) wszystkie próbki do rekonstrukcji głębokości wody oparte na zgrupowaniach subkoplanych Cladocera reprezentowały bardzo słabe współczesne analogi. W przypadku rekonstrukcji opartej na zgrupowaniach subkoplanych Chironomidae ze strefy brzegowej (STII M25) tylko jedna próbka z 124 cm pozostała poniżej progu 2 percentyla, reprezentując bardzo dobre współczesne analogi, sześć zostało w granicach 5-10 percentyla, reprezentujący umiarkowane współczesne analogi, natomiast 24 próbki pozostały powyżej progu 10 percentyla, co oznacza, że są to próbki o słabych i bardzo słabych współczesnych analogach (Mroczkowska i in., 2021b). Zmiany w strukturze zgrupowań wioślarek i ochotek reprezentowane przez wyniki DCA Ax1 nie są też zbieżne z przebiegiem rekonstrukcji poziomu wody w oparciu o te proxy, przebiegają natomiast podobnie do rekonstrukcji temperatury lata. W sekwencji zgrupowań Cladocera ze strefy głębokowodnej (ST IIa) wszystkie próbki miały bardzo słabe współczesne analogi jednak trend DCA Ax1 jest wyraźnie zbieżny z przebiegiem rekonstruowanego poziomu wody, bardziej niż z rekonstrukcją temperatury lata (Płociennik i in., 2022).

Dolna część rdzenia strefy głębokowodnej (ST IIa) zbudowana jest z osadów wodnolodowcowych (limnoglacialnych), które akumulowane były w starszej części późnego vistulianu (zlodowacenia valdai) (Kittel i in., 2018). Jeziora polodowcowe w obrębie WSBP, zasilane przez wody proglacialne, mogły pojawić się wkrótce po wycofaniu lądolodu z tego obszaru w późnym vistulianie, być może w fazie epe (kamion) pomiędzy 18000–17000 cal BP

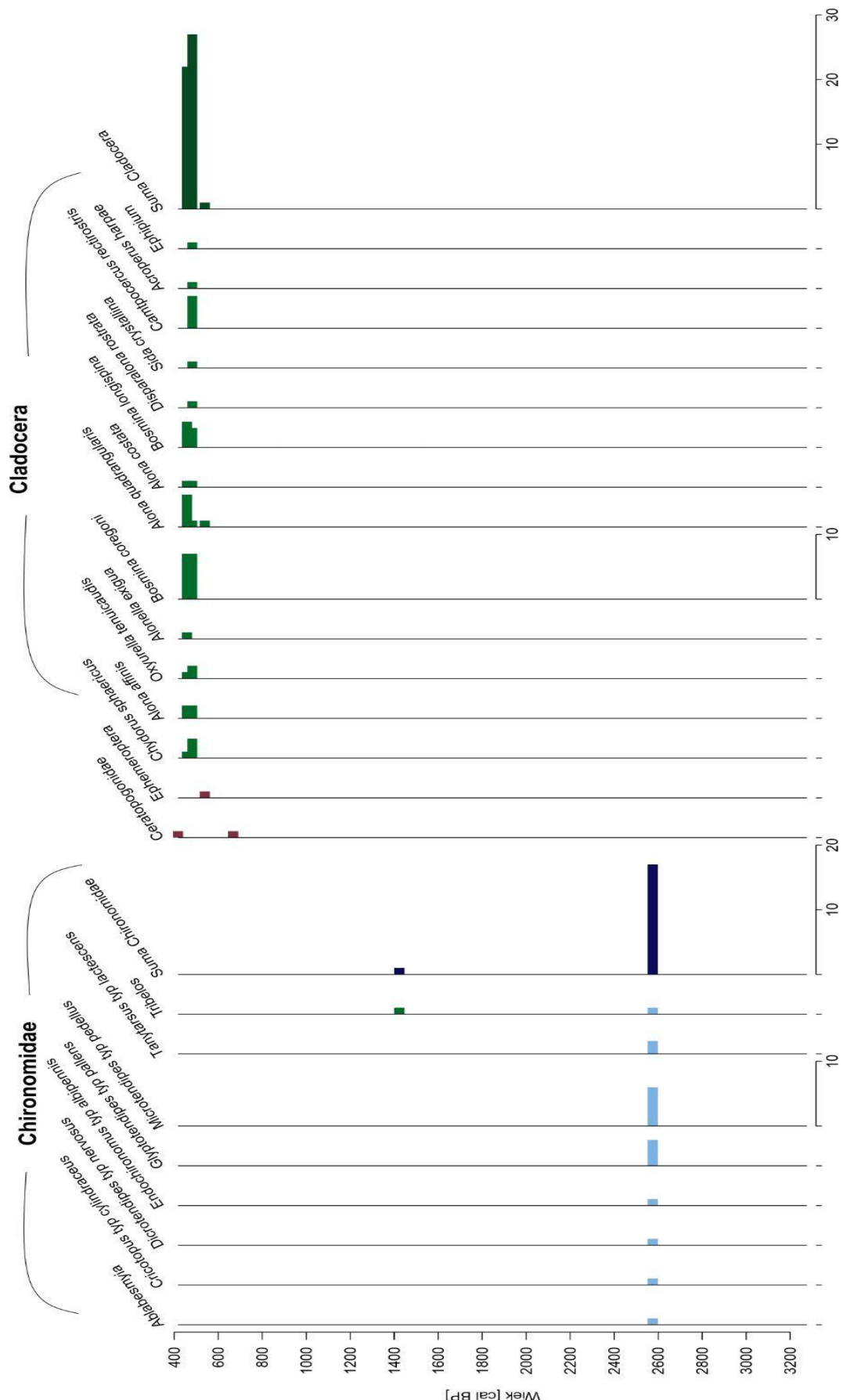
(Płociennik i in., 2022). Ten początkowy etap rozwoju jezior charakteryzował się bardzo niską liczebnością zarówno ochockowatych i kuczmanów, jak też zapisał się niską zawartością makroskopowych szczątków roślin oraz okrzemek. Warunki musiały być wówczas bardzo zmienne i niekorzystne dla organizmów wodnych (Wieckowska-Lüth, 2021). Obecność makrobentosu i meiobentosu (Chironomidae, Ceratopogonidae i Cladocera) wskazała jednak, że zbiornik wodny funkcjonował w tym okresie co najmniej sezonowo. W młodszej części późnego vistulianu rozwinał się sezonowy zbiornik, skolonizowany przez przypadkowe gatunki odporne na niskie temperatury. Były to w większości taksony typowe dla strefy borealnej (Hofmann i Winn, 2000, Nazarova i in., 2015). Na podstawie rekonstrukcji głębokości opartej o Cladocera wynika, że zbiornik był głęboki. Symulacja przedstawiona w Płociennik i in., (2022) może być przeszacowana z powodu m.in. 1) elastyczności ekologicznej występujących taksonów, 2) szybkiego tempa ich rozmnażania bezpłciowego kiedy jezioro jest wolne od pokrywy lodowej (Sarmaja-Korjonen, 2003, Pawłowski i in., 2013) i dużej zdolności do dyspersji.

W oparciu o wyniki badań osadów WSBP można stwierdzić, że w młodszej części greenlandianu (około 9000-8200 cal BP) klimat prawdopodobnie był wilgotniejszy niż w okresie wcześniejszym. Zapis tego odcinka w rdzeniu ST IIa zawiera dwie przerwy w sedimentacji osadu (hiatusy) we wczesnym holocenie. Osady zbudowane są głównie z mułku piaszczystego z domieszkami organicznymi, które mogły być redeponowane podczas transgresji wczesnoholoceńskiej (Wieckowska-Lüth i in., 2021). Około 9000 cal BP koncentracja i bogactwo gatunkowe subfosylnych bezkręgowców wzrosły w osadach z rdzenia ze strefy głębokowodnej (ST IIa), wśród Cladocera liczne są taksony pelagiczne, obecne są też licznie gatunki litoralne i fitofilne (Płociennik i in., 2022). Równocześnie dochodzi do spadku poziomu wody i zmiany stosunków geochemicznych w jeziorze (niższy stosunek Fe/Mn i wyższe Ca/Fe). Badania hydrologiczne wskazują, że podczas holoceńskiego optimum klimatycznego epizody wezbrań wiosennych stały się częstsze (Płociennik i in., 2022, por. też Pawłowski i in., 2016b, Danilovich i in., 2019).

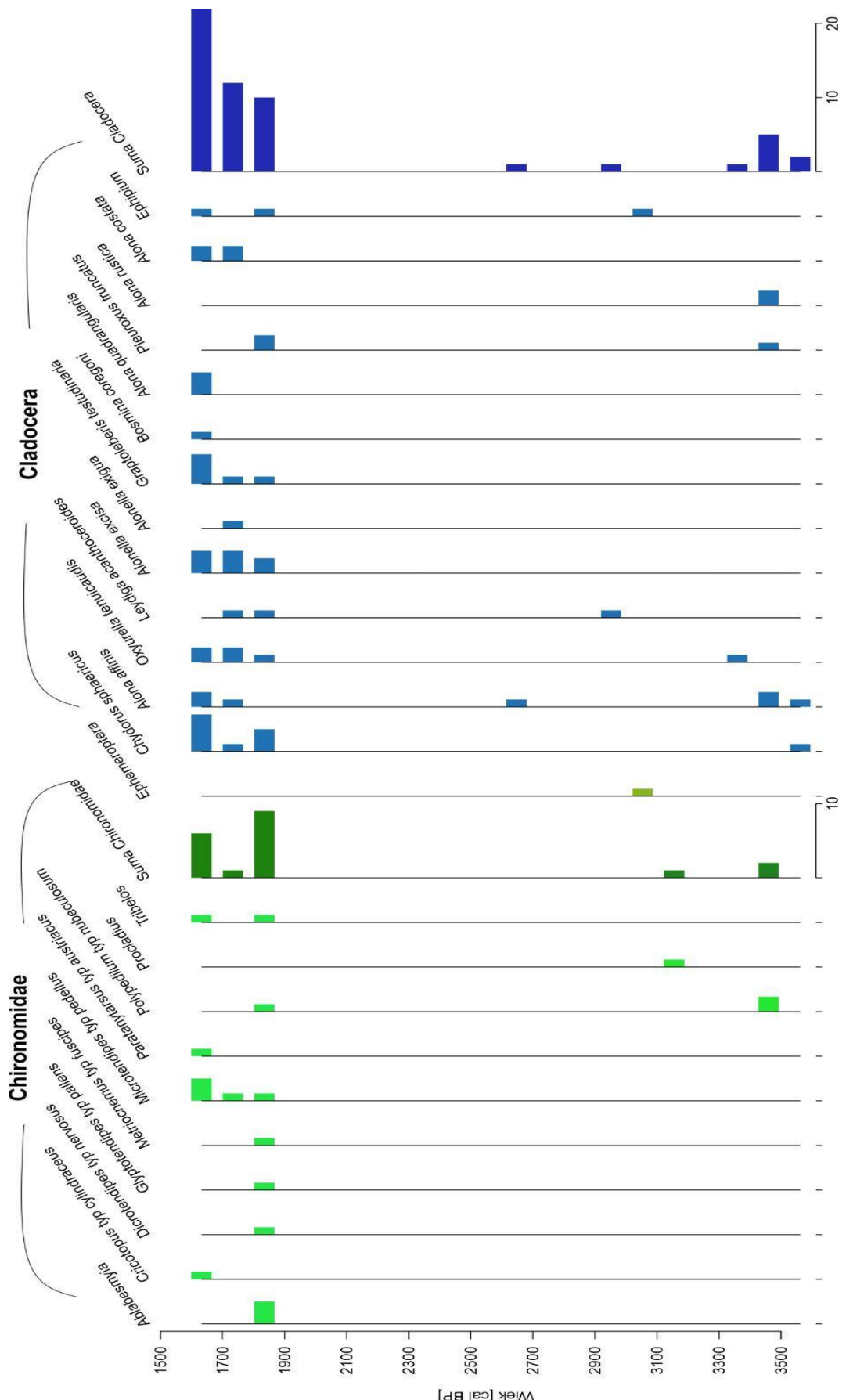
Warunki środowiskowe (na stanowisku ST IIa) w northgrippianie (8200–4200 cal BP) sprzyjały bardziej ochockowatym i okrzemkom litoralnym, niż pelagicznym wioślarkom (patrz Problem 3). Okres podniesienia poziomu wody przed 6310 cal BP udokumentowany został również w rdzeniu części okresowo zalewanej (STII L29), kiedy to wystąpiła najwyższa liczebność wioślarek. W tej fazie występowały gatunki pelagiczne, takie jak *Bosmina longispina* i *Bosmina coregoni* (Kittel i in., 2020).



Rycina 14. Zestawienie rekonstrukcji zmian poziomu wody w oparciu o FN ZT dla Chironomidae oraz Cladocera ze stratygrafią zgrupowań Chironomidae, Cladocera i Coleoptera z rdzeni ze strefy brzegowej WSBP



Rycina 15. Zgrupowania subfosylnych Chironomidae i Cladocera w rdzeniu STP I



Rycina 16. Zgrupowania subfosylnych Chironomidae i Cladocera w rdzeniu STP II

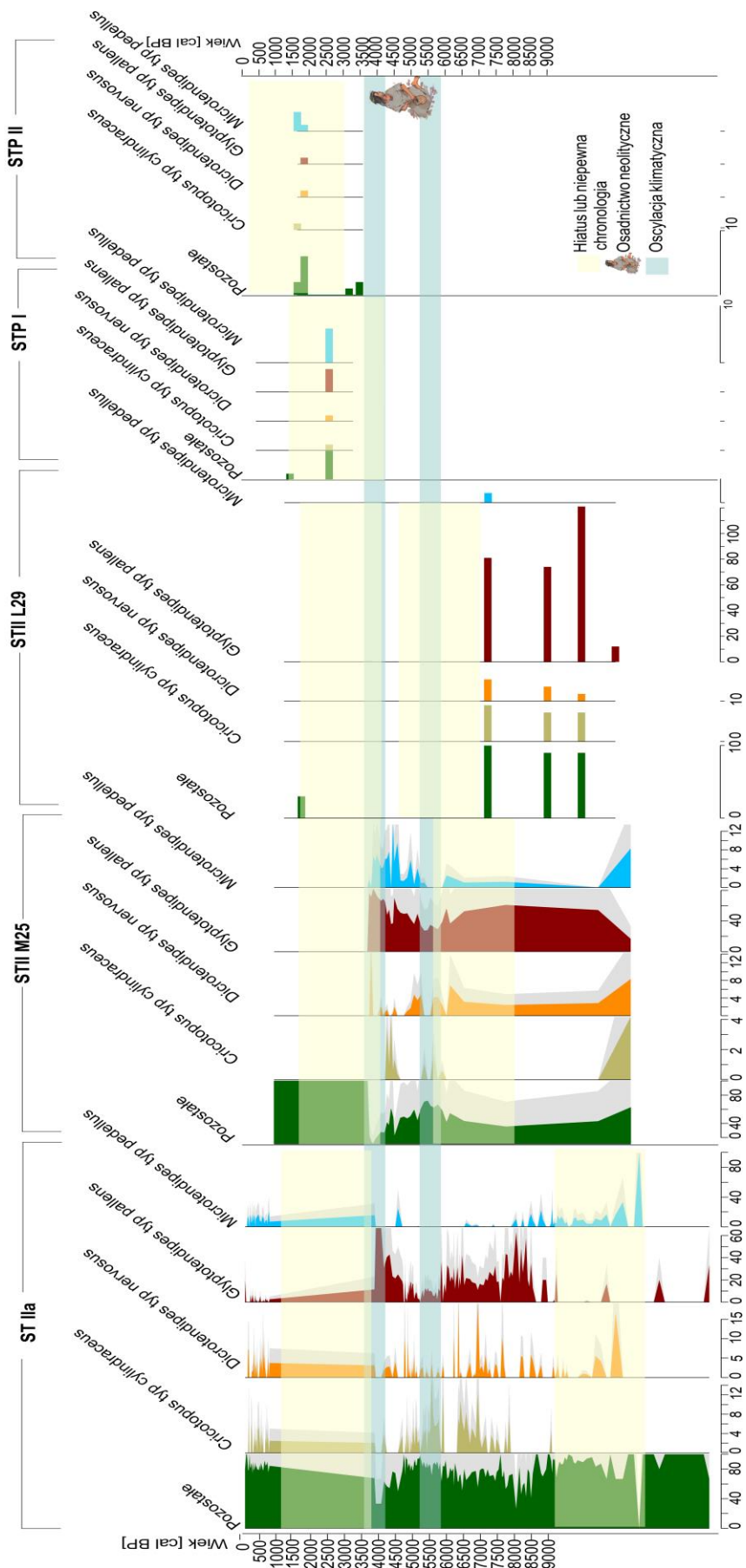
Do około 6200 cal BP w profilu głębokowodnym (ST IIa) poziom wody stale się obniżała, na co wskazała mniejsza liczebność wioślarek (głównie obecnych gatunków makrofitowych i kosmopolitycznych) oraz zwiększały się udział makroszczątków roślin wodnych porastających dno zbiornika. Wśród Chironomidae dominowały gatunki typowe dla płytowych wód z organicznym dnem (Płociennik i in., 2022). W strefie brzegowej jeziora (STII M25) do 6100 cal BP obecność makrofitów zanurzonych, takich jak *Potamogeton* spp. i *Chara*, oraz pelagicznych gatunków Cladocera (szczątki *Bosmina longirostris*) wskazują na wyższy poziom wody (głębokość około 1,2 do 2 m, z krótkim wzrostem poziomu wody około 5900 cal BP). Różnorodność gatunkowa zgrupowań Chironomidae sugerowała zaś epizydyczny lub sezonowy charakter tych zmian. Następnie (około 4950 cal BP) pojawiają się gatunki litoralne Cladocera, np. *Alona quadrangularis*, oraz gatunki litoralne Chironomidae - *Glyptotendipes* typ *pallens*, *Endochironomus albipennis* i *Dicrotendipes* typ *nervosus*, świadczące o funkcjonowaniu płytowego zbiornika z sezonowymi wezbraniami (Mroczkowska i in., 2021b, Kittel i in., 2021).

Około 4400 cal BP w profilu ze strefy brzegowej (STII M25), niższa koncentracja puszek głowowych Chironomidae świadczy o być może jedynie sezonowej obecności płytowego lustra wody, jednak w kolejnych próbkach przypadających na oscylację 4200 cal BP rekonstrukcja oparta o Chironomidae wskazała na wyraźny wyższy poziom wody. Świadczy to o dużej zmienności warunków hydrologicznych w okresie funkcjonowania osady palafitowej ówczesnego jeziora w obrębie WSBP. Analiza rdzenia strefy głębokowodnej (ST IIa) wskazała na to, że wahania te mogły być spowodowane roztopowymi(?) wezbraniami w górnym odcinku rzeki Serteki (Płociennik i in., 2022). Jednocześnie w rdzeniach ze strefy brzegowej STII L22 (około 4500-4300 cal BP) oraz STII N24 (około 4400-4300 cal BP) pojawiły się gatunki chrząszczy związane z materią organiczną naniesioną podczas zdarzeń wezbraniowych (Mroczkowska i in., w przyg.). Od około 4400 cal BP nastąpił spadek nagromadzenia szczątków makrofitów, Chironomidae i Cladocera w profilu ze strefy głębokowodnej ST IIa, co wskazało na niekorzystne warunki dla zbiorowisk roślinności wodnej takiej jak nymfeidy i elodeidy oraz bezkręgowców wodnych w strefie brzegowej (STII M25) WSBP (Więckowska-Luth i in., 2021, Mroczkowska i in., 2021). Najprawdopodobniej odzwierciedla to znaczny spadek poziomu wody i postępujący proces terrestrializacji jeziora. Dane paleozoologiczne wskazują też, że epizody znacznych wahań poziomu wody i zalania w miejscu rdzeni ze strefy brzegowej (STII N24 i STII L22) miały miejsce odpowiednio około 4200-4100 cal BP oraz 4100-3800 cal BP (Mroczkowska i in., w przyg.). Podobny zapis odnotowano w rdzeniu

STII L29 dla okresu około 3900 cal BP (Kittel i in., 2020). Na powtarzające się wezbrania wskazał także wzrost nagromadzenia makroszczątków hydrofitów w osadzie oraz piki dominacji gatunków planktonowych Cladocera około 3900 cal BP i 3800 cal BP. Obok planktonowych gatunków z rodziny Bosminidae pojawiły się inne wioślarki pelagiczne (m.in. *Daphnia pulex*). Skład taksonomiczny wioślarek w tym okresie sugerował rozwój strefy otwartej toni wodnej przez okres kilku tygodni w ciągu roku. Nagromadzenie statoblastów Bryozoa (głównie *Cristatella mucedo*) w profilach ST IIa i STII M25 również dowodzi obecności wody w tym czasie. Analiza fenologiczna Chironomidae stwierdzonych w rdzeniach ze strefy brzegowej paleojeziora wskazuje, że wysokie stany wody powodujące podtopienia w profilu ze strefy okresowo zalewanej (STII L29) miały miejsce w okresie wiosennym, kiedy gwałtowne podniesienie poziomu wody rzeki Sertejki zasilającej WSBP powodowały intensywne roztopy (Kittel i in., 2020). Jest to zgodne z współczesnym reżimem wodnym cieków w dorzeczu Dźwiny.

Krótkotrwałe wezbrania odnotowano jeszcze około 3350 cal BP w rdzeniu STII M25 ze strefy brzegowej (Kittel i in., 2021). Wystąpiły w tym czasie pelagiczne gatunki z rodziny Bosminidae oraz gatunki bentosowe. Liczne wśród nich były gatunki kosmopolityczne Cladocera obficie notowane w jeziorach strefy umiarkowanej (Pawłowski i in., 2016a, 2016b). Wzrost udziału wioślarek i taksonów pelagicznych związanych z osadami był w tym czasie ściśle skorelowany z nanoszeniem osadów mineralnych podczas wezbrań (por. Pawłowski i in., 2015, Kittel i in., 2016). W tym czasie w rejonie rdzenia ST I istniał płytki, niewielki zbiornik, funkcjonujący prawdopodobnie jedynie okresowo (być może sezonowo?), o czym świadczą nieliczne notowane epizodyczne Cladocera i Chironomidae (Piech i in., w przyg.).

W rdzeniu STP II na podstawie wyników analiz subkopalnych Chironomidae udokumentowano wezbranie, które miało miejsce około 2600 cal BP (Ginter i in., 2023). W rdzeniu osadów STP I Chironomidae występowały około 750-620 cal BP, kiedy to pojawiają się gatunki związane ze strefą litoralną jeziora (Piech i in., w przyg.). Pod koniec tego okresu pojawiły się Ceratopogonidae, które są ściśle związane z makrofitami, co może świadczyć o dalszym wypłycaniu się zbiornika.



Rycina 17. Rozkład gatunków wspólnych Chironomidae dla wszystkich badanych rdzeni

Od późnego średniowiecza do około 200 cal BP zbiornik ulegał eutrofizacji i zarastaniu, o czym świadczy wystąpienie gatunku Cladocera *Leydigia acanthocercoides*, zasiedlających wody o niskiej przezroczystości (Piech i in., w przyg.). Postępującą terrestrializację potwierdza występowanie taksonów typowych dla siedlisk ziemnowodnych, np. *Metriocnemus* typ *fuscipes*. Po tym czasie niewielki wzrost poziomu wody notowany był jedynie podczas trwania Małej Epoki Lodowcowej (350-150 cal BP) (Piech i in., w przyg.).

Przeprowadzone studia wykazały, że zbiornik wodny funkcjonujący w obrębie WSBP był znacznie głębszy w późnym vistulianie niż w środkowym i późnym holocenie. Ponadto w późnym okresie wczesnego holocenu i w środkowym holocenie funkcjonowało stabilne, płytke jezioro. W późnym holocenie, szczególnie w małej epoce lodowej, odnotowano znacznie wyraźniejszy spadek poziomu wody i funkcjonowanie płytkego, być może okresowego jeziora. Ponadto udokumentowano również interesującą zmienność subkopalnych zgrupowań Chironomidae w badanych strefach dawnego zbiornika. W rdzeniach ze strefy okresowo zalewanej (STII L29, STP I) występowały gatunki jeziorne, brak natomiast gatunków ziemnowodnych. Gatunki te prawdopodobnie były nanoszone z osadem podczas wezbrań w górnej części zlewni Sertejki.

Zestawiając różnorodność gatunkową zgrupowań ze wszystkich badanych rdzeni (rycina 17) można zauważyć, że rdzeń ze strefy głębokowodnej cechuje największa bioróżnorodność. Interesujące jest także, że jedynie 4 gatunki były wspólne dla wszystkich czterech rdzeni: *Glyptotendipes* typ *pallens*, *Cricotopus* typ *cylindraceus*, *Dicrotendipes* typ *nervosus*, *Microtendipes* typ *pedellus*. Są to gatunki litoralne preferujące warunki mezo-eutroficzne, na ogół związane z makrofitami. Wskazało to, że strefy paleojeziora w WSBP bardzo różniły się składem i różnorodnością gatunkową Chironomidae. Rdzenie strefy brzegowej STII L29 i STP I także lepiej dokumentują wahania poziomów wody. Lokalizacja poboru rdzenia powinna zostać odpowiednio dostosowana do celów zakładanych w badaniach. Jeżeli mają być śledzone procesy regionalne - takie jak zmiany klimatyczne czy inne środowiskowe zachodzące w całym jeziorze, lepsze wyniki daje badanie profilu głębokowodnego z środkowej części zbiornika. Procesy lokalne, wahania poziomu wody i np. wpływ miejscowych społeczności ludzkich lepiej odzwierciedlają profile ze strefy brzegowej zbiornika.

5.3 Problem badawczy nr 3

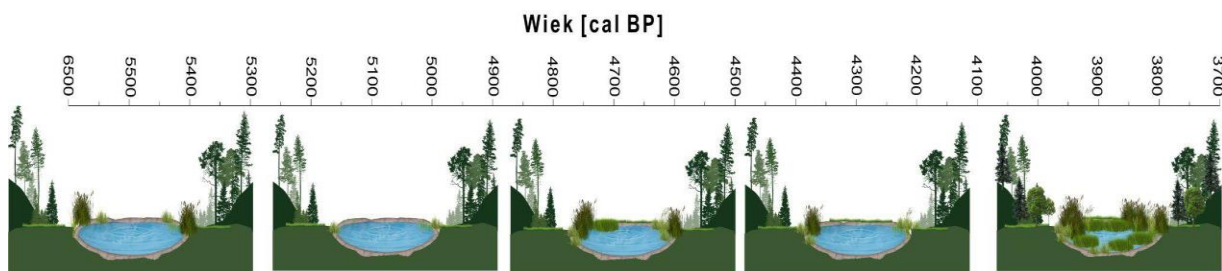
Zmiany siedliskowe na stanowisku Serteya jako obraz naturalnej sukcesji jeziornej

We wszystkich badanych rdzeniach osadów biogenicznych udokumentowanych zostało ogółem 129 gatunków Chironomidae. Jedynie 4 taksony są obecne w każdym rdzeniu. Wskazało to na wysoką różnorodność gatunkową i siedliskową. Również w rdzeniach obejmujących dłuższy okres sedymentacji wystąpiła duża zmienność gatunków w czasie. Także Coleoptera wskazywały na dużą różnorodność ekologiczną terenu (gatunki wodne, koprofilne, lasów liściastych, bagien i mokradeł czy łąk i wrzosowisk). W dwóch rdzeniach udokumentowane zostały aż 84 gatunki Coleoptera. Stwierdzono też szczątki gatunków Coleoptera związane z napływkami (*Cercyon tristis*, *Coelostoma orbicular*, *Hydrochus brevis*, *Stenus cicindeloides*, *Tanysphyrus lemnae*) czy taksony korpopilne, takie jak *Aphodius* sp. i *Staphylinus* sp.

Warunki środowiskowe, takie jak: trofia zbiornika, stopień pokrycia dna roślinnością wodną, pH zostały zrekonstruowane z zastosowaniem metod jakościowych, w oparciu o spektralną tolerancję warunków występowania poszczególnych taksonów Chironomidae, Cladocera oraz Coleoptera (rycina 18, 19, 20). Początek rozwoju zbiornika WSBP wiąże się z procesami wytapiania brył martwego lodu (Kittel i in., 2018, Płociennik i in., 2022). Procesy te zachodziły najprawdopodobniej w okresie bølling-allerød, tj. między 14200 a 12600 cal BP wg Dzieduszyńskiej (2019). W jeziorze stopniowo rosła liczelnosc wioślarek. Na początku były to głównie taksony litoralne, później zwiększała się dominacja gatunków pelagicznych. Wczesna faza rozwoju ekosystemu zbiornika charakteryzowała się niekorzystnymi warunkami dla bezkręgowców, okrzemek i makrofitów. Żaden takson z badanych grup bioindykatorów nie znalazł warunków optymalnych w tym okresie (Płociennik i in., 2022).

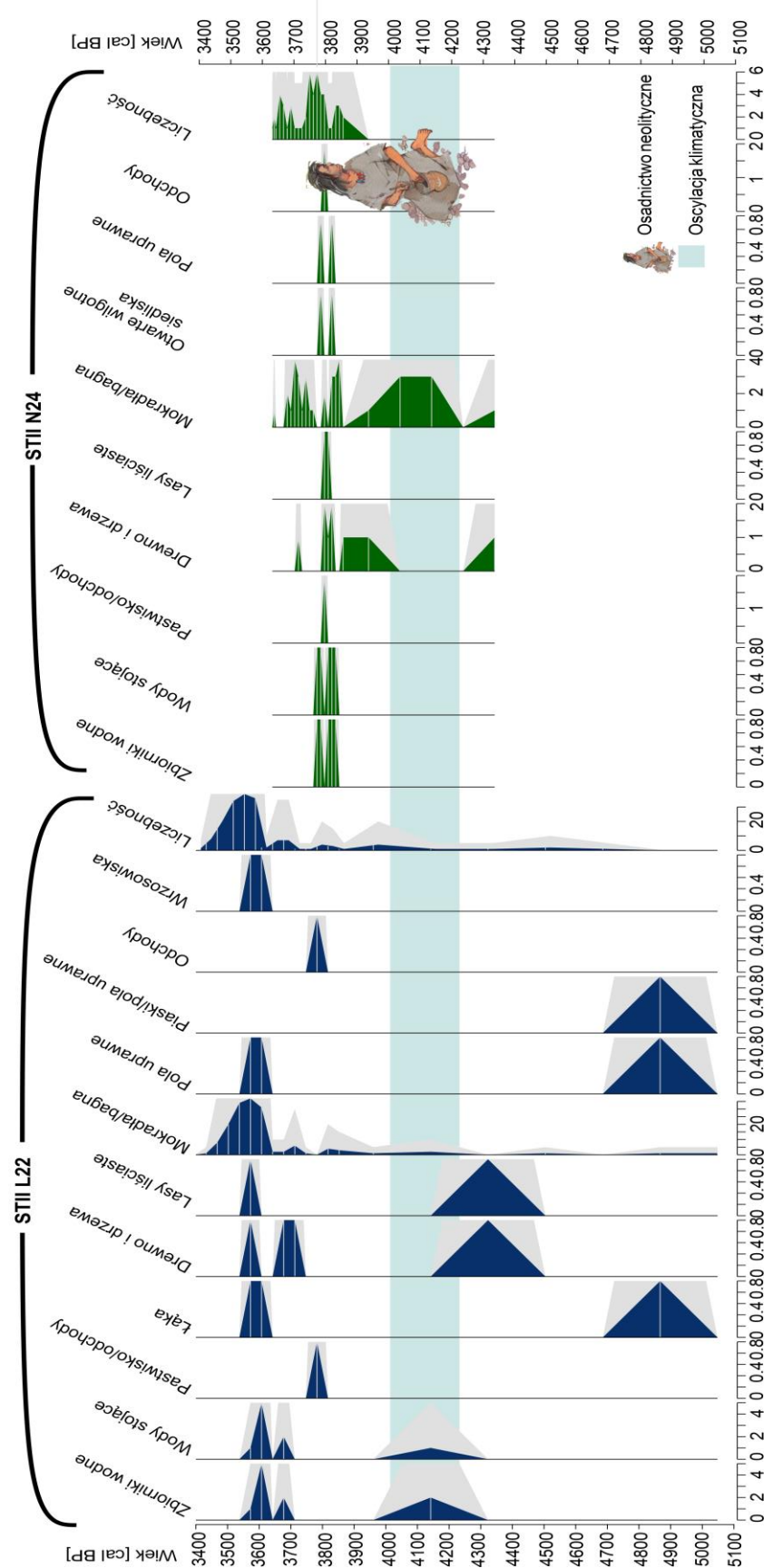
Okres 9000–5700 cal BP charakteryzował się bardzo dużą liczebnością i wysoką różnorodnością gatunkową wioślarek odnotowaną w osadach rdzenia ST IIa. Skład gatunkowy wskazał na mezotroficzny charakter wód, natomiast współwystępowanie gatunków związanych ze strefą pelagialną (Bosmnidae), zasiedlających osady mineralne jeziora oraz żyjących w asocjacji z roślinnością świadczyło o dużej różnorodności siedlisk. Wyniki analizy SOM wykonane dla strefy głębokowodnej (ST IIa) pozwoliły na wyodrębnienie tego okresu jako fazy optymalnej dla rozwoju zgrupowań wioślarek (Płociennik i in., 2022). Liczne szczątki taksonów związanych z wodami mętnymi wskazywały na napływ materii mineralnej i organicznej ze zlewni jeziora, głównie z wodami rzeki Sertejki podczas częstych wiosennych

wezbrań (Płociennik i in., 2022). W okresowo zalewanej strefie brzegowej zbiornika (rdzeń STII L29) występowały prawdopodobnie w tym okresie bogate zgrupowania Cladocera. Pojawiły się wśród nich gatunki eutroficzne m.in. *Leydigia leydigia* oraz ciepłolubne *Graptoleberis testudinaria*, *Chydorus* sp., *Kurzia lattisima*. Wśród Chironomidae został odnotowany głównie *Glyptotendipes* typ *pallens*, który jest związany m.in. z podłożem bogatym w gruby detrytus roślinny. Jego larwy mają stosunkowo dużą odporność na zamarzanie i żyją w obficie zarośniętym litoralu. Ponadto zostały udokumentowane szczątki *Cricotopus* typ *cylindraceus*, *Endochironomus* typ *albibennis* i *Dicrotendipes* typ *nervosus*, czyli gatunki typowe dla litoralu jezior mezo/eutroficznych oraz Ceratopogonidae, które żyją na roślinach wodnych (Brooks i in., 2007) i larwy Ephemeroptera (Kittel i in., 2020).

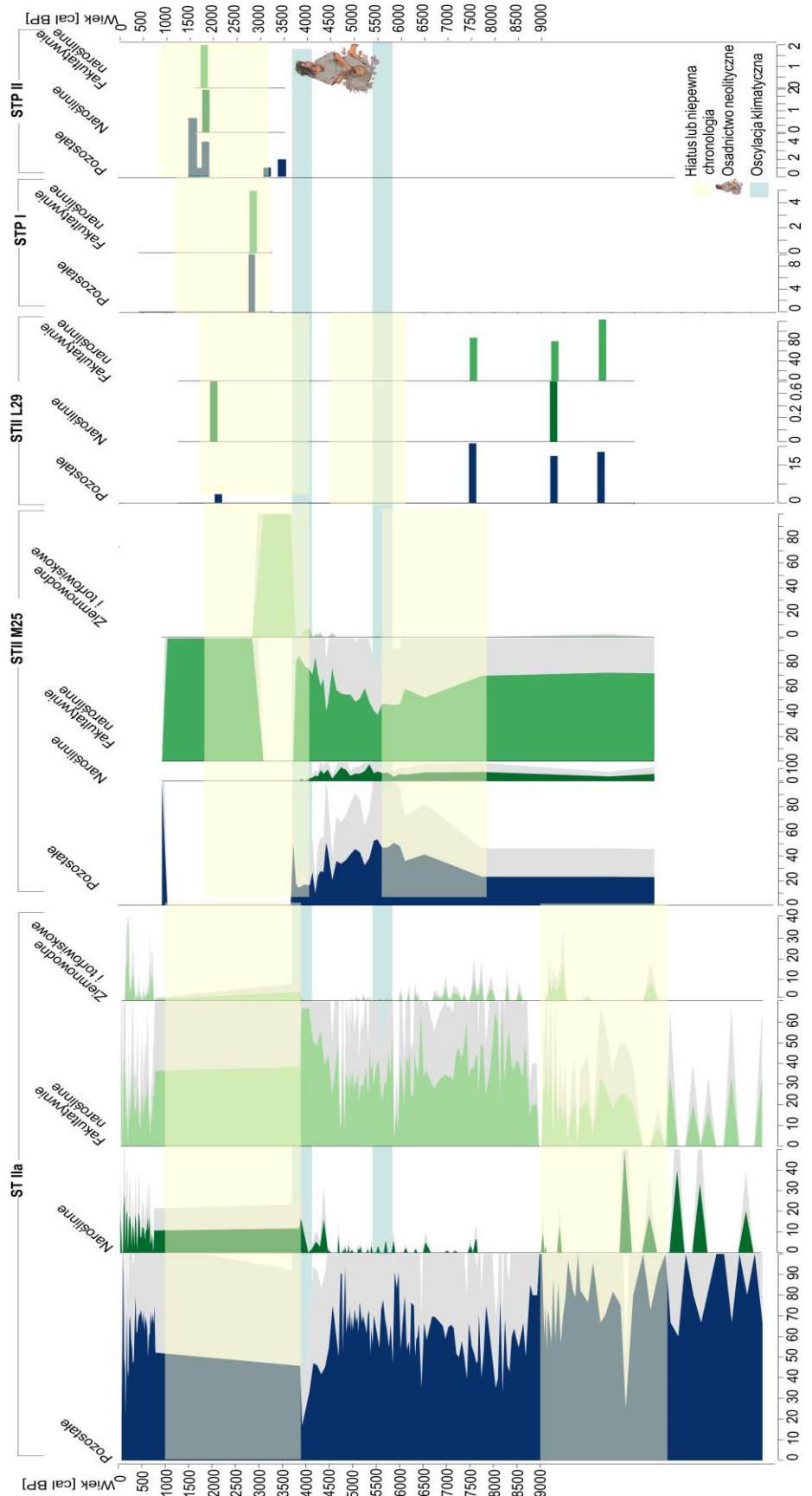


Rycina 18. Rozwój WSBP na podstawie składu gatunkowego Coleoptera

W strefie brzegowej (STII M25), w okresie 6200-5500 cal BP, także dominowały gatunki fakultatywnie fitofilne. Skład gatunkowy makroskopowych szczątków roślinnych i Chironomidae wskazał na rozwój roślinności wodnej (na tym etapie zapewne elodeidów inymfeidów), który mógł być spowodowany zwiększoną zawartością nutrientów w wodach zbiornika w tym czasie. Wzrost roślinności wodnej i żywotności zbiornika widoczny był w zapisie pyłkowym i makroskopowych szczątków roślinnych (Kittel i in., 2021, Mroczkowska i in., 2021b). W tym okresie wzrosła również liczelnosc i różnorodność wioślarek. Objęła ona dużą liczbę taksonów bentosowych, będących wskaźnikami wód eutroficznych (*Alona rectangula*, *Chydorus sphaericus*, *Leydigia acanthocercoides*) i bogatej roślinności w strefie litoralnej jeziora (*Alona affinis*, *Acroperus harpae*, *Eury cercus lamellatus*, *Camptocercus rectirostris*, *Graptoleberis testudinaria*, rodzaj *Pleuroxus*). Sytuacja ta wskazała na proces eutrofizacji, który mógł być spowodowany zwiększoną podażą nutrientów, a przede wszystkim wzrostem temperatury w trakcie holocenejskiego optimum klimatycznego (Kittel i in., 2021).



Rycina 19. Diagram stratygraficzny zgrupowań subfosylnych Coleoptera w rdzeniach STII N24 i STII L22



Rycina 20. Zestawienie zgrupowań Chironomidae związanych z roślinnością i naturalną sukcesją jeziorną w badanych rdzeniach

W kolejnym etapie rozwoju ekosystemu strefy głębokowodnej WSBP (ST IIa) pomiędzy około 5700 a 4800 cal BP nastąpiła faza, w której wioślarki są zastępowane przez ochotki i okrzemki jako grupy najważniejszych bioindykatorów. Może to wskazywać na zmianę warunków siedliskowych charakterystycznych dla panujących w strefie pelagicznej na optymalne dla zgrupowań bentosowych i peryfitonowych związanych z rdestnicami i ramienicami. Wiąże się to ze zmianami hydrologicznymi w jeziorze (stopniowym wypłycaniem). W tym czasie spośród ochotek gatunki eutroficzne (jak *Cricotopus* typ *intersectus*, *Einfeldia* typ *dissidens*, *Endochironomus* typ *albibennis* i *Polypedilum* typ *nubeculosum*) są charakterystyczne dla biocenozy jeziora. Wśród okrzemek *Pantocsekiella comensis* znalazł odpowiednie warunki do życia, co wskazało na długotrwałe zalodzenie, również wczesną wiosną (Płociennik i in., 2022).

W strefie brzegowej basenu, w rdzeniu ze strefy okresowo zalewanej (STII L29), w northgrippianie udokumentowano bardzo niską frekwencję wioślarek, zdominowanych jeszcze w tym czasie przez pelagiczną *Bosmina* (E.) *longirostris* i taksony bentosowe (Kittel i in., 2020). W strefie brzegowej (STII M25) zmiany te rozpoczynają się później od około 4400 cal BP, kiedy dochodzi do spadku liczebności taksonów planktonowych Cladocera oraz dominacji taksonów związanych z niższym pH oraz makrofitami i/lub osadami mineralnymi, co jest wskaźnikiem postępującego spadku poziomu wody (Mroczkowska i in., 2021b, Kittel i in., 2021). Wyniki analiz szczątków chrząszczy (rycina 19) w brzegowych profilach (STII L22 i STII N24) wskazywały na wilgotne, ale jednak bardziej telmatyczne niż typowo wodne siedliska na początku meghalayanu (Mroczkowska i in., w przyg.). Wśród Chironomidae w strefie głębokowodnej (ST IIa) dominował takson typowy dla płytkiego, żyznego litoralu (*Glyptotendipes* typ *pallens*). Było to związane z funkcjonowaniem osadnictwa neolitycznego. Trofia wody (przejście od morfotypów eutroficznych-ciepłolubnych do mezotroficznych-chłodnolubnych) po zakończeniu funkcjonowania osady palafitowej prawdopodobnie spowodowane było zmniejszeniem wpływu człowieka na funkcjonowanie zbiornika lub mogło też wynikać ze stopniowego ochłodzenia klimatu w meghalayanie (około 4200–0 cal BP) (Kittel i in., 2021). Na większą rolę czynnika klimatycznego wskazał wynik analizy DCA dla ochotek zarówno z profilu ze strefy brzegowej (STII M25) jak strefy głębokowodnej (ST IIa) (Mroczkowska i in., 2021b, Płociennik i in., 2022).

Około 4300 cal BP w osadach akumulowanych w rdzeniu ze strefy okresowo zalewanej (STII L29) wykazano pojedyncze szczątki *Paratanytarsus* typ *austriacus*, *Pseudochironomus* typ *praslinatus* i *Tanytarsus* typ *pallidicornis*. Gatunki te są związane często z piaszczystym

dnem (Pinder, 1983), a także częściowo z chłodniejszymi warunkami klimatycznymi (Buskens, 1987, Brooks i in., 2007). Larwy wszystkich trzech gatunków w trzecim i czwartym stadium rozwojowym występują w środkowej Europie zimą i wiosną (do kwietnia) (Moller Pillot, 2009; Gińska 2001, 2011), co zbiega się z zasadniczym okresem wezbrań rzeki Sertejki, która wiosną mogła tworzyć rozlewiska i zasilać WSBP w wodę wraz z krą (Kittel i in., 2020). W tym okresie dochodziło do zwiększenia różnorodności chrząszczy. Pojawiają się gatunki zarówno wodne, świadczące o okresowo wyższym poziomie wody około 4300-4100 cal BP, ale też gatunki związane z koprolitami, martwym drewnem oraz mętnieniem wody (Mroczkowska i in., w przyg.).

W późniejszym okresie około 4200-4100 cal BP w strefie brzegowej basenu (STII M25), pojawiają się gatunki typowe dla źródlisk i wysięków glebowych takie jak *Paracricotopus* i *Zavrelimyia* (Mroczkowska i in., 2021b). W profilu STII L22 (rycina 19) podobny wzrost różnorodności pojawia się nieco później od około 4100 cal BP do 3900 cal BP jednak przy znacznie niższych frekwencjach indykatatorów typowo wodnych, a większej dominacji gatunków związanych z warunkami telmatycznymi. Około 4150 cal BP widoczne były niekorzystne warunki dla rozwoju zbiorowisk roślin wodnych i zgrupowań bezkręgowców. Obecność niektórych gatunków Chironomidae (STII M25) wskazała na występowanie roślinności wodnej, choć w niewielkiej ilości. Duża liczebność Cladocera (takich jak *Chydorus sphaericus* i *Alona affinis*) wskazała na wypływanie zbiornika. Wśród Chironomidae liczne też były gatunki wód eutroficznych, ciepłych, płytowych z osadami organicznymi (Kittel i in., 2021).

Po około 4000 cal BP w strefie głębokowodnej (ST IIa) a po 3600 cal BP w osadach ze strefy brzegowej na stanowisku STII M25 wystąpił hiatus. W strefie brzegowej nastąpił wtedy zanik szczątków Chironomidae (Kittel i in., 2021), natomiast w profilach STII L22 i STII N24 notowane były jedynie gatunki Coleoptera siedlisk telmatycznych, co może świadczyć o regresji wód jeziora z tego obszaru i jedynie okresowych wezbraniach (Mroczkowska i in., w przyg.). Na stanowisku spod stożka (STP II) około 3320 cal BP funkcjonowało płytke zagłębienie epizodycznie wypełnione wodą (Piech i in., w przyg.). W osadach z STP I między 700 a 600 cal BP istniał niewielki, zarośnięty zbiornik. W średniowieczu zbiornik był w małym stopniu porośnięty roślinnością wodną oraz dochodziło do znacznego dopływu wód wezbraniowych, o czym świadczył zapis osadów z obu rdzeni STP I i STP II. Później (około 450 cal BP do 300 cal BP) doszło do eutrofizacji i zarastania zbiornika (Piech i in., w przyg.). W ostatnim etapie rozwoju paleojeziora udokumentowanym w strefie głębokowodnej WSBP

(rdzeń ST IIa) wystąpiła około 250 cal BP faza rozwoju wielu płytakowodnych okrzemek peryfitonowych. Zbiornik był wówczas bardzo płytka, porośnięty szuwarami, ograniczony do okresowego występowania wody w centralnej części basenu. Był on też w tym czasie przeżyźniony, na co wskazała obecność okrzemek typowych dla wód hipertroficznych (por. Wiklund i in., 2010, Besse-Lototskaya i in., 2011, Ejarque i in., 2015).

5.4 Problem badawczy nr 4

Wzajemne relacje człowiek-środowisko

Krajobraz i zasoby naturalne, które ukształtowały się na badanym obszarze w późnym vistulianie i holocenie przyciągały w region WSBP nie tylko lokalne społeczności łowców-rybaków-zbieraczy, ale także społeczności kultur stepowych zajmujących się hodowlą bydła. Po ustąpieniu ostatniego lądolodu pierwsze grupy ludzkie w regionie Serteji pojawiły się w epoce epipaleolitycznej, a następnie w mezolicie. Później ze stepów Morza Azowskiego oraz stepowych i półpustynnych regionów północnego Morza Kaspijskiego przybyli osadnicy wczesnoneolityczni. Migracja ta mogła być spowodowana zmianą warunków środowiskowych związanych z ochłodzeniem klimatycznym określonym jako event 8200 cal BP (Kulkova i in., 2001, 2015, Mazurkevich i in., 2009c, 2020a). Zimna oscylacja klimatyczna i powiązane z nią zmiany hydrologiczne wywoływały kryzysy w funkcjonowaniu społeczeństw pierwotnych. Chłodne lato i surowe zimy wpływały na długość okresu wegetacyjnego, to natomiast oddziaływało negatywnie na źródła pożywienia (Dolbunova i in., 2022). Utrzymujący się dugo lód na wodzie mógł także zmniejszać produktywność jezior i rzek. Pogarszające się warunki środowiska wymuszały zmianę trybu i miejsca życia. W późnym paleolicie, mezolicie i wczesnym neolicie, w badanych bioarchiwach brakuje wiarygodnego zapisu paleoekologii. W eneolicie funkcjonowały najprawdopodobniej głównie okresowe obozowiska posadowione na brzegach jezior (Mazurkevich, 2011a, Mazurkevich i Dolbunova, 2015). Zakładały je w dalszym ciągu społeczności łowiecko-zbierackie. Intensywna działalność osadnicza w strefie brzegowej jeziora w obrębie WSBP przejawiała się zbieractwem dzikich roślin (orzechów i jagód, a także ziół i kłączy grążeli), intensywnym rybołówstwem i łowiectwem (w tym przetwórstwem ryb na miejscu, o czym świadczą pozostałości konstrukcji rybackich i fragmentów wioseł czy ślady uboju zwierząt). Zioła takie jak *Urtica*, *Allium* oraz rośliny z rodziny Chenopodiaceae (np. *Chenopodium album*) i rodziny Apiaceae (np. *Angelica archangelica*, *Daucus carota*) mogły być wykorzystywane jako warzywa (Bos i Urz, 2003,

Itkonen, 1921, Vanhanen i Pesonen, 2016). Bogate w skrobię nasiona Chenopodiaceae mogą być przechowywane przez pewien czas ze względu na ich stosunkowo twardą okrywę nasienną. To samo dotyczy roślin z rodziny Polygonaceae (np. *Persicaria lapathifolia*, *Persicaria maculosa*) (Vanhanen i Pesonen, 2016). *Filipendula ulmaria* i *Solanum dulcamara* mogły być wykorzystywane jako rośliny lecznicze (Bos i Urz, 2003, O'Neill i Rana, 2016, Wolters, 2016). Oprócz ziół lądowych osadnicy mogli żywić się także roślinami wodnymi, jak np. bogatymi w skrobię nasionami i kłączami *Nuphar* (por. Kubiak-Martens, 2002, Warren i in., 2013, Wolters, 2016, Kirleis i in., 2020). Zapis tych aktywności udokumentowany został na obszarze stanowiska Serteya II w rdzeniu STII M25 w okresie około 6100-5500 cal BP (Kittel i in., 2021).

W tym czasie dochodziło w przylegającej do obozowiska części jeziora do intensywniejszego wzrostu hydrofitów, co wskazało na wzbogacenie wody w składniki odżywcze. Jednocześnie dominowały fitofilne bezkręgowce wodne (rycina 21), związane ze strefą litoralną jezior eutroficznych. Wzrosła frekwencja i różnorodność wioślarek, w tym wskaźników wód eutroficznych (*Alona rectangula*, *Chydorus sphaericus*, *Leydigia acanthocercoides*) oraz makrofitów (*Alona affinis*, *Acroperus harpae*, *Eury cercus lamellatus*, *Camptocercus rectirostris*, *Graptoleberis testudinaria*, *Pleuroxus* spp.). Także liczebność Chironomidae gwałtownie wzrosła, zwłaszcza eutroficzne gatunki bytujące na dnie i taksony fitofilne. Wskazało to na eutrofizację jeziora, która mogła być spowodowana zwiększoną podażą składników pokarmowych w wyniku działalności człowieka. Pojawienie się mszywiołów i nagromadzenie kości ryb i ssaków również świadczy o zwiększonej dostępności pokarmu. Ponadto obecność szczątków makrofitów, które mogą występować w głębokiej wodzie, takich jak *Potamogeton* spp. i *Chara* dowodzi, że poziom wody musiał być stosunkowo wysoki. Zwiększoną koncentrację węgli drzewnych, obecność husek i kości ryb w osadach oraz szczątków roślin jadalnych można powiązać ze stosunkowo intensywną lokalną aktywnością osadniczą w tym czasie. Gdyby działalność człowieka spowodowała dostawę nutrientów spoza basenu WSBP do jeziora, wywołoby to wzrost jego żyźności. Dzięki temu zwiększyłaby się produkcja pierwotna i wtórna ekosystemu, co przyniosłoby dodatkowe korzyści gospodarcze - zwiększone połowy ryb i biomasę zebranych makrofitów wodnych. Na skalę lokalną, w pobliżu osady, taki efekt mogło wywołać oprawianie zwierząt nad brzegiem jeziora, co potwierdzają pozostałości archeologiczne (Kittel i in., 2021). Zgrupowania Chironomidae w głębokowodnym profilu ST IIa wykazują, że dopływ allochtonicznych biogenów do wody nie był w tym okresie wystarczająco intensywny, aby spowodować dodatkową eutrofizację

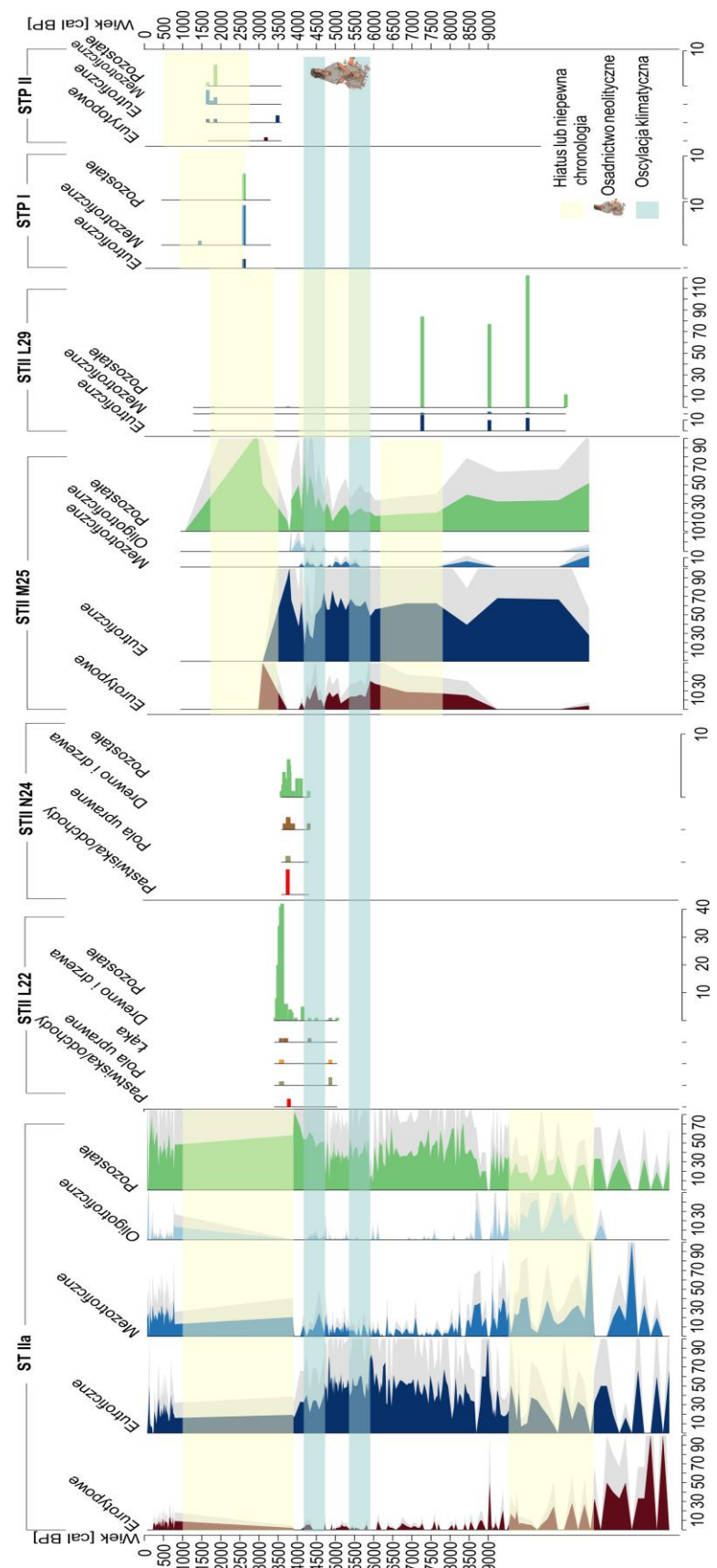
całego jeziora. Wysoka produkcja ekosystemu jeziora w tym czasie wynikała w głównej mierze ze wzrostu średnich temperatur powietrza latem. Nie mniej jednak siedliska w pobliżu stanowiska Sertaya II zostały lokalnie zeutrofizowane przez funkcjonowanie osady oraz działalność gospodarczą jej mieszkańców i były odpowiednie dla rozwoju Chironomidae żerujących na detrytusie, takich jak *Chironomus typ plumosus*, *Glyptotendipes typ pallens* lub *Polypedilum typ nubeculosum*. Duża liczbedo larw Chironomidae i odpadki mogły przyciągać ryby w otoczenie osady. Te wszystkie aspekty prowadziły zapewne do dłuższego utrzymania się gospodarki przyswajalnej w regionie Serteji, podczas gdy w południowych regionach Niziny Wschodnioeuropejskiej społeczeństwa przechodziły już w tym okresie na hodowlę zwierząt i uprawę roślin (Bondetti i in., 2020).

Najwyższą zawartość węgli drzewnych w rdzeniu STII M25 udokumentowano dla okresu około 4500 cal BP, w poziomie powiązanym z zaleganiem szkieletów ludzkich. Złożenie ciał kobiet w miejscu funkcjonowania osady można interpretować jako specyficzny zabieg pogrzebowy, ale mógł to też być rodzaj ofiary bagiennej lub efekt incydentalnego wydarzenia. Trudno na podstawie zebranych materiałów odtworzyć zarówno przyczynę śmierci, jak i kontekst złożenia odnalezionych szkieletów. Ciała te zostały złożone w strefie brzegowej zbiornika w fazie obniżania się poziomu wody w paleojeziorze (Kittel i in., 2021; Mroczkowska i in., 2021). Koncentracja szczątków Chironomidae w poziomie złożenia szczątków ludzkich, około 4500-4350 cal BP, jest o 4 razy wyższa niż w sąsiednich próbkach. Tak nagły wzrost liczności ochotek na stanowisku STII M25, nie notowany równolegle w profilu ST IIa, mógł wynikać tylko z wyjątkowo wysokiej dostępności pokarmu, takiej jak lokalna akumulacja gnijącej materii organicznej. Żerowanie ochotek na zwłokach kobiety zdeponowanych w wodzie opisali m.in. Medina i in., (2015). Podczas sekcji zwłok zebrano larwy *Chironomus riparius* rozmieszczone między długimi włosami na głowie (Gonzalez Medina i in., 2015). Włosy mogły w tym wypadku imitować nitkowate glony lub rozkładające się liście roślin, a tym samym zapewniać odpowiednie mikrosiedlisko dla larw ochotkowatych. Ciała dwóch kobiet, których szkielety znaleziono w sąsiedztwie STII M25, musiały rozkładać się w wodzie, ponieważ stwierdzono szczątki larw ochotkowatych typowych tylko dla środowiska wodnego. Śmierć musiała również nastąpić w cieplejszych miesiącach (późną wiosną i latem) na co wskazało nagromadzenie szczątków larw Chironomidae. W niskich temperaturach, w okresie zimowym pozostają one w diapauzie. Alternatywnie, tak szybki wzrost populacji ochotkowatych można tłumaczyć wzrostem trofii jeziora lub wyjątkowo ciepłym i długim okresem wegetacji. Gdyby jednak nastąpił wzrost trofii jeziora, konsekwencje

ekologiczne i wzrost liczebności Chironomidae byłyby obserwowane w kolejnych próbach (Mroczkowska i in., 2021b). Byłoby to też widoczne w odpowiednich wiekowo odcinkach rdzenia ST IIa (Mroczkowska i in., 2021, Płociennik i in., 2022) czy rdzeni STII L22 i STII N24.

Od około 4500 cal BP wpływ człowieka w strefie brzegowej (rdzeń STII M25) był coraz słabszy. Wskazał na to spadek koncentracji makroszczątków roślin wskaźnikowych dla wysokich warunków edaficznych. Obniżała się równolegle frekwencja planktonowych Cladocera. Rozwijały się natomiast populacje taksonów związanych z niższym pH (*Alonella excisa* i *Alona guttata* var. *tuberculata*) zasiedlających makrofity. Wskazało to na intensyfikację procesów terrestrializacji w lokalizacji STII M25. Chironomidae dają spójny sygnał z wioślarkami i makrofitami. Wzrost *M. typ pedellus*, przy spadku prawie wszystkich innych taksonów (z wyjątkiem typu *G. pallens*), wskazała na spadek trofii jeziora i słabszą antropopresję (Mroczkowska i in., 2021b). Z charakterystyki geomorfologicznej wynika, że po 4500 cal BP dochodziło do okresowego wkraczania (rozwijania) koryt rzecznych w obrębie (części) basenu jeziornego w trakcie krótkotrwałych faz obniżenia poziomu wód jeziora (Kittel i in., 2018). Mogło to zbiegać się z główną fazą istnienia osady palafitowej. Osada palafitowa udokumentowana na stanowisku Serteya II funkcjonowała bezpośrednio na odsłoniętej powierzchni osadów jeziornych (gytia grubodetrytusowa), co potwierdzają dane archeologiczne (Mazurkevich i in., 2017, 2020; Kittel i in., 2018). Jej założenie mogło mieć miejsce podczas obniżania poziomu wody w paleojeziorze, gdy dno zbiornika zostało (częściowo) odsłonięte lub podczas krótkotrwałego (sezonowego) obniżenia zwierciadła wody w jeziorze.

Gatunki Chironomidae w rdzeniu STII M25 wskazywały na wyraźną zmienność warunków hydrologicznych podczas funkcjonowania osady (Mroczkowska i in. 2020). Wahania te mogły być spowodowane roztopowymi wezbraniami w górnym odcinku rzeki Serteki (Płociennik i in., 2022). Także chrząszcze w tym okresie wskazywały na epizody wezbraniowe podczas okresu osadnictwa na palach (Mroczkowska i in., w przyg.). Na podstawie wyników badań makroskopowych szczątków roślin także zaobserwowano zaburzenia w ekosystemie jeziora, co może świadczyć o funkcjonowaniu osadnictwa na palach, jako przystosowaniu do warunków hydrologicznych (Więckowska-Luth i in., 2021).



Rycina 21. Zmiany trofii zrekonstruowane w badanych rdzeniach w oparciu o zbiorowiska Chironomidae skorelowane z indykatorem człowieka z gatunków Coleoptera

Od około 4450 cal BP nastąpił dalszy spadek nagromadzenia makroszczątków hydrofitów. Jednocześnie zniknęły helofity, rosnące w głębszych obszarach strefy litoralu (*Schoenoplectus lacustris*). Regres zbiorowisk roślin wodnych pokazuje, że poziom wody dalej się obniża i prawdopodobnie mogły zachodzić dłuższe fazy przesuszenia. Potwierdza to tezę o występowaniu dużych wahań poziomu wody w WSBP (Płociennik i in., 2022).

Aktywność osadnicza do około 4400 cal BP przyczyniła się do uruchamiania procesów stokowych, które mogły powodować akumulację materii organicznej w strefie brzegowej jeziora, udokumentowanych w rdzeniu STII L29 (Kittel i in., 2020). Na wzmożoną erozję wskazywały również zgrupowania subfosylnych chrząszczy w rdzeniu STII L22. Gatunki chrząszczy związane z wypasem, koprofilne i bytujące na drewnie pojawiły się około 4300 cal BP także w pobliskim profilu STII N24. Następnie doszło do zmiany fauny na gatunki Coleoptera żyjące w wodach zaburzonych, zanieczyszczonych z niską przejrzystością, jak też odżywiające się martwą materią organiczną i odchodami. Udokumentowano także wzrost trofii, spowodowany dostawą szczątków organicznych w wyniku działalności człowieka (Mroczkowska i in., w przyg.). Tym samym osadę palafitową można uznać za przystosowanie do sezonowych wahań poziomu wody. W czasie ochłodzenia 4,2 ka cal BP intensywność osadnicza zaczynała słabnąć (Mazurkevich, 2011a, Mazurkevich i in., 2017, Wieckowska-Lüth i in., 2021).

Ponowną fazę wzmożonej aktywności człowieka można skorelować z okresem około 4100–3800 cal BP, kiedy udokumentowano w profilu STII M25 podwyższoną obecność makroszczątków malin w osadach (Kittel i in., 2021). Na stanowisku ze strefy głębokowodnej (ST IIa) odnotowano wskaźniki związane z funkcjonowaniem konstrukcji palafitowych, m.in. szczątki mchu, kory i drewna, a także duże ilości kości ryb, owoce kotewki wodnej. Także wskaźniki geochemiczne potwierdzają obecność osadnictwa człowieka (Więckowska-Luth i in., 2021, Płociennik i in., 2022). W tym czasie rejestrowana była jedynie epizydyczna działalność człowieka na brzegu jeziora – schyłek funkcjonowania osady palafitowej. Świadczy to o istotnej przebudowie warunków paleośrodowiskowych wymuszonych globalnymi zmianami klimatycznymi (Kittel i in., 2021).

Dynamiczna sytuacja geomorfologiczna (zmienne funkcjonowanie systemów jeziornego, bagiennego i rzecznego) silnie wpłynęły na styl życia społeczności neolitycznych i formę przystosowania do warunków ekologicznych, co mogło znaleźć odzwierciedlenie w powstawaniu osad palafitowych. Osada przetrwała wiele sezonów, zanim ponownie została zalana wodami zbiornika (Mazurkevich, Dolbunova 2011; Mazurkevich i in.. 2011; Kul'kova

i in.. 2015a, 2015b). Przejściowy wzrost poziomu wody w jeziorze odnotowano dla zdarzenia 4,2 ka BP. Potem nastąpił spadek poziomu wody w jeziorze, a później były już tylko sezonowe wezbrania spowodowane wiosennymi roztopami (Kittel i in., 2021). Późniejsze podniesienie poziomu wody w jeziorze doprowadziło do dewastacji osady palafitowej, przez co osadnictwo przeniosło się na wyżej położone miejsca. Z tego okresu notowana jest epizodyczna działalność człowieka na brzegu jeziora (Kittel i in., 2021). Około 3800 cal BP doszło do wzrostu wietrzenia w obszarze zlewni, co mogło być spowodowane obecnością człowieka na badanym obszarze i wylesianiem (nieudokumentowanym jednak w zapisie pyłkowym) (Kittel i in., 2021). W rdzeniu strefy przybrzeżnej (STII L22), dochodziło do przekształcania ekosystemu jeziornego w kierunku terenów podmokłych oraz intensyfikacji procesów stokowych (Mroczkowska i in., w przyg.).

Obniżenie poziomu wody w strefie litoralu jeziora w okresie 3250-2300 cal BP przypadło na czas funkcjonowania ludności kultury ceramiki kreskowanej mającej stałe osady w oddaleniu od stanowiska Serteya II (Kittel i in., 2020). Jej społeczności bazowały już na uprawie roślin i hodowli zwierząt (Więckowska-Luth i in., 2021). Działalność człowieka w tym okresie mogła prowadzić do intensyfikacji procesów stokowych. Zanik jeziora jednak ograniczył możliwość pozyskania pożywienia z rybołówstwa, co doprowadziło do opuszczenia jego otoczenia przez osadników. Dlatego zaobserwowane wahania geochemiczne między 3800 cal BP i 3100 cal BP nie są skorelowane z wpływami kulturowymi. Mają one naturalne pochodzenie, wynikając z sezonowych wałań poziomu wody w WSBP wywołanych roztopami lub silnymi opadami (Kittel i in., 2020).

W średniowieczu (900 cal BP) na stanowisku STP II występował pyłek *Picea abies*, *Juniperus communis* i *Tilia cordata* oraz gatunki roślin związane z działalnością człowieka, takie jak *Cirsium arvense*, *Fragaria vesca* czy *Oxalis acetosella* (Ginter in in. 2023). W sąsiednim profilu (tj. STP I) wyniki analizy palinologicznej również wykazały, że krajobraz charakteryzował się znaczącymi przekształceniami pod wpływem działalności człowieka. Wskazywały na to dane dotyczące wylesiania, a także liczne taksony synantropijne, a przede wszystkim rośliny uprawne, takie jak *Secale*, *Triticum*, *Cannabis* i *Fagopyrum* (Piech i in., w przyg.). Wyniki badań paleoekologicznych z torfowiska kotłowego (KH) wskazywały na stały wzrost oddziaływania człowieka w średniowieczu i wczesnej nowożytności. Przede wszystkim udokumentowany został wzrost wylesiania i rozwój upraw rolnych. Do około 450 cal BP w rdzeniu STP II odnotowano niewielki wpływ człowieka, wcześniej roślinność występująca na badanym obszarze odpowiadała potencjalnej roślinności w regionalnych

biomach. Po tym czasie i w okresie wczesnonowożytnym doszło do stopniowo rosnącej antropopresji. Działalność ta prowadziła do wylesiania terenu i rozwoju upraw rolnych (Piech i in., w przyg.). Wyniki uzyskane z rdzenia z torfowiska KH dowodzą, że wylesianie terenu w regionie Serteki rozpoczęło się około 230 cal BP. Na podstawie danych paleoekologicznych wiadomo, że w tym czasie pojawiały się rośliny uprawne, chwasty i epifyty (*Secale*, *Fagopyrum*, *C. cyanus*, *P. lanceolata*), wraz ze wzrostem liczby *Cerealia*, *Cyperaceae*, *Poaceae*, *R. acetosa* i *Artemisia*, co świadczy o wzmożonej działalności rolniczej i wylesieniu na tym obszarze (Mroczkowska i in., 2021b). Po około 190 cal BP pojawiły się także gatunki ziemnowodne i bagienne Chironomidae, takie jak: *Pseudorthocladius*, *Pseudosmittia* i *Lasiodiamesa* (Mroczkowska i in., 2021b), które związane są z niskim pH (por. De Vleeschouwer i in., 2009, Hamerlik i in., 2019). Zwiększenie ich liczebności oraz pojawienie się gatunków typowo wodnych mogło być spowodowane wzrostem wilgotności na torfowisku lub, co bardziej prawdopodobne w przypadku torfowiska Sertety, z neutralizacją niskiego pH spowodowanego namywaniem frakcji mineralnych na tereny podmokłe, w trakcie wylesiania. Wyniki analizy pyłkowej wykazały, że od około 120 cal BP nastąpił lokalny spadek udziału roślin uprawnych, które zostały zastąpione przez rośliny ruderalne, takie jak *Plantago lanceolata*, *Rumex acetosa*, *Artemisia*, *Chenopodiaceae* i *Urticaceae* (Mroczkowska i in., 2021b). Grzyby koprofilne (*Sporormiella*, *Podospora*, *Cercophora*) wystąpiły w tym okresie liczniej, co sugeruje wypas bezpośrednio na badanym torfowisku (van Geel i Aptroot, 2006). Wzrost wskaźników antropogenicznych mógł być związany z reformą rolną Aleksandra II która spowodowała ożywienie na krótki czas gospodarki rolnej w Rosji. Po 80 cal BP wzrosło zalesienie obszaru, zaś od 60 cal BP niska frekwencja *Chenopodiaceae*, *Cerealia* i *Cyperaceae* świadczy o zmniejszeniu wpływu człowieka. Faza ta charakteryzuje się ograniczeniem działalności człowieka po reformie agrarnej P. Stołypina, która spowodowała odpływ ludności ze wsi i naturalną regenerację ekosystemów leśnych (Mroczkowska i in., 2021b).

6. Wnioski

W toku rozprawy wykonano analizy zgrupowań subfosylnych Chironomidae, Cladocera oraz Coleoptera. Na podstawie powyższych analiz zrekonstruowano średnie temperatury powietrza lipca i zmiany warunków hydrologicznych niemal dla całego holocenu. Na podstawie wyników badań udało się wysunąć następujące wnioski:

1) Wszystkie rekonstrukcje temperatur ze stanowiska położonego w strefie głębokowodnej (ST IIa) dokumentują podobny trend zmian średnich temperatur lata, od niskich temperatur w późnym vistulianie, najwyższych we wczesnej fazie środkowego holocenu (8400-7800 cal BP), po wyraźnie widoczną tendencję spadkową w późnym holocenie, oraz ochłodzenie podczas małej epoki lodowej. Na podstawie danych z profilu ST IIa udokumentowano chłodne oscylacje około 6900 i 5800 cal BP, zaś z profilu STII M25 5800 cal BP i 4200 cal BP. Oscylacje te dają się korelować z epizodami Bonda. Na fluktuacje średnich temperatur lata nakładają się zmiany hydrologiczne w obrębie WSBP, częściowo powiązane z reżimem rzeki Serteki, w tym epizody wezbraniowe i stopniowe wypływanie i zarastanie paleojeziora. Spadek temperatur związany z tzw. oscylacjami klimatycznymi 5,9 i 4,2 ka cal BP był mniejszy na Pojezierzu Witebskim niż na Półwyspie Skandynawskim. W regionach bardziej kontynentalnych, odległych od wpływów Atlantyku oscylacje Bonda zaznaczają się mniej wyraźnie, stąd niewidoczna w rekonstrukcjach ilościowych jest oscylacja 8,2 ka cal BP. Na podstawie przeprowadzonych badań należy odrzucić hipotezę H1.

2) W holocenie dochodziło do zmian warunków hydrologicznych zbiornika jeziornego w obrębie WSBP i rosnących wpływów systemu rzecznego. Potwierdza to wyraźna sukcesja zgrupowań bezkręgowców (wioślarek i ochotek) w profilu ST IIa. Rosnący wpływ systemu rzecznego był związany z obniżaniem poziomu wody w WSBP, a także procesami zachodzącymi w wyżej położonej części zlewni. Wahania poziomu wody wywołane wezbraniami Serteki są dobrze widoczne w profilach ze strefy brzegowej i zaznaczają się pojawianiem się gatunków jeziornych w czasie epizodów wezbraniowych. Wyniki przeprowadzonych badań pozwoliły na częściowe utrzymanie hipotez H2 i H8, hipotezy te są odporne na falsyfikację.

3) Głównym czynnikiem determinującym skład gatunkowy Chironomidae w WSBP były fluktuacje średnich temperatur lata, co oznacza że bioarchiwa ze strefy głębokowodnej (ST IIa) oraz brzegowej (STII M25) stanowią dobry zapis zmian paleoklimatycznych. Natomiast zgrupowania Cladocera w rdzeniu ze strefy głębokowodnej były silniej kształtowane przez zmiany poziomu wody niż wahania temperatury. Jednocześnie zgrupowania Cladocera w strefie brzegowej są związane ze zmianami temperatury na co wskazała analiza DCA, jednak rekonstrukcje paleoklimatyczne oparte o analizy subkopalnych zespołów wioślarkowych z profilu STII M25 są mało wiarygodne ze względu na brak współczesnych analogów. W rdzeniach ze strefy brzegowej (STII M25, STII N24 i STII L22) bardzo dobrze uwidaczniają się lokalne wahania poziomu wody i trofii co udokumentowano nie tylko w składzie

gatunkowym ale i koncentracji szczątków Chironomidae, Cladocera i Coleoptera. Należy zatem przyjąć hipotezę H3, w której oba komponenty są odporne na falsyfikację.

4) Analiza SOM danych pochodzących z rdzenia ze strefy głębokowodnej pozwoliła na określenie głównych faz sukcesji ekosystemu paleojeziora i wyznaczenie gatunków wskaźnikowych dla poszczególnych faz rozwoju zbiornika. Pozwoliło to na uzyskanie szczegółowego obrazu zmian w ekosystemie i przez to możliwe było rozpoznanie lokalnych, innych niż klimatyczne czynników środowiskowych wpływających na zgrupowania ochotek i wioślarek. Hipoteza H4 jest odporna na falsyfikację.

5) W okresie atlantyckim i subborealnym wahania lustra wody były na tyle częste, że budowle mieszkalne o konstrukcji palafitowej zakładane były w III tys. p.n.e. na obszarach sezonowo (?) podmokłych w strefach brzegowych jeziora lub na równinach pojeziornych w okresach regresji. Wynika to z analizy zgrupowań Chironomidae, Cladocera i Coleoptera, wyraźnie zależnych w tym okresie od sezonowych wałań stanów wody w WSBP. Społeczności neolityczne jako oparte na zasobach środowiska naturalnego były najmocniej warunkowane zasobami żywności (dostępność zwierząt i roślin), te zaś uwarunkowane klimatem. Wyniki przeprowadzonych analiz udowodniły że hipoteza H5 jest odporna na falsyfikację.

6) Zarówno regionalne zmiany klimatyczne jak i lokalne fluktuacje hydrologiczne decydowały o produktywności ekosystemów wodnych i lądowych, a przez to o uwarunkowaniach naturalnych funkcjonowania i rozwoju gospodarczym społeczności zamieszkujących region Serteki w neolicie. Chłodne oscylacje wymuszały na społecznościach neolitycznych niestandardowe działania przystosowujące do nowych, trudniejszych warunków środowiska. Należy odrzucić oba komponenty H6.

7) Wyniki studiów archeologicznych wyraźnie wskazują na bardzo silne powiązanie społeczności neolitycznych w regionie Serteki ze środowiskiem jeziornym. Wyniki badań paleoekologicznych potwierdzają to, że jezioro było głównym źródłem surowców i pożywienia dla wspólnot ze stanowiska Serteya II i miejscem, na którym przede wszystkim koncentrowała się ich aktywność życiowa oraz na którym zaznaczała się okresowa wyraźna antropopresja. Należy odrzucić pierwszy komponent H7 natomiast komponent drugi jest odporny na falsyfikację.

Analiza ilościowa i jakościowa subfosylnych Chironomidae umożliwia wiarygodne rekonstruowanie średniej paleotemperatury powietrza lipca dla w dalszym ciągu słabo przebadanego z punktu widzenia rekonstrukcji paleoklimatycznych obszaru Niziny Wschodnioeuropejskiej. Dzięki szczegółowym badaniom paleoekologicznym

udokumentowano przebieg i skutki zmian warunków klimatycznych i ich wpływ m.in. na bio- i antroposferę. Znając przebieg procesów zmian klimatu, możemy lepiej projektować środki zaradcze i aktywnie chronić klimat.

Spis rycin i zdjęć

- Rycina 1. Lokalizacja terenu badań A) na mapie świata, B) na mapie Federacji Rosyjskiej
- Rycina 2. Lokalizacja terenu badań na tle śródkowej Europy i Obwody Smoleńskiego
- Rycina 3. Lokalizacja terenu badań stanowiska Serteya II (STII), profili STP i torfowiska Serteya (KH)
- Rycina 4. Lokalizacja stanowisk wchodzących w zespół stanowisk Serteya II
- Rycina 5. Położenie stanowisk poboru rdzeni na tle rzeźby terenu regionu Serteji
- Rycina 6. Plan rozmieszczenia badanych rdzeni na stanowisku archeologicznym Serteya II (za (Kittel i in., 2021)
- Rycina 7. Litologia badanych rdzeni z regionu Serteji
- Rycina 8. Szczegółowa lokalizacja rdzeni STII M25 i ST IIa
- Rycina 9. Przykładowe szczątki Chironomidae z rdzeni osadów biogenicznych (wyk. A. Mroczkowska 2019)
- Rycina 10. Przykładowe szczątki Cladocera z rdzenia KH (fot. A. Mroczkowska)
- Rycina 11. Kolekcja szczątków subfosylnych chrząszczy użytych do identyfikacji i analizy
- Rycina 12 Zestawienie średnich paleotemperatur lipca odtworzonych w oparciu o szczątki Chironomidae i Cladocera ze stanowisk ST IIa i STII M25
- Rycina 13. Zakres temperatur letnich (wzajemny zakres klimatyczny - ang. MCR (Mutual Climate Range) w oparciu o zgrupowania subfosylnych Coleoptera dla rdzeni STII N24, STII L22 zestawione z wykresem paleotemperatury lipca SNP ZT dla rdzenia STII M25
- Rycina 14. Zestawienie rekonstrukcji zmian poziomu wody w oparciu o FN ZT dla Chironomidae oraz Cladocera ze stratygrafią zgrupowań Chironomidae, Cladocera i Coleoptera z rdzeni ze strefy brzegowej WSBP
- Rycina 15. Zgrupowania subfosylnych Chironomidae i Cladocera w rdzeniu STP I
- Rycina 16. Zgrupowania subfosylnych Chironomidae i Cladocera w rdzeniu STP II
- Rycina 17. Rozkład gatunków wspólnych dla wszystkich badanych rdzeni z analizą Chironomidae
- Rycina 18. Rozwój WSBP na podstawie składu gatunkowego Coleoptera
- Rycina 19. Diagram stratygraficzny zgrupowań subfosylnych Coleoptera w rdzeniach STII N24 i STII L22
- Rycina 20. Zestawienie zgrupowań Chironomidae związanych z roślinnością i naturalną sukcesją jeziorną w badanych rdzeniach

Rycina 21. Zmiany trofii zrekonstruowane w badanych rdzeniach w oparciu o zbiorowiska Chironomidae skorelowane z indykatorem człowieka z gatunków Coleoptera

Fotografia 1. Badania archeologiczne prowadzone metodą archeologii podwodnej na stanowisku archeologicznym Serteya II (fot. A. Mroczkowska 2017)

Fotografia 2. Pozostałości pali konstrukcji budynków osady palafitowej Serteya II-1 sub. (fot. A. Mroczkowska 2017)

Fotografia 3. Wykop archeologiczny w obrębie osadów jeziornych na stanowisku STII-2 (fot. A. Mroczkowska 2017)

Fotografia 4. Grot kościany ze stanowiska Serteya II-2 z epoki mezolitu (fot. A. Mroczkowska 2017)

Fotografia 5. Kręg jelenia ze stanowiska Serteya II (fot. A. Mroczkowska 2017)

Fotografia 6. Wykop archeologiczny na stanowisku STII-1 (fot. A. Mroczkowska 2017)

Fotografia 7. Pobór rdzenia ST IIa (fot. P. Kittel 2016)

Fotografia 8. Stanowisko STII-2-prace archeologiczne (fot. B. Kotrys 2016)

Spis tabel i rycin

Tabela 1. Rdzenie i wykonane z nich analiz wraz z opisującymi je publikacjami

Tabela 2. Litologia rdzenia ST IIa

Bibliografia

1. <http://www.tutiempo.net>. [Accessed 9.12.2019].
2. www.meteoblue.com/en [Accessed 9.12.2019].
3. <http://www.geomonitoring.ru>. Center of state monitoring of natural resources, 2007 [Accessed 9.12.2019].
4. <https://github.com/nsj3/rioja> [Accessed 02.02.2022].
5. ABRAMOW, L. 1972. *Opisaniya prirody nashey strany: Razvitiye fiziko-geograficheskikh kharakteristik*, Mysl'. Moskva.
6. ALEKSEEV, L. 1980. Smolenskaia zemlia v IX—XIII vv. Ocherki istorii Smolenshchiny i Vostochnoi Belorussii (The Smolensk Land in 9th—13th Centuries: Essays on the History of the Smolensk Oblast and Eastern Belorussia). Nauka. Moskwa.
7. AMMER, C., FICHTNER, A., FISCHER, A., GOSSNER, M. M., MEYER, P., SEIDL, R., THOMAS, F. M., ANNIGHÖFER, P., KREYLING, J. & OHSE, B. 2018. Key ecological research questions for Central European forests. *Basic and Applied Ecology*, 32, 3-25.
8. ANDREEV, A., TARASOV, P., SCHWAMBORN, G., ILYASHUK, B., ILYASHUK, E., BOBROV, A., KLIMANOV, V., RACHOLD, V. & HUBBERTEN, H.-W. 2004. Holocene paleoenvironmental records from Nikolay Lake, Lena river delta, arctic Russia. *Palaeogeography, Palaeoclimatology, Palaeoecology*, 209, 197-217.
9. ANDRONIKOV, A., SUBETTO, D., LAURETTA, D., ANDRONIKOVA, I., DROSENKO, D., KUZNETSOV, D., SAPELKOV, T. & SYRYKH, L. 2014. In search for fingerprints of an extraterrestrial event: Trace element characteristics of sediments from the lake Medvedevskoye (Karelian Isthmus, Russia). *Doklady Earth Sciences* 457, Springer, 819-823.
10. ARSLANOV, K. A., SAVELIEVA, L., GEY, N., KLIMANOV, V., CHERNOV, S., CHERNOVA, G., KUZMIN, G., TERTYCHNAYA, T., SUBETTO, D. & DENISENKOV, V. 1999. Chronology of vegetation and paleoclimatic stages of northwestern Russia during the Late Glacial and Holocene. *Radiocarbon*, 41, 25-45.
11. ARSLANOV, K. A., SAVELIEVA, L., KLIMANOV, V., CHERNOV, S., MAKSIMOV, F., TERTYCHNAYA, T. & SUBETTO, D. 2001. New data on chronology of landscape-paleoclimatic stages in Northwestern Russia during the Late Glacial and Holocene. *Radiocarbon*, 43, 581-594.
12. ARTYUSHENKO, A., ARAP, R. Y. & BEZUSKO, L. 1982. Istoria rastitelnosti zapadnyh oblastei Ukrayny v chetvertichnom periode. Naukova dumka, Kiev.

13. ATKINSON, T., BRIFFA, K., COOPE, G., JOACHIM, M. & PERRY, D. 1986. *Climatic calibration of coleopteran data*, Wiley, Chichester.
14. ATKINSON, T. C., BRIFFA, K. R. & COOPE, G. 1987. Seasonal temperatures in Britain during the past 22,000 years, reconstructed using beetle remains. *Nature*, 325, 587-592.
15. BENDREY, R., RICHARDSON, A., ELLIOTT, S. & WHITLAM, J. 2015. Environmental archaeologies of Neolithisation: Old World case studies. *Environmental Archaeology* 20(3):221-224 .
16. BENNETT, K. D. 1996. Determination of the number of zones in a biostratigraphical sequence. *New Phytologist*, 132, 155-170.
17. BERNTSSON, A., ROSQVIST, G. C. & VELLE, G. 2014. Late-Holocene temperature and precipitation changes in Vindelfjällen, mid-western Swedish Lapland, inferred from chironomid and geochemical data. *The Holocene*, 24, 78-92.
18. BESSE-LOTOTSKAYA, A., VERDONSCHOT, P. F., COSTE, M. & VAN DE VIJVER, B. 2011. Evaluation of European diatom trophic indices. *Ecological Indicators*, 11, 456-467.
19. BIRKS, H. H. & HH, B. 1980. Plant macrofossils in Quaternary lake sediments. *Archiv für Hydrobiologie - Ergebnisse der Limnologie*, 15,1–60.
20. BOGDANOVA, S., GORBATSCHEV, R. & GARETSKY, R. G. 2005. EUROPE: East European Craton. *Encyclopedia of Geology*, 2 (eds. R. C. Selley, L. R. Cocks and I. R. Plimer): 34-49. Elsevier, Amsterdam.
21. BOHN, U., GOLLUB, G. & HETTWER, C. 2000. *Karte der natürlichen Vegetation Europas*.Karte der natürlichen Vegetation Europas. Massstab 1:2.500.000 Karten und Legende. Bundesamt für Naturschutz,Landwirtschaftsverlag, Bonn, Germany
22. BOLTE, A., HILBRIG, L., GRUNDMANN, B., KAMPF, F., BRUNET, J. & ROLOFF, A. 2010. Climate change impacts on stand structure and competitive interactions in a southern Swedish spruce-beech forest. *European Journal of Forest Research*, 129, 261-276.
23. BOND, G., KROMER, B., BEER, J., MUSCHELER, R., EVANS, M. N., SHOWERS, W., HOFFMANN, S., LOTTI-BOND, R., HAJDAS, I. & BONANI, G. 2001. Persistent solar influence on North Atlantic climate during the Holocene. *Science*, 294, 2130-2136.
24. BONDETTI, M., SCOTT, S., LUCQUIN, A., MEADOWS, J., LOZOVSAYA, O., DOLBUNOVA, E., JORDAN, P. & CRAIG, O. E. 2020. Fruits, fish and the introduction of pottery in the Eastern European plain: Lipid residue analysis of ceramic vessels from Zamostje 2. *Quaternary International*, 541, 104-114.

25. BOS, J. A. & URZ, R. 2003. Late Glacial and early Holocene environment in the middle Lahn river valley (Hessen, central-west Germany) and the local impact of early Mesolithic people—pollen and macrofossil evidence. *Vegetation History and Archaeobotany*, 12, 19-36.
26. BRAY, P., BLOCKLEY, S., COOPE, G., DADSWELL, L., ELIAS, S., LOWE, J. & POLLARD, A. 2006. Refining mutual climatic range (MCR) quantitative estimates of palaeotemperature using ubiquity analysis. *Quaternary Science Reviews*, 25, 1865-1876.
27. BROOKS, S. J., HEIRI, O. & LANGDON, P. G. 2007. *The identification and use of palaearctic chironomidae larvae in palaeoecology*, Quaternary Research Association, London.
28. BUCKLAND, P. I. & BUCKLAND, P. C. 2006. BugsCEP: Coleopteran Ecology Package (software).
29. BURGER, J. R. & FRISTOE, T. S. 2018. Hunter-gatherer populations inform modern ecology. *Proceedings of the National Academy of Sciences*, 115, 1137-1139.
30. BUSKENS, R. 1987. The chironomid assemblages in shallow lentic waters differing in acidity, buffering capacity and trophic level in the Netherlands. *Entomologica Scandinavica*, 217-224.
31. COOPE, G. 1986. Coleoptera analysis. Berglund B.E. (ed.), *Handbook of Holocene palaeoecology and palaeohydrology*, Wiley Chichester, United Kingdom, 703-713.
32. DANILOVICH, I., ZHURAVLEV, S., KUROCHKINA, L. & GROISMAN, P. 2019. The Past and Future Estimates of Climate and Streamflow Changes in the Western Dvina River Basin. *Frontiers in Earth Science*, 7, 204.
33. DAVIS, S., BROWN, A. & DINNIN, M. 2007. Floodplain connectivity, disturbance and change: a palaeoentomological investigation of floodplain ecology from south-west England. *Journal of Animal Ecology*, 76, 276-288.
34. DAVYDOVA, N. & SERVANT-VILDARY, S. 1996. Late Pleistocene and Holocene history of the lakes in the Kola Peninsula, Karelia and the north-western part of the east European plain. *Quaternary Science Reviews*, 15, 997-1012.
35. DE VLEESCHOUWER, F., PIOTROWSKA, N., SIKORSKI, J., PAWLÝTA, J., CHEBURKIN, A., LE ROUX, G., LAMENTOWICZ, M., FAGEL, N. & MAUQUOY, D. 2009. Multiproxy evidence of 'Little Ice Age' palaeoenvironmental changes in a peat bog from northern Poland. *The Holocene*, 19, 625-637.

36. DOLBUNOVA, E., LUCQUIN, A., MCLAUGHLIN, T.R., BONDETTI, M., COUREL, B., ORAS, E., PIEZONKA, H., ROBSON, H.K., TALBOT, H., ADAMCZAK, K., ANDREEV, K., ASHEICHYK, V., CHARNIAUSKI, M., CZEKAJ-ZASTAWNÝ, A., EZEPENKO, I., GRECHKINA, T., GUNNARSSONE, A., GUSENTSOVA, T.M., HASKEVYCH, D., IVANISCHEVA, M., KABACIŃSKI, J., KARMANOV, V., KOSORUKOVA, N., KOSTYLEVA, E., KRIISKA, A., KUKAWKA, S., LOZOVSAYA, O., MAZURKEVICH, A., NEDOMOLKINA, N., PILICIAUSKAS, G., SINITSYNA, G., SKOROBOGATO, A., SMOLYANINOV, R.V., SURUKOV, A., TKACHOV, O., TKACHOVA, M., TSYBRIJ, A., TSYBRIJ, V., VYBORNOV, A.A., WAWRUSIEWICZ, A., YUDIN, A.I., MEADOWS, J., HERON, C., CRAIG, O.E. 2022. The transmission of pottery technology among prehistoric European hunter-gatherers. *Nature Human Behaviour*.
37. DOLUKHANOV, P. & MIKLYAYEV, A. 1986. Prehistoric lacustrine pile dwellings in the north-western part of the USSR. *Fennoscandia archaeologica*, 3, 81-89.
38. DOLUKHANOV, P., GEY, N., MIKLYAYEV, A. & MAZURKEWICZ, A. 1989. Rudnya-Serteya, a stratified dwelling-site in the Upper Duna basin (a multidisciplinary research). *Fennoscandia archaeologica*, 6, 23-27.
39. DOLUKHANOV, P. M., SARSON, G. R. & SHUKUROV, A. M. 2009. *BAR International Series 1964*. Archaeopress, Oxford, 109-121.
40. DZIEDUSZYŃSKA, D. A. 2019. Timing of environmental changes of the Weichselian decline (18.0–11.5 ka cal BP) using frequency distribution of ¹⁴C dates for the Łódź region, Central Poland. *Quaternary International*, 501, 135-146.
41. EJARQUE, A., BEAUGER, A., MIRAS, Y., PEIRY, J.-L., VOLDOIRE, O., VAUTIER, F., BENBAKKAR, M. & STEIGER, J. 2015. Historical fluvial palaeodynamics and multi-proxy palaeoenvironmental analyses of a palaeochannel, Allier River, France. *Geodinamica Acta*, 27, 25-47.
42. ELIAS, S. A. 1994. *Quaternary insects and their environments*, Smithsonian Institution Press. Washington-London, 284.
43. FEI, S., JO, I., GUO, Q., WARDLE, D. A., FANG, J., CHEN, A., OSWALT, C. M. & BROCKERHOFF, E. G. 2018. Impacts of climate on the biodiversity-productivity relationship in natural forests. *Nature Communications*, 9, 1–7.
44. FEURDEAN, A., PERŞOIU, A., TANȚĂU, I., STEVENS, T., MAGYARI, E. K., ONAC, B. P., MARKOVIĆ, S., ANDRIĆ, M., CONNOR, S. & FĂRCAŞ, S. 2014. Climate

- variability and associated vegetation response throughout Central and Eastern Europe (CEE) between 60 and 8 ka. *Quaternary Science Reviews*, 106, 206-224.
45. FREY, D. 1986. Cladocera Analysis. Handbook of Holocene Palaeoecology and Palaeohydrology. (ed.) Berglund, BE. John Wiley & Sons, Chichester, United Kingdom.
46. GAŁKA, M., MIOTK-SZPIGANOWICZ, G., GOSLAR, T., JĘŚKO, M., VAN DER KNAAP, W. O. & LAMENTOWICZ, M. 2013. Palaeohydrology, fires and vegetation succession in the southern Baltic during the last 7500 years reconstructed from a raised bog based on multi-proxy data. *Palaeogeography, Palaeoclimatology, Palaeoecology*, 370, 209-221.
47. GAŁKA, M., MIOTK-SZPIGANOWICZ, G., MARCZEWSKA, M., BARABACH, J., VAN DER KNAAP, W. O. & LAMENTOWICZ, M. 2015. Palaeoenvironmental changes in Central Europe (NE Poland) during the last 6200 years reconstructed from a high-resolution multi-proxy peat archive. *The Holocene*, 25, 421-434.
48. GIŁKA, W. 2001. Sezonowa dynamika pojawi wybranych gatunków ochockowatych z plemienia Tanytarsini Pojezierza Kaszubskiego (Diptera: Chironomidae). *Acta Entomologica Silesiana* 7-8: 31-42.
49. GIŁKA, W. 2011. Six unusual *Cladotanytarsus* Kieffer: towards a systematics of the genus and resurrection of *Lenziella* Kieffer (Diptera: Chironomidae: Tanytarsini). *Zootaxa*, 3100, 1–34.
50. GINTER, A., PIECH, W., KRĄPIEC, M., MOSKA, P., SIKORSKI, J., HRYNOWIECKA, A., STACHOWICZ-RYBKA, R., CYWA, K., PIOTROWSKA, N. & MROCZKOWSKA, A. 2023. Intense and quick land relief transformation in the Little Ice Age: The age of accumulative fan deposits in Seretka River Valley (Western East European Plain). *Quaternary International* 644-645, 160-177.
51. GLAIS, A., LÓPEZ-SÁEZ, J. A., LESPEZ, L. & DAVIDSON, R. 2016. Climate and human–environment relationships on the edge of the Tenaghi-Philippon marsh (Northern Greece) during the Neolithization process. *Quaternary International*, 403, 237-250.
52. GONZALEZ MEDINA, A., SORIANO HERNANDO, O. & JIMÉNEZ RÍOS, G. 2015. The use of the developmental rate of the aquatic midge *Chironomus riparius* (Diptera, Chironomidae) in the assessment of the postsubmersion interval. *Journal of forensic sciences*, 60, 822-826.
53. GRIMM, E. 1991. Tilia and tiliograph. *Illinois State Museum, Springfield*.

54. HAMERLIK, L., VESELSKA, M., NOVIKMEC, M. & SVITOK, M. 2019. Lasiodiamesa (Podonominae, Chironomidae), first record of the genus from Slovakia. *CHIRONOMUS Journal of Chironomidae Research*, 32, 79-82.
55. HEIKKILAE, M. E. & SEPPÄ, H. 2010. Holocene climate dynamics in Latvia, eastern Baltic region: a pollen based summer temperature reconstruction and regional comparison. *Boreas*, 39, 705-719.
56. HEINSALU, A. & VESKI, S. 2007. The history of the Yoldia Sea in Northern Estonia: palaeoenvironmental conditions and climatic oscillations. *Geological Quarterly*, 51, 295-306.
57. HOFMANN, W. 2000. Response of the chydorid faunas to rapid climatic changes in four alpine lakes at different altitudes. *Palaeogeography, Palaeoclimatology, Palaeoecology*, 159, 281-292.
58. HOFMANN, W. & WINN, K. 2000. The littorina transgression in the Western Baltic Sea as indicated by subfossil Chironomidae (Diptera) and Cladocera (Crustacea). *International Review of Hydrobiology: A Journal Covering all Aspects of Limnology and Marine Biology*, 85, 267-291.
59. ITKONEN, T. 1921. The population and settlements. *Theodor Homén and others, Fennia*, 42, 25-30.
60. JUGGINS, S. 2007. C2 version 1.5. 0: a program for plotting and visualising stratigraphic data. *University of Newcastle, UK*.
61. KALICKI, T., KITTEL, P., PAWŁOWSKI, D., PŁÓCIENNIK, M., STACHOWICZ-RYBKA, R., MAZURKEVICH, A., KRUPA, J. & ALEXANDROVSKIY, A. 2015. Postglacial evolution of Lower Serteya river valley (Western Russia). Quaternary Conference, 27 November 2015 2015 Brno. ÚGV PřF MU, 23.
62. KAUFMAN, D., MCKAY, N., ROUTSON, C., EEB, M., DAVIS, B., HEIRI, O., JACCARD, S., TIERNEY, J., DATWYLER, C., AXFORD, Y., BRUSSEL, T., CARTAPANIS, O., CHASE, B., DAWSON, A., DE VERNAL, A., ENGELS, S., JONKERS, L., MARSICEK, J., MOFFA-SANCHEZ, P., MORILL, C., ORSI, A., REHFELD, K., SAUNDERS, K., SOMMER, P.S., THOMAS, E., TONELLO, M., TOTH, M., VACHULA, R., ANDREEV, A., BERTRAND, S., BISKABORN, B., BRINGUE, M., BROOKS, S., CANIUPAN, M., CHEVALIER, M., CWYNAR, L., EMILE-GEAY, J., FEGYVERESI, J., FEURDEAN, A., FINSINGER, W., FORTIN, M.C., FOSTER, L., FOX, M., GAJEWSKI, K., GROSEJEAN, M., HAUSMANN, S., HEINRICHS, M.,

- HOLMES, N., ILYASHUK, B., ILYASHUK, E., JUGGINS, S., KHIDER, D., KOINIG, K., LANGDON, P., LAROCQUE-TOBLER, I., LI, J., LOTTER, A., LUOTO, T., MACKAY, A., MAGYARI, E., MALEVICH, S., MARK, B., MASSAFERRO, J., MONTADE, V., NAZAROVA, L., NOVENKO, E., PARIL, P., PEARSON, E., PEROS, M., PIENITZ, R., PŁÓCIENNIK, M., PORINCHYU, D., POTITO, A., REES, A., REINEMANN, S., ROBERTS, S., ROLLAND, N., SALONEN, S., SELF, A., SEPPA, H., SHALA, S., ST-JACQUES, J.M., STENNI, B., SYRYKH, L., TARRATS, P., TAYLOR, K., VAN DEN BOS, V., VELLE, G., WAHL, E., WALKER, I., WILMSHURST, J., ZHANG, E., ZHILICH, S. 2020. A global database of Holocene paleotemperature records. *Scientific Data*. 2020.04.14;7(1):115.
63. KHRUSTALEVA, I. 2016. The earliest dwellings of the stone age in Smolensk and Pskov regions of Russia. *Samara Journal of Science* 5.4: 77-85.
64. KIRLEIS, W., WIECKOWSKA-LÜTH, M., PIEZONKA, H., NEDOMOLKINA, N., LORENZ, S., ELBERFELD, V. & SCHNEEWEIß, J. 2020. The Development of Plant Use and Cultivation in the Sukhona Basin, Northwest Russian Taiga Zone. *Archaeobotanical Studies of Past Plant Cultivation in Northern Europe. Advances in Archaeobotany*, 5, 101-118.
65. KITTEL, P., MAZURKEVICH, A., DOLBUNOVA, E., KALICKI, T., KUL'KOVA, M., PAWŁOWSKI, D., PŁÓCIENNIK, M., STACHOWICZ-RYBKA, R. & ZAITSEVA, G. 2016. Evolution of lake basins in the Serteya region (Western Russia) in the context of Neolithic settlement's development. W: S. LEVINA, R. G., I. YADRIKHINSKI, P. DAVYDOVA (ed.) *Paleolimnology of Northern Eurasia. Experience, Methodology, Current Status: Proceedings of the International Conference*. North-Eastern Federal University. Yakutsk.
66. KITTEL, P., MAZURKEVICH, A., DOLBUNOVA, E., KAZAKOV, E., MROCKOWSKA, A., PAVLOVSKAIA, E., PIECH, W., PŁÓCIENNIK, M., SIKORA, J. & TELTEVSKAYA, Y. 2018. Palaeoenvironmental reconstructions for the Neolithic pile-dwelling Serteya II site case study, Western Russia. *Acta Geographica Lodzienia*, 107, 191-213.
67. KITTEL, P., MAZURKEVICH, A., ALEXANDROVSKIY, A., DOLBUNOVA, E., KRUPSKI, M., SZMANDA, J., STACHOWICZ-RYBKA, R., CYWA, K., MROCKOWSKA, A. & OKUPNY, D. 2020. Lacustrine, fluvial and slope deposits in the

- wetland shore area in Serteya, Western Russia. *Acta Geographica Lodzienia*, 110, 103-124.
68. KITTEL, P., MAZURKEVICH, A., WIECKOWSKA-LÜTH, M., PAWŁOWSKI, D., DOLBUNOVA, E., PŁOCIENNIK, M., GAUTHIER, E., KRĄPIEC, M., MAIGROT, Y. & DANGER, M. 2021. On the border between land and water: the environmental conditions of the Neolithic occupation from 4.3 until 1.6 ka BC at Serteya, Western Russia. *Geoarchaeology*, 36, 173-202.
69. KITTEL, P., MAZURKEVICH, A., GAUTHIER, E., KAZAKOV, E., KUBITSKY, Y., RZODKIEWICZ, M., MROCKOWSKA, A., OKUPNY, D., SZMAŃDA, J., DOLBUNOVA, E. 2022. A deep history within a small wetland: 13 000 years of human-environment relations on the East European Plain. *Antiquity*. Cambridge University Press 1–8.
70. KOBYSHEVOY, N. V. AKENT'YEVA Ye., BOGDANOV E., 2001. The Climate of Russia. *Gidrometeoizdat*, 655.
71. KOFF, T. 2010. Pollen profile LIIVJARV, Liivjarve Bog, Estonia. PANGAEA.
72. KOHONEN, T. 1982. Self-organized formation of topologically correct feature maps. *Biological cybernetics*, 43, 59-69.
73. KOHONEN, T. 1995. Learning vector quantization. Self-organizing maps. *Springer Series in Information Sciences*, Springer, Berlin, Heidelberg, 30, 175-189.
74. KOHONEN, T. 2001. Learning vector quantization. Self-organizing maps. *Springer Series in Information Sciences*, Springer, Berlin, Heidelberg, 256-261.
75. KONDRAKCI, J. 1992. Fizycznogeograficzna regionalizacja republik Litewskiej i Białoruskiej w układzie dziesiętnym. *Przegląd Geograficzny. Instytut Geografii i Przestrzennego Zagospodarowania Polskiej Akademii Nauk*, LXIV, 344.
76. KORHOLA, A. 1999. Distribution patterns of Cladocera in subarctic Fennoscandian lakes and their potential in environmental reconstruction. *Ecography*, 22, 357-373.
77. KOTRYS, B., PŁOCIENNIK, M., SYDOR, P. & BROOKS, S. J. 2020. Expanding the Swiss-Norwegian chironomid training set with Polish data. *Boreas*, 49, 89-107.
78. KREMENETSKI, K., BORISOVA, O. & ZELIKSON, E. 2000. The Late Glacial and Holocene history of vegetation in the Moscow region. *Paleontological Journal c/c Paleontologicheskii Zhurnal*, 34, 67-74.

79. KUBIAK-MARTENS, L. 2002. New evidence for the use of root foods in pre-agrarian subsistence recovered from the late Mesolithic site at Halsskov, Denmark. *Vegetation History and Archaeobotany*, 11, 23-32.
80. KUBLITSKIY, I., SUBETTO, D., DRUZHININA, O., KULKOVA, M. & ARSLANOV, K. 2016. Paleolimnological reconstruction of environmental variability during the Late Pleistocene and Holocene in the south-east Baltic region. EGU General Assembly Conference Abstracts, EPSC2016-521.
81. KULKOVA, M., MAZURKEVICH, A. & DOLUKHANOV, P. 2001. Chronology and paleoclimate of prehistoric sites in Western Dvina-Lovat area of North-western Russia. *Geochronometria: Journal on Methods & Applications of Absolute Chronology*, 20, 87-94.
82. KULKOVA, M., MAZURKEVICH, A., DOLBUNOVA, E. & LOZOVSKY, V. 2015a. The 8200 calBP climate event and the spread of the Neolithic in Eastern Europe. *Documenta Praehistorica*, 42, 77–92.
83. KULKOVA, M., MAZURKEVICH, A., DOLBUNOVA, E., REGERT, M., MAZUY, A., NESTEROV, E. & SINAI, M. 2015b. Late Neolithic Subsistence Strategy and Reservoir Effects in ¹⁴C Dating of Artifacts at the Pile-Dwelling Site Serteya II (NW Russia). *Radiocarbon*, 57, 611-623.
84. KUZ'MIN, S. L. 1988. Kurgannaya gruppa u d. Berezno-pamyatnik kul'tury dlinnykh kurganov v basseyne g. Plyussy. *Arkheologiya i istoriya Pskova i Pskovskoy zemli (tezisy dokladov nauchno-prakticheskoy konferentsii)*. [Dostęp online 12.01.2022]. <https://arheologi.livejournal.com/20892.html>
85. KUZ'MINA, S. 2003. Novye faunisticheskie dannye po rezul'tatam raskopok neoliticheskikh pamyatnikov Smolenskoi i Pskovskoi oblastei. *Drevnosti Podvin'ya: istoricheskii aspekt. St Petersburg, Izdatelstvo Gosudarstvennogo Jermitaja*, 300-316.
86. LAMENTOWICZ, M., LAMENTOWICZ, Ł., VAN DER KNAAP, W. O., GĄBKA, M. & MITCHELL, E. A. D. 2010. Contrasting Species—Environment Relationships in Communities of Testate Amoebae, Bryophytes and Vascular Plants Along the Fen–Bog Gradient. *Microbial Ecology*, 59, 499-510.
87. LI, C. & BORN, A. 2019. Coupled atmosphere-ice-ocean dynamics in Dansgaard-Oeschger events. *Quaternary Science Reviews*, 203, 1-20.
88. LINE, J. & BIRKS, H. 1996. BSTICK Version 1.0. *Unpublished computer program. Botanical Institute, University of Bergen.*

89. LUOTO, T. P., KULTTI, S., NEVALAINEN, L. & SARMAJA-KORJONEN, K. 2010. Temperature and effective moisture variability in southern Finland during the Holocene quantified with midge-based calibration models. *Journal of Quaternary Science*, 25, 1317-1326.
90. LUOTO, T. P. & NEVALAINEN, L. 2017. Quantifying climate changes of the Common Era for Finland. *Climate Dynamics*, 49, 2557-2567.
91. ŁUCÓW, D., LAMENTOWICZ, M., OBREMSKA, M., ARKHIPOVA, M., KITTEL, P., ŁOKAS, E., MAZURKEVICH, A., MRÓZ, T., TJALLINGII, R. & SŁOWIŃSKI, M. 2020. Disturbance and resilience of a Sphagnum peatland in western Russia (Western Dvina Lakeland) during the last 300 years: A multiproxy, high-resolution study. *The Holocene*, 30, 1552-1566.
92. MACARTHUR, R. H. 1957. On the relative abundance of bird species. *Proceedings of the National Academy of Sciences of the United States of America*, 43(3): 293–295.
93. MAKOTINSKAYA, Y., DUDAREV, V. A., YEVSEYEVA, N. A. 1980. SSSR: administrativno-territorial'noye deleniye soyuznykh respublik na 1 yanvarya 1980 goda. *Izvestia*, 515 - 623.
94. MARCISZ, K., GAŁKA, M., PIETRALA, P., MIOTK-SZPIGANOWICZ, G., OBREMSKA, M., TOBOLSKI, K. & LAMENTOWICZ, M. 2017. Fire activity and hydrological dynamics in the past 5700 years reconstructed from Sphagnum peatlands along the oceanic–continental climatic gradient in northern Poland. *Quaternary Science Reviews*, 177, 145-157.
95. MARTIN, C., MENOT, G., THOUVENY, N., PERYRON, O., ANDRIEU-PONEL, V., MONTADE, V., DAVTIAN, N., REILLE, M., BARD, E. 2020 Early Holocene Thermal Maximum recorded by branched tetraethers and pollen in Western Europe (Massif Central, France). *Quaternary Science Reviews* 228, 106-109.
96. MATERO, I. S. O., GREGOIRE, L. J., IVANOVIC, R. F., TINDALL, J. C. & HAYWOOD, A. M. 2017. The 8.2 ka cooling event caused by Laurentide ice saddle collapse. *Earth and Planetary Science Letters*, 473, 205-214.
97. MAZEI, Y. A., TSYGANOV, A. N., BOBROVSKY, M. V., MAZEI, N. G., KUPRIYANOV, D. A., GAŁKA, M., ROSTANETS, D. V., KHAZANOVA, K. P., STOIKO, T. G. & PASTUKHOVA, Y. A. 2020. Peatland Development, Vegetation History, Climate Change and Human Activity in the Valdai Uplands (Central European Russia) during the Holocene: A Multi-Proxy Palaeoecological Study. *Diversity*, 12 (2), 462.

98. MAZURKEVICH, A. N. 2003. Pervyye svidetelstva proyavleniya proizvodyashchego khozyaystva na Severo-Zapade Rossii. W: SEDYKH, D. G. S. V. N., ed. Pushkarevskiy sbornik II. Wyd. II, 77-84.
99. MAZURKEVICH, A., SABLIN, M. V., DOLBUNOVA, E. V., KITTEL, P., MAIGROT, Y. & KAZAKOV, E. 2020b. Landscape, seasonality and natural resources use in the 3rd millennium BC by pile-dwelling communities (NW Russia). W: A. HAFNER, E. DOLBUNOVA, A. MAZURKEVICH, E. PRANCKENAITĖ & HINZ, M. (eds.) *Settling waterscapes in Europe: The archaeology of Neolithic and Bronze Age pile-dwellings*. OSPA – Open Series in Prehistoric Archaeology, Band 1, Propylaeum, Heidelberg. 17–35.
100. MAZURKEVICH, A. N., DOLUKHANOV, P., SHUKUROV, A. & ZAITSEVA, G. 2009b. Mesolithic and Neolithic in the Western Dvina–Lovat Area. *The East European Plain on the Eve of Agriculture, BAR International Series*, 164, 145–153.
101. MAZURKEVICH, A. N., KOROTKEVICH, B. N., DOLUKHANOV, P. M., SHUKUROV, A. M., ARSLANOV, K. A., SAVEL'EVA, L. A., DZINORDZE, E. N., KULKOVA, M. A. & ZAITSEVA, G. I. 2009c. Climate, subsistence and human movements in the Western Dvina - Lovat River Basins. *Quaternary International*, 203, 52–66.
102. MAZURKEVICH, A. N., & DOLBUNOVA, Y. V. 2011a. Podvodnyye issledovaniya neoliticheskikh pamyatnikov Severo-Zapada Rossii. *Trudy III (XIX) Vserossiyskogo Arkheologicheskogo S"yezda*, 174–175.
103. MAZURKEVICH, A. N., DOLBUNOVA, E.V., MAIGROT, Y, HOOKK, D. 2011b. Results of underwater excavations of Serteya II and research of pile-dwellings in Northwest Russia. *Archaeologia Baltica*, 14, 47–64.
104. MAZURKEVICH, A., DOLBUNOVA, E., KUL'KOVA, M., ALEXANDROVSKIY, A., SAVELEVA, L., POLKOVNIKOVA, M., KHRUSTALEVA, I., KOLOSOVA, M., HOOKK, D. & MAZURKEVICH, K. 2012a. Dynamics of landscape developing in early-middle Neolithics in Dnepr-Dvina region. International conference “Geomorphic Processes and Geoarchaeology: from Landscape Archaeology to Archaeotourism”, Moscow-Smolensk. Russia, Universum, 192–194.
105. MAZURKEVICH, A., KULKOVA, M. & SAVEL'EVA, L. 2012b. Geoarchaeology of the Serteya Microregion, the Upper Dvina Basin. *Geoarchaeological Issues of the Upper Dnieper–Western Dvina River Region (Western Russia)*. Universum, Moscow-Smolensk, 49-104.

- 106.MAZURKEVICH, A. & DOLBUNOVA, E. 2015. The oldest pottery in hunter-gatherer communities and models of Neolithisation of Eastern Europe. *Documenta Praehistorica*, 42, 13-66.
- 107.MAZURKEVICH, A., DOLBUNOVA, E., KITTEL, P., FASSBENDER, J., MAIGROT, Y., MROCKOWSKA, A., PŁOCIENNIK, M., SIKORA, J., SŁOWIŃSKI, M., SABLIN, M. & I. S. 2017. Multi-disciplinary research on the Neolithic pile-dwelling Serteya II site (Western Russia) and the landscape reconstruction. W: A. MARCINIAK-KAJZER, A. A., A. GOLAŃSKI, S. RZEPECKI (ed.) *Nie tylko krzemienie. Not only flints*. Łódź: Instytut Archeologii Uniwersytetu Łódzkiego, Łódzka Fundacja Badań Naukowych, Stowarzyszenie Naukowe Archeologów Polskich Oddział w Łodzi, 103-128.
- 108.MAZURKEVICH, A., DOLBUNOVA, E. & OTTONELLO, L. 2018. Archaeological excavations and reconstructions of disappeared archaeological heritage (based on excavations in North-Western Russia). Prehistoric Networks in Southern and Eastern Europe, *Vita Antiqua*, 10, 165-175.
- 109.MAZURKEVICH, A., DOLUKHANOV, P. & SHUKUROV, A. 2009a. Mesolithic and Neolithic in the Western Dvina–Lovat Area. *The East European Plain on the Eve of Agriculture, BAR International Series*, 164, 145-153.
- 110.MAZURKEVICH, A., KITTEL, P., MAIGROT, Y., DOLBUNOVA, E., MROCKOWSKA, A., WIECKOWSKA-LÜTH, M. & PIECH, W. 2020a. Natural and anthropogenic impact on the formation of archaeological layers in a lake shore area: case study from the Serteya II site, Western Russia. *Acta Geographica Lodziensia*, 110, 81-102.
- 111.MIKLYAEV, A. 1969. Pamyatniki Usvyatskogo mikrorayona. Pskovskaya oblast'. Arkheologicheskiy sbornik Gosudarstvennogo Ermitazha. Wyd. 11. 18-40.
- 112.MIKLJAEV, A. 1995. *Kamenny — zheleznyy vek v mezhdurech'ye Zapadnoy Dviny i Lovati*. Peterburgskiy arkheologicheskiy vestnik. ed. B.S.Korotkevich, A. Mazurkevich. Wyd. 9. Sankt Petersburg, 7-39.
- 113.MIKLYAEV, A. M., MAZURKEVICH, A. N., & ANISYUTKIN, N. K. 1995. Yeshche raz o nakhodkakh arkhaichnykh kremnevykh izdeliy v verkhov'yakh Zapadnoy Dviny. In *Drevnosti Severo-Zapadnoy Rossii*, 11-16.
- 114.MOLLER PILLOT, H. K. 2009. *Chironomidae larvae of the Netherlands and adjacent lowlands: biology and ecology of the Chironomini*, KNNV publishing, Zeist, 270.
- 115.MORENO, A., SVENSSON, A., BROOKS, S. J., CONNOR, S., ENGELS, S., FLETCHER, W., GENTY, D., HEIRI, O., LABUHN, I. & PERŞOIU, A. 2014. A

- compilation of Western European terrestrial records 60–8 ka BP: towards an understanding of latitudinal climatic gradients. *Quaternary Science Reviews*, 106, 167-185.
116. MROCKOWSKA, A., KITTEL, P., MARCISZ, K., DOLBUNOVA, E., GAUTHIER, E., LAMENTOWICZ, M., MAZURKEVICH, A., OBREMSKA, M., PŁOCIENNIK, M. & KRAMKOWSKI, M. 2021a. Small peatland with a big story: 600-year paleoecological and historical data from a kettle-hole peatland in Western Russia. *The Holocene*, 31, 1761-1776.
117. MROCKOWSKA, A., PAWŁOWSKI, D., GAUTHIER, E., MAZURKEVICH, A., LUOTO, T. P., PEYRON, O., KOTRYS, B., BROOKS, S. J., NAZAROVA, L. B., SYRYKH, L., DOLBUNOVA, E. V., THIEBAUT, E., PŁOCIENNIK, M., ANTCZAK-ORLEWSKA, O. & KITTEL, P. 2021b. Middle Holocene Climate Oscillations Recorded in the Western Dvina Lakeland. *Water*, 13, 1611.
118. MROCKOWSKA, A., WANAT, M., PRZEWOŹNY, M., RUTA R., STACHOWIAK, M., MAZURKEVICH, A., PŁOCIENNIK, M., JAŁOSZYŃSKI P., KITTEL P., KARBOWIAK, G., OKUPNY, D., WJITEHOUSE, N. J., KRUK A., SŁOWIŃSKI M. Coleoptera as ecological indicators of Neolithic human impact: Western Russia (Serteya II site - case study) (w przygotowaniu)
119. NATANSON-LESKI, J. 1922. *Dzieje granicy wschodniej Rzeczypospolitej: Granica moskiewska w epoce jagiellońskiej*, Książnica Polska Towarzystwa Nauczycieli Szkół Wyższych, Lwów-Warszawa.
120. NAZAROVA, L. B., SAPELKO, T. V., KUZNETSOV, D. D. & SYRYKH, L. S. 2015. Palaeoecological and palaeoclimatical reconstructions of Holocene according chironomid analysis of Lake Glubokoye sediments. *Doklady Biological Sciences*, 460, 57-60.
121. NAZAROVA, T., FOMIN, I., DMITRIEV, P., WENDT, J. & JANALEYEVA, K. 2019. Landscape and limnological research of lake systems of the northeastern borderlands of the Republic of Kazakhstan and assesment of their recreational capacity. *GeoJournal of Tourism and Geosites*, 25 (2), 485–495.
122. NAZAROVA, L., SYRYKH, L. S., MAYFIELD, R. J., FROLOVA, L. A., IBRAGIMOVA, A. G., GREKOV, I. M. & SUBETTO, D. A. 2020. Palaeoecological and palaeoclimatic conditions on the Karelian Isthmus (northwestern Russia) during the Holocene. *Quaternary Research*, 95, 65-83.
123. NEVALAINEN, L. & LUOTO, T. P. 2017. Relationship between cladoceran (Crustacea) functional diversity and lake trophic gradients. *Functional Ecology*, 31, 488-498.

- 124.NOSOVA, M. B., NOVENKO, E. Y., SEVEROVA, E. E. & VOLKOVA, O. A. 2019. Vegetation and climate changes within and around the Polistovo-Lovatskaya mire system (Pskov Oblast, north-western Russia) during the past 10,500 years. *Vegetation History and Archaeobotany*, 28, 123-140.
- 125.NOVIK, A. 2014. The development of Belarusian lakes during the Late Glacial and Holocene. *Estonian Journal of Earth Sciences*, 59(1), 63-79.
- 126.O'NEILL, A. R. & RANA, S. K. 2016. An ethnobotanical analysis of parasitic plants (Parijibi) in the Nepal Himalaya. *Journal of ethnobiology and ethnomedicine*, 12, 1-15.
- 127.OSBORNE, P. 1988. A Late Bronze Age insect fauna from the River Avon, Warwickshire, England: its implications for the terrestrial and fluvial environment and for climate. *Journal of archaeological science*, 15, 715-727.
- 128.OSHIBKINA, S. 1987. Eneolith i bronzovy vek Severa Evropejskoj chasti SSSR. *Arkheologija SSSR. Epokha bronzy lesnoj polosy SSSR*, ON Bader, DA Krajnov and MF Kosarev (eds), 147-156.
- 129.PANIN, A. V., ADAMIEC, G., ARSLANOV, K. A., BRONNIKOVA, M. A., FILIPPOV, V. V., SHEREMETSKAYA, E. D., ZARETSKAYA, N. E. & ZAZOVSKAYA, E. P. 2014. Absolute chronology of fluvial events in the Upper Dnieper river system and its palaeogeographic implications. *Geochronometria*, 41, 278-293.
- 130.PAWŁOWSKI, D. 2011. Evolution of an Eemian lake based on Cladocera analysis (Konin area, Central Poland). *Acta Geologica Polonica*, 61, 441-450.
- 131.PAWŁOWSKI, D., GRUSZKA, B., GALLAS, H. & PETERA-ZGANIACZ, J. 2013. Changes in the biota and sediments of glacial Lake Koźmin, Poland, during the late Saalian (Illinoian). *Journal of Paleolimnology*, 49, 679-696.
- 132.PAWŁOWSKI, D., KOWALEWSKI, G., MILECKA, K., PŁOCIENNIK, M., WOSZCZYK, M., ZIELIŃSKI, T., OKUPNY, D., WŁODARSKI, W. & FORYSIAK, J. 2015a. A reconstruction of the palaeohydrological conditions of a flood-plain: a multi-proxy study from the Grabia River valley mire, central Poland. *Boreas*, 44, 543-562.
- 133.PAWŁOWSKI, D., BORÓWKA, R. K., KOWALEWSKI, G., LUOTO, T. P., MILECKA, K., NEVALAINEN, L., OKUPNY, D., PŁOCIENNIK, M., WOSZCZYK, M. & TOMKOWIAK, J. 2016a. The response of flood-plain ecosystems to the Late Glacial and Early Holocene hydrological changes: A case study from a small Central European river valley. *Catena*, 147, 411-428.

- 134.PAWŁOWSKI, D., BORÓWKA, R. K., KOWALEWSKI, G. A., LUOTO, T. P., MILECKA, K., NEVALAINEN, L., OKUPNY, D., TOMKOWIAK, J. & ZIELIŃSKI, T. 2016b. Late Weichselian and Holocene record of the paleoenvironmental changes in a small river valley in Central Poland. *Quaternary Science Reviews*, 135, 24-40.
- 135.PEYRON, O., MAGNY, M., GORING, S., JOANIN, S., de BEAULIEU, J.L., BRUGGIAPAGLIA, E., SADORI, L., GARFI, G., KOULI, K., IOAKIM, C. 2013. Contrasting patterns of climatic changes during the Holocene across the Italian Peninsula reconstructed from pollen data. *Climate of the Past*, 9, 1233–1252.
- 136.PIECH, W. 2021. Sedimentological features and depositional conditions of accumulative fans in the lower Serteyka River valley, Western Russia. *Acta Geographica Lodziensia*, 111, 159-188.
- 137.PIECH, W., HRYNOWIECKA, A., STACHOWICZ-RYBKA, R., CYWA, K., MROCKOWSKA, A., SŁOWIŃSKI, M., OKUPNY, D., KRĄPIEC, M., GINTER, A., MAZURKEVICH, A., KITTEL, P. Natural and anthropogenic factors of the intense slope processes in Eastern Europe in the Modern Period; case study in Serteyka River valley (w przygotowaniu)
- 138.PINDER, L. C. V. 1983. The larvae of Chironominae (Diptera : Chironomidae) of the Holarctic region-Keys and diagnoses. *Chironomidae of the Holarctic Region. Keys and Diagnoses, 1. Larvae, Entomologica Scandinavica Supplement*, 19, 149-294.
- 139.PINNEKER, E. V. 1983. *General hydrogeology*, Cambridge University Press.
- 140.PŁOCIENNIK, M., KRUK, A., MICHCZYŃSKA, D. J. & BIRKS, J. 2015. Kohonen artificial neural networks and the indval index as supplementary tools for the quantitative analysis of palaeoecological data. *Geochronometria*, 42, 189--201.
- 141.PŁOCIENNIK, M., PAWŁOWSKI, D., VILIZZI, L. & ANTczAK-ORLEWSKA, O. 2020. From oxbow to mire: Chironomidae and Cladocera as habitat palaeoindicators. *Hydrobiologia*, 847, 3257-3275.
- 142.PŁOCIENNIK, M., MROCKOWSKA, A., PAWŁOWSKI, D., WIECKOWSKA-LÜTH, M., KURZAWSKA, A., RZODKIEWICZ, M., OKUPNY, D., SZMAŃDA, J., MAZURKEVICH, A. & DOLBUNOVA, E. 2022. Summer temperature drives the lake ecosystem during the Late Weichselian and Holocene in Eastern Europe: A case study from East European Plain. *Catena*, 214, 106206.
- 143.PODBielkowski, Z. 1995. *Fitogeografia części świata. Europa, Azja, Afryka*. PWN. Warszawa, 400.

- 144.RENSSEN, H., SEPPÄ, H., CROSTA, X., GOOSSE, H. & ROCHE, D. M. 2012. Global characterization of the Holocene thermal maximum. *Quaternary Science Reviews*, 48, 7-19.
- 145.SABLIN, M. & SIROMYATNIKOVA, E. 2009. Animal Remains from Neolithic Sites in Northwestern Russia. W: P.M. DOLUKHANOV, G. R. S., A.M. SHUKUROV (ed.) *The East European Plain on the Eve of Agriculture*. BAR International Series 1964. Oxford: Archaeopress. 153-158.
- 146.SAN'KO, A. F. 1987. *Neoplejstocen severo-vostočnoj Belorussii i smežnych pajonov RSFSR*, Nauka i technika, 176.
- 147.SAPELKO, T.V. 2006. Dinamika razvitiâ rastitel'nosti na territorii Kenozerskogo nacional'nogo parka v golocene. *Izvestiya Russkogo geograficheskogo obshchestva*. 138, 70-76.
- 148.SARMAJA-KORJONEN, K. 2003. Chydoid ephippia as indicators of environmental change biostratigraphical evidence from two lakes in southern Finland. *The Holocene*, 13, 691-700.
- 149.SARMAJA-KORJONEN, K., NYMAN, M., KULTTI, S. & VÄLIRANTA, M. 2006. Palaeolimnological development of Lake Njargajavri, northern Finnish Lapland, in a changing Holocene climate and environment. *Journal of Paleolimnology*, 35, 65-81.
- 150.SCHAD, P., DONDEYNE, S. 2016. World reference base for soil resources. 1-4.
- 151.SCHMIDT, E. A. 1992. *Plemena verkhov'yev Dnepr'a do obrazovaniya Drevnerusskogo gosudarstva. Dnepro-dvinskiye plemena (VIII v. do n. e. - III v. n. e.)*. Prometey, 207.
- 152.SHMIDT, E. A. 2003. *Verkhneye podneprov'ye i podvin'ye v III-VII vv. n. e. Tushemlinskaya kul'tura*, Rossiiskaia arkheologija Smolensk, 4. 53-65.
- 153.ŠEIRIENĖ, V., KABAILIENĖ, M., KASPEROVIČIENĖ, J., MAŽEIKA, J., PETROŠIUS, R. & PAŠKAUSKAS, R. 2009. Reconstruction of postglacial palaeoenvironmental changes in eastern Lithuania: evidence from lacustrine sediment data. *Quaternary International*, 207, 58-68.
- 154.SEPPÄ, H. & POSKA, A. 2004. Holocene annual mean temperature changes in Estonia and their relationship to solar insolation and atmospheric circulation patterns. *Quaternary Research*, 61, 22-31.
- 155.SHELEKHOVA, T., VAS' KO, O. & DEMIDOV, I. 2005. Paleoekologicheskie usloviya razvitiya severo-zapadnogo Prionezh'ya v pozdnelednikov'e i golotsene. *Geologiya i poleznyye iskopayemyye Karelii. Petrozavodsk: KarRC RAS*, 149-157.

- 156.SHELEKHOVA, T. S. & LAVROVA, N. B. 2020. Paleograficheskiye rekonstruktsii razvitiya territorii severo-zapadnoy Karelii v golotsene (po dannym izucheniya donnykh otlozheniy malykh ozer. *Trudy Karel'skogo nauchnogo tsentra Rossiyskoy akademii nauk*, 9, 101-122.
- 157.SHELOMANOVA, N. B. 1967. *K voprosu ob izuchenii istochnikov po istorii vneshney politiki Rossii v kontse XVIv*. Novoye o proshlom nashey strany: pamyati akademika M. N. Tikhomirova: sbornik statey. Akademiya nauk SSSR, Otdeleniye istorii, Arkheograficheskaya komissiya; [ed. V. A. Aleksandrov], Moskva, Nauka, Glavnaya redaktsiya vostochnoy literatury.
- 158.SHKALIKOV, V., YERASHOV, M. & BORISOVSKAYA, I. 2005. Osobo okhranyayemye prirodnyye territorii Smolenskoi oblasti. Smolensk, 464.
- 159.SILLASOO, U., MAUQUOY, D., BLUNDELL, A., CHARMAN, D., BLAAUW, M., DANIELL, J. R. G., TOMS, P., NEWBERRY, J., CHAMBERS, F. M. & KAROFELD, E. 2007. Peat multi-proxy data from Männikjärve bog as indicators of late Holocene climate changes in Estonia. *Boreas*, 36, 20-37.
- 160.SMITH, D. N. & HOWARD, A. J. 2004. Identifying changing fluvial conditions in low gradient alluvial archaeological landscapes: can coleoptera provide insights into changing discharge rates and floodplain evolution? *Journal of Archaeological Science*, 31, 109-120.
- 161.SOHAR, K. & KALM, V. 2008. A 12.8-ka-long palaeoenvironmental record revealed by subfossil ostracod data from lacustrine freshwater tufa in Lake Sinijärv, northern Estonia. *Journal of Paleolimnology*, 40, 809-821.
- 162.SPIRIDONOVA, E. 1991. *Evolyutsiya rastitel'nogo pokrova basseyna Dona v verkhнем pleystotsene - golotsene*, Nauka, Moscow, 221.
- 163.STARKEL, L., SOJA, R. & MICHĘŻYŃSKA, D. J. 2006. Past hydrological events reflected in Holocene history of Polish rivers. *Catena*, 66, 24-33.
- 164.STARKEL, L., MICHĘŻYŃSKA, D. J., KRĄPIEC, M., MARGIELEWSKI, W., NALEPKA, D. & PAZDUR, A. 2013. Progress in the Holocene chrono-climatostigraphy of Polish territory. *Geochronometria*, 40, 1-21.
- 165.STIVRINS, N., KALNINA, L., VESKI, S. & ZEIMULE, S. 2014. Local and regional Holocene vegetation dynamics at two sites in eastern Latvia. *Boreal Environment Research*, 19, 310-322.
- 166.STOLBOVOI, V. 2002. Carbon in Russian Soils. *Climatic Change*, 55, 131-156.

167. SUBETTO, D., NAZAROVA, L., PESTRYAKOVA, L., SYRYKH, L., ANDRONIKOV, A., BISKABORN, B., DIEKMANN, B., KUZNETSOV, D., SAPELKO, T. & GREKOV, I. 2017. Paleolimnological studies in Russian northern Eurasia: A review. *Contemporary problems of Ecology*, 10, 327-335.
168. SYRYKH, L., NAZAROVA, L. & SUBETTO, D. 2015. Preliminary data on climate development in the territory of the Karelian Isthmus during the Holocene based on the results of chironomid and lithological analyses. *Trudy Karel'skogo nauchnogo tsentra Rossiyskoy akademii nauk, Seriya Limnologiya*, 53-59.
169. SYRYKH, L., SUBETTO, D. & NAZAROVA, L. 2021. Paleolimnological studies on the East European Plain and nearby regions: the PaleoLake Database. *Journal of Paleolimnology*, 65, 369-375.
170. SZEROCZYŃSKA, K. 1998. Wioślarki (Cladocera, Crustacea) jako źródło informacji w badaniach osadów jeziornych. *Studia Geologica Polonica*, 112, 9-28.
171. TARASOV, P. E., SAVELIEVA, L. A., LONG, T. & LEIPE, C. 2019. Postglacial vegetation and climate history and traces of early human impact and agriculture in the present-day cool mixed forest zone of European Russia. *Quaternary International*, 516, 21-41.
172. TERASMAA, J., PUUSEPP, L., MARZECOVÁ, A., VANDEL, E., VAASMA, T. & KOFF, T. 2013. Natural and human-induced environmental changes in Eastern Europe during the Holocene: a multi-proxy palaeolimnological study of a small Latvian lake in a humid temperate zone. *Journal of Paleolimnology*, 49, 663-678.
173. TERSKII, P., KULESHOV, A., CHALOV, S., TERSKAIA, A., BELYAKOVA, P., KARTHE, D. & PLUNTKE, T. 2019. Assessment of water balance for Russian subcatchment of western dvina river using SWAT model. *Frontiers in Earth Science*, 7: 241.
174. TRET'YAKOV, P. N. 1966. Finno-ugry, balty i slavyane na Dnepre i Volge. *Nauka*, Moscow, 276.
175. VAN GEEL, B. & APTROOT, A. 2006. Fossil ascomycetes in Quaternary deposits. *Nova Hedwigia*, 82, 313-330.
176. VANHANEN, S. & PESONEN, P. 2016. Wild plant gathering in stone age Finland. *Quaternary International*, 404, 43-55.
177. VELICHKO, A., TIMIREVA, S., KREMENETSKI, K., MACDONALD, G. & SMITH, L. 2011. West Siberian Plain as a late glacial desert. *Quaternary International*, 237, 45-53.

178. VESKI, S., SEPPÄ, H. & OJALA, A. E. 2004. Cold event at 8200 yr BP recorded in annually laminated lake sediments in eastern Europe. *Geology*, 32, 681-684.
179. VESKI, S., SEPPÄ, H., STANČIKAITĖ, M., ZERNITSKAYA, V., REITALU, T., GRYGUC, G., HEINSALU, A., STIVRINS, N., AMON, L. & VASSILJEV, J. 2015. Quantitative summer and winter temperature reconstructions from pollen and chironomid data between 15 and 8 ka BP in the Baltic–Belarus area. *Quaternary International*, 388, 4-11.
180. WALANUS, A. & NALEPKA, D. 1999. Program for counting pollen grains, diagrams plotting and numerical analysis. *Acta Paleobotanica*, Suppl. 2: 659-661.
181. WARREN, R., VANDERWAL, J., PRICE, J., WELBERGEN, J. A., ATKINSON, I., RAMIREZ-VILLEGRAS, J., OSBORN, T. J., JARVIS, A., SHOO, L. P. & WILLIAMS, S. E. 2013. Quantifying the benefit of early climate change mitigation in avoiding biodiversity loss. *Nature Climate Change*, 3, 678-682.
182. WENINGER, B. & HARPER, T. 2015. The geographic corridor for rapid climate change in Southeast Europe and Ukraine. *Archäol in Eurasien*, 31, 475-505.
183. WIECKOWSKA-LÜTH, M., THIEBAUT, E., GAUTHIER, E., SŁOWIŃSKI, M., KRĄPIEC, M., DOLBUNOVA, E., MAZURKEVICH, A., MAIGROT, Y., DANGER M., KITTEL, P. 2021. Palaeoenvironment and settlement history of a lakeshore setting: an interdisciplinary study from the multi-layered archaeological site of Serteya II, Western Russia. *Journal of Archaeological Science: Reports* 40: 103219.
184. WIKLUND, J. A., BOZINOVSKI, N., HALL, R. I. & WOLFE, B. B. 2010. Epiphytic diatoms as flood indicators. *Journal of Paleolimnology*, 44, 25-42.
185. WOHLFARTH, B., TARASOV, P., BENNIKE, O., LACOURSE, T., SUBETTO, D., TORSSANDER, P. & ROMANENKO, F. 2006. Late glacial and Holocene palaeoenvironmental changes in the Rostov-Yaroslavl'area, West Central Russia. *Journal of Paleolimnology*, 35, 543-569.
186. WOLTERS, S. 2016. Die pflanzlichen Makroreste der Mesolithstation Friesack. *Subsistenz und Umwelt der Feuchtbodenstation Friesack*, 4, 189-203.
187. ZEKTSER, I. S. Contamination and vulnerability of groundwater resources in Russia. International Seminar On Nuclear War And Planetary Emergencies—30th Session: Anniversary Celebrations: The Pontifical Academy of Sciences 400th—The “Ettore Majorana” Foundation and Centre for Scientific Culture 40th—HH John Paul II Apostolate 25th—Climate/Global Warming: The Cosmic Ray Effect; Effects on Species and

Biodiversity; Human Effects; Paleoclimate Implications Evidence for Global Warming—Pollution: Endocrine Disrupting Chemicals; Hazardous Material; Legacy Wastes and Radioactive Waste Management in USA, Europe, Southeast Asia and Japan—The Cultural Planetary Emergency: Role of the Media; Intolerance; Terrorism; Iraqi Perspective; Open Forum Debate—AIDS and Infectious Diseases: Ethics in Medicine; AIDS Vaccine Strategies—Water: Water Conflicts in the Middle East—Energy: Developing Countries; Mitigation of Greenhouse Warming—Permanent Monitoring Panels Reports—Workshops: Long-Term Stewardship of Hazardous Material; AIDS Vaccine Strategies and Ethics, 2004. World Scientific, 545-548.

- 188.ZERNITSKAYA, V., MATVEYEV, A., RAKOVICH, I. & KOLOSOV 2019. Korrelyatsiya dinamiki okruzhayushchey sredy yugo-vostochnoy periferii Poozerskogo (Valdayskogo) oledeneneniya oledeneneniya oledeneneniya vedleniya v'neniya. *Litasfera*, 1(50), 28-43.

Opis wkładu autorki w artykuły włączone do rozprawy:

Summer temperature drives the lake ecosystem during the Late Vistulian and Holocene in Eastern Europe: a case study from Western Russia, Płociennik M., Mroczkowska A., Pawłowski D., Kruk A., Wieckowska-Lüth M., Kurzawska A., Rzodkiewicz M., Okupny D., Szmańda J., Mazurkevich A., Dolbunova E., Luoto TP., Kotrys B., Nazarova L., Syrykh L., Krąpiec M., Kittel P.

Mój udział w przygotowanie tej publikacji obejmował:

1. zebraniu i analizy danych literaturowych dotyczących taksonomii i ekologii Chironomidae oraz stanu badań paleoekologicznych w Zachodniej Rosji;
2. pobór rdzenia i prace terenowe
3. podział rdzenia na analizy;
4. preparatyka chemiczna prób do analizy Chironomidae
5. wykonanie analizy subfosylnych Chironomidae;
6. identyfikacja puszek głowowych;
7. analiza jakościowa i ilościowa.
8. udział w przygotowaniu koncepcji artykułu
9. udział w przygotowaniu draftu artykułu
10. przygotowanie wykresów i części grafiki

On the border between land and water: The environmental conditions of the Neolithic occupation from 4.3 until 1.6 ka BC at Serteya, Western Russia, Kittel P., Mazurkevich A., Wieckowska-Lüth M., Pawłowski D., Dolbunova E., Płociennik M., Gauthier E., Krąpiec M., Maigrot Y., Danger M., Mroczkowska A., Okupny D., Szmańda J., Thiebaut E., Słowiński M., 2021, Geoarchaeology, 36, 2, s. 173-202.

Mój udział w przygotowanie tej publikacji obejmował:

1. zebraniu i analizy danych literaturowych dotyczących archeologii stanowiska Serteya
2. pobór rdzenia i prace terenowe
3. podział rdzenia na analizy;
4. preparatyka chemiczna prób do analizy Chironomidae
5. wykonanie analizy subfosylnych Chironomidae;
6. identyfikacja puszek głowowych;
7. analiza jakościowa i ilościowa.
8. udział w przygotowaniu koncepcji artykułu

9. udział w przygotowaniu draftu artykułu

Middle Holocene climate oscillations recorded in the Western Dvina Lakeland,

Mroczkowska A., Pawłowski D., Gauthier E., Mazurkevich A., Luoto T., Peyron O., Kotrys B., Brooks S., Nazarova L., Syrykh L., Dolbunova E., Thiebaut E., Płociennik M., Antczak-Orlewska O., Kittel P., 2021, Water, 13, 11, s. 1611

Mój udział w przygotowanie tej publikacji obejmował:

1. zebraniu i analizy danych literaturowych dotyczących taksonomii i ekologii Chironomidae;
2. pobór rdzenia i prace terenowe
3. podział rdzenia na analizy
4. preparatyka chemiczna prób do analizy Chironomidae
5. wykonanie analizy subfosylnych Chironomidae
6. identyfikacja puszek głowowych
7. analiza jakościowa i ilościowa
8. udział w przygotowaniu koncepcji artykułu
9. przygotowanie draftu artykułu
10. wykonanie części wykresów i diagramów
11. Poprawienie manuskryptu i przygotowanie odpowiedzi na recenzję

Lacustrine, fluvial and slope deposits in the wetland shore area in Serteya, Western Russia, Acta Geographica Lodzienia, Kittel P., Mazurkevich A., Alexandrovskiy A., Dolbunova E., Krupski M., Szmańda J., Stachowicz-Rybka R., Cywa K., Mroczkowska A., Okupny D., 2020, 110, s. 103-124.

Mój udział w przygotowanie tej publikacji obejmował:

1. zebraniu i analizy danych literaturowych dotyczących taksonomii i ekologii Chironomidae i Cladocera;
2. prace terenowe i pobór rdzenia;
3. podział rdzenia na analizy;
4. preparatyka chemiczna prób do analizy Chironomidae;
5. wykonanie analizy subfosylnych Chironomidae;
6. identyfikacja puszek głowowych Chironomidae;
7. preparatyka chemiczna prób do analizy Cladocera;
8. wykonanie analizy subfosylnych Cladocera;

9. identyfikacja szczątków Cladocera;
10. analiza jakościowa i ilościowa;
11. udział w przygotowaniu draftu;
12. stworzenie diagramów i wykresów.

Załączniki



Summer temperature drives the lake ecosystem during the Late Weichselian and Holocene in Eastern Europe: A case study from East European Plain

Mateusz Płociennik^{a,*}, Agnieszka Mroczkowska^{b,c}, Dominik Pawłowski^d, Magda Wieckowska-Lüth^e, Aldona Kurzawska^f, Monika Rzodkiewicz^g, Daniel Okupny^h, Jacek Szmańdaⁱ, Andrey Mazurkevich^j, Ekaterina Dolbunova^j, Tomi P. Luoto^k, Bartosz Kotrys^l, Larisa Nazarova^m, Liudmila Syrykhⁿ, Marek Krapiec^o, Piotr Kittel^c

^a University of Łódź, Department of Invertebrate Zoology and Hydrobiology, Łódź, Poland

^b Polish Academy of Sciences, Institute of Geography and Spatial Organization, Warsaw, Poland

^c University of Łódź, Faculty of Geographical Sciences, Department of Geology and Geomorphology, Łódź, Poland

^d Adam Mickiewicz University, Institute of Geology, Poznań, Poland

^e University of Kiel, Institute of Prehistoric and Protohistoric Archaeology, Archaeobotanical and Palynological Laboratory, Kiel, Germany

^f Polish Academy of Sciences, Institute of Archaeology and Ethnology, Poznań, Poland

^g Adam Mickiewicz University, Institute of Geocology and Geoinformation, Biogeochemistry Research Unit, Poznań, Poland

^h University of Szczecin, Institute of Marine and Environmental Sciences, Szczecin, Poland

ⁱ Pedagogical University of Cracow, Institute of Geography, Krakow, Poland

^j The State Hermitage Museum, St. Petersburg, Russia

^k University of Helsinki, Faculty of Biological and Environmental Sciences, Ecosystems and Environment Research Programme, Lahti, Finland

^l Polish Geological Institute – National Research Institute, Pomeranian Branch in Szczecin, Szczecin, Poland

^m Alfred Wegener Institute Helmholtz Centre for Polar and Marine Research, Potsdam, Germany

ⁿ Herzen State Pedagogical University of Russia, St. Petersburg, Russia

^o AGH – University of Science and Technology, Faculty of Geology, Geophysics and Environmental Protection, Krakow, Poland

ARTICLE INFO

ABSTRACT

Keywords:

Palaeoecology
Palaeoclimatic reconstructions
Clusters of neurons
SOM
Lake evolution
Eastern Europe
Holocene

East European lake-river systems have hydrological regimes typical for continental climate zones. The Postglacial development of the basins and regional palaeoclimatic pattern in the Holocene implied a specific succession of biota communities passing through lakes' subsequent stages in the water level, trophic state and habitat availability. The Great Serteya Palaeolake Basin is the largest palaeolake within the Serteya lake-river system, which has been functioning since the Late Weichselian (Vistulian). Presented below is a multi-proxy study on the sequence from the paleolake within the present-day valley. During the Late Weichselian, it formed an astatic, and later a permanent, water body of Postglacial origin. The associated melting, flooding and aeolian processes acted as sources of various Late Weichselian sediments. Summer mean air temperature drove the lake ecosystem development. The Holocene Thermal Optimum in 8.5–7.7 kyr cal BP was followed by subsequent lower temperature. There is weak evidence of cool oscillations at 8.2 kyr cal BP, 7.0–6.8 kyr cal BP and 5.8–5.9 kyr cal BP and the Little Ice Age (480–395 yr cal BP), until modern time (~65 yr cal BP). Five stages of lake ecosystem development were identified based on the biota: 1) an initial stage during the Late Weichselian with glaciolastrine and later lacustrine accumulation of inorganic deposits, 2) the stage with Cladocera as a leading indicators of mesotrophic water body with a well-developed pelagic zone supplied by early spring floods of the Serteya River, carrying melting snow and ice floes to the lake basin, 3) the stage dominated by Chironomidae and diatoms typical to high trophic states reflecting widespread open bottom sediment and macrophyte habitats 4) a stage with distinct Neolithic community impact reflected by macrofossils remain after pile-dwelling

* Corresponding author.

E-mail addresses: mplociennik10@outlook.com (M. Płociennik), agnieszka.mroczkowska@twarda.pan.pl (A. Mroczkowska), dominikp@amu.edu.pl (D. Pawłowski), mwieckowska@ufg.uni-kiel.de (M. Wieckowska-Lüth), aldona.kurzawska@wp.pl (A. Kurzawska), lutynska@amu.edu.pl (M. Rzodkiewicz), daniel.okupny@usz.edu.pl (D. Okupny), jacek.szmania@gmail.com (J. Szmańda), a-mazurkevich@mail.ru (A. Mazurkevich), katjer@mail.ru (E. Dolbunova), tomi.luoto@helsinki.fi (T.P. Luoto), bkotr@pgi.gov.pl (B. Kotrys), Larisa.Nazarova@awi.de (L. Nazarova), lssyryh@herzen.spb.ru (L. Syrykh), mkrapiec@agh.edu.pl (M. Krapiec), piotr.kittel@geo.uni.lodz.pl (P. Kittel).

<https://doi.org/10.1016/j.catena.2022.106206>

Received 21 April 2021; Received in revised form 10 December 2021; Accepted 5 March 2022

0341-8162/© 2022 Elsevier B.V. All rights reserved.

settlement, fish and aquatic plants consumption 5) a final stage dominated by diatoms typical to shallow, semi-permanent, eutrophic bulrush swamp.

1. Introduction

The palaeoarchives of Eastern Europe have been extensively investigated over the previous decades. A number of studies have examined the Late Weichselian and the entire Holocene sequence of lakes located in Vologda Oblast, Moscow Oblast and Leningrad Oblast, Arkhangelsk Oblast with Republic of Karelia, the Arctic region of Russia, Estonia and Poozerye and Polesye of Belarus (cf [Syrykh et al., 2021, Table 1](#)).

Most of the records mentioned by [Syrykh et al. \(2021\)](#) include qualitative palaeogeographic and pollen data supported by bulk-based ^{14}C dates. The areas from South Karelia, through the Valday Upland and Smolensk Upland to the Western Dvina Lakeland, have been investigated, mostly by [Nazarova et al. \(2015; 2019\)](#), [Novenko et al. \(2013; 2005\)](#) and [Syrykh et al. \(2015\)](#). These studies provide quantitative palaeoclimatic reconstructions inferred mainly from chironomids and pollen, and some have been summarized by [Kaufman et al. \(2020a\)](#). Although palaeoclimatic studies have been extensively conducted in the East European Plain, no comprehensive picture of the climate history of the region yet exists, at least for the Late Weichselian and Holocene, mostly due to the lack of sufficient multi-proxy studies that would allow multiple palaeoclimatic reconstructions. Moreover, previous studies have rarely been linked to age-depth models based on AMS dating.

The 5.9 kyr cal BP and 4.2 kyr cal BP Bond Events are well-documented in Europe ([Bond et al., 2001; 1997](#)), but little is known of them in the East. [Mroczkowska et al. \(2021\)](#) indicate that clear cooling episodes took place at the time of the two Bond events (5.9 kyr cal BP and 4.2 kyr cal BP), but they note that the events occurring in Central Europe have little in common with those of Eastern Europe; in addition, the events reflect a temperature trend and fluctuations in precipitation that are unusual for mid-to-late Holocene. It is believed that in the South and East of Europe, wet weather conditions alternate with dry ones ([Spinoni et al., 2015; Utkuzova et al., 2015](#)), which influences the hydrology of eastern water courses ([Danilovich et al., 2019](#)).

In the Late Weichselian landscape, many Postglacial lake-river systems stand out in central-eastern Europe ([Błaszkiewicz et al., 2015](#)). One of the best recognized in East European Plain is the Serteyka lake-river system ([Kittel et al., 2018, 2020](#)) in the Western Dvina Lakeland. It is regarded as a crucial area for the development of Neolithic communities in Eastern Europe ([Kulkova et al., 2015a; Mazurkevich et al., 2020b; Mazurkevich et al., 2009a](#)). Over the last 30 years, relicts of numerous Neolithic settlements dating from 8.2 kyr cal BP to ca. 4.2 kyr cal BP have been discovered in the lower course of the Serteyka River valley, a left tributary of the western Dvina River ([Mazurkevich and Dolbunova, 2015; Mazurkevich et al., 2020b; Wieckowska-Lüth et al. 2021](#)). The archaeological evidence suggests the occurrence of short-term episodes of lake regressions (ex. ca. 4.2 kyr cal BP). These findings suggest that it is possible to date short palaeohydrological episodes using geoarchaeological methods ([Kittel et al., 2021; Wieckowska-Lüth et al., 2021](#)); however, these findings should also be confirmed by palaeoecological reconstructions indicating long-time water level fluctuations in the state of biota dynamics and geochemical sediment structure.

Pollen, diatom and basic geochemical analyses have been performed in the lower Serteyka River valley but they have only been carried out at two locations ([Dolukhanov et al., 1989; Kulkova et al., 2015a; Mazurkevich et al., 2009b; Tarasov et al., 2019](#)), and the findings are hampered by low resolution, a lack of palaeozoological analysis, weak geochemical analyses of the mineral fraction in the biogenic sediments, and a lack of AMS dating of selected plant remains. The only multi-proxy study of the Great Serteya Palaeolake Basin (GSPB) concerns the Middle Holocene from ca. 5.9 kyr cal BP to ca 4.2. kyr cal BP ([Kittel et al., 2021; Mroczkowska et al., 2021](#)) however, it is obvious that human

communities continued to influence the lake after these dates. This implies the need for extensive research on the whole GSPB development from deglaciation through lake history to terrestrialisation of the basin.

The lake-river systems in central Europe underwent well-defined changes in the pre-Holocene development of the basin. These were primarily associated with Post-glacial depositional and later fluvial processes. The accumulation of allochthonous and autochthonous organic matter, together with human impact, led to an increase in productivity in the area.

The global fluctuations in the state of biota in the lakes can only be determined by holistic analyses based on palaeoecological studies (e.g. [Hakala et al., 2004; Schroeder et al., 2018; Zander et al., 2021](#)). The history of the biota in lakes can reveal both local patterns dependent on the catchment and more global ones, like climate change. Biocenoses have also a more complicated structure than abiotic components of ecosystems. For example, extreme events are much more likely to be apparent in biological than abiotic components of ecosystems. In addition, biota are much more likely to demonstrate extremes driven by within-year dynamics, and thus be more indicative of processes occurring at short time scales ([Batt et al., 2017](#)). However, the recognition of the biotic ecosystem components is more demanding than palaeogeographic or archaeological reconstructions, requiring more variables, higher sampling resolutions and higher numbers of long-term series replicates.

The temperature and habitat conditions are the leading factors that influence invertebrate communities over large spatial and temporal scales ([Pawlowski, 2017; Płociennik et al., 2020](#)). [Beaver et al. \(2020\)](#) analysed body sizes of cladoceran populations across the Nearctic. Multiple regressions revealed complex environmental influences on cladoceran body size, with temperature-related variables and trophic state-related variables. Climate change and eutrophication drive lake ecosystems but the local watershed land use and microclimate affect water flea' populations (i.e. [Hillbrand et al. 2014](#)). [Telford \(2019\)](#) revised the phenological context of palaeolimnological reconstructions. He considered summer air temperature to be the key variable affecting chironomid assemblages but the phenology of midges in northern temperate regions is diverse. There are taxa that emerge in colder early spring (April to May) or late summer (August or September) but majority of univoltine species swarm in warm July and early summer ([Vallenduuk and Moller Pillot, 2007; Moller Pillot, 2009, 2013](#)). This is associated with air temperature but also humidity and day length ([Płociennik et al., 2018](#)). Over a spatial calibration set, the correlation between air temperature reconstructed for different months of a season can be high but difference of each month (i.e. June or July or August) temperature values may be insignificant ([Telford, 2019](#)).

The present paper describes a multi-proxy study of the palaeoecology of the GSPB from Late Weichselian to modern times. It aims to identify the main environmental drivers of change in the lake ecosystem and community succession under the influence of ancient human communities. To that end, a high resolution analysis of the plant macrofossils and diatoms, molluscs, Cladocera and Chironomidae subfossils present in the deposits was performed, and the geochemical composition of the sediment was examined. The GSPB is not only a very good study site for testing the complex interactions between the environment and lake biota, but also between the lake biota and humans, due to the presence of a well-documented human settlement in the area since the Stone Age and the influence of specific hydrological and climatic conditions ([Kulkova et al., 2015b](#)).

A particularly significant element of the study on palaeoclimatic pattern in the Holocene development of the lake is that it reconstructs the climate-driven evolution of lake-fluvial systems from the late

Table 1

List of the references concerning some of previous studies in Eastern Europe. Comprehensive literature review gives [Syrykh et al. \(2021\)](#).

Study site	Time period	Proxy	References
Imandra Lake, Murmansk Oblast, Russia ($67^{\circ}30'N$, $33^{\circ}00'E$), Kovozero Lake, Murman Oblast, Russia ($66^{\circ}30'N$, $33^{\circ}00'E$), Oltushskoe Lake, Polesye District, Belarus ($51^{\circ}55'N$, $24^{\circ}03'E$) Naroch Lake Myadzeyel District, Belarus ($54^{\circ}05'N$, $26^{\circ}45'E$)	Late Glacial, Holocene	pollen, diatom, geochemical	Davydova and Servant-Vildary, 1996
Valday Lake, Novgorod Oblast, Russia ($57^{\circ}59'N$, $33^{\circ}16'E$) Kubenskoye Lake, Karelian Isthmus, Russia ($59^{\circ}42'N$, $39^{\circ}30'E$) Vishnevskoye Lake, Karelian Isthmus, Russia ($60^{\circ}30'N$, $29^{\circ}31'E$)	Late Glacial, Holocene	pollen, diatom	Davydova et al. 2001
Myshetskoe-Dolgoe Lake, Moscow Oblast, Russia ($56^{\circ}04'N$, $37^{\circ}20'E$)	Late Glacial, Holocene	pollen	Kremenetski et al. 2000
Lembolovskoye Lake, Leningrad Oblast, Russia ($60^{\circ}21'45''N$, $30^{\circ}18'80''E$) Mshinskoye bog, Leningrad Oblast, Russia ($59^{\circ}52'00''N$, $29^{\circ}55'00''E$)	Holocene	pollen	Arslanov et al., 2001.
Nikolay Lake, Arga Island, Russia ($73^{\circ}20'N$, $124^{\circ}12'E$)	Holocene	pollen Rhizopod Chironomidae	Andreev et al., 2004
Ratasjärv lake, Rouge Parish, Estonia ($57^{\circ}44'N$, $26^{\circ}54'E$)	9400–7200 BP	pollen	Veski et al. 2004
Shavnillampi Lake, Karelian Isthmus ($62^{\circ}32'N$, $33^{\circ}42'E$)	Holocene	geochemical composition, pollen	Shelekhova et al. 2005
Lazoviki Lake, Vitebsk Oblast, Belarus ($55^{\circ}16'N$, $28^{\circ}07'E$), Mezhuzhol Lake, Vitebsk Oblast, Belarus ($55^{\circ}00'N$, $28^{\circ}04'E$) Kryvoe Lake, Vitebsk Oblast, Belarus ($55^{\circ}10'N$, $29^{\circ}00'E$) Sudoble Lake, Minsk Oblast, Belarus ($54^{\circ}03'N$, $28^{\circ}24'E$) Bobrovichskoe Lake, Polesye District, Belarus ($52^{\circ}37'N$, $25^{\circ}47'E$) Oltushskoe Lake, Polesye District, Belarus ($51^{\circ}41'N$, $23^{\circ}57'E$) Glubokoe Lake, Vitebsk Oblast, Belarus ($55^{\circ}76'N$, $36^{\circ}51'E$)	Late Glacial Holocene	pollen pollen pollen	Novik et al. 2010
	Holocene	pollen, diatom, chironomids	Nazarova et al. 2015

Table 1 (continued)

Study site	Time period	Proxy	References
Medvedevskoe Lake, Leningrad Oblast, Russia ($60^{\circ}23'N$, $29^{\circ}9'E$)	Younger Dryas, Holocene	pollen, lithological, diatom, chironomids, cladocera, geochemical	Subetto et al. 2006 , Andronikov et al. 2014 , Syrykh et al. 2015 , Subetto, 2009
Mount Vottovaara Karelian Isthmus Russia ($63^{\circ}04'N$, $27^{\circ}37'32'E$)	Holocene	pollen, diatoms	Shelekhova & Lavrova 2019

Greenlandian (Early Holocene 9–8.2 kyr cal BP) through Northgrippian (Middle Holocene 8.2–4.2 kyr cal BP) to the Meghalayan (Late Holocene 4.2–0 kyr cal BP) stages, based on a core of organic deposits taken from the archaeological Serteya II site in 2016 ([Kittel et al., 2018](#)). The palaeoecological research was based on the central part of the Serteya ST IIa core, containing remnants of pile-dwellings ([Fig. 1](#)). The core itself comprises 790 cm of lacustrine deposits from the Late Weichselian and the Holocene.

Detailed quantitative climatic and hydrological reconstructions were necessary, as fluvial conditions and temperature changed remarkably since the Late Weichselian, and varied considerably between Early, Middle and Late Holocene ([Panin and Matlakhova, 2015](#)). Thus, new detailed reconstructions from ST IIa based on independent proxies are needed to understand the lake ecosystems functioning in Eastern Europe during the Holocene. We hypothesise that: 1) silty-clayey deposits of the core bottom part were accumulated in lacustrine conditions of cool-water lake. 2) mean July air temperature was the main driver of the ecosystem; 3) short, but distinctive, cool oscillations (on 8.2 kyr cal BP, 5.9 kyr cal BP, 4.2 kyr cal BP) are visible in the region during this period; 4) the connection of the lake to the Serteya River influenced diatom and invertebrate communities; 5) the humans in the pile-dwelling location had an insignificant influence on the trophic state of the water.

1.1. Study area

The study site ($55^{\circ}37'53''N$; $31^{\circ}32'28''E$; 152.5 m a.s.l.) is situated at East European Plain; more precisely in the Western Dvina Lakeland, according to [Abramow \(1972\)](#), or the Vitebsk Lakeland, after [Kondracki \(1992\)](#) ([Fig. 1](#)). This area is located in the Western Dvina River Basin (WDB), more than 650 km eastward from the Baltic Sea coast, not far from the European watershed of three catchments: the Baltic Sea, the Black Sea and the Caspian Sea. Although the main watercourse of the area is the Western Dvina River, the study site is in the Serteya River valley, an approximately 40-km-long left tributary of the Western Dvina.

The present-day lower Serteya River valley developed within a tunnel valley from the Valdai (Weichselian, Vistulian) Glaciation, which also included a system of lakes in the Late Valdai and the Holocene. A few palaeolake basins have been documented within the valley floor of the lower section of the valley. The river channel drained subsequent water bodies during the Holocene as a result of fluvial headward erosion. Hence, the area includes numerous biogenic plains filled with organic deposits of lacustrine and swamp origin, the largest of which is the GSPB ([Kittel et al., 2018](#)), where the study site is located.

In this area, the main traits of the land relief were formed during and after the Valdai Glaciation ([Gorlach et al., 2015](#); [Velichko et al., 2011](#); [Kittel et al., 2018](#)). Currently, its prevailing climatic conditions are moderately continental with an influence of oceanic Atlantic air masses ([Alpat'yev et al., 1976](#)). Winters are moderately cold with stable snow cover from November to April, and summers are moderately cool and humid. Most of the annual precipitation (ca. 60%) occurs from May to October. For Velizh, situated 20 km to the west of the site, mean annual air temperature ranges from $3.6^{\circ}C$ to $8.4^{\circ}C$, while mean annual atmospheric precipitation varies from 488 to 1296 mm. The mean temperature of the warmest month (July) ranges from $14.8^{\circ}C$ to $23.01^{\circ}C$.

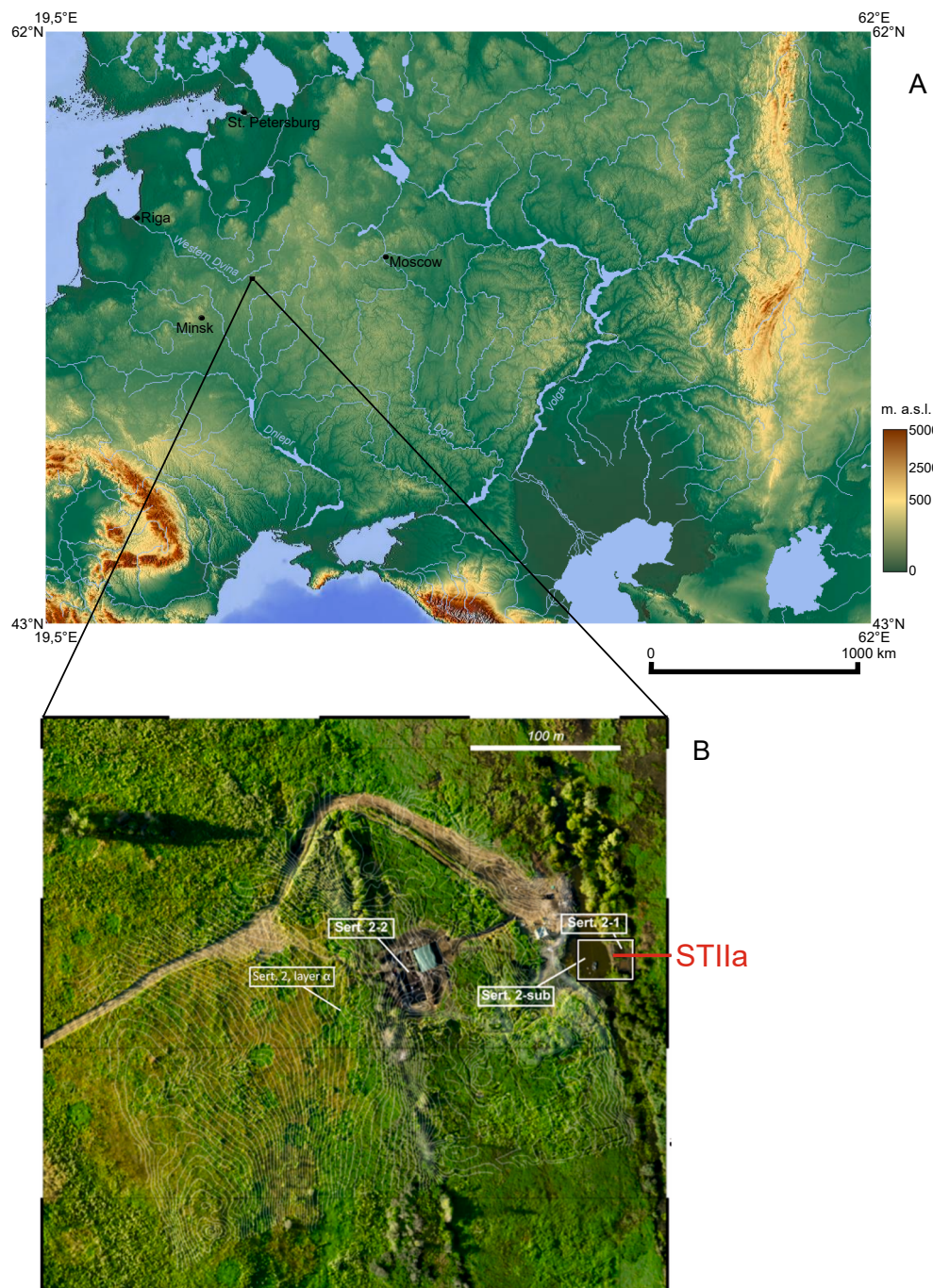


Fig. 1. The location of the Serteya II site and the ST IIa core; A. on the physical map of Eastern Europe; B. on the aerial photo of the Serteya II site (Sert. 2-1; Sert. 2-sub; Sert. 2-2; Sert. 2, layer α - markings of parts of the site).

and the mean temperature of the coldest month (January) from -17.7°C to -0.8°C (<http://www.tutiempo.net>; date of last access: 9th Dec. 2019).

The samples were taken from the pile-dwelling settlement found at archaeological site Serteya II, which had been explored from 2008 with underwater and wetland archaeological methods. The site is an archaeological multilayered complex with relicts indicating occupation from the Mesolithic to the Middle Ages, but mostly by hunter-fisher-gatherer communities in the Middle and Late Neolithic (i.e. from the 5th to 4th millennium BP). The archaeological layers with wooden structures and fish traps were discovered within the lacustrine deposits, and are therefore well-preserved. The site revealed several late Neolithic pile-dwelling constructions from ca. 4.9–4.0 cal BP (Mazurkevich et al.,

2020a, 2020b, 2011a; Wieckowska-Lüth et al., 2021). Most of the remnants are located within the deep-water part, as well as at the shore zone of the GSPB (Kittel et al., 2018, 2020, 2021).

2. Materials and methods

2.1. Field investigation

The location of the core was inside one of the constructions identified in the pile-dwelling settlement at archaeological site Serteya II-1. Geological mapping has been performed with the use of geological hand auger in the immediate area of the Serteya site II (totally ca. 100 drillings). Then, they were continued by geological trenching along with

geological and geoarchaeological research within geological outcrops and archaeological excavations. The results (i.e. the geological and geomorphological situation of the site, along with the palaeogeography of the area) are described in detail in our previous papers - [Kittel et al., 2018, 2020, 2021](#); [Mazurkevich et al., 2020b](#). The results indicated the range and thickness of organic deposits within the biogenic plain of the GSPB.

2.2. Core chronology

The core chronology has already been described by [Wieckowska-Lüth et al. \(2021\)](#). Briefly speaking, a total of 13 samples of selected terrestrial plant macrofossils from the ST IIa core were subjected to radiocarbon (^{14}C) dating using accelerator mass spectrometry (AMS). The plant macrofossils were dated in the Laboratory of Absolute Dating in Krakow (Poland); the samples were chemically pretreated with the

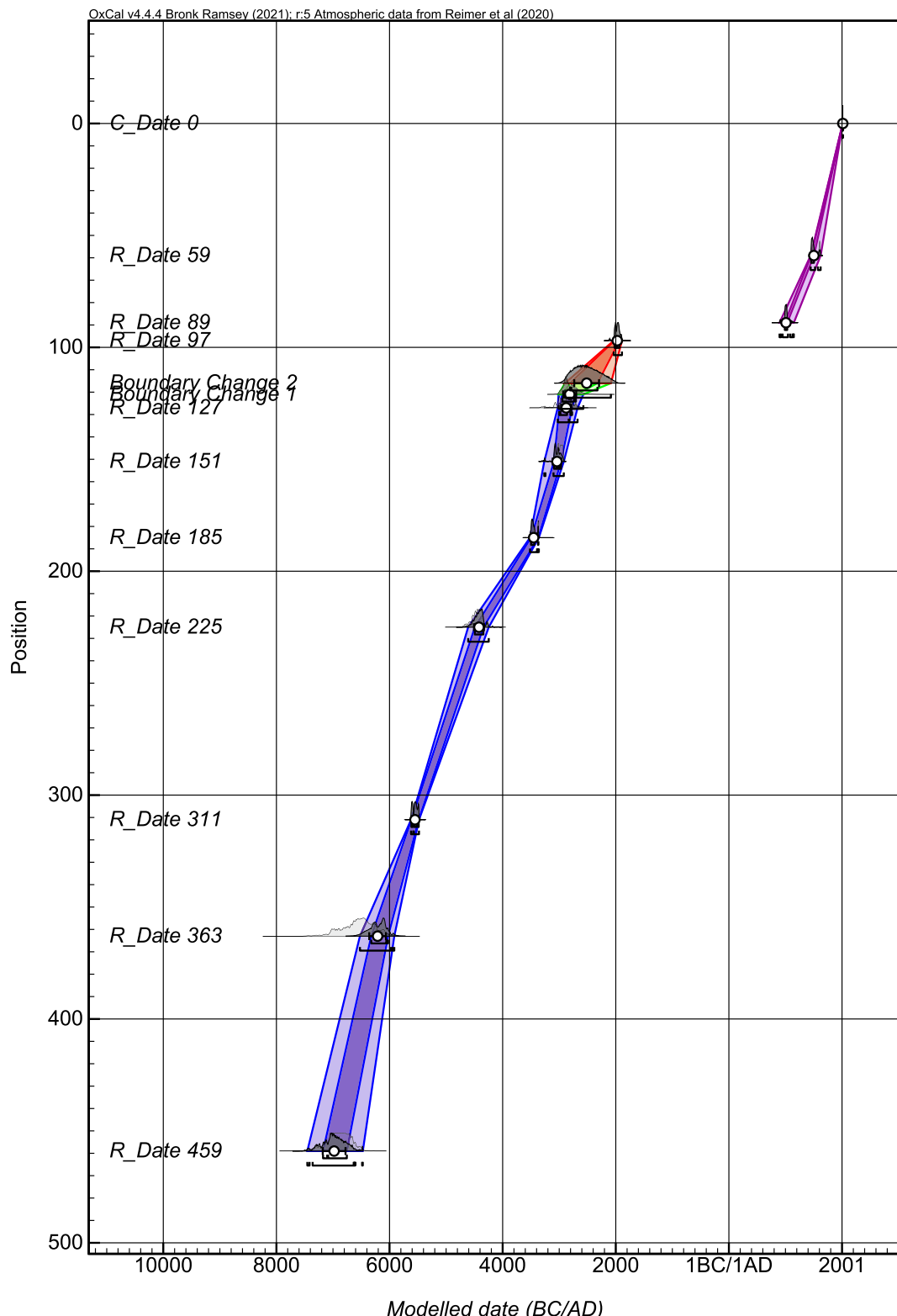


Fig. 2. The depth/age model for the deposits of the ST IIa core (prepared by M. Krapiec, after [Wieckowska-Lüth et al., 2021](#)).

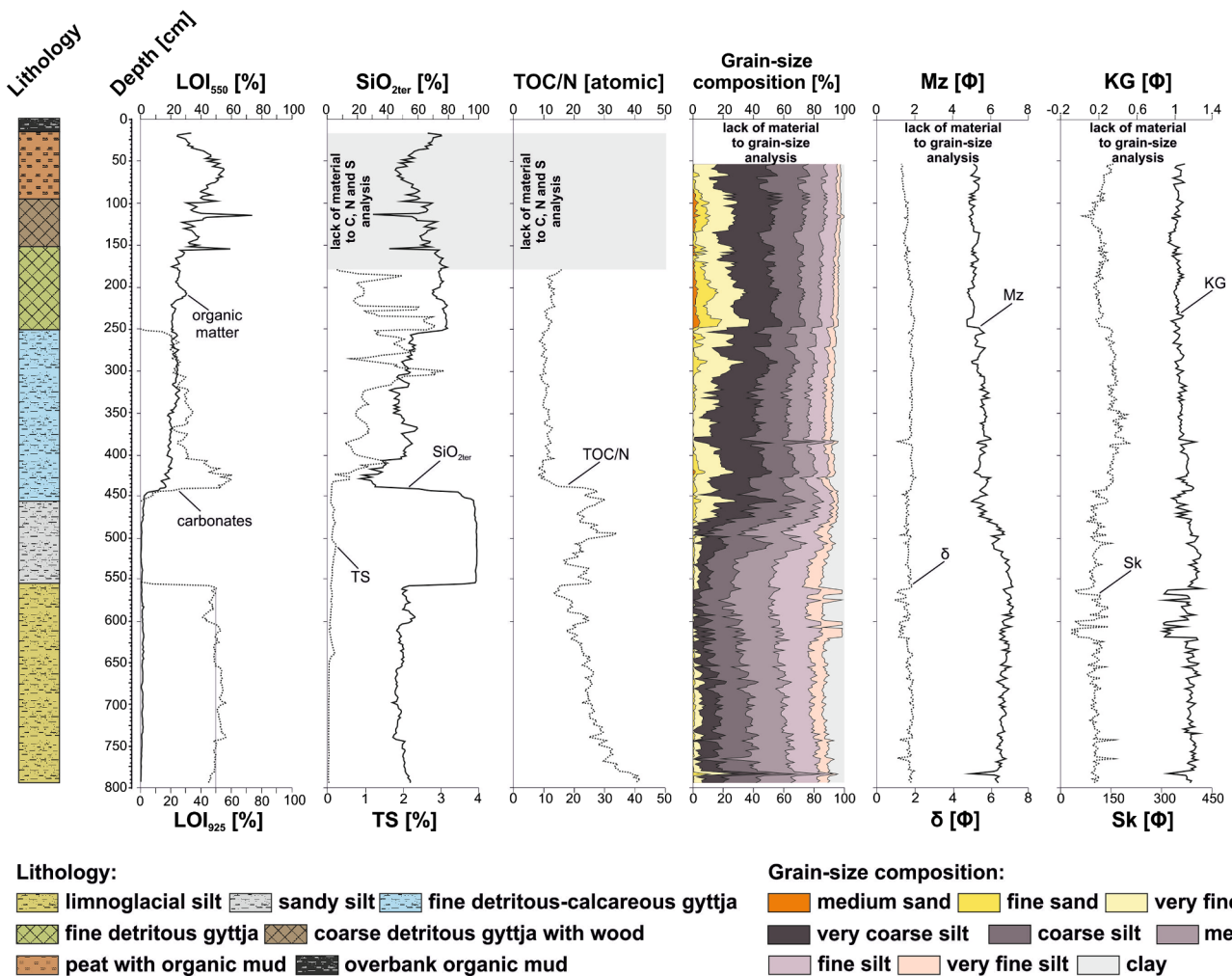


Fig. 3. Geochemical (organic matter, carbonates, $\text{SiO}_{2\text{ter}}$, TS contents and TOC/N ratio) and sedimentological (grain-size content, Folk and Ward coefficients) results of the ST IIa core against age and lithology of deposits (analysis by D. Okupny).

AAA (acid-alkali-acid) method.

Radiocarbon ages (cal yr BP) were calibrated based on the IntCal20 radiocarbon calibration dataset (Reimer et al., 2020) and the OxCal 4.4.2 calibration software (Bronk Ramsey et al., 2020). The chronology (age-depth curve) (Fig. 2) of the core based on the OxCal P_Sequence model (Ramsey, 2008) is presented in detail by Wieckowska-Lüth et al. (2021).

2.3. Laboratory methods

2.3.1. Geochemical analyses and sedimentology

Geochemical composition was determined in 390 samples after drying at 105 °C and homogenisation in an agate mortar. The based geochemical analysis (Fig. 3) comprised the identification of organic matter (OM) and carbonate content (CaCO_3) using loss on ignition (LOI) in a muffle furnace at a temperature of 550 and 925 °C, as defined by Heiri et al. (2001). The samples of ash were dissolved in a mixture of 10% HCl, 65% HNO_3 and H_2O_2 in Teflon bombs using a Berghof microwave mineraliser. The concentrations of Na, K, Ca, Mg, Fe, Mn, Cu, Zn and Pb were determined using atomic absorption spectrometry (AAS), with the results, expressed in mg dm^{-3} , converted to mg g^{-1} or ug g^{-1} dry weight (d.w.) (Fig. 4). The total C, N and S contents were determined in a Vario Max CNS elemental analyser (Elementar Analyse systeme, GmbH, Germany). Terrigenous silica ($\text{SiO}_{2\text{ter}}$) was calculated as the weight difference between the total mineral matter and carbonate content, because the calculated mass of residue sample

dissolved with 0.5n NaOH (treated as biogenic silica - $\text{SiO}_{2\text{biog}}$) differed by only 1–2% from the mass of sample before two-step extraction described by Apolinarska et al. (2012).

The ash samples remaining after the solutions were prepared ($n = 317$) were analysed for grain size according to Clift et al. (2019) using a Mastersizer 3000 laser particle size analyser with a Hydro MU dispersion unit (Malvern Panalytical). To determine the genesis and deposition conditions of sediments, textural features were evaluated using Folk and Ward (1957) coefficients. The obtained proportions of the geochemical elements and selected grain-size components were used to classify deposits and to reconstruct environmental change in the sedimentologic basin and catchment as a whole (Okupny et al., 2020; Pawłowski et al., 2016b).

2.3.2. Diatom analysis

Diatoms were used to reconstruct Total Phosphorus ($\mu\text{g dm}^{-3}$) in the lake and to track habitat changes in lake pelagic and littoral zone. The diatom analysis was performed on 195 sediment samples taken from depths of 19–795 cm. Microscope slides were prepared from the sediment samples according to the standard method proposed by Battarbee (1986). Diatoms were counted to a maximum of 300, and classified to species level. For identification, a selection of published keys was used: Krammer and Lange-Bertalot (2008; 2010; 2011), Lange-Bertalot et al. (2011a), Lange-Bertalot and Metzeltin (1996), Lange-Bertalot et al. (2011b) and AlgaeBase (Guiry and Guiry, 2017). Diatom analysis of ST IIa sediments showed medium to very poor condition of diatom

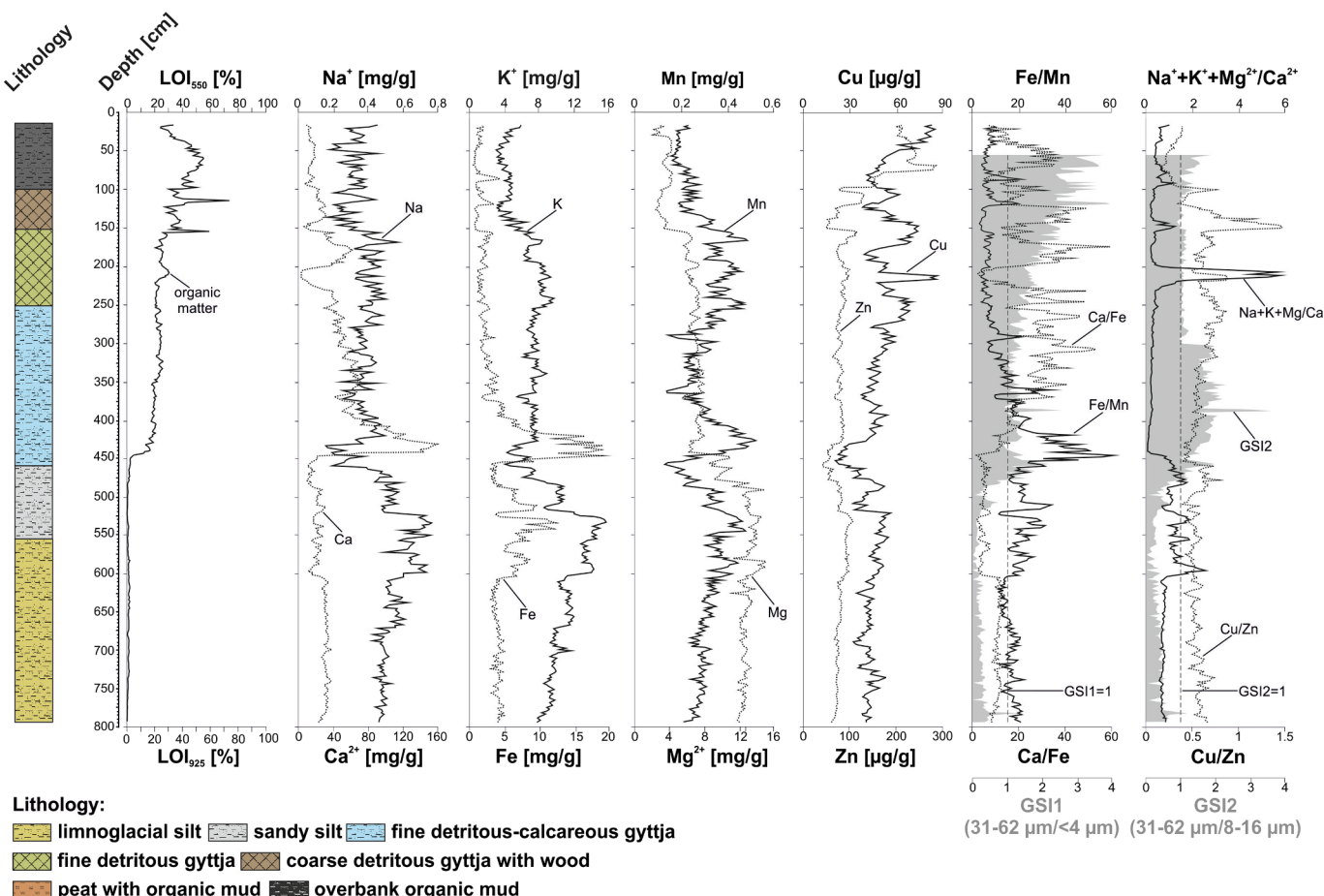


Fig. 4. Geochemical results (organic matter, Na, Ca, K, Fe, Mn, Mg, Cu, Zn contents and palaeoenvironmental ratios: Fe/Mn, Ca/Fe, (Na + K + Mg)/Ca and Cu/Zn) and grain-size indicators (GSI1 and GSI2) of the ST IIa core against age and lithology of deposits (analysis by D. Okupny).

frustules, with numerous traces of destruction or dissolution. In total, 162 species of diatoms were identified in the examined core (Fig. S1). It was found that 35 species constituted more than 2% of the total population.

2.3.3. Plant macrofossils

Plant macrofossils were used to track habitat changes in lake littoral zones and human activity. As much as 192 sediment samples were taken from the core. The weight of the samples ranged from 2.46 to 28.81 g. Briefly, the samples were treated with KOH to reduce the amount of sediment and remove humic matter, and washed through a sieve with mesh size of 0.3 mm. The remnants were dispersed in water and identified at up to $\times 40$ magnification with a binocular microscope. The plant remains and other macrofossils were determined according to Beijerinck et al. (1976), Birks (1980), Mauquoy and van Geel (2007), and Cappers et al. (2012), as well as the reference collection of the Institute of Pre- and Protohistoric Archaeology, University of Kiel. The results of the macrofossil analysis are presented in absolute values (Fig. S2). The macrofossil diagram was produced using TILIA version 2.1.1 software (Grimm, 2016). In the macrofossil diagram, the ecological classification is mainly based on the indicator values according to Ellenberg (1991).

2.3.4. Subfossil Cladocera

Cladocera were used to reconstruct lake level fluctuations and July temperature, and to track habitat changes in pelagic and littoral zones. The Subfossil Cladocera were examined at varying intervals depending on the sediment layer of the ST IIa core. At depths of 16–232 cm, samples were taken every 2 cm (106 samples), from 232 to 500 cm they were taken every 4 cm (66 samples) and from 500 to 795 cm they were taken

at 8–12 cm intervals (27 samples). In total, 199 samples were analysed (Fig. S3). Each sample, comprising 1 cm^3 of deposit, was processed according to Frey (1986): briefly, the deposit was treated with HCl to eliminate carbonates, and boiled for 30 min in a 10% KOH solution, with a magnetic stirrer to deflocculate the material and remove humic matter. The residue was then washed and sieved (using 33 µm mesh), and the final residue was colored with safranin dye before counting. A solution of 0.1 ml was added to a microscope slide and analysed using a Leica DMLB biological microscope. All Cladocera remains were counted. For each taxon, the most abundant body part was taken to represent the number of individuals, and percentages were calculated from the sum of individuals. The cladoceran remains were classified according to Szeroczyńska and Sarmaja-Korjonen (2007), Van Damme and Dumont (2008), Van Damme et al. (2010), and Faustová (2011). The ecological preferences of the cladoceran taxa were determined according to keys published by Flössner (1972; 2000), Bjerring et al. (2009) and by Błedzki and Rybak (2016).

2.3.5. Subfossil Chironomidae

Chironomidae were used to reconstruct mean July air temperature and to track habitat changes on the lake bottom. Subfossil Chironomidae were examined with 2 cm resolution for the core section 32–234 cm and with 4 cm resolution for the core sections 238–500 cm and over 500 cm. In total, 199 deposit samples were subjected to subfossil midge analysis, with a mass ranging from 3 to 25 g (Fig. S4). The samples were prepared according to Brooks et al. (2007). Briefly, the sediments were passed through a 90 µm mesh sieve and all head capsules (h.c.) were fixed in Euparal® on microscope slides. The Chironomidae collection was determined to the lowest possible taxonomic level according to Brooks

et al. (2007) and Andersen et al. (2013). The ecological preferences of identified taxa were determined based mainly on Brooks et al. (2007), Vallendauk and Moller Pillot (2007), Moller Pillot (2013, 2009).

2.3.6. Molluscs remains

Mollusks were used to track habitat changes on the lake bottom. Malacological analysis was based on shell remains preserved in the sediments; these were systematically selected from the 192 samples intended for macrofossil analysis. The malacological analysis was conducted using standard methods described by Alexandrowicz (1987). The shell remains were identified according to Welter-Schultes (2012), Killeen et al. (2004), Gittenberger et al. (2004) and reference collection of the Institute of Archaeology and Ethnology Polish Academy of Sciences in Poznań. The ecological and palaeoenvironmental values of the mollusk shells were described according to Ložek (1964), and Alexandrowicz and Alexandrowicz (2011). The malacological composition of the described fauna is presented in Fig. S5.

2.3.7. Total phosphorus and palaeohydrological reconstructions

The total phosphorus (TP) concentration was reconstructed based on changes in diatom species composition (Diatom I-TP). The reconstruction was performed using the European Diatom Database (EDDI) in the ERNIE software (Juggins, 2001). The model, based on inverse regression, had a root mean square error of prediction (RMSEP) of $0.33 \mu\text{g dm}^{-3}$ and a coefficient of determination (R^2) of 0.64. The TP level was reconstructed based on diatom taxa presenting a dominance of more than 2% of the total abundance. The Diatom I-TP was calculated using the combined TP dataset (derived from nine datasets with 347 samples in total), covering a TP range of $2\text{--}1189 \mu\text{g dm}^{-3}$, with a mean of $98.6 \mu\text{g dm}^{-3}$. The weighted averaging (WA) method with good empirical predictive ability was used (Juggins, 2001).

Lake level fluctuations were estimated using the Finnish cladoceran-based inference model (Clado-I lake depth Fn TS) (Nevalainen et al., 2011). The cladoceran-based lake level training set uses a modern analogue technique (MAT) transfer function which yielded a coefficient of determination, $R^2_{\text{jack}} = 0.56$ and RMSEP = 1.084 m with mean and maximum biases of 0.05 and 2.86 m, respectively.

2.3.8. Palaeoclimatic reconstructions

July air temperature was inferred based on chironomid subfossils (Chiro-I) according to Luoto and Nevalainen (2017), Kotrys et al. (2020) and Nazarova et al. (2015, unpublished data). The Finnish Training Set (Fn TS) 2-component WA-PLS model had a coefficient of determination (R^2_{jack}) of 0.86, a Root Mean Squared Error of Prediction (RMSEP) of 0.85°C and a maximum bias of 0.75°C . The temperature gradient in the Fn TS (180 lakes and 129 taxa) varied from 7.9°C to 17.6°C . The Swiss-Norwegian-Polish TS (SNP TS) included 357 lakes, 134 taxa and a temperature range of $3.5\text{--}20.1^\circ\text{C}$. The Russian TS (Rn TS) (WA-PLS, 2 components; R^2_{boot} was 0.8; RMSEP boot was 1.43°C) was based on a modern calibration dataset of 310 lakes and 172 taxa from northern Russia Euroasia ($61\text{--}75^\circ\text{N}, 50\text{--}140^\circ\text{E}$, T July range was $1.8\text{--}18.8^\circ\text{C}$; Nazarova et al., 2015, unpublished data). The Fn TS, SNP TS and Russian TS used the Weighted Averaging-Partial Least Squares transfer function (WA-PLS); the SNP TS also used the Artificial Neural Network (ANN). The SNP TS RMSEP and R^2_{jack} for WA-PLS component 3 was 1.39 °C and 0.91, respectively. The SNP TS RMSEP and R^2_{jack} for the ANN was 1.34°C and 0.95, respectively.

The cladoceran-based inference of July air temperature (Clado-I T Jul Fn TS) was based on the Finnish Cladocera-inferred mean July air temperature training set (Nevalainen et al., 2012). The Weighted Averaging-Partial Least Squares regression (WA-PLS) technique was used. The cladoceran-based July air temperature inference model parameters were the $R^2_{\text{jack}} = 0.67$, Root Mean Squared Error of Prediction (RMSEP) of 0.86°C , and mean and maximum biases of -0.017°C and 1.732°C , respectively (Luoto et al., 2011).

2.3.9. Detrended Correspondence analysis

Detrended Correspondence Analysis (DCA) was also implemented to explore patterns in assemblages. It was performed with CANOCO 4.5 (Ter Braak and Šmilauer, 2002). The procedure was run with detrending by segments on percentage-transformed data, nonlinear rescaling, and down-weighting of rare species.

2.3.10. Self-Organising Map

Kohonen's artificial neural network, also referred to as a Self-Organising Map (SOM) (Kohonen, 1982; Kohonen, 2001) was applied to identify periods that were similar in terms of biota. The data used for the SOM analysis comprised log-transformed abundances of 233 palaeoindicators present in at least three samples: 70 chironomids, 29 cladocerans, 39 macrofossils, 92 diatoms and three mollusks. The samples came from 177 core depths (1-cm sample intervals) that were common for all proxies included in SOM.

Kohonen's artificial neural networks (SOM) are simple structural and functional models of the brain. They are constructed from data processing units (neurons) arranged in layers. Kohonen's SOMs comprise two layers: an input layer used for data input and an output layer responsible for data structuring and output.

The data set used in this study (log-transformed abundances of 233 palaeoindicators \times 177 depths) was displayed on the input layer comprising 233 neurons (one input neuron per palaeoindicator). Each input neuron was connected to all output neurons and repeatedly transmitted signals to them. During the network training process, the signals travelling from the input to the output layer were strengthened or weakened by modifying the weight of the connections between neurons. On this basis, a virtual core sample (VCS) was created in each output neuron.

The output layer exists as a two-dimensional rectangular grid. The number of output neurons was determined according to the heuristic rule stating that it should be close to $5\sqrt{n}$, where n is the number of samples (177 in this study); in this case the result was 66.5 (see: Vesanto and Alhoniemi, 2000). Therefore, the final size of the output layer was $9 \times 7 (=63)$ neurons.

The distance between the output neurons on the two-dimensional grid reflects the mutual dissimilarity of the respective VCSs, or rather, the VCSs assigned to distant neurons are different, while those assigned to neighboring neurons are similar; however, the latter may not be true when the neighboring neurons are in different (sub)clusters. The (sub) clusters of output neurons, or more precisely clusters of their respective VCSs, were distinguished using hierarchical cluster analysis (Ward linkage method with Euclidean distance measure) (Vesanto and Alhoniemi, 2000; Ward, 1963).

Finally, each real core sample (RCS) was assigned to the best matching VCS and the respective output neuron. The mutual position of the RCSs on the SOM is a derivative of the mutual similarity and position of VCSs on the SOM; therefore, significantly dissimilar RCSs are located in distant neurons, while similar RCSs are located in the same neuron or in adjoining neurons (Lek et al., 2005).

Network training was performed using the batch training algorithm because it is not necessary to specify the training rate factor (Park and Chung, 2006). The network training and VCS clustering methods were performed with the use of the SOM Toolbox (Alhoniemi et al., 1999) developed by the Laboratory of Information and Computer Science at the Helsinki University of Technology (<http://www.cis.hut.fi/projects/somtoolbox/>) with the algorithm optimisation methods suggested by Vesanto et al. (2000).

Additionally, the SOM Toolbox was also used to visualise the associations between palaeoindicators and SOM regions (clusters of neurons) as greyness gradients over a two-dimensional grid. Palaeoindicators with the same pattern of greyness over a SOM co-occurred in time. In the case of taxa, similar patterns usually indicated similar habitat preferences.

The associations between each palaeoindicator and each (sub)cluster

of neurons, and its respective environmental conditions, were also expressed in a numeric form with the Indicator Species Analysis (ISA) based on indicator values (IndVals) by Dufrene and Legendre (1997). An IndVal (range 0–100%) of the palaeoindicator *i* in all RCSs of each (sub) cluster *j* is a product of three variables: (1) A_{ij} – the mean abundance of the palaeoindicator *i* in RCSs assigned to the (sub)cluster *j* divided by the sum of its average abundances in all subclusters (%), (2) F_{ij} – the constancy of occurrence of the palaeoindicator *i* (%) in RCSs assigned to the (sub)cluster *j*, and (3) the constant 100 in order to obtain the percentages as follows:

$$\text{IndVal}_{ij} = A_{ij} \times F_{ij} \times 100$$

$$A_{ij} = \text{abundance}_{ij} / \text{abundance}_i$$

$$F_{ij} = N \text{ real core samples}_{ij} / N \text{ real core samples}_i$$

The maximum IndVal (100%) is observed when all RCSs with the palaeoindicator *i* are assigned to a single (sub)cluster of output neurons and when the palaeoindicator *i* is present in all RCSs assigned to that (sub)cluster (Dufrêne and Legendre, 1997).

Finally, the palaeoindicators significantly associated with a given SOM (sub)cluster, i.e. those demonstrating a significant maximum IndVal obtained for the RCSs assigned to that (sub)cluster, were identified with a Monte Carlo randomization test performed in PC-ORD (McCune and Mefford, 2011). IndVals complement the visualisation in the form of greyness gradients.

Additionally, geochemical variables were compared between SOM subclusters with the Kruskal-Wallis test and the post hoc Dunn test (TIBCO Software (Inc, 2017; Zar, 1984).

Self-Organizing Map was implemented in palaeoecology first by Plóciennik et al. (2015a, 2015b) and Słowiński et al. (2018).

3. Results

3.1. Relationship between the lithology and geochemical composition of the core deposits

The present palaeoecological study focuses on samples taken from the core of organic deposits, called ST IIa. The core, with a total length 795 cm, was collected in 2016 with a 78 cm-long Instorf sampler. It consists of:

0–15 cm b.g.l. overbank organic mud

15–95 cm brownish peat with organic mud

95–149 cm brownish coarse detritus gyttja, with charcoal wood fragments and sandy admixtures in places, archaeological layer within

at 109–113 cm two fragments of Late Neolithic potsherds (in vertical position)

at 115–120 cm Ulmus wood fragment (laying almost horizontally)

149–314 cm olive-greyish or olive fine detritus gyttja with sand and silt admixtures

314–444 cm olive-brownish muddy fine detritus gyttja with fine sand admixtures in places

444–474 cm light brownish silt with fine-grained sand, with organic admixtures

474–780 cm beige clayey silt

780–795 cm beige clayey silt with fine-grained sand laminations

Successive samples of deposits were taken as 1 cm slices with 2 cm intervals between them. Material used for radiocarbon dating was collected from the remains of the selected terrestrial plants after plant macrofossil analysis.

The bottom part of the ST IIa core (from 788 to 554 cm b.g.l.; sub-cluster V) was dominated by inorganic sediments, composed mainly of CaCO_3 (average is 50.2%) and $\text{SiO}_{2\text{ter}}$ (between 42.2 and 58.2%)

(Fig. 3). In the group of glacio-lacustrine silt deposits, it was found that 76.6%, 80.8% and 64.8% of the total number of samples corresponded to the following respective mode value ranges: 5.75–6.00, 6.50–6.75 and 7.00–7.25 phi. Almost all elements, particularly Ca (mean 28.9 mg g^{-1}), Cu (mean $42.5 \mu\text{g g}^{-1}$) and Zn (mean $78.5 \mu\text{g g}^{-1}$) were found at constant concentrations in every deposit. Proportions of coarse (31–62 μm) to fine silt (8–16 μm) and clay (<4 μm) fractions ranged from 0.01 to 1.2 (GSI1 at Fig. 4) and 0.01 to 1.17 (GSI2 at Fig. 4).

A lithological change regarding the concentrations of lithophilic elements was observed between 554 and 456 cm b.g.l. (subcluster V) of the core; the values initially increased to a maximum at the depth of 526 cm (for example: Na to 0.78 mg g^{-1} , K to 15.7 mg g^{-1} and Mg to 14.9 mg g^{-1}), followed by a three-fold decrease. This subcluster was formed from inorganic sediments ($\text{SiO}_{2\text{ter}} > 96\%$), mainly silt (Mz range 6.1–7.08 phi, δ range 1.34–1.87 phi), to a lesser extent by sandy silt (Mz range 5.02–5.85 phi, δ range 1.34–1.87 phi), while CaCO_3 was completely absent. These sediments were characterised by an increased molar TOC/N ratio (mean 23.8; maximum higher than 30) and a highly variable Fe/Mn ratio (mean 19.8, range 9.3–31).

The sandy silt layer was overlain by mixed sediments (fine detritus-calcareous gyttja; depth: 456–250 cm b.g.l.; subclusters X₁ and X₂), which comprised 2–60% of CaCO_3 , up to 26% of organic matter, while $\text{SiO}_{2\text{ter}}$ decreased from the bottom to top 91 to 20%. In addition, an abrupt enrichment in Ca (to 159.3 mg g^{-1}), Fe (to 18.8 mg g^{-1}) and Mn (to 0.51 mg g^{-1}) was observed. In these clusters, the sand fraction became more predominant, particularly very fine sand, ranging from 3.2 to 22%.

At depths between 250 and 150 cm b.g.l. (subclusters X₂ and Y₁), the sediments were mainly composed of $\text{SiO}_{2\text{ter}}$ (mean 74.4%; range 40–78%) and characterised by an increase in the concentration of S (up to 3%), Na (up to 0.57 mg g^{-1}), Mn (up to 0.48 mg g^{-1}) and Cu (up to $85.3 \mu\text{g g}^{-1}$). Between 245–230 and 215–200 cm (subcluster X₂), higher proportions of sand fractions, particularly of fine- and medium-grained sand were observed, reaching above 25%, as well as a decreased GSI2 ratio. In the upper part, coarse silt was enriched in relation to the clay fraction (GSI1 even exceeded 3). Atomic TOC/N ratio was relatively low (often < 12) and slightly increased in an upwards direction, reaching 15. The Ca/Fe and (Na + K + Mg)/Ca ratios displayed considerable variability, especially between 230 and 200 cm (subcluster X₂).

In the upper part of the ST IIa core (depth: 150–16 cm b.g.l., cluster Y and Z), the amount of organic matter was relatively high and continued to increase from 27% in the coarse detritus gyttja to 55% in the peat with organic mud. A significant decrease of sand fractions (even below 15%), accompanied by variable levels of Na, K and Cu, was noted between 150 and 130 cm (subcluster Y₁). Ca concentrations decreased only to 7.7 mg g^{-1} , (Na + K + Mg)/Ca ratio increased to 2, and GSI2 decreased below 1. Lithogegeochemical changes consisting of supply of mineral matter, mainly very fine sand and very coarse silt, were documented in the upper part of the core (depth: 60–16 cm; cluster Z). The clusters Y and Z were also characterised by the highest levels of the trace elements Zn ($285 \mu\text{g g}^{-1}$ between 75 and 70 cm) and Cu ($84 \mu\text{g g}^{-1}$ between 50 and 16 cm).

3.2. Hydroclimatic reconstructions

3.2.1. Diatom-inferred total phosphorus

The diatom-inferred total phosphorus (Diatom I-TP) reconstruction values ranged from $59.2 \mu\text{g dm}^{-3}$ (27 cm) to $91.8 \mu\text{g dm}^{-3}$ (259 cm) (Fig. 5). The Diatom I-TP kept high values at 283–251 cm (74.5 – $91.8 \mu\text{g dm}^{-3}$) (7.1–6.7 kyr cal BP), peaking at 259–251 cm (6.8–6.7 kyr cal BP). The TP values for the 247–95 cm core range (6.7–3.9 kyr cal BP) were moderate (69.3 – $81.7 \mu\text{g dm}^{-3}$). Finally, the top sequence, falling within the Little Ice Age (89–19 cm) demonstrated generally low TP content (59.2 – $68.0 \mu\text{g dm}^{-3}$); however, it increased to 69.5 – $78.0 \mu\text{g dm}^{-3}$ between 65 and 43 cm (ca. 700/500–300 cal BP).

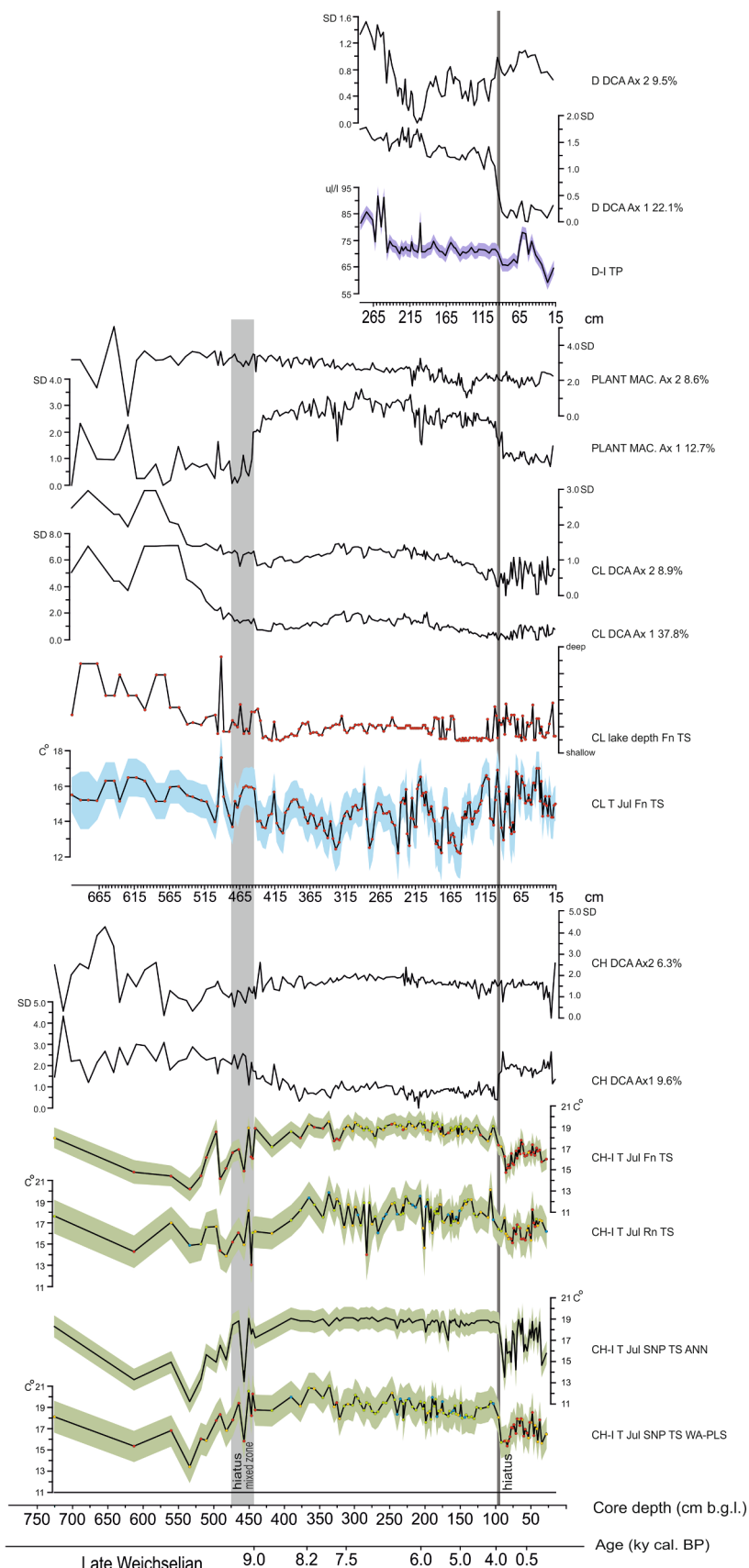


Fig. 5. Palaeoclimatic reconstructions for the Serteya region based on the results from the ST IIa core. D- diatoms, PLANT MAC – plant macrofossils, CL – Cladocera, CH – Chironomidae.

3.2.2. Cladocera-inferred summer temperature and GSPB depth reconstructions

The mean July air temperature (Clado-I T Jul) Fn TS reconstruction values inferred by Cladocera content ranged from 12.2 °C (152 cm; 154 cm; 178 cm; 240 cm) to 17.6 °C (492 cm) (Fig. 5). The Clado-I T Jul indicated higher temperatures at 704–436 cm (Late Weichselian to Early Holocene) with a constant downward trend; low to very low, highly variable values were observed in the Middle Holocene at 368–150 cm (8.2–5.0 kyr cal BP); following this, the temperature increased up to the 40 cm core depth (ca. 280 cal BP, LIA), before finally falling at the top of the sequence (38–16 cm) (ca. 265–70 cal BP). All Cladocera samples revealed very poor modern analogues (minDC > 20 percentile: minDC > 4.30013).

The Clado-I depth Fn TS reconstruction values did not correspond well with the geological or geomorphological situation of the core site. Both the geomorphological and geological findings, along with reconstructions based on the Cladocera subfossil analysis, clearly indicated greater palaeolake depths than revealed by Fn TS. In addition, the Clado-I lake depth Fn TS data corresponded with the trends demonstrated by CL DCA Ax1 and Ax2, suggesting that the reconstructed lake depth trends correspond with changes in assemblage composition.

The reconstruction indicated that the palaeolake was much deeper during the Late Weichselian than throughout the Holocene. In addition, constant, shallow conditions were observed during the late stage of Early Holocene and in the Middle Holocene; in addition, much more pronounced Clado-I lake level variation was recorded for the Late Holocene, particularly in the Little Ice Age. All Cladocera samples had very poor modern analogues (minDC > 20 percentile: minDC > 12.383).

3.2.3. Chironomidae-inferred mean July temperature

The mean July air temperature (Chiro-I T Jul) SNP TS reconstruction values, inferred by Chironomidae analysis, ranged from 11.2 to 13.4 °C at 536 cm (ANN and WA-PLS respectively) to 19.1–21.1 °C (276 cm, 316 cm, 326 cm ANN – 338 cm WA-PLS respectively) (Fig. 5). The Rn TS reconstruction values ranged from 13.2 °C (448 cm) to 20.2 °C (107 cm). The Fn TS reconstruction ranged from 13.1 °C (536 cm) to 19.6 °C (338 cm). All reconstructions reveal a similar trend consisting of low summer temperatures in the Late Weichselian (615–458 cm), highest in the early stage of the Middle Holocene (391–338 cm: 8.4–7.8 kyr cal BP) with unclear 8.2 kyr cal BP event (at ca. 369 cm); this is followed by a clearly visible (SNP WA-PLS, Rn TS) or weakly defined (SNP ANN, Fn TS) decreasing trend towards the early phase of Late Holocene, and finally cooling during the Little Ice Age. Interestingly, from the Late Weichselian to the mid-phase of Late Holocene, temperature variability is weakest according to SNP ANN, and strongest according to Rn TS. Both SNP WA-PLS and Rn TSs reconstructions reveal weak cooling to 18.9–14.0 °C (Rn TS) – 19.5–18.7 °C (SNP TS) on 276–268 cm (ca. 7.0 kyr cal BP). Additionally, Rn TS reveals exceptionally low temperature values in samples at 204–202 cm, corresponding to ca. 5.85–5.8 kyr cal BP, which also coincides with the 5.9 kyr cal BP Bond event.

SNP TS and Fn TS reconstructions indicate a strong cold oscillation between 15.9–16.9 °C (SNP ANN), 16.1–16.9 °C (SNP WA-PLS), 16.2–16.7 °C (Fn TS) between 60 and 54 cm, which falls in the early Little Ice Age (ca. 465–400 yr cal BP). SNP WA-PLS reconstructions reveal generally poor (minDC > 10 percentile: 10.0564) to moderate (10 percentile > minDC > 5 percentile: 10.0564 > minDC > 8.57757) modern analogues for the 728–442 cm and 88–28 cm sections, and moderate to good and very good (minDC < 5 percentile: minDC < 8.57757) modern analogues for the 419–92 cm section. Rn TS reconstructions indicate generally poor (minDC > 10 percentile: 40.7224) to moderate (10 percentile > minDC > 5 percentile: 40.7224 > minDC > 36.5794) modern analogues for 498–448 cm and 88–44 cm, and moderate to good and very good (minDC < 5 percentile: minDC < 36.5794) modern analogues for the 728–512 cm, 446–82 cm and 42–28 cm sections. The Fn TS reconstructions suggest generally poor (minDC > 10 percentile: 9.75318) to moderate (10 percentile > minDC > 5 percentile:

9.75318 > minDC > 8.50537) modern analogues for 728–300 cm and 122–28 cm, and moderate to good (minDC < 5 percentile: minDC < 8.50537) modern analogues for the 296–127 cm section.

3.2.4. Results of DCA

The first DCA axis of the Chironomidae sequence explains 9.6% of the cumulative variance of taxa data and has a gradient length of 4.330, indicating that the data have a unimodal distribution. The second DCA axis of the Chironomidae sequence explains 6.3% of the cumulative variance of species data. The first DCA axis (DCA Ax1) of chironomid assemblages reveals a similar (reversed) trend to mean July air temperature estimations from the SNP, Fn and Rn Training Sets (TSs) (Fig. 5), indicating that summer temperature was the main driver of the midge communities.

The first DCA axis of the Cladocera communities explains 37.8% of the cumulative variance of taxa data and has a gradient length of 5.588. The second DCA axis of Cladocera assemblages explains 8.9% of the cumulative variance of species data. The cladoceran DCA Ax1 and Ax2 reflect the palaeolake depth oscillations reconstructed from the Fn TS, indicating that water level was the main driver of the Cladocera communities.

The first DCA axis of plant macrofossil communities explains 12.7% of the cumulative variance of taxa data and has a gradient length of 6.410. The second DCA axis explains 8.6% of the cumulative variance of species data. The plant macrofossil DCA Ax1 correlates with Chiro-I mean July temperature reconstruction, suggesting that macrophyte communities in the palaeolake, and on its shore, were also influenced by climatic conditions, mostly during the vegetation season.

The first diatom DCA axis of diatom communities explains 22.1% of the cumulative variance of taxa data and has a gradient length of 1.771, which indicates that the data have a linear distribution. The second DCA axis explains 9.5% of the cumulative variance of species data. The diatom DCA Ax1 has a similar trend to the top part of the Chiro-I mean July temperature reconstruction, indicating that diatom communities were also affected by summer temperatures. Diatom DCA Ax2 shares to some extent a common trend with DI-TP reconstruction, as such, palaeolake trophic state can be regarded as a second important factor for the diatom assemblages.

3.2.5. Biota stratification with SOM and subsequent geochemical analysis

Four main clusters were distinguished in the output layer of the SOM: V, X, Y and Z, with the last three clusters comprising the respective pairs of subclusters: X₁ and X₂, Y₁ and Y₂, Z₁ and Z₂ (Fig. 6).

The samples were assigned to output neurons according to their temporal origin. The oldest material, core depth 788–443 cm, was assigned to (sub)cluster V. The next younger samples, from 440–287 cm, were assigned to subcluster X₁, those from 284–196 cm to X₂, those from 195–132 cm to Y₁, and those from 131–95 cm to Y₂. The youngest samples, i.e. from 89–38 cm and 35–19 cm of core depth, were assigned to subclusters Z₁ and Z₂, respectively (Fig. 6). There were only two exceptions: the sample from 136–135 cm was assigned to X₂ and those from 92–91 cm to Z₂. They come from transitional zones and, as they do not match chronologically the palaeolake developmental stages, they were excluded from further analysis of associations between palaeoindicators and the periods demonstrating homogenous biota.

A total of 168 palaeoindicators were significantly associated with some subcluster (period). Among them, 68 exhibited IndVals significant at $p \leq 0.001$ (Fig. 7), 54 were significant at $p \leq 0.01$, and 46 at $p \leq 0.05$ (Table S1). A clear temporal trend was observed in the number of palaeoindicators significantly associated with SOM subclusters. Generally, the number of associated palaeoindicators increased from 4 to 67 from subclusters V to Z₁ (788–38 cm), but then decreased to 29 in Z₂ (35–19 cm) (Table S1). Therefore, the palaeolake became increasingly favorable for rich biota development over successive stages, but the trend reversed in the last stage.

Among the 233 palaeoindicators analysed with SOM and IndVal, the

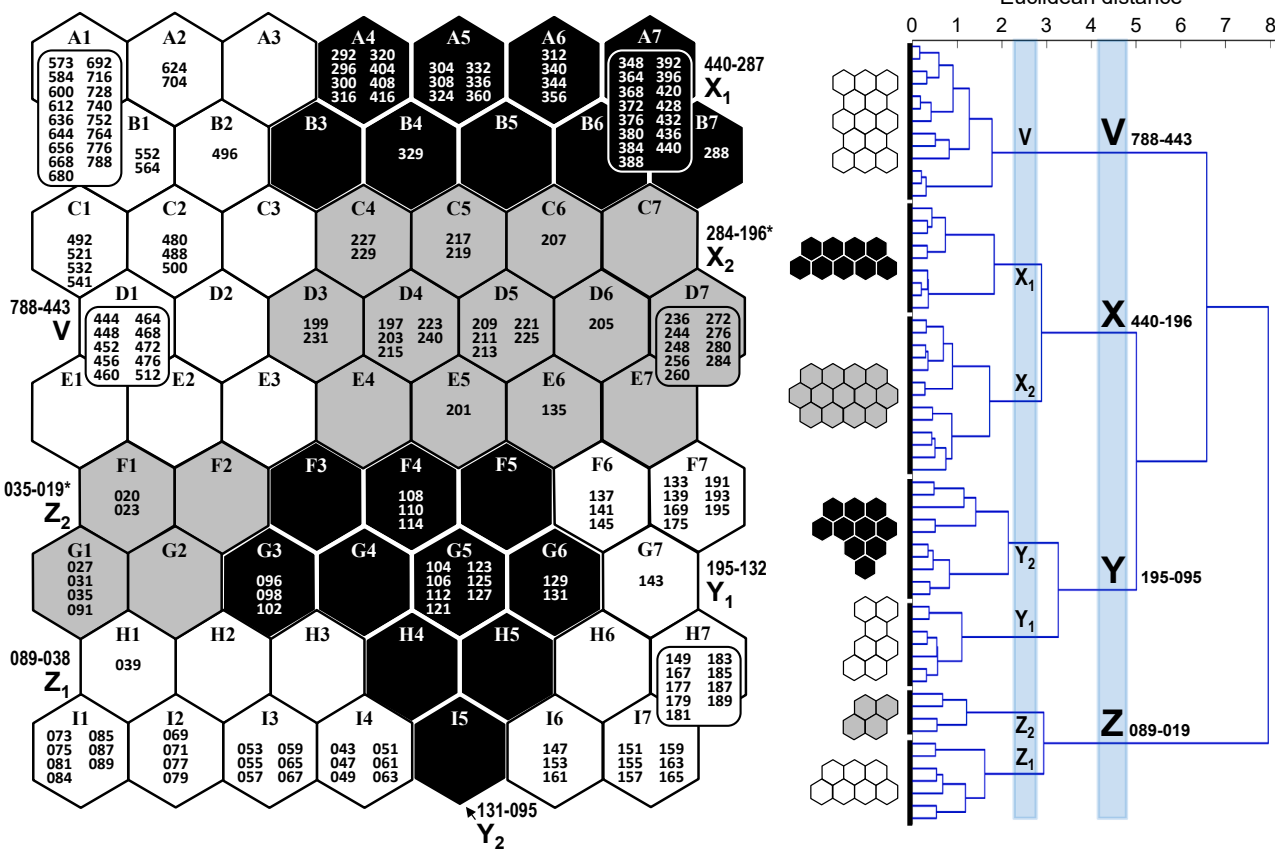


Fig. 6. Core samples (each 1 cm thick) from 177 core depths (in cm) assigned to 63 Self-Organising Map (SOM) output neurons (A1–I7). The neurons are arranged into a two-dimensional grid (9 × 7). Clusters (V, X, Y, Z) and sub-clusters (V, X₁, X₂, Y₁, Y₂, Z₁ and Z₂; shown in different degrees of greyness) of neurons have been identified with the use of hierarchical cluster analysis. A core-depth range (in cm; with derogation if marked with an asterisk) is presented above each sub-cluster symbol.

most indicative of environmental conditions in the SOM-recognised palaeolake developmental stages were diatoms (86% of palaeoindicators; 79 of 92) and macrofossils (77%; 30 of 39). Of chironomids and cladocerans, 59% of morphotypes (41 of 70 and 17 of 29, respectively) were indicative of any subcluster. Of molluscs, one taxon (33%) was associated with subcluster Y₁.

There was a clear downward trend in the amount of mineral matter from V to Z₁ subclusters (788–38 cm) (Fig. 8). A similar trend was observed for the percentage of the finest fractions: clay, very fine silt and fine silt. Medium and coarse silt were the least abundant in X₂ (284–196 cm) and the most abundant, respectively, in V (788–443 cm) and Z₁ (89–38 cm). For the very coarse silt, the lowest median level was observed in V, and the highest in Z₁. In turn, sand of various grain sizes was the most abundant in X₂ (284–196 cm), Y₁ (195–132 cm) and/or Y₂ (131–95 cm), i.e. between 284 and 95 cm b.g.l. An upward trend in the content of zinc (Zn), and a downward trend in the content of Mg and Fe were also observed (Fig. 9). The amounts of K and Mn were generally significantly lower than for other subclusters in Y₂ (131–95 cm), Z₁ (89–38 cm) and Z₂ (35–19 cm), i.e. from 131 to 19 cm b.g.l. The highest medians for Na and Ca were recorded in V (788–443 cm) and X₁ (440–287 cm), respectively. Generally, the Na/K ratio showed an upward trend (Fig. 10). The highest medians for the Fe/Mn ratio were recorded in V and X₁ (from 788 to 287 cm b.g.l.), and for the Cu/Zn ratio in X₂ and Y₁ (from 284 to 132 cm b.g.l.). The lowest percentage of S, N and C were recorded in V (788–443 cm) compared to X₁–Y₁ (440–132 cm b.g.l.) (Fig. 10). The TOC/N atomic ratio was highest in V.

4. Discussion

4.1. Pre-Holocene development of the basin

Our constructed depth/age model for the ST IIa core indicates that the inorganic deposits from the lower part of the profile were deposited before 9.0 kyr cal BP (Fig. 2). In addition, reconstructions based on Fe/Mn, Ca/Fe, S/Fe and Cu/Zn ratios confirm generally high palaeolake level phases (Fig. 4). The relatively high carbonate and decrease in Ca/Fe and Fe/Mn ratios were commonly reported for European lakes during pre-Holocene period, which has been associated with deposition in lake of detrital material from catchment such as detrital carbonates (remains of crushed malacofauna), epidote, limonite and zircon (Enters et al., 2010; Pleskot et al., 2018). This reconstruction corresponds with the results of the Clado-I lake depth modeling. The proportion of fine silt and clay fractions appear to increase upwards, distinguished in GZI (795–555 cm b.g.l., corresponding to the deeper samples of the V cluster on SOM); this section can be treated as a whole as glaciolacustrine sediments (Figs. 3, 6, 8, 9, 10).

In addition, very high SiO₂ter and K content is observed, particularly in the range 795–555 cm; this indicates the existence of cold climatic conditions with very poor vegetation and intense mechanical denudation in the catchment. Sediments of this type have been documented in many sites in Eurasia (Wohlfarth et al., 2006; Yanina, 2013) and are correlated with Upper Pleniweichselian (>22 kyr BP), exactly at the time of the West Siberian lake described by Grosswald (1980). The lower part of ST IIa core consists of glaciolacustrine deposits that accumulated during the older part of the Late Valdai according to Arslanov (1993) and Velichko et al. (2011), or during the Late Vistulian (Marks, 2012).

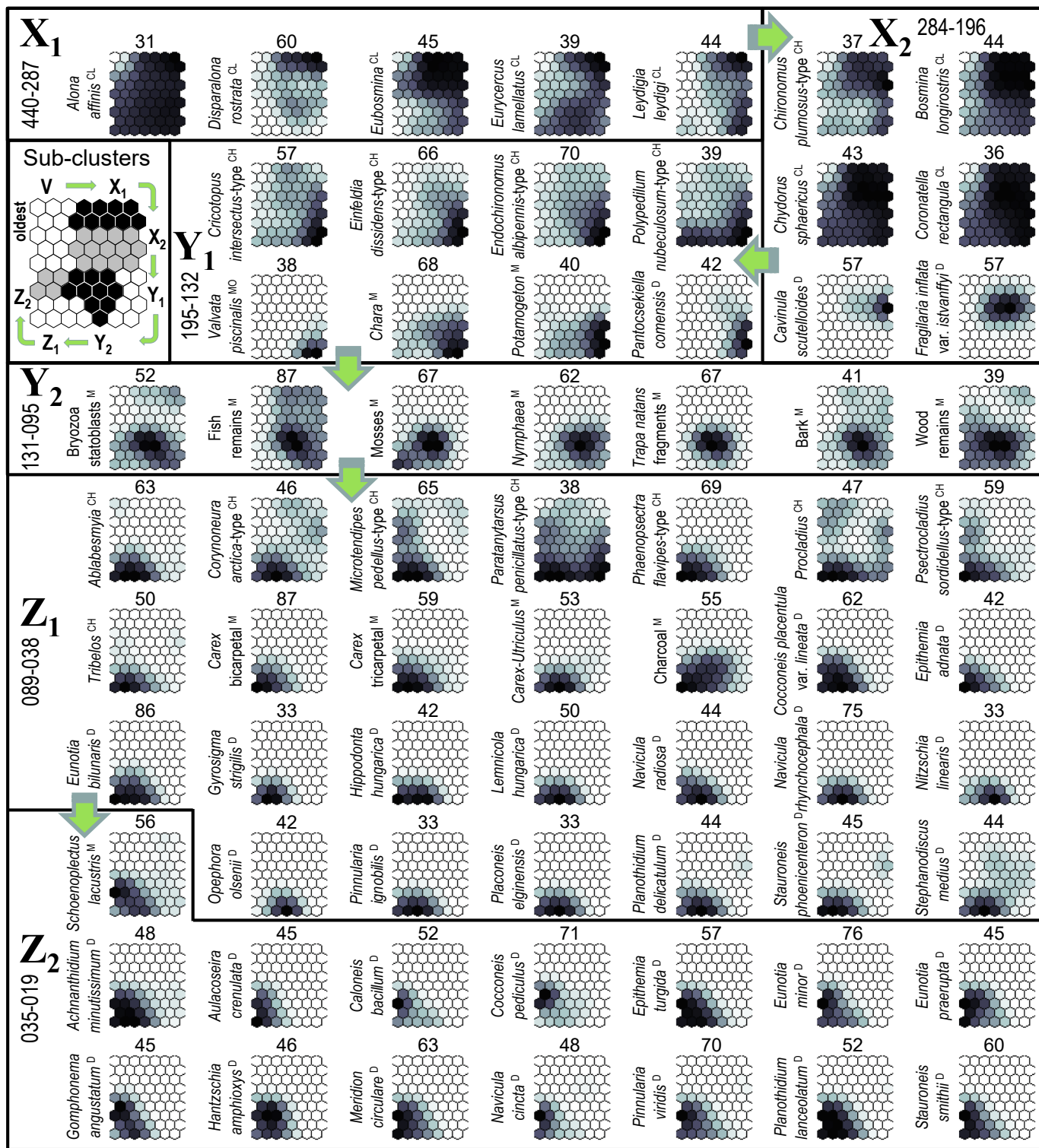


Fig. 7. All 68 palaeoindicators associated with SOM subclusters (V–Z₂) at $p \leq 0.001$ (remaining 100 palaeoindicators are listed in Table S1). CH = chironomids, CL = cladocerans, M = macrofossils, D = diatoms, MO = mollusks. The shading is scaled independently for each palaeoindicator; it is darker for a stronger association in virtual core samples. Maximum observed indicator value (IndVal) is shown above each palaeoindicator plane; IndVals and their significance levels were calculated on the basis of real core samples.

The initial phase of the gradual retreat of the Valdai ice margin in the East European Plain began prior to 16 kyr BP (Velichko et al., 2011).

In Eastern Europe, the Late Glacial Maximum was formed by different ice streams during successive phases in the period between 24 and 19 kyr BP, although this took place later in Eastern Poland (Marks, 2012). The first glacial lakes in the Serteya region, fed by proglacial

waters, may have appeared shortly after the retreat of the Late Valdai ice sheet from the area. However, without any absolute chronology for the discussed sediments, we can only suggest that this lake stage took place in the Epe (Kamion) Phase, dated to 18–17 kyr cal BP (Dzieduszyńska, 2019; Dzieduszyńska and Forysiak, 2019), correlated with the Meien-dorf interstadial (Litt et al., 2001).

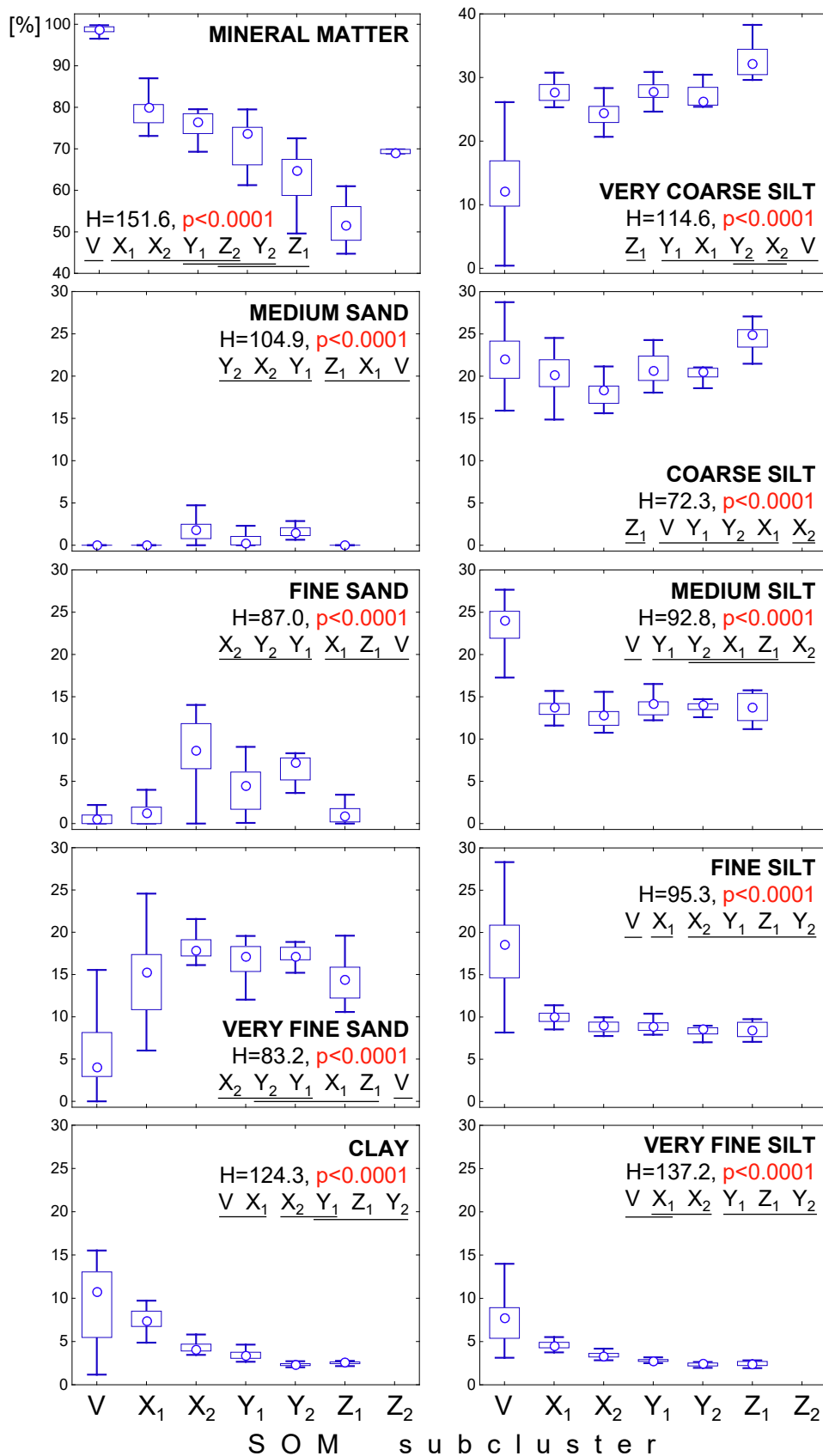


Fig. 8. The percentage of mineral matter and its fractions in the core samples assigned to SOM subclusters (see Fig. 6). Due to the insufficient amount of sediment, the percentages of individual fractions for the depths of 20–53 cm were not determined. Circle – median, box – interquartile range, whiskers – variability (min–max) range, H – statistic of the Kruskal-Wallis test (mineral matter: d.f. = 6, n_V = 39, n_{X1} = 35, n_{X2} = 28, n_{Y1} = 29, n_{Y2} = 15, n_{Z1} = 24, n_{Z2} = 5; fractions: d.f. = 5, n_V = 39, n_{X1} = 35, n_{X2} = 28, n_{Y1} = 29, n_{Y2} = 15, n_{Z1} = 18). For subclusters whose symbols are underlined with the same line, no significant difference in post-hoc comparisons was recorded.

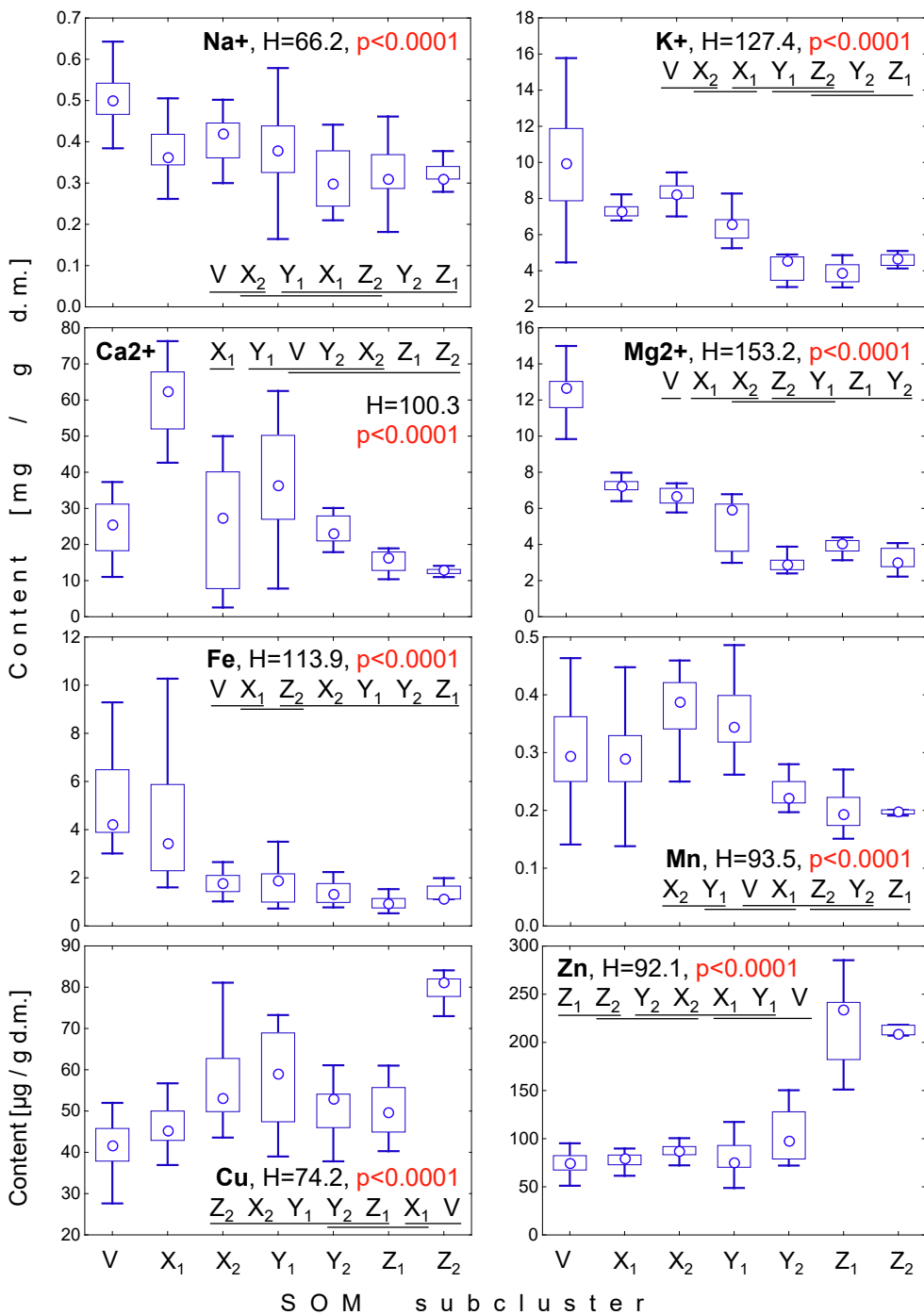


Fig. 9. The content of selected elements in dry matter (d.m.) of the core samples assigned to SOM subclusters (see Fig. 6). Circle – median, box – interquartile range, whiskers – variability (min–max) range, H – statistic of the Kruskal-Wallis test (d.f. = 6, n_V = 39, n_{X1} = 35, n_{X2} = 28, n_{Y1} = 29, n_{Y2} = 15, n_{Z1} = 24, n_{Z2} = 5). For subclusters whose symbols are underlined with the same line, no significant difference in post-hoc comparisons was recorded.

The increasing content of clay and very fine silt could be interpreted primarily as a reflection of the regression of the ice sheet. Indeed, the low values of the GSI 1 and 2 ratios suggest that mineral material was delivered to the proglacial lake from increasingly greater distances. Furthermore, the geochemical changes, particularly the increased sum of lithophilic elements and complete lack of CaCO₃ content, suggest the input material could reflect the development of a river water network and increased mechanical denudation. The enrichment of terrigenous silica and lithophilic elements in the sediments are attributed to flood events and slope processes under condition of less developed plant cover (Mendyk et al., 2016; Pawłowski et al., 2016a). As the grain-size and

geochemical properties are characterized by a short delay in response to changes in the water regime, they could represent palaeoenvironmental proxies in the set of studied variables (Vasskog et al., 2012).

The lower part of the ST IIa profile is characterized by a low concentration of Cladocera and Chironomidae subfossils, and a few plant macrofossils. The number of Cladocera was relatively low and characterised by the dominance of cold-tolerant taxa, such as pelagic forms of Bosminidae, e.g. *Eubosmina* spp., *Bosmina longirostris*, and Daphniidae, e.g. *Daphnia longispina*-group, as these taxa have been found in northern Finnish Lapland (Korhola, 1999; Sarmaja-Korjonen et al., 2006). Additionally, the Bosminidae and littoral taxon, *Chydorus sphaericus*, are

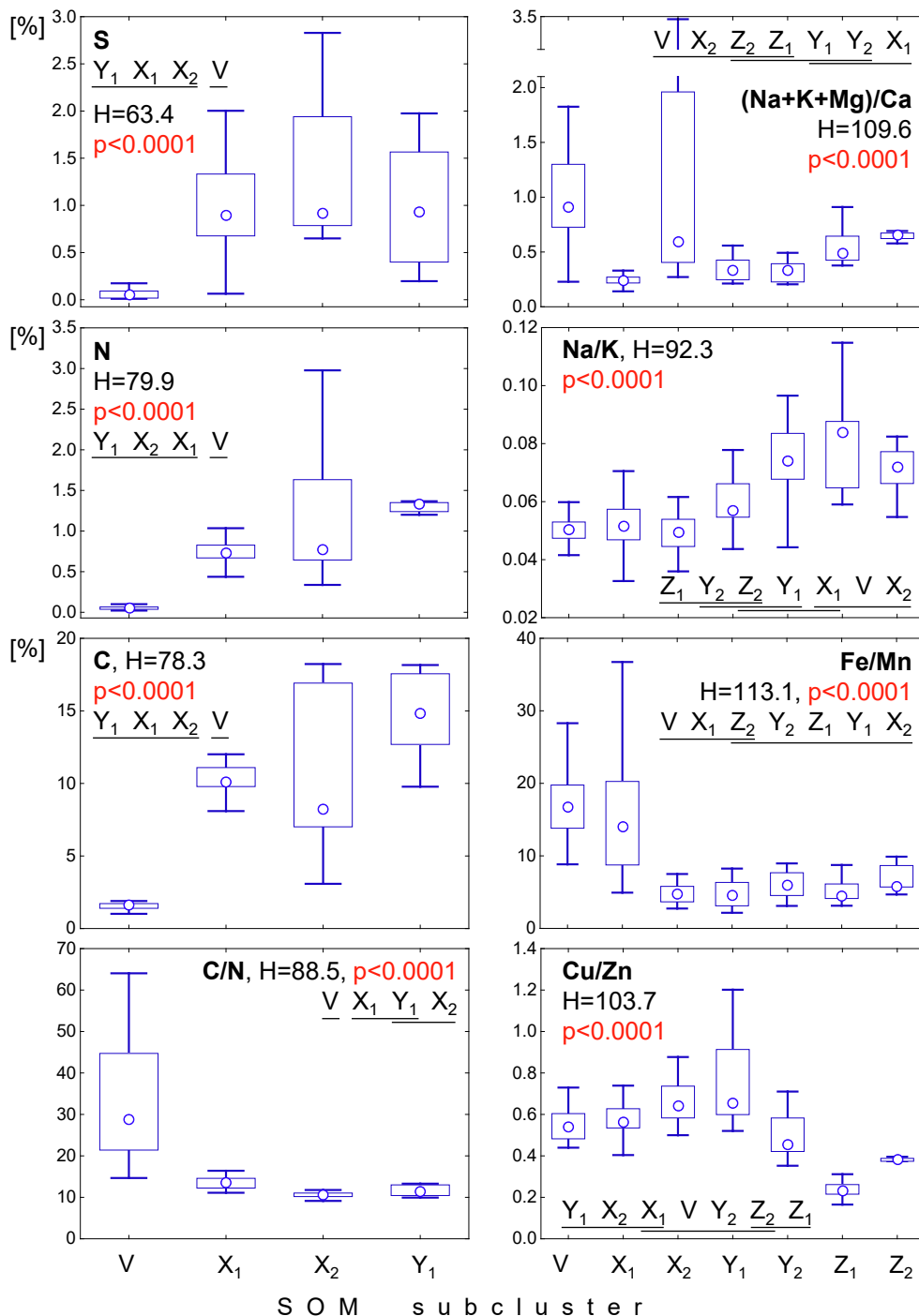


Fig. 10. The percentage of sulphur (S), nitrogen (N) and carbon (C), the erosion index $[(\text{Na} + \text{K} + \text{Mg})/\text{Ca}]$ and selected other ratios of the elements (C/N, Na/K, Fe/Mn, Cu/Zn) in the core samples assigned to SOM sub-clusters (see Fig. 6). Due to the insufficient amount of sediment, the percentages of S, C and N, and C/N ratio for the depths of 20–179 cm were not determined. Circle – median, box – interquartile range, whiskers – variability (min–max) range, H – statistic of the Kruskal-Wallis test (left column: d.f. = 3, $n_V = 39$, $n_{X_1} = 35$, $n_{X_2} = 28$, $n_{Y_1} = 8$; right column: d.f. = 5, $n_V = 39$, $n_{X_1} = 35$, $n_{X_2} = 28$, $n_{Y_1} = 29$, $n_{Y_2} = 15$, $n_{Z_1} = 18$). For subclusters whose symbols are underlined with the same line, no significant difference in post-hoc comparisons was recorded.

believed to be early immigrants following the ice retreat (Hofmann, 2000; Pawłowski, 2011)

The Clado-I lake depth Fn TS analysis suggests that the palaeolake was deep at this time (Fig. 5); however, it is possible that this depth was overestimated. The ecological plasticity and fast reproduction of Cladocera favor their rapid population growth and maintenance, especially in glacial lakes (Pawłowski et al., 2013). For example, some pelagic species lack a dormant stage and may have a greater ability to disperse (Hairston, 1996). In turn, chydorids reproduce asexually during a large part of the season when the lake is free from ice cover, as noted by Sarmaja-Korjonen (2003) in northern boreal and subarctic lakes. Additionally, it is possible that some of the first colonists following the ice retreat that were tolerant of severe climate conditions mainly

reproduced asexually. Therefore, we assume that the frequency of Cladocera observed at this time in GSPB was mainly a reaction to the seasonality of the ice sheet melting, during summers with a longer open-water season. Chironomids in the GZI phase, i.e. corresponding to the deeper samples of the V cluster on SOM, are represented by cold-stenotherm taxa like *Micropsectra contracta*-type, eurytopic (*Procladius*, *Polypedilum nubeculosum*-type) (Fig. S4) and warm-stenotherm morphotypes (*Paratanytarsus penicillatus*-type). In the same period, the sandy-silty deposits accumulated; these are recognised by Kittel et al. (2018) as kames or kame terraces. The range of these relief forms allows for the reconstruction of the area of the first-generation water body in the tunnel valley (used by the present-day Serteyka River) after partial melting of ice blocks.

The inorganic sediments deposited during the latter part of the Late Weichselian (depth: 555–450 cm b.g.l., corresponding to the upper samples of the V cluster on SOM) may largely come from areas distant from the research site, resulting in it being characterised by a greater admixture of fine fraction (Fig. 3). A threefold increase in the Fe/Mn (above 30) and a slightly elevated concentration of S (from 0.01 to 0.20%) indicate decreasing redox conditions in the lake (Fig. 4), which may indicate microbial decomposition of the organic remains or cloudy lake water (Eusterhues et al., 2005; Apolinarska et al., 2012). By contrast, a partial correlation was observed between Fe and lithophilic content (Na, K and Mg) and with non-carbonated mineral matter ($\text{SiO}_{2\text{ter}}$), indicating a high intensity of mechanical denudation/slope erosion (Mendyk et al., 2016). In turn, input organic matter from terrestrial sources was indicated by the high values of TOC/N (Meyers and Teranes, 2001).

Comparing analogous sediments from different morphogenetic zones in Central Europe, it can be concluded that the Late Weichselian deposits could be rich in ice and (partly) deposited on buried ice blocks (Błaszkiewicz, 2005, 2007), which may have resulted from thermokarst processes. The thermokarst activity appeared to be divergent at various spatial and temporal scales; this could be related mainly to climate and hydrogeological conditions, as well as the development of local plant cover (Balwierz and Goździk, 1997; Forysiak et al., 2014). In this case, this stage of GSPB development can be treated as a relatively warmer and wetter period than the earlier phase of proglacial lake development.

In many localities of Eurasia, the lithology and geochemical record of environmental changes during the Late Weichselian (Apolinarska et al., 2012; Hinderer, 2001; Lotter and Hölzer, 1994; Ryabogina et al., 2019; Vyse et al., 2020) is influenced by the intensity of detrital input to lakes. However, it is important to consider that the gradual filling of the palaeolake basin with deposits may have influenced the decline in denudation processes or resulted in changes in the type of deposit. The rapid disappearance of CaCO_3 in the Late Weichselian sediments could be explained by the application of a large amount of mineral cover, possibly a moraine material, derived from deposits melted from the upper ice surface; this is supported by the change in the relationship between the percentage share of individual fractions and the textural indexes. Many studies of the dynamics of lithology changes have indicated the possibility of sedimentation of a given sediment series under extreme conditions (Błaszkiewicz, 2008; Kokorowski et al., 2008; Lenz et al., 2021). The observed lack of carbonates could also have been caused by the depth of the permafrost bottom, i.e. continuous permafrost cover, which had slightly responded to environmental changes resulting from the warming climate in the Late Weichselian.

The upper part of the inorganic sector of the ST IIa core (555–450 cm b.g.l.) accumulated after the depositional hiatus, marked by very sharp changes in geochemical indicators, mostly carbonates and $\text{SiO}_{2\text{ter}}$ (Fig. 3). This hiatus resulted from a lowering of the water table or a reorganisation of the hydrological situation following the drainage of the first-generation lake. Velichko et al. (2011) describe a cold interval in the East European Plain followed by a short and pronounced readvance of the Valdai ice sheet, called the Vepovo or Pomeranian advance, dated to about 15.5 kyr BP. Following this, in the Bølling, a second stage of deglaciation occurred, characterised by a rapid transition from active to passive ice, and the East European Plain became free of ice (Faustova, 1994; Velichko et al., 2011, 2017); this resulted in intense melting of the dead ice blocks and a consequent rise in the water level within the tunnel valley. This period was also characterised by the recession of permafrost.

These processes occurred most probably in the Bølling-Allerød period, i.e. between 14.2 and 12.6 kyr cal BP (Dzieduszyńska, 2019), although the beginning of the Bølling-Allerød chronozone was dated to 14.6 kyr b2k by Rasmussen et al. (2014). Błaszkiewicz (2005; 2007) argues that the melting of the dead ice and formation of postglacial lakes in the recently glaciated zone was most intensive during this period. Silty clay deposits also accumulated in Kamyshevoye Lake in the

Kaliningrad Region between 15.0 and 11.4 cal BP (Kublitskiy et al., 2020). During this period, the number of Cladocera systematically increased, especially the frequency of littoral taxa. Although pelagic taxa constituted over 60% of total Cladocera abundance at the onset of this period (ca. 550–500 cm depth), littoral, macrophyte-associated and macrophyte/sediment-associated taxa were also common; following this, from ca. 500 cm, the frequency of the former systematically decreased and the latter increased (Fig. S3). This situation is reflected on the Clado-I lake depth Fn TS reconstruction as a gradual decrease in palaeolake depth (Fig. 5)

Again, sharp changes in geochemical indicators (organic matter, carbonates, $\text{SiO}_{2\text{ter}}$ and, Fe and TS) at ca. 450 cm b.g.l. of the core indicate a rapid change of sedimentological conditions (Figs. 3, 4). The deposition hiatus must be taken into consideration. Increased CaCO_3 in the deposits again indicates alkalinity of the lake water, while the low values of TOC/N are typical for algal phytoplankton (Meyers and Teranes, 2001). Similar changes in lithology and geochemical composition of biogenic sediments, reflecting trophy, development soil cover with humic acids and dissolution of gypsum in the catchment, have been observed in sediments of the Early Holocene lakes (Engstrom and Wright, 1984; Lauterbach et al., 2010; Apolinarska et al., 2012). Lacustrine organic deposits present in the core from ca. 450 cm b.g.l. appear to have accumulated from ca. 9.0 kyr cal BP, based on the ^{14}C age of plant macrofossils (*Betula* fruit) found at a depth of 459 cm b.g.l., i.e. from the upper part of sandy silt with organic admixtures (Wieckowska-Lüth et al., 2021). This demonstrates that the uppermost part of the Late Weichselian deposits could be washed and redeposited during Early Holocene transgression. From the depth of ca. 450 cm, the abundance of Cladocera rapidly increased, with the littoral taxa dominating, especially macrophyte/sediment-associated taxa. Nevertheless, sediment-associated taxa still appear frequently in the sequence.

4.2. Palaeoclimatic pattern in the Holocene development of the lake

The global mean annual sea surface temperatures have been steadily increasing since the start of the early Holocene stage, along with retreating ice sheets, up to 6.5 kyr cal BP. Global mean annual sea surface temperature then grew at $0.25 \pm 0.21^\circ\text{C}$ as a result of rising greenhouse gas concentrations, although at the continents level, the temperature decreased during the Late Holocene (Bova et al., 2021). The CH-I mean air T Jul reconstructions of Holocene temperature fit the global pattern presented by the ‘Temperature 12k database’.

Kaufman et al. (2020a; 2020b) outline a relatively cool Early Holocene at 30–60N, the Holocene Thermal Maximum (HTM) falling on 8–6 kyr cal BP, followed by steady decreasing temperature until Modern Times. The same Chiro-I T Jul analysis of ST IIa core found the HTM to fall on the Early Holocene/Middle Holocene transition and early phase of Middle Holocene, 8.5–7.7 kyr cal BP. This period was marked by the arrival of early Neolithic communities to the Western Dvina Lakeland (Mazurkevich et al., 2020a, 2020b). Renssen et al. (2012) indicated earlier that mid- and high latitude European pollen and chironomid data are considered to give warmest conditions between 7 and 5 kyr BP, with summer temperatures being 0.5–1.5 °C above the preindustrial level but their simulation suggest somewhat warmer summer conditions during the HTM in central Europe (i.e. 3 °C above the preindustrial value). The ST IIa palaeotemperature records indicate a 3.5–5.5 °C deviation from Modern Times, depending on the used model. In North-Western Eurasia, the month with the largest positive temperature deviation from the preindustrial mean was June (Renssen et al., 2012). The June–August season was used as a temperature inference time for the TSs (Kotrys et al., 2020; Luoto et al., 2019; Nazarova et al., 2015, unpublished data), because the Chironomidae are more indicative of the temperature of the summer season than of individual months (Telford, 2019). Indeed, Bova et al. (2021) argue that global temperature in the Holocene reflects the evolution of seasonal, rather than annual, temperatures.

Novenko et al. (2019) also place the HTM within 8.8–5.7 kyr BP, and

Mazei et al. (2020) place it within 8–6 kyr cal BP in the East European Uplands. Although both estimates are based on palaeobotanical-based reconstructions, Novenko et al. (2009) draw different conclusions: they place the HTM in the late phase of Middle Holocene with the temperature of the coldest month being 3 °C higher, summer temperature 1 °C higher, and precipitation close to modern values, based on the climagrams method (Grichuk et al., 1985). The winter temperature inferred from pollen collected from GSPB littoral zone (ST M25 core), fell from 6 kyr cal BP to at least 4 kyr cal BP (Mroczkowska et al., 2021), and the summer temperature ranged from 16.4 °C to 18.5 °C (Payron and Gauthier unpublished).

Our estimation of HTM is consistent with the results presented by Novenko et al. (2019), based on more recent data. They also indicate the 6.7–5.5 kyr BP period as mildly dry, which correlates well with the decrease in ST IIa Clado-I water level to very low, as well as slightly lower Fe/Mn and much higher Ca/Fe ratios, which were confirmed by the results from ST M25 core (Kittel et al., 2021; Mroczkowska et al., 2021).

None of the reconstructions conducted from ST IIa core provide clear indication of the 8.2 kyr cal BP cooling event. Although the Chironomidae could be analysed with a high (4 cm) resolution, only two temperature points were used for 8.25–7.75 kyr cal BP due to some samples being merged because of low head capsule concentration. Still, after 8.2 kyr cal BP, the mean rate of lacustrine deposit accumulation decreased from ca. 1.25 mm yr⁻¹ to ca. 0.8 mm yr⁻¹. In addition, a distinct decrease in Fe and S concentrations in these sediments may indicate oxidising conditions in the palaeolake or limited particulate supply from the catchment. The first situation can be explained by specific hydrogeology properties and rapid early decrease in groundwater level, because the main source of dissolved iron to the lakes is groundwater (Pleskot et al., 2020). Li and Born (2019) clearly indicate a weak response by the plant communities to the 8.2 kyr cal BP cooling event in Eastern Europe compared to Scandinavia. The 8.2 kyr BP event was first recorded by Alley et al. (1997) and von Grafenstein et al. (1998). It has been mainly attributed to the collapse of the North Atlantic circulation (Matero et al., 2017). This event was generally cold and dry, particularly during the winter seasons; however, the summers could be cool and wet in NW Europe (Alley and Ágústsdóttir, 2005; Baker, 2012). Northern and southern Europe experienced drier conditions, while central Europe experienced wet conditions, according to Magny and Bégeot (2004), Magny et al. (2003, 2007) and Morrill et al. (2013). The cool, dry climatic conditions of the 8.2 kyr cal BP event are believed to have lasted 150.0–160.5 years, between 8.3 kyr BP and 8 kyr BP, with the cooling reaching a peak 60–69 yrs into this interval (Baker, 2012; Thomas et al., 2007). The climate of the East European Plain is more driven by the continental air masses, and it is likely that the North Atlantic may have had only an insignificant influence on cooling.

Instead of 8.2 kyr cal BP, the temperature analysis ST IIa records a cool oscillation at 7.0–6.8 kyr cal BP. This may correlate with the 7.4–6.8 kyr cal BP wet climatic event, which was also observed in speleothems in caves of the Lesser Poland Upland (Starkel et al., 2006, 2013). A cool oscillation at 7.4 kyr cal BP was also noticed in the East European Uplands by Mazei et al. (2020). It coincided with the end of the earliest ceramic traditions and changes of cultural vectors from south-north to west-east directions at ca. 7.0 kyr cal BP, as new ceramic-bearing cultures penetrated the Western Dvina Lakeland from the early Narva culture area. The Rn TS reconstruction also shows a cold oscillation at ca. 5.8 kyr cal BP. A 5.9 kyr cal BP event has also been identified from the ST M25 core situated at the shallow littoral zone of the GSPB (Mroczkowska et al., 2021). However, it is questionable whether this cold oscillation in the region could be associated with the Bond Events and North Atlantic Oscillation, as the quantitative reconstructions from Eastern Europe do not suggest any common trend in summer or winter temperatures, or precipitation (Kaufman et al., 2020b; Mroczkowska, et al. 2021), and this oscillation may just be a coincidence.

It needs to be stated, that the reconstructions from Eastern Europe

given in the Temperature 12 k database are based mainly on old pollen records, often have low resolution, and may be obscured by old, large bulk-sampled radiocarbon dates. The influence of the North Atlantic Oscillation in Eastern Europe might be weak, but the causes of the 5.9 kyr cal BP event on the East European Plain remain open due to lack of modern quantitative reconstructions. Bednorz (2004) indicates no negative correlation between snow cover and the North Atlantic Circulation in the region. However, vegetation-based reconstructions by Velichko et al. (1997) suggest that the Atlantic circulation had some influence; this in turn could indicate that in the Holocene, the climate fluctuations were more pronounced in Eastern Europe than in Siberia due to some influence of westerly air masses. Although all northern Eurasia underwent Mid-Holocene warming, the east European region faced stronger cooling during the late Holocene than Siberia, due to the influence of continental air masses in Siberia. Bailey et al. (2021) demonstrate clearly that the loss of Arctic sea-ice has been implicated in the occurrence of a number of severe cold and snowy mid-latitude winters in the 21st Century. An anomalously warm Barents Sea, with a 60% ice-free surface, contributes moisture flux to the cold northeasterly airflow, which then supplies up to 88% of the fresh snow over northern Europe.

The concurrence between the continental and Atlantic air masses was also well documented by ice ¹⁸O and K⁺ dust in GISP2 and archaeological data from the south-east Mediterranean and Pontic regions. During the 6.2–5.0 kyr cal BP events and the Little Ice Age, strong shifts in Siberian air masses occurred in north-eastern Europe, reaching as far south as Ukraine and the Balkans (Weninger and Harper, 2015). The 5.8 kyr cal BP oscillation recorded by Rn TS is weakly remarked, but all Chiro-I reconstructions from the ST IIa core suggest clearly lower summer temperatures for the Late Holocene. The stable isotope data from Romania indicate that south-east Europe was under North Atlantic Circulation during the Little Ice Age but, compared to the Medieval Warm Period, it was characterised by a weaker temperature decrease in summer and a stronger one in winter (Bădăluță et al., 2020). In the ST IIa core, a change in lithology was observed, which was associated with the disappearance of carbonates and constantly high concentrations of lithophilic elements, as well as a periodic decrease in the content of Ca. The periods of higher mechanical denudation also correspond to decreases in the Ca/Fe ratio, especially for the fine and coarse detritus gyttja. This geochemical stratification may also be the result of a wetter climate phase and nutrient delivery due to wildfires, both in the catchment and in other localities, as noted by Pleskot et al. (2018) and Kittel et al. (2020).

While weak evidence exists for the 5.9 kyr cal BP episode, the 4.2 kyr cal BP event remains unmarked in ST IIa Chiro-I reconstructions, despite being documented in the nearby ST M25 (Mroczkowska, et al. 2021). This could be due to the partial mixing of archaeological layers and essential human impact on deposit formation.

No clear results for the last millennium were obtained from ST IIa core, which is partly due to the uncertainty of our depth/age model between 95 and 59 cm. Surprisingly, some reconstructions based on SNP TS and Fn TS suggest that the Middle Ages (ca. 0.75–0.60 kyr cal BP) and the last two centuries were colder than early Modern Times (0.60–0.20 kyr cal BP), while others, based on Rn TS, indicate cool events at ca. 0.65–0.55 kyr cal BP and 0.45–0.35 kyr cal BP. The Rn TS records are closer to historical sources. An increasing trend was observed in the sedimentology of GS1, indicating stronger continentality (Mikolaskova, 2009).

4.3. The global fluctuations in the state of biota and lakes

According to the SOM, the GSPB biocoenosis has gone through four well defined stages from Late Weichselian to Modern Times: 1) Late Weichselian initial stage (and later hiatus in the early Holocene) (SOM V cluster), 2) late phase of Early Holocene – Middle Holocene stage 9.0–5.7 kyr cal BP (X cluster), 3a) late phase of Middle Holocene up to

early Modern Times (5.7–0.25 kyr cal BP) (Y_1 - Z_1 subclusters), 3b) archaeological layer on 4.85–3.9 kyr cal BP (Y_2 subcluster), 4) Modern Times (0.25–0.10 kyr cal BP; Z_2 subcluster (Fig. 6).

The initial stage of GSPB biocenosis development is characterised by a very low abundance of both chironomids and water fleas, and a near absence of plant macrofossils and diatoms. No highly-significant indicator taxa were found for subcluster V of SOM (Fig. 7, Tab. S1), suggesting that the conditions were very changeable and unfavorable for aquatic organisms. Nonetheless, it appears that at least a seasonal water body existed in the basin from the beginning, because both midges and Cladocera were frequent through stage V and were represented by relatively diverse communities. In the early part of stage V, corresponding to the Late Weichselian, only very few head capsules were found, representing various species. Similarly, the initial cladoceran species were immigrants that colonised the area following the retreat of the ice; their frequency was connected with the seasonality of the ice sheet, which melted during the summers with a longer open-water period as a result of melting. This indicates that astatic water bodies derived from melting dead ice blocks were accidentally colonised by random species (but cold-adapted), although colonisation of the local landscape by midges and water fleas started very early, even during deglaciation. These would have been mostly taxa typical of the boreal zone rather than the high arctic (Hofmann, 2000; Nazarova et al., 2015). Later, from ca. 555 cm, the community composition became better defined, and the subfossil concentration increased, indicating that the permanent water body may have been inhabited by ecologically diverse, stable communities during the late stage, maybe from the Late Weichselian or even the early Holocene. Similar was stated by Birks et al., (2012) and Flössner, (2000).

The X-cluster stage is defined by a very high abundance of Cladocera and the presence of a group of cladoceran indicator taxa (Fig. 7, S3). The palaeolake was predominated by species typical of more mesotrophic conditions, dwelling at the lake bottom sediment, as well as various macrophytes dwelling in the lake bottom sediment (*Alona affinis*, *Eurycerus lamellatus*, *Leydigia leydigii*, *Coronatella rectangula*, *Chydorus sphaericus*, *Disparalona rostrata*, *Pleuroxus uncinatus*, *Acroperus harpae*, *Monospilus dispar*), and in the pelagic zone (Bosminidae). The ample subfossils of sediment-associated taxa may indicate an inwash of both mineral and organic matter from the lake basin, or with the Serteyka River waters during spring floods (Pawlowski et al., 2016a). Although the water would have been more turbid during intense precipitation or snowmelt in spring, populations of sediment-associated water fleas could develop (Plóciennik et al., 2020). The WDB study case predicts that spring flood episodes would become more frequent with global warming, suggesting that spring flood episodes could also become more intense during the HTM (Danilovich et al., 2019). The water quality was good, as confirmed by diatom indicators of cluster stage X_2 – *Cavinula scutelloides* and *Fragilaria inflata*. Thanks to the clear water, phytoplankton (algae and diatoms) would have reached high populations during the dry, warm season and hosted abundant water flea guilds.

In cluster stages Y_1 - Z_1 , the presence of macrophyte-associated cladocerans and periphyton diatoms suggests the existence of macrophyte vegetation in the lake, with patches of *Chara* spp. and *Potamogeton* spp. However, the identified midge indicator taxa indicate that the conditions among the macroinvertebrates at that time were particularly suitable for sediment-associated dwellers (Moller Pillot, 2009, 2013). An interesting finding is the occurrence of the diatom *Pantocsekia comensis*, which grows on ice floes in early spring (Rühland et al., 2008; Saros and Anderson, 2015; Winder et al., 2009). Its presence confirms that the GSPB was supplied by ice floes and snow from the Serteyka River in early spring, also during the HTM. It was during cluster stages Y_1 - Z_1 that the chironomids, and later diatoms, found the best conditions to develop; in addition, during this period, the Cladocera dominated among the sediment-associated taxa typical of more turbid conditions. In addition, these changes were correlated with short-term increases in the frequency of pelagic species, which may indicate occasional

flooding, resulting in an added inflow of mineral matter from the Serteyka River basin (Luoto et al., 2011; Pawłowski et al., 2015b; Richardson, 1992).

The only mollusc indicator of the Y_1 -cluster samples was *Valvata cristata*. It inhabits small, strongly overgrown water bodies and marshes, and is often found in places where the bottom is covered with macrophytes (Piechocki and Wawrzyniak-Wydrowska, 2016). The other mollusc shells were left by species preferring permanent water bodies such as lakes, ponds and bays, and tend to demonstrate wide ecological preference. During cluster Z_1 , i.e. in the Middle Ages and early Modern Times, the sediment-associated taxa were replaced by phytophilous in chironomid guilds, suggesting that the palaeolake was substantially shallow (Brooks et al., 2007; Moller Pillot, 2013; Vallenduuk and Pillot, 2007). The GSPB shores were overgrown by sedge rushes. The diatoms were represented by species characteristic of shallow, eutrophic littoral areas overgrown by aquatic vegetation, which might reflect the input of nutrients to the water (Niyatbekov and Barinova, 2018; Sládeček, 1986; Zawiska et al., 2019, 2020). The environmental conditions, despite being favorable for littoral chironomids and diatoms, were not so suitable for the Cladocera assemblages, and no characteristic taxa were observed; it is likely that this was due to progressive terrestrialisation, which would have occurred during dry phases. In this case, only a few taxa would have appeared in ephemeral pools (Pawlowski et al., 2015a, 2015b). The conditions were oxidizing, as demonstrated by low Fe/Mn ratios, with the Ca/Fe ratio remaining highly variable throughout most of the Holocene sedimentary section. This may suggest that interpretation of these elements is dependent on catchment-scale variables, such as lithology, forestation and nutrient input (Zander et al., 2021).

The stage defined by midges and diatoms, representing the natural palaeolake ecosystem development, was interrupted by archaeological layer Y_2 , similar to those described from the shore zone sequence (Kittel et al., 2021). It included a number of indicators that were elements of the pile-dwellings constructions, e.g. moss, bark, and wood remains, as well as accumulated fish bones and water chestnut fruits that had been consumed by the Late Neolithic inhabitants. There were also numerous bryozoan statoblasts concentrated in the vicinity of the pile-dwellings (Kittel et al., 2021). Law (2013) indicates that the presence of statoblasts at archaeological excavations generally reflect flooding phases, as bryozoans are aquatic sedentary benthic organisms, similarly to many diatoms. Bryozoan colonies overgrow underwater constructions, and hence they may be synanthropic organisms on pile-dwellings. They do not decompose wooden underwater constructions as they just use hard substrate for sedent and not mine inside the wood. The SOM and ISA analyses clearly associate them with other macrofossils in the Y_2 Neolithic archaeological layer. The geochemical ratios confirm human settlement at layer Y_2 (Figs. 8, 9).

The final stage of the palaeolake development (cluster Z_2), beginning in the 18th c. AD, was defined by the occurrence of a number of littoral peryphitic diatoms. The water body was very shallow at that time and overgrown by lakeshore bulrush (Cejudo-Figueiras et al., 2011; Ludi-kova, 2016). The water quality was probably poor, as indicated by the presence of diatoms typical of hypertrophic waters. The final stage of the basin was not paludified to a mire, but rather transformed to a semi-aquatic swampy habitat influenced by floods (Besse-Lototskaya et al., 2011; Ejarque et al., 2015; Wiklund et al., 2010); this would have succeeded to wet rush, which was probably used by local people for their households.

5. Conclusion

The present paper is the first high-resolution multi-proxy study to include quantitative reconstructions from the Western Dvina Lakeland encompassing the long Late Weichselian and Holocene sequence. The findings of the multi-proxy study of the Great Serteyka Palaeolake Basin system contribute significantly to our understanding of the palaeolimnology of East European lakes. The high resolution of the

palaeozoological and geochemical analyses of the mineral fraction in the biogenic sediments, along with reliable depth/age model, document the reaction of the lake's ecosystem to: i) climate change and its impact on the type of denudation processes during the Late Weichselian and the Holocene, ii) hydrology with frequent water level extremes in winter and spring, and iii) the human impact from the Neolithic to the Modern period. For this reason, we used the Self-Organizing Map and different hydroclimatic reconstructions based on the chironomid and cladoceran assemblages.

The SOM method enabled five stages of presented ecosystem development to be defined. Firstly, the initial stage after the Valdai ice sheet regression, from ca. 18 to 9.0 kyr cal BP indicated the presence of astatic water bodies derived from melting dead ice blocks.

The second stage (ca. 9.0–5.7 kyr cal BP) represents mesotrophic lakes with well-developed pelagic zone, which have been interrupted by an inwash of mineral and organic matter, transported from the lake basin and material borne by the Serteyka River waters during spring floods, during the HTM.

The third stage (ca. 5.7–4.9 kyr cal BP) is indicative of the lake habitats transitioning from an open sediment bottom to once covered by macrophytes with simultaneous eutrophication. It also has been supplied by ice floes and snow from the Serteyka River in early spring, as well as during the HTM.

The fourth stage (ca. 4.8–3.9 kyr cal BP) was characterised by rich remains of moss, bark, wood remains that were elements of the Middle and Late Neolithic pile-dwellings constructions. A hiatus in sedimentation was observed between the late Neolithic and early Modern Times, followed by the final stage of the basin evolution (ca. last 250 yr cal BP) which was characterised by shallow, semiaquatic swampy habitat, eutrophicated by the local human settlement and influenced by floods.

The chironomid-based summer mean air temperature reconstruction from GSPB displays the HTM at 8.5–7.7 kyr cal BP (ca. 17–20 °C), no clear cool oscillations at 8.2 kyr cal BP but remarkable 7.0–6.8 kyr cal BP and 5.8–5.9 oscillations. 4.2 kyr cal BP event is better documented by previous reconstructions provided by Mroczkowska et al. (2021) from the shallow zone core of the lake. The Little Ice Age cooling is reflected by all four CH-I temperature reconstructions but its timing and trends are inconsistent between reconstructions. In turn, the Cladocera-inferred summer temperature reconstruction indicates higher temperatures at Late Weichselian and Holocene than chironomid reconstruction. We suppose that this situation was connected with the fact that the water level was the main driver of the water fleas communities. Although cladoceran-depth reconstruction values during the Late Weichselian did not correspond very well with the geological or geomorphological situation (reconstruction indicated that the palaeolake was much deeper), this method shows much more pronounced lake level variation for the Late Holocene than other proxy. All of this suggests that the GSPB could be regarded as representative of the regional lake-river systems which exist(ed) in Eastern Europe.

Declaration of Competing Interest

The authors declare that they have no known competing financial interests or personal relationships that could have appeared to influence the work reported in this paper.

Acknowledgements

The research project is financed by a grant from the "National Science Centre", Poland based on the decision No. 2017/25/B/HS3/00274. Archaeological research at the Serteya II site was supported by the Russian Science Foundation (project N°19-78-00009). We want to thank M. Słowiński, Ph.D. for the very constructive discussions during the paper preparation, English native speaker Edward Lowczowski, MSc and Jarosław Sawiuk, MSc for linguistic correction.

Appendix A. Supplementary data

Supplementary data to this article can be found online at <https://doi.org/10.1016/j.catena.2022.106206>.

References

- Abramow, L., 1972. Opisaniya prirody nashey strany: Razvitiye fiziko-geograficheskikh kharakteristik. Moskva, Mysl, p. 448.
- Alexandrowicz, S.W., 1987. Analiza malakologiczna w badaniach osadów czwartorzędowych. Geologia 13, 1–240.
- Alexandrowicz, S.W., Alexandrowicz, W.P., 2011. Analiza malakologiczna: metody badania i interpretacji. Kraków, Polska Akademia Umiejętności, p. 304.
- Alhoniemi, E., Hollmén, J., Simula, O., Vesanto, J., 1999. Process monitoring and modeling using the self-organizing map. Integr. Comput.-Aided Eng. 6, 3–14.
- Alley, R.B., Agustsdóttir, A.M., 2005. The 8k event: cause and consequences of a major Holocene abrupt climate change. Quat. Sci. Rev. 24, 1123–1149.
- Alley, R.B., Mayewski, P.A., Sowers, T.A., Stuiver, M., Taylor, K.C., Clark, P.U., 1997. Holocene climatic instability: A prominent, widespread event 8200 yr ago. Geology 25, 483–486.
- Alpat'ev, A.M., Arkhangel'skiy, A.M., Podoplelov, N.Y.A., Stepanov, A.Y.A., 1976. Fizicheskaya geografiya SSSR (A ziatksaya chast'). Moskva, Vysshaya shkola, p. 448.
- Andersen, T., Cranston, P., Epler, J., 2013. Chironomidae of the Holarctic Region: Keys and Diagnoses: Larvae. Scandinavian Soc. Entomol. 573.
- Andreev, A.A., Tarasov, P.E., Schwamborn, G., Ilyashuk, B.P., Ilyashuk, E.A., Bobrov, A., Klimanov, V.A., Rachold, V., Hubberten, H., 2004. Holocene paleoenvironmental records from Nikolay Lake, Lena river delta, arctic Russia. Palaeogeogr. Palaeoclimatol. Palaeoecol. 209, 197–217.
- Andronikov, A.V., Subetto, D., Lauretta, D.S., Andronikova, I.E., Drosenko, D., Kuznetsov, D.D., Sapelko, T.V., Syrykh, L., 2014. In search for fingerprints of an extraterrestrial event: Trace element characteristics of sediments from the lake Medvedevskaya (Karelian Isthmus, Russia). Dokl. Earth Sci. 457, 819–823.
- Apolinarska, K., Woszczyk, M., Obrembska, M., 2012. Late Weichselian and Holocene palaeoenvironmental changes in northern Poland based on the Lake Skrzynka record. Boreas 41, 292–307.
- Arslanov, K.A., 1993. Late Pleistocene geochronology of European Russia. Radiocarbon 35, 421–427.
- Arslanov, K.A., Saveljeva, L.A., Klimanov, V.A., Chernov, S.B., Maksimov, F., Tertychnaya, T.V., Subetto, D.A., 2001. New data on chronology of landscape-paleoclimatic stages in Northwestern Russia during the Late Glacial and Holocene. Radiocarbon 43, 581–594.
- Badałuć, C.-A., Persoou, A., Ionita, M., Piotrowska, N., 2020. Stable isotopes in cave ice suggest summer temperatures in east-central Europe are linked to Atlantic Multidecadal Oscillation variability. Clim. Past 16, 2445–2458.
- Bailey, H.L., Hubbard, A., Klein, E.S., Mustonen, K., Akers, P.D., Marttila, H., Welker, J. M., 2021. Arctic sea-ice loss fuels extreme European snowfall. Nat. Geosci. 1–6.
- Baker, C.A., 2012. The Holocene 8200 BP event: its origin, character and significance. Mercian Geol. 18, 47–54.
- Bałwierz, Z., Goździk, J., 1997. Paleśrodowiskowe zmiany w świetle analiz palinologicznych późnovidzialińskich osadów węglanowych w zagłębiach bezodpływowych w Bełchatowie. Acta Universitatis Lodzienensis. Folia Geographica Physica 1, 7–21.
- Batt, R.D., Carpenter, S.R., Ives, A.R., 2017. Extreme events in lake ecosystem time series. Limnol. Oceanogr. Lett. 2, 63–69.
- Battarbee, R.W., 1986. Diatom analysis. in: Berglund B.E. (Ed.), Handbook of Holocene palaeoecology and palaeohydrology. John Wiley & Sons Ltd., London, pp. 527–70.
- Beaver, J.R., Tausz, C.E., Black, K.M., Bolam, B.A., 2020. Cladoceran body size distributions along temperature and trophic gradients in the conterminous USA. J. Plankton Res. 42, 613–629.
- Bednorz, E., 2004. Snow cover in eastern Europe in relation to temperature, precipitation and circulation. Int. J. Climatol.: A J. Royal Meteorol. Soc. 24, 591–601.
- Beijerinck, H., Stevens, M., Verster, N., 1976. Monte-Carlo of molecular flow through a cylindrical channel. Physica B+C 83, 209–219.
- Besse-Lototskaya, A., Verdonschot, P.F., Coste, M., Van de Vijver, B., 2011. Evaluation of European diatom trophic indices. Ecol. Ind. 11, 456–467.
- Birks, H.H., 1980. Plant macrofossils in Quaternary lake sediments. Archiv für Hydrobiologie, Stuttgart 15, 1–60.
- Birks, H.H., Jones, V.J., Brooks, S.J., Birks, H.J., Telford, R.J., Juggins, S., Peglar, S.M., 2012. From cold to cool in northernmost Norway: Lateglacial and early Holocene multi-proxy environmental and climate reconstructions from Jansvatnet, Hammerfest. Quat. Sci. Rev. 33, 100–120.
- Bjerring, R., Bécarès, E., Declerck, S.A., Gross, E.M., Hansson, L., Kairesalo, T., Nykänen, M., Halkiewicz, A., Korniłow, R., Conde-Porcuna, J.M., Seferlis, M., Nöges, T., Moss, B., Amsinck, S.L., Odgaard, B.V., Jeppesen, E., 2009. Subfossil Cladocera in relation to contemporary environmental variables in 54 Pan-European lakes. Freshw. Biol. 54, 2401–2417.
- Błaszkiewicz, M., 2005. Północnoatlantyczna ewolucja obniżeń jeziornych na Pojezierzu Kociewskim (wschodnia część Pomorza). IGiPZ PAN, Warszawa 201, 192.
- Błaszkiewicz, M., 2007. Geneza i ewolucja mis jeziornych na młodoglacjalnym obszarze Polski – wybrane problemy. Studia Limnologica et Telmatologica 1, 5–16.
- Błaszkiewicz, M., 2008. Wytapianie się pogrzebanych brył martwego lodu w północnym głacjalnym holocenie a zdarzenia ekstremalne. Landform Analysis 8, 9–12.

- Błaszkiewicz, M., Piotrowski, J.A., Brauer, A., Gierszewski, P., Kordowski, J., Kramkowski, M., Lamparski, P., Lorenz, S., Noryskiewicz, A.M., Ott, F., Słowiński, M., Tyszkowski, S., 2015. Climatic and morphological controls on diachronous postglacial lake and river valley evolution in the area of Last Glaciation, northern Poland. *Quat. Sci. Rev.* 109, 13–27.
- Bledzki, L.A., Rybak, J.I., 2016. Cladocera Morphology. Freshwater Crustacean Zooplankton of Europe. Springer, Cham, pp. 95–101.
- Bond, G.C., Kromer, B., Beer, J., Muscheler, R., Evans, M.N., Showers, W.J., Hoffmann, S.S., Lotti-Bond, R., Hajdas, I., Bonani, G., 2001. Persistent solar influence on North Atlantic climate during the Holocene. *Science* 294, 2130–2136.
- Bond, G.C., Showers, W.J., Cheseby, M., Lotti, R., Almasi, P.F., de Menocal, P.B., Priore, P., Cullen, H.M., Hajdas, I., Bonani, G., 1997. A pervasive millennial-scale cycle in North Atlantic Holocene and glacial climates. *Science* 278, 1257–1266.
- Bova, S., Rosenthal, Y., Liu, Z., Godad, S.P., Yan, M., 2021. Seasonal origin of the thermal maxima at the Holocene and the last interglacial. *Nature* 589, 548–553.
- Bronk Ramsey, C., Heaton, T.J., Blaauw, M., Blackwell, P.G., Reimer, P.J., Scott, M., 2020. New approaches to radiocarbon calibration arising from statistical developments in IntCal20. *EGU General Assembly Conference Abstracts*, pp. 9422.
- Brooks, S.J., Heiri, O., Langdon, P.G., 2007. The identification and use of palaeartic chironomidae larvae in palaeoecology. Quaternary Research Association, London, p. 276.
- Cappers, R.T., Bekker, R.M., Jans, J.E., 2012. Digital seed atlas of the Netherlands. Barkhuis, Netherlands, p. 528.
- Cejudo-Figueiras, C., Álvarez-Blanco, I., Bécares, E., Blanco, S., 2011. Epiphytic diatoms and water quality in shallow lakes: the neutral substrate hypothesis revisited. *Mar. Freshw. Res.* 61, 1457–1467.
- Clift, P.D., Olson, E.D., Lechnowskyj, A.N., Moran, M.G., Barbato, A.K., Lorenzo, J.M., 2019. Grain-size variability within a mega-scale point-bar system, False River, Louisiana. *Sedimentology* 66, 408–434.
- Danilovich, I., Zhuravlev, S., Kurochkina, L., Groisman, P., 2019. The Past and Future Estimates of Climate and Streamflow Changes in the Western Dvina River Basin. *Front. Earth Sci.* 7, 204. <https://doi.org/10.3389/feart.2019.00204>.
- Davydova, N., Servant-Vildary, S., 1996. Late Pleistocene and Holocene history of the lakes in the Kola Peninsula, Karelia and the north-western part of the east European plain. *Quat. Sci. Rev.* 15, 997–1012.
- Davydova, N.N., Subetto, D.A., Khomutova, V.I., Sapelko, T.V., 2001. Late Pleistocene-Holocene paleolimnology of three north-western Russian lakes. *J. Paleolimnol.* 26, 37–51.
- Dolukhanov, P., Gey, N., Miklyayev, A., Mazurkewicz, A., 1989. Rudnya-Serteya, a stratified dwelling-site in the Upper Dvina basin (a multidisciplinary research). *Fennoscandia Archaeologica* 6, 23–27.
- Dufrène, M., Legendre, P., 1997. Species assemblages and indicator species: the need for a flexible asymmetrical approach. *Ecological Monographs* 67, 345–366.
- Dzieduszyńska, D.A., 2019. Timing of environmental changes of the Weichselian decline (18.0–11.5 ka cal BP) using frequency distribution of ^{14}C dates for the Łódź region, Central Poland. *Quaternary International* 501, 135–146.
- Dzieduszyńska, D.A., Forysiak, J., 2019. Chronostratigraphy of the late Vistulian in Central Poland and the correlation with Vistulian glacial phases. *Stud. Quat.* 137–145.
- Ejnarque, A., Beauger, A., Miras, Y., Peiry, J., Volodire, O., Vautier, F., Benbakkar, M., Steiger, J., 2015. Historical fluvial palaeodynamics and multi-proxy palaeoenvironmental analyses of a palaeochannel, Allier River, France. *Geodin. Acta* 27, 25–47.
- Ellenberg, H., 1991. Zeigerwerte von pflanzen in Mitteleuropa. *Scripta Geobotanica* 18, 1–248.
- Engstrom, D.R., Wright Jr, H., 1984. Chemical stratigraphy of lake sediments as a record of environmental change. Lake sediments and environmental history: studies in paleolimnology and palaeoecology in honour of Winifred Tutin/edited by EY Haworth and JWG Lund. Leicester University Press, Leicester, pp. 11–67.
- Enters, D., Kirilova, E., Lotter, A.F., Lücke, A., Parplies, J., Jahns, S., Kuhn, G., Zolitschka, B., 2010. Climate change and human impact at Sacrower See (NE Germany) during the past 13,000 years: a geochemical record. *J. Paleolimnol.* 43, 719–737.
- Eusterhues, K., Rumpel, C., Kögel-Knabner, I., 2005. Organo-mineral associations in sandy acid forest soils: Importance of specific surface area, iron oxides and micro pores. *Eur. J. Soil Sci.* 56, 753–763.
- Faustova, M., 1994. Deglyatsiatsiya i tipy lednikovogo rel'yfa na territorii yevropeyskoy chasti USSR. In: Velichko, A.A., Starke, L. (Eds.), Paleogeograficheskaya osnova sovremennykh landshaftov. Nauka, Moscow, pp. 30–40.
- Faustová, M., 2011. Phylogeny, taxonomy and systematics of selected members of the family Bosminidae. Charles University in Prague Faculty of Science Department of Ecology, Prague. PhD thesis.
- Flössner, D., 1972. Kiemen-und Blattfüßer, Branchiopoda-Fischläuse, Branchiura: Krebstiere. Veb Gustav Fischer Verlag, Jena. Die Tierwelt Deutschlands 60, Jena, pp. 499.
- Flössner, D., 2000. The Haplopoda and Cladocera (without Bosminidae) in Central Europe. Backhuys Publishers, Leiden, Backhuys, Leiden, The Netherlands, p. 428.
- Folk, R.L., Ward, W.C., 1957. Brazos River bar [Texas]; a study in the significance of grain size parameters. *J. Sediment. Res.* 27, 3–26.
- Forysiak, J., Kloss, M., Obrembska, M., Żurek, S., 2014. Lateglacial and Holocene sediments of some valley peatlands in the Łódź region in relation to palaeoenvironmental changes. *Folia Quaternaria* 82, 5–30.
- Frey, D., 1986. Cladocera Analysis. In: Berglund, B.E. (Ed.), *Handbook of Holocene Palaeoecology and Palaeohydrology*. John Wiley & Sons, London, pp. 677–692.
- Gittenberger, E., Piel, W., Groenenberg, D., 2004. The Pleistocene glaciations and the evolutionary history of the polypolyt snail species *Arianta arbustorum* (Gastropoda, Pulmonata, Helicidae). *Mol. Phylogen. Evol.* 30, 64–73.
- Gorlach, A., Kalm, V., Hang, T., 2015. Thickness distribution of quaternary deposits in the formerly glaciated part of the East European plain. *J. Maps* 11, 625–635.
- Grichuk, D.V., Borisov, M.V., Mel'nikova, G.L., 1985. Thermodynamic Modelling of a Hydrothermal System in Oceanic Crust: the Evolution of Fluid Compositions. *Int. Geol. Rev.* 27 (9), 1097–1115.
- Grimm, E.C., 2016. TILIA 2.1. 1. Illinois state museum, Springfield.
- Grosswald, M., 1980. Late Weichselian ice sheet of northern Eurasia. *Quat. Res.* 13, 1–32.
- Guiry, M., Guiry, G., 2017. AlgaeBase. World-wide electronic publication, National University of Ireland, Galway. 2017. URL: <http://www.algaebase.org>.
- Hairston, J.N., G., 1996. Zooplankton egg banks as biotic reservoirs in changing environments. *Limnology and Oceanography*, 41, 1087–1092.
- Hakala, A., Sarmaja-Korjonen, K., Miettinen, A., 2004. The Origin and Evolution of Lake Vähä-Pitkusta, SW Finland – A Multi-Proxy Study of a Meromictic Lake. *Hydrobiologia* 527, 85–97.
- Heiri, O., Lotter, A.F., Lemcke, G., 2001. Loss on ignition as a method for estimating organic and carbonate content in sediments: reproducibility and comparability of results. *J. Paleolimnol.* 25, 101–110.
- Hillbrand, M., van Geel, B., Hasenfratz, A., Hadorn, P., Haas, J.N., 2014. Non-pollen palynomorphs show human- and livestock-induced eutrophication of Lake Nussbaumersee (Thurgau, Switzerland) since Neolithic times (3840 BC). *The Holocene* 24, 559–568.
- Hinderer, M., 2001. Late Quaternary denudation of the Alps, valley and lake fillings and modern river loads. *Geodin. Acta* 14, 231–263.
- Hofmann, W., 2000. Response of the chydorid faunas to rapid climatic changes in four alpine lakes at different altitudes. *Palaeogeogr. Palaeoclimatol. Palaeoecol.* 159, 281–292.
- Inc, T.S., 2017. Statistica (data analysis software system), version 13.
- Juggins, S., 2001. The European diatom database. User Guide, Version 1, 72.
- Kaufman, D.S., McKay, N.P., Routson, C.C., Erb, M.P., Dätwyler, C., Sommer, P.S., Heiri, O., Davis, B.A., 2020a. Holocene global mean surface temperature, a multi-method reconstruction approach. *Sci. Data* 7, 1–13.
- Kaufman, D.S., McKay, N.P., Routson, C.C., Erb, M.P., Davis, B.A., Heiri, O., Jaccard, S.L., Tierney, J.E., Dätwyler, C., Axford, Y., Brussel, T.V., Cartapanis, O., Chase, B.M., Dawson, A., de Vernal, A., Engels, S., Jonkers, L., Marsicek, J.P., Moffa-Sánchez, P., Morrill, C., Orsi, A.J., Rehfeld, K., Saunders, K.M., Sommer, P.S., Thomas, E.K., Tonello, M.S., Toth, M., Vachula, R.S., Andreev, A.A., Bertrand, S., Biskaborn, B.K., Bringué, M., Brooks, S.J., Caniupán, M., Chevalier, M., Cwynar, L.C., Emile-Geay, J., Fegyveresi, J.M., Feurdean, A., Finsinger, W., Fortin, M.C., Foster, L.C., Fox, M.J., Gajewski, K., Grosjean, M., Hausmann, S., Heinrichs, M.L., Holmes, N., Ilyashuk, B.P., Ilyashuk, E.A., Juggins, S., Khider, D., Koinig, K.A., Langdon, P.G., Larocque-Tobler, I., Li, J., Lotter, A.F., Luoto, T.P., Mackay, A.W., Magyari, E.K., Malevich, S.B., Mark, B.G., Massaferro, J., Montade, V., Nazarova, L.B., Novenko, E.Y., Pařil, P., Pearson, E.J., Peros, M.C., Pienitz, R., Plöciennik, M., Porinchu, D.F., Potito, A., Rees, A., Reinemann, S.A., Roberts, S.J., Rolland, N., Salonen, S., Self, A., Seppä, H., Shala, S., St-Jacques, J., Stenni, B., Syrykh, L.S., Tarrats, P., Taylor, K.J., van den Bos, V., Velle, G., Wahl, E.R., Walker, I., Wilmshurst, J.M., Zhang, E., Zhilich, S., 2020b. A global database of Holocene paleotemperature records. *Sci. Data* 7, 1–34.
- Killeen, I.J., Aldridge, D., Oliver, G., 2004. Freshwater bivalves of Britain and Ireland. Field Studies Council, London, p. 119.
- Kittel, P., Mazurkevich, A.N., Dolbunova, E., Kazakov, E., Mroczkowska, A., Pavlovskaya, E., Piech, W., Plöciennik, M., Sikora, J., Teltevskaya, Y., Wieckowska-Lüth, M., 2018. Palaeoenvironmental reconstructions for the Neolithic pile-dwelling Serteya II site case study, Western Russia. *Acta Geographica Lodzienia* 107, 191–213.
- Kittel, P., Mazurkevich, A.N., Alexandrovskiy, A., Dolbunova, E., Krupski, M., Szmańda, J.B., Stachowicz-Rybka, R., Cywa, K., Mroczkowska, A., Okupny, D., 2020. Lacustrine, fluvial and slope deposits in the wetland shore area in Serteya, Western Russia. *Acta Geographica Lodzienia* 110, 103–124.
- Kittel, P., Mazurkevich, A.N., Wieckowska-Lüth, M., Pawłowski, D., Dolbunova, E., Plöciennik, M., Gauthier, E., Krapiec, M., Maigrot, Y., Danger, M., Mroczkowska, A., Okupny, D., Szmańda, J.B., Thiebaut, E., Słowiński, M., 2021. On the border between land and water: the environmental conditions of the Neolithic occupation from 4.3 until 1.6 ka BC at Serteya, Western Russia. *Geoarchaeology* 36, 173–202.
- Kohenen, T., 1982. Self-organized formation of topologically correct feature maps. *Biol. Cybern.* 43, 59–69.
- Kohenen, T., 2001. Learning Vector Quantization. In: Self-Organizing Maps. Springer Series in Information Sciences, vol 30. Springer, Berlin, Heidelberg. https://doi.org/10.1007/978-3-642-56927-2_6.
- Kokorowski, H., Anderson, P., Sletten, R., Lozhkin, A., Brown, T., 2008. Late glacial and early Holocene climatic changes based on a multiproxy lacustrine sediment record from northeast Siberia. *Arct. Antarct. Alp. Res.* 40, 497–505.
- Kondracki, J., 1992. Fizycznogeograficzna regionalizacja republik Litewskiej i Białoruskiej w układzie dziesiętnym. *Przegląd Geograficzny* 64 (3–4), 341–346.
- Korholka, A., 1999. Distribution patterns of Cladocera in subarctic Fennoscandian lakes and their potential in environmental reconstruction. *Ecography* 22, 357–373.
- Kotrys, B., Plöciennik, M., Sydor, P., Brooks, S.J., 2020. Expanding the Swiss-Norwegian chironomid training set with Polish data. *Boreas* 49, 89–107.
- Krammer, K., Lange-Bertalot, H., 2008. Bacillariophyceae 2. Ephitemiaceae. Bacillariaceae. Surirellaceae. In: Ettl, H., Gerloff, J., Heyning, H., Mollenhauer, D. (Eds.), *Süsswasserflora von Mitteleuropa* 4th. Fisher, Stuttgart, p. 596.
- Krammer, K.-L.-B., Lange-Bertalot, H., 2011. Bacillariophyceae 4. Achanthaceae. In: Ettl, H., Gärtnner, G., Gerloff, J., Heyning, H., Mollenhauer, D. (Eds.), *Süsswasserflora von Mitteleuropa*, 3rd ed. Gustav Fisher Verlag, Stuttgart, p. 437.

- Kremenetski, K., Borisova, O., Zelikson, E., 2000. The Late Glacial and Holocene history of vegetation in the Moscow region. *Paleontol. Zh.* 34, 67–74.
- Kublitsky, Y., Kulkova, M.A., Druzhinina, O., Subetto, D.A., Stančikaitė, M., Gedminienė, L., Arslanov, K.A., 2020. Geochemical Approach to the Reconstruction of Sedimentation Processes in Kamyshovoye Lake (SE Baltic, Russia) during the Late Glacial and Holocene. *Minerals* 10, 764.
- Kulkova, M., Mazurkevich, A., Dolbunova, E., Lozovsky, V., 2015a. The 8200 calBP climate event and the spread of the Neolithic in Eastern Europe. *Documenta Praehistorica* 42, 77–92.
- Kulkova, M.A., Mazurkevich, A.N., Dolbunova, E., Regert, M., Mazuy, A., Nesterov, E., Sinai, M.Y., 2015b. Late Neolithic Subsistence Strategy and Reservoir Effects in ^{14}C Dating of Artifacts at the Pile-Dwelling Site Serteya II (NW Russia). *Radiocarbon* 57, 611–623.
- Lange-Bertalot, H., Hofmann, G., Werum, M., 2011. Diatomene im Süßwasser-Benthos von Mitteleuropa. Koeltz Scientific Books, Königstein, p. 908.
- Lange-Bertalot, H.B., M.; Witkowski, A.; Tagliaventi, N., 2011b. Diatoms of Europe Vol. 6: Eunotia and some related genera. Ruggell: ARG Gantner Verlag KG, pp. 747.
- Lange-Bertalot, H.M., D., 1996. Indicators of Oligotrophy. 800 taxa representative of three ecologically distinct lake types. In: Lange-Bertalot, H. (Ed.), *Iconographia Diatomologica: Annotated Diatom Micrographs*, Ed.; A. R. G. Gantner Verlag K. G. Ruggell, Liechtenstein, pp. 390.
- Law, M., 2013. Bryozoans in archaeology. *Internet Archaeology*. 35. <https://doi.org/10.11141/ia.35.3>.
- Leck, S., Scardi, M., Verdonschot, P.F.M., Descy, J.P., Park, Y.S., 2005. Modelling Community Structure in Freshwater Ecosystems. Springer-Verlag, Berlin, p. 518.
- Lenz, M., Savelieva, L.A., Frolova, L.A., Cherezova, A.A., Moros, M., Baumer, M., Gromig, R., Kostromina, N., Nigmatullin, N., Kolka, V., Wagner, B., Fedorov, G.B., Melles, M., 2021. Lateglacial and Holocene environmental history of the central Kola region, northwestern Russia revealed by a sediment succession from Lake Imandra. *Boreas* 50, 76–100.
- Li, C., Born, A., 2019. Coupled atmosphere-ice-ocean dynamics in Dansgaard-Oeschger events. *Quat. Sci. Rev.* 203, 20.
- Litt, T., Brauer, A., Goslar, T., Merkt, J., Balaga, K., Müller, H., Ralska-Jasiewiczowa, M., Stebich, M., Negendank, J.F., 2001. Correlation and synchronisation of Lateglacial continental sequences in northern central Europe based on annually laminated lacustrine sediments. *Quat. Sci. Rev.* 20, 1233–1249.
- Lotter, A.F., Höller, A., 1994. A high-resolution late-glacial and early Holocene environmental history of Rotmeier, southern Black Forest (Germany). *Dissertationes Botanicae* 234, 365–388.
- Ložek, V., 1964. Quartärmollusken der Tschechoslowakei. (Rozpravy Ústředního ústavu geologického 31) Verlag der Tschechoslowakischen Akademie der Wissenschaften, Praha, pp. 374.
- Ludikova, A., 2016. Surface-sediment diatom assemblages of the urban ponds of St. Petersburg, Russia. *Inland Water Biology* 9, 274–282.
- Luoto, T.P., Kotrys, B., Plöciennik, M., 2019. East European chironomid-based calibration model for past summer temperature reconstructions. *Climate Research* 77, 63–76.
- Luoto, T.P., Nevalainen, L., 2017. Quantifying climate changes of the Common Era for Finland. *Clim. Dyn.* 49, 2557–2567.
- Luoto, T.P., Nevalainen, L., Kultti, S., Sarmaja-Korjonen, K., 2011. An evaluation of the influence of water depth and river inflow on quantitative Cladocera-based temperature and lake level inferences in a shallow boreal lake. *Hydrobiologia* 676, 143–154.
- Magny, M., Bégeot, C., 2004. Hydrological changes in the European midlatitudes associated with freshwater outbursts from Lake Agassiz during the Younger Dryas event and the early Holocene. *Quat. Res.* 61, 181–192.
- Magny, M., Bégeot, C., Guiot, J., Peyron, O., 2003. Contrasting patterns of hydrological changes in Europe in response to Holocene climate cooling phases. *Quat. Sci. Rev.* 22, 1589–1596.
- Magny, M., Beaulieu, J.L., Drescher-Schneider, R., Vanniére, B., Walter-Simonnet, A., Miras, Y., Millet, L., Bossuet, G., Peyron, O., Brugia, E., Leroux, A., 2007. Holocene climate changes in the central Mediterranean as recorded by lake-level fluctuations at Lake Accesa (Tuscany, Italy). *Quat. Sci. Rev.* 26, 1736–1758.
- Marks, L., 2012. Timing of the Late Vistulian (Weichselian) glacial phases in Poland. *Quat. Sci. Rev.* 44, 81–88.
- Matero, I.S.O., Gregoire, L.J., Ivanovic, R.F., Tindall, J.C., Haywood, A.M., 2017. The 8.2 ka cooling event caused by Laurentide ice saddle collapse. *Earth Planet. Sci. Lett.* 473, 205–214.
- Mauquoy, D., Van Geel, B., 2007. Plant macrofossil methods and studies. *Mire and Peat Macros*. In: Elias, S.A. (Ed.), *Encyclopedia of Quaternary Science*. Elsevier, Oxford, pp. 2315–2336.
- Mazei, Y.A., Tsyanov, A.N., Bobrovsky, M.V., Mazei, N.G., Kupriyanov, D.A., Gaika, M., Rostanets, D.V., Khazanova, K.P., Stoiko, T.G., Pastukhova, Y.A., Fatynina, Y.A., Komarov, A.A., Babeshko, K.V., Makarova, A.D., Saldaev, D.A., Zazovskaya, E.P., Dobrovolskaya, M.V., Tiunov, A.V., 2020. Peatland Development, Vegetation History, Climate Change and Human Activity in the Valdai Uplands (Central European Russia) during the Holocene: A Multi-Proxy Palaeoecological Study. *Diversity* 12, 462.
- Mazurkevich, A., Dolbunova, E., 2015. The oldest pottery in hunter-gatherer communities and models of Neolithisation of Eastern Europe. *Documenta Praehistorica* 42, 13–66.
- Mazurkevich, A.N., Kittel, P., Maigrot, Y., Dolbunova, E., Mroczkowska, A., Wieckowska-Lüth, M., Piech, W., 2020. Natural and anthropogenic impact on the formation of archaeological layers in a lake shore area: case study from the Serteya II site, Western Russia. *Acta Geographica Lodzienia* 110, 81–102.
- Mazurkevich, A. N., Sablin, M. V., Dolbunova, E. V., Kittel, P., Maigrot, Y., Kazakov, E., 2020b. Landscape, seasonality and natural resources use in the 3rd millennium BC by pile-dwelling communities (NW Russia). In: A. Hafner, E.D., A. Mazurkevich, E. Pranckienė, M. Hinze (Eds.), *Settling waterscapes in Europe: The archaeology of Neolithic and Bronze Age pile-dwellings*, OSPRA – Open Series in Prehistoric Archaeology, Band 1, Propylaeum, Heidelberg, pp. 17–35.
- Mazurkevich, A.N., Dolukhanov, P., Shukurov, A., G., Z., 2009a. Mesolithic and Neolithic in the Western Dvina-Lovat Area. The East European Plain on the Eve of Agriculture. BAR International Series, 164, 145–153.
- Mazurkevich, A.N., Korotkevich, B.N., Dolukhanov, P.M., Shukurov, A., Arslanov, K.A., Savel'eva, L.A., Dzinoridze, E.N., Kulkova, M.A., Zaitseva, G.I., 2009b. Climate, subsistence and human movements in the Western Dvina – Lovat River Basins. *Quaternary International*, 203, 52–66.
- McCune, B., Mefford, M., 2011. Nonparametric multiplicative regression for habitat modeling. Oregon State University. Version 1.0.MJM Software, Gleneden Beach, OR, US. Mendyk, Ł., Markiewicz, M., Bednarek, R., Świtoniak, M., Gamrat, W., Krzesiak, Ł., Sykula, M., Gerszten, L., Kupniewska, A., 2016. Environmental changes of a shallow kettle lake catchment in a young glacial landscape (Sumowskie Lake catchment), North-Central Poland. *Quaternary International* 418, 116–131.
- Meyers, P.A., Teranes, J.L., 2001. Sediment organic matter. In: Last, W.M., Smol, J.P., (Eds.) *Tracking Environmental Change Using Lake Sediments*, vol 2: Physical and Geochemical Methods, Kluwer Academic Publishers, Dordrecht, pp. 239–269.
- Mikolaskova, K., 2009. Continental and oceanic precipitation régime in Europe. *Central European J. Geosci.* 1, 176–182.
- Moller Pillot, H.K., 2009. Chironomidae larvae of the Netherlands and adjacent lowlands: biology and ecology of the Chironomini. KNNV Publishing, Zeist, p. 270.
- Moller Pillot, H., 2013. Chironomidae Larvae of the Netherlands and Adjacent Lowlands, *Biology and Ecology of the aquatic Orthocladiinae*. KNNV Publishing, Zeist, p. 320.
- Morrill, C., Le Grande, A.N., Renssen, H., Bakker, P., Otto-Bliesner, B., 2013. Model sensitivity to North Atlantic freshwater forcing at 8.2 ka. *Clim. Past* 9, 955–968.
- Mroczkowska, A., Pawłowski, D., Gauthier, E., Mazurkevich, A., Luoto, T.P., Peyron, O., Kotrys, B., Brooks, S.J., Nazarova, L.B., Syrykh, L.S., Dolbunova, E., Thiebaud, E., Plöciennik, M., Antczak-Orlewska, O., Kittel, P., 2021. Middle Holocene Climate Oscillations Recorded in the Western Dvina Lakeland. *Water* 13, 1611.
- Nazarova, L.B., Sapelko, T.V., Kuznetsov, D.D., Syrykh, L.S., 2015. Palaeoecological and palaeoclimatical reconstructions of Holocene according chironomid analysis of Lake Glubokoye sediments. *Doklady Biol. Sci.* 460, 57–60.
- Nazarova, T., Fomin, I., Dmitriev, P., Wendt, J., Janalejeva, K., 2019. Landscape and limnological research of lake systems of the northeastern borderlands of the Republic of Kazakhstan and assessment of their recreational capacity. *GeoJournal of Tourism and Geosites* 25 (2), 485–495.
- Nevalainen, L., Luoto, T.P., Kultti, S., Sarmaja-Korjonen, K., 2012. Do subfossil Cladocera and chydorid ephippia disentangle Holocene climate trends? *The Holocene* 22, 291–299.
- Nevalainen, T., Raumolin-Brunberg, H., Mannila, H., 2011. The diffusion of language change in real time: Progressive and conservative individuals and the time depth of change. *Language Variation and Change* 23, 1–43.
- Niyatbekov, T., Barinova, S., 2018. Bioindication of aquatic habitats with diatom algae in the Pamir Mountains, Tajikistan. *MOJ Ecol. Environ. Sci.* 3, 117–120.
- Novenko, E., Glasko, M., Volkova, E., Ziuganova, I., 2013. Dinamika landshaftov i klimata basseyina verkhnei Donya v sredinem i pozdnem golotsene. *Izvestiya RAN. Seriya Geograficheskaya* 2, 68–82.
- Novenko, E., Olchev, A., Desherevskaya, O., Ziganova, I., 2009. Paleoclimatic reconstructions for the south of Valdai Hills (European Russia) as paleo-analogs of possible regional vegetation changes under global warming. *Environ. Res. Lett.* 4, 045016.
- Novenko, E.Y., Tsyanov, A.N., Babeshko, K.V., Payne, R.J., Li, J., Mazei, Y.A., Olchev, A.V., 2019. Climatic moisture conditions in the north-west of the Mid-Russian Upland during the Holocene. *Geography, Environment, Sustainability* 12, 188–202.
- Novenko, E.Y., Velichko, A.A., Ziganova, I., Boettger, T., Junge, F., 2005. Dynamics of vegetation at the Late Pleistocene Glacial/Interglacial transition (new data from the center of the East European Plain). *Polish Geological Institute Special Papers* 16, 77–82.
- Novik, A., Punning, J.-M., Zernitskaya, V., 2010. The development of Belarusian lakes during the Late Glacial and Holocene. *Estonian J. Earth Sci.* 59, 63–79.
- Okupny, D., Borówka, R.K., Cedro, B., Ślawińska, J., Tomkowiak, J., Michczyński, A., Kozłowska, D., Kowalski, K., Siedlik, K., 2020. Geochemistry of a sedimentary section at the Wawelnicza archaeological site, Szczecin Hills (Western Pomerania). *Acta Geographica Lodzienia* 110, 169–186.
- Panin, A., Matlakhova, E., 2015. Fluvial chronology in the East European Plain over the last 20 ka and its paleohydrological implications. *Catena* 130, 46–61.
- Park, Y.-S., Chung, Y.-J., 2006. Hazard rating of pine trees from a forest insect pest using artificial neural networks. *For. Ecol. Manage.* 222, 222–233.
- Pawlowski, D., 2011. Evolution of an Eemian lake based on Cladocera analysis (Konin area, Central Poland). *Acta Geol. Pol.* 61, 441–450.
- Pawlowski, D., 2017. Younger Dryas climatic reconstructions in central Poland. *Acta Geol. Pol.* 67, 441–450.
- Pawlowski, D., Borówka, R.K., Kowalewski, G., Luoto, T.P., Milecka, K., Nevalainen, L., Okupny, D., Plöciennik, M., Woszczyk, M., Tomkowiak, J., Zielinski, T., 2016a. The response of flood-plain ecosystems to the Late Glacial and Early Holocene hydrological changes: a case study from a small Central European river valley. *Catena* 147, 411–428.
- Pawlowski, D., Borowka, R.K., Kowalewski, G.A., Luoto, T.P., Milecka, K., Nevalainen, L., Okupny, D., Tomkowiak, J., Zielinski, T., 2016b. Late Weichselian and Holocene

- record of the paleoenvironmental changes in a small river valley in Central Poland. *Quat. Sci. Rev.* 135, 24–40.
- Pawlowski, D., Gruszka, B., Gallas, H., Petera-Zganiacz, J., 2013. Changes in the biota and sediments of glacial Lake Koźmin, Poland, during the late Saalian (Illinoian). *J. Paleolimnol.* 49, 679–696.
- Pawlowski, D., Kowalewski, G., Milecka, K., Płociennik, M., Woszczyk, M., Zieliński, T., Okupny, D., Włodarski, W., Forysiak, J., 2015a. A reconstruction of the palaeohydrological conditions of a flood-plain: a multi-proxy study from the Grabia River valley mire, central Poland. *Boreas* 44, 543–562.
- Pawlowski, D., Płociennik, M., Brooks, S.J., Luoto, T.P., Milecka, K., Nevalainen, L., Peyron, O., Self, A., Zieliński, T., 2015b. A multiproxy study of Younger Dryas and Early Holocene climatic conditions from the Grabia River paleo-oxbow lake (central Poland). *Palaeogeogr. Palaeoclimatol. Palaeoecol.* 438, 34–50.
- Piechocki, A., Wawrzyniak-Wydrowska, B., 2016. Guide to freshwater and marine Mollusca of Poland. Bogucki Wydawnictwo Naukowe, Poznań, p. 280.
- Pleskot, K., Apolinarska, K., Kołaczek, P., Suchora, M., Fojutowski, M., Joniak, T., Kotrys, B., Kramkowski, M., Słowiński, M., Woźniak, M.M., Lamentowicz, M., 2020. Searching for the 4.2 ka climate event at Lake Spore. Poland. *Catena* 191, 104565.
- Pleskot, K., Tjallingii, R., Makohonienko, M., Nowaczyk, N., Szczuciński, W., 2018. Holocene paleohydrological reconstruction of Lake Strzeszyńskie (western Poland) and its implications for the central European climatic transition zone. *J. Paleolimnol.* 59, 443–459.
- Płociennik, M., Kruk, A., Forysiak, J., Pawłowski, D., Mianowicz, K., Elias, S.A., Borówka, R.K., Kloss, M., Obremska, M., Coope, R., Krapiec, M., Kittel, P., Żurek, S.J., 2015a. Fen ecosystem responses to water-level fluctuations during the early and middle Holocene in central Europe: a case study from Wilczków, Poland. *Boreas* 44, 721–740.
- Płociennik, M., Kruk, A., Michczyńska, D.J., Birks, J., 2015b. Kohonen artificial neural networks and the indval index as supplementary tools for the quantitative analysis of palaeoecological data. *Geochronometria* 42, 189–201.
- Płociennik, M., Pawłowski, D., Vilizzi, L., Antczak-Orlewska, O., 2020. From oxbow to mire: Chironomidae and Cladocera as habitat palaeoindicators. *Hydrobiologia* 847, 3257–3275.
- Płociennik, M., Skonieczka, M., Antczak, O., Siciński, J., 2018. Phenology of non-biting midges (Diptera Chironomidae) in peatland ponds, Central Poland. *Entomologica Fennica* 29, 61–74.
- Ramsey, C.B., 2008. Deposition models for chronological records. *Quat. Sci. Rev.* 27, 42–60.
- Rasmussen, S.O., Bigler, M., Blockley, S., Blunier, T., Buchardt, S.L., Clausen, H.B., Cvijanović, I., Dahl-Jensen, D., Johnsen, S.J., Fischer, H., Gkinis, V., Guillevic, M., Hoek, W.Z., Lowe, J.J., Pedro, J.B., Popp, T.J., Seierstad, I.K., Steffensen, J.P., Svensson, A., Vallelonga, P.T., Vinther, B.M., Walker, M., Wheatley, J.J., Winstrup, M., 2014. A stratigraphic framework for abrupt climatic changes during the Last Glacial period based on three synchronized Greenland ice-core records: refining and extending the INTIMATE event stratigraphy. *Quat. Sci. Rev.* 106, 14–28.
- Reimer, P.J., Austin, W.E., Bard, E., Bayliss, A., Blackwell, P.G., Bronk Ramsey, C., Butzin, M., Cheng, H., Edwards, R.L., Friedrich, M., Grootes, P.M., Guilderson, T.P., Hajdas, I., Heaton, T.J., Hogg, A.G., Hughen, K.A., Kromer, B., Manning, S.W., Muscheler, R., Palmer, J.G., Pearson, C., van der Plicht, J., Reimer, R.W., Richards, D.A., Scott, E.M., Southon, J.R., Turney, C.S., Wacker, L., Adolphi, F., Büntgen, U., Capone, M., Fahrni, S.M., Fogtmann-Schulz, A., Friedrich, R., Köhler, P., Kudsk, S.G., Miyake, F., Olsen, J., Reinig, F., Sakamoto, M., Sookdeo, A., Talamo, S., 2020. The IntCal20 Northern Hemisphere radiocarbon age calibration curve (0–55 cal kBP). *Radiocarbon* 62, 725–757.
- Renssen, H., Seppä, H., Crosta, X., Goosse, H., Roche, D.M., 2012. Global characterization of the Holocene thermal maximum. *Quat. Sci. Rev.* 48, 7–19.
- Richardson, W.B., 1992. Microcrustacea in flowing water: experimental analysis of washout times and a field test. *Freshw. Biol.* 28, 217–230.
- Rühland, K., Paterson, A.M., Smol, J.P., 2008. Hemispheric-scale patterns of climate-related shifts in planktonic diatoms from North American and European lakes. *Glob. Change Biol.* 14, 2740–2754.
- Rybogina, N., Borisov, A., Idrisov, I., Bakushev, M., 2019. Holocene environmental history and populating of mountainous Dagestan (Eastern Caucasus, Russia). *Quat. Int.* 516, 111–126.
- Sarmaja-Korjonen, K., 2003. Chydoid ephippia as indicators of environmental change biostratigraphical evidence from two lakes in southern Finland. *The Holocene* 13, 691–700.
- Sarmaja-Korjonen, K., Nyman, M., Kultti, S., Välijanta, M., 2006. Palaeolimnological development of Lake Njargajavri, northern Finnish Lapland, in a changing Holocene climate and environment. *J. Paleolimnol.* 35, 65–81.
- Saros, J., Anderson, N., 2015. The ecology of the planktonic diatom *Cyclotella* and its implications for global environmental change studies. *Biol. Rev.* 90, 522–541.
- Schroeder, T., van't Hoff, J., López-Sáez, J.A., Viehberg, F.A., Melles, M., Reicherter, K., 2018. Holocene climatic and environmental evolution on the southwestern Iberian Peninsula: A high-resolution multi-proxy study from Lake Medina (Cádiz, SW Spain). *Quaternary Science Reviews*, 198, 208–225.
- Shelekhova, T., Lavrova, N., 2019. Paleoenvironmental reconstructions and a sedimentological evidence of paleoseismic activity ca 9000 yr BP in Karelia, NW Russia, based on lake sediment studies on Mount Vottovaara. *Baltica* 32, 190–201.
- Shelekhova, T., Vas'ko, O., Demidov, I., 2005. Paleokologicheskie usloviya razvitiya severo-zapadnogo Prionezh'ya v pozdnelednikov'e i golotsene. *Geologiya i Poleznye I skopae mye Karelii*, 8, 149–157.
- Sládeček, V., 1986. Diatoms as indicators of organic pollution. *Acta Hydroch. Hydrob.* 14, 555–566.
- Słowiński, M., Skubala, P., Zawiska, I., Kruk, A., Obremska, M., Milecka, K., Ott, F., 2018. Cascading effects between climate, vegetation, and macroinvertebrate fauna in 14,000-year palaeoecological investigations of a shallow lake in eastern Poland. *Ecol. Ind.* 85, 329–341.
- Spinoni, J., Naumann, G., Vogt, J.V., Barbosa, P., 2015. The biggest drought events in Europe from 1950 to 2012. *J. Hydrol.: Reg. Stud.* 3, 509–524.
- Starkel, L., Soja, R., Michczyńska, D.J., 2006. Past hydrological events reflected in Holocene history of Polish rivers. *Catena* 66, 24–33.
- Starkel, L., Michczyńska, D.J., Krapiec, M., Margielewski, W., Nalepka, D., Pazdur, A., 2013. Progress in the Holocene chrono-climatostratigraphy of Polish territory. *Geochronometria* 40, 1–21.
- Subetto, D., 2009. Donnye Otlozheniya Ozer: Paleolimnologicheskie Rekonstruktsii. /Nauchnaya Monografiya. RGPU im. A.I. Gertsena, Saint Petersburg, pp. 339.
- Subetto, D., Davydova, N., Kuznetsov, D., Ludikova, A., Sapelko, T., 2006. Climate and environment reconstructions of the Lake Ladoga area during the Late Holocene. In: European Large Lakes Symposium: Ecosystem changes and their ecological and socioeconomic impacts 11–15 September. Springer, Tartu, Estonia, pp. 11–15.
- Sirykh, L., Nazarova, L., Subetto, D., 2015. Preliminary data on climate development in the territory of the Karelian Isthmus during the Holocene based on the results of chironomid and lithological analyses. Trudy Karel'skogo Nauchnogo Tsentr, Rossiyskaya Akademiya Nauk, Seria Limnologiya, pp. 53–59.
- Sirykh, L., Subetto, D., Nazarova, L., 2021. Paleolimnological studies on the East European Plain and nearby regions: the PaleoLake Database. *J. Paleolimnol.* 65, 369–375.
- Szeroczyńska, K., Sarmaja-Korjonen, K., 2007. Atlas of subfossil Cladocera from Central and Northern Europe. Friends of the Lower Vistula Society, Gruczno, p. 84.
- Tarasov, P.E., Saveljeva, L.A., Long, T., Leipe, C., 2019. Postglacial vegetation and climate history and traces of early human impact and agriculture in the present-day cool mixed forest zone of European Russia. *Quat. Int.* 516, 21–41.
- Telford, R.J., 2019. Review and test of reproducibility of subdecadal resolution palaeoenvironmental reconstructions from microfossil assemblages. *Quat. Sci. Rev.* 222, 105893.
- Ter Braak, C.J., Šmilauer, P., 2002. CANOCO reference manual and CanoDraw for Windows user's guide. Software for canonical community ordination (version 4.5). Microcomputer Power, Ithaca, New York, pp. 500.
- Thomas, E.R., Wolff, E.W., Mulvaney, R., Steffensen, J.P., Johnsen, S.J., Arrowsmith, C., White, J.W., Vaughn, B.H., Popp, T.J., 2007. The 8.2 ka event from Greenland ice cores. *Quat. Sci. Rev.* 26, 70–81.
- Utkuzova, D.N., Han, V.M., Vil'fand, R.M., 2015. Statistical analysis of extreme drought and wet events in Russia. *Atmospheric and Oceanic Optics*, 28, 336–346.
- Vallenduk, H.J., Moller Pillot, H.K.M., 2007. Chironomidae Larvae. In: Tanypodinae: General Ecology and Tanypodinae, Vol. 1. KNNV Publishing, Zeist, p. 172.
- Van Damme, K., Dumont, H.J., 2008. Further division of Alona Baird, 1843: separation and position of Coronatella Dybowski & Grochowski and Ovalona gen. n. (Crustacea: Cladocera). *Zootaxa* 1960, 1–44.
- Van Damme, K., Kotov, A.A., Dumont, H.J., 2010. A checklist of names in Alona Baird 1843 (Crustacea: Cladocera: Chydoridae) and their current status: an analysis of the taxonomy of a lump genus. *Zootaxa* 2330, 1–63.
- Vasskog, K., Paasche, Ø., Nesje, A., Boyle, J.F., Birks, H., 2012. A new approach for reconstructing glacier variability based on lake sediments recording input from more than one glacier. *Quat. Res.* 77, 192–204.
- Velichko, A., Borisova, O., Kononov, Y.M., Konstantinov, E., Kurbanov, R.N., Morozova, T.D., Panin, P., Semenov, V.V., Tesakov, A.S., Timireva, S.N., Titov, V.V., Frolov, P., 2017. Reconstruction of Late Pleistocene events in the periglacial area in the southern part of the East European Plain. *Doklady Earth Science* 475, 895–899.
- Velichko, A., Timireva, S., Kremenetski, K., MacDonald, G., Smith, L., 2011. West Siberian Plain as a late glacial desert. *Quat. Int.* 237, 45–53.
- Velichko, A.A., Andreev, A., Klimanov, V., 1997. Climate and vegetation dynamics in the tundra and forest zone during the Late Glacial and Holocene. *Quat. Int.* 41, 71–96.
- Vesanto, J., Alhoniemi, E., 2000. Clustering of the self-organizing map. *IEEE Trans. Neural Networks* 11, 586–600.
- Veski, S., Seppä, H., Ojala, A.E., 2004. Cold event at 8200 yr BP recorded in annually laminated lake sediments in eastern Europe. *Geology* 32, 681–684.
- Von Grafenstein, U., Erlenkeuser, H., Müller, J., Jouzel, J., Johnsen, S., 1998. The cold event 8200 years ago documented in oxygen isotope records of precipitation in Europe and Greenland. *Climate Dynamics* 14, 73–81.
- Vyse, S.A., Herzschuh, U., Andreev, A.A., Pestryakova, L.A., Diekmann, B., Armitage, S.J., Biskaborn, B.K., 2020. Geochemical and sedimentological responses of arctic glacial Lake Ilirney, chukotka (far east Russia) to palaeoenvironmental change since ~ 51.8 ka BP. *Quat. Sci. Rev.* 247, 106607.
- Ward, J., 1963. Hierarchical grouping to optimize an objective function. *J. Am. Statistical Assoc.* 58, 236–244.
- Welter-Schultes, F.W., 2012. Case 3581Turbo bidens Linnaeus, 1758 (Gastropoda, clausiliidae): request for setting aside the neotype. *The Bulletin of Zoological Nomenclature* 69, 85–87.
- Weninger, B., Harper, T., 2015. The geographic corridor for rapid climate change in Southeast Europe and Ukraine. *Archäologie in Eurasie* 31, 475–505.
- Wieckowska-Lüth, M., Gauthier, E., Thiebaut, E., Słowiński, M., Krapiec, M., Dolbunova, E., Mazurkovich, A., Maigret, Y., Danger, M., Kittel, P., 2021. The palaeoenvironment and settlement history of a lakeshore setting: An

- interdisciplinary study from the multi-layered archaeological site of Serteya II, Western Russia. *J. Archaeol. Sci.: Rep.* 40, 103219.
- Wiklund, J.A., Bozinovski, N., Hall, R.I., Wolfe, B.B., 2010. Epiphytic diatoms as flood indicators. *J. Paleolimnol.* 44, 25–42.
- Winder, M., Reuter, J.E., Schladow, S.G., 2009. Lake warming favours small-sized planktonic diatom species. *Proceedings of the Royal Society B: Biological Sciences* 276, 427–435.
- Wohlfarth, B., Tarasov, P.E., Bennike, O., Lacourse, T., Subetto, D.A., Torsander, P., Romanenko, F.A., 2006. Late glacial and Holocene palaeoenvironmental changes in the Rostov-Yaroslavl'area, West Central Russia. *J. Paleolimnol.* 35, 543–569.
- Yanina, T.A., 2013. Biostratigraphy of the Middle and Upper Pleistocene of the Caspian region. *Quat. Int.* 284, 85–97.
- Zander, P.D., Żarczyński, M., Vogel, H., Tylmann, W., Wacnik, A., Sanchini, A., Grosjean, M., 2021. A high-resolution record of Holocene primary productivity and water-column mixing from the varved sediments of Lake Żabińskie, Poland. *Science of The Total Environment* 755, 143713.
- Zar, J., 1984. Simple linear regression. *Biostatistical Analysis* 4, 324–359.
- Zawiska, I., Dimante-Deimantovica, I., Luoto, T.P., Rzodkiewicz, M., Saarni, S., Stivrins, N., Tylmann, W., Lanka, A., Robeznieks, M., Jilbert, T., 2020. Long-term consequences of water pumping on the ecosystem functioning of Lake Sekšu, Latvia. *Water* 12, 1459.
- Zawisza, E., Zawiska, I., Szeroczyńska, K., Correa-Metrio, A., Mirosław-Grabowska, J., Obremska, M., Rzodkiewicz, M., Słowiński, M., Woszczyk, M., 2019. Dystrophication of lake Suchar IV (NE Poland): an alternative way of lake development. *Limnetica* 38, 391–416.



On the border between land and water: The environmental conditions of the Neolithic occupation from 4.3 until 1.6 ka BC at Serteya, Western Russia

Piotr Kittel¹ | Andrey Mazurkevich² | Magda Wieckowska-Lüth³ | Dominik Pawłowski⁴ | Ekaterina Dolbunova^{2,5} | Mateusz Płociennik⁶ | Emilie Gauthier⁷ | Marek Krąpiec⁸ | Yolaine Maigrot⁹ | Maxime Danger⁹ | Agnieszka Mroczkowska^{1,10} | Daniel Okupny¹¹ | Jacek Szmańda¹² | Eva Thiebaut⁷ | Michał Słowiński¹⁰

¹Department of Geology and Geomorphology, Faculty of Geographical Sciences, University of Łódź, Łódź, Poland

²The State Hermitage Museum, St. Petersburg, Russia

³Archaeobotanical and Palynological Laboratory, Institute of Prehistoric and Protohistoric Archaeology, University of Kiel, Kiel, Germany

⁴Department of Palaeoenvironmental Research, Institute of Geology, Adam Mickiewicz University, Poznań, Poland

⁵The British Museum, London, UK

⁶Department of Invertebrate Zoology and Hydrobiology, University of Łódź, Łódź, Poland

⁷Laboratoire de Chrono-Environnement, UMR CNRS 6249, Université Bourgogne Franche-Comté, Besançon, France

⁸Faculty of Geology, Geophysics, and Environmental Protection, AGH University of Science and Technology, Krakow, Poland

⁹UMR 8215 Trajectoires, CNRS-Université Paris 1 Panthéon—Sorbonne, Nanterre, France

¹⁰Past Landscape Dynamics Laboratory, Institute of Geography and Spatial Organization, Polish Academy of Sciences, Warsaw, Poland

¹¹Institute of Marine and Environmental Sciences, University of Szczecin, Szczecin, Poland

¹²Institute of Geography, Pedagogical University of Krakow, Krakow, Poland

Correspondence

Piotr Kittel, Department of Geology and Geomorphology, Faculty of Geographical Sciences, University of Łódź, ul. Narutowicza 88, PL 90-139 Łódź, Poland.
Email: piotr.kittel@geo.uni.lodz.pl

Scientific editing by Dr Kevin Walsh

Funding information

Narodowe Centrum Nauki,
Grant/Award Number: 2017/25/B/HS3/
00274; Russian Science Foundation,
Grant/Award Number: 19-78-00009; French
Ministry for Europe and Foreign Affairs

Abstract

The paper presents the results of a palaeoecological study of Neolithic archaeological layers from a wetland, multilayer site, Serteya II (Western Russia). It contains, domestic structures, rich organic artefacts, skeletons, and ecofacts preserved within lacustrine deposits that are extremely important on a European scale. We employed a set of specialised palaeoecological analyses and accelerator mass spectrometry radiocarbon dating to identify the principal environmental conditions which attracted Neolithic hunter-fisher-gatherer communities from 4300 to 1600 cal. BC. The distinct impact of communities using a nonproductive economy on the ecology of the palaeolake shore zone was recorded. Also, palaeolake water level changes influenced the palaeoeconomic activity of local Neolithic societies, such as gathering of plants (for the medicinal use or serving as dietary components), fishing activities, and possible funeral practices. In addition, the identified phases of high-water level changes, which were responses to climatic oscillations, were correlated

with supraregional climatic events, especially ca. 6.2, 5.9, and 4.2 ka cal. BP. Thus, our results allowed for the reconstruction of environment transformations and conditions of Neolithic communities' activity, as well as for a better understanding of the relationships between local Neolithic communities' way of life and neolithisation processes in Eastern Europe.

KEY WORDS

Eastern Europe, multiproxy study, Neolithic, palaeoecology, palaeoeconomy, pile-dwelling settlement, Western Dvina Lakeland

1 | INTRODUCTION

Neolithisation processes played a crucial role in the rebuilding of the economic structure of ancient human groups and human-environment relationships. Those processes, however, had a specific way of developing in Eastern Europe compared to the situation in the central and western parts of the continent. The studied region occupies a particular place in research on the development of Neolithic cultures in Eastern Europe, being attractive to ancient communities for several millennia. Those communities left sites with some of the earliest pottery in Eastern Europe and much later pile-dwelling settlements (Kul'kova et al., 2015; Mazurkevich & Dolbunova, 2015; see also Jordan et al., 2016; Piezonka et al., 2016). The nonproductive economy survived there until the 2nd millennium BC (Dolukhanov & Mazurkevich, 2000; Dolukhanov et al., 2004; Mazurkevich et al., 2009; Tarasov et al., 2019).

Archaeological research of the Serteya II site revealed the continuity of habitation and use of this place. The oldest single artefacts found here can be attributed to the Mesolithic. A short-term episode is dated to the Early Neolithic (the Serteya Culture and the Rudnya Culture) represented by several eroded pottery fragments of the 7–6th millennia BC (Mazurkevich et al., 2017). Here, for the first time in the forest zone so far in the north, materials of southern Eneolithic steppe cultures (the Khvalyn Culture, Sredny Stog Culture, and Mariupol Culture) of the 5–4th millennia BC were recorded. These remains evidence the first wave of penetration of steppe tribes with pastoral cattle breeding, which can be archaeologically traced only through specific pottery. Findings of the Middle and Late Neolithic belong to the culture of pile-dwelling builders of the 4–3rd millennia BC. The productive economy and metal objects (a copper awl was found at the Usviaty IV site) might have resulted from the penetration of bearers of the Globular Amphora Culture, and possibly the Corded Ware Culture, in the first half-middle of the 3rd millennium BC. That migration could be linked with the spread of Indo-European languages (Kristiansen et al., 2017; Vander Linden, 2016), and it was connected with climatic changes in the mid-3rd millennium BC (Shishlina, 2004). A genetic analysis of skeletons from this region dated to the first half of the 3rd millennium BC confirms the penetration of the Indo-European population (Chekunova et al., 2014).

Sites containing domestic structures (i.e., pile-dwellings), artefacts, and ecofacts, preserved within lacustrine sediments, are extremely important on a European scale. Archaeological layers of these sites are often discovered within lacustrine deposits as a result of later lake transgression, and therefore artefacts and ecofacts are in a unique state of preservation (Kittel et al., 2018a; Mazurkevich & Dolbunova, 2011). The disappearance (or at least a decrease in the importance) of the pile-dwelling culture coincided with the 4.2 ka BP cooling event, however, infrequently found relicts indicate further rare local presence of this tradition until the end of the 3rd millennium BC (Dolukhanov & Miklyayev, 1986; Kul'kova et al., 2015; Mazurkevich & Dolbunova, 2011). The construction of pile-dwellings might have been an adaptation to environmental changes (Kul'kova et al., 2015; Mazurkevich et al., 2017). They existed at about the same time as in the eastern Baltic region and the foothills of the Alps (Bolliger-Schreyer, 2004; Dolukhanov & Mazurkevich, 2000; Hafner et al., 2017; Menotti, 2004; Merkl, 2016; Schlichtherle, 1997). The main phase of development of the pile-dwelling settlement at the Serteya II site is dated to ca. 2400–2000 cal. BC and lasted for almost 140 years. The archaeological context suggests that it functioned in a period when a palaeolake existed, which was affected, however, by water table fluctuations (Kittel et al., 2018a).

Generally, palaeoecological reconstructions for Neolithic archaeological investigations are focused mostly on determining the character of local vegetation and its changes during the human occupation (e.g., Berglund & Ralska-Jasiewiczowa, 1986), as well as on presenting indicators of palaeoenvironments (e.g., Nevalainen et al., 2011; Ruiz et al., 2006), including trophic status (e.g., Brooks et al., 2001; Kittel et al., 2014, 2018b; Luoto, 2011; Pawłowski et al., 2016a; Płociennik et al., 2015). The first palaeoecological reconstructions in the Serteya microregion were conducted in the 2000s (e.g., Dolukhanov et al., 2004; Kul'kova et al., 2001; Mazurkevich et al., 2009; Mazurkevich, 2003; Tarasov et al., 2019) and were mostly focused on vegetation development and lake water level fluctuations studies based on pollen, diatom and geochemical analyses. However, those studies did not address the anthropogenic aspects of the landscape evolution and resource availability, based on plant macrofossils and palaeozoological proxies, or provided a detailed palaeoecological reconstruction for the time period of the occupation.

Thus, a detailed survey was necessary for a comprehensive reconstruction of the palaeoecological milieu in which ancient societies chose to live and adapt to evolving conditions.

Due to the deposition of well-preserved Neolithic remnants within lacustrine sediments, wetland and underwater archaeological excavations were undertaken at the Serteya II site. Wet sites usually yield unparalleled quality and quantity of artefacts (also made from organic materials) as well as ecofacts, and also offer a good opportunity for reliable reconstructions (Coles, 2018). A typical practice is to undertake off-site examinations during the environmental archaeology field work, developed as part of an extensive study of archaeological sites or complexes (e.g., Dimbleby, 1985; Edwards, 2016). At wetland sites, such as the Serteya II site, it is possible to undertake multiproxy palaeoecological analyses (such as pollen, plant macrofossils, charcoal, Cladocera, Chironomidae, fish remains, geochemistry, and sedimentology) based on the core collected directly from the archaeological site and archaeological outcrop. This way, we used lacustrine deposits with archaeological layers as an archive of traces of ancient societies' occupation and palaeoeconomic activity as well as landscape evolution and human-environment relationships. Our on-site palaeoecological investigations, as an integral part of archaeological research, allowed for a detailed reconstruction of: (a) natural environment transformations, (b) natural conditions of the activity of ancient communities, and (c) human adaptation to palaeoenvironmental conditions and human induced changes. An accelerator mass spectrometry (AMS) radiocarbon dating sequence provided an absolute chronology of the profile and for correlation with the archaeological chronology of the site.

We tested the influence of palaeoenvironmental changes on the human settlement pattern, and the extent that human impact had affected landscape changes in the period between ca. 4300 cal. BC and ca. 1600 cal. BC. This period covers two cooling periods called Bond events: the 4th (5.9 ka BP) and the 3rd (4.2 ka BP; Bond et al., 2001). The latter event marks the onset of the Late Holocene, called the Meghalayan stage, starting ca. 2250 BC (Cohen et al., 2019). The strong impact of landscape geo- and biodiversity, as well as climate and hydrologic fluctuations, on the local settlement and economy in the period between ca. 4300 cal. BC and ca. 1600 cal. BC make this a key study region for precise reconstructions of socio-biocenoses.

The palaeoenvironmental reconstruction presented here, based on multiproxy analyses, is focused on: (a) changes of natural environment components, (b) environmental conditions during the existence of the Neolithic community, (c) natural resources available to the Neolithic communities, and (d) human-environment relationships in the period from ca. 4.3 to ca. 1.6 ka cal. BC in the recently glaciated area of the East European (Russian) Plain.

2 | STUDY AREA

The study site (55°37'53"N; 31°32'28"E; 152.5 m above sea level) is situated in Western Russia (Figure 1) on the border between three administrative regions—the Pskov, Smolensk, and Tver oblasts. The

area is part of the Western Dvina Lakeland according to Abramov (1972), or the Vitebsk Lakeland after Kondracki (1992). It lies near the Central Russian Upland and close to the European watershed of three catchments: the Baltic Sea, the Black Sea, and the Caspian Sea. The main watercourse of the area is the Western Dvina River, but the main axis of the studied region is the Serteyka River, an approximately 40-km-long left tributary of the Western Dvina River. The main traits of the land relief of this recently glaciated area were formed during and after the Valdai (Weichselian, Vistulian) Glaciation (Gorlach et al., 2015; Velichko et al., 2011). The geology and geomorphology of the area is described by Kittel et al. (2018a).

The present-day lower Serteyka River valley was developed within a tunnel valley which incised the neighbouring morainic plateaus and glaciofluvial plains from the Valdai Glaciation. Lakes of different sizes existed within the enlargement of the tunnel valley in the Late Valdai (Late Weichselian) and during the Holocene. This is the reason why numerous biogenic plains occurring in the valley floor are separated by narrow sections of the valley. The river presumably drained subsequent water bodies during the Holocene, as a result of fluvial headward erosion. A few in-filled lake basins, filled with organic deposits of lacustrine and swamp origin as well as alluvial sands and silts, have been documented within the lower section of the valley. The largest is the Great Serteya Palaeolake Basin (GSPB; Kittel et al., 2018a).

The area is located within the temperate deciduous forest zone in the East European Plain. Contemporary climatic conditions of the study area are moderately continental with the influence of oceanic Atlantic air masses (Alpat'ev et al., 1976). Winters are moderately cold with a stable snow cover from November to April, and summers are moderately cool and humid. Most of the annual precipitation (ca. 60%) falls from May to October. The climate data for Velizh, situated 20 km to the West from the site, reveal for the Years 1955–2017 an average annual temperature ranging from 3.6°C to 8.4°C and average annual atmospheric precipitation varying from 488 to 1296 mm per year. The mean temperature of the warmest month (July) is between 14.8°C and 23.01°C and the mean temperature of the coldest month (January) is from -17.7°C to -0.8°C (<http://www.tutiempo.net>; date of last access: 9th Dec. 2019).

3 | ARCHAEOLOGICAL DATA

The Serteya II site is an archaeological multi-layered complex with several settlements and relicts indicating occupation of the area since the Mesolithic up to the Middle Ages. It was studied in the 1970s and subsequently since 2008. It is situated in the present day Serteyka River valley, on the southern border of the GSPB. The archaeological remains are on the surface of a sandy kame terrace formed by clastic sediments and within lacustrine biogenic deposits filling the palaeolake basin of the GSPB (Kittel et al., 2018a, 2020). The core zone of the site, located within the drainage channel and its shores, revealed several late Neolithic pile-dwelling constructions from the period between ca. 2900 and ca. 2000 cal. BC. The layer with pile-dwelling constructions, within coarse detritus gyttja ca. 1.1–1.5 m below ground level (b.g.l.),

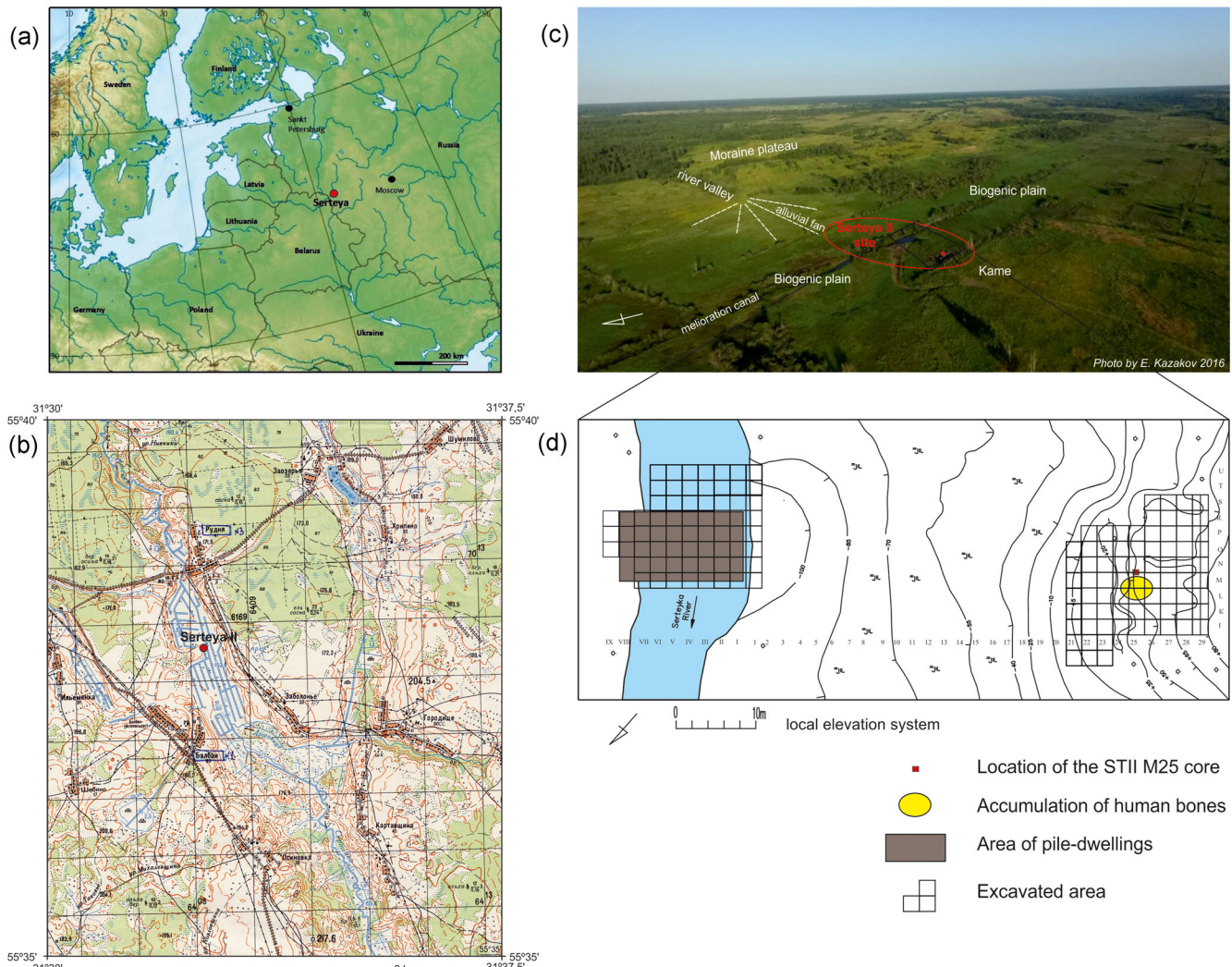


FIGURE 1 The location of the Serteya II site and the STII M25 core. (a) On the physical map of Europe, (b) on the topographical map of the Serteya region, (c) on the airborne photo of the Serteya II site, (d) on the plan of archaeological excavation of the Serteya II site [Color figure can be viewed at wileyonlinelibrary.com]

was excavated using underwater and wetland archaeological methods (Dolukhanov & Miklyayev, 1986; Mazurkevich & Dolbunova, 2011; Mazurkevich et al., 2017). Six pile-dwellings, with floor remains made from large wooden bark placed on poles, and wooden planks, as well as fireplaces with sand bases, attributed to the Zhizhitsa Culture were discovered (squares M-U/I-VII (Figure 1d); Mazurkevich & Dolbunova, 2011).

Two earlier archaeological layers were documented there as well, marked by an increase in the amount of charcoal and a number of fish bones: 1/ca. 1.2–1.5 and 2/ca. 2.0 m b.g.l. (Kittel et al., 2018a). The constructions were established most probably on a marshy shore or on the exposed bottom of a palaeolake. This fact is attested by the accumulation of clay, sand, and shells around the piles in which occurred during the periods of seasonal or perennial water level rises. Discoveries of pits of a different kind may evidence a settlement made on the periodically dry surface. It could indicate that the remains of the pile-dwelling settlement were uncovered (mostly) during periods

of a lower water level, later they were submerged and eroded during water level increases, and finally, they became covered with gyttja deposition. Thus, the archaeological context suggests episodes of palaeolake water level fluctuations at ca. 4.2 ka BP. Thereafter, the pile-dwellings were gradually abandoned, the settlements might have been moved to higher places. At the same time, the penetration of new cultural groups can be recorded.

The STII M25 core area (squares I-S/21–29; Figure 1d) has more complex stratigraphy owing to the location of the transect in the palaeolake shore area and the repeated periods of habitation due to the better accessibility of this area at different times. This is in contrast to the area where the pile-dwellings were located, which was accessible only during a definite period of time. Archaeological layers are situated on the sandy surface and also within the lacustrine deposits in the GSPB shore zone (Kittel et al., 2018a). Numerous features and artefacts were recorded within lacustrine coarse-detritus gyttja and underlying sands with organic mud admixtures.

The oldest potsherd assemblage is attributed to the Serteya Culture dated to the 7–6th millennia BC and the Rudnya Culture (5300–4900 cal. BC). These materials occur within the layer of sands with organic mud. Fragments of Rudnya Culture vessels were also found in the lower part of the gyttja layer. They are eroded as a result of redeposition of the Early Neolithic layer in the palaeolake shore zone (Kittel et al., 2018a; Mazurkevich et al., 2020). This indicates that the archaeological layer of the neighbouring part of the site, situated at a higher level, was destroyed, and then redeposited in the palaeolake shore zone. This can also be evidenced by the joint occurrence of finds dated to different periods of time. It is important to note the findings of a single Rudnya Culture arrowhead and one Mesolithic bone arrowhead within the grey sand layer. They might have been deposited there as a result of unsuccessful hunting or fishing in the lake shore zone.

The coarse-detritus gyttja in the excavated area of the squares I-S/21–27 reached a thickness of up to 1 m. A particular event in the history of this site is represented by ceramic fragments of the Eneolithic cultures of the steppe and forest-steppe zone of Eastern Europe which were dated to the boundary of the 5th and 4th millennia BC. Some of the vessels may have been dug into the gyttja and left there, further transgression led to the partial destruction of the vessels, which is marked by small washed-out fragments at one depth, clearly marking the level of the ancient washout.

A large group of Eneolithic steppe vessels was found within the area of the squares I-P/21–25. The inhabited area of this time is located down the slope in the square I-L/23–21. Near this, the lake shore zone is marked by a complete absence of single scattered artefacts (such as flint debris or pottery sherds) and the presence of objects related to aquatic activities (such as paddles). The analysis of sieved materials indicates the absence of macro remains typical of the settlement layer, and only numerous fragments of charcoal, fish bones, burnt bones, hazelnut shells, *Trapa natans*, and acorns were present. Those artefacts were deposited together with single vessels of the Usviaty Middle Neolithic local culture. They are covered with the materials of the Zhizhitsa Culture, including a butchering area.

The Middle and Late Neolithic materials of the Usviaty Culture (3100–2900 cal. BC) and the Zhizhitsa Culture (3000–2300 cal. BC) were found mostly in the lower part of the lake gyttja at a depth of ca. 1.2–1.5 cm b.g.l. (Photo 1). Numerous flint, bone, antler, and wooden artefacts, as well as ecofacts, were found as well as the potsherds in the gyttja layer. Here, in the palaeolake shore zone, household areas, synchronous to the time of the pile-dwelling inhabitation were discovered. The area includes the remains of open constructions without fireplaces, and possibly places of butchering (elk, bear, boar, and otter; Mazurkevich et al., 2017). A new sedentary economic model in the Middle and Late Neolithic, connected also to landscape changes, is evidenced by different categories of archaeological finds.

Most spectacular is the discovery (M-L/24–25 square; Figure 1d) of bones of two almost complete skeletons of young

women, deposited in a nonanatomical order, and a small part of a third skeleton found in the upper part of coarse-detritus gyttja. They were associated with rich wood fragments, deposited most probably during palaeolake water level fluctuations, placed there intentionally, or accumulated there later.

4 | MATERIALS AND METHODS

4.1 | Field work and sampling

Investigations of the Serteya II site were renewed in 2008 and a wide range of underwater as well as wetland archaeological methods was used. In recent years, a geological survey was carried out in the site area and its surroundings including detailed geological mapping and trenching as an integral part of archaeological investigations of the site (Kittel et al., 2018a; Mazurkevich et al., 2017). To document its surficial geology, geological mapping with hand augering was undertaken, mostly to determine the range and thickness of organic deposits as well as overlaying fluvial overbank deposits.

Our palaeoecological study is focused on the core of organic deposits (called STII M25) collected in 2016 from the southern wall of the geological outcrop in the square M/25 (Figures 1 and 2). After a full excavation of the archaeological outcrop in the place where human skeletons were discovered (i.e., squares M/24–26), a core of organic deposits was collected for detailed multiproxy palaeoecological analyses. The core was taken as monoliths into three metal boxes with dimensions of 50 × 10 × 10 cm and covers deposits between 23 and 160 cm b.g.l. This method preserves an undisturbed sediment structure.

Successive samples of deposits were taken in 1 cm slices at 2 cm intervals between 24 and 72 cm b.g.l. and at 1 cm intervals between 73 and 159 cm b.g.l. for pollen, Cladocera, geochemical, and sedimentological analyses and as contiguous 2 cm slices for plant macrofossils, charcoal, subfossil Chironomidae, and fish remains analyses. The samples for diatoms and mollusc were also collected, however, those remains were not recognised within studied deposits. Material for radiocarbon dating was collected after plant macrofossils analysis elaboration from the remains of selected terrestrial plants.

The STII M25 core was situated in the shore zone of the studied wetland ecosystem. Such location might have determined specific conditions of microdiscontinuity in the record of environmental changes (Dietze et al., 2016; Digerfeldt, 1986). It was a kind of compromise between the nearest location of the core and the archaeological layers. In addition, it was related to the consequences resulting from the shore zone character of the studied geoarchive (see also Kittel et al., 2020). Therefore, it is planned to compare in the near future the presented results with the results of a study of a new deep water core representing a comparable continuous record of the evolution of this ecosystem (Kittel et al., 2018a).

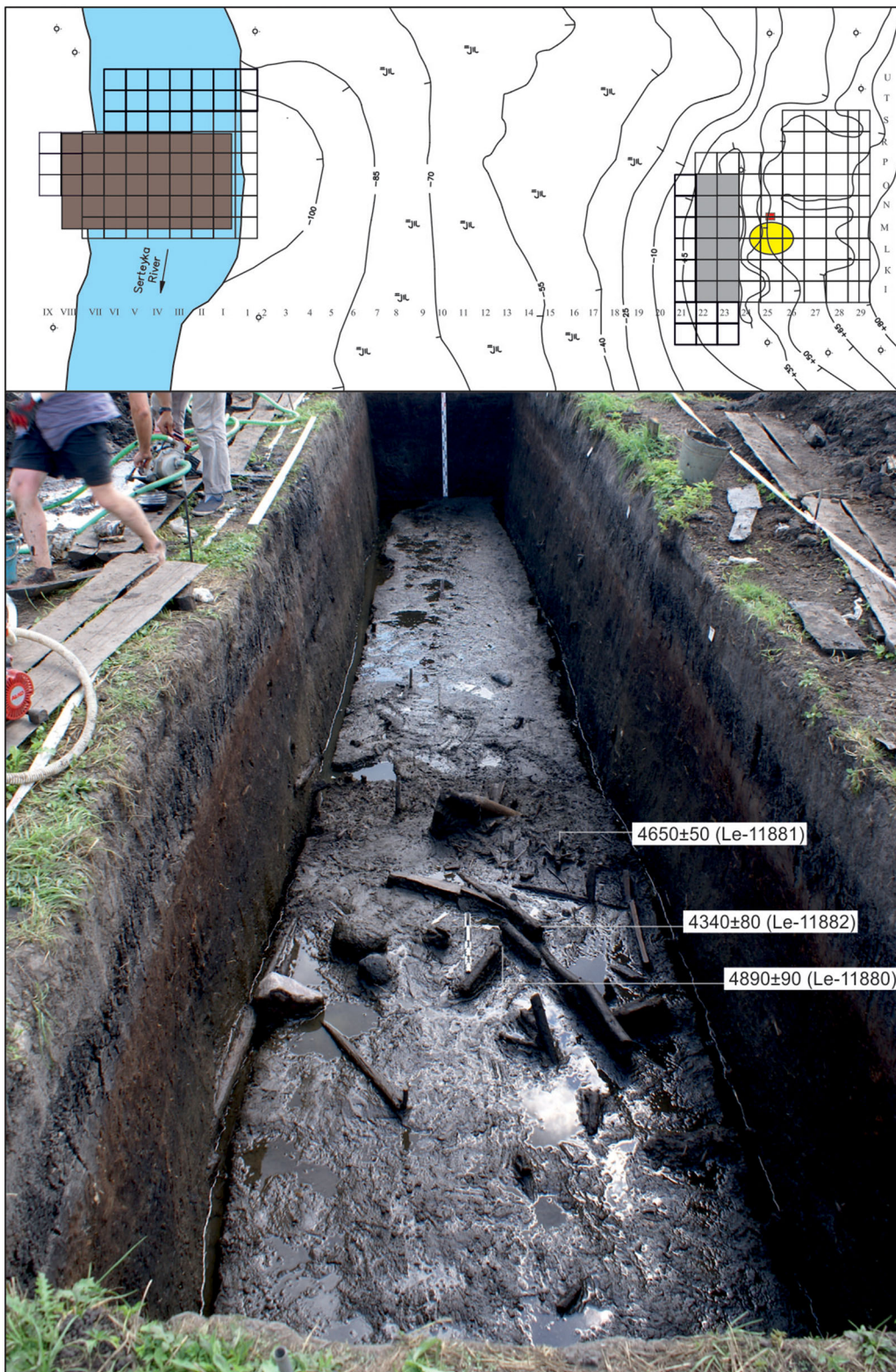


PHOTO 1 The view of the archaeological outcrop in the squares I-O/22-23 (see Figure 1) with ^{14}C data for wooden construction elements (see Table 5) [Color figure can be viewed at wileyonlinelibrary.com]

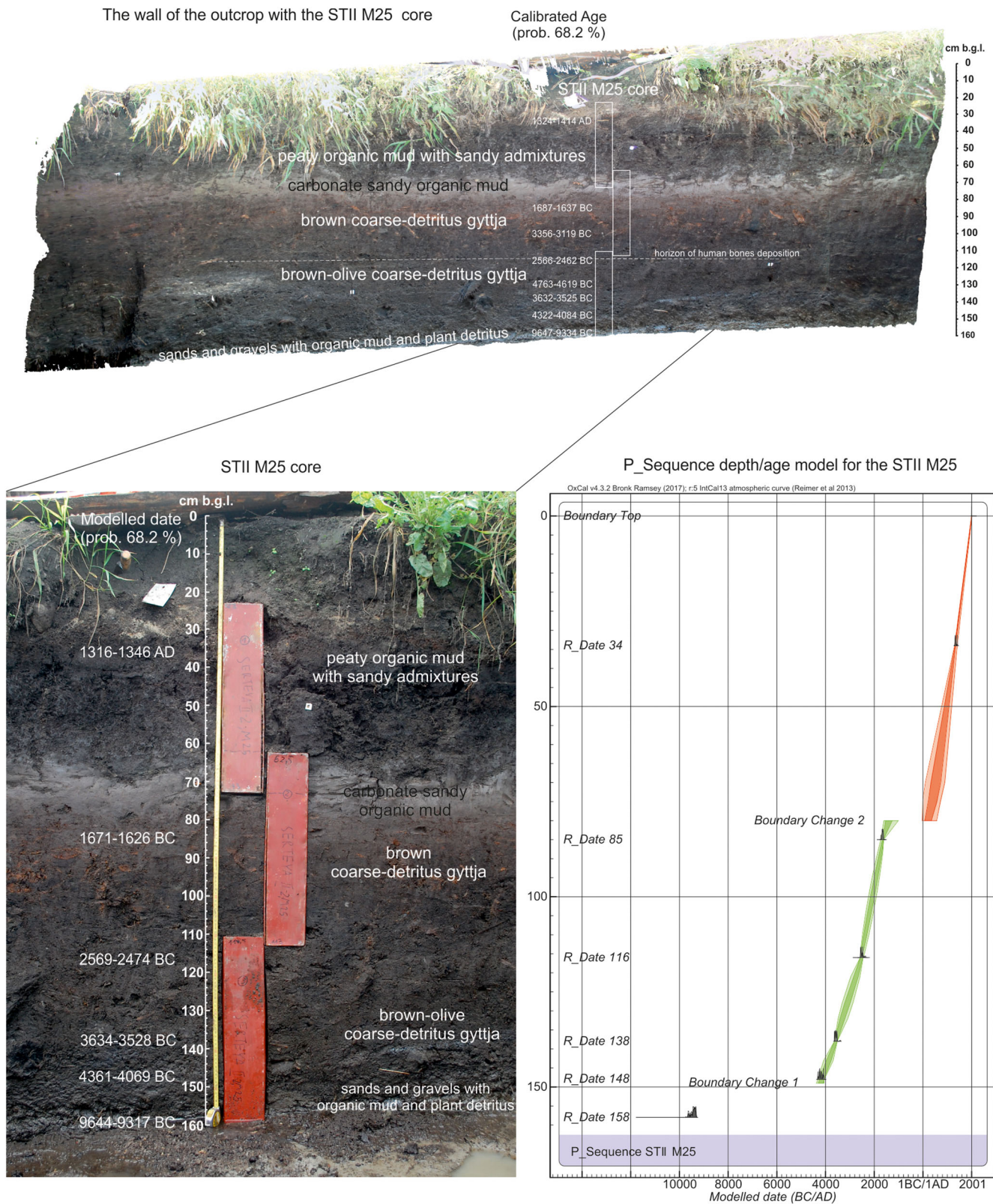


FIGURE 2 The lithology and depth/age model for the deposits of the STII M25 core (prepared by M. Krapiec) [Color figure can be viewed at wileyonlinelibrary.com]

4.2 | Geochemical and sedimentological analyses

Chemical composition was determined in 120 samples after drying at 105°C and homogenisation in an agate mortar. The basic geochemical analysis conducted included the identification of: organic matter (the loss on ignition method [LOI] in a muffle furnace at a temperature of 550°C) and calcium carbonate (CaCO_3 ; the volumetric method by means of Scheibler's apparatus; methods after: Bengtsson & Enell, 1986). The ash samples were dissolved (using HCl, HNO_3 , and H_2O_2) in Teflon bombs using a microwave mineraliser for 30 samples. The solution obtained was analysed for concentrations of Na, K, Ca, Mg, Fe, Mn, Cu, Zn, and Pb using atomic absorption spectrometry (Figure 3). The proportions of these compounds were used to classify deposits and to reconstruct environmental change in the sedimentologic basin and in the catchment (Pawlowski et al., 2016a). The total C, N, and S contents were analysed in a Vario Max CNS elemental analyser (Elementar Analysensysteme, GmbH).

The grain size composition of the 68 ash samples remaining after the LOI analysis was determined using the laser particle size analyser Mastersizer 3000 with a Hydro MU dispersion unit (Malvern). The textural features, using Folk and Ward (1957) coefficients, were evaluated for inferences about the genesis and deposition conditions of sediments.

Standardised values of organic matter and nine macro- and microelements were used as input variables in principal component analysis (PCA; Figure 4). The calculations were run using PAST version 2.17c software (Hammer et al., 2001). The cluster analysis was applied to geochemical data that described 68 sediment samples. As grouping variables, 15 lithogeochemical properties were adopted that reflect, for example, the type and dynamics of denudation processes and the supply type. The calculations employed Ward's method of hierarchical grouping, which uses estimates of distance between clusters in a variance analysis approach (Zhou et al., 2018). The identified lithogeochemical facies form three main groups of sediments (organic, mineral, and mixed).

4.3 | Palaeoecological analyses

A total of 55 samples for pollen analysis contained 1 cm³ of sediment and only 22 of them comprised sufficient quantities of pollen grains. Organic deposit samples were processed for pollen and nonpollen palynomorph (NPP) analysis using standard techniques (Moore et al., 1991) following modified Erdtman's acetolysis method (Berglund & Ralska-Jasiewiczowa, 1986). They were treated with HCl (10%), NaOH (10%), HF (40%), and acetolysis (8 min). A minimum of 400 pollen grains of terrestrial plants was counted in each sample to ensure statistical significance. Cyperaceae, hygrophilous plant, spores, and NPPs were excluded from the pollen sum. Pollen grains were identified with the aid of a reference collection of modern pollen types and keys (Fægri & Iversen, 1989; Moore

et al., 1991), as well as photographs (Beug, 2004; Reille, 1992). NPPs were identified according to van Geel et al. (2003), van Geel and Aptroot (2006), and Cugny et al. (2010), and percentages were calculated on the basis of the same pollen sum used for a pollen diagram (van Geel et al., 1981). The pollen diagram was drawn using TILIA and TGView software (Grimm, 1992). Pollen zones were delimited with the help of CONISS (Grimm, 1987; Figure 5). The basic sum used for percentage calculation consists of pollen grains of terrestrial plants (AP + NAP = 100%).

For macrofossil analysis, 55 sediment samples were taken from the core. Since the uppermost samples (26 and 30 cm) did not contain any relevant botanical macro-remains, those were removed from data processing. The samples were treated with KOH to reduce the amount of sediment and remove humic matter and washed through a sieve with a mesh size of 0.3 mm. The remnants were dispersed in water and identified at up to $\times 40$ magnification with a binocular microscope. Identification of plant remains and other macrofossils was done by the references to Beijerinck (1976), Birks (1980), Mauquoy and van Geel (2007), and Cappers et al. (2012) as well as the reference collection of the Institute of Pre-and Protohistoric Archaeology, University of Kiel. The ecological classification of the plant macro-remains recorded is mainly based on the indicator values, according to Ellenberg et al. (1991). Based on their life-form, macrophytes (plants that grow in or near water), such as *Mentha aquatica*, *Ranunculus sceleratus*, *Lycopus europaeus*, *Juncus* spp., *Glyceria* spp., *Eleocharis* spp., *Typha* spp., *Scirpus sylvaticus*, *Schoenoplectus* spp., and *S. lacustris* were summarised as helophytes. *Sagittaria sagittifolia* and *Alisma* spp. were grouped into amphiphytes. Aquatic macrophytes were classified into hydrophytes and further subdivided into floating-leaved plants, including *Nymphaea alba* and *Nuphar lutea*, and submerged plants, consisting of *Najas marina*, *Potamogeton* spp., *Zannichellia palustris*, and *Chara* spp. In addition, further sum curves were generated for vegetation of moist to wet habitats (*Carex* spp., *C. spp. bicarpetal*, *C. spp. tricarpetal*, *Filipendula ulmaria*, *Solanum dulcamara*, *Potentilla erecta*, *Apiaceae*, *Brassicaceae*, *Poaceae*, *Allium* spp.) as well as nutrient-loving herbs (*Bidens* spp., *Persicaria* spp., *P. hydropiper*, *P. lapathifolia*, *P. maculosa*, *Urtica dioica*, *Ranunculus acris/repens*, cf. *Ranunculus*, *Chenopodium* spp., *Ch. glaucum/rubrum*, *Ch. album*). The results of the macrofossil analysis are presented in absolute values (Figure 6). The diagram of macrofossils was produced with the help of the program TILIA version 2.1.1 (Grimm, 2016). Plant macrofossil zones were defined according to visual criteria.

To reconstruct local past fire activity, samples for macroscopic charcoal were prepared following standard procedures for Whitlock (Whitlock & Larsen, 2001). The charcoal particles were then categorised into three charcoal sizes: 150–300 µm, 300–500 µm, and more than 500 µm, which gives information about distances of fires from the study site. Then, the macro charcoal influx or accumulation rates (CHAR) were calculated and expressed as charcoal particles/cm²/year (Davis & Deevey, 1964).

The analysis of subfossil Cladocera was conducted for 67 samples of 1 cm³ of deposit. All were processed according to the standard procedure (Frey, 1986). A solution of 0.1 ml was used for each

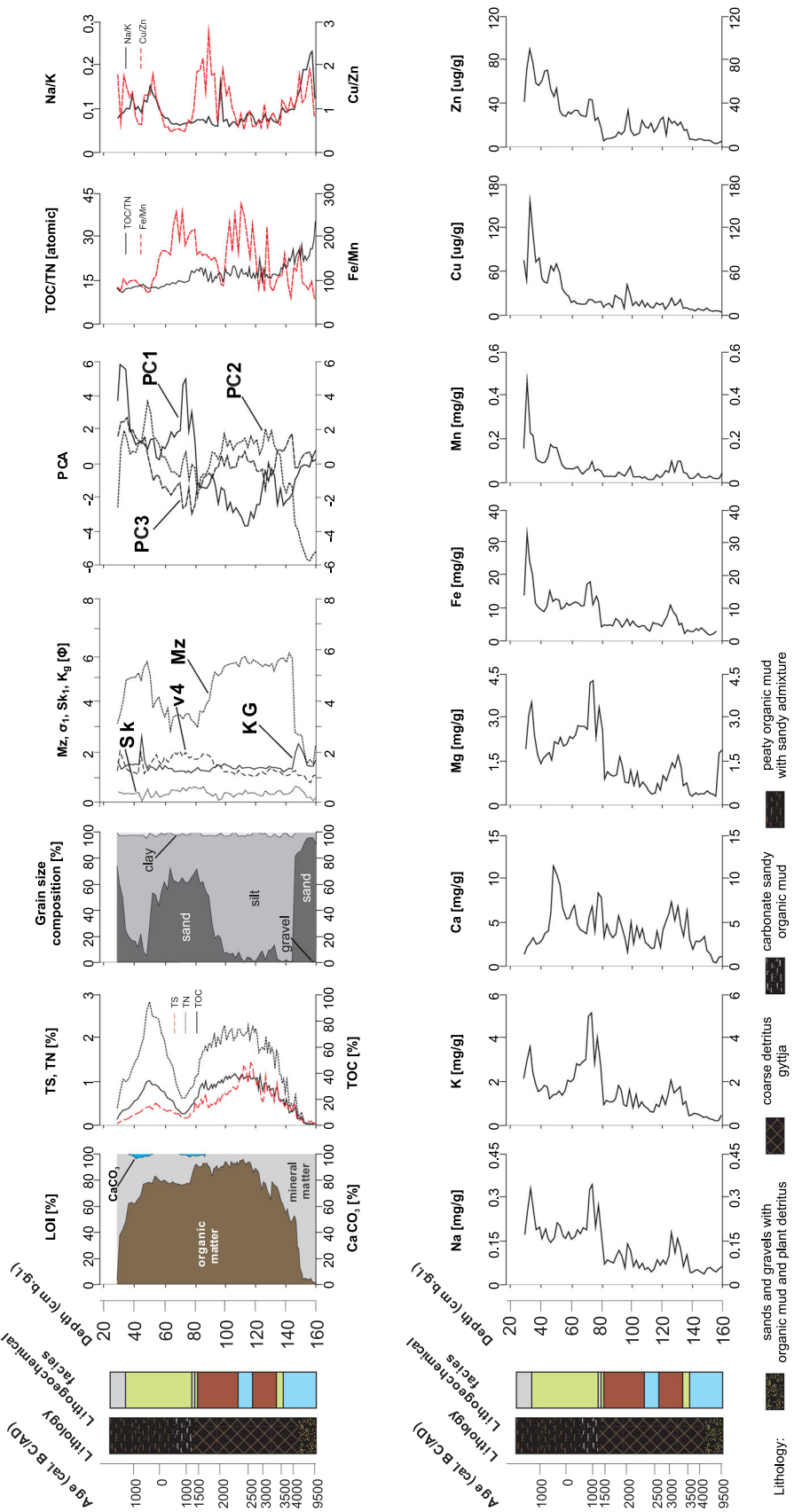


FIGURE 3 Results of sedimentological and geochemical analyses for the deposits of the STII M25 core (analysis by D. Okupny & J. Szmańda) [Color figure can be viewed at wileyonlinelibrary.com]

Analysis: D. Okupny & J. Szmańda (2019)

FIGURE 4 Principal component analysis (PCA) biplot of geochemical and grain-size data for the deposits of the STII M25 core (analysis by D. Okupny) [Color figure can be viewed at wileyonlinelibrary.com]

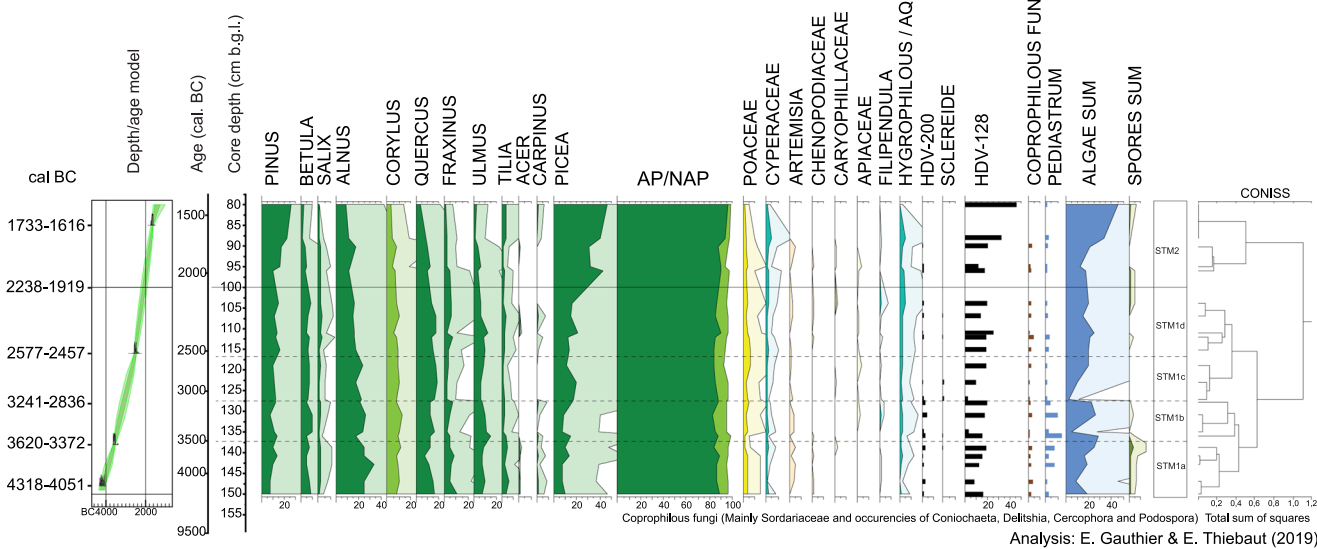
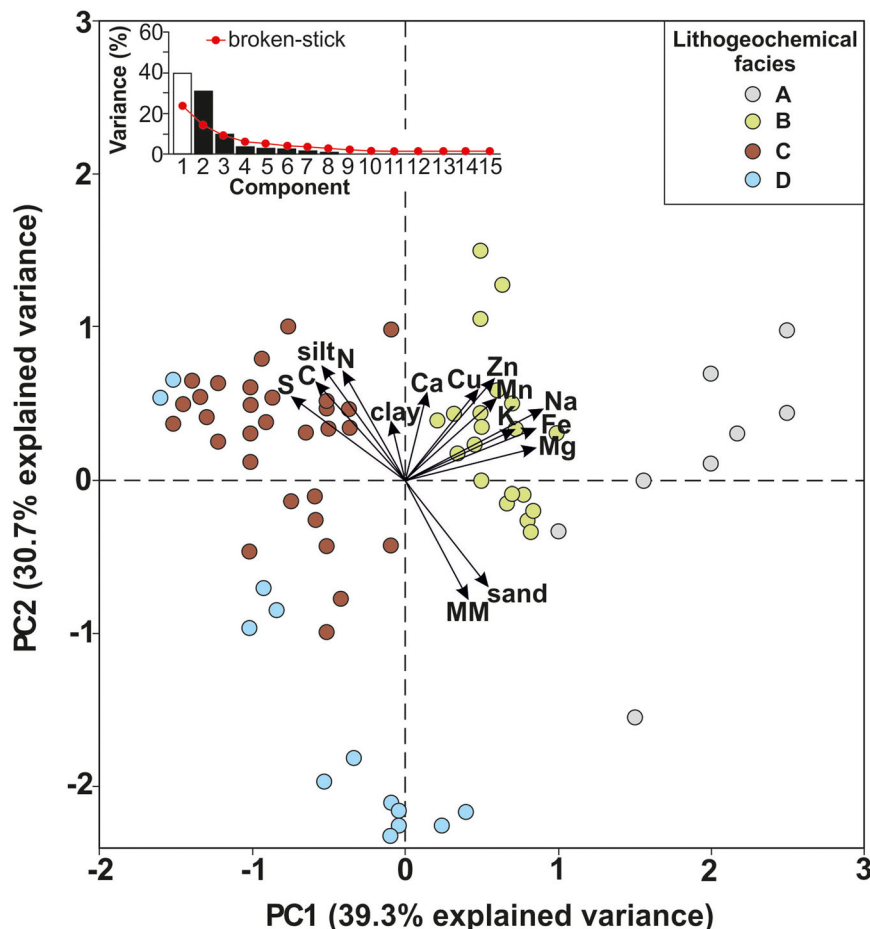


FIGURE 5 Percentage pollen diagram of selected taxa for the deposits of the STII M25 core (analysis by E. Gauthier & E. Thiebaut) [Color figure can be viewed at wileyonlinelibrary.com]

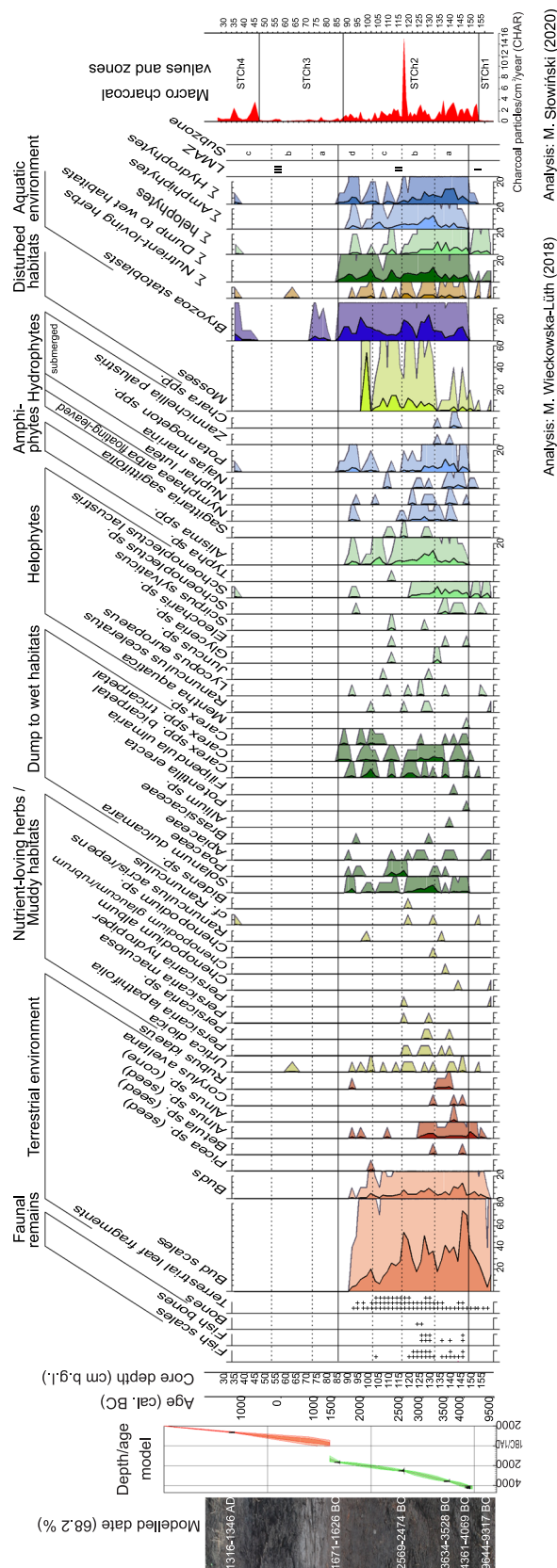


FIGURE 6 Plant and other macrofossil diagram (analysis by M. Wieckowska-Lüth) and charcoal accumulation rate (CHAR, particles/cm²/year) for the deposits of the STII M25 core (analysis by M. Stowński) [Color figure can be viewed at wileyonlinelibrary.com]

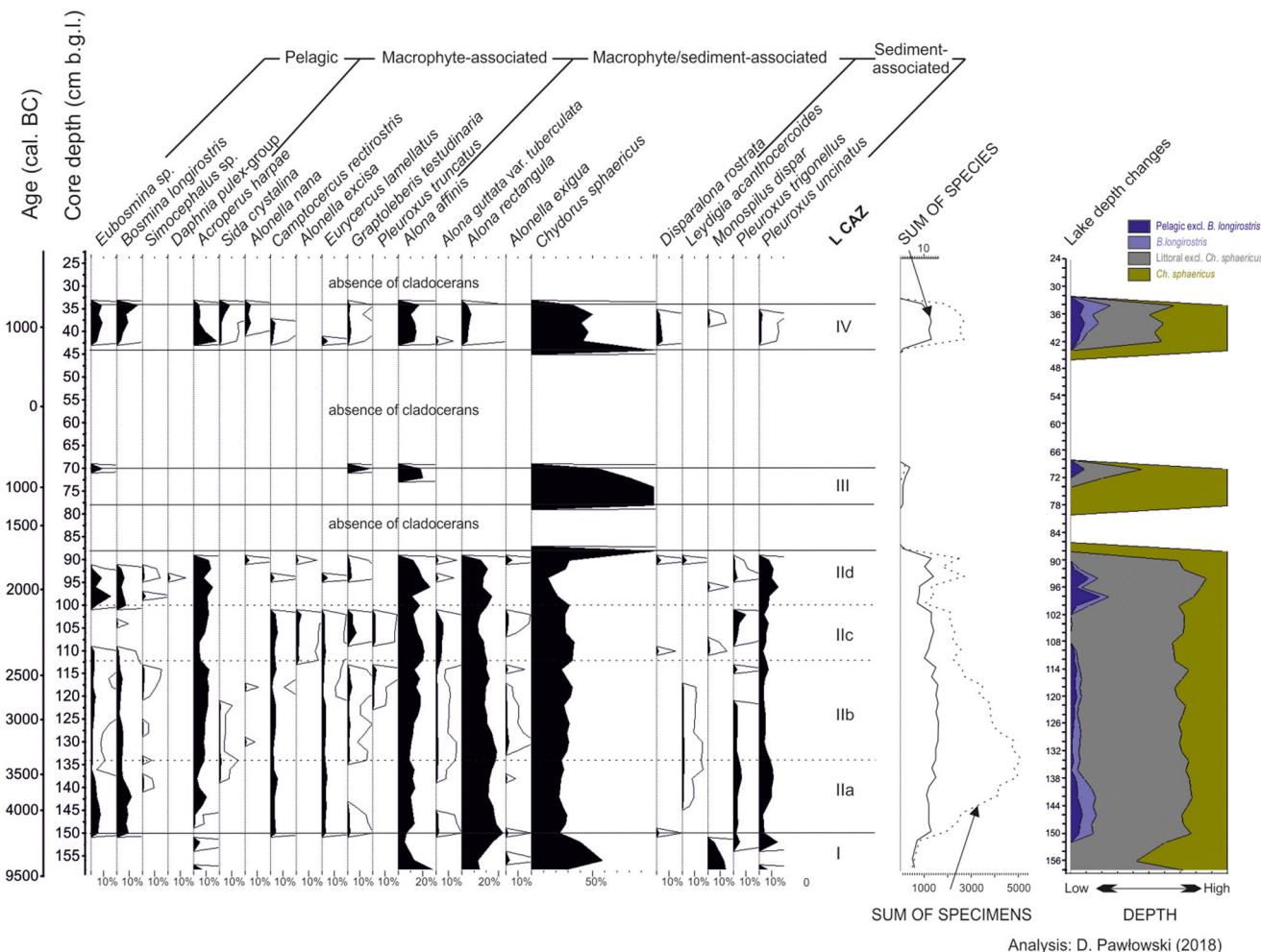


FIGURE 7 Percentage Cladocera diagram for the deposits of the STII M25 core (analysis by D. Pawłowski) [Color figure can be viewed at wileyonlinelibrary.com]

microscope slide ($\times 100$ magnification). All Cladocera remains were counted. For each taxon, the most abundant body parts were taken to represent the number of individuals, and percentages were calculated from the sum of individuals. The taxonomy of cladoceran remains in this paper follows that presented by Szerocyńska and Sarmaja-Korjonen (2007). The ecological preferences of cladoceran taxa were determined on the basis of the published key after Bjerring et al. (2009). The results of those calculations were presented in a diagram (Figure 7). A stratigraphically constrained cluster analysis (CONISS) was conducted to distinguish cladoceran zones. The ratio of pelagic to littoral Cladocera species was calculated to reconstruct water depth fluctuations. As the frequency of *Bosmina longirostris* and *Chydorus sphaericus* could be strongly dependent on trophy increases (Whiteside, 1970), those taxa were excluded.

The weight of deposit samples for the chironomid analysis ranged between 3 and 25 g out of 42 samples of deposits. Preparation methods followed Brooks et al. (2007). The sediments were passed through a 90 μm mesh sieve. All the head capsules (h.c.) were fixed in the Euparal® on microscope slides. The Chironomidae collection was determined to the lowest possible taxonomic level using the keys of Brooks et al. (2007)

and Andersen et al. (2013). Ecological preferences of identified taxa are based mainly on Brooks et al. (2007), Vallenduuk and Moller Pillot (2007), and Moller Pillot (2009, 2013). The Chironomidae diagram was plotted using C2 software (Juggins, 2007; Figure 8).

Analysed ichthyofaunal remains come from 15 sediment samples. Every piece of fish remains was identified under a $\times 10$ magnifying glass and determined by the references to Baglinière and LE Louarn (1987), Radu (2005) as well as on the basis of our personal reference collection.

4.4 | Geochronology: radiocarbon dating and age-depth model

A total of eight samples of selected terrestrial plant macrofossils from the STII M25 core were dated with the radiocarbon (^{14}C) method, using the AMS technique (Table 1).

Plant macrofossils for AMS dating were processed in the Laboratory of Absolute Dating, Krakow (Poland). Samples were chemically pretreated with the AAA (acid-alkali-acid) method. The mixture of graphite and Fe powder was pressed into a target holder and measured

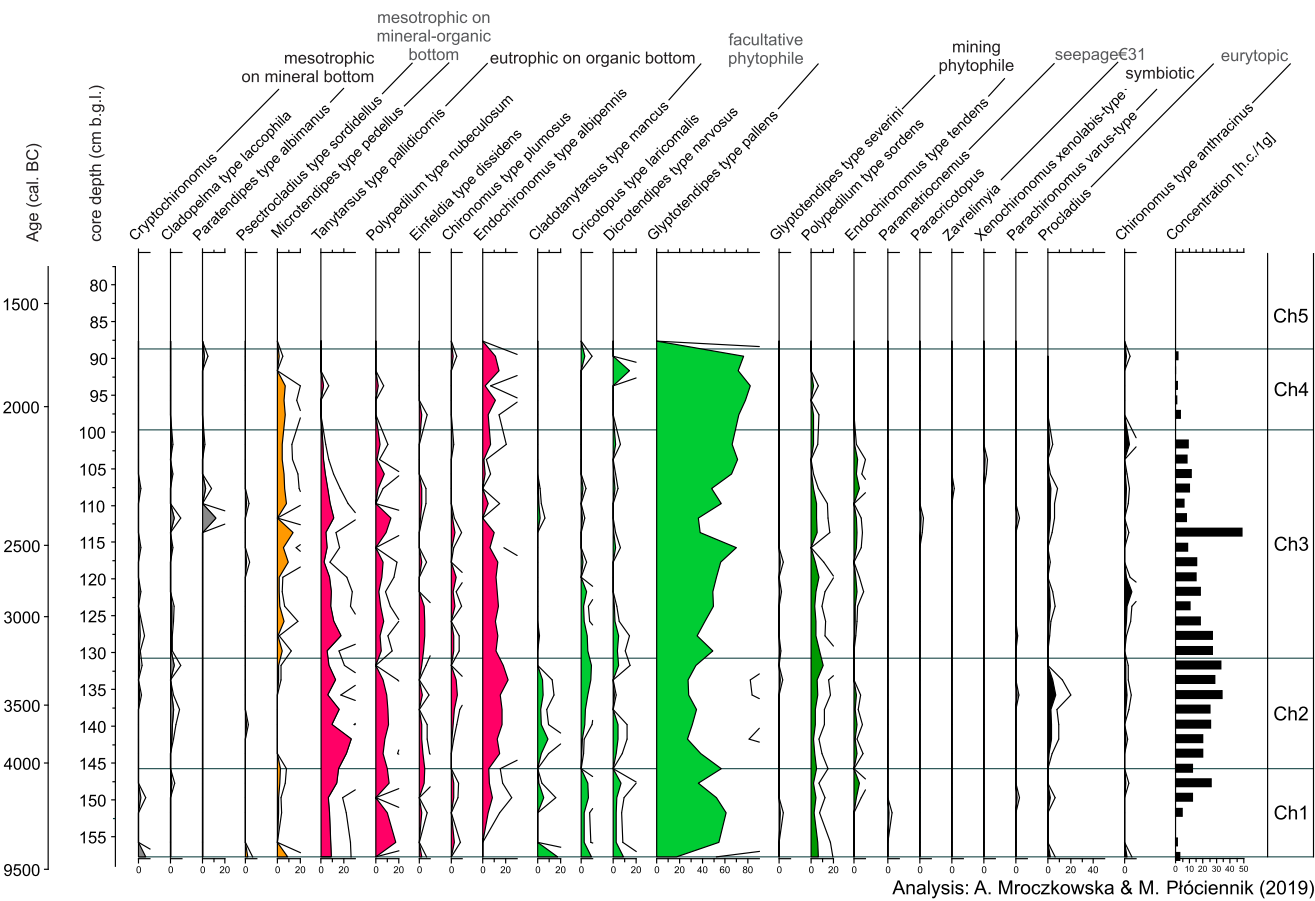


FIGURE 8 Percentage Chironomidae diagram for the deposits of the STII M25 core (analysis by A. Mroczkowska & M. Płociennik) [Color figure can be viewed at [wileyonlinelibrary.com](#)]

with the AMS system at the Center for Applied Isotope Studies at the University of Georgia, USA (Cherniksky et al., 2010).

Calibrated radiocarbon ages (cal. yr BP) were made using the IntCal13 radiocarbon calibration data set (Reimer et al., 2013) and OxCal 4.2 calibration software (Bronk Ramsey, 2009). All presented margins of error are the uncertainties at a 68.2% probability.

The chronology (age-depth curve) of the core is based on the OxCal P_Sequence model (Bronk Ramsey, 2008). In total, six radiocarbon dates were used for the construction of the age-depth model (Table 2). The changes in the pattern of accumulation were taken into account during the age-depth model construction. Therefore, in our model, single-boundary constraints were introduced, assigned to depths of 149 and 80 cm b.g.l. (Figure 2). On the basis of the age-depth model, we calculated the probability distributions of the modelled calendar ages for selected events related to local palaeoenvironmental changes.

5 | RESULTS

5.1 | Geological and geochemical traits of deposits

The STII M25 profile consists of five main lithological units (Figure 2). The bottommost sediments of the studied depositional sequence are

sands and gravels with organic mud and plant detritus (depth: 148.5–160 cm b.g.l.). Above, at a depth of 75/80–148.5 cm b.g.l., coarse detritus gyttja is found. Carbonate sandy organic mud (depth: 65–75/80 cm b.g.l.) and peaty organic mud with sandy admixtures (depth: 23–65 cm b.g.l.) are recorded upward. The uppermost layers are silty sands and silts of earthwork from the 1970s (depth: 0–23 cm b.g.l.).

Based on textural features of clastic fractions as well as variations in the chemical composition of deposits and the macro- and microelements contents, four lithogeochemical facies were distinguished (Table 3; Figures 3 and 4).

Lithogeochemical facies A (24–34 and 78–80 cm b.g.l.) are represented by mineral-organic deposits with an increased content of lithophilic elements, such as K (between 1.53 and 3.59 mg/g), Mg (between 1.45 and 3.55 mg/g), and Na (between 0.17 and 0.33 mg/g). It creates two thin layers at the top of the profile. In addition to the large variable value of the content of organic matter (from 2% to 90%), these sediments are generally characterised by a decrease of geochemical ratios such as TOC/TN (from 18.6 to 10.9) and Cu/Zn (from 1.79 to 0.69).

Lithogeochemical facies B (34–78, 80–82, and 134–138) cover organic-mineral deposits with an increasing content of Ca and CaCO₃. The calcium carbonate varied between 0.8% and 5.28% and

TABLE 1 The results of radiocarbon dating of the deposits of the STII M25 core

Dated deposits	Depth b.g.l. (cm)	Dated macrofossils	^{14}C age yr BP	Laboratory code	Calibrated age (prob. 68.2%)	Calibrated age (95.4%)
Peaty organic mud	34	Schoenoplectus and cf. Ranunculus (2 seeds)	561 ± 26	MKL-A3888	1324–1414 AD	1311–1425 AD
Coarse detritus gyttja	85	wood	3371 ± 21	MKL-A3936	1687–1637 BC	1736–1621 BC
Coarse detritus gyttja	100	Picea (seed)	4532 ± 28 ^a	MKL-A3886	3356–3119 BC	3361–3104 BC
Coarse detritus gyttja	116	Sagittaria (fruit) and Alisma (seed)	3967 ± 33	MKL-A3979	2566–2462 BC	2575–2348 BC
Coarse detritus gyttja	130	Alnus (2 seeds)	5831 ± 26 ^a	MKL-A3885	4763–4619 BC	4780–4612 BC
Coarse detritus gyttja	138	Rubus (2 seeds)	4761 ± 21	MKL-A3937	3632–3525 BC	3636–3519 BC
Sandy coarse detritus gyttja	148	Alnus (4 seeds)	5368 ± 28	MKL-A3884	4322–4084 BC	4329–4067 BC
Organic mud layer within sands	158	cf. Rosaceae (seed)	9973 ± 35	MKL-A3887	9647–9334 BC	9661–9317 BC

Abbreviation: b.g.l., below ground level.

^aDate recognised as outlier (redeposited material).

displayed two periods corresponding to distinct enrichment in Zn (up to 70.9 µg/g). These deposits, with a total thickness of 47 cm, are characterised by the highest average share of TN (88.7%), a decrease in the content of sand (from 78% to 4%) and the Fe/Mn ratio (from 258 to 72.4), as well as an increase of average content of TS (0.31%) and Mg (2.47 mg/g), as well as the Cu/Zn ratio (from 0.49 to 1.79).

Lithogeochemical facies C (82–109 and 118–134) are organic deposits with an increasing content of lithophilic elements: K (between 0.77 and 1.84 mg/g), Mg (between 0.52 and 1.65 mg/g), and Na (between 0.05 and 0.13 mg/g). A significant enrichment of S (often above 0.8%) accompanied by increasing contents of organic matter (above 91%) is observed. Admixtures of sand decrease to only a few per cent and very fine sand dominates (average is 85%). The silt fraction dominates, and the very coarse and coarse silt share is three to five times greater than the sum of the share of fine and very fine silt.

Lithogeochemical facies D (109–118 and 138–160) are represented by mineral-organic deposits with decreasing content of all elements. Here, silty sand (M_2 : 1.63–2.92 phi) and sandy silt (M_2 : 5.32–5.86 phi) with moderate sorting (σ_1 average is 1.07 phi) dominate. The deposits in the lower part of the profile were characterised by a decreased content of organic matter (average is 4.9%) and a lack of carbonates. Towards the top of this zone, the sediments became progressively enriched in TOC (above 30%), TN (above 2%), and TS (above 1.3%). In the lower part of the core, a distinct peak of Mg (about 2 mg/g) was observed.

5.2 | The age of deposits

Due to the location of the archaeological layers and artefacts in the palaeolake shore zone, their depth differs significantly within different areas in the vicinity of the studied core. Neolithic archaeological layers were distinguished mostly from a depth of ca. 100 cm b.g.l. in the immediate vicinity of the STII M25 core. Single fragments of Eneolithic vessels were found at a depth of 57 cm and major fragments within 105–158 cm. Fragments of Usviaty Culture vessels were found at depths of 113, 120–126, 131, 137, and 140–143 cm; Zhizhitsa Culture vessels were found mainly at a depth of 117–125 cm, while, fragments of Serteya Culture vessels were located at 131, 140, and 149 cm.

Changes in the categories of inventory within lacustrine deposits show various uses of the area and evidence changes of the water regime in the Neolithic—the existence of the lake marked by fragments of fishing gear and the wetland area with a solid shoreline where living areas remained. Selected plant macrofossils from the organic mud lamination within sands and gravel were ^{14}C dated at a depth of 158 cm b.g.l. to 9973 ± 35 BP (MKL-A3887), that is, 9647–9334 BC. It must be noted that there is an absence of sediments dated to the 7–6th millennia BC resulting from depositional hiatus or erosion. This period is synchronous with the time of the Serteya Culture and Rudnya Culture and the location of pottery shreds attributed to these horizons in later sediments, which means that they were redeposited.

TABLE 2 The P_Sequence depth/age model for the STII M25 core

Name	Depth b.g.l. (cm)	¹⁴ C age year BP	Unmodelled (BC/ AD; prob. 68.2%)	Unmodelled (BC/ AD; prob. 95.4%)	Modelled (BC/AD; prob. 68.2%)	Modelled (BC/AD; prob. 95.4%)	Indices	
							Amodel 89.7	Aoverall 89.7
							A	C
Boundary top	0				2012–2018 AD	2012–2037 AD		99
R_Date 34	34	561±26	1324–1414 AD	1311–1425 AD	1316–1346 AD	1301–1411 AD	89.6	99.9
Boundary change 2	80				1535–1259 BC	1607–1015 BC		99.7
R_Date 85	85	3371±21	1687–1637 BC	1736–1621 BC	1671–1626 BC	1731–1613 BC	101.1	100
R_Date 116	116	3967±33	2566–2462 BC	2575–2348 BC	2569–2474 BC	2577–2459 BC	104.2	99.9
R_Date 138	138	4761±21	3632–3525 BC	3636–3519 BC	3634–3528 BC	3636–3522 BC	100.6	99.9
R_Date 148	148	5368±28	4322–4084 BC	4329–4067 BC	4261–4069 BC	4322–4053 BC	80.7	99.7
Boundary change 1	149				4286–4085 BC	4373–4067 BC		99.6
R_Date 158	158	9973±35	9647–9334 BC	9661–9317 BC	9644–9317 BC	9656–9305 BC	97.9	96.6
Boundary bottom	160				9646–9317 BC	9665–9300 BC		95.9

Note: OxCal v4.3.2 Bronk Ramsey (2017): r.5 IntCal13 atmospheric curve (Reimer et al., 2013).

The sample from the very bottom of the gyttja layer (148 cm b.g.l.) was dated to the ¹⁴C age 5368±28 BP (MKL-A3884), that is, 4322–4084 BC. This date should document the earliest phases of an increase of the palaeolake water level. At the top (85 cm b.g.l.), the gyttja layer was dated to 3371±21 BP (MKL-A3936), that is, 1687–1637 BC. The gyttja from the horizon at which the skeletons were deposited (116 cm b.g.l.) was dated to 3967±33 BP (MKL-A3979), that is, 2566–2462 BC, and one of the bones was dated to 4080±35 BP (Poz-103947), that is, 2836–2504 BC (Lorkiewicz et al., in prep.). Two wooden elements in the immediate surroundings of the bones, at a depth of ca. 90–80 cm b.g.l., were dated to 3760±20 BP (Le-11161), that is, 2202–2142 BC, and 3450±50 BP (Le-11162), that is, 1876–1691 BC (Mazurkevich et al., 2017).

The age-depth curve demonstrates that the continuous accumulation of lacustrine coarse-detritus gyttja began ca. 6300 cal. BP (4300 BC), and it was replaced by the fluvial overbank deposition after 3600 cal. BP (1650 BC). Thus, our palaeoecological reconstructions are focused on the period between 4300 and 1600 cal. years BC (ca. 150–85 cm b.g.l. of the core sequence; Figure 2). The obtained chronology of human bones fits well with the gained age-depth model.

5.3 | Palaeoecological study

The Serteya STII M25 pollen diagram is divided into two major pollen zones called STM1 and STM2. STM1 is itself divided into four subzones (STM1a, STM1b, STM1c, and STM1d; Figure 5). The archaeological levels are located at a depth of 150–100 cm b.g.l. and correspond to the pollen zone STM1 dated between

4300 cal. BC and 2200/2000 cal. BC according to the age-depth model.

STM1a (150–138 cm b.g.l. of the core sequence): the first subzone is characterised by a forested environment (95% of tree and shrub pollen) mainly represented by *Alnus*. Taxa of the mixed oak forest, such as *Quercus*, *Ulmus*, *Tilia*, *Fraxinus*, and *Acer*, are also present, with values between 5% and 18%. *Picea* and *Pinus* are represented by 20% each in this sequence. Herbaceous taxa are mainly represented by *Poaceae*, *Cyperaceae*, *Artemisia*, and *Chenopodiaceae*. Coprophilous fungi are present in small quantities. The presence of HdV-200 is correlated with a decrease in algae spores.

In the STM1b (138–128 cm) subzone, the percentages of trees and shrubs decrease a little but are still close to 90%. A slight decrease in *Pinus*, *Picea*, *Alnus*, *Betula*, and *Carpinus* values is observed. The percentage of *Artemisia* is continuous but *Chenopodiaceae* decrease and disappear at the end of the phase. At the beginning of this phase, the share of algae spores is very small and increases significantly during this phase to reach almost 30%, while HdV-200 is still present. Coprophilous fungi are absent and reappear when algae spores increase.

In STM1c (128–117 cm), the tree and shrub pollen sum remains at ca. 90%. *Carpinus* and *Chenopodiaceae* are absent in this phase. The percentage of algae increases during this phase, while HdV-200 decreases and disappears. *Poaceae* seem to increase slightly. *Pinus* and *Picea* generally increase while the share of *Alnus* generally decreases. Quite low values of coprophilous fungi spores are recorded during this phase.

In STM1d (117–100 cm), *Pinus* percentages stay stable but the share of *Picea* increases a lot at the end of this phase, reaching 20%. HdV-200 is present but in very low concentrations. In the meantime,

TABLE 3 Lithogeochemical facies and lithofacies of the deposits in the STII M25 core

Lithogeo-chemical facies symbol ^a	Depth (cm b.g.l.)	Lithology	Facies/lithofacies ^b	Depositional environment	Total thickness for all profile in m (% of sum)
A	24–34, 78–80	Coarse detritus gyttja, peaty organic mud with sandy admixture	Limnic, telmatic/C, FS FCS, FS	Lake/mire	0.12 (9)
B	34–78, 80–82, 134–138	Coarse detritus gyttja, carbonate sandy organic mud, peaty organic mud with sandy admixture	Limnic, telmatic/C, C, FCS, FS	Lake/mire	0.54 (38)
C	82–109, 118–134	Coarse detritus gyttja	Limnic/C	Lake	0.43 (31)
D	109–118, 138–160	Sands and gravels with organic mud and plant detritus, coarse detritus gyttja	Limnic/S, G, CF	Lake, river	0.31 (22)

Abbreviation: b.g.l., below ground level.

^aSymbols as in Figure 4.^bLithofacial–textural symbols of clastic sediments after Zieliński and Pisarska-Jamrozy (2012).

algae spores are quite stable at around 30%. Poaceae slightly decrease but stay under 10% as in the entire core. *Ulmus*, *Quercus* and *Corylus* tend to decrease a little. Tree and shrub pollen values increase slowly. Chenopodiaceae reappear in very low percentages.

In the following STM2 (100–80 cm) zone, *Picea* percentages increase and reach almost 50% and the share of *Pinus* increases to 25%. Meanwhile, the percentage of *Alnus* decreases a lot to reach less than 10%, and the share of *Quercus* also decreases. At the end, tree pollen combined with shrub pollen reach almost 100%. HdV-200 percentages become null, and algae spores increase to more than 40% (the highest value in the core). Coprophilous fungi spores are absent at the end of this phase. *Artemisia* and Chenopodiaceae occur occasionally.

The Serteya STII M25 macro charcoal diagram is divided into four charcoal zones called STCh—from STCh1 to STCh4. The STCh1 zone (159–152 cm) is characterised by low CHAR_{macro} values with fluctuations, averaging approximately 0.05 particles/cm²/year, and not exceeding 0.2 particles/cm²/year. In the STCh2 zone (152–87 cm), the highest CHAR_{macro} values were recorded, averaging approximately 1.65 particles/cm²/year with the maximum of more than 15 particles/cm²/year (at 115 cm). The STCh3 zone (87–46 cm) is characterised again by low CHAR_{macro} values with fluctuations, averaging approximately 0.2 particles/cm²/year, and not exceeding 1.1 particles/cm²/year. The last zone STCh4 (46–26 cm) is characterised by an increase in CHAR_{macro} values also with fluctuations, averaging approximately 1.0 particles/cm²/year, and not exceeding 3.4 particles/cm²/year (Figure 6).

Based on major changes in macrofossil proportions, three local plant macrofossil assemblage zones (LMAZs) were distinguished in the macrofossil diagram. These zones, I–III, were further subdivided into subzones based on minor changes (Figure 6).

In LMAZ I (depth: 158–147 cm), the most frequently found helophyte is *Schoenoplectus lacustris*. Among hydrophytes, *Najas marina* appears in the upper part of this zone. Terrestrial plant remains, such as leaf fragments, buds, and bud scales, as well as seeds of *Alnus* sp., are also present, increasing in the course of this zone.

The following LMAZ II (147–84 cm) is characterised by a distinct rise in macrophyte assemblages. In LMAZ IIa (147–131 cm), the strongest evidence of hydrophytes was recorded, of which *Potamogeton* spp. is the most representative of submerged vegetation, along with *Najas marina*, *Zannichellia palustris*, and *Chara* spp. The presence of helophytes, in particular *Schoenoplectus lacustris*, is somewhat smaller, and the occurrence of amphiphytes, represented by *Alisma* spp., is even lesser. Other remains of aquatic organisms, such as dormant stages of Bryozoa, also appear. At the same time, increased proportions of terrestrial remains (buds, bud scales, and *Alnus* spp. seeds) were documented, along with evidence of fish remnants (scales, bones). Shell fragments of *Corylus avellana* and seeds of *Rubus idaeus* were also recorded, parallel to finds of nutrient-loving herbs of muddy habitats, such as *Urtica dioica*, *Chenopodium album*, *Ch. glaucum/rubrum*, *Persicaria lapathifolia*, and *Ranunculus acris/repens*.

In LMAZ IIb (131–115 cm), there is a visible increase in amphiphytes represented by *Sagittaria sagittifolia* and *Alisma* spp., whereas

finds of submerged hydrophytes (*Najas marina*, *Potamogeton* spp.) diminish or even disappear (*Zannichellia palustris*, *Chara* spp.). The proportion of floating-leaved hydrophytes—in particular *Nymphaea alba*—increases slightly. The evidence of helophytes also decreases, whereas the share of plant representatives of moist to wet habitats increases, in particular sedges (*Carex* spp. bicarpetal, *Carex* spp. tricarpetal) and *Solanum dulcamara*. The same is true for Bryozoa, but they show a sharp reduction in the middle of this subzone. Fish remains were detected in large quantities, whereas bone fragments were documented in two samples. Shell fragments of *Corylus avellana* occur too, along with finds of *Alnus* sp. seeds. However, their evidence disappears in the course of this subzone. Different nutrient-loving herbs of muddy habitats (*Urtica dioica*, *Persicaria lapathifolia*, *P. maculosa*, *P. hydropiper*, *Bidens* sp.) are also still present. Furthermore, elevated records of mosses were documented, along with increased finds of terrestrial leaf fragments.

In the subsequent LMAZ IIc (115–101 cm), there is a distinct decrease in the amounts of both submerged and floating-leaved hydrophytes. At some levels, their evidence even vanishes completely. Representatives of helophytes, such as *Schoenoplectus lacustris*, disappear. The abundance of amphiphytes becomes smaller, whereas the presence of mosses is still high. The evidence of Bryozoa is also reduced. The amount of wetland vegetation varies a lot and there is an increase in terrestrial leaf remains, whereas the share of other plant remains, such as buds and bud scales, diminishes. Nutrient-loving herbs show a distinct reduction. Evidence of fish remains was recorded only once.

In the uppermost LMAZ IId (101–84 cm), there is renewed stronger evidence of submerged hydrophytes (*Potamogeton* spp.), but this fluctuates visibly. Finds of floating-leaved aquatic plants, amphiphytes, and helophytes were made only sporadically. The proportions of Bryozoa increase in general, but they are also affected by fluctuations. The abundances of nutrient-loving herbs of muddy habitats and representatives of moist to wet sites are at somewhat higher levels than before. Since the beginning of this subzone, an almost continuous decrease in the proportions of terrestrial remains (buds, bud scales, leaf fragments) was documented. However, evidence of seeds of *Alnus* sp., *Pinus* sp., and *Rubus idaeus* could be found here.

The following LMAZ III (84–34 cm) is distinguished by the disappearance of almost all plant macrofossils.

A total of 15 fish remains were gathered from the core samples. The depth of these finds ranges from 104 to 146 cm. The sample from a depth of 130 cm is the richest, with five remains; samples from depths of 124 and 126 cm both yield three remains, and then samples from depths of 104, 120, 136, and 146 cm are represented by only one piece of ichthyological remains (Table 4). Perch is the most well-represented taxon with seven remains. Pike and one of cyprinids are both pictured from one piece of remains. No anthropogenic trace could be observed on the bones; also no seasonality or size reconstruction could be obtained. Concerning environmental conditions, perch, and pike are present in water bodies such as rivers, lakes and ponds with rich aquatic vegetation (Kottelat &

Freyhof, 2007) which is used for spawning. Cyprinids are other phytophilous species, too.

The sediments contain 22 Cladocera species, belonging to four families: Bosminidae, Daphniidae, Sidiidae, and Chydoridae. We identified four zones in the local cladoceran development for Cladocera fossils in the STII M25 core (Figure 7).

The zone LCAZ I (158–150 cm) is characterised by relatively low finds of cladocerans with the dominance of *Chydorus sphaericus*, *Alona affinis*, and *Alona rectangula* remains.

LCAZ II (150–86 cm) is the zone with the greatest cladoceran frequency and diversity within the whole section, thus, four subzones were distinguished: LCAZ IIa (150–134 cm) is composed mainly of *Ch. sphaericus*, *A. rectangula*, and *A. affinis*. Remains of *Camptocercus rectirostris*, *Eurycericus lamellatus*, *Graptoleberis testudinaria*, *Alona guttata* var. *tuberculata*, *Leydigia acanthoceroides*, and *Disparalona rostrata* as well as pelagic forms, *Bosmina* (*Eubosmina*) *coregoni*, *Bosmina longirostris*, and *Simocephalus* sp. are recorded for the first time; LCAZ IIb (134–112 cm) sees a decline in *A. rectangula* and *B.(E.) coregoni*, *B. longirostris* as well as *Simocephalus* sp. remains. *Pleuroxus truncatus* and *Alonella nana* appear for the first time; in LCAZ IIc (112–100 cm), Cladocera numbers significantly decrease and pelagic forms are represented by only *B. longirostris*. The share of *A. guttata* var. *tuberculata* remains relatively increases, and at the same time, the frequency of *A. rectangula* continues to decrease; LCAZ IId (100–88 cm) sees an increase in cladocerans at the onset, especially pelagic taxa, but at the end of this subzone, cladocerans disappear. The *Daphnia pulex*-group appears for the first time. Although *Ch. sphaericus*, *A. affinis*, and *A. rectangula* dominate, the presence of *Pleuroxus uncinatus* is also significant.

LCAZ III (78–70 cm) is characterised by only three littoral and one pelagic taxa while LCAZ IV (44–34 cm) by a relatively high number of Cladocera.

In total, 3561 specimens of Chironomidae were identified and classified into three subfamilies (Figure 8).

In the phase ST-Ch1 (158–146 cm), an increase in the number of h.c. starts from about 150 cm b.g.l. This zone is over-dominated by *Glyptotendipes pallens*-type. There also appear six other phytophile—both mining and facultative phytophile taxa. The subdominant morphotypes are *Tanytarsus pallidicornis*-type and *Polypedilum nubeculosum*-type. *Endochironomus albipennis*-type starts to occur from 150 cm b.g.l. From the ST-Ch1 to ST-Ch3 zone, *Parachironomusvarus*-type, which is a symbiotic species of snails, is also present.

In ST-Ch2 (146–131 cm), communities are dominated by facultative phytophile species (mainly *G. pallens*-type reaching 37%, although its share is the lowest in the whole sequence). The share of taxa typical of the organic bottom is the highest through the M25 Chironomidae stratigraphy. They are mainly *E. albipennis*-type (13%), *T. pallidicornis*-type (22%), *P. nubeculosum*-type (7%), and *Einfeldia dissidens*-type with *Chironomus pulmosus*-type as secondary taxa. There is a significant increase in the concentration of subfossils. The average concentration of midge h.c. in the ST-Ch2 zone is the highest in the whole sequence (26 h.c./1 g).

TABLE 4 The fish remains from the STII M25 core (analysis by M. Danger)

Depth b.g.l. (cm)	Anatomical part 1	Anatomical part 2	State of completeness	Taxon	Vernacular name	Measurement 1
104	Scale	n/a	Fragmented	<i>Perca fluviatilis</i> (Linnaeus, 1758)	Perch	n/a
120	Scale	n/a	Full	<i>Perca fluviatilis</i> (Linnaeus, 1758)	Perch	0.34 cm
124	Scale	n/a	Fragmented	undetermined	n/a	n/a
124	Cranial bone	n/a	Fragmented	undetermined	n/a	n/a
124	Vertebrate	n/a	Fragmented	undetermined	n/a	n/a
126	Pharyngeal tooth	n/a	Full	Cyprinid	Cyprinidae	n/a
126	Tooth	n/a	Full	<i>Esox lucius</i> (Linnaeus, 1758)	Pike	0.53 cm
126	Precaudal vertebrae	thoracic	Full	<i>Perca fluviatilis</i> (Linnaeus, 1758)	Perch	0.19 cm
130	Rib	n/a	Fragmented	undetermined	n/a	n/a
130	Scale	n/a	Fragmented	<i>Perca fluviatilis</i> (Linnaeus, 1758)	Perch	n/a
130	Scale	n/a	Fragmented	<i>Perca fluviatilis</i> (Linnaeus, 1758)	Perch	n/a
130	Scale	n/a	Fragmented	<i>Perca fluviatilis</i> (Linnaeus, 1758)	Perch	n/a
130	Scale	n/a	Fragmented	Undetermined	n/a	n/a
136	Rib	n/a	Fragmented	Undetermined	n/a	n/a
146	Precaudal vertebrae	thoracic	Full	<i>Perca fluviatilis</i> (Linnaeus, 1758)	Perch	0.32 cm

Abbreviation: b.g.l., below ground level.

In ST-Ch3 (131–100 cm), the subfossils concentration varies from 50 to 7 h.c./1 g. In this zone, optionally phytophilic species and taxa typical of the organic bottom also reveal the highest dominance. The *G. pallens*-type (52%), *E. albipennis*-type (8%), and *P. nubeculosum*-type (5% of individuals) remain the main dominants. The share of *G. pallens*-type increases whereas other phytophilic taxa decline. The species richness of mesotrophic guilds typical of the mineral and mineral-organic bottom increases. In this group, *Microtendipes pedellus*-type plays a dominant role. At the end of the zone, the species typical of seepages and small brooks, such as *Paracricotopus* and *Zavrelimya*, appear. Two h.c. of *Xenochironomus xenolabis*, which mines sponge and bryozoans, were collected at depths 106–104 cm b.g.l.

In the initial part of the ST-Ch4 (100–89 cm) zone, the abundance of organic bottom dwellers declines. Among organic bottom taxa, only *E. albipennis*-type reveals a higher share within the communities (7%). *G. pallens*-type reaches the highest domination (78%). The share of the mesotrophic *M. pedellus*-type is ca. 5% at the bottom of the zone, later on, this species disappears. The chironomid species richness and h.c. concentration rapidly decline in the ST-Ch4 zone to twelve morphotypes and 0–3.8 h.c./1 g, respectively.

In the upper—not included here—sections of ST-Ch5, there are a few midge h.c. recorded but the concentration of midge subfossils never reaches over 0.1 h.c./g in this zone.

6 | DISCUSSION

6.1 | Local palaeoenvironment reconstruction

6.1.1 | Regional vegetation

The results of pollen analysis document a dense forest cover during the entire period studied by this study. Nevertheless, a change occurred between 2550 and 2475 cal. BC and 2150–2000 cal. BC. The forest, largely dominated by *Alnus* in the wetland and the mixed oak forest beyond, was replaced by a cover of *Pinus* and *Picea*. This event was linked to cooler and wetter conditions at the onset of the Neoglacial period, as has already been observed in the Serteya region (Tarasov et al., 2019). It is important to note that the main wooden building material during this period was spruce, though a tradition of broad-leaved wood use for household objects was maintained (Mazurkevich & Dolbunova, 2011). There is no

overrepresentation of some taxa in the archaeological layer (between 4300 cal. BC and 2200/2000 cal. BC), it is not easy therefore to evidence particular activities linked to plant consumption at the site. Few indicators characterising farming activities (Behre, 1981) are present. *Artemisia* and *Chenopodiaceae* are heliophilous and nitrophilous, and their presence in the pollen record is associated with nitrogen-rich areas around dwellings (Behre, 1981). However, their presence here might have been totally natural too, and there is no evidence of any large clearances favouring their growth. Coprophilous fungi spores occur regularly and could be related to wild or domesticated herbivores. So, there is no unambiguous evidence of human impact at Serteya II based on pollen analysis. Nevertheless, the increased evidence of *Artemisia* and *Chenopodiaceae* between ca. 4300 and 3450 cal. BC correlates with finds of berries and nutshells, which may be attributed to local human activity. Numerous finds of fish traps left by Eneolithic tribes and dated from the end of the 5th millennium BC to the middle of the 4th millennium BC were present. It is interesting to note a settlement hiatus, based on a radiocarbon data set for artefacts between the beginning of the 5th millennium BC (the end of the Rudnya Culture existence) and ca. 4300 cal. BC (the appearance of Eneolithic tribes), which could indicate that this area was not populated during this period of time.

During the same period, there was a sharp increase of CHAR_{macro} (from sample to sample) from 0.2 to 3.1 particles/cm²/year. Earlier works on vegetation, human, and fire relationships through the Holocene in Eastern and Central Europe (Dietze et al., 2018; Feurdean et al., 2020) indicate that the use of fire increased around 2900 cal. BC when there was a transition from the Funnel Beaker Culture towards the Corded Ware Culture can be recorded (Dietze et al., 2018; Warden et al., 2017).

6.1.2 | Increase of lake water level (ca. 4300–3300 cal. BC)

Generally, the Serteya STII M25 core represents the littoral part of the lake and shows permanent water cover between 4300 and 1600 cal. BC, but with a continuous trend of shallowing, and finally with only periodic flooding. However, plant, palaeozoological and geochemical records suggest various episodes of palaeolake water level fluctuations (Mroczkowska et al., 2020).

Fungal spore analysis suggests there were frequent fluctuations of water depth and periodic emersions of the shoreline (Laine et al., 2010; van Geel et al., 1989). Indeed, shoreline emersion can activate fungal decomposition of organic materials. So, the presence of HdV-200 together with the decrease of algal spores suggests some phases of temporary drying from ca. 4300/4100 cal. BC to ca. 3050 cal. BC, and probably also between ca. 2500 and 1800 cal. BC. However, this situation does not exclude short-term episodes of increases of water-level and periodic flooding, as suggested by palaeozoological proxies.

Before ca. 4150 cal. BC, unfavourable conditions for the development of aquatic plant and invertebrate communities were

apparent (Figure 9). During that time *Schoenoplectus lacustris* was abundant. This reed is able to tolerate higher water levels than other helophytes, thus suggesting permanent water cover up to 6 m (Hannon & Gaillard, 1997). However, with the exception of *Najas marina*, which appears in the upper part of this zone, no further macrophytes were recorded. This indicates unfavourable conditions for the development of species-rich aquatic vegetation. Nevertheless, the presence of some water plants is suggested by the occurrence of phytophilic chironomids, although in low abundance until 4.3 ka BC (i.e., below 150 cm b.g.l.). The scarcity of macrophytes could be due to insufficient nutrients in the water limiting aquatic plant colonisation. This interpretation is supported by evidence of few nutrient-loving herbs of muddy habitats. In addition, the continuously increasing presence of terrestrial plants (seeds of *Alnus* spp., leaf fragments, buds, and bud scales) could be an indication that the water level steadily decreased over time. This is also indicated by the low frequency of, mostly cosmopolitan cladoceran taxa (such *Chydorus sphaericus* and *Alona affinis*). As well as a high frequency of facultative phytophilic chironomids, chironomids typical of eutrophic, warm, shallow waters with organic sediments are dominant. As indicated by the high values of TOC/TN (often >25), the organic matter is derived mainly from terrestrial sources (Meyers & Teranes, 2001). The Fe/Mn ratio, which is an indicator of palaeoredox conditions (Eusterhues et al., 2005), was generally low (average is 97), but reached a maximum value of 130–174 at the upper part of the lithogeochimical facie "D". The proportion of sand increased to 82%–96%, and fine-grained sand dominates (average 36%). The dominance of coarse silt (four to five times) over fine silt indicates sediment transport under conditions of short-term suspension and saltation. Human occupation during relatively warm climatic conditions probably caused an increase in erosion, as is reported at other archaeological sites (Kittel, 2015; Sobkowiak-Tabaka et al., 2020).

The distinct rise of hydrophytes from approximately 4150 cal. BC onwards indicates nutrient enrichment of the water. At the same time, phytophilic aquatic invertebrates, associated with the littoral zone of eutrophic lakes, dominate. The frequency and diversity of Cladocera increases (Figures 7 and 9), including a many benthic taxa of which a few are indicators of eutrophic water (*A. rectangula*, *Ch. sphaericus*, *L. acanthocercoides*), rich vegetation in the littoral zone and warm waters (*A. affinis*, *Ac. harpae*, *E. lamellatus*, *C. rectirostris*, *G. testudinaria*, *Pleuroxus* spp.). The abundance of Nonbiting midges rapidly increases, especially of eutrophic organic bottom dwellers and phytophilic taxa. This indicates eutrophication of the lake which could have been caused by increased supply of nutrients as a result of human activity. The appearance of Bryozoa and fish, also demonstrates increased food availability. Furthermore, the presence of submerged macrophytes that can occur in deep water, such as *Potamogeton* spp. and *Chara*, shows that the water level must have been relatively high up to ca. 3250 cal. BC. The occurrence of planktonic Cladocera indicates a significant increase in the palaeolake water level ca. 4150–3600 cal. BC. This correlates with the arrival of Eneolithic tribes from the steppe area in this region, marked by the

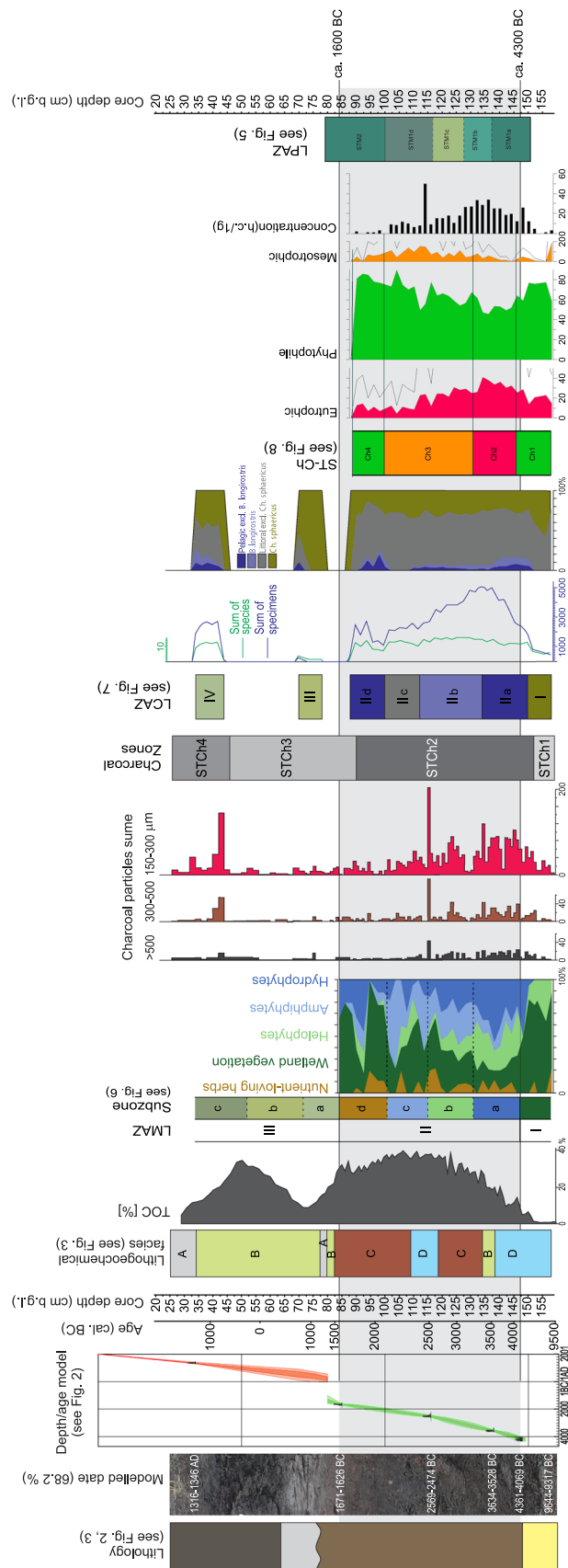


FIGURE 9 Palaeoecology reconstruction for the Setteya II site based on selected results [Color figure can be viewed at wileyonlinelibrary.com]

remains of different types of fish traps, parts of paddles and large boats (Photo 1; Table 5). The pelagic cladoceran *B. longirostris*, which lives in both in the open water and the littoral, and indicates eutrophic conditions (Pawłowski, 2011), was common. Chironomid larval h.c. concentrations were also at their highest during this period. In this period, organic-rich (LOI increase to 74%) coarse detritus gyttja was deposited in the highly productive lake. Nevertheless, fluctuations of TN and TS content as well as the Na/K ratio suggests periodic changes in biological productivity and denudation processes in the catchment. This is confirmed by the frequent (but not abundant) appearance of chironomids such as *Cryptochironomus*, which favour mineral sediments. Apart from short-term variations, a general increase in TN (from 0.4% to 1.69%) from the base of the lacustrine sediments to ca. 3250 cal. BC indicates a gradual increase in productivity, while a decrease in sand content (from 12% to 0.5%) and coarse silts twice as abundant as fine silt indicates a relatively small increase in weathering and soil processes in the catchment.

6.1.3 | Decrease of lake water level (ca. 3300–2500 cal. BC)

From ca. 3250 cal. BC, there is an increase in floating-leaf plant communities and amphiphytes, and gradual decrease in submerged hydrophytes. These rooted aquatic plants colonise shallow waters and indicate the lowering of the water level lowering. Other indicators of lowering water level are the increase of herbs of moist habitats, mosses that indicate disturbed, exposed sites, and the low

frequency of chironomids and pelagic Cladocera. Although, as the number of chironomids stays high, this suggests that water level reduction did not occur for long periods of time. Chironomid taxa typical of a eutrophic, detritus-rich littoral (e.g., *G. pallens*-type) are still present, but the proportion of taxa typical of mesotrophic conditions rises. This indicates that water trophic level decreased probably due to reduced human activity and/or climate cooling.

Highly oxidizing conditions are recorded by a very low Fe/Mn ratio (values between 75 and 80) throughout most of the "B" and "C" lithogeochemical facies. A short-term decreasing trend in PC3 (Figure 3), and an increase of weathering and soil processes are manifested in the high values of the coarse/fine silt ratio (above 5). The rise in the Na + K + Mg/Ca (to 1.3–1.72) ratio in the bottom part of these sedimentary sequences can be linked to enhanced soil erosion. Two, about 1-cm thick, intercalations of mineral matter where sand is almost completely lacking (below 2.5%), and a sharp increase in the Fe/Mn ratio (above 220, ca. 3050 and 2650 cal. BC) indicate high-water level episodes in the lake or weathering processes. The distinct decline in oxygenation of lake water since ca. 2800 cal. BC was presumably caused by the microbial decomposition of organic matter. Changes of Fe fixation inorganic deposits are also related to bacterial production of H₂S in the environmental lake accumulation (Apolinarska et al., 2012). This is confirmed by the Fe/S ratio which falls to 0.04 in the organic-rich sediments (LOI between 65–93%).

The concentration of chironomid larval h.c. in the sample at 114 cm b.g.l. (modelled ¹⁴C cal. age: 2535–2435 cal. BC) is 50 h.c./g., higher than all the other values in the core sequence. Such high

TABLE 5 The results of radiocarbon dating of archaeological materials from the western part of the Sertya II site (in the vicinity of the STII M25 core)

Square (see Figure 1)	Dated material	Layer-context (local elev. system)	¹⁴ C Age yr BP	Laboratory code	Calibrated Age (prob. 68.2%)	Calibrated Age (95.4%)
O27	Bone (mandible of the cow)	Top of brown gyttja (-0.258)	1685 ± 30	Poz-108410	335–400 AD	257–419 AD
M22	Food crust	(-0.984)	4255 ± 35	Poz-108832	2912–2873 BC	2922–2704 BC
K23	Wood ^a	Wooden pile, №224	4340 ± 80	Le-11882	3090–2888 BC	3336–2708 BC
N24	Food crust	Olive gyttja (-0.772)	4505 ± 35	Poz-108583	3339–3106 BC	3352–3095 BC
L23	Food crust	(-0.930)	4560 ± 35	Poz-108833	3368–3124 BC	3489–3104 BC
N24	Food crust	Olive gyttja (-0.743)	4570 ± 35	Poz-108986	3485–3127 BC	3496–3104 BC
L22	Food crust	(-1.113)	4625 ± 35	Poz-108827	3498–3360 BC	3517–3348 BC
K23	Wood ^a	Wooden treated sticks from construction, №247	4650 ± 50	Le-11881	3514–3365 BC	3630–3345 BC
N24	Food crust	Olive gyttja (-0.826)	4670 ± 35	Poz-108598	3516–3372 BC	3622–3366 BC
K23	Wood ^a	№229, wooden pile	4890 ± 90	Le-11880	3789–3536 BC	3943–3385 BC
N22	Food crust	(-1.073)	4940 ± 35	Poz-108581	3761–3661 BC	3786–3651 BC
N25	Food crust		5115 ± 35	Poz-108597	3969–3812 BC	3981–3800 BC
P27	Bone	Brown gyttja (-0.513)	5180 ± 40	Poz-108409	4039–3960 BC	4218–3813 BC

^aSee Photo 1.

midge abundance may come from exceptionally high food availability, such as the local accumulation of rotting organic matter, and this coincides with the deposition of human skeletons in the same layer. Non-biting midges are often associated with submerged carcasses and are used in forensic entomology (Keiper & Casamatta, 2001). Medina et al. (2015) analysed the case of a female carcass found in a river near Granada similar to the one reported from the STII M25 excavation. The only entomological evidence collected during the autopsy consisted of *Chironomus riparius* larvae interposed among the long hair of the head, in the area close to the scalp. Human hair may imitate filamentous algae or decaying plant leaves and thus provide a suitable habitat for chironomid larvae. The decaying bodies of two females (and also probably one male) whose skeletons were found at M25 must have been deposited in the water because aquatic chironomid larvae do not develop in terrestrial conditions. The death must also have taken place during the growing season as midge larvae usually do not grow at low temperatures and remain in diapause during the winter. Larvae may have gathered in the hair after moving from the lake sediments or eggs may have been oviposited and larvae completed the life cycle on the body. If the latter, that would mean the women's death occurred most probably between May and August, as this is the period that eggs are deposited in most of the chironomid species collected in the sample 114 cm b.g.l. (Moller Pillot, 2009). Alternatively, such a rapid increase in the chironomid population could be explained by an increase in lake trophy, or an exceptionally warm and long growing season. However, if a wider increase in lake trophy had occurred, the ecological consequences and an increase in midge abundance would be observed in subsequent samples. However, this is not the case. Also, the Chironomidae-inferred mean July air temperature reconstruction for the 114 cm b.g.l. remains the same as temperatures inferred from samples above and below (Mroczkowska et al., 2020). Simultaneously, a very distinct peak of charcoal admixture in gyttja deposits is also recorded at 115 cm b.g.l. (Figure 9).

6.1.4 | Lake water level fluctuations with desiccation phases (ca. 2500–2100 cal. BC)

From ca. 2500 cal. BC, there is a further drop of the abundance of submerged water plants and floating-leaved hydrophytes. Synchronously, helophytes, growing in the deeper areas of the littoral zone (*Schoenoplectus lacustris*), disappear. This general decrease in the macrophyte assemblage shows that the water level decreased further, and probably that there may have been longer desiccation phases. In this context, the concurrent high frequency of mosses suggests the presence of remnants of disturbed hummocks. However, as amphiphytes (i.e., plants that are particularly well adapted to fluctuating water levels) continue to be present, this indicates that the water did not retreat permanently. Ca. 2300–2200 cal. BC, the Chironomidae *X. xenolabis*, which as a larva mines Bryozoa colonies, is present, proving that not only resting statoblasts but also fully aquatic bryozoan zooids were present at the site. Such changes in

macrofossil remains, along with changes of the organic matter content, and the Fe/Mn and Fe/S ratios for lithohgeochemical facie "D", reflect a varying water level in the lake. At the beginning of this phase, the high Fe/Mn ratio (above 200) indicates strongly reducing conditions in the lake. The gradual change in soil erosion is reflected in the peaks of the TOC/TN ratio, which corresponds to the grain-size composition of inorganic admixtures (an increase in the proportion of sand from 0.5% to 8%), an increase of the erosion ratio (Na + K + Mg/Ca—from 0.4 to 0.8), and a high sedimentation rate. Later, highly oxidizing conditions are demonstrated by a decrease of the Fe/Mn ratio (from 275 to 167), reaching a minimum at ca. 2250 and 2150 cal. BC. Cladocera reveal conditions. At ca. 2500 cal. BC, a decreased frequency of planktonic cladoceran taxa and the presence of cladoceran taxa associated with decreasing pH and lower lake productivity (*Alonella excisa* and *Alona guttata* var. *tuberculata*), as well as macrophytes and/or sediments, show the intensification of terrestrialization processes. Chironomids give a consistent signal with Cladocera and macrophytes. Low h.c. concentrations show seasonal, though the long-term presence of shallow water conditions. An increase of the mesotrophic *M. pedellus*-type, with a decline of nearly all the other taxa (except *G. pallens*-type), indicates a decrease in lake trophic levels, and a lower human impact. The geomorphological characteristics show that since the 2nd half of the 3rd millennium BC the lake system could have been replaced by a fluvial one. Fluvial deposits from that period are cut within lacustrine sediments (Kittel et al., 2018a). This could have coincided with the main phase of the existence of the pile-dwellings, shown by an increase of radiocarbon dated wooden constructions and artefacts. Throughout Eastern and Central Europe, this period is characterised by a progressive decrease in lake levels between 3300 and 2000 cal. BC, suggesting a drier climate (Dietze et al., 2016; Harrison et al., 1996; Lamentowicz et al., 2019; Słowiński et al., 2016; Tarasov et al., 1994, 1996; Warden et al., 2017).

6.1.5 | Lake water level fluctuations with flooding phases (ca. 2100–1600 cal. BC)

From ca. 2100 cal. BC, chironomids nearly disappear, indicating unfavourable conditions for benthic insects. This suggests water was only present episodically, although submerged hydrophytes increase. This could be indicative of recurring phases of deep-water conditions. This is confirmed by peaks of planktonic Cladocera at ca. 2000 cal. BC and 1900 cal. BC, especially in Bosminidae, and other deep-water cladocerans (among others, from the *Daphnia pulex*-group; Figures 7 and 9). Palaeolake eutrophication is also suggested at this time from the periodic occurrences of pelagic and benthic Cladocera species (e.g., *Ac. harpae*, *Ch. sphaericus*, *M. dispar*), which are abundant in temperate lakes amongst macrophytes, and which can tolerate changes in hydrological conditions (Błędzki & Rybak, 2016; Pawłowski et al., 2016a).

An increase in cladocerans is observed after 2000 cal. BC and later (after ca. 1800 cal. BC) chironomids disappear. This suggests

seasonal flooding of the site, mostly in the spring, before the main growth period of Chironomidae larvae. The cladoceran assemblage suggests that open water may have been present for periods as short as a few weeks. In accordance with this, plant macrofossils (*Potamogeton* spp. and *Schoenoplectus lacustris*) are recorded only sporadically, whereas aquatic Bryozoa (mostly *Cristatella mucedo*) are more frequent but with longer periods of absence. This may be indicative of phases with a temporary water cover at the site, probably as periodic inundations. On the other hand, Bryozoa species are capable of enduring dry periods by producing dormant structures—the statoblasts—which, however, does not exclude the recurring water level fluctuations. Bryozoa statoblasts are dispersible “survival pods” that may be transported over a large distance, even from another part of the lake or from another basin, and can be left on the shore by waves or incidental inundation (Ruppert et al., 2004). Furthermore, Bryozoa are sensitive to temperature, often absent in water colder than 16°C in summer (Økland et al., 2003), and they prefer alkaline habitats with a pH of at least 6.6 and a well-developed littoral zone (Økland and Økland, 2002; Økland et al., 2003; Słowiński et al., 2018; Zawisza et al., 2019). Thus, their presence may be indicative of flood events, when alkaline water conditions prevailed due to catchment run-off.

Such observations are confirmed partly by geochemical and sedimentological records, mostly the mineral matter content, variable values of the Fe/Mn, Cu/Zn, Na + K + Mg/Ca ratios, and grain-size composition. The enrichment in the mineral matter (from 6% to 12%) is observed only from ca. 1900 cal. BC and shows seasonal fluctuations (between 9% and 13.6%). Flood events are more reflected in peaks of the TOC/TN ratio (increased from 17 to 19 at ca. 2100 cal. BC and from 14 to 17 at ca. 1800 cal. BC). In both periods, the increase of sand content (from 6% to 21%) and coarse silt five times more abundant than fine silt indicates a relative increase of catchment weathering. This interpretation is supported by an increased trend in PCA, which indicates intensification of the erosional capability of allochthonous materials and enhanced accumulation of fine-grained sand. Changes in the trend of the C/N ratio and mineral grain-size composition are commonly related to human presence in the area and deforestation (Ochiai et al., 2015; Routh et al., 2007), although deforestation is not recorded in the pollen sequence. The C/N ratio of the sediment is between 14 and 19, indicating that both algal inputs and terrestrial organic matter are significant contributors to the sedimentary organic matter in the lake. Thus, a lower shift in the C/N ratio may indicate a change to a more aquatic source of organic matter in the spring. This interpretation is supported by an increasing trend of the Na + K + Mg/Ca ratio, which indicates an increase in erosion of allochthonous materials. A change in the Na + K + Mg/Ca ratio (between 0.6 and 1.4) is interpreted as a signal of seasonal floods. Observed geochemical fluctuations between 2100 cal. BC and 1800 cal. BC are not correlated with strong cultural influences and must, therefore, be of a natural, probably climatic origin, such as freshet floods caused mostly by unusual high snowmelt or heavy rains. Seasonal (spring-thaw) floods and latter stagnation of flood waters in a shallow lake, followed by periods of

desiccation is recorded for GSPB by Kittel et al. (2020). This correlates well with archaeological data: we trace only episodic visiting by people of the lacustrine shores.

At ca. 2000 cal. BC and from 1800 cal. BC onwards, the cladoceran record reveals an initially short-term and later a permanent drop of the water level. From ca. 1750 cal. BC onwards, there is a general reduction in macrophyte assemblages, pointing to unfavourable conditions for littoral and water plants. In contrast, plants of swampy and drier habitats, such as sedges and grasses, occur. Therefore, this probably reflects a significant decrease of the water level and a subsequent terrestrialization process. After ca. 1700 cal. BC, there was a process of natural succession of the lake towards wetland.

Sedimentary succession (change of lithogeochemical facies from “C” to “B” and “A”) and an increase of fine sand (up to 30%) in the gyttja deposits suggest conditions of standing water with floods. These sediments are composed of organic matter (mean values of 88.6%) with 1%–3.63% mixture of CaCO₃, as well as stable values of the TOC/TN (approximately 15–16) and Fe/Mn (approximately 140–160) ratios. A rapid change of grain-size composition in the sediment from sandy silt (mean value of M_z is 5.2 phi) to silty sand (mean values of M_z is 4.1 phi) and a low value of the coarse/fine silt ratio (about 3) suggests intensification of slope processes in the period between ca. 1850 and ca. 1600 cal. BC. These values are representative of the substratum deposits of the catchment. The period of higher mechanical denudation corresponds also with a decrease of the Ca/Fe ratio. Distinct, concurrent changes in geochemical proxies can be the result of wetter climatic conditions and nutrient delivery due to wildfires in the catchment (Pleskot et al., 2018).

The record of flooding after ca. 1500 cal. BC is manifested by an increase of the inorganic matter in sediments (from 8.2% to 23.7%) and the Fe/Mn ratio (from 159 to 216). This signal is very significant in changes in the content of TOC (a decrease from 21% to 12%; Figure 9) and an increase of the Fe/S ratio, whose values between 0.6 and 0.7 may indicate the presence of pyrite and strongly reducing conditions in the lake (Engstrom & Wright, 1984; Pędziżewska et al., 2015). This is also distinctly documented by the change in grain-size composition (the mean value of sand is 68.9%).

Such short-term rises of the water level were noted after 1400 cal. BC onwards, as confirmed by the Cladocera record (Figure 9). An improvement in habitat conditions, such as a trophic increase after ca. 1400 cal. BC, was favourable for periodic occurrences of pelagic Cladocera from the family Bosminidae, and benthic, mostly cosmopolitan species, which are abundant in temperate lakes and can tolerate changes in water velocity (Pawlowski et al., 2016a, 2016b). It is possible that an increase in the proportion of sediment-associated Cladocera and pelagic taxa at this time was closely correlated with floods (Kittel et al., 2016, 2020; Pawłowski et al., 2015).

6.2 | Palaeoeconomic reconstruction

The previous study conducted in the Serteya region reveals intense settlement activity during the Neolithic since ca. 6300 cal. BC.

Early Neolithic communities were hunter-gatherers, while Middle and Late Neolithic communities might have introduced agriculture and cattle-breeding. However, according to bioarchaeological analyses, the productive economy did not play a significant role for Serteya II Neolithic societies (Mazurkevich et al., 2009; Mazurkevich, 2003; Tarasov et al., 2019).

The Neolithic remains at the Serteya II site have been dated to 6000/5500 cal. BC to 2000 cal. BC (Kul'kova et al., 2001; Mazurkevich et al., 2009). The shore zone of the site and its immediate vicinity were used in the Mesolithic and the Early Neolithic, and later, in the 1st half of the 3rd millennium BC, when it became a place of possible unique human burial. It was also the household area of the pile-dwelling settlement in the 3rd millennium BC (Mazurkevich et al., 2017).

Presented results confirm a progressing process of the lowering of the palaeolake water level in the Neolithic since ca. 3250 cal. BC. A long-term water level decrease can be certainly seen ca. 2500–2100 cal. BC. Before, the macrofossil record shows a rather shallow but permanent water cover. A distinct drop of water level is revealed by the Cladocera record between ca. 2050 and 1850 cal. BC. The results document that human bodies were deposited during the lowering of the water level in the palaeolake shore zone. Similarly, the pile-dwellings documented at the Serteya II site functioned (almost periodically) directly on the uncovered surface of lacustrine deposits (coarse detritus gyttja), as confirmed by archaeological data (Kittel et al., 2018a; Mazurkevich et al., 2017). It was during the decrease of the palaeolake water level when the bottom of the reservoir was (partly) uncovered, or it could have taken place during at least the short-term (rather seasonal) lowering of the lake water table. The Serteya II pile-dwelling settlement appeared before the 4.2 ka BP cooling event (Mazurkevich & Dolbunova, 2011; Mazurkevich et al., 2017). This event is globally recorded (e.g. Bond et al., 2001; Cullen et al., 2000; Marchant & Hooghiemstra, 2004; Roland et al., 2014). However, contrasting environmental responses were identified in different zones with cooler and wetter conditions at higher latitudes (Bini et al., 2019; Booth et al., 2005; Wanner et al., 2011). Recent palaeoenvironmental reconstructions indicate that the 4.2 ka event in Eurasia was characterised by strong seasonality (Persioiu et al., 2019; Pleskot et al., 2020). Palaeoecological and archaeological data show that the pile-dwelling constructions at the Serteya II site were finally flooded (Kittel et al., 2018a; Kul'kova et al., 2015; Mazurkevich & Dolbunova, 2011).

Based on the multiproxy palaeoecological study of the STII M25 core, some conclusions can be drawn regarding the economic activity of the Neolithic communities in the Serteya II area. The results of pollen analysis show a dense forest cover recorded in the archaeological layers and a lack of anthropogenic indicators. However, the results of plant macrofossils analysis of the studied core are helpful for the palaeoeconomic reconstruction of the ancient societies which occupied the Serteya II area.

Considering the botanical macrofossil record, which is the first such comprehensive study made for this area and this period, there is evidence of wild plants which could have been gathered as a supplement to the agriculturally produced foodstuffs, in particular,

between ca. 4150 and 3250 cal. BC. During this time, quite high records of *Alnus* sp. seeds and other land plant remains (buds and bud scales) were documented within coarse detritus gyttja deposits. This evidence indicates, on the one hand, a close proximity of the sampling site to the shoreline, not the deep-water zone. On the other hand, the elevated numbers of remnants of terrestrial origin could be associated with increased settlement activities in the shore zone. Perhaps they indicate, for example, the use of young branches for several construction purposes, as well as fuel for fire. Since the macrophyte evidence clearly supports high water levels at this point in time, the latter assumption is more likely. In the period between ca. 3500 and ca. 3100 cal. BC, a slight decrease of AP in pollen data was also recorded—mostly for *Picea*, *Carpinus*, *Tilia*, as well as *Fraxinus* and *Salix*. The increased presence of nitrophilous plant remains, such as *Urtica dioica* and *Persicaria lapathifolia*, can probably also be linked to human agency, or to natural eutrophic, muddy locations close to the shore, respectively. Another indication of the human use of the site is the presence of the remains of nuts and berries. In addition, the increased evidence of fish remains, all associated with Neolithic layers, point to fishing-related activities. Nonetheless, the number of remains is too small to discuss further fishing strategies. Ample fish populations were supplied by rich food resources—midge larvae and cladocerans. These invertebrate groups are one of the most important prey pools for benthivorous and planktivorous fish. This implies that if human activity had induced lake eutrophication (fertilisation), it should have also favoured the production of settlers' main food component—fish meat.

Remains of nuts (*Corylus avellana*) and berries (*Rubus idaeus*) from the 4150–3250 cal. BC period can indicate their on-site use by the Middle and Late Neolithic cultures, as well as steppe communities (Photo 1; Table 5). In addition, some locally occurring herbs had the potential to be used as additional food sources (Kaliečyc, 2018; Navahroński, 2000). Herbs such as *Urtica*, *Allium* and representatives of both the family Chenopodiaceae (e.g., *Chenopodium album*) and the family Apiaceae (e.g., *Angelica archangelica*, *Daucus carota*) could have been used as vegetables (Bos & Urz, 2003; Itkonen, 1921; Vanhanen & Pesonen, 2016). Starch-rich seeds of Chenopodiaceae can be stored for some time due to their relatively hard seed coat. The same is true for the family Polygonaceae (e.g. *Persicaria lapathifolia*, *Persicaria maculosa*; Vanhanen & Pesonen, 2016; Wolters, 2016). *Filipendula ulmaria* and *Solanum dulcamara* may have been used as medicinal plants (Bos & Urz, 2003; O'Neill & Rana, 2016). Apart from terrestrial herbs, macrophytes can also be consumed. For example, the starch-rich seeds and rhizomes of *Nuphar* are suggested as a dietary component at several archaeological sites (Kirleis et al., 2020; Kubiak-Martens, 2002; Warren et al., 2013; Wolters, 2016). In summary, these macro-botanical data, along with the concurrent evidence of increased amounts of charcoal and the presence of fish scales and fish bones in the sediment, can be linked to a relatively high level of local settlement activity during this time.

If human activity had induced lake fertilisation, it would have enhanced primary and secondary production of the GSPB ecosystem, which would have further benefited the economy increasing fish

catches and aquatic macrophyte biomass. However, this would have influenced the entire lake ecosystem only when the nutrients had been added in large amounts by human activity from the terrestrial environment. Alternatively, butchering mammals and birds from the forests at the lake shore, as confirmed by archaeological remnants, and then leaving organic remains in the water could have caused such an effect on a local scale. Although fish, wild plants, and boars fed by mussels collected from the lake were the main sources of food, the lake autochthonous matter and local offshore plants were transferred to the lake by Serteya II settlers. However, as demonstrated by the Chironomidae record, the input of allochthonous nutrients (N and P) to the water was not intense enough to cause extra eutrophication of the whole lake. Accordingly, another factor must have been decisive for the increase in the primary and secondary production during that time. The mean summer temperature, for instance, could have been the main driver of fish prey pools—chironomids and cladocerans (Luoto et al., 2019; Nevalainen et al., 2012). To put it in a nutshell, human activity would not have affected the lake trophy and indirectly fish resources on a large scale. Nonetheless, habitats in the site vicinity might have been locally more eutrophic and suitable for organic bottom dwellers feeding on detritus such as *Chironomus plumosus*-type, *Glyptotendipes pallens*-type or *Polypedilum nubeculosum*-type. Potentially more dense midge larvae populations and food remains could have attracted fish to the pile-dwelling. It is an open question whether this was an elaborate model developed specially by ancient people.

Since ca. 3250 cal. BC, the occurrence of shell fragments of *Corylus avellana*, along with the finds of, in particular, bones must be associated with the presence of dwellings at the investigated site. However, the temporary disappearance of nutrient-loving herbs around 2800 cal. BC in parallel to a distinct decline of both terrestrial bud scales and Bryozoa remains may represent a response to lesser water eutrophication, probably due to a short phase of a reduced human impact at that time. It correlates with the density of radiocarbon dates (Mazurkevich et al., 2017) and a possible settlement on another shore of the lake. However, the highest content of charcoal is noted ca. 2500 cal. BC, in the horizon where the human bodies were found, which can be probably linked to the burial rite. After ca. 2500 cal. BC, there seems to have been a reduced human impact at the site (see Table 5), as shown by the general decrease in the number of nutrient-loving herbs and the nonexistence of other macro-fossils attributed to human activity (nuts, berries, and fish remains) in this particular place. A renewed phase of increased human activity can be correlated with the period between ca. 2100–1800 cal. BC, when an elevated presence of wild berries was again documented in the sediment record.

Our results showed neither the palaeoeconomic transition from the hunter-gatherer economy into the productive one in the Late Neolithic before ca. 1500 cal. BC nor minor inputs of productive economy indicated by previous palynological data (Mazurkevich et al., 2009; Mazurkevich, 2003; Tarasov et al., 2019). In other words, we could not find any evidence of cultivated plants and animal husbandry record in archaeobotanical proxies until this period.

7 | CONCLUSIONS

The detailed multiproxy palaeoenvironmental research undertaken based on the lacustrine deposits core from the Serteya II site contributes greatly to broadening the knowledge of the functioning and transformation of the natural environment in the Neolithic between ca. 4300 and 1600 cal. BC. This is a period of global climate changes ca. 6.2, 5.9 and 4.2 ka cal. BP. The most intense settlement activity in the studied shore area of the GSPB is documented by palaeoecological proxies in the period 4150–3250 cal. BC, when the water table was relatively high. A strong impact of hunter-fisher-gatherer communities on the lake environment in the shore zone is recorded as significant water eutrophication, but only at the local level. The pile-dwellings constructions from the 3rd millennium BC existed during the period of lake water level decreasing with fluctuations and seasonal desiccation. In our record, the period of the 4.2 ka BP event can be correlated with a phase of temporal increase of the lake water level and later with its further drop. After ca. 2100 cal. BC only seasonal floodings, which resulted mostly from spring thawing, were recorded. This shows an important rebuilding of palaeoenvironmental conditions forced by global climatic changes. Thus, the pile-dwellings should be recognised as an adaptation to the changeable ecological conditions.

The general agenda of palaeoenvironmental changes and archaeological events in the GSPB was as follows:

1. Before 4150 cal. BC: a permanent shallow water cover, the water level decreased steadily over time, the organic and inorganic matter originated mostly from terrestrial sources. During the 6th millennium BC, early Neolithic sites were situated on lacustrine shores, those archaeological layers were destroyed by later transgressions. The remains of human activity show shoreline activity connected with some household needs, not with a dwelling area.
2. 4150–3250 cal. BC: the water level relatively high (the most significant increase at ca. 4150–3600 cal. BC), significant eutrophication (an impact of human activity only at the local level—fertilisation of the water body), rich vegetation, denudation processes in the catchment; intense settlement activity in the lake shore zone—gathering of wild plants (nuts and berries, as well as herbs and possibly also water-lilies), the use of young branches of trees, and intense fishing (including on-site fish processing). Groups of the Eneolithic steppe tradition penetrated into this region. Household activity can be traced in the shore zone, marked by fishing constructions, and later on—different household remains, big vessels possibly put in pits located on the shore, fragments of paddles, and traces of animal butchering.
3. 3250–2500 cal. BC: water level lowering (fluctuating with possible disappearance during the dry season), water trophy decrease, erosion in the shore zone and increased weathering, soil erosion; periodic settlement activity with dwellings at the site—gathering of wild plants (nuts) and fishing (ca. 2800 cal. BC—reduction of settlement activity). Formation of the Middle Neolithic Usiyati Culture—traces of animal butchering, accumulation of coprolites and a variety of artefacts.

4. ca. 2500 cal. BC—human bodies deposition in the shore zone.
5. 2500–2100 cal. BC: further water level decreasing with fluctuations and seasonal desiccation phases (ca. 2300–2200 cal. BC an increase of the water level), low trophy, increasing catchment erosion. Pile-dwellings in the eastern part of the site. The M25 area used as a butchering zone with terrain constructions.
6. 2100–1700 cal. BC: a short seasonal (spring) or episodic deep eutrophic water cover (the highest water level ca. 2000–1900 cal. BC)—seasonal flooding, an increase of catchment weathering, human activity record (barriers deposition). Renewal of the lacustrine system led to the devastation of the pile-dwellings, the settlement moved to higher places. Episodic shoreline human activity.
7. After 1700 cal. BC: a drop of the water level—natural succession of the lake towards the wetland (terrestrialization) with only short-time floods (ca. 1400 cal. BC), an intense slope process in the catchment. Change of the lacustrine system into the fluvial system.

As for the neolithisation process, it seems that the transition to the productive economy was strongly linked not only to environmental conditions but was also determined by social-cultural choice. Culturally driven technologies were to abate in different ways the multiple ecological drivers that restricted hunter-gatherers (Burger & Fristoe, 2018). While in southern regions of the Eastern European Plain neolithisation was already initiated, in other areas, such as in Serteya, the lifeways of hunter-fisher-gatherers was largely maintained. One explanation could be favourable local conditions in the Serteya region, which offered a variety of different environmental resources with a stable ecosystem promoted by biodiversity (Hooper et al., 2005), thus delaying the onset of agriculture. In this context, macro remains can point to different resource use. We may assume different hunter-gatherer-fisher strategies employed during different time periods, all pointing to multiple economic ways practised by these societies determined both by environmental factors and social-cultural choices.

ACKNOWLEDGEMENTS

The research project is financed by a grant from the National Science Centre, Poland based on the decision No. 2017/25/B/HS3/00274.

Archaeological research was supported by a grant of the Russian Science Foundation (Project No: 19-78-00009). The archaeological mission 2NOR was supported by the French Ministry for Europe and Foreign Affairs (including ^{14}C dating—Table 5).

Detailed geochemical analysis was carried in the Geochemical Laboratory of the Institute of Marine and Environmental Sciences University of Szczecin (with the help of Mrs. Julita Tomkowiak and Mrs. Joanna Ślawińska).

We are grateful to two anonymous reviewers and the journal editors for their very constructive remarks which have greatly improved the final version of the paper. Special thanks also go to Dr. Steve J. Brooks from the Department of Life Sciences, Natural History Museum, London, UK, for very constructive remarks and copy editing of our manuscript.

AUTHOR CONTRIBUTIONS

Piotr Kittel: conceptualization, data curation, funding acquisition, investigation, methodology, project administration, resources, supervision, visualization, writing original draft, writing review, and editing. Andrey Mazurkevich: conceptualization, data curation, formal analysis, funding acquisition, investigation, methodology, resources, supervision, and visualization. Ekaterina Dolbunova: data curation, investigation, methodology, and visualization. Emilie Gauthier: data curation, formal analysis, and investigation. Yolaine Maigrot: data curation, formal analysis, and investigation. Maxime Danger: data curation, formal analysis, and investigation. Agnieszka Mroczkowska: data curation, formal analysis, and investigation. Daniel Okupny: data curation, formal analysis, and investigation.

ORCID

Piotr Kittel  <http://orcid.org/0000-0001-6987-7968>
 Magda Wieckowska-Lüth  <http://orcid.org/0000-0002-1940-6700>
 Dominik Pawłowski  <http://orcid.org/0000-0003-4616-6666>
 Mateusz Płociennik  <http://orcid.org/0000-0003-1487-6698>
 Emilie Gauthier  <http://orcid.org/0000-0002-9238-8190>
 Marek Krąpiec  <http://orcid.org/0000-0003-4270-1668>
 Agnieszka Mroczkowska  <http://orcid.org/0000-0002-3534-7843>
 Daniel Okupny  <http://orcid.org/0000-0002-8836-6044>
 Jacek Szmařida  <http://orcid.org/0000-0002-4058-8334>
 Michał Ślawiński  <http://orcid.org/0000-0002-3011-2682>

REFERENCES

- Abramov, L. S. (1972). *Opisaniya prirody nashey strany: Razvitiye fiziko-geograficheskikh kharakteristik. Mysl'.*
- Alpat'ev, A. M., Arkhangel'skii, A. M., Podoplelov, N. Y., & Stepanov, A. Y. (1976). *Fizicheskaya Geografiya SSSR (Evropeiskaya Chast'). Vysshaya Shkola.*
- Andersen, T., Cranston, P. S. & Epler, J. H.(Eds.) (2013). *Chironomidae of the Holarctic Region: Keys and Diagnoses. Part 1. Larvae, Insect Systematics and Evolution Supplements 66.*
- Apolinarska, K., Woszczyk, M., & Obremska, M. (2012). Late Weichselian and Holocene palaeoenvironmental changes in northern Poland based on Lake Skrzynka record. *Boreas*, 41, 292–307.
- Baglinière, J. L., & LE Louarn, H. (1987). Caractéristiques scalimétriques des principales espèces de poissons d'eau douce de France. *Bulletin Français de la Pêche et de la Pisciculture*, 306, 1–39.
- Behre, K. E. (1981). The interpretation of anthropogenic indicators in pollen diagrams. *Pollen et Spores*, 23(2), 225–245.
- Beijerinck, W. (1976). *Zadenatlas der Nederlandsche Flora. Ten Behoeve van de Botanie, Palaeontologie, Bodemcultuur en Warenkennis.* Backhuys & Meesters.
- Bengtsson, L., & Enell, M. (1986). Chemical analysis. In Berglund, B. E. (Ed.), *Handbook of Holocene Palaeoecology and Palaeohydrology* (pp. 423–451). John Wiley and Sons Ltd.
- Berglund, B. E., & Ralska-Jasiewiczowa, M. (1986). Pollen analysis and pollen diagrams. In Berglund, B. E. (Ed.), *Handbook of Holocene Palaeoecology and Palaeohydrology* (pp. 455–484). John Wiley and Sons Ltd.
- Beug, H.-J. (2004). *Leitfaden der Pollenbestimmung für Mitteleuropa und angrenzende Gebiete.* Verlag Dr. Friedrich Pfeil, München.
- Bini, M., Zanchetta, G., Persouli, A., Cartier, R., Català, A., Cacho, I., Dean, J. R., Di Rita, F., Drysdale, R. N., Finnè, M., Isola, I., Jalali, B., Lirer, F., Magri, D., Masi, A., Marks, L., Mercuri, A. M., Peyron, O., Sadori, L., ... Brisset, E. (2019). The 4.2 ka BP event in the

- mediterranean region: An overview. *Climate of the Past*, 15, 555–577.
- Birks, H. H. (1980). Plant macrofossils in Quaternary lake sediments. *Archiv für Hydrobiologie*, 15, 1–60.
- Bjerring, R., Becares, E., Declerck, S., Gross, E. M., Hansson, L.-A., Kairesalo, T., Nykänen, M., Halkiewicz, A., Kornijów, R., Conde-Porcuna, J. M., Seferlis, M., Noges, T., Moss, B., Amsinck, S. L., Vad Odgaard, B., & Jeppesen, E. (2009). Subfossil Cladocera in relation to contemporary environmental variables in 54 Pan-European lakes. *Freshwater Biology*, 54, 2401–2417.
- Błędzki, L. A., & Rybak, J. I. (2016). *Freshwater Crustacean Zooplankton of Europe. Cladocera & Copepoda (Calanoida, Cyclopoida)* Key to species identification, with notes on ecology, distribution, methods and introduction to data analysis. Springer.
- Bolliger-Schreyer, S. (2004). *Pfahlbau und Uferdorf -Leben in der Steinzeit und Bronzezeit*. Glanzlichter aus dem Bernischen HistorischenMuseum.
- Bond, G., Kromer, B., Beer, J., Muscheler, R., Evans, M. N., Showers, W., Hoffmann, S., Lotti-Bond, R., Hajdas, I., & Bonani, G. (2001). Persistent solar influence on north Atlantic climate during the Holocene. *Science*, 294(5549), 2130–2136.
- Booth, R. K., Jackson, S. T., Forman, S. L., Kutzbach, J. E., Bettis, I.I.I., E. A., Kreig, J., & Wright, D. K. (2005). A severe centennial-scale drought in midcontinental North America 4200 years ago and apparent global linkages. *The Holocene*, 15(3), 321–328.
- Bos, J. A. A., & Urz, R. (2003). Late Glacial and early Holocene environment in the middle Lahn river valley (Hessen, central-west Germany) and the local impact of early Mesolithic people-pollen and macrofossil evidence. *Vegetation History and Archaeobotany*, 12, 19–36.
- Bronk Ramsey, C. (2008). Deposition models for chronological records. *Quaternary Science Reviews*, 27(1-2), 42–60.
- Bronk Ramsey, C. (2009). Bayesian analysis of radiocarbon dates. *Radiocarbon*, 51(1), 337–360.
- Brooks, S. J., Bennion, H., & Birks, H. J. B. (2001). Tracing lake trophic history with a chironomid-total phosphorus inference model. *Freshwater Biology*, 46(4), 513–533.
- Brooks, S. J., Langdon, P. G., & Heiri, O. (2007). *The identification and use of Palaearctic Chironomidae larvae in palaeoecology*. QRA Technical Guide No. 10, Quaternary Research Association, London.
- Burger, R. J., & Fristoe, S. T. (2018). Hunter-gatherer populations inform modern ecology. *Proceedings of the National Academy of Sciences*, 115(6), 1137–1139.
- Cappers, R. T. J., Bekker, R. M., & Jans, J. E. A. (2012). Digitale Zadenatlas van Nederland. In *Digital Seed Atlas of the Netherlands*. Groningen Archaeological Studies 4 (2 ed.), Auflage, Barkhuis & Groningen University Library, Groningen.
- Chekunova, E. M., Yarceva, N. V., Chekunov, M. K., & Mazurkevich, A. N. (2014). The first results of genetic typing of local population and ancient humans in Upper Dvina region, in: Mazurkevich, A.N., Polkovnikova, M.E., Dolbunova, E.V. (Eds.), *Archaeology of lake settlements IV-II mil. BC: Chronology of cultures, environment and palaeoclimatic rhythms. Material of international conference dedicated the semi-centennial anniversary of the researches of lake dwellings in North-Western Russia, Saint-Petersburg, 13-15 November 2014*. The State Hermitage Museum, Saint-Petersburg, pp. 290–294.
- Cherkinsky, A., Culp, R. A., Dvoracek, D. K., & Noakes, J. E. (2010). Status of the AMS facility at the University of Georgia. *Nuclear Instruments and Methods in Physics Research, B*, 268(7–8), 867–870.
- Cohen, K. M., Harper, D. A. T., & Gibbard, P. L. (2019, May 15). ICS International Chronostratigraphic Chart. International Commission on Stratigraphy, IUGS. www.stratigraphy.org
- Coles, J. M. (2018). A wetland perspective. In Purdy, B. A. (Ed.), *Wet Site Archaeology*. (pp. 1–14). CRC Press Taylor & Francis Group.
- Cugny, C., Mazier, F., & Galop, D. (2010). Modern and fossil non-pollen palynomorphs from the Basque mountains (western Pyrenees, France): The use of coprophilous fungi to reconstruct pastoral activity. *Vegetation history and Archaeobotany*, 19(5–6), 391–408.
- Cullen, H. M., deMenocal, P. B., Hemming, S., Hemming, G., Brown, F. H., Guilderson, T., & Sirocko, F. (2000). Climate change and the collapse of the Akkadian empire: Evidence from the deep sea. *Geology*, 28(4), 379–382.
- Davis, M. B., Deevey, E. S., Jr. (1964). Pollen Accumulation Rates: Estimates from Late-Glacial Sediment of Rogers Lake. *Science*, 145, 1293–1295.
- Dietze, E., Słowiński, M., Zawiska, I., Veh, G., & Brauer, A. (2016). Multiple drivers of Holocene lake level changes at a lowland lake in northeastern Germany. *Boreas*, 45, 828–845.
- Dietze, E., Theuerkauf, M., Bloom, K., Brauer, A., Dörfler, W., Feeser, I., Feurdean, A., Gedminienė, L., Giesecke, T., Jahns, S., Karpińska-Kołaczek, M., Kołaczek, P., Lamentowicz, M., Latałowa, M., Marcisz, K., Obremska, M., Pędziżewska, A., Poska, A., Rehfeld, K., ... Słowiński, M. (2018). Holocene fire activity during low-natural flammability periods reveals scale-dependent cultural human-fire relationships in Europe. *Quaternary Science Reviews*, 201, 44–56.
- Digerfeldt, G. (1986). Studies on past lake-level fluctuations. In Berglund, B. E. (Ed.), *Handbook of Holocene Palaeoecology and Palaeohydrology* (pp. 127–143). John Wiley and Sons Ltd.
- Dimbleby, G. W. (1985). *The Palynology of Archaeological Sites*. Academic Press, INC.
- Dolukhanov, P. M., & Miklyayev, A. M. (1986). Prehistoric lacustrine pile dwellings in the north-western part of the USSR. *Fennoscandia Archaeologica*, 3, 81–89.
- Dolukhanov, P., & Mazurkevich, A. (2000). Sites lacustres néolithiques de Russie. *Archeologia*, 369, 69–70.
- Dolukhanov, P. M., Shukurov, A., Arslanov, K.hA., Mazurkevich, A. N., Savel'eva, L. A., Dzinoridze, E. N., Kulkova, M. A., & Zaitseva, G. I. (2004). The holocene environment and transition to agriculture in Boreal Russia (Serteya Valley Case Study). *Internet Archaeology*, 17. <http://intarch.ac.uk/journal/issue17>
- Edwards, K. J. (2016). Using space in cultural palynology: the value of the off-site pollen record. In Harris, D. R. & Thomas, K. D. (Eds.), *Modelling Ecological Change: Perspectives from Neoeontology, Palaeoecology and Environmental Archaeology* (pp. 61–74). University Collage London Institute of Archaeology Publications, Vol. 15, Routledge Taylor & Francis Group.
- Ellenberg, H., Weber, H. E., Düll, R., Wirth, V., Werner, W., & Paulißen, D. (1991). *Zeigerwerte von Pflanzen in Mitteleuropa*. Scripta geobotanica 18, Verlag Erich Goltze KG.
- Engstrom, D. R., & Wright, H. E. (1984). Chemical stratigraphy of lake sediments as a record of environmental change. In Haworth, E. Y. & Lund, J. W. G. (Eds.), *Lake Sediments and Environmental History* (pp. 11–67). Leicester University Press.
- Eusterhues, K., Heinrichs, H., & Schneider, J. (2005). Geochemical response on redox fluctuations in Holocene lake sediments, Laek Steisslingen, Southern Germany. *Chemical Geology*, 222(1-2), 1–22.
- Fægri, K., & Iversen, J. (1989). *Textbook of pollen analysis*. John Wiley & Sons.
- Feurdean, A., Vannière, B., Finsinger, W., Warren, D., Connor, S. C., Forrest, M., Liakka, J., Panait, A., Werner, C., Andrič, M., Bobek, P., Carter, V. A., Davis, B., Diaconu, A.-C., Dietze, E., Feeser, I., Florescu, G., Gałka, M., Giesecke, T., ... Hickler, T. (2020). Fire hazard modulation by long-term dynamics in land cover and dominant forest type in eastern and central Europe. *Biogeosciences*, 17(5), 1213–1230.
- Folk, R., & Ward, W. (1957). Brazos River bar: A study in the significance of grain size parameters. *Journal of Sedimentary Petrology*, 27(1), 3–26.
- Frey, D. G. (1986). Cladocera analysis. In Berglund, B. E. (Ed.), *Handbook of Holocene paleoecology and paleohydrology* (pp. 667–692). John Wiley and Sons.

- Gorlach, A., Kalm, V., & Hang, T. (2015). Thickness distribution of quaternary deposits in the formerly glaciated part of the East European plain. *Journal of Maps*, 11(4), 625–635.
- Grimm, E. C. (1987). CONISS: A FORTRAN 77 program for stratigraphically constrained cluster analysis by the method of incremental sum of squares. *Computers & Geosciences*, 13, 13–35.
- Grimm, E. C. (1992). TILIA and TILIA GRAPH: Pollen spreadsheet and graphics program, in: *8th International Palynological Congress. Program and Abstracts*. Aix-en-Provence, France, pp. 1–56.
- Grimm, E. C. (2016). *TiliaT*. Available at <https://www.tiliait.com/>
- Hafner, A., Brunner, M., & Laabs, J. (2017). Archaeology of the Alpine Space. Research on the foothills, valley systems and high mountain landscapes of the Alps. *Via Antiqua*, 9, 16–37.
- Hammer, Ø., Harper, D. A. T., & Ryan, P. D. (2001). PAST: Paleontological Statistics software package for education and data analysis. *Paleontologia Electronica*, 4, 1–9.
- Harrison, S. P., Yu, G., & Tarasov, P. E. (1996). Late Quaternary lake-level record from northern Eurasia. *Quaternary Research*, 45, 138–159.
- Hannon, G. E., & Gaillard, M.-J. (1997). The plant-macrofossil record of past lake-level changes. *Journal of Paleolimnology*, 18, 15–28.
- Hooper, D. U., Chapin, F. S., Ewel, J. J., Hector, A., Inchausti, P., Lavorel, S., Lawton, J. H., Lodge, D. M., Loreau, M., Naeem, S., Schmid, B., Setala, H., Symstad, A. J., Vandermeer, J., & Wardle, D. A. (2005). Effects of biodiversity on ecosystem functioning: a consensus of current knowledge. *Ecological Monographs*, 75(1), 3–35.
- Itkonen, T. I. (1921). *Lappalaisten ruokatalous. Suomalais-ugrilaisen seuran toimituksia* LI.
- Jordan, P., Gibbs, K., Hommel, P., Piezonka, H., Silva, F., & Steele, J. (2016). Modelling the diffusion of pottery technologies across Afro-Eurasia: Emerging insights and future research. *Antiquity*, 90(351), 590–603.
- Juggins, S. (2007). *C2 version 1.5 user guide. Software for Ecological and Palaeoecological Data Analysis and Visualisation*. Newcastle University, Newcastle upon Tyne.
- Kaliečyc, A. H. (2018). *Čalaviek i asiardonnie: Kamiennyj viek, Zachodniaje Paliesie*. Bielaruskaja navuka.
- Keiper, J. B., & Casamatta, D. A. (2001). Benthic organisms as forensic indicators. *Journal of the North American Benthological Society*, 20(2), 311–324.
- Kirleis, W., Wieckowska-Lüth, M., Piezonka, H., Elberfeld, V., & Nedomolkina, N. (2020). The Development of Plant Use and Cultivation in the Northwest Russian Taiga Zone, in: In (Eds.) Vanhanen, S., Grabowski, R. & Hambro Mikkelsen, P., *Development of plant cultivation in the Nordic countries from the Prehistoric to the Early Historic Period*. Barkhuis Publishing.
- Kittel, P. (2015). The prehistoric human impact on slope development at the archaeological site in Smólsk (Kuyavian Lakeland). *Bulletin of Geography. Physical Geography Series*, 8, 107–122.
- Kittel, P., Mazurkevich, A., Alexandrovskiy, A., Dolbunova, E., Krupski, M., Szmarida, J., Stachowicz-Rybka, R., Cywa, K., Mroczkowska, A., & Okupny, D. (2020). Lacustrine, fluvial and slope deposits in the wetland shore area in Serteya, Western Russia. *Acta Geographica Lodziensia*, 109. In press.
- Kittel, P., Mazurkevich, A., Dolbunova, E., Kazakov, E., Mroczkowska, A., Pavlovskaya, E., Piech, W., Płociennik, M., Sikora, J., Teltevskaya, Y., & Wieckowska-Lüth, M. (2018a). Palaeoenvironmental reconstructions for the Neolithic pile-dwelling Serteya II site case study, Western Russia. *Acta Geographica Lodziensia*, 107, 191–213.
- Kittel, P., Muzolf, B., Płociennik, M., Elias, S., Brooks, S. J., Lutyńska, M., Pawłowski, D., Stachowicz-Rybka, R., Wacnik, A., Okupny, D., Głab, Z., & Mueller-Bieniek, A. (2014). A multi-proxy reconstruction from Lutomiersk-Koziówka, Central Poland, in the context of early modern hemp and flax processing. *Journal of Archaeological Science*, 50, 318–337.
- Kittel, P., Płociennik, M., Borówka, R. K., Okupny, D., Pawłowski, D., Peyron, O., Stachowicz-Rybka, R., Obremska, M., & Cywa, K. (2016). Early Holocene hydrology and environments of the Ner River (Poland). *Quaternary Research*, 85, 187–203.
- Kittel, P., Sikora, J., Antczak, O., Brooks, S. J., Elias, S., Krapiec, M., Luoto, T. P., Borówka, R. K., Okupny, D., Pawłowski, D., Płociennik, M., Rzodkiewicz, M., Stachowicz-Rybka, R., & Wacnik, A. (2018b). The palaeoecological development of the Late Medieval moat—Multiproxy research at Rozprza, Central Poland. *Quaternary International*, 482, 131–156.
- Kondracki, J. (1992). Fizycznoogeograficzna regionalizacja republik Litewskiej i Białoruskiej w układzie dziesiętnym. *Przegląd Geograficzny*, 64(3–4), 341–346.
- Kottelat, M., & Freyhof, J. (2007). *Handbook of European Freshwater Fishes*. Publications Kottelat.
- Kristiansen, K., Allentoft, M., Frei, K., Iversen, R., Johannsen, N., Kroonen, G., Pospiszny, Ł., Price, T. D., Rasmussen, S., Sjögren, K.-G., Sikora, M., & Willerslev, E. (2017). Re-theorising mobility and the formation of culture and language among the Corded Ware Culture in Europe. *Antiquity*, 91(356), 334–347.
- Kubiak-Martens, L. (2002). New evidence for the use of root foods in pre-agrarian subsistence recovered from the late Mesolithic site at Halsskov, Denmark. *Vegetation History and Archaeobotany*, 11, 23–32.
- Kul'kova, M. A., Mazurkevich, A. N., & Dolukhanov, P. M. (2001). Chronology and palaeoclimate of prehistoric sites in Western Dvina-Lovat area of North-western Russia. *Geochronometria*, 20, 87–94.
- Kul'kova, M. A., Mazurkevich, A., & Gerasimov, D. (2015). Stone Age archaeological sites and environmental changes during the Holocene in the NW region of Russia. In Harff, J., Bailey, G. & Lüth, F. (Eds.), *Geology and Archaeology: Submerged Landscapes of the Continental Shelf* (pp. 27–50). Geological Society.
- Lamentowicz, M., Kołaczek, P., Mauquoy, D., Kittel, P., Łokas, E., Słowiński, M., Jassey, V. E. J., Niedziółka, K., Kajukało-Drygalska, K., & Marcisz, K. (2019). Always on the tipping point—A search for signals of past societies and related peatland ecosystem critical transitions during the last 6500 years in N Poland. *Quaternary Science Reviews*, 225, 105954.
- Laine, A., Gauthier, E., Garcia, J. P., Petit, C., Cruz, F., & Richard, H. (2010). A three-thousand-year history of vegetation and human impact in Burgundy (France) reconstructed from pollen and non-pollen palynomorphs analysis. *Comptes Rendus Biologies*, 333(11–12), 850–857.
- Lorkiewicz, W., Borówka, P., Shirobokov, I., Mazurkevich, A., Dolbunova, E., Wieckowska-Lüth, M., Płociennik, M., & Kittel, P. (in prep.). Human remains from the wet land in Western Dvina Lakeland: anthropological, genetic, cultural, and environmental context.
- Luoto, T. P. (2011). The relationship between water quality and chironomid distribution in Finland—A new assemblage-based tool for assessments of long-term nutrient dynamics. *Ecological Indicators*, 1, 255–262.
- Luoto, T. P., Kotrys, B., & Płociennik, M. (2019). East European chironomid-based calibration model for past summer temperature reconstructions. *Climate Research*, 77, 63–76.
- Marchant, R., & Hooghiemstra, H. (2004). Rapid environmental change in African and South American tropics around 4000 years before present: A review. *Earth-Science Reviews*, 66(3–4), 217–260.
- Mauquoy, D., & van Geel, B. (2007). Mire and peat macros. In Elias, S. A. (Ed.), *Encyclopedia of quaternary science* (3, pp. 2315–2336). Elsevier.
- Mazurkevich, A. N. (2003). Pervyye svидetelstva proyavleniya proizvodyashchego khozyaystva na Severo-Zapade Rossii. In Savinov, D. G. & Sedykh, V. N. (Eds.), *Pushkarevskiy sbornik II* (pp. 77–84). Izd-vo S-Peterburgskogo un-ta.
- Mazurkevich, A., & Dolbunova, E. (2011). Underwater Investigations in Northwest Russia: lacustrine archaeology of Neolithic pile dwellings. In Benjamin, J., Bonsall, C., Pickard, C. & Fischer, A. (Eds.), *Submerged Prehistory*. (pp. 158–172). Oxbow Books.

- Mazurkevich, A., & Dolbunova, E. (2015). The oldest pottery in hunter-gatherer communities and models of Neolithisation of Eastern Europe. *Documenta Praehistorica*, 42, 13–66.
- Mazurkevich, A., Dolbunova, E., Kittel, P., Fassbender, J., Maigrot, Y., Mroczkowska, A., Płociennik, M., Sikora, J., Słowiński, M., Sablin, M., & Shirobokov, I. (2017). Multi-disciplinary research on the Neolithic pile-dwelling Serteya II site (Western Russia) and the landscape reconstruction. In Marciniak-Kajzer, A., Andrzejewski, A., Golański, A. & Rzepecki, S. (Eds.), *Nie tylko krzemienie. Not only flints* (pp. 103–128). Instytut Archeologii Uniwersytetu Łódzkiego, Łódzka Fundacja Badań Naukowych, Stowarzyszenie Naukowe Archeologów Polskich Oddział w Łodzi.
- Mazurkevich, A., Kittel, P., Maigrot, Y., Dolbunova, E., Mroczkowska, A., Wieckowska-Lüth, M., & Piech, W. (2020). Natural and anthropogenic impact on formation of archaeological layers in the lake shore area: Case study from the Serteya II site, Western Russia. *Acta Geographica Lodzienia*, 109. In press.
- Mazurkevich, A., Korotkevich, B. N., Dolukhanov, P. M., Shukurov, A. M., Arslanov, K.hA., Savel'eva, L. A., Dzinoridze, E. N., Kul'kova, M. A., & Zaitseva, G. I. (2009). Climate, subsistence and human movements in the Western Dvina–Lovat River Basins. *Quaternary International*, 203, 52–66.
- Medina, A. G., Hernando, O. S., & Ríos, G. J. (2015). The Use of the Developmental Rate of the Aquatic Midge Chironomus riparius (Diptera, Chironomidae) in the Assessment of the Postsubmersion Interval. *Journal of Forensic Science*, 60, 822–826.
- Menotti, F., (Ed.). (2004). *Living on the lake in prehistoric Europe. 150 years of lake-dwelling research*. Routledge.
- Merkl, M. B. (2016). Corded Ware, Bell Beakers and the Earliest Bronze Age in the Hegau and the Western Lake Constance Region. *Musaica Archaeologica*, 1, 59–80.
- Meyers, P. A., & Teranes, J. L. (2001). Sediment organic matter. In Last, W. M. & Smol, J. P. (Eds.), *Tracking Environmental Change Using Lake Sediments* (2, pp. 239–269). Kluwer Academic Publishers.
- Moller Pillot, H. K. M. (2009). *Chironomidae larvae. Biology and Ecology of the Chironomini*. KNNV Publishing.
- Moller Pillot, H. K. M. (2013). *Chironomidae larvae of the Netherlands and adjacent lowlands, Biology and Ecology of the aquatic Orthocladiinae, Prodiamesinae, Diamesinae, Buchonomyiinae, Podonominae, Telmatogotoninae*. KNNV Publishing.
- Moore, P. D., Webb, J. A., & Collinson, M. E. (1991). *Pollen analysis*. Blackwell Scientific Publications.
- Mroczkowska, A., Płociennik, M., Pawłowski, D., Gauthier, E., Mazurkevich, A., Luoto, T. P., Peyron, O., Kotrys, B., Nazarova, L., Syrykh, L., Dolbunova, E., Thiebaut, E., Antczak-Orlewska, O., & Kittel, P. (2020 – in press). Northgrippian climate oscillations recorded at the Western Dvina Lakeland (Serteya Valley). Water.
- Navahrodski, T. A. (2000). *Tradycyi narodnaha charčavannia bielarusai*. NIA.
- Nevalainen, L., Luoto, T. P., Kultti, S., & Sarmaja-Korjonen, K. (2012). Do subfossil Cladocera and chydorid ephippia disentangle Holocene climate trends? *The Holocene*, 22, 291–299.
- Nevalainen, L., Sarmaja-Korjonen, K., & Luoto, T. P. (2011). Sedimentary Cladocera as indicators of past water-level changes in shallow northern lakes. *Quaternary Research*, 75(3), 430–437.
- O'Neill, A. R., & Rana, S. K. (2016). An ethnobotanical analysis of parasiticplants (Parijibi) in the Nepal Himalaya. *Journal of Ethnobiology and Ethnomedicine*, 12, 14.
- Ochiai, S., Nagao, S., Yonebayashi, K., Fukuyama, T., Suzuki, T., Yamamoto, M., Kashiwaya, K., & Nakamura, K. (2015). Effect of deforestation on the transport of particulate organic matter inferred from the geochemical properties of reservoir sediments in the Noto Peninsula, Japan. *Geochemical Journal*, 49, 513–522.
- Økland, K. A., & Økland, J. (2000). Freshwater bryozoans (Bryozoa) of Norway: Distribution and ecology of Cristatella mucedo and Paludicella articulate. *Hydrobiologia*, 421, 1–24.
- Økland, K. A., Økland, J., Geimer, G., & Massard, J. A. (2003). Freshwater bryozoans (Bryozoa) of Norway IV: Distribution and ecology of four species of Plumatella with notes on Hyalinella punctata. *Hydrobiologia*, 501, 179–198.
- Pawlowski, D. (2011). Evolution of an Eemian lake based on Cladocera analysis (Konin area, Central Poland). *Acta Geologica Polonica*, 61, 441–450.
- Pawlowski, D., Borówka, R. K., Kowalewski, G., Luoto, T. P., Milecka, K., Nevalainen, L., Okupny, D., Płociennik, M., Woszczyk, M., Tomkowiak, J., & Zieliński, T. (2016a). The response of flood-plain ecosystems to the Late Glacial and Early Holocene hydrological changes: A case study from a small Central European river valley. *Catena*, 147, 411–428.
- Pawlowski, D., Borówka, R. K., Kowalewski, G. A., Luoto, T. P., Milecka, K., Nevalainen, L., Okupny, D., Zieliński, T., & Tomkowiak, J. (2016b). Late Weichselian and Holocene record of the paleoenvironmental changes in a small river valley in Central Poland. *Quaternary Science Review*, 135, 24–40.
- Pawlowski, D., Milecka, K., Kittel, P., Woszczyk, M., & Spychaliski, W. (2015). Palaeoecological record of natural changes and human impact in a small river valley in Central Poland. *Quaternary International*, 370, 12–28.
- Peršou, A., Ionita, M., & Weiss, H. (2019). Atmospheric blocking induced by the strengthened Siberian High led to drying in west Asia during the 4.2kaBP event—A hypothesis. *Climate of the Past*, 15, 781–793.
- Pędziżewska, A., Tylmann, W., Witak, M., Piotrowska, N., Maciejewska, E., & Latałowa, M. (2015). Holocene environmental changes reflected by pollen, diatoms, and geochemistry of annually laminated sediments of Lake Suminko in the Kashubian Lake District (N Poland). *Review of Palaeobotany and Palynology*, 216, 55–73.
- Piezonka, H., Meadows, J., Hartz, S., Kostyleva, E., Nedomolkina, N., Ivanishcheva, M., Kosorukova, N., & Terberger, T. (2016). Stone age pottery chronology in the Northeast European Forest Zone: New AMS and EA-IRMS Results on Foodcrusts. *Radiocarbon*, 58(2), 267–289.
- Pleskot, K., Tjallingii, R., Makohonienko, M., Nowaczyk, N., & Szczuciński, W. (2018). Holocene paleohydrological reconstruction of Lake Strzeszyńskie (western Poland) and its implications for the central European climatic transition zone. *Journal of Paleolimnology*, 59, 443–459.
- Pleskot, K., Apolinarska, K., Kołaczek, P., Suchora, M., Fojutowski, M., Joniak, T., Kotrys, B., Kramkowski, M., Słowiński, M., Woźniak, M., & Lamentowicz, M. (2020). Searching for the 4.2 ka climate event at Lake Spore, Poland. *CATENA*, 191, 104565.
- Płociennik, M., Kruk, A., Forysiak, J., Pawłowski, D., Mianowicz, K., Elias, S., Borówka, R. K., Kloss, M., Obremska, M., Cope, R., Krapiec, M., Kittel, P., & Żurek, S. (2015). Fen ecosystem responses to water-level fluctuations during the early and middle Holocene in central Europe: A case study from Wilczków, Poland. *Boreas*, 44(4), 721–740.
- Radu, V. (2005). *Atlas For The Identification of Bony Fish Bones From Archaeological Sites*. Contrast Bucaresti, Studii de Preistorie, Supplementum 1, Contrast, Bucuresti.
- Reille, M. (1992). *Pollen et spores d'Europe et d'Afrique du Nord*. Laboratoire de Botanique Historique et Palynologie, Marseille.
- Reimer, P. J., Bard, E., Bayliss, A., Beck, J. W., Blackwell, P. G., Bronk Ramsey, C., Grootes, P. M., Guilderson, T. P., Haflidason, H., Hajdas, I., Hatt, C., Heaton, T. J., Hoffmann, D. L., Hogg, A. G., Hughen, K. A., Kaiser, K. F., Kromer, B., Manning, S. W., Niu, M., ... van der Plicht, J. (2013). IntCal13 and Marine13 Radiocarbon Age Calibration Curves 0–50,000 Years cal BP. *Radiocarbon*, 55(4), 1869–1887.
- Roland, T. P., Caseldine, C. J., Charman, D. J., Turney, C. S. M., & Amesbury, M. J. (2014). Was there a '4.2 ka event' in Great Britain

- and Ireland? Evidence from the peatland record. *Quaternary Science Reviews*, 83, 11–27.
- Routh, J., Meyers, P. A., Hjorth, T., Baskaran, M., & Hallberg, R. (2007). Sedimentary geochemical record of recent environmental changes around Lake Middle Marviken, Sweden. *Journal of Paleolimnology*, 37, 529–545.
- Ruiz, Z., Brown, A. G., & Langdon, P. G. (2006). The potential of chironomid (Insecta: Diptera) larvae in archaeological investigations of floodplain and lake settlements. *Journal of Archaeological Science*, 33, 14–33.
- Ruppert, E. E., Fox, R. S., & Barnes, R. D. (2004). *Invertebrate Zoology: A Functional Evolutionary Approach*. Thomson-Brooks/Cole.
- Schlüchter, H., (Ed.). (1997). *Pfaulbauten rund um die Alpen*. Konrad Theiss Verlag.
- Shishlina, N. I. (2004). North-West Caspian Sea Steppe: Environment and Migration Crossroads of Pastoral Culture Population During the Third Millennium BC. In Marian Scott, E., Alekseev, A. Y. & Zaitseva, G. (Eds.), *Impact of the Environment on Human Migration in Eurasia* (NATO Science Series: IV: Earth and Environmental Sciences, 42, pp. 91–106). Springer.
- Słowiński, M., Marcisz, K., Płociennik, M., Obremska, M., Pawłowski, D., Okupny, D., Słowińska, S., Borówka, R., Kittel, P., Forsyak, J., Michczyńska, D. J., & Lamentowicz, M. (2016). Drought as a stress driver of ecological changes in peatland - A palaeoecological study of peatland development between 3500 BCE and 200 BCE in central Poland. *Palaeogeography, Palaeoclimatology, Palaeoecology*, 461, 272–291.
- Słowiński, M., Skubała, P., Zawiska, I., Kruk, A., Obremska, M., Milecka, K., & Ott, F. (2018). Cascading effects between climate, vegetation, and macroinvertebrate fauna in 14,000-year palaeoecological investigations of a shallow lake in eastern Poland. *Ecological Indicators*, 85, 329–341.
- Sobkowiak-Tabaka, I., Pawłowski, D., Milecka, K., Kubiak-Martens, L., Kostecki, R., Janczak-Kostecka, B., Goslar, T., & Ratajczak-Szczerba, M. (2020). Multi-proxy records of Mesolithic activity in the Lubuskie Lakeland (western Poland). *Vegetation History and Archaeobotany*, 29, 153–171.
- Szeroczyńska, K., & Sarmaja-Korjonen, K. (2007). *Atlas of subfossil Cladocera from central and northern Europe*. Friends of Lower Vistula Society.
- Tarasov, P. E., Harrison, S. P., Saarse, L., Pushenko, M.Y.a, Andreev, A. A., Aleshinskaya, Z. V., Davydova, N. N., Dorofeyuk, N. I., Efremov, Y.uV., Khomutova, V. I., Sevastyanov, D. V., Tamozaitis, J., Uspenskaya, O. N., Yakushko, O. F., & Tarasova, I. V. 1994. *Lake Status Records from the Former Soviet Union and Mongolia: Data Base Documentation*. NOAA Paleoclimatology Publications Series Report, 2. Boulder, Colorado.
- Tarasov, P. E., Pushenko, M.Y.a, Harrison, S. P., Saarse, L., Andreev, A. A., Aleshinskaya, Z. V., Davydova, N. N., Dorofeyuk, N. I., Efremov, Y.uV., Elina, G. A., Elovicheva, Y.aK., Filimonova, L. V., Gunova, V. S., Khomutova, V. I., Kvavadze, E. V., Neustrueva, I.Y.u, Pisareva, V. V., Sevastyanov, D. V., Shelekhova, T. S., ... Zernitskaya, V. P. (1996). *Lake Status Record from the Former Soviet Union and Mongolia: Documentation of the Second Version of the Database*. NOAA Paleoclimatology Publication Series Report, 5. Boulder, Colorado.
- Tarasov, P. E., Savelieva, L. A., Long, T., & Leipe, C. (2019). Postglacial vegetation and climate history and traces of early human impact and agriculture in the present-day cool mixed forest zone of European Russia. *Quaternary International*, 516, 21–41.
- Vanhanen, S., & Pesonen, P. (2016). Wild plant gathering in Stone Age Finland. *Quaternary International*, 404, 43–55.
- Vallenduuk, H. J., & Moller Pillot, H. K. M. (2007). *Chironomidae Larvae of the Netherlands and Adjacent Lowlands. General ecology and Tanypodinae*. KNNV Publishing.
- van Geel, B., & Aptroot, A. (2006). Fossil ascomycetes in Quaternary deposits. *Nova Hedwigia*, 82, 313–329.
- van Geel, B., Bohncke, S. J. P., & Dee, H. (1981). A palaeoecological study of an Upper Late Glacial and Holocene sequence from 'De Borchert', The Netherlands. *Review of Palaeobotany and Palynology*, 31, 367–448.
- van Geel, B., Buurman, J., Brinkkemper, O., Schelvis, J., Aptroot, A., van Reenena, G., & Hakbijl, T. (2003). Environmental reconstruction of a Roman Period settlement site in Uitgeest (The Netherlands), with special reference to coprophilous fungi. *Journal Archaeological Sciences*, 30, 873–883.
- van Geel, B., Coope, G. R., & Van Der Hammen, T. (1989). Palaeoecology and stratigraphy of the Lateglacial type section at Usselo (The Netherlands). *Review of Palaeobotany and Palynology*, 60(1-2), 25–129.
- Vander Linden, M. (2016). Population history in third-millennium BC Europe: Assessing the contribution of genetics. *World Archaeology*, 48, 714–728.
- Velichko, A. A., Faustova, M. A., Pisareva, V. V., Gribchenko, Y.uN., Sudakova, N. G., & Lavrentiev, N. V. (2011). Glaciations of the East European Plain: Distribution and Chronology. *Developments in Quaternary Science*, 15, 337–359.
- Wanner, H., Solomina, O., Grosjean, M., Ritz, S. P., & Jetel, M. (2011). Structure and origin of Holocene cold events. *Quaternary Science Reviews*, 30(21–22), 3109–3123.
- Warden, L., Moros, M., Neumann, T., Shennan, S., Timpson, A., Manning, K., Sollai, M., Wacker, L., Perner, K., Häusler, K., Leipe, T., Zillén, L., Kotilainen, A., Jansen, E., Schneider, R. R., Oeberst, R., Arz, H., & Sinninghe Damsté, J. S. (2017). Climate induced human demographic and cultural change in northern Europe during the mid-Holocene. *Scientific Reports*, 7(1), 15251, 1–11.
- Warren, G., Davis, S., McClatchie, M., & Sands, R. (2013). The potential role of humans in structuring the wooded landscapes of Mesolithic Ireland: A review of data and discussion of approaches. *Vegetation History and Archaeobotany*, 23, 629–646.
- Whiteside, M. C. (1970). Danish chydorid Cladocera: Modern ecology and core studies. *Ecological Monographs*, 40, 79–118.
- Whitlock, C., & Larsen, C. (2001). Charcoal as a fire proxy. In Smol, J. P., Birks, H. J. B. & Last, W. M. (Eds.), *Tracking Environmental Change Using lake Sediments* (pp. 75–97). Springer.
- Wolters, S. (2016). Die pflanzlichen Reste der Mesolithstation Friesack. In Benecke, N., Gramsch, B. & Jahns, S. (Eds.), *Subsistenz und Umwelt der Feuchtbodenstation Friesack 4 im Havelland. Ergebnisse der naturwissenschaftlichen Untersuchungen* (pp. 189–203). Brandenburgisches Landesamt für Denkmalpflege und Archäologisches Landesmuseum.
- Zawisza, E., Zawiska, I., Szeroczyńska, K., Correa-Metrio, A., Mirosław-Grabowska, M., Obremska, M., Rzodkiewicz, M., Słowiński, M., & Woszczyk, M. (2019). Dystrophication of lake Suchar IV (NE Poland): An alternative way of lake development. *Limnetica*, 38, 391–416.
- Zhou, S., Zhou, K., Wang, J., Yang, G., & Wang, S. (2018). Application of cluster analysis to geochemical compositional data for identifying ore-related geochemical anomalies. *Frontiers of Earth Science*, 12(3), 491–505.
- Zieliński, T., & Pisarska-Jamroży, M. (2012). Jakie cechy litologiczne osadów warto kodować, a jakie nie? *Przegląd Geologiczny*, 60, 387–397.

How to cite this article: Kittel P, Mazurkевич A, Wieckowska-Lüth M, et al. On the border between land and water: The environmental conditions of the Neolithic occupation from 4.3 until 1.6 ka BC at Serteya, Western Russia. *Gearchaeology*. 2020;1–30.
<https://doi.org/10.1002/gea.21824>

Article

Middle Holocene Climate Oscillations Recorded in the Western Dvina Lakeland

Agnieszka Mroczkowska ^{1,2,*}, Dominik Pawłowski ³, Emilie Gauthier ⁴, Andrey Mazurkevich ⁵, Tomi P. Luoto ⁶, Odile Peyron ⁷, Bartosz Kotrys ⁸, Stephen J. Brooks ⁹, Larisa B. Nazarova ^{10,11}, Liudmila Syrykh ¹², Ekaterina V. Dolbunova ⁵, Eva Thiebaut ⁴, Mateusz Płociennik ¹³, Olga Antczak-Orlewska ¹⁴ and Piotr Kittel ¹

¹ Department of Geology and Geomorphology, Faculty of Geographical Sciences, University of Lodz, Narutowicza 88, 90-139 Lodz, Poland; piotr.kittel@geo.uni.lodz.pl

² Stanisław Leszczycki Institute of Geography and Spatial Organisation, Polish Academy of Sciences, Twarda 51/55, 00-818 Warsaw, Poland

³ Faculty of Geographical and Geological Sciences, Institute of Geology, Adam Mickiewicz University, B. Krygowskiego 12, 61-680 Poznan, Poland; dominikp@amu.edu.pl

⁴ Laboratoire Chrono-Environnement, UMR CNRS/6249, Université de Bourgogne Franche-Comté, 25000 Besançon, France; emilie.gauthier@univ-fcomte.fr (E.G.); tanyopodinae1@wp.pl (E.T.)

⁵ The State Hermitage Museum, Dvortsovaya Naberezhnaya 34, 190000 St. Petersburg, Russia; a-mazurkevich@mail.ru (A.M.); katjer@mail.ru (E.V.D.)

⁶ Ecosystems and Environment Research Programme, Faculty of Biological and Environmental Sciences, University of Helsinki, 73 Niemenkatu, FI-15140 Lahti, Finland; tomi.luoto@helsinki.fi

⁷ Institut des Sciences de l'Evolution de Montpellier ISEM, Université de Montpellier, CNRS, IRD, EPHE, 34095 Montpellier, France; odile.peyron@umontpellier.fr

⁸ Polish Geological Institute—National Research Institute, Pomeranian Branch in Szczecin, 71-130 Szczecin, Poland; bkotr@pgi.gov.pl

⁹ Department of Life Sciences, Natural History Museum, Cromwell Road, London SW7 5BD, UK; s.brooks@nhm.ac.uk

¹⁰ Institute of Geoscience, Potsdam University, 14476 Potsdam, Germany; larisa.nazarova@awi.de

¹¹ Institute of Management and Territorial Development, Kremlevskaya, Kazan Federal University, Kremlyovskaya Str., 18, 420008 Kazan, Russia

¹² Department of Physical Geography & Environment, Herzen State Pedagogical University of Russia, 191186 St. Petersburg, Russia; lyudmilasd@gmail.com

¹³ Department of Invertebrate Zoology & Hydrobiology, Faculty of Biology and Environmental Protection, University of Lodz, Banacha 12/16, 90-237 Lodz, Poland; mateusz.plociennik@biol.uni.lodz.pl

¹⁴ Laboratory of Palaeoecology and Archaeobotany, Department of Plant Ecology, Faculty of Biology, University of Gdańsk, Wita Stwosza 59, 80-308 Gdańsk, Poland; olga.antczak-orlewska@ug.edu.pl

* Correspondence: agnieszka.mroczkowska@twarda.pan.pl



Citation: Mroczkowska, A.; Pawłowski, D.; Gauthier, E.; Mazurkevich, A.; Luoto, T.P.; Peyron, O.; Kotrys, B.; Brooks, S.J.; Nazarova, L.B.; Syrykh, L.; et al. Middle Holocene Climate Oscillations Recorded in the Western Dvina Lakeland. *Water* **2021**, *13*, 1611. <https://doi.org/10.3390/w13111611>

Academic Editors: Michał Ślowiński and Natalia Rudaya

Received: 19 April 2021

Accepted: 28 May 2021

Published: 7 June 2021

Publisher's Note: MDPI stays neutral with regard to jurisdictional claims in published maps and institutional affiliations.



Copyright: © 2021 by the authors. Licensee MDPI, Basel, Switzerland. This article is an open access article distributed under the terms and conditions of the Creative Commons Attribution (CC BY) license (<https://creativecommons.org/licenses/by/4.0/>).

Abstract: Although extensive archeological research works have been conducted in the Serteya region in recent years, the Holocene climate history in the Western Dvina Lakeland in Western Russia is still poorly understood. The Neolithic human occupation of the Serteya lake–river system responded to climate oscillations, resulting in the development of a pile-dwelling settlement between 5.9 and 4.2 ka cal BP. In this paper, we present the quantitative paleoclimatic reconstructions of the Northgrippian stage (8.2–4.2 ka cal BP) from the Great Serteya Palaeolake Basin. The reconstructions were created based on a multiproxy (Chironomidae, pollen and Cladocera) approach. The mean July air temperature remained at 17–20 °C, which is similar to the present temperature in the Smolensk Upland. The summer temperature revealed only weak oscillations during 5.9 and 4.2 ka cal BP. A more remarkable feature during those events was an increase in continentality, manifested by a lower winter temperature and lower annual precipitation. During the third, intermediate oscillation in 5.0–4.7 ka cal BP, a rise in summer temperature and stronger shifts in continental air masses were recorded. It is still unclear if the above-described climate fluctuations are linked to the North Atlantic Oscillation and can be interpreted as an indication of Bond events because only a few high-resolution paleoclimatic reconstructions from the region have been presented and these reconstructions do not demonstrate explicit oscillations in the period of 5.9 and 4.2 ka cal BP.

Keywords: paleolimnology; lake sediment; multiproxy reconstruction; 5.9 and 4.2 climate event; climate change; Western Russia

1. Introduction

Neolithization processes in Central and Northern Europe were mainly caused by climate fluctuations, especially during the period between 8.2 and 6 ka cal BP [1]. The cold event in 8.2 ka cal BP caused the migration of Neolithic communities northward from the steppe area of the Black Sea Lowland region toward the coniferous and mixed forest belt of the East European Plain [2]. The rise of temperature in Northern Europe in ca. 6 ka cal BP favored agriculture dispersion and an increase of population in the circum-Baltic Region [3]. In the Central–Western European territories, the expansion of Linear Pottery Culture communities appears to coincide with wet and relatively warm winters and cool summers [1], which was also supported by quantitative paleoclimatic studies. Several paleotemperature records from the E Scandinavia and NW Russia were cited by Kaufman et al. [4], e.g., two quantitative reconstructions based on pollen data [5,6] and one based on Chironomidae [7,8].

Paleoclimatic research is less developed in Eastern Europe compared to the western part of the continent [2,9–11]. Thus, the paleoclimatic background for archeological discoveries on Mesolithic and Neolithic cultures in Eastern Europe is still insufficient. Good qualitative data, unfortunately, the temperature reconstructions are not available for the following publication: Tallinn region (Estonia) [12], Myshetskoe-Dolgoe Lake in Moscow [13], Lake Kenozero [14], Ukraine and Belarus [15,16]. However, plant communities in the area reveal a lagged response to short-lived temperature oscillations that might have been crucial for human settlement, which made it possible to adopt different nutritional strategies at different times.

Aquatic invertebrates are more reactive and sensitive to short-term changes in temperature than plants [17]. Chironomids (Chironomidae), a midge group within the Culicomorpha (Diptera) infraorder, have short life cycles and respond sensitively to climate changes with a decadal resolution [18]. Their development is strongly influenced by environmental conditions [19,20]. The characteristics of Chironomids, namely species diversity, short life cycles, and sensitivity to environmental conditions, make them one of the most reliable proxies for summer air reconstructions [18,21].

Although the summer temperature is crucial for vegetation in temperate to boreal biomes, and influences the economy of the Neolithic communities, precipitation also determines primitive agriculture as well as a hunter-gatherer subsistence strategy. The effective long-term precipitation may be estimated from changes in lake level [22]. Alongside chironomids, small crustaceans of the order Cladocera are very sensitive to lake level fluctuations, as many of the Cladocera taxa are planktonic [23,24]. Therefore, cladocerans can be successfully used for water level reconstructions [25,26]. These microcrustaceans also indicate changes in the trophic status of lakes, including human–environment relationships [27], lake levels [28] including overbank episodes in floodplain areas [29,30], and climate change [31,32]. The Holocene lake level changes are very well documented for Eastern Europe. In the case of the East Peribaltic Region, lake levels and climate wetness were recorded from Northern Poland [33–35] and Baltic States [36–40]. Currently, the entire Holocene sequence from the East European Plain can be found in as many as 50 lake records [41,42]. From Eastern Europe quantitative reconstruction have been made from pollen-inferred paleotemperature and precipitation at Mshinskoye raised bog and Lembolovskoye Lake [43], Bobrovichskoe and Oltushskoe (Polesye) [44], Upper Don [45] and Myshetskoe-Dolgoe Lake [13]. Also pollen-inferred Holocene paleotemperature data from Nikokolsko-Lutinskoye bog, Shirinsky Mokh bog, Lammin-Suo bog, Vishnevskoye Lake and Sakkala bog [46] are available. Chironomid-based mean July air temperature reconstructions are available from Nikolay Lake [47], Lake Medvedevskoe [48] and Lake

Glubokoye [49,50]. One of the important regions in terms of East European paleoclimatology is the Western Dvina Lakeland (Western Russia), where the terrain relief was formed after the recession of the Valdai Ice Sheet [51]. This region was considered crucial for studying the development of human settlement [52–55]. The Neolithic occupation in this area began at ca. 8.3 ka cal BP, and the development of Neolithic communities lasted up to around 3.8 ka cal BP [53,54,56,57]. The pile-dwelling settlement existed in the region during the Middle and Late Neolithic period (between 5.9 and 4.2 ka cal BP) [53,58]. The existence of Neolithic communities in this part of Europe was based on a hunter-gatherer subsistence strategy. The elements of agriculture were adopted gradually only in the Late Neolithic (from ca. 3.8 ka cal BP) [59–62]. However, the local production of biocenoses was influenced by climate variability, particularly mean July air temperature (T_{Jul}), precipitation, and duration of the growing season. Hunter-gatherer communities were also dependent on climate conditions [55]. Thus, the sudden climate fluctuations linked to the Bond events, during 5.9 and 4.2 ka cal BP, might have triggered cultural changes in the Serteya region, forcing a lifestyle change due to the lower productivity of lake and terrestrial ecosystems, lake level fluctuations, and changes in snow cover.

Bond events are climate fluctuations in the Holocene which are based on petrological traces of drifting ice in the North Atlantic over a 1000-year cycle [63,64]. The possible causes for these events include: (1) Orbital insolation—changes in the Earth's orbit are, however, a process too long to cause a 1000-year fluctuation [65]. Solar irradiance—it is contested at event 4.2, where the peak values of ^{14}C and ^{10}Be were very low [66], and is speculated as a possible cause of a decrease in the amount of ultraviolet radiation that may have cooled the ozone layer. These changes could ignite the negative North Atlantic oscillation (NAO) phase, which transported cold and dry air masses over Northern Europe [67,68]. The NAO phenomena in the Holocene correspond chronologically to a decrease in solar activity (increase in ^{14}C and ^{10}Be) [63]. NAO is a circulation system that determines mostly autumn and winter weather conditions in Europe. It is the transition between the positive and negative phases which are distinguished by the amount of atmospheric pressure. Based on the observations of the fluctuations connected with global air circulation and oceanic water, it is known that the NAO is characterized by two phases: positive and negative. The positive phase involves the transfer of warm and humid air masses from the Atlantic Ocean in the direction of Northeastern Europe, while in the negative phase warm and humid air masses move toward the Mediterranean area, causing drought due to decreased snowfall in the northeastern part of Europe [69–71]. (2) Volcanic activity—it is possible only with huge eruptions, but according to Cronin et al. [72] even the largest ones may cause a reduction of the global temperature by only 0.2–0.3 °C for one to several years. There were 12 volcanic eruptions during the Little Ice Age [73]. (3) Ice-sheet dynamics—the melting of icebergs lowers salinity, while decreasing THC (thermohaline circulation) causes negative feedback leading to ice growth in Laurentide [72,74,75].

This paper presents quantitative reconstructions of the main climate factors (mean summer and winter air temperature, and precipitation) influencing the neolithization processes in Eastern Europe, especially the activities related to human occupation in the Western Dvina Lakeland from the 5.9 ka cal BP event (at 6.0–5.75 ka cal BP) to the 4.2-ka cal BP event (at 4.43–3.97 ka cal BP). The T_{Jul} , lake water level related to effective precipitation, mean temperature of the coldest month (TCM), and annual precipitation (AnP) were inferred from the analyses of Chironomidae, Cladocera, and pollen assemblages [18,25,76] and Nazarova et al. unpublished data). We aimed to identify the scale of temperature fluctuations in the region and climate wetness phases. According to the null hypothesis, during the Northgrippian stage (Middle Holocene), the mean July temperature and climate humidity did not vary significantly in the Eastern European Plain and were not decisive for the late emergence of agriculture in the Serteya area. Alternatively, we hypothesized that significant climate changes, coincident with global events, took place during the mid-Holocene. These changes might influence the long-term development of the Serteya II settlement, e.g.: a switch to the Neolithic culture at 8.2 ka cal BP, the development of

the pile-dwelling settlement at 4.2 ka cal BP, the prolonged existence of a hunter-gatherer subsistence strategy, and the late emergence of agriculture after 4.2 ka cal BP [57,77].

2. Study Area

The Serteya region, including the Serteya River valley, is situated in Western Russia (the Smolensk Oblast of the Russian Federation), in the vicinity of the European watershed of the Western Dvina (Daugava) River and the Dnieper River Basin (Figure 1). The Serteya River is a left-bank tributary of the Western Dvina River. According to the physico-geographical division, the Serteya region belongs to the Western Dvina Lakeland [78] or the Vitebsk Lakeland [79]. It lies in the temperate continental climate zone characterized by high-dynamic changes in modern meteorological conditions which strongly influence the natural environment of the area [80]. Winters are moderately cold, with a stable snow cover from November to April, and summers are moderately cool and humid. Much of the AnP (ca. 60%) falls between the months of May and October. The climate data of Velizh, situated 20 km west of the site, has an average annual temperature of 3.6 °C to 8.4 °C and average annual atmospheric precipitation varying from 488 to 1296 mm per year for the years 1955–2017. The mean temperature of the warmest month (TWM) (July) varies between 14.8 °C and 23.0 °C, while that of the coldest month (January) ranges from –17.7 °C to –0.8 °C [81].

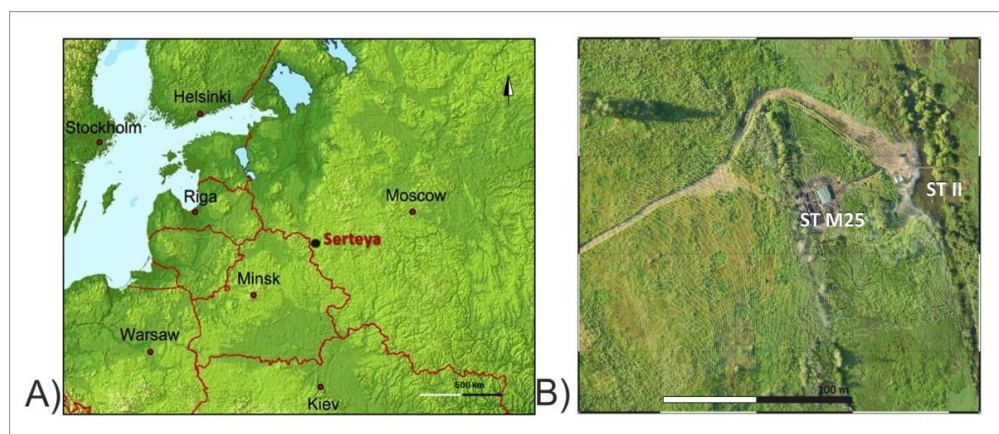


Figure 1. (A) Location of the study area; (B) location of the studied core.

At the end of the Valdai Glaciation, geomorphological processes led to the formation of the land relief framework in the area [82,83]. Within the tunnel valley, which is occupied in modern times by the lower Serteya River valley, a few lake basins existed in the Late Vistulian and during the Holocene. Previous reports indicate that, in the Late Holocene, the lake landscape was gradually replaced by a fluvial system due to the headward erosion and subsequent draining of the lake basins during the development of the Serteya River valley [84,85]. This scheme is similar to that described by Błaszkiewicz [86,87] for the Kociewskie Lakeland, Poland. At present, the Great Serteya Palaeolake Basin is the largest extension of the valley, with a length of ca. 1.2 km and a width of over 0.5 km [85].

During the last 30 years of intense archaeological survey, about 60 archaeological sites, originating from different periods since the Late Paleolithic to the Middle Ages, have been discovered in the surrounding area. The results of the long-term archeological research formed the basis for the reconstruction of the human settlement development and economic foundations of communities in the subsequent periods. The human settlement in this area was strongly affected by paleoenvironmental conditions. Previous palynological, diatom, and geochemical research of biogenic sediment cores M25 from the Serteya region provided an insight into the general paleoclimatic situation of the study area. Kittel et al. [57] explained the paleoecological changes of the Great Serteya Palaeolake Basin in the last 6.3 ky BP. Based on previous research of the Neolithic environmental con-

ditions between ca. 4300 and 1600 cal BC, the period 4150–3250 cal BC is distinguished as a time of increased settlement activity of Neolithic hunter-gatherers on the paleolake shore. On the basis of ecological proxies, fluctuations in the lake water level and the increase in the lake trophic state caused by human influence were also reconstructed. The results show that the Neolithic community and its functioning were strongly influenced by changing environmental conditions, including climate change. Łuców et al. [88] described the last 300-year ecological history of the Serteya region, based on analysis of the organic sediments of an ombrotrophic fen, which revealed the influence of local anthropogenic disturbances on the functioning of the fen. This work reconstructed climate and lake level change based on three proxies (testate amoeba and pollen, plant macrofossils). In the present study, a complete chronology of the sediment was obtained from AMS radiocarbon dating based on the macrofossils of terrestrial plants [cf. 57]. The chronology used follows Kittel et al. [57]. The results presented below are a further analysis of the data obtained from the deposits of the STII M25 core.

Archeological Investigation

Two main areas of the Serteya II have been explored so far [52,57]. The eastern part of the site contains the remains of the pile-dwelling structures, which are dated to 5–4 ka cal BP. The western part of the site was first inhabited in the Late Mesolithic period. During the Early Neolithic, periodic settlements were established at 9–6 ka cal BP. At 6–5 ka cal BP, people of Eneolithic steppe cultures were active in the area. Numerous wooden and bone objects, remnants of residential structures, and fishing devices were found at these complexes. In addition, finds from ca. 5–4 ka cal BP belonging to the Usviaty Culture and Zhizhitsa Culture were recorded, similar to materials from pile dwellings found in the eastern part of the site. At ca. 4.5 ka cal BP, the bodies of two young women were deposited in the paleolake shore zone of site's western part [52,57,89,90].

3. Materials and Methods

3.1. Field Studies and Coring

The geological and geomorphological survey made in 2013–2019 enabled a detailed reconstruction of the geology of the Serteya II site and its vicinity [52,85]. In 2016, a 1.4-m core (STII M25) was taken from the wall of the archeological outcrop in close proximity to the human bones discovered in 2015 [57] covering deposits from 23 to 160 cm below ground level (b.g.l.). The core was placed in three metal boxes measuring 50 cm × 10 cm × 10 cm in size. It consists of the following deposits [57]:

- 0–23 cm b.g.l.—20th century AD embankment
- 23–65 cm b.g.l.—peaty organic mud with sandy admixtures
- 65–75/80 cm b.g.l.—carbonate sandy organic mud
- 75/80–148.5 cm b.g.l.—coarse detritus gyttja
- 148.5–160 cm b.g.l.—sand and gravel with organic mud and plant detritus

The age of the deposits was determined by Kittel et al. [57] from selected macrofossils of terrestrial plants through ^{14}C AMS (accelerator mass spectrometry) analysis. The calibration and chronology were estimated using OxCal v. 4.4.3 with IntCal 20 calibration curve and P_Sequence model [91,92]. For the 1.4-m-long core, a total of six AMS dates, from depths 34, 85, 116, 138, 148, and 158 cm b.g.l., were used for the construction of the depth-age model (not shown) [57].

3.2. Paleoecological Analyses

3.2.1. Chironomidae—Laboratory Techniques, Identification, and Statistics

The subfossil Chironomidae assemblage analysis was carried out on the STII M25 core with a resolution of 2 cm. For this purpose, the sediment samples were sieved on 90 μm sieves. The laboratory methods described by Brooks et al. [18] were used for the analysis. In total, 3503 specimens were identified and classified into three Chironomidae subfamilies and undetermined Ceratopogonidae. The subfossils were identified to the lowest possible

taxonomic level, mainly using the keys of Brooks et al. [18] and Andersen et al. [93]. The sequence zonation was determined using the optimal sum-of-squares partitioning method described by Birks [94], Birks and Gordon [95], and Bennett [96]. The statistically significant number of zones was calculated based on the broken-stick model [97]. The number of zones was determined using ZONE software [98] and BSTICK [99], and the stratigraphic diagram was made using C2 software [100].

3.2.2. Cladocera—Laboratory Techniques, Identification, and Statistics

The sediments the Serteya STII M25 core were examined at 2-cm intervals. Each 1-cm³ sample of the deposit was processed according to the standard procedure [101]. A minimum of 200 cladoceran remains per sample were identified. The taxonomy follows Szeroczyńska and Sarmaja-Korjonen [102] and Van Damm et al. [103]. The ecological preferences of cladoceran taxa were determined using Bjerring et al. [104]. The cladoceran zones were determined by a stratigraphically constrained cluster analysis (CONISS) using POLPAL software [105].

3.2.3. Pollen—Laboratory Techniques, Identification, and Statistics

A total of 55 one cm³ samples (2-cm interval) were treated following the standard pollen preparation procedures (treated with HCl and NaOH, sieved using a 250-μm sieve, treated with HF, acetolysis) [106]. Pollen and NPPs were identified at a magnification of ×400 and ×630 with reference to published illustrations, morphological keys—including those of Fægri and Iversen [106], Reille [107], van Geel [108], van Geel and Aptroot [109], and Beug [110], and a laboratory reference collection. Pollen percentage and influx diagrams were constructed using Tilia software [111,112]. Aquatic and hygrophilous plants, undetermined pollen, ferns, moss, and NPPs were excluded from the pollen sum. The percentages of excluded taxa were calculated using the total pollen sum [113].

3.3. Temperature, Precipitation, and Water Depth Reconstructions

Climate parameters are inferred from chironomids, cladocerans, and pollen assemblages, and water level fluctuations are estimated using chironomids and cladoceran data. The characteristics of the training sets used are presented in Table 1.

Table 1. Training sets used in the analysis and their characteristics.

Training Set	R ² jack	RMSEP	Number of Lakes	Number of Taxa	Temperature/Water Depth Gradient	References
Finnish chironomid Training Set Fn TS Ch-I T Jul	0.86	0.85 °C	180	129	7.9 °C–17.6 °C	Luoto and Nevalainen [114]
Swiss-Norwegian-Polish chironomid Training Set SNP TS Ch-I T Jul	0.91	1.39 °C	357	134	3.5 °C–20.1 °C	Kotrys et al. 2020 [21]
Russian chironomid Training Set Rn TS Ch-I T Jul	0.8	1.43 °C	310	172	1.8 °C–18.8 °C	Nazarova in prep.
Finish Cladocera Training Set Fn TS CL-I T Jul	0.67	0.86 °C	76	38	11.3 °C–20.1 °C	Luoto et al. 2011 [115], Nevalainen et al. 2012 [31]
Finnish Cladocera Depth Training Set Fn TS CL-I depth	0.56	1.084	55	56	0.5–7.0 m	Luoto et al. 2020 [25]

The pollen-inferred (P-I) reconstructions of temperature and precipitation at Serteya across the Holocene were performed using the Modern Analogue Technique (MAT) [116]. This method has been utilized at a global scale for samples from Europe [117,118] and at a more regional scale for samples from Mediterranean pollen sequences [119,120]. The MAT is not a transfer function (cf. the WA-PLS) but an “assemblage approach,” and is based on the primary assumption that pollen samples sharing a similar composition are

a by-product of comparable vegetation assemblages. Using MAT, the composition and abundance of fossil pollen samples are compared with those of modern pollen surface samples, and the similarity between each fossil sample and modern pollen assemblage is evaluated by a squared chord distance.

Once a set of modern pollen samples has been selected as analogues (samples with the smallest distance), climate parameters are assigned to each fossil sample as the weighted average of the climate parameters of the modern samples which are the best analogues. In this study, the number of analogues chosen was five, which were selected using a leave-one-out cross-validation test. The training set of modern pollen samples contains more than 3000 samples from Europe and the Mediterranean area [76]. We also calculated and plotted the chord distance of the first best analogue (Distmin1) and the last analogue selected (Distmin2) (not illustrated) based on a threshold defined by a Monte Carlo method, in order to check the accuracy of the pollen-based climatic reconstruction. The minimum distance (Distmin1) calculated was low for P-I TCM, P-I AnP, indicating that the analogues selected are consistent. Based on previous studies, we reconstructed the climate for precipitation and mean TCM so that the results would be comparable across the region. These reconstructions were carried out using the package Rioja with R software [121].

A Detrended Correspondence Analysis (DCA) was carried out on the percentage data for the Chironomidae, Cladocera, and pollen datasets, with detrending by segments and down-weighting of rare species using Canoco 4.5 [122]. The temperature, water depth, and precipitation reconstructions used C2 and NeuroGenetic Optimizer software (NGO, version 2.6.130, ©BioComp Systems, Inc.) [100,123].

4. Results and Interpretation

4.1. Chironomidae, Cladocera, and Pollen Assemblage Stratigraphy

The detailed ecological description of the zones can be found in Kittel et al. [54], here we present only a summary of the ecological interpretation and diagrams (Figure S1). Based on the similarity analysis using CONISS and BSTICK [99,124], the zones are divided as follows for each proxy. The Chironomidae STII M25 sequence is divided into five significant zones (Figure S1, Figure 2) as follows: ST-Ch1 (158–146 cm b.g.l.), ST-Ch2 (146–131 cm b.g.l.), ST-Ch3 (131–100 cm b.g.l.), ST-Ch4 (100–89 cm b.g.l.), and ST-Ch5 (89–34 cm b.g.l.). The Cladocera sequence is divided into four zones (Figure S1, Figure 3) as follows: ST-Cl1 (158–150 cm b.g.l.), ST-Cl2 (150–78 cm b.g.l.), ST-Cl3 (78–44 cm b.g.l.), and ST-Cl4 (44–34 cm b.g.l.).

The pollen sequence is divided into two zones as follows: ST-P1 (150–100 cm b.g.l.) and ST-P2 (100–80 cm b.g.l.). The ST-P1 has four subzones: ST-P1a (150–138 cm b.g.l.), ST-P1b (138–128 cm b.g.l.), ST-P1c (128–117 cm b.g.l.), and ST-P1d (117–100 cm b.g.l.) (Figure S1, Figure 4).

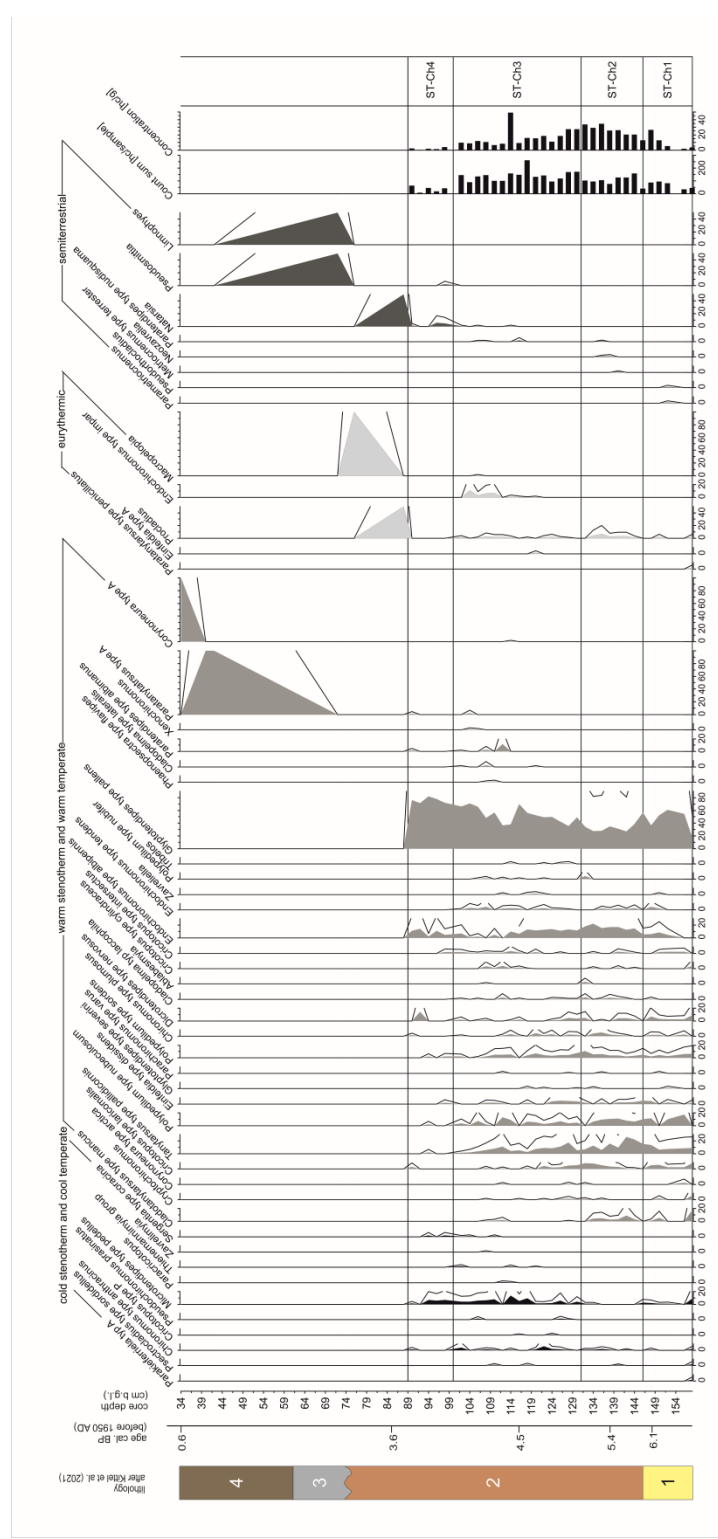


Figure 2. Chironomidae stratigraphic diagram presenting the main chironomid taxa. Taxa are grouped according to summer temperature and lake depth preferences. Exaggeration is with a three times multiplier. Lithology: 1—sand and gravel with organic mud and plant detritus; 2—coarse detritus gyttja; 3—carbonate sandy organic mud; 4—peaty organic mud with sandy admixtures.

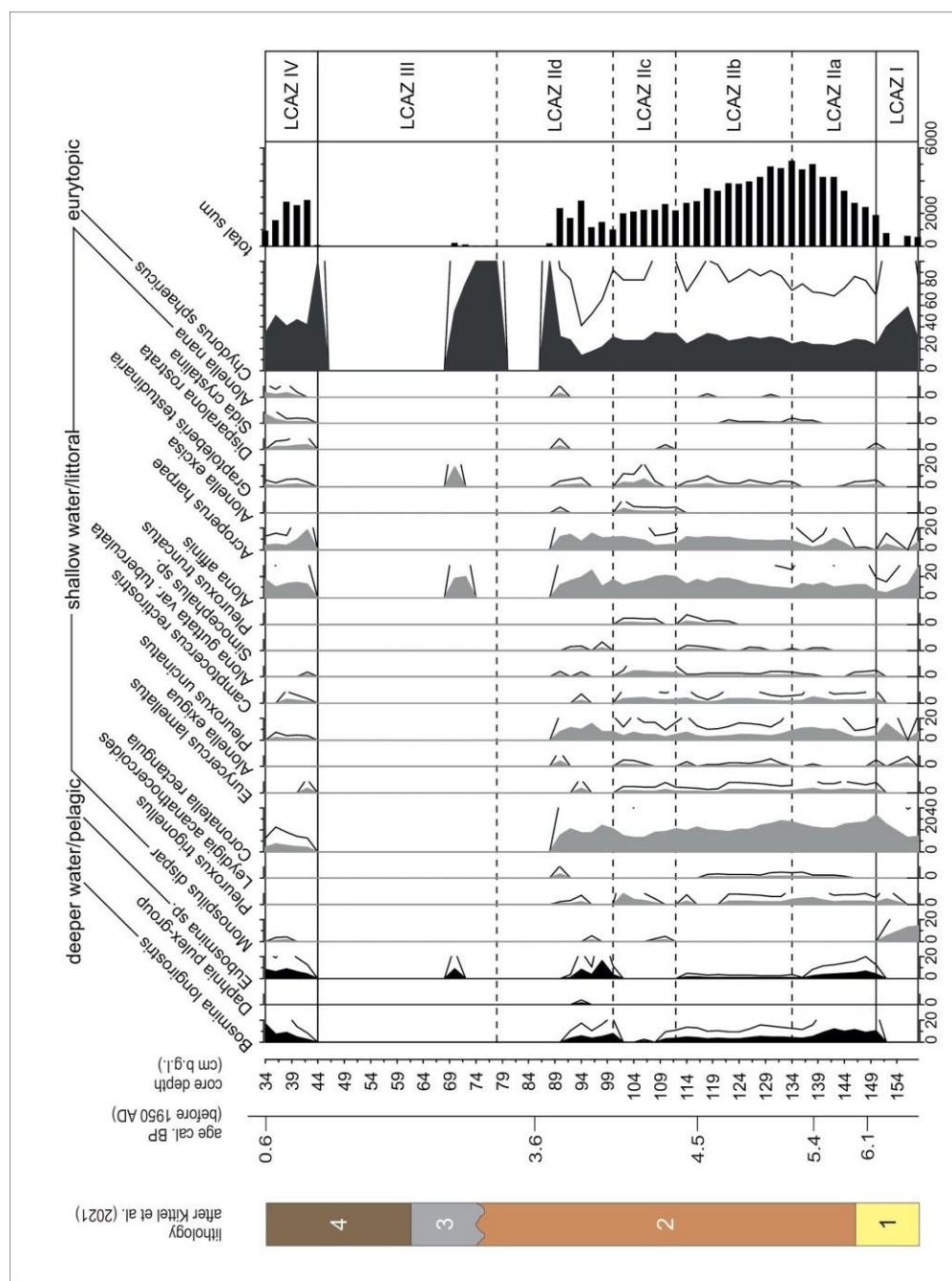


Figure 3. Cladocera stratigraphic diagram presenting the classification of taxa according to lake depth preferences. Exaggeration is with a three times multiplier. Lithology: 1—sand and gravel with organic mud and plant detritus; 2—coarse detritus gyttja; 3—carbonate sandy organic mud; 4—peaty organic mud with sandy admixtures.

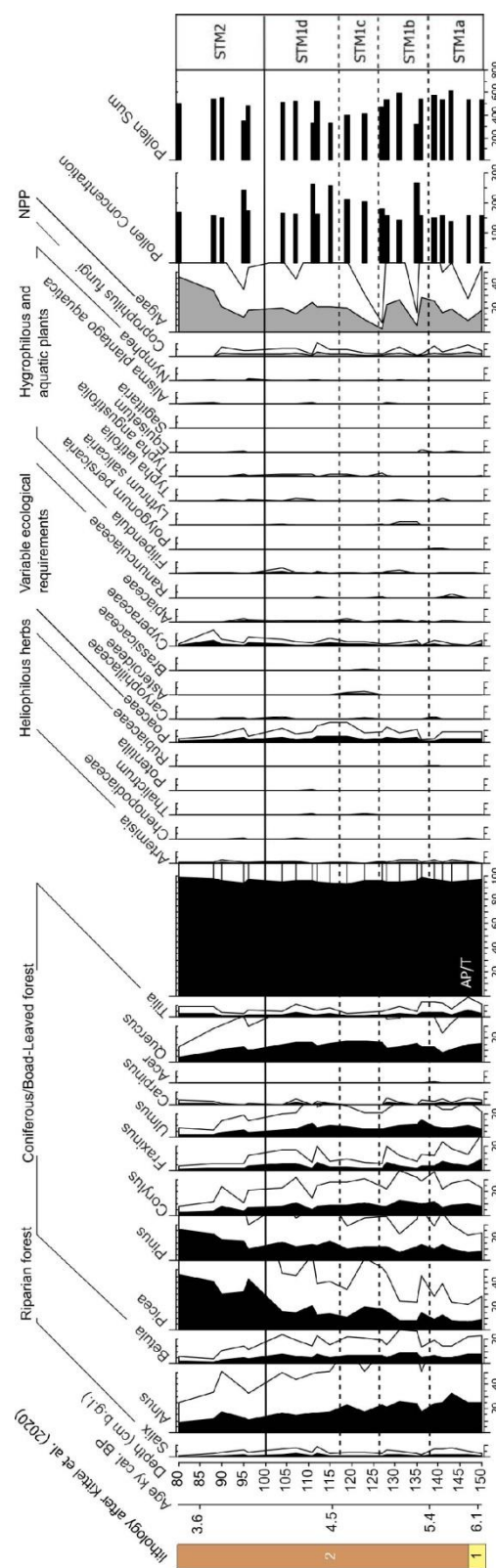


Figure 4. Pollen stratigraphic diagram. Exaggeration is with a three times multiplier. Lithology: 1—sand and gravel with organic mud and plant detritus; 2—coarse detritus gyttja.

4.2. Results and Interpretation of Climatic and Hydroclimatic Reconstructions

4.2.1. Detrended Correspondence Analysis

The first DCA axis of the Chironomidae sequence explained 23.6% of the cumulative variance of species data and had a gradient length of 1.742, proving the linear distribution of the data. The second DCA axis explained 7.7% of the cumulative variance of species data. The DCA Ax1 of chironomid assemblages revealed a similar trend to the estimations of mean July air temperature from the Fn TS and SNP TS WA-PLS (Figure 5), which indicates that the summer temperature was the main driver of the midge communities. Furthermore, the estimations of mean July air temperature from the SNP TS artificial neural network (ANN) were similar to DCA Ax2 of Chironomidae assemblages, but it is a completely different trend than that marked on Ax1. The reconstruction based on the SNP of ANN reflects the influence of another unknown factor. Regarding Cladocera communities, the first DCA axis explained 27.3% of the cumulative variance of species data, with a gradient length of 1.339, proving the linear distribution of the data. The second DCA axis explained 9.9% of the cumulative variance. Similar to chironomid assemblages, the DCA Ax1 of cladoceran communities also reflected the mean July air temperature estimations from the Fn TS (Figure 5), indicating that the summer temperature was the main driver of the water flea communities, whereas Ax2 revealed a different trend.

4.2.2. The Chironomidae-Inferred and Cladocera-Inferred Mean Summer Air Temperature Reconstructions

According to the CH-I T Jul of the 31 Fn TS samples, seven samples remained below the 2 percentile threshold ($\text{minDC} < 7.40328$), representing that they are samples with very good modern analogues, 14 remained below the 5 percentile threshold ($\text{minDC} < 8.85913$), representing good modern analogues, and only two had values over the 10 percentile threshold ($\text{minDC} > 10.1025$), representing poor or very poor modern analogues. Referring to the SNP TS WA-PLS reconstruction, among the 31 samples, only one was below the 2 percentile threshold ($\text{minDC} < 6.98983$) and three were below the 5 percentile threshold ($\text{minDC} < 8.57757$), representing that they are samples with very good and good modern analogues, respectively. As many as 16 samples remained over the 10 percentile threshold ($\text{minDC} > 10.0564$), representing poor or very poor modern analogues. Regarding the Rn TS reconstruction, out of the 31 samples, two topmost ones were below the 5 percentile threshold ($\text{minDC} < 36.57936$), representing good modern analogues. Sixteen samples remained over the 10 percentile threshold ($\text{minDC} > 40.72241$), representing poor and very poor modern analogues.

All the samples from the Cladocera-inferred (CL-I) T Jul Fn TS reconstruction represented very poor modern analogues ($\text{minDC} > 4.30013$), falling over the 20 percentile threshold.

The values of Fn TS CH-I T Jul reconstruction varied from 16.3 °C (158 cm) to 20.9 °C (96 cm) (Figure 5), SNP TS WA-PLS reconstruction from 15.9 °C (142 cm) to 21.3 °C (96 cm), and Rn TS reconstruction from 16.8 °C (158 cm) to 21.6 °C (146 cm). Generally, the Fn TS and SNP TS reconstructions revealed similar trends, but the SNP TS reconstruction showed a higher temperature amplitude and variability. Both reconstructions indicated an increase of summer temperature from the bottom to the top of the sequence, in two phases: the first, cooler phase (158–126 cm) with an average CH-I T Jul of 17.2 °C (SNP TS WA-PLS)–18.3 °C (Fn TS), and the second, warmer phase (124–94 cm) with an average CH-I T Jul of 18.9 °C (Fn TS)–19.0 °C (SNP TS WA-PLS). The Rn TS reconstruction revealed a different trend, with a higher average temperature in the first phase (19.5 °C) and a slightly lower temperature in the second phase (19.1 °C). The weak cool oscillation took place at core depth 146–134 cm (6.0–5.75 ka cal BP), culminating at 146–142 cm. The temperature at the culmination of this episode was in the range 15.9–18.5 °C (SNP TS WA-PLS), 18.4–19.1 °C (Fn TS), and 18.4–21.6 °C (Rn TS).

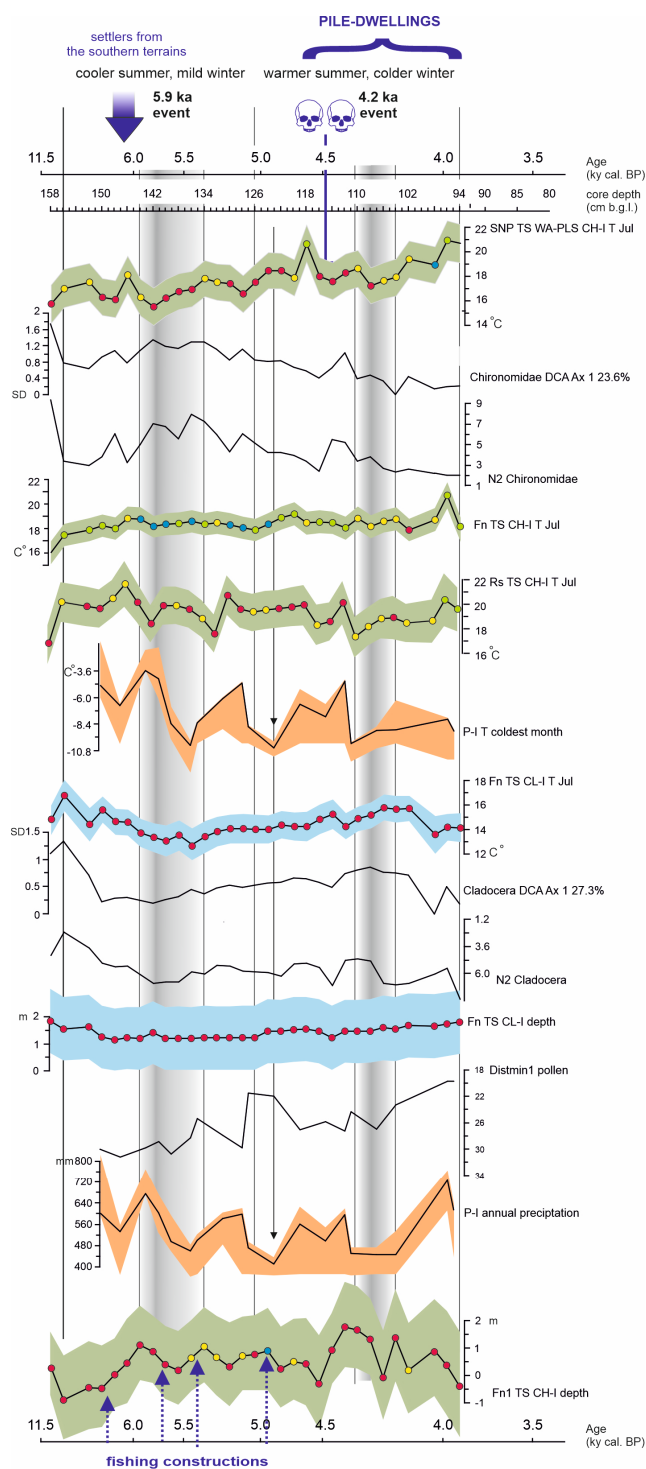


Figure 5. Results of quantitative climatic and water depth reconstructions: SNP TS WA-PLS CH-I T Jul; Chironomidae DCA Ax1 23.6%; N2 Chironomidae (the number of occurrences of Chironomidae species); Fn TS CH-I T Jul; Rs TS CH-I T Jul; P-I TCM; Fn TS CL-I T Jul; Cladocera DCA Ax1 27.3%; N2 Cladocera (the number of occurrences of Cladocera species); Fn TS CL-I depth; Distmin1 pollen (Euclidean distances calculated between the eight modern pollen assemblages considered as the best analogues and the fossil assemblage—nearest and furthest); P-I AnP; and Fn TS CH-I depth. Skulls with an arrow indicate the depth of the skeleton deposition. The arrows at 4.9 ka indicate peaks in precipitation and TCM (i.e., maximum continentality).

The second small temperature decrease took place at core depth 120–94 cm (4.6–3.8 ka cal BP), culminating at 108–104 cm (4.3–4.1 ka cal BP). The temperature at the culmination of this episode was in the range of 17.6–18.3 °C (SNP TS WA-PLS), 18.2–18.9 °C (Rn TS), and 18.4–19.0 °C (Fn TS). In the sample located directly at the skeleton deposition site (115 cm), there was no distinct change of the SNP TS and Fn TS mean summer temperature compared to the adjacent samples, but the Rn TS revealed a decrease of ca. 1.5 °C at 114–116 cm. The average CH-I T Jul for the period of the pile-dwelling location (116–94 cm) was 18.8 °C (Fn TS, Rn TS)–19.0 °C (SNP TS WA-PLS). The SNP TS ANN-based CH-I T Jul (not illustrated) revealed trends that are not consistent with the other mean summer temperature reconstructions for STII M25. Two clear phases were distinguished: the first with a rising temperature trend from 12.9 °C (156 cm) to 18.1 °C (132 cm), and the second with a temperature decline to 13.4–13.6 °C (104 and 94 cm).

The values of Fn TS CL-I T Jul reconstruction ranged from 12.9 °C (136 cm) to 16.9 °C (156 cm) (Figure 5). The CL-I T Jul also revealed two phases, but they are not consistent with the Fn TS and SNP WA-PLS CH-I T Jul. The first phase was characterized by a clear decrease of temperature from 156 cm/10.5 ka cal BP (16.9 °C) to 136 cm (12.9 °C), falling on the ca. 5.9-ka cal BP event. From that point on, there was a steady increase in temperature, up to 106–102 cm/ca. 4.2–4.1 ka cal BP (15.8–15.9 °C). During the 4.2-ka cal BP event, the summer temperature slightly decreased, reaching ca. 15.7 °C. In the case of the last three samples (98–94 cm), the summer temperatures inferred were lower again (13.7–14.3 °C). In the sample where the skeletons were located (115 cm), the mean summer temperature was 15.3 °C and slightly higher compared to the adjacent samples and the average CL-I T Jul for the period of the pile-dwelling location was 15.0 °C.

4.2.3. The Pollen-Inferred Temperature of the Coldest Month and Annual Precipitation Reconstructions

The P-I TCM values ranged from -10.0 °C (123 cm) to -3.0 °C (143 cm) (Figure 5), and P-I AnP values varied from 409 mm (123 cm) to 725 mm (96 cm). Both P-I reconstructions revealed a similar trend indicating phases of more continental (cold winter and arid years) and more Atlantic (mild winter and humid years) conditions. The reconstructions indicated a general decrease of P-I TCM and P-I AnP from the bottom to the top of the sequence. There were three alternate cold-winter and arid phases (Ic—141–135 cm; IIc—127–123 cm; IIIc—111–104 cm) and mild-winter and humid phases (Ia—150–141 cm; IIa—135–128 cm; IIIa—119–112 cm). The topmost samples from 96–95 cm revealed cold winters and high AnP. The cold-winter arid phase Ic fell on the 5.9-ka cal BP event and phase IIIc on the 4.2-ka cal BP event. Phase IIc coincided with a distinct rise of CH-I and CL-I summer temperature reconstructions derived from all three TSs. The minimum distance (Distmin1) calculated was low, indicating that the selected analogues are consistent and that our reconstruction is acceptable considering the possible bias due to the human impact on the pollen data. However, no indicator of farming activities was identified in the pollen diagram [57].

4.2.4. The Cladocera-Inferred and Chironomidae-Inferred Lake Water Level Reconstructions

All the samples of CL-I water depth reconstruction (CL-I depth) represented very poor modern analogues, which were over the 20 percentile threshold ($\text{minDC} > 3.68913$). According to the CH-I water depth reconstruction (CH-I depth), only one sample from 124 cm remained below the 2 percentile threshold ($\text{minDC} < 8.57652$), representing very good modern analogues, and six remained within the 5–10 percentile threshold ($9.81504 < \text{minDC} < 10.8182$), representing moderate modern analogues. All the other 24 samples remained over the 10 percentile threshold ($\text{minDC} > 10.8182$), representing that they are samples with poor and very poor modern analogues.

The Fn TS CL-I depth reconstruction showed a constantly shallow littoral depth ranging from 1.2 to 2 m. However, this reconstruction indicated a relative increase in water level at 142 cm/ca. 5.9 ka cal BP (from 1.2 to 1.5 m) as well as at 96 cm, where the highest water depth—ca. 2 m—was recorded. In turn, at a depth of 114 cm (ca. 4.4 ka cal BP), the

Fn TS CL-I depth showed a decrease of water level from 1.6 to 1.3 m. The CL-I depth followed the general trend of the Fn TS and SNP TS WA-PLS CH-I T Jul, manifesting a lower average value for the first, cooler phase (1.4 m) and a slightly higher average value for the second, warmer phase (1.6 m). The CH-I depth revealed four phases. At the Greenlandian (Preboreal—Early Atlantic) period, up to 6.1 ka cal BP (158–148 cm), there was only astatic, possibly seasonal water inundation of the STII M25 site. At 146–142 cm falling on 6.0–5.75 ka cal BP, i.e. the culmination of the 5.9-ka cal BP event, a clear transgression of the lake (increase from 0.4 to 1.1 m) was observed, followed by a very shallow phase of occasional seasonal water conditions up to a core depth of 116 cm (average CH-I depth = 0.5 m). The human bodies were deposited in astatic or seasonal water conditions at the horizon of ca. 115-cm core depth. From 114 to 98 cm of the core length, the second lake transgression to the average depth value of 1.2 m (excluding the 106 cm sample) took place, falling on the 4.2-ka cal BP event: 4.4–4.0 ka cal BP. At the topmost 96–94 cm, low or even seasonal water conditions were recorded again. The average CH-I depth and CL-I depth for the period of the pile-dwelling location (116–94 cm) were 0.7 and 1.6 m, respectively.

5. Discussion

The CH-I T Jul reconstructions were based on three different models. As the training sets originated from different regions—Western and Central Europe (SNP TS), Central and Northern Europe (Fn TS), and Eastern Eurasia (Rn TS), we obtained different results. Nonetheless, the reconstructions were consistent, giving similar values and showing more or less similar trends. It is not surprising that the SNP TS and Fn TS showed similar trends compared to the more dissimilar Rn TS, because they shared ca. 100 sites from Poland. The SNP TS revealed high temperature variability because it combines three different climatic regions representing separate midge fauna, with a wide range of temperatures. The Fn TS gave the closest modern analogues as it uses samples from the nearby geographical region. The results of the Fn TS reconstruction are strongly flattened. The Rn TS gave the highest temperature values, in the range of continental climates of Central Siberia. This reconstruction indicates an overall slightly decreasing trend, but is erratic. The DCA and N2 showed similar trends to the SNP TS reconstruction indicating that the summer temperature was a dominant driver for Chironomidae communities. The cold oscillations took place at about 5.9 and 4.2 ka. Generally, these oscillations are weak and are apparent in a few consecutive samples (1–4) and indicate a drop in T Jul of ca. 1–2 °C. This exceeds the RMSEP of the models, which suggests this is not noise. It can be seen from the reconstructions that during the Northgrippian stage the summer air temperature was high, mostly in the range of 17–20 °C. These values are similar to the current July air temperatures in the Serteya region [80,125]. A comparison with other sites in Eastern Europe indicates that the values of P-I TWM and CH-I T Jul were usually 2 °C lower in the circum-Baltic region, whereas on the Central Polish Plain (e.g., Żabieniec, Błędowo) and the Central Russian Plain (Staroselsky Moch, Peatland Klukva) the values were similar to those at the Serteya STII M25 (Table S1, Figure S2). The data from the Leningrad Oblast shows a cold oscillation between 5.9 and 4.2 ka cal BP [43]. This result indicates that in more continental regions, distant from the Baltic influence, the summer temperatures were slightly higher.

The SNP TS reconstructions showed a increasing temperature trend from 5.9 to 4.2 ka cal BP, punctuated by two cool oscillations indicated at 5.9 and 4.2 ka. However, the Rn TS showed a weakly decreasing trend. An increasing trend is also indicated from Upper Don [45]. The global temperature trend of terrestrial records from 30° to 60° latitude is decreasing after 6 ka cal BP [126,127]. In addition, the simulations of Renssen et al. [128] indicated that the Holocene Thermal Maximum (HTM) occurred in Eastern Europe earlier than 6 ka cal BP. A comparison of the temperature of both cooling events in Table S1 indicated a similar trend in the East European Lowland. At some sites in the southern part of the region, the temperatures were slightly higher at 5.9 ka cal BP. However, in the northern part, some sites had slightly higher TWM during 4.2 ka cal BP. Warden et al. [3] clearly indicated that the HTM in the peri-Baltic region occurred at ca. 5.9–5.5 ka cal BP,

with a cooling trend to 4.2 ka cal BP. The nearby P-I TWM reconstruction from Staroselsky Moch revealed more or less the same values through 6–4 ka cal BP. Tarasov et al. [62] also suggested that in the Western Dvina Lakeland HTM occurred in ca 8.6–6.9 ka cal BP and in the Karelian Isthmus in ca 7.8 cal BP [40]. It started and ended some centuries earlier than suggested for the neighboring Baltic region—ca 8.1–5.6 ka cal BP. Based on pollen data, Tarasov et al. [62] reported that the climate in Middle Holocene was drier and warmer, whereas after 5.4 ka cal BP the climate was cooler and wetter. Nonetheless, the authors did not perform quantitative reconstructions from the investigated sites, but their results seem to be more consistent with the Rn TS reconstruction.

The SNP TS and Fn TS revealed a cold oscillation from the Mid- to Late Northgrippian (5.9–4.2 ka cal BP) stage. It may be a microclimate pattern that is dependent on local factors such as lake transgressions. The warm-stenotherm chironomid taxa usually have preferences for a higher trophic state [17]. Human-induced eutrophication might have overridden the influence of July air temperature resulting in higher reconstructed temperatures [57].

Juggins [129] suggested that only one quantitative reconstruction should be obtained from a particular proxy. Here, we decided to illustrate both reconstructions from the pollen data. Both revealed very similar trends and were consistent with Distmin1 (Figure 5). This suggests that plant communities were influenced by one climatic factor: continentality fluctuations. Such a coincidence of decreased precipitation and TCM indicates that continentality is the main driving factor of plant communities in the region. At about 4.9 ka occurs sudden drop in precipitation and TCM. The values of TCM, TWM/T Jul, and AnP were compared for a wide group of 22 sites from Eastern Europe (Table S1), no clear signal of the 5.9- and 4.2-ka cal BP oscillations in the region was noted.

Knowledge about the cold episode at ca 5.9 ka BP is still insufficient. There is no consensus on the magnitude and timing of the 5.9 Bond event oscillation in eastern Europe [36,128–131]. This raises a doubt whether there are any well-documented quantitative reconstructions of these Bond events in Eastern Europe. Where there are some records indicating oscillations in a few consecutive samples, the signal is weak and unclear. Hence, climatic records of much better resolution are needed from the region to verify the hypothesis of the presence of these Bond events.

Because the Bond events are linked to the NAO fluctuations, they might be more significant in Western Europe than in the East. The European territory along the North Atlantic is the main area to be affected by this climatic phenomenon. The STII M25 site is located in the Western Dvina Lakeland in the contact zone of transitional and continental climate, which could have made it sensitive to the paleoclimatic regime changes (NAO circulation). Based on their studies, Yao and Luo [130] and Rousi et al. [131] concluded that the eastern and western types of NAO differently influence the temperature and precipitation regimes in Europe. To study the magnitude of the NAO influence and the relationship between NAO and the temperate climate zone, the domain size must also be considered [132]. For this zone, the optimal domain sizes are lower in summer compared to winter, and for continental rather than oceanic regions. The NAO will likely have a stronger impact on the climate of Northeast Europe in winter in continental regions. From the results (Figure 5), one can speculate that the positive NAO phases during the 4.2 and 5.9 ka events was characterized by cool summers and severely cold winters, as well as intense precipitation mostly in autumn. The differences between the dynamics of precipitation during these events may result from changes in the activity of ultraviolet radiation and glacier size. For further conclusions, it is necessary to study more sites in Eastern Europe at high temporal resolution. However, for the LIA, correlated with the Bond Event no. 0, a predominance of negative NAO phases is postulated by Trouet [133]. Moreover, a positive NAO phase is postulated for the MCA-LIA period [134,135]. It must be also stressed that Moreno-Chamarro et al. [136] emphasize a reduction in the heat transport by the subpolar gyre rather than a NAO impact on the LIA cooling, mostly during the winter seasons.

The boundary of boreal plant assemblages and temperate deciduous forest in the studied area also reflect the climate zones. Thus, P-I reconstructions should reflect the change in the range of vegetation composition in Eastern Europe. Pleskot et al. [137] questions the presence of the 4.2-ka cal BP oscillation in Poland. At the STII M25 P-I, the higher continentality signal is clear at both events and has also been recorded in a few subsequent samples. Pleskot et al. [137] performed only CH-I T Jul reconstruction. The STII M25 CH-I T Jul reconstruction also gave a weak and ambiguous signal of 4.2- and 5.9-ka cal BP oscillations. P-I reconstructions revealed a much clearer pattern at the STII M25 site, but not at the nearby Staroselsky Moch and Klukva Peatland [138,139].

The P-I TCM/AnP and CH-I T Jul reconstructions from STII M25 indicated the third intermediate oscillation falling on 5.0–4.7 ka cal BP. This oscillation manifests by a small increase of T Jul at 5.1 ka and distinct increase in continentality. Its maximum effect falls on 4.9–4.8 ka cal BP, and its magnitude is comparable with the 5.9-ka cal BP signal and stronger than the 4.2-ka cal BP one. Modern maps indicate that this microregion differs from the wider Smolensk region. The oscillation may have had a more local character as there are warmer and colder microregions within the Western Dvina Lakeland. Besides P-I and CH-I, the present study performed CL-I summer temperature and lake depth reconstructions. Although water level fluctuations are regarded as the primary factor influencing Cladocera communities in the long term [28], the DCA (Figure 5) results were consistent with the CL-I summer temperature reconstruction, indicating it as the primary driver of cladoceran communities. The values of temperature are lower than CH-I T Jul because midges are more linked to air temperature while water fleas are linked to water temperature [6,24,140,141]. Thus, the lower values of CL-I temperature are not surprising; however, the decrease of CL-I T Jul also differs from CH-I. From 136 to 104 cm b.g.l., the temperature increasing was observed, similar to the SNP and Fn TS CH-I T Jul reconstructions, although the earlier (158–134 cm b.g.l.) oscillation was opposite. In addition, the reconstruction from the three topmost samples revealed a dissimilar pattern to all CH-I reconstructions. This can also be explained by the differences and complexity of proxy responses to temperature which merges with water trophic state and other environmental factors [142]. Moreover, it needs to be mentioned that CL-I reconstructions from STII M25 gave poor and very poor modern analogues.

Finally, the question of CH-I water level reconstruction remains. Because the site is located in the lakeshore zone [57,85], water level fluctuations at STII M25 are crucial for explaining the environmental causes of Neolithic settlements. The results showed by CL-I and CH-I lake depth reconstructions are consistent with general observations that STII M25 is located in the shallow littoral zone [57]. The CH-I lake depth suggests that the water level was unstable and may have even been seasonal before the 5.9-ka cal BP event, and then there were very shallow water conditions up to ca. 4.5 ka cal BP. According to the CH-I lake depth, the bodies of women recovered at ca. 115 cm b.g.l. should have been placed when the water level was increasing before the 4.2-ka cal BP event. During this event, the lake revealed a higher water level than during the 5.9-ka cal BP event. Nonetheless, the CH-I depth gave generally better modern analogues between the 5.9- and 4.2-ka cal BP event in comparison to the CL-I depth, and the fluctuations of both reconstructions remained within the RMSEP range. The mean July temperature was the leading factor in the case of both Chironomidae and Cladocera, overriding water level fluctuations in the permanently shallow littoral zone. Therefore, the constructed quantitative reconstructions of water level fluctuations are doubtful, and in this case, qualitative reconstructions of the habitat change presented in a previous study [57] are more valid.

The above-presented reconstructions prove that climate conditions during the Northgrippian stage were suitable for human communities. The local microclimate in the Serteya could have been buffered by the lake–river system, weakening the fluctuations of summer temperature during 5.9 and 4.2 ka cal BP. Summer temperature was relatively high during the whole Northgrippian stage, due to which tribes from the Black Sea Lowland settled here after 8.2 ka cal BP [1,55]. Stable climate conditions would imply constant primary and

secondary production of an ecosystem supporting a hunter-gatherer economy for a long time after agricultural development in localities in the West and the North [3]. However, plant communities here consist of those that clearly reacted negatively to the 5.9- and 4.2-ka cal BP event. This suggests that the Bond events might have indeed influenced the ecology of local settlers triggering a change in their culture to altered, more difficult (higher continentality) conditions. The intermediate climate oscillation falling on 5.0–4.7 ka cal BP coincides with the appearance of relicts of the Globular Amphora culture at the Serteyka River Valley. It indicates that local settlers participated in spreading trails of amber to the East. Hence, the Western Dvina Lakeland must have had high economic status in the region [57,85] which can be attributed to productive local ecosystems, high geodiversity, and favorable [142] climate conditions.

6. Conclusions

In recent years, quantitative reconstructions have impacted paleoecology mainly by providing precise quantitative records, though they have their own limitations. One of them is the reconstructed chronology of non-laminated lake sediments, another is sedimentation rate in lakes, and the lag in the reaction of plant biota to climate change that limits reconstruction to decadal resolution [143]. Moreover, the methods used for quantitative reconstructions have their own statistical limitations which can be accessed from the R₂, RMSEP, and modern analogues. The climatic records may be obscured by local impacts from non-climatic influences on the proxies [129,142]. The present study has included several reconstructions using three different proxies: chironomids, cladocerans, and pollen. Summer mean air temperature appeared to have a stronger influence than the lake depth on the midges and water fleas, which is in line with the general observations of their ecology [144,145]. This indicates that local water level fluctuations had only a secondary effect on the littoral lake ecosystem. The CH-I mean air temperature and CL-I mean water temperature of the summer season are similar to the recent, Late Holocene values. Although STII M25 is located in the western part of the archaeological site, not within a major dwelling area of the pile-dwelling settlement, human-induced local eutrophication might have still reinforced the effect of temperature, to produce a false signal of temperature increase inferred from Chironomidae as well as Cladocera. The pollen analysis indicated an increase in continentality during the investigated period. Furthermore, P-I TCM and AnP showed clearer oscillations at the 5.9- and 4.2-ka cal BP events than the chironomids and Cladocera. Hence, the P-I reconstructions may be considered as the primary result of the presented studies. It is difficult to recognize mid-Holocene (Northgrippian) oscillations, especially in Eastern Europe where the influence of NAO is weaker [24,69,137]. In order to speculate about their time shift (5.9 ka cal BP and 4.2 cal BP), it would be useful to increase the number of quantitative reconstructions for the area of Eastern Europe. The comparison of the results obtained with broad-spectrum quantitative reconstructions from the region (Table S1) shows that the SNP TS results do agree with other global reconstructions. Most reconstructions from Eastern Europe have insufficient resolution to capture Bond oscillations in the Northgrippian stage. Considering all the methodological cautions in the interpretation of the presented results, we are inclined to support the alternative hypothesis presented in the Introduction, though with some reservations. Nevertheless, we cannot prove that the oscillations are at a regional or global scale and result from NAO. We assume that these climate changes might have influenced the progression of the Serteya II settlement over time, including the possible collapse of the pile-dwelling settlement at 4.2 ka cal BP and the prolonged existence of a hunter-fisher-gatherer subsistence strategy as the conditions were favorable for the productivity of local ecosystems.

Supplementary Materials: The following are available online at <https://www.mdpi.com/article/10.3390/w13111611/s1>, Table S1. Review of quantitative climatic and water level reconstructions from the region in 5.9 ka cal BP and 4.2 ka cal BP. Part of the records is based on Kaufman et al. (2020) [146–160]: http://lipdverse.org/Temp12k/current_version/. Data access: 1 January 2021; Figure S1. Zonation of Cladocera, Chironomidae, and pollen communities based on Kittel et al. 2021.

Lithology: 4-peaty organic mud with sandy admixtures; 3-carbonate sandy organic mud, 2-coarse detritus gyttja, 1-sand and gravel with organic mud and plant detritus; Figure S2. Map of sites mentioned in Table S1.

Author Contributions: A.M. (Agnieszka Mroczkowska) conducted the Chironomidae analysis, proposed the idea of the main text, constructed the manuscript, and contributed to the figures. D.P. conducted the Cladocera analysis, and contributed to the main text and figures. E.G. and E.T. conducted the pollen analysis, and contributed to the main text and figures. A.M. (Andrey Mazurkevich) and E.V.D. conducted the archaeological field research, and contributed to the main text and the concept of paleoecological studies at the STII site. T.P.L. conducted the climatic and hydrological reconstructions from the Fn TS and East European TSs. O.P. conducted the pollen climatic reconstructions. B.K. conducted the climatic reconstruction from the SNP TS and contributed to the field investigation at the STII site. S.J.B. conducted the climatic reconstruction from the SNP TS. L.B.N. conducted the climatic reconstruction from the Rs TS. L.S. conducted the climatic reconstruction from the Rs TS. DE conducted field research at the STII site. E.T. conducted the pollen analysis. M.P. provided comments to the manuscript, statistics, and figures. O.A.-O. contributed to the main text. P.K. is the head of the project, invented the concept of paleoclimatic and paleoecological studies at the STII site, conducted paleoenvironmental field research at the site, and contributed to the main text and figures. All authors have read and agreed to the published version of the manuscript.

Funding: The author(s) disclosed receipt of the following financial support for the research, authorship, and/or publication of this article: This research was supported by grants 2017/25/B/HS3/00274 and 2018/31/B/ST10/02498 from the National Science Center (Poland). N.L. was supported by the Russian Scientific Foundation, grant 20-17-00135.

Institutional Review Board Statement: Not applicable.

Informed Consent Statement: Not applicable.

Data Availability Statement: The data presented in this study are available on request from the corresponding author.

Conflicts of Interest: The authors declare no conflict of interest.

References

1. Sánchez Goñi, M.F.; Ortú, E.; Banks, W.E.; Giraudieu, J.; Leroyer, C.; Hanquiez, V. The expansion of Central and Northern European Neolithic populations was associated with a multi-century warm winter and wetter climate. *Holocene* **2016**, *26*, 1188–1199. [[CrossRef](#)]
2. Kulkova, M.; Mazurkevich, A.; Dolbunova, E.; Lozovsky, V. The 8200 calBP climate event and the spread of the Neolithic in Eastern Europe. *Doc. Praehist.* **2015**, *42*, 77–92. [[CrossRef](#)]
3. Warden, L.; Moros, M.; Neumann, T.; Shennan, S.; Timpson, A.; Manning, K.; Sollai, M.; Wacker, L.; Perner, K.; Häusler, K. Climate induced human demographic and cultural change in northern Europe during the mid-Holocene. *Sci. Rep.* **2017**, *7*, 15251. [[CrossRef](#)] [[PubMed](#)]
4. Kaufman, D.; McKay, N.; Routson, C.; Erb, M.; Davis, B.; Heiri, O.; Jaccard, S.; Tierney, J.; Dätwyler, C.; Axford, Y. A global database of Holocene paleotemperature records. *Sci. Data* **2020**, *7*, 115. [[CrossRef](#)]
5. Khomutova, V.I.; Elina, G.A. Stratigraphy of lake sediments by palynological data. Istorya Ladozhskogo, Onezhskogo, Pskovsko-Chudskogo ozer, Baikala i Khanki [The history of Ladoga, Onego, Pskovsko-Chudskoe, Baikal and Khanki lakes]. 1990. pp. 92–96.
6. Elina, G.; Filimonova, L.; Raukas, A.; Saarse, L. Late-Glacial Vegetation on the Territory of Karelia. In *Palaeohydrology of the Temperate Zone III: Mires and Lakes*; Valgus: Tallinn, Estonia, 1987; pp. 53–69.
7. Nazarova, L.; Syrykh, L.S.; Mayfield, R.J.; Frolova, L.A.; Ibragimova, A.G.; Grekov, I.M.; Subetto, D.A. Palaeoecological and palaeoclimatic conditions on the Karelian Isthmus (northwestern Russia) during the Holocene. *Quat. Res.* **2020**, *95*, 65–83. [[CrossRef](#)]
8. Nazarova, L.B.; Subetto, D.A.; Syrykh, L.S.; Grekov, I.M.; Leontev, P.A. Reconstructions of Paleoenvironmental and Paleoclimatic Conditions of the Late Pleistocene and Holocene according to the Results of Chironomid Analysis of Sediments from Medvedevskoe Lake (Karelian Isthmus). *Dokl. Earth Sci.* **2018**, *480*, 710. [[CrossRef](#)]
9. Feurdean, A.; Persoiu, A.; Tanțău, I.; Stevens, T.; Magyari, E.K.; Onac, B.P.; Marković, S.; Andrič, M.; Connor, S.; Fărcaș, S. Climate variability and associated vegetation response throughout Central and Eastern Europe (CEE) between 60 and 8 ka. *Quat. Sci. Rev.* **2014**, *106*, 206–224. [[CrossRef](#)]

10. Moreno, A.; Svensson, A.; Brooks, S.J.; Connor, S.; Engels, S.; Fletcher, W.; Genty, D.; Heiri, O.; Labuhn, I.; Peršoiu, A. A compilation of Western European terrestrial records 60–8 ka BP: Towards an understanding of latitudinal climatic gradients. *Quat. Sci. Rev.* **2014**, *106*, 167–185. [[CrossRef](#)]
11. Berntsson, A.; Rosqvist, G.C.; Velle, G. Late-Holocene temperature and precipitation changes in Vindelfjällen, mid-western Swedish Lapland, inferred from chironomid and geochemical data. *Holocene* **2014**, *24*, 78–92. [[CrossRef](#)]
12. Heinsalu, A.; Veski, S. The history of the Yoldia Sea in Northern Estonia: Palaeoenvironmental conditions and climatic oscillations. *Geol. Q.* **2007**, *51*, 295–306.
13. Kremenetski, K.; Borisova, O.; Zelikson, E. The Late Glacial and Holocene history of vegetation in the Moscow region. *Paleontol. J. C/C Paleontol. Zhurnal* **2000**, *34*, 67–74.
14. Sapelko, T.V. Dinamika razvitiâ rastitel'nosti na territorii Kenozerskogo nacional'nogo parka v golicene. *Izv. Rus. Geogr. Obšestva* **2006**, *138*, 70–76.
15. Velichko, A.A.; Andreev, A.; Klimanov, V. Climate and vegetation dynamics in the tundra and forest zone during the Late Glacial and Holocene. *Quat. Int.* **1997**, *41*, 71–96. [[CrossRef](#)]
16. Velichko, A.A.; Catto, N.; Drenova, A.N.; Klimanov, V.A.; Kremenetski, K.V.; Nechaev, V.P. Climate changes in East Europe and Siberia at the Late glacial–holocene transition. *Quat. Int.* **2002**, *91*, 75–99. [[CrossRef](#)]
17. Kołaczek, P.; Karpińska-Kołaczek, M.; Marcisz, K.; Gałka, M.; Lamentowicz, M. Palaeohydrology and the human impact on one of the largest raised bogs complex in the Western Carpathians (Central Europe) during the last two millennia. *Holocene* **2018**, *28*, 595–608. [[CrossRef](#)]
18. Brooks, S.J.; Heiri, O.; Langdon, P.G. *The Identification and Use of Palaearctic Chironomidae Larvae in Palaeoecology*; Quaternary Research Association: London, UK, 2007.
19. Oliver, D. Life history of the Chironomidae. *Annu. Rev. Entomol.* **1971**, *16*, 211–230. [[CrossRef](#)]
20. Eggermont, H.; Heiri, O. The chironomid-temperature relationship: Expression in nature and palaeoenvironmental implications. *Biol. Rev.* **2012**, *87*, 430–456. [[CrossRef](#)]
21. Kotrys, B.; Płociennik, M.; Sydor, P.; Brooks, S.J. Expanding the Swiss-Norwegian chironomid training set with Polish data. *Boreas* **2020**, *49*, 89–107. [[CrossRef](#)]
22. Magny, M.; Combourieu-Nebout, N.; De Beaulieu, J.-L.; Bout-Roumazeilles, V.; Colombaroli, D.; Desprat, S.; Francke, A.; Joannin, S.; Ortú, E.; Peyron, O. North–south palaeohydrological contrasts in the central Mediterranean during the Holocene: Tentative synthesis and working hypotheses. *Clim. Past* **2013**, *9*, 2043–2071. [[CrossRef](#)]
23. Frolova, L.; Nazarova, L.; Pestryakova, L.; Herzschuh, U. Analysis of the effects of climate-dependent factors on the formation of zooplankton communities that inhabit arctic lakes in the Anabar River Basin. *Contemp. Probl. Ecol.* **2013**, *6*, 1–11. [[CrossRef](#)]
24. Płociennik, M.; Pawłowski, D.; Vilizzi, L.; Antczak-Orlewska, O. From oxbow to mire: Chironomidae and Cladocera as habitat palaeoindicators. *Hydrobiologia* **2020**, *847*, 3257–3275. [[CrossRef](#)]
25. Luoto, T.P.; Kivilä, E.H.; Kotrys, B.; Płociennik, M.; Rantala, M.V.; Nevalainen, L. Air temperature and water level inferences from northeastern Lapland (69°N) since the Little Ice Age. *Pol. Polar Res.* **2020**, *23*–40. [[CrossRef](#)]
26. Pawłowski, D.; Płociennik, M.; Brooks, S.J.; Luoto, T.P.; Milecka, K.; Nevalainen, L.; Peyron, O.; Self, A.; Zieliński, T. A multiproxy study of Younger Dryas and Early Holocene climatic conditions from the Grabia River paleo-oxbow lake (central Poland). *Palaeogeogr. Palaeoclimatol. Palaeoecol.* **2015**, *438*, 34–50. [[CrossRef](#)]
27. Pawłowski, D.; Kowalewski, G.; Milecka, K.; Płociennik, M.; Woszczyk, M.; Zieliński, T.; Okupny, D.; Włodarski, W.; Forysiak, J. A reconstruction of the palaeohydrological conditions of a flood-plain: A multi-proxy study from the Grabia River valley mire, central Poland. *Boreas* **2015**, *44*, 543–562. [[CrossRef](#)]
28. Nevalainen, L.; Sarmaja-Korjonen, K.; Luoto, T.P. Sedimentary Cladocera as indicators of past water-level changes in shallow northern lakes. *Quat. Res.* **2011**, *75*, 430–437. [[CrossRef](#)]
29. Pawłowski, D.; Borówka, R.K.; Kowalewski, G.; Luoto, T.P.; Milecka, K.; Nevalainen, L.; Okupny, D.; Płociennik, M.; Woszczyk, M.; Tomkowiak, J. The response of flood-plain ecosystems to the Late Glacial and Early Holocene hydrological changes: A case study from a small Central European river valley. *Catena* **2016**, *147*, 411–428. [[CrossRef](#)]
30. Pawłowski, D.; Borówka, R.K.; Kowalewski, G.A.; Luoto, T.P.; Milecka, K.; Nevalainen, L.; Okupny, D.; Tomkowiak, J.; Zieliński, T. Late Weichselian and Holocene record of the paleoenvironmental changes in a small river valley in Central Poland. *Quat. Sci. Rev.* **2016**, *135*, 24–40. [[CrossRef](#)]
31. Nevalainen, L.; Luoto, T.P.; Kultti, S.; Sarmaja-Korjonen, K. Do subfossil Cladocera and chydorid ephippia disentangle Holocene climate trends? *Holocene* **2012**, *22*, 291–299. [[CrossRef](#)]
32. Pawłowski, D. Younger Dryas climatic reconstructions in central Poland. *Acta Geol. Pol.* **2017**, *67*, 567–584. [[CrossRef](#)]
33. Marcisz, K.; Gałka, M.; Pietrala, P.; Miotk-Szpiganowicz, G.; Obremska, M.; Tobolski, K.; Lamentowicz, M. Fire activity and hydrological dynamics in the past 5700 years reconstructed from Sphagnum peatlands along the oceanic–continental climatic gradient in northern Poland. *Quat. Sci. Rev.* **2017**, *177*, 145–157. [[CrossRef](#)]
34. Gałka, M.; Miotk-Szpiganowicz, G.; Marczewska, M.; Barabach, J.; van der Knaap, W.O.; Lamentowicz, M. Palaeoenvironmental changes in Central Europe (NE Poland) during the last 6200 years reconstructed from a high-resolution multi-proxy peat archive. *Holocene* **2015**, *25*, 421–434. [[CrossRef](#)]

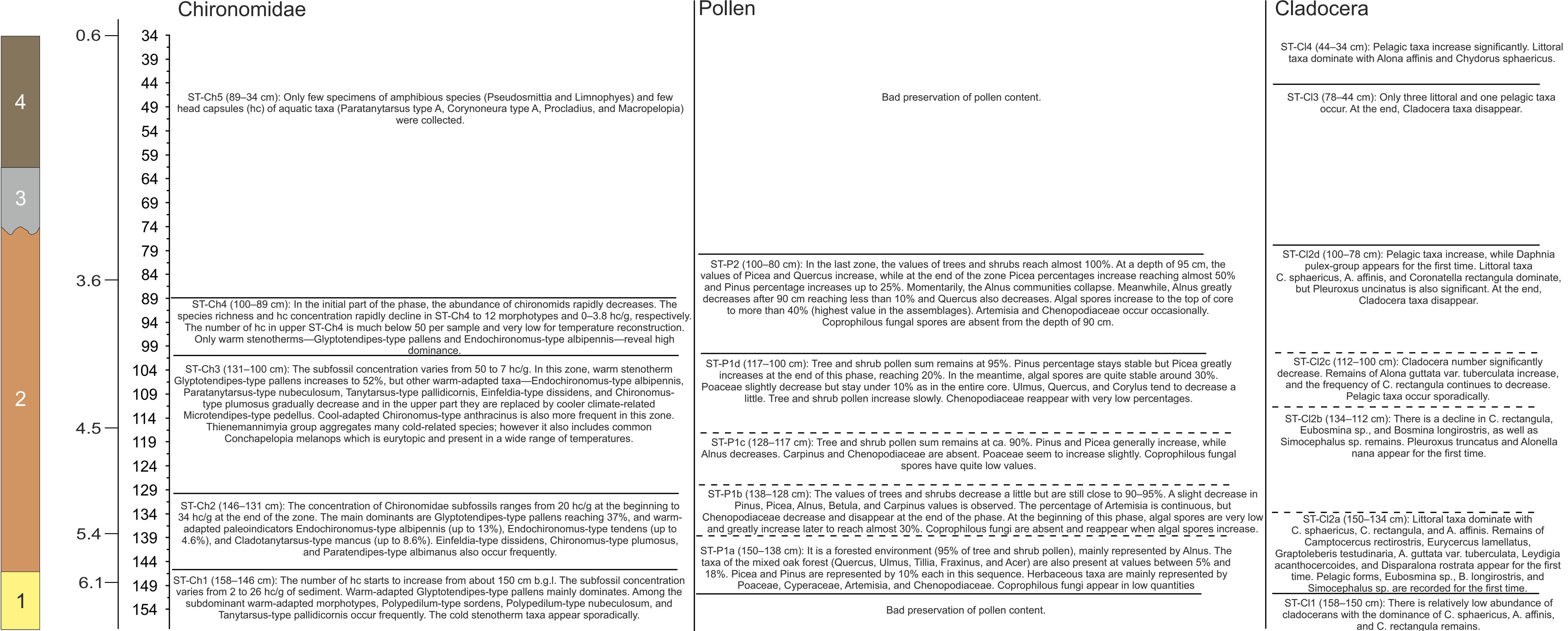
35. Lamentowicz, M.; Lamentowicz, Ł.; van der Knaap, W.O.; Gąbka, M.; Mitchell, E.A.D. Contrasting Species—Environment Relationships in Communities of Testate Amoebae, Bryophytes and Vascular Plants Along the Fen–Bog Gradient. *Microb. Ecol.* **2010**, *59*, 499–510. [[CrossRef](#)] [[PubMed](#)]
36. Heikkilae, M.E.; Seppä, H. Holocene climate dynamics in Latvia, eastern Baltic region: A pollen based summer temperature reconstruction and regional comparison. *Boreas* **2010**, *39*, 705–719. [[CrossRef](#)]
37. Sohar, K.; Kalm, V. A 12.8-ka-long palaeoenvironmental record revealed by subfossil ostracod data from lacustrine freshwater tufa in Lake Sinijärvi, northern Estonia. *J. Paleolimnol.* **2008**, *40*, 809–821. [[CrossRef](#)]
38. Šeiriene, V.; Kabailienė, M.; Kasperovičienė, J.; Mažeika, J.; Petrošius, R.; Paškauskas, R. Reconstruction of postglacial palaeoenvironmental changes in eastern Lithuania: Evidence from lacustrine sediment data. *Quat. Int.* **2009**, *207*, 58–68. [[CrossRef](#)]
39. Stivrins, N.; Kalnina, L.; Veski, S.; Zeimule, S. Local and regional Holocene vegetation dynamics at two sites in eastern Latvia. *Boreal Environ. Res.* **2014**, *19*, 310–322.
40. Terasmaa, J.; Puusepp, L.; Marzecová, A.; Vandel, E.; Vaasma, T.; Koff, T. Natural and human-induced environmental changes in Eastern Europe during the Holocene: A multi-proxy palaeolimnological study of a small Latvian lake in a humid temperate zone. *J. Paleolimnol.* **2013**, *49*, 663–678. [[CrossRef](#)]
41. Syrykh, L.; Subetto, D.; Nazarova, L. Paleolimnological studies on the East European Plain and nearby regions: The PaleoLake Database. *J. Paleolimnol.* **2021**, *65*, 369–375. [[CrossRef](#)]
42. Subetto, D.; Nazarova, L.; Pestryakova, L.; Syrykh, L.; Andronikov, A.; Biskaborn, B.; Diekmann, B.; Kuznetsov, D.; Sapelko, T.; Grekov, I. Paleolimnological studies in Russian northern Eurasia: A review. *Contemp. Probl. Ecol.* **2017**, *10*, 327–335. [[CrossRef](#)]
43. Arslanov, K.A.; Saveljeva, L.; Klimanov, V.; Chernov, S.; Maksimov, F.; Tertychnaya, T.; Subetto, D. New data on chronology of landscape-paleoclimatic stages in Northwestern Russia during the Late Glacial and Holocene. *Radiocarbon* **2001**, *43*, 581–594. [[CrossRef](#)]
44. Novik, A.; Punning, J.-M.; Zernitskaya, V. The development of Belarusian lakes during the Late Glacial and Holocene. *Est. J. Earth Sci.* **2010**, *59*, 63–79. [[CrossRef](#)]
45. Novenko, E.; Glasko, M.; Volkova, E.; Ziuganova, I. Dinamika landšaftov i klimata bassejna verhnego Dona v sredнем i pozdnem goloocene. *Izvestiâ Akademii nauk SSSR. Seria geografičeskâ* **2013**, *2*, 68–82.
46. Arslanov, K.A.; Saveljeva, L.; Gey, N.; Klimanov, V.; Chernov, S.; Chernova, G.; Kuzmin, G.; Tertychnaya, T.; Subetto, D.; Denisenkov, V. Chronology of vegetation and paleoclimatic stages of northwestern Russia during the Late Glacial and Holocene. *Radiocarbon* **1999**, *41*, 25–45. [[CrossRef](#)]
47. Nazarova, L.; Herzschuh, U.; Wetterich, S.; Pestryakova, L. Chironomid-based inference models for estimating mean July air temperature and water depth from lakes in Yakutia, northeastern Russia. *J. Paleolimnol.* **2011**, *45*, 57–71. [[CrossRef](#)]
48. Nazarova, T.; Fomin, I.; Dmitriev, P.; Wendt, J.; Janaleyeva, K. Landscape and limnological research of lake systems of the northeastern borderlands of the Republic of Kazakhstan and assesment of their recreational capacity. *Geoj. Tour. Geosites* **2019**, *25*, 485–495. [[CrossRef](#)]
49. Druzhinina, O.; Kublitskiy, Y.; Stančikaitė, M.; Nazarova, L.; Syrykh, L.; Gedminiene, L.; Uogintas, D.; Skipityte, R.; Arslanov, K.; Vaikutiene, G. The Late Pleistocene–Early Holocene palaeoenvironmental evolution in the SE Baltic region: A new approach based on chironomid, geochemical and isotopic data from Kamyshovoye Lake, Russia. *Boreas* **2020**, *49*, 544–561. [[CrossRef](#)]
50. Nazarova, L.B.; Sapelko, T.V.; Kuznetsov, D.D.; Syrykh, L.S. Palaeoecological and Palaeoclimatical Reconstructions of Holocene According Chironomid Analysis of Lake Glubokoye Sediments. In *Doklady Biological Sciences: Proceedings of the Academy of Sciences of the USSR, Biological Sciences Sections; Pleiades Publishing*: New York, NY, USA, 2015; Volume 460, pp. 57–60. [[CrossRef](#)]
51. Rinterknecht, V.; Hang, T.; Gorlach, A.; Kohv, M.; Kalla, K.; Kalm, V.; Subetto, D.; Bourlès, D.; Léanni, L.; Guillou, V. The Last Glacial Maximum extent of the Scandinavian Ice Sheet in the Valday Heights, western Russia: Evidence from cosmogenic surface exposure dating using ^{10}Be . *Quat. Sci. Rev.* **2018**, *200*, 106–113. [[CrossRef](#)]
52. Mazurkevich, A.; Dolbunova, E.; Kittel, P.; Fassbender, J.; Maigrot, Y.; Mroczkowska, A.; Płociennik, M.; Sikora, J.; Ślowiński, M.; Sablin, M. *Multi-Disciplinary Research on the Neolithic Pile-Dwelling Serteya II Site (Western Russia) and the Landscape Reconstruction. Nie tylko Krzemienie. Not only flints.*; Instytut Archeologii Uniwersytetu Łódzkiego, Łódzka Fundacja Badań Naukowych, Stowarzyszenie Naukowe Archeologów Polskich Oddział w Łodzi: Łódź, Poland, 2017; pp. 103–128.
53. Mazurkevich, A.; Kulkova, M.; Savel'eva, L. Geoarchaeology of the Serteya Microregion, the Upper Dvina Basin. In *Geoarchaeological Issues of the Upper Dnieper–Western Dvina River Region (Western Russia)*; Universum: Moscow-Smolensk, Russia, 2012; pp. 49–104.
54. Mazurkevich, A.N.; Arslanov, K.A.; Savel'eva, L.A.; Kulkova, M.A.; Zaitseva, G.I. Mesolithic and Neolithic in the Western Dvina–Lovat Area. In *The East European Plain on the Eve of Agriculture*; BAR International Series; Archaeopress: Oxford, UK, 2009; Volume 164, pp. 145–153.
55. Kulkova, M.; Mazurkevich, A.; Dolbunova, E.; Regert, M.; Mazuy, A.; Nesterov, E.; Sinai, M. Late Neolithic Subsistence Strategy and Reservoir Effects in ^{14}C Dating of Artifacts at the Pile-Dwelling Site Serteya II (NW Russia). *Radiocarbon* **2015**, *57*, 611–623. [[CrossRef](#)]
56. Mazurkevich, A.N.; Korotkevich, B.N.; Dolukhanov, P.M.; Shukurov, A.M.; Arslanov, K.A.; Savel'eva, L.A.; Dzinoridze, E.N.; Kulkova, M.A.; Zaitseva, G.I. Climate, subsistence and human movements in the Western Dvina–Lovat River Basins. *Quaternary International*. *Quat. Int.* **2009**, *203*, 52–66. [[CrossRef](#)]

57. Kittel, P.; Mazurkevich, A.; Wieckowska-Lüth, M.; Pawłowski, D.; Dolbunova, E.; Płociennik, M.; Gauthier, E.; Krapiec, M.; Maigrot, Y.; Danger, M. On the border between land and water: The environmental conditions of the Neolithic occupation from 4.3 until 1.6 ka BC at Serteya, Western Russia. *Geoarchaeology* **2021**, *36*, 173–202. [[CrossRef](#)]
58. Kulkova, M.; Mazurkevich, A.; Dolukhanov, P. Chronology and paleoclimate of prehistoric sites in Western Dvina-Lovat area of North-western Russia. *Geochronometria: J. Methods Appl. Absol. Chronol.* **2001**, *20*, 87–94.
59. Mazurkevich, A.; Dolbunova, E.; Kul'kova, M.; Alexandrovskiy, A.; Saveleva, L.; Polkovnikova, M.; Khrustaleva, I.; Kolosova, M.; Hook, D.; Mazurkevich, K. Dynamics of landscape developing in early-middle Neolithics in Dnepr-Dvina region. In *Proceedings of the International Conference “Geomorphic Processes and Geoarchaeology: From Landscape Archaeology to Archaeotourism”*; Universum: Moscow-Smolensk, Russia, 2012; pp. 20–24.
60. Mazurkevich, A.N.; Hook, D.Y.; Fassbinder, J. Magnetometry and susceptibility prospecting on Neolithic-early Iron Age sites at Serteya, North-West Russia. *ArcheoSciences Revue D’archéométrie* **2009**, *33*, 81–85. [[CrossRef](#)]
61. Mazurkevich, A.N. Pervyye svидетельства проявления производящего khozyaystva na Severo-Zapade Rossii. In *Pushkarevskiy sbornik II*; Izd-vo S-Peterburgskogo un-ta: Sankt Petersburg, Russia, 2003; pp. 77–84.
62. Tarasov, P.E.; Savelieva, L.A.; Long, T.; Leipe, C. Postglacial vegetation and climate history and traces of early human impact and agriculture in the present-day cool mixed forest zone of European Russia. *Quat. Int.* **2019**, *516*, 21–41. [[CrossRef](#)]
63. Bond, G.; Kromer, B.; Beer, J.; Muscheler, R.; Evans, M.N.; Showers, W.; Hoffmann, S.; Lotti-Bond, R.; Hajdas, I.; Bonani, G. Persistent solar influence on North Atlantic climate during the Holocene. *Science* **2001**, *294*, 2130–2136. [[CrossRef](#)]
64. Obrochta, S.P.; Miyahara, H.; Yokoyama, Y.; Crowley, T.J. A re-examination of evidence for the North Atlantic “1500-year cycle” at Site 609. *Quat. Sci. Rev.* **2012**, *55*, 23–33. [[CrossRef](#)]
65. Bütkofer, J. Millennial Scale Climate Variability during the Last 6000 Years—Tracking down the Bond Cycles. Verlag nicht ermittelbar. 2007.
66. Solanki, S.; Usoskin, I.; Kromer, B.; Schüssler, M.; Beer, J. How unusual is today’s solar activity?(reply). *Nature* **2005**, *436*, E4–E5. [[CrossRef](#)]
67. Wang, W.; Feng, Z.; Ran, M.; Zhang, C. Holocene climate and vegetation changes inferred from pollen records of Lake Aibi, northern Xinjiang, China: A potential contribution to understanding of Holocene climate pattern in East-central Asia. *Quat. Int.* **2013**, *311*, 54–62. [[CrossRef](#)]
68. Mayewski, P.A.; Rohling, E.E.; Stager, J.C.; Karlén, W.; Maasch, K.A.; Meeker, L.D.; Meyerson, E.A.; Gasse, F.; van Kreveld, S.; Holmgren, K. Holocene climate variability. *Quat. Res.* **2004**, *62*, 243–255. [[CrossRef](#)]
69. Newman, M.; Alexander, M.A.; Ault, T.R.; Cobb, K.M.; Deser, C.; Di Lorenzo, E.; Mantua, N.J.; Miller, A.J.; Minobe, S.; Nakamura, H. The Pacific decadal oscillation, revisited. *J. Clim.* **2016**, *29*, 4399–4427. [[CrossRef](#)]
70. Trigo, R.M.; Osborn, T.J.; Corte-Real, J.M. The North Atlantic Oscillation influence on Europe: Climate impacts and associated physical mechanisms. *Clim. Res.* **2002**, *20*, 9–17. [[CrossRef](#)]
71. Visbeck, M.H.; Hurrell, J.W.; Polvani, L.; Cullen, H.M. The North Atlantic Oscillation: Past, present, and future. *Proc. Natl. Acad. Sci. USA* **2001**, *98*, 12876–12877. [[CrossRef](#)]
72. Cronin, T.; Hayo, K.; Thunell, R.; Dwyer, G.; Saenger, C.; Willard, D. The medieval climate anomaly and little ice age in Chesapeake Bay and the North Atlantic Ocean. *Palaeogeogr. Palaeoclimatol. Palaeoecol.* **2010**, *297*, 299–310. [[CrossRef](#)]
73. Wanner, H.; Beer, J.; Bütkofer, J.; Crowley, T.J.; Cubasch, U.; Flückiger, J.; Goosse, H.; Grosjean, M.; Joos, F.; Kaplan, J.O.; et al. Mid- to Late Holocene climate change: An overview. *Quat. Sci. Rev.* **2008**, *27*, 1791–1828. [[CrossRef](#)]
74. Seidov, D.; Maslin, M. North Atlantic deep water circulation collapse during Heinrich events. *Geology* **1999**, *27*, 23–26. [[CrossRef](#)]
75. Jennings, A.E.; Grönvold, K.; Hilberman, R.; Smith, M.; Hald, M. High-resolution study of Icelandic tephras in the Kangerlussuaq Trough, southeast Greenland, during the last deglaciation. *J. Quat. Sci. Publ. Quat. Res. Assoc.* **2002**, *17*, 747–757. [[CrossRef](#)]
76. Peyron, O.; Combourieu-Nebout, N.; Brayshaw, D.; Goring, S.; Andrieu-Ponel, V.; Desprat, S.; Fletcher, W.; Gambin, B.; Ioakim, C.; Joannin, S. Precipitation changes in the Mediterranean basin during the Holocene from terrestrial and marine pollen records: A model-data comparison. *Clim. Past* **2017**, *13*, 249–265. [[CrossRef](#)]
77. Kulkova, M.; Chadov, F.; Davidochkina, A. Radiocarbon in vegetation of coastal zone of Finnish Bay (Russia). *Procedia Environ. Sci.* **2011**, *8*, 375–381. [[CrossRef](#)]
78. Abramov, L. *Opisaniya Prirody Nashey Strany: Razvitiye Fiziko-Geograficheskikh Kharakteristik*; Akademiya nauk SSSR, Institut Geografii: Moskva, Russia, 1972.
79. Kondracki, J. Fizycznogeograficzna regionalizacja republik Litewskiej i Białoruskiej w układzie dziesiętnym. *Przegląd Geograficzny* **1992**, *64*, 341–346.
80. Kobyshevoy, N.V. The Climate of Russia [Klimat Rossii], Habil. (geography). *Gidrometeoizdat* **2001**, 655.
81. El tiempo. Available online: <http://www.tutiempo.net> (accessed on 9 December 2019).
82. Arslanov, K.A.; Savel'eva, L.; Dzinoridze, E.; Mazurkevich, A.; Dolukhanov, P. *The Holocene Environments in North-Western and Central Russia; The East European Plain on the Eve of Agriculture*. BAR International Series 1964; Dolukhanov, P.M., Sarson, G.R., Shukorov, A.M., Eds.; Archaeopress: Oxford, UK, 2009; pp. 109–121.
83. Velichko, A.A.; Faustova, M.A.; Pisareva, V.V.; Gribchenko, Y.N.; Sudakova, N.G.; Lavrentiev, N.V. Chapter 26—Glaciations of the East European Plain: Distribution and Chronology. In *Developments in Quaternary Sciences*; Ehlers, J., Gibbard, P.L., Hughes, P.D., Eds.; Elsevier: Amsterdam, The Netherlands, 2011; Volume 15, pp. 337–359.

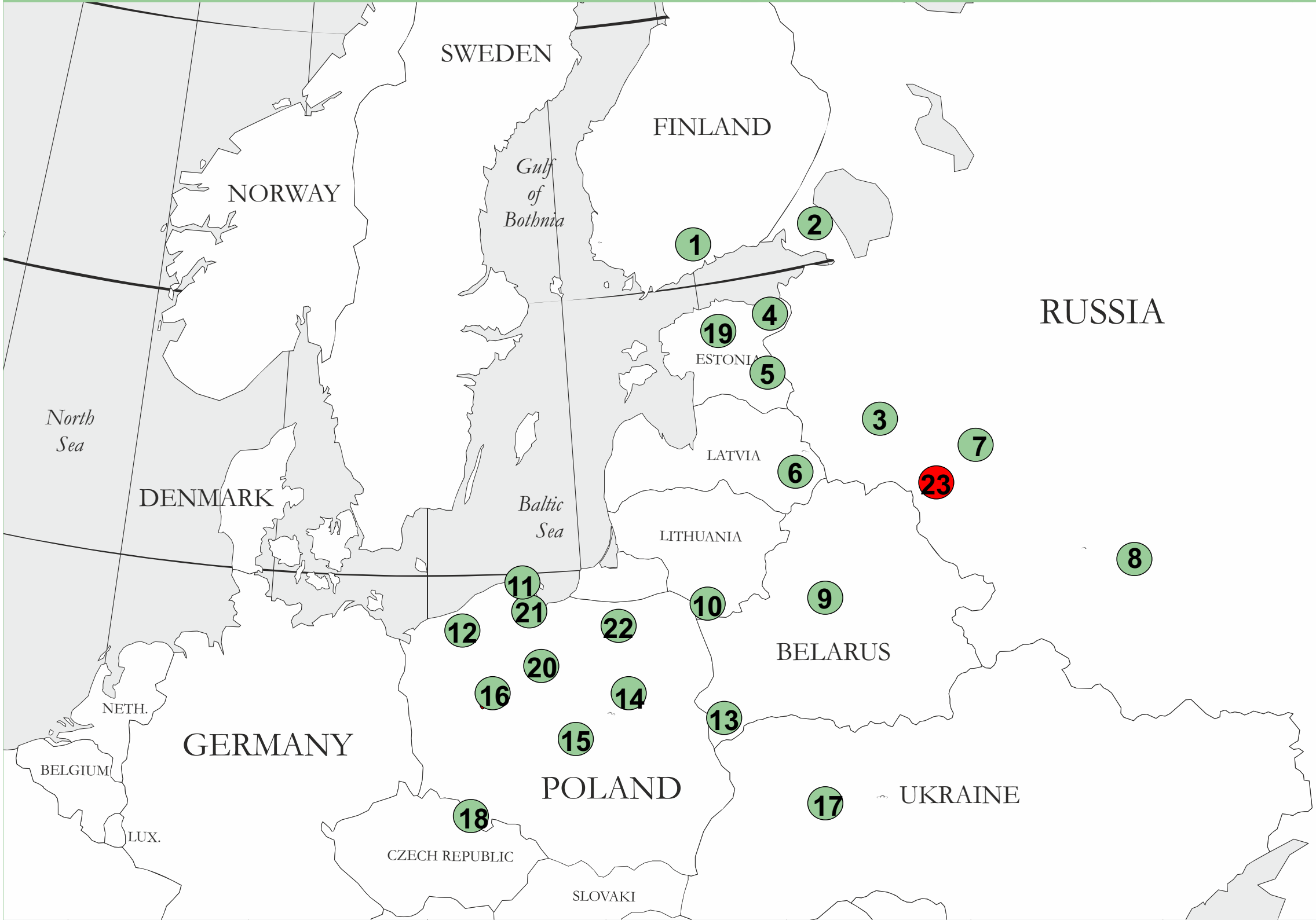
84. Piech, W.; Kittel, P.; Mazurkevich, A.; Pavlovskaia, E.; Kazakov, E.; Teltevskaia, Y.; Błaszczyk, K.; Kotrys, B. Cechy sedymentologiczne i warunki depozycji osadów stożka akumulacyjnego w dolinie rzeki Sertejki (zachodnia Rosja). *Acta Geogr. Lodz.* **2018**, *107*, 215–238.
85. Kittel, P.; Mazurkevich, A.; Dolbunova, E.V.; Kazakov, E.; Mroczkowska, A.; Pavlovskaia, E.; Piech, W.; Płociennik, M.; Sikora, J.; Teltevskaia, Y.; et al. Palaeoenvironmental reconstructions for the Neolithic pile-dwelling Serteya II site case study, Western Russia. *Acta Geogr. Lodz.* **2018**, *107*, 191–213.
86. Błaszkiewicz, M. Wytapianie się pogrzebanych brył martwego lodu w późnym glaciale i wczesnym holocenie a zdarzenia ekstremalne. *Landf. Anal.* **2008**, *8*, 9–12.
87. Błaszkiewicz, M. *Późnoglacialna i Wczesnoholocenecka Ewolucja Obniżeń Jeziornych na Pojezierzu Kociewskim (wschodnia część Pomorza)*; IGiPZ PAN: Warszawa, Poland, 2005; Volume 201.
88. Łuców, D.; Lamentowicz, M.; Obremska, M.; Arkhipova, M.; Kittel, P.; Łokas, E.; Mazurkevich, A.; Mróz, T.; Tjallingii, R.; Słowiński, M. Disturbance and resilience of a Sphagnum peatland in western Russia (Western Dvina Lakeland) during the last 300 years: A multiproxy, high-resolution study. *Holocene* **2020**, *30*, 1552–1566. [[CrossRef](#)]
89. Mazurkevich, A.; Kittel, P.; Maigrot, Y.; Dolbunova, E.; Mroczkowska, A.; Wieckowska-Lüth, M.; Piech, W. Natural and anthropogenic impact on the formation of archaeological layers in a lake shore area: Case study from the Serteya II site, Western Russia. *Acta Geogr. Lodz.* **2020**, *110*, 81–102.
90. Mazurkevich, A.; Sablin, M.V.; Dolbunova, E.V.; Kittel, P.; Maigrot, Y.; Kazakov, E. Landscape, Seasonality and Natural Resources Use in the 3rd Millennium BC by Pile-Dwelling Communities (NW Russia). In *Settling Waterscapes in Europe: The Archaeology of Neolithic and Bronze Age Pile-Dwellings*; Hafner, A.E.D., Mazurkevich, A., Pranckenaite, E., Hinz, M., Eds.; OSPA—Open Series in Prehistoric Archaeology, Band 1; Propylaeum: Heidelberg, Germany, 2020; pp. 17–35.
91. Ramsey, C.B. Bayesian analysis of radiocarbon dates. *Radiocarbon* **2009**, *51*, 337–360. [[CrossRef](#)]
92. Ramsey, C.B. Deposition models for chronological records. *Quat. Sci. Rev.* **2008**, *27*, 42–60. [[CrossRef](#)]
93. Andersen, T.; Cranston, P.; Epler, J. *Chironomidae of the Holarctic Region: Keys and Diagnoses: Larvae*; Scandinavian Society of Entomology, Entomological Society of Lund: Lund, Sweden, 2013.
94. Birks, H. Late-Quaternary biotic changes in terrestrial and lacustrine environments, with particular reference to north-west Europe. *Handb. Holocene Palaeoecol. Palaeohydrology* **1986**, *3*, 65.
95. Birks, H.J.B.; Gordon, A.D. *Numerical Methods in Quaternary Pollen Analysis*; Academic Press: Orlando, FL, USA, 1985.
96. Bennett, K.D. Determination of the number of zones in a biostratigraphical sequence. *New Phytol.* **1996**, *132*, 155–170. [[CrossRef](#)]
97. MacArthur, R.H. On the relative abundance of bird species. *Proc. Natl. Acad. Sci. USA* **1957**, *43*, 293. [[CrossRef](#)]
98. Lotter, A.; Juggins, S. POLPROF, TRAN and ZONE: Programs for Plotting, Editing and Zoning Pollen and Diatom Data. INQUA-Subcommission for the Study of the Holocene Working Group on Data-Handling Methods, Newsletter. 1991; Volume 6, pp. 4–6.
99. Line, J.; Birks, H. BSTICK Version 1.0; Unpublished Computer Program; Botanical Institute, University of Bergen: Bergen, Norway, 1996.
100. Juggins, S. C2 Version 1.5.0: A Program for Plotting and Visualising Stratigraphic Data; University of Newcastle: Newcastle upon Tyne, UK, 2007.
101. Frey, D. Cladocera Analysis. In *Handbook of Holocene Palaeoecology and Palaeohydrology*; Berglund, B.E., Ed.; Wiley: Chichester, UK, 1986.
102. Szeroczyńska, K.; Sarmaja-Korjonen, K. *Atlas of Subfossil Cladocera from Central and Northern Europe*; Friends of Lower Vistula Society: Świecie, Poland, 2007; pp. 1–87.
103. Van Damme, K.; Kotov, A.A.; Dumont, H.J. A checklist of names in Alona Baird 1843 (Crustacea: Cladocera: Chydoridae) and their current status: An analysis of the taxonomy of a lump genus. *Zootaxa* **2010**, *2330*, 1–63. [[CrossRef](#)]
104. Bjerring, R.; Becares, E.; Declerck, S.; Gross, E.M.; Hansson, L.-A.; Kairesalo, T.; Nykanen, M.; Halkiewicz, A.; Kornijów, R.; Conde-Porcuna, J.M.; et al. Subfossil Cladocera in relation to contemporary environmental variables in 54 Pan-European lakes. *Freshw. Biol.* **2009**, *54*, 2401–2417. [[CrossRef](#)]
105. Walanus, A.; Nalepka, D. Program for counting pollen grains, diagrams plotting and numerical analysis. *Trees* **1999**, *9*, 3.
106. Faegri, K.; Iversen, J. Finding the grain: Laboratory Techniques. *Textbook of Pollen Analysis*. 1989; pp. 69–89.
107. Svobodová, H. M. Reille: Pollen et spores d'europe et d'afrique du nord. *Folia Geobot.* **1997**, *32*, 24. [[CrossRef](#)]
108. Van Geel, B. Non-pollen palynomorphs. In *Tracking environmental change using lake sediments*; Springer: Berlin/Heidelberg, Germany, 2002; pp. 99–119.
109. Van Geel, B.; Aptroot, A. Fossil ascomycetes in Quaternary deposits. *Nova Hedwig.* **2006**, *82*, 313–330. [[CrossRef](#)]
110. Beug, H. 2004: *Leitfaden der Pollenbestimmung für Mitteleuropa und angrenzende Gebiete*; Verlag Dr. Friedrich Pfeil.: München, Germany, 2004.
111. Grimm, E. *Tilia Software v. 1.7.16*; Illinois State Museum: Springfield, IL, USA, 2011.
112. Grimm, E. *Tilia software 2.0.2.*; Illinois State Museum Research and Collection Center: Springfield, IL, USA, 2004.
113. Blackford, J.; Innes, J. Linking current environments and processes to fungal spore assemblages: Surface NPM data from woodland environments. *Rev. Palaeobot. Palynol.* **2006**, *141*, 179–187. [[CrossRef](#)]
114. Luoto, T.P.; Nevalainen, L. Quantifying climate changes of the Common Era for Finland. *Clim. Dyn.* **2017**, *49*, 2557–2567. [[CrossRef](#)]

115. Luoto, T.P.; Nevalainen, L.; Kultti, S.; Sarmaja-Korjonen, K. An evaluation of the influence of water depth and river inflow on quantitative Cladocera-based temperature and lake level inferences in a shallow boreal lake. *Hydrobiologia* **2011**, *676*, 143–154. [[CrossRef](#)]
116. Guiot, J. Methodology of the last climatic cycle reconstruction in France from pollen data. *Palaeogeogr. Palaeoclimatol. Palaeoecol.* **1990**, *80*, 49–69. [[CrossRef](#)]
117. Marsicek, J.; Shuman, B.N.; Bartlein, P.J.; Shafer, S.L.; Brewer, S. Reconciling divergent trends and millennial variations in Holocene temperatures. *Nature* **2018**, *554*, 92–96. [[CrossRef](#)] [[PubMed](#)]
118. Mauri, A.; Davis, B.; Collins, P.; Kaplan, J. The climate of Europe during the Holocene: A gridded pollen-based reconstruction and its multi-proxy evaluation. *Quat. Sci. Rev.* **2015**, *112*, 109–127. [[CrossRef](#)]
119. Martin, C.; Menot, G.; Thouveny, N.; Peyron, O.; Andrieu-Ponel, V.; Montade, V.; Davtian, N.; Reille, M.; Bard, E. Early Holocene Thermal Maximum recorded by branched tetraethers and pollen in Western Europe (Massif Central, France). *Quat. Sci. Rev.* **2020**, *228*, 106109. [[CrossRef](#)]
120. Peyron, O.; Magny, M.; Goring, S.; Joannin, S.; de Beaulieu, J.-L.; Bruggiapaglia, E.; Saduri, L.; Garfi, G.; Kouli, K.; Ioakim, C. Contrasting patterns of climatic changes during the Holocene across the Italian Peninsula reconstructed from pollen data. *Clim. Past* **2013**, *9*, 1233–1252. [[CrossRef](#)]
121. Juggins, S. Rioja: Analysis of Quaternary Science Data: R package versión (0.9–21). 2017.
122. Ter Braak, C.J.; Šmilauer, P. *CANOCO Reference Manual and CanoDraw for Windows User's Guide*; Software for Canonical Community Ordination (Version 4.5); Microcomputer Power: Ithaca, NY, USA, 2002; p. 500.
123. Malmgren, B.A.; Nordlund, U. Application of artificial neural networks to paleoceanographic data. *laoeogeogr. Palaeoclimatol. Palaeoecol.* **1997**, *136*, 359–373. [[CrossRef](#)]
124. Grimm, E.C. CONISS: A FORTRAN 77 program for stratigraphically constrained cluster analysis by the method of incremental sum of squares. *Comput. Geosci.* **1987**, *13*, 13–35. [[CrossRef](#)]
125. Alpat'ev, A.M.; Arkhangel'skiy, A.M.; Podoplelov, N.Y.; Stepanov, A.Y. *Fizicheskaya Geografiya SSSR (Aziatskaya Chast')*; Vysshaya shkola: Moskva, Russia, 1976; Volume 2, p. 360.
126. Kaufman, D.; McKay, N.; Routson, C.; Erb, M.; Dätwyler, C.; Sommer, P.S.; Heiri, O.; Davis, B. Holocene global mean surface temperature, a multi-method reconstruction approach. *Sci. Data* **2020**, *7*, 201. [[CrossRef](#)] [[PubMed](#)]
127. Levitan, M.; Lavrushin, Y.A. The Late Glacial Time and Holocene of Northern Eurasia. In *Sedimentation History in the Arctic Ocean and Subarctic Seas for the Last 130 kyr*; Springer: Berlin/Heidelberg, Germany, 2009; pp. 43–45.
128. Renssen, H.; Seppä, H.; Heiri, O.; Roche, D.; Goosse, H.; Fichefet, T. The spatial and temporal complexity of the Holocene thermal maximum. *Nat. Geosci.* **2009**, *2*, 411–414. [[CrossRef](#)]
129. Juggins, S. Quantitative reconstructions in palaeolimnology: New paradigm or sick science? *Quat. Sci. Rev.* **2013**, *64*, 20–32. [[CrossRef](#)]
130. Yao, Y.; Luo, D. Do European blocking events precede North Atlantic Oscillation events? *Adv. Atmos. Sci.* **2015**, *32*, 1106–1118. [[CrossRef](#)]
131. Rousi, E.; Rust, H.W.; Ulbrich, U.; Anagnostopoulou, C. Implications of winter NAO flavors on present and future European climate. *Climate* **2020**, *8*, 13. [[CrossRef](#)]
132. Beck, C.; Philipp, A.; Streicher, F. The effect of domain size on the relationship between circulation type classifications and surface climate. *Int. J. Climatol.* **2016**, *36*, 2692–2709. [[CrossRef](#)]
133. Trouet, V.; Esper, J.; Graham, N.E.; Baker, A.; Scourse, J.D.; Frank, D.C. Persistent Positive North Atlantic Oscillation Mode Dominated the Medieval Climate Anomaly. *Science* **2009**, *324*, 78–80. [[CrossRef](#)] [[PubMed](#)]
134. Mann, M.E.; Zhang, Z.; Rutherford, S.; Bradley, R.S.; Hughes, M.K.; Shindell, D.; Ammann, C.; Faluvegi, G.; Ni, F. Global Signatures and Dynamical Origins of the Little Ice Age and Medieval Climate Anomaly. *Science* **2009**, *326*, 1256–1260. [[CrossRef](#)] [[PubMed](#)]
135. Ortega, P.; Lehner, F.; Swingedouw, D.; Masson-Delmotte, V.; Raible, C.C.; Casado, M.; Yiou, P. A model-tested North Atlantic Oscillation reconstruction for the past millennium. *Nature* **2015**, *523*, 71–74. [[CrossRef](#)]
136. Moreno-Chamarro, E.; Zanchettin, D.; Lohmann, K.; Luterbacher, J.; Jungclaus, J.H. Winter amplification of the European Little Ice Age cooling by the subpolar gyre. *Sci. Rep.* **2017**, *7*, 9981. [[CrossRef](#)]
137. Pleskot, K.; Apolinarska, K.; Kołaczek, P.; Suchora, M.; Fojutowski, M.; Joniak, T.; Kotrys, B.; Kramkowski, M.; Słowiński, M.; Woźniak, M. Searching for the 4.2 ka climate event at Lake Spore, Poland. *Catena* **2020**, *191*, 104565. [[CrossRef](#)]
138. Novenko, E.Y.; Eremeeva, A.P.; Chepurnaya, A.A. Reconstruction of Holocene vegetation, tree cover dynamics and human disturbances in central European Russia, using pollen and satellite data sets. *Veg. Hist. Archaeobotany* **2014**, *23*, 109–119. [[CrossRef](#)]
139. Novenko, E.Y.; Tsyganov, A.N.; Pisarchuk, N.M.; Volkova, E.M.; Babeshko, K.V.; Kozlov, D.N.; Shilov, P.M.; Payne, R.J.; Mazei, Y.A.; Olchev, A.V. Forest history, peatland development and mid-to late Holocene environmental change in the southern taiga forest of central European Russia. *Quat. Res.* **2018**, *89*, 223–236. [[CrossRef](#)]
140. Lotter, A.F.; Birks, H.J.B.; Hofmann, W.; Marchetto, A. Modern diatom, cladocera, chironomid, and chrysophyte cyst assemblages as quantitative indicators for the reconstruction of past environmental conditions in the Alps. II. Nutrients. *J. Paleolimnol.* **1998**, *19*, 443–463. [[CrossRef](#)]
141. Brodersen, K.P.; Quinlan, R. Midges as palaeoindicators of lake productivity, eutrophication and hypolimnetic oxygen. *Quat. Sci. Rev.* **2006**, *25*, 1995–2012. [[CrossRef](#)]

142. Chevalier, M.; Davis, B.A.; Heiri, O.; Seppä, H.; Chase, B.M.; Gajewski, K.; Lacourse, T.; Telford, R.J.; Finsinger, W.; Guiot, J. Pollen-based climate reconstruction techniques for late Quaternary studies. *Earth Sci. Rev.* **2020**, *210*, 103384. [[CrossRef](#)]
143. Telford, R.J. Review and test of reproducibility of subdecadal resolution palaeoenvironmental reconstructions from microfossil assemblages. *Quat. Sci. Rev.* **2019**, *222*, 105893. [[CrossRef](#)]
144. Brooks, S.J. Fossil midges (Diptera: Chironomidae) as palaeoclimatic indicators for the Eurasian region. *Quat. Sci. Rev.* **2006**, *25*, 1894–1910. [[CrossRef](#)]
145. Flössner, D. Krebstiere, Crustacea. Kiemen-und Blattfüßer, Branchiopoda Fischläuse, Branchiura. Die Tierwelt Deutschlands 60. Teil. Jena **1972**.
146. Luoto, T.P.; Kultti, S.; Nevalainen, L.; Sarmaja-Korjonen, K. Temperature and effective moisture variability in southern Finland during the Holocene quantified with midge-based calibration models. *J. Quat. Sci.* **2010**, *25*, 1317–1326. [[CrossRef](#)]
147. Nosova, M.B.; Novenko, E.Y.; Severova, E.E.; Volkova, O.A. Vegetation and climate changes within and around the Polistovo-Lovatskaya mire system (Pskov Oblast, north-western Russia) during the past 10,500 years. *Veg. Hist. Archaeobotany* **2019**, *28*, 123–140. [[CrossRef](#)]
148. Koff, T. *Pollen Profile LIIVJARV*; Liivjarve Bog: Estonia, 2010. [[CrossRef](#)]
149. Pirrus, R.; Rouk, A.; Liiva, A. Geology and stratigraphy of the reference site of Lake Raigastvere in Saadjärv drumlin field. *Palaeohydrology Temp. Zone II. Lakes* **1987**, *101–122*.
150. Novenko, E.Y.; Tsyanov, A.N.; Volkova, E.M.; Babeshko, K.V.; Lavrentiev, N.V.; Payne, R.J.; Mazei, Y.A. The Holocene paleoenvironmental history of central European Russia reconstructed from pollen, plant macrofossil, and testate amoeba analyses of the Klukva Peatland, Tula Region. *Quat. Res.* **2015**, *83*, 459–468. [[CrossRef](#)]
151. Elovicheva, Y. *Novye razrezy golotsena Belarusii* (New Holocene sections in Byelorussia). Geologicheskoe stroenie osadochnoi tolshchi Belorusii (Geological composition of sedimentary sequence of Byelorussia). 1985; pp. 141–169.
152. Shulija, K.; Lujanas, V.; Kibilda, Z.; Banys, J.; Genutiene, I. Stratigraphy and chronology of lacustrine and bog deposits of the Bebrukas Lake hollow. *Tr. Instituta Geol. Vilnius* **5**. *1967*.
153. Ralska-Jasiewiczowa, M.; Latalowa, M. Poland. Palaeoecological events during the last 15,000 years: Regional syntheses of palaeoecological studies of lakes and mires in Europe. 1996.
154. Yelovich, Y. Pleistocene nature events of the Central and Middle-East Europe for the comprehension of their development in the future (by palynological data). Quaternary stratigraphy and paleontology of the southern russia: Connections between Europe, Africa and Asia. 2010; p. 198.
155. Binka, K.; Madeyska, T.; Marcińska, B.; Seroczynska, K.; Wieckowski, K. Bledowo Lake (central Poland): History of vegetation and lake development during the last 12 kyr. *Bull. Acad. Pol. Sci.* **1988**, *36*, 147–158.
156. Noryśkiewicz, B. Zmiany szaty roślinnej okolic Jeziora Biskupińskiego pod wpływem czynników naturalnych i antropogenicznych w późnym glacjale i holocenie. In *Zarys zmian środowiska geograficznego okolic Biskupina pod wpływem czynników naturalnych i antropogenicznych w późnym glacjale i holocenie*; Turpress: Toruń, Poland, 1995; pp. 147–179.
157. Bezusko, L. History of vegetation of the north western part of Small Polesye in Holocene. *Ukr. Bot. J.* **1977**, *3*, 294–298.
158. Peichlová, M. *Historie vegetace Broumovska. [Vegetation history of the Broumovsko Region]*; Ms. Cand. diss.; Academy of Science CR: Pruhonice, Czech Republic, 1979.
159. Sillasoo, U.; Mauquoy, D.; Blundell, A.; Charman, D.; Blaauw, M.; Daniell, J.R.; Toms, P.; Newberry, J.; Chambers, F.M.; Karofeld, E. Peat multi-proxy data from Männikjärve bog as indicators of late Holocene climate changes in Estonia. *Boreas* **2007**, *36*, 20–37. [[CrossRef](#)]
160. Lamentowicz, M.; Kołaczek, P.; Mauquoy, D.; Kittel, P.; Łokas, E.; Słowiński, M.; Jassey, V.E.J.; Niedziółka, K.; Kajukało-Drygalska, K.; Marcisz, K. Always on the tipping point—A search for signals of past societies and related peatland ecosystem critical transitions during the last 6500 years in N Poland. *Quat. Sci. Rev.* **2019**, *225*, 105954. [[CrossRef](#)]

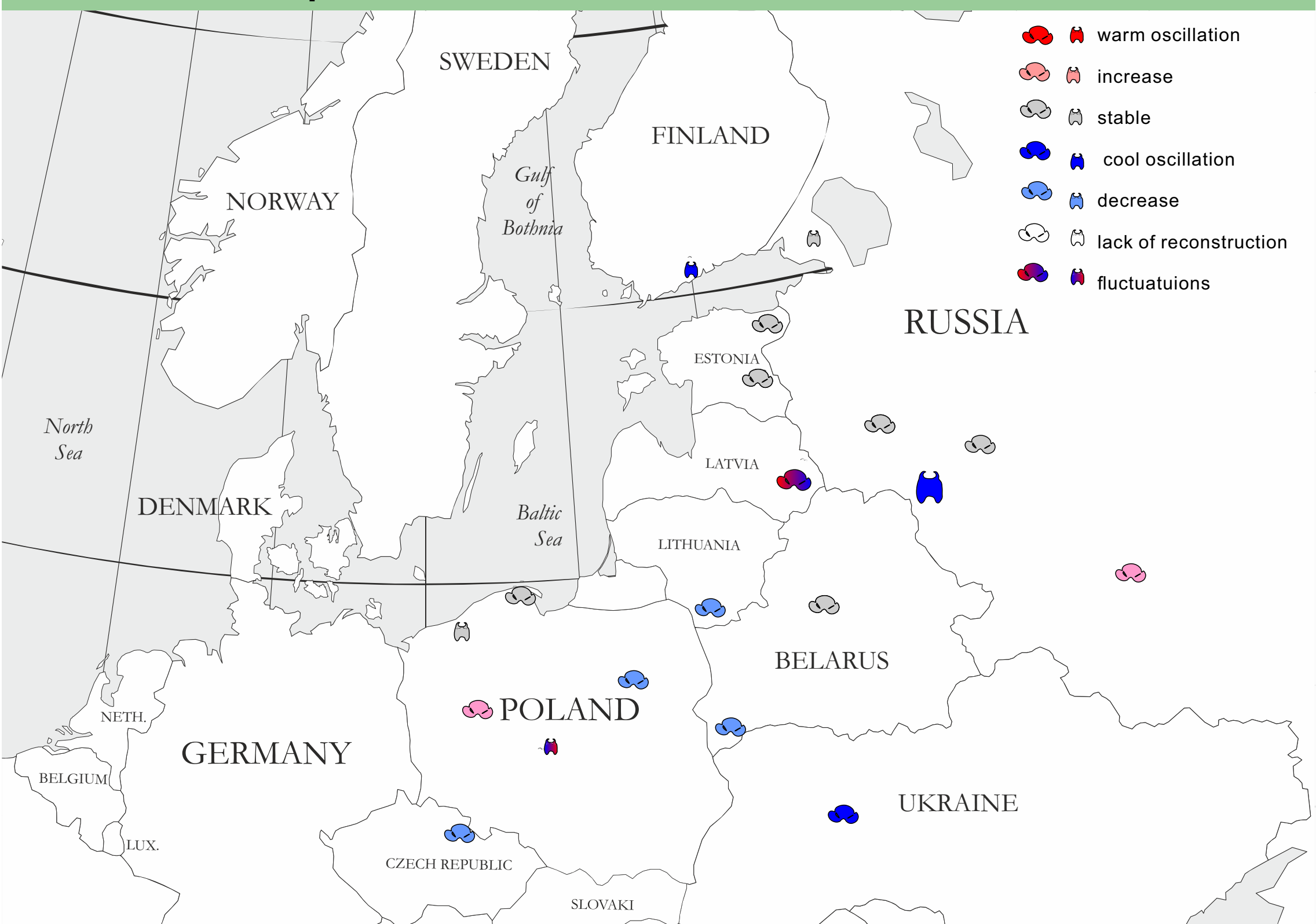


Map of sites mentioned in Table S1

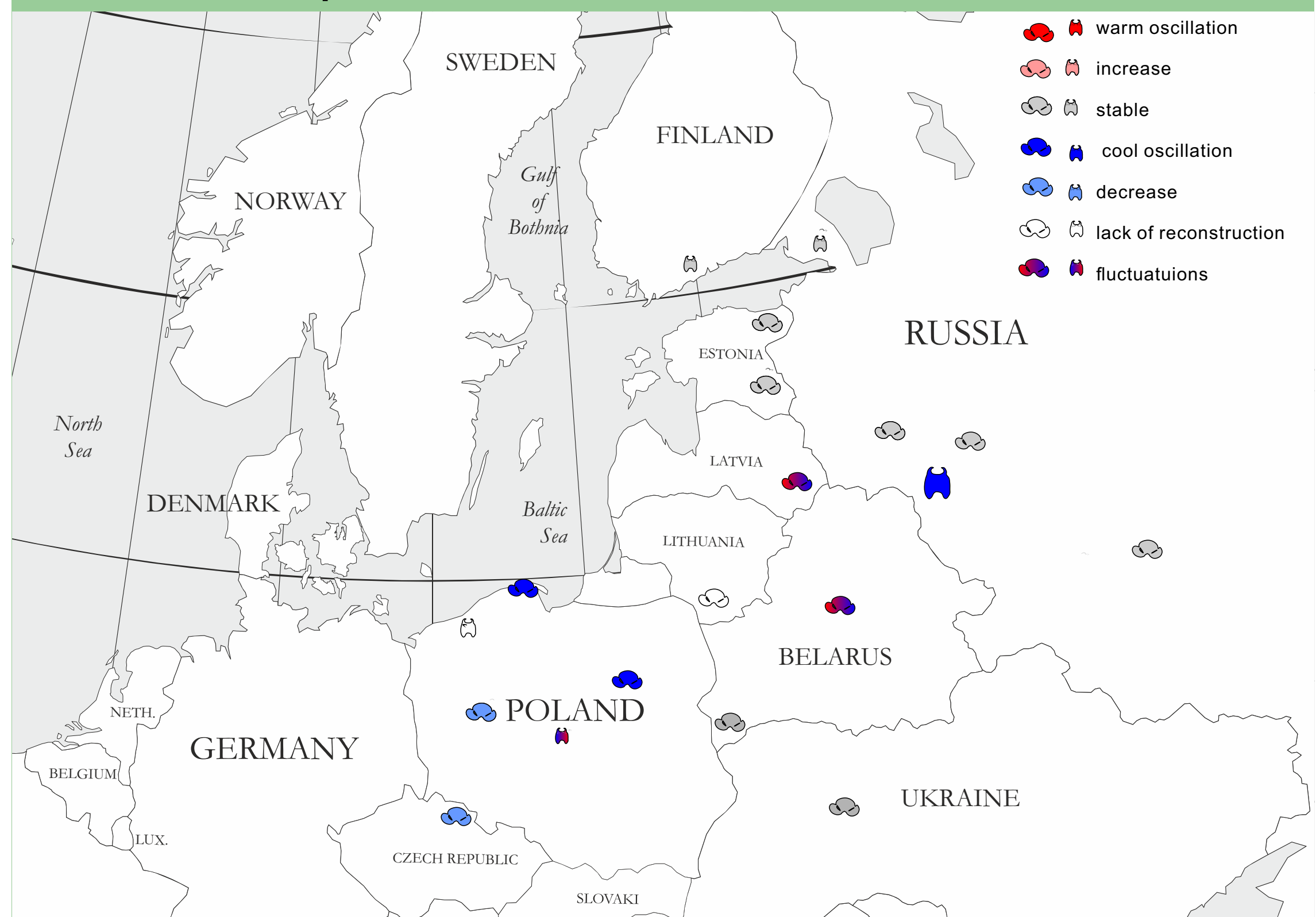


1. Hirvijärvi, Finland
2. Medvedevskoe, Russia
3. Polistovo-Lovatskaya mire system, Russia
4. Liivjarve Bog, Estonia
5. Raigastvere Lake, Estonia
6. Lake Kurjanova, Latvia
7. Staroselsky Moch, Russia
8. Peatland Klukva, Russia
9. Sudoble Lake, Belarus
10. Bebrukas Lake, Lithuania
11. Darzlubie Bog, Poland
12. Lake Spore, Poland
13. Oltush Lake, Belarus
14. Blędowo Lake, Poland
15. Żabieniec Bog, Poland
16. Biskupińskie Lake, Poland
17. Zalozhtsy, Ukraine
18. Vernéřovice, Czech Republic
19. Männikjärve bog, Estonia
20. Głęboczek, Poland
21. Stążki, Poland
22. Gązwa, Poland
23. Serteya

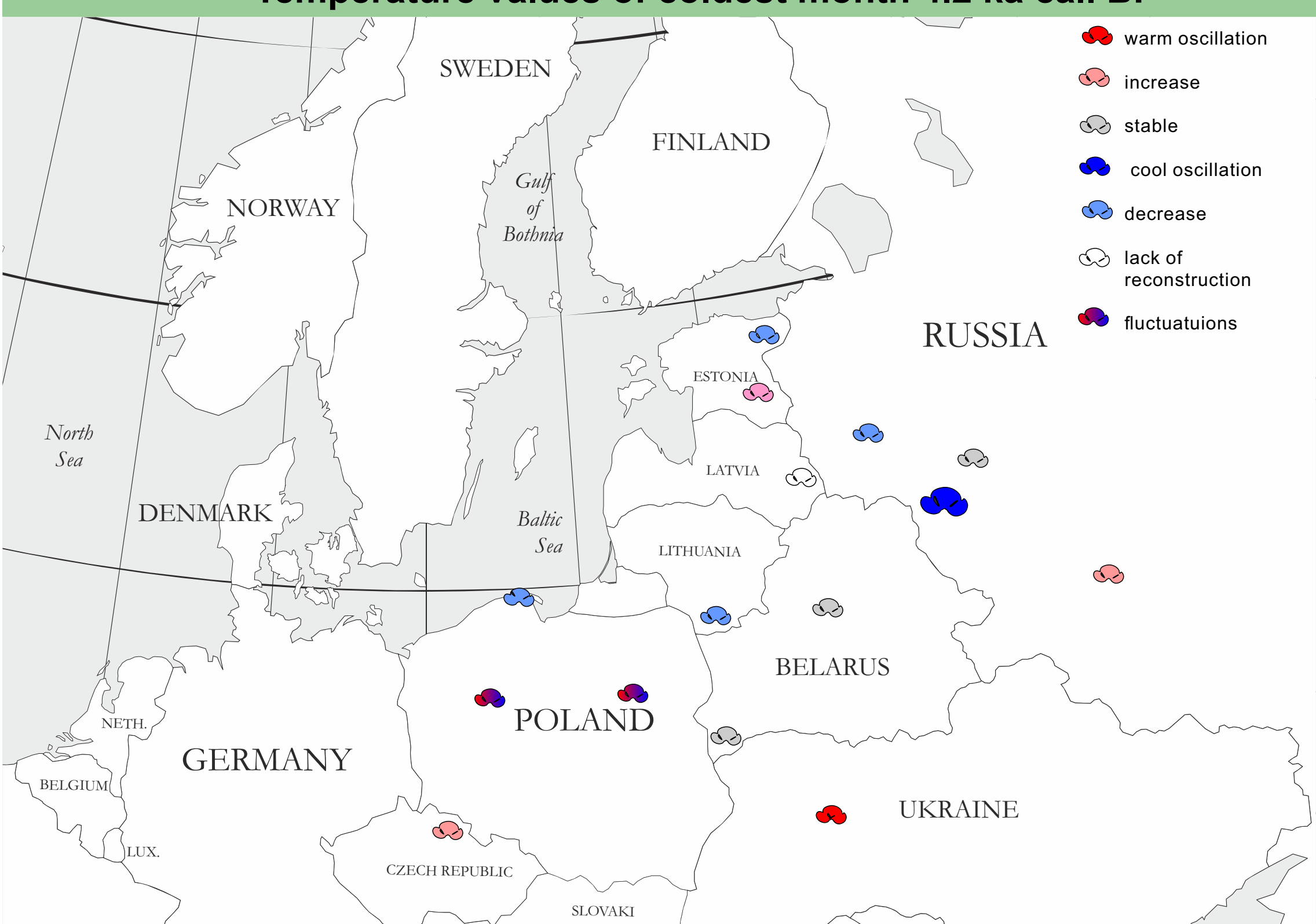
Temperature values of warmest month 4.2 ka cal. BP



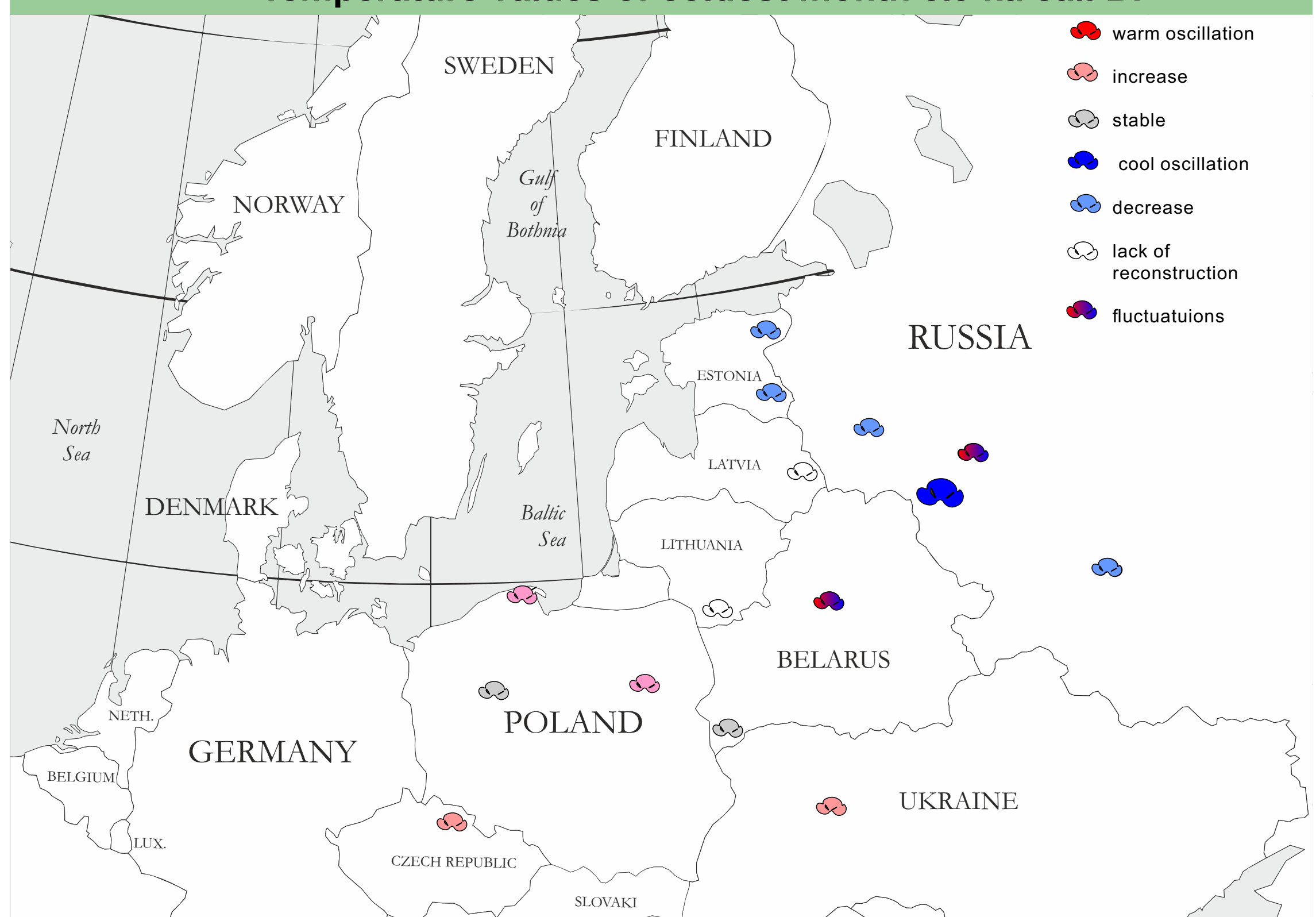
Temperature values of warmest month 5.9 ka cal. BP



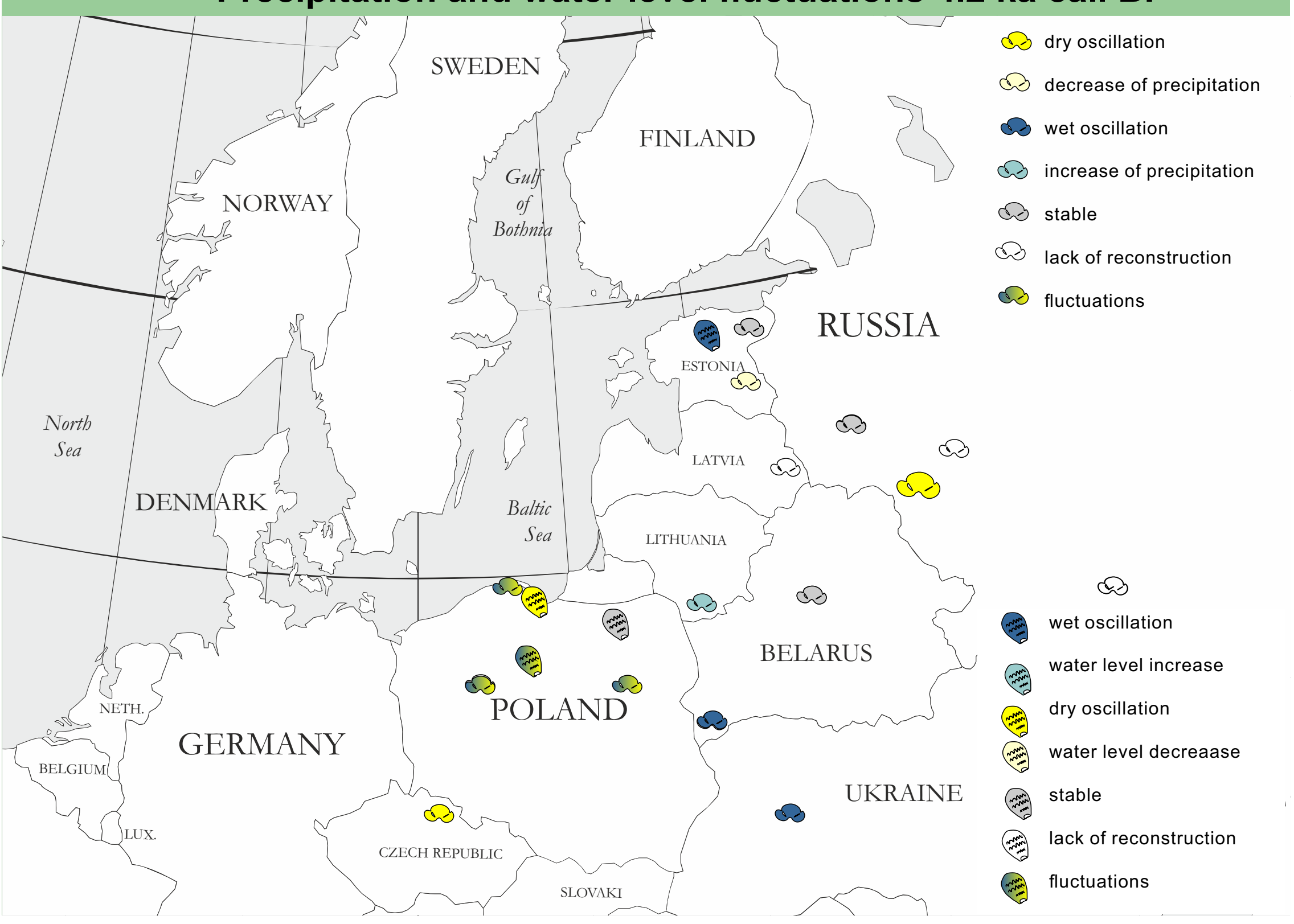
Temperature values of coldest month 4.2 ka cal. BP



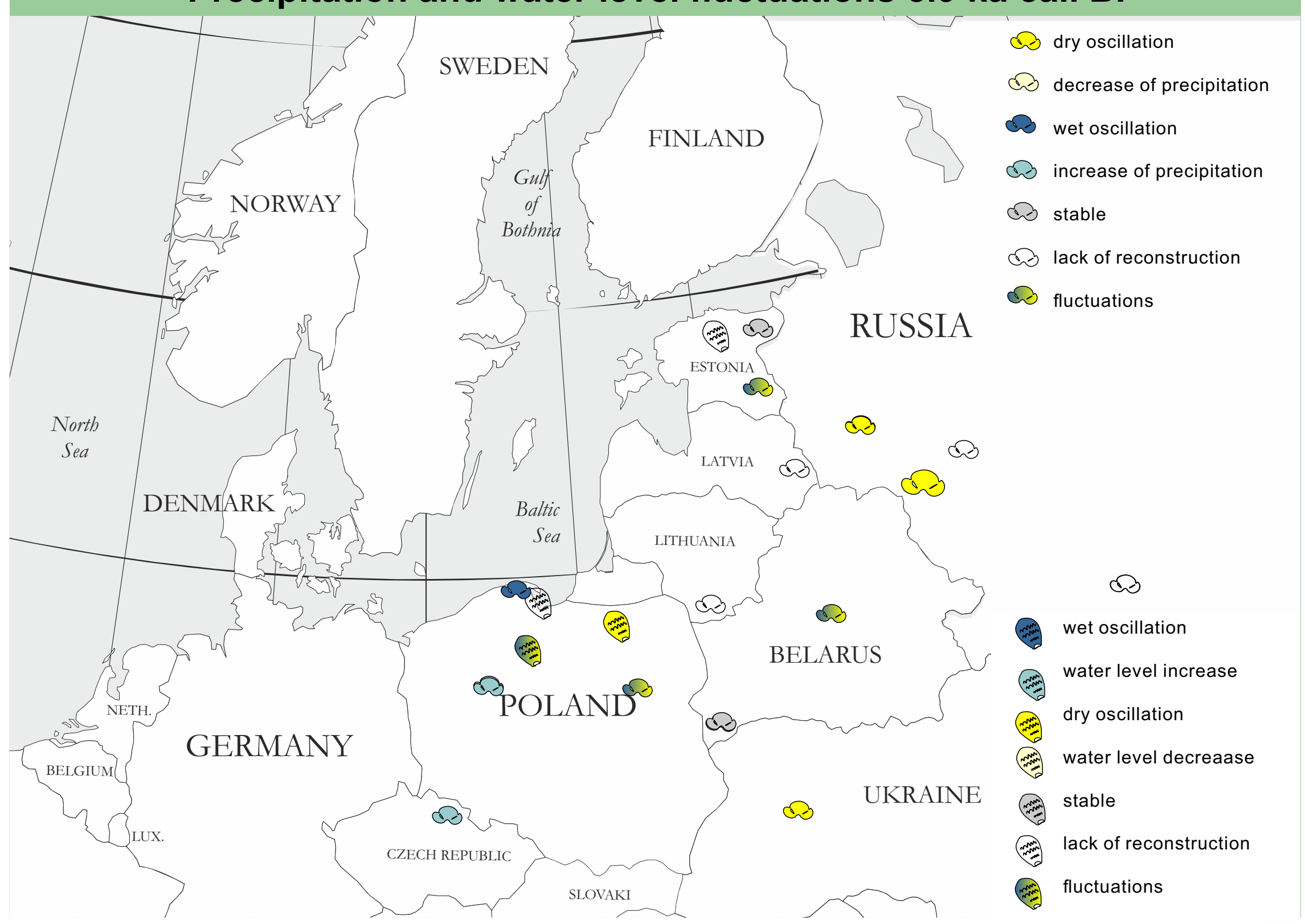
Temperature values of coldest month 5.9 ka cal. BP



Precipitation and water level fluctuations 4.2 ka cal. BP



Precipitation and water level fluctuations 5.9 ka cal. BP



	4.2 ka cal BP event (4.43-3.97 ka cal BP)				5.9 ka cal BP event (6.0-5.75 ka cal PB)			
	before event	event		after event	before event	event		after event
		CH-I, P-I temper ature	P-I AnP			CH-I, P-I temper ature	P-I AnP	
	Temperature and precipitation fluctuations							
1. Hirvijärvi, Finland [144]	5.4-4.7 ka cal BP: higher T Jul values	CH-I T Jul 15.3°C cooling oscillat ion on 4.2 ka cal BP	no reconstr uction	3.9-3.2 ka cal BP: higher T Jul values	6.6 ka cal BP: the same level of T Jul values	CH-I T Jul ca. 17°C	no reconstr uction	5.6 ka cal BP: the same level of T Jul values
2. Medvedevsk oe, Russia [8]	5.5 ka cal BP: 14.7°C	CH-I T Jul 14.0°C	no reconstr uction	3.8 ka cal BP: 14.1°C	6.35 ka cal BP: the same level of T Jul	CH-I T Jul 14.6°C	no reconstr uction	5.6 ka cal BP: the same level of T Jul
3. Polistovo- Lovatskaya mire system, Russia [13]	4.4-5.2 ka cal BP: TWM similar values, TCM similar to higher records, AnP similar values	P-I TCM ca. - 7°C TWM 17.0-	P-I AnP 670- 700 mm	3.9-3.5 ka cal BP: similar values of TCM, TWM, AnP	6.1-6.4 ka cal BP: TCM and TWM similar values; AnP higher value	P-I TCM - 4°C TWM 18°C	P-I AnP 620 mm	5.6-5.5 ka cal BP: lower TCM, similar TWM and higher to same AnP

		17.5°C						
4. LLiivjarve Bog, Estonia [145]	5.2-4.6 ka cal BP: similar level of TCM, TWM and AnP	P-I TCM - 11.0°C to - 6.4°C TWM 16.3- 16.5°C	P-I AnP 617- 640 mm	3.8-3.6 ka cal BP: similar to lower TCM, similar TWM, AnP	6.2-6.5 ka cal BP: similar level of AnP, TCM and TWM	P-I TCM - 9.6°C to - 8.6°C- TWM ca.16.5 °C	P-I AnP ca. 635 mm	5.7-5.2 ka cal BP: lower TCM, similar TWM, AnP
5. Raigastvere Lake, Estonia [146]	5.2-4.6 ka cal BP: similar level of TCM, TWM and AnP	P-I TCM - 10.7°C to - 9.7°C TWM 16.2- 16.5°C except one outlier sample.	P-I AnP 640- 680 mm except one outlier sample.	3.8-3.6 ka cal BP: similar to higher TCM, similar TWM, lower AnP	6.4-6.2 ka cal BP: P-I TCM, TWM, AnP reveal similar values at values to 6.0 ka cal BP	P-I TCM - 2.6°C to 1.5°C on 6.0 ka cal BP and 5.85- 5.75 ka cal BP, 0.8°C on 5.9 ka cal BP TWM variate	P-I AnP in two phases: ca. 775 mm on 6.0-5.9 ka cal BP and 885 mm on 5.85- 5.75 ka cal BP	5.6-5.4 ka cal BP: lower TCM, similar TWM and lower AnP

						within 16.2- 17.4°C		
6. LLake Kurjanova, Latvia [35]	Two phases: first warm (4.43-4.2 ka cal BP) with +0.7°C of P-I sum. T, and second cool oscillation of -1C in P-I summer T at 4.0-3.9 ka cal BP comparing to 4.4-5.0 ka cal BP	no reconstruction	3.9-3.8 ka cal BP: higher T summer (ca. + 1°C), 3.7-3.5 ka cal BP: similar values of T summer	Gradual decreasing trend of P-I summer T compared to 6.4-6.2 ka cal BP but no clear oscillation.	no reconstruction	ca. 5.6 ka cal BP: lower T summer by -0.7°C, 5.5 ka cal BP: similar values of T summer		
7. Staroselsky Moch, Russia [137]	5.2-4.5 ka cal BP: similar level	P-I TCM - 9.5- 5.9°C TWM 17.5- 18.7°C	no reconstruction	3.9-3.7 ka cal BP: similar values of TCM and TWM	6.1-6.5 ka cal BP: similar level of TWM and much lower TCM	P-I TCM - 4.4°C TWM 17.5°C	no reconstruction	5.7-5.4 ka cal BP: high variability of TCM and similar values of TWM
8. Peatland Klukva, Russia [14]	5.2-4.5 ka cal BP: similar level of TCM and TWM	P-I TCM - 5.8°C to - 4.4°C TWM 18.0-	no reconstruction	3.8-3.4 ka cal BP: higher TCM and similar to higher TWM	6.2-6.5 ka cal BP: higher values of TCM and similar level of TWM	P-I TCM - 4.8°C TWM 18.9°C	no reconstruction	5.6-5.2 ka cal BP: similar TCM and TWM

		18.6°C						
9. Sudoble Lake, Belarus [147]	5.0-4.7 ka cal BP: similar values of P-I TCM, TWM and AnP	P-I TCM - 7.2°C to -8°C TWM 15.9- 16.5°C	P-I AnP ca. 632 mm,	3.8-3.4 ka cal BP: TCM, TWM and AnP reveal similar values	6.5-6.2 ka cal BP: TCM values are lower compared to 6.0 ka cal BP and much higher compared to 5.9 ka cal BP; TWM reveal variable values on 6.5-6.2 ka cal BP; AnP reveal big fluctuations.	P-I TCM - 2.7°C on 6.0 ka cal BP -7.2°C on 5.9 ka cal BP TWM 17.6°C on 6.0 ka cal BP 15.9°C on 5.9 ka cal BP	P-I AnP variete from 734 to 630mm (6.0 to 5.9 ka cal BP)	5.7-5.4 ka cal BP: similar to lower TCM, similar and variable TWM and AnP

10. Bebrukas Lake, Lithuania [148]	5.2-4.8 ka cal BP: sharp decrease of TCM and TWM and increase of AnP starting on 4.5 ka cal BP	P-I TCM - 5°C to - 8.5°C TWM 16.2- 16.8°C	P-I AnP 590- 630 mm;	3.9-3.6 ka cal BP: similar values of TCM, TWM, AnP		no data	no data	
11. Darzlubie Bog, Poland [149]	4.8-4.55 ka cal BP: P-I TCM, TWM on similar level; AnP reveal long-time fluctuations	P-I TCM 1.5°C TWM 16.4- 16.8°C;	P-I AnP stays on ca. 815 mm fluctuations from 4.8- 4.55 ka cal BP	3.8-3.4 ka cal BP: lower to similar TCM, similar TWM, higher to similar AnP	6.4 ka cal BP: similar values of TCM, higher values of TWM, lower values of AnP	P-I TCM - 0.4°C TWM 17.5°C;	P-I AnP 904 mm;	5.7-5.2 ka cal BP: similar to higher TCM, TWM, similar to lower AnP
12. Lake Spore, Poland [135]	CH-I T Jul variate within 18–19 °C; Slightly higher temperatures, reaching up to 20 °C were reconstructed at ~3.9–4.05 and 4.18–4.27 cal ka BP					no data	no data	
13. Oltush Lake, Belarus [150]	5.6-4.7 ka cal BP: TCM on the similar level, TWM higher	P-I TCM -	P-I AnP 743	3.8-3.4 ka cal BP: similar to lower TCM, TWM, lower AnP	6.4 ka cal BP: TCM, TWM and AnP on similar level	P-I TCM -	P-I AnP 571 mm.	5.6 ka cal BP: similar TCM, TWM and AnP

	values ca. 18.0°C; AnP - much lower values	2.3°C TWM 17.3°C	mm;			2.9°C TWM 18.0°C		
14. Błędowo Lake, Poland [151]	5.2-4.5 ka cal BP: TCM and TWM keep decreasing trend toward 4.2 ka cal BP event;	P-I TCM - 4.4°C to - 0.8°C TWM decrease from 20°C to 15.51° C;	At first phase the same P-I AnP compared to 5.7-4.43 ka cal BP (622-706 mm), at second phase increase to 894 mm	3.9-3.6 ka cal BP: similar values of TCM and TWM but much lower variability; AnP of similar values to first phase of 4.2 ka cal BP event and much lower than in the second phase of one	6.5-6.1 ka cal BP: higher TCM; 6.1 ka cal BP higher TWM; 6.5-6.2 ka cal BP higher AnP	P-I TCM - 6.0°C on 5.9 ka cal BP TWM 15.7°C on 5.8 ka cal BP Clear cold oscillation summer	P-I AnP ca. 620 mm exactly on 6.0-5.8 ka cal BP	after 5.9 ka cal BP event TCM and TWM sharply increase, AnP variable
15. Żabieniec Bog, Poland [20]	5.0-4.6 ka cal BP: T Jul reveal slightly higher values - ca. 16.7-17.2°C	CH-I T Jul fluctuates 15.9-	No data	3.9-3.5 ka cal BP: generally similar values of T Jul: 15.3-16.9°C except outlier on 3.8 ka	6.6-6.2 ka cal BP: values higher then on 6.0 ka cal BP	CH-I TJul is 14.0°C exactly on 6.0	No data	5.6-5.2 ka cal BP: similar values as in second phase of 5.9 ka cal BP event

		16.9°C		cal BP (13.8°C)		ka cal BP, in second phase of 5.9 ka event, temperature increases to 16.5°C;		
16. Biskupińskie Lake, Poland [152]	5.2 -4.5 ka cal BP: TCM and TWM on similar level; AnP at similar level to second phase of 4.2 event	P-I TCM - 5.0°C to - 3.0°C TWM with increasing trend from 15.8°C to 19.2°C;	P-I AnP: at first phase high value (818 mm) then much lower ca. 550 mm;	3.9-3.6 ka cal BP: TCM, TWM ranging in variability of 4.2 ka cal BP event to higher values, AnP higher	6.0-6.4 ka cal BP: TCM, TWM and AnP on the similar level	P-I TCM - 3.7°C to - 5.1°C TWM 18.0- 17.1°C;	P-I AnP: ca 590 mm	5.7-5.2 ka cal BP: TCM, TWM similar to lower values, AnP similar to higher values

17. Zalozhtsy, Ukraine [153]	5.1 ka cal BP: TCM lower, TWM higher and AnP substantially lower then on 4.2 ka event	P-I TCM - 0.9°C TWM 15.3°C	P-I AnP 1110 mm	3.4 ka cal BP: TCM, AnP reveal lower, TWM higher values	6.6 ka cal BP: TCM and TWM on similar level, substantially higher AnP	P-I TCM - 3.9°C TWM 16.0°C	P-I AnP 830mm	5.1 ka cal BP: TCM, AnP reveal higher, TWM similar values
18. Vernéřovice, Czech Republic [154]	4.9 ka cal BP: similar values of TCM and TWM, slightly higher values of AnP	P-I TCM - 9.0 °C TWM 16.3°C	P-I AnP 654 mm	3.3 ka cal BP: TCM, AnP reveal much higher, TWM lower values	6.3 ka cal BP: lower TCM, higher TWM and lower AnP (630 mm)	P-I TCM - 7.8°C TWM 15.8°C	P-I AnP: ca. 760 mm	5.8 ka cal BP: TCM, AnP reveal higher, TWM similar values
fluctuations of water level								
	before event	4.2 ka cal BP event (4.43-3.97 ka cal BP)		after event	before event	5.9 ka cal BP event (6.0-5.75 ka cal PB)		after event
19. Männikjärve bog, Estonia [155]	no data	TA-I DWT (Testate Amoebae- Inferred water table depth (cm)) reveal wet oscillation		3.9-3.7 ka cal BP: DWT reveal much drier conditions with tendency to decrease of water table		no data		

20. Głęboczek, Poland [156]	DWT on 4.2 ka cal BP event similar water level comparing to 4.3-4.5 ka cal BP and 3.8-3.4 ka cal BP, wetter than multi-millennial mean			6.2 ka cal BP: wet oscillation	DWT on 5.9 ka cal BP event on multi-millenial mean	5.4 ka cal BP: dry oscillation
21. Stążki, Poland [34]	3.7-3.4 ka cal BP: increase of water table	TA-I DWT dry oscillation	4.4.-4.7 ka cal BP: water level on multi-century mean			
22. Gązwa, Poland [33]	4.4-4.8 ka cal BP: water level on multi-millenial mean	TA-I DWT small fluctuations	3.9-3.5 ka cal BP: water level on multi-millenial mean		TA-I DWT clear dry oscillation	5.8: clear wet oscillation then water level stays on multi-millenial mean

LACUSTRINE, FLUVIAL AND SLOPE DEPOSITS IN THE WETLAND SHORE AREA IN SERTEYA, WESTERN RUSSIA

PIOTR KITTEL¹, ANDREY MAZURKEVICH², ALEXANDER ALEXANDROVSKIY³,
EKATERINA DOLBUNOVA², MATEUSZ KRUPSKI^{4,9}, JACEK SZMAŃDA⁵,
RENATA STACHOWICZ-RYBKA⁶, KATARZYNA CYWA⁶,
AGNIESZKA MROCZKOWSKA^{1,7}, DANIEL OKUPNY⁸

Abstract. The article presents the results of a study on sediment deposition processes in the palaeolake shore zone, at the multi-layered Serteya II archaeological site in Western Russia. In recent years, geomorphological, palaeopedological and palaeoecological research was undertaken in strict cooperation with archaeological fieldwork. The Serteya II site occupies a substantial area of a kame terrace and biogenic plain within a palaeolake basin. From an archaeological point of view, the site is represented by few Mesolithic artefacts, but mostly by remnants of hunter-gatherer-fisher communities attributed in the Russian scientific tradition to the Neolithic period and dated from 6300 BC to 2000 BC. Later, the area was used by people in the Bronze Age, Early Iron Age and Early Middle Ages. The integration of archaeological and multidisciplinary palaeoenvironmental research allowed the natural and human induced deposition of mineral-organic and minerogenic sediments to be reconstructed, as well as the development of structures in the lake shore zone. The changes from lacustrine to fluvial system were documented and the human impact is recorded mostly in the acceleration of slope processes.

Key words: sedimentology, micromorphology, micro- and macrofossils, geochemistry, palaeolake shore zone, archaeological layers

Introduction

The western part of the multi-layered Serteya II archaeological complex (Western Russia) is situated in a palaeolake shore area. It is characterised by a complex cultural stratigraphy due to its diversified geomorphological setting and different periods of inhabitation. The geomorphological

condition of the Serteya II site was recently described by Kittel *et al.* (2018), and the latest archaeological discoveries have recently been presented by Mazurkevich *et al.* (2017) and Kittel *et al.* (2020).

The diversified geomorphological situation results from the studied site's location in a recently glaciated area. The terrain relief has been

¹ University of Lodz, Faculty of Geographical Sciences, Department of Geology and Geomorphology, ul. Narutowicza 88, 90-139 Łódź, Poland; e-mail: piotr.kittel@geo.uni.lodz.pl, ORCID: 0000-0001-6987-7968

² The State Hermitage Museum, Department of Archaeology of Eastern Europe and Siberia, Dvortsovaya Naberezhnaya 34, 190000 Saint Petersburg, Russia; e-mail: a-mazurkevich@mail.ru, ORCID: 0000-0002-4947-0498; katjer@mail.ru, ORCID: 0000-0003-1843-9620

³ Russian Academy of Sciences, Institute of Geography, Department of Soil Geography and Evolution, Staromonetnyi lane, 29, 119017 Moscow, Russia, Russia; e-mail: alexandrovskiy@mail.ru

⁴ Archeolodzy.org Foundation, ul. Bolesława Prusa 81/3i, 50-316 Wrocław, Poland; e-mail: mateusz@archeolodzy.org, ORCID: 0000-0001-7992-967X

⁵ Pedagogical University of Cracow, Institute of Geography, ul. Podchorążych 2, 30-084 Krakow, Poland; e-mail: jacek.szmanda@up.krakow.com, ORCID: 0000-0002-4058-8334

⁶ W. Szafer Institute of Botany, Polish Academy of Sciences, ul. Lubicz 46, 31-512 Kraków, Poland; e-mail: k.cywa@botany.pl, r.stachowicz@botany.pl

⁷ Polish Academy of Sciences, Institute of Geography and Spatial Organization, ul. Twarda 51/55, 00-818 Warsaw, Poland; e-mail: A_Mroczkowska@outlook.com, ORCID: 0000-0002-3534-7843

⁸ University of Szczecin, Institute of Marine and Environmental Sciences, ul. Mickiewicza 16, 70-383 Szczecin, Poland; e-mail: daniel.okupny@usz.edu.pl

⁹ Wrocław University of Environmental and Life Sciences, Institute of Soil Science and Environmental Protection, ul. Grunwaldzka 53, 50-357 Wrocław, Poland

formed since the Late Weichselian (Late Valdai) and the site lies within a subglacial channel that was earlier occupied by a few lake basins and later by the Serteya River Valley. The site is located within a valley, at the point where the valley crosses the border between areas of moraine and glaciofluvial sediments. Soil-forming rocks are heterogeneous, often layered, from sand to loams. The latter are found on terraces, and sands predominate in the valley floor. In general, sandy podzols predominate on the studied territory, while in the area of Serteya II α there are podzols on sands, in some places underlain by moraine diamicton.

Archaeological relicts, features and layers are found on a kame terrace, which is formed by clastic sediments (at part of the site called Serteya II layer α), as well as within lacustrine organic deposits of the palaeolake basin (Serteya II-2) (Fig. 1).

The surface of the kame occupied by the Serteya II layer α is slightly inclined east-north-eastwards and formed by glaciofluvial sands with admixtures of gravels and limnoglacial fine sands and silts. Numerous Neolithic artefacts and features were discovered at the Serteya II-2 site in: a brown coarse-detritus, a brown-olive coarse-detritus gyttja, and underlying sands with organic mud and clay admixture (see also Mazurkevich *et al.* 2020). The upper part of the muddy brown gyttja layer may be synchronous with the time when communities of the Textile Ceramics Culture dwelled at the higher part of the site, which is represented by Serteya II layer α and belongs to the Late Bronze Age of the first half-middle of the 2nd millennium BC, based on the dates obtained for similar complexes in other regions. These cultural layers are covered with sandy and silty organic mud deposits.

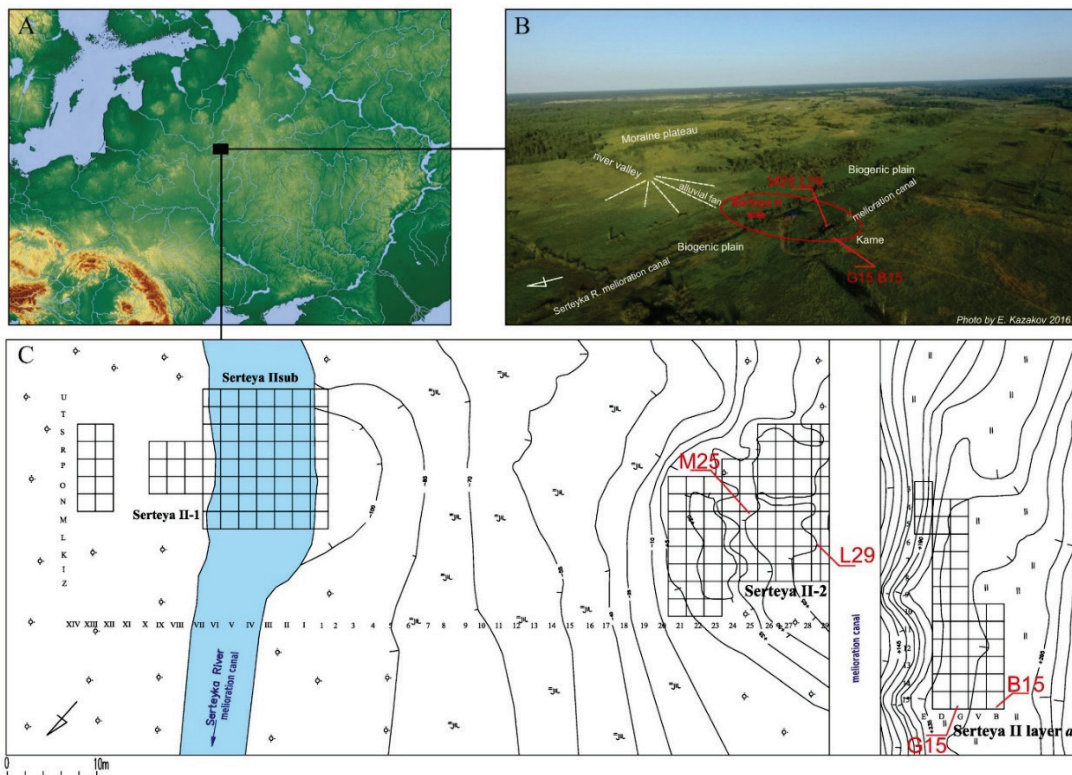


Fig. 1. Research area: Serteya II site plan indicating location of L29, M25, G15 and B15 cores

- A. On the physical map of Europe (based on DEM)
- B. On an aerial photo of the Serteya II site (photo by E. Kazakov 2016)
- C. On the Serteya II site archaeological excavation plan

The accumulation of lacustrine deposits was replaced in the studied area by fluvial overbank deposition after 1650 BC (after 3371 ± 21 BP) (Kittel *et al.* 2020). It may have occurred even later, as

indicated by the discovery of a cow mandible in squares O26–O27 at the Serteya II-2 site (Fig. 1) at the border of muddy brown gyttja and a silty organic mud layer. This bone was dated to 1685 ± 30

BP (Poz-108410), i.e. 335–400 AD. Moreover, plant macrofossils from the overbank deposits obtained a date of 561±26 BP (MKL-A3888), i.e. 1324–1414 AD (Kittel *et al.* 2018, 2020). This demonstrates that the palaeolake water level possibly decreased in the studied area between 1500 BC and 300 AD and fluvial overbank deposition started before 1300 AD.

Our study is focused on Late Holocene changes in deposition processes in the palaeolake shore zone – from a lacustrine system to a fluvial system and with slope processes playing a role. These transitions were influenced by palaeoenvironmental conditions and the episodic impact of small human groups. The palaeoenvironmental conditions were reconstructed based on sedimentological, palaeopedological and palaeoecological traits of deposits of the palaeolake shore zone.

Material and study methods

The western shore zone part of the Serteya II site has been excavated since 2015 using wetland archaeological methods. The surficial geology of the site surroundings was recognised by detailed mapping with the use of hand augering. A more detailed study was undertaken in archaeological trenches. After a full excavation of the archaeological outcrop, a core of deposits was collected in square L29 for detailed multi-proxy analyses (Fig. 1). The L29 core was taken as a monolith in a metal box with dimensions of 50×10×10 cm (Fig. 2) and it covers the deposits between 65 and 115 cm below ground level (b.g.l.). This sampling method preserves the undisturbed structure of sediments. Sub-samples of the L29 core deposits were taken in 1-cm slices at 2-cm intervals for geochemical, sedimentological, palaeozoological (subfossil Cladocera and Chironomidae) and plant macrofossil analyses. Thin sections for micromorphological analysis were manufactured from the remainder of deposits protected in the metal box.

For the L29 core, chemical composition was determined for 21 samples after drying at 105 °C and homogenisation in an agate mortar. The geochemical analysis included identification of: organic matter (LOI) in a muffle furnace at 550 °C, calcium carbonate – CaCO₃ (volumetric method by means of Scheibler's apparatus) (methods after: Bengtsson, Enell 1986). The ash samples were dissolved (with HCl, HNO₃ and H₂O₂) in Teflon bombs using a microwave mineraliser for 21 samples. The obtained solution was analysed for concentrations of selected elements, using atomic

absorption spectrometry (SOLAAR 969 Unicam). The proportions of these compounds (such as: Fe/Mn, Cu/Zn, Ca/Fe, Na/K, Ca/Mg and Na+K+ +Mg/Ca) were used to classify deposits and to reconstruct environmental change in the sedimentary basin and in its catchment (Pawlowski *et al.* 2016). The key assumption of these interpretations is that lithophilic and biogenic elements derive from different sources and that they accumulate in deposits in different physico-chemical conditions. The grain-size composition of the ash samples remaining after Loss-On-Ignition analysis, was determined using a laser particle size analyser Mastersizer 3000 with a Hydro MU dispersion unit (Malvern).

The origins and conditions of sediment deposition were interpreted on the basis of Mycielska-Dowgiatło and Ludwikowska-Kędzia (2011), using the Folk and Ward (1957) indices based on the distribution of samples on the relationship diagram of mean grain size (M_z) and sorting (σ_1). Moreover, the momentary indices of grain-size composition of the samples were calculated, and the conditions of sediment deposition were interpreted by analysing the distribution of the samples on the mean grain size (M_1) versus standard deviation (M_2) diagram, referring to the views of Sly *et al.* (1983). Depositional velocities of water flow were calculated based on the values of the mean grain-size diameter, according to Koster's (1978) formula. Shear velocities of water flow were estimated based on the first percentile and Sundborg (1967) diagram.

Three undisturbed soil blocks were sub-sampled from the L29 monolith sample for soil micromorphology analysis, at depth ranges 80–90, 90–100 and 100–110 (cm b.g.l.), capturing horizons described as: 1 – organic mud (called OM, 110–109 cm), 2 – sand with organic mud (SOM, 109–100/96 cm), and 3 – muddy sand with organic matter and silty organic mud at the top (OSOM, at 100/96–80 cm) (Fig. 2). The samples were air-dried, impregnated with resin, cut and polished to a thickness of *ca* 30 µm in the Laboratory of Mineralogy and Petrology, Ghent University. The procedure of thin section production did not include acetone replacement. Air drying of samples causes shrinkage of organic matter, which leads to an artificial increase in porosity. Thus, the estimates of porosity in thin sections have to be taken with caution. The thin sections were first scanned and analysed macroscopically to allow correlation with field observations and preliminary identification of microstructure. Microscopic observations were conducted using a Zeiss Axio Lab A1 in plane polarised light (PPL), cross-polarised light (XPL) and

oblique incident light (OIL), in magnifications ranging from $25\times$ to $200\times$ (Courty *et al.* 1989; Goldberg, Macphail 2006; Nicosia, Stoops 2017). Standard terminology of Bullock *et al.* (1985) and

Stoops (2003) was used for descriptions of micro-morphological features, whereas phytolith distribution patterns were recognised following Vrydaghs *et al.* (2016).

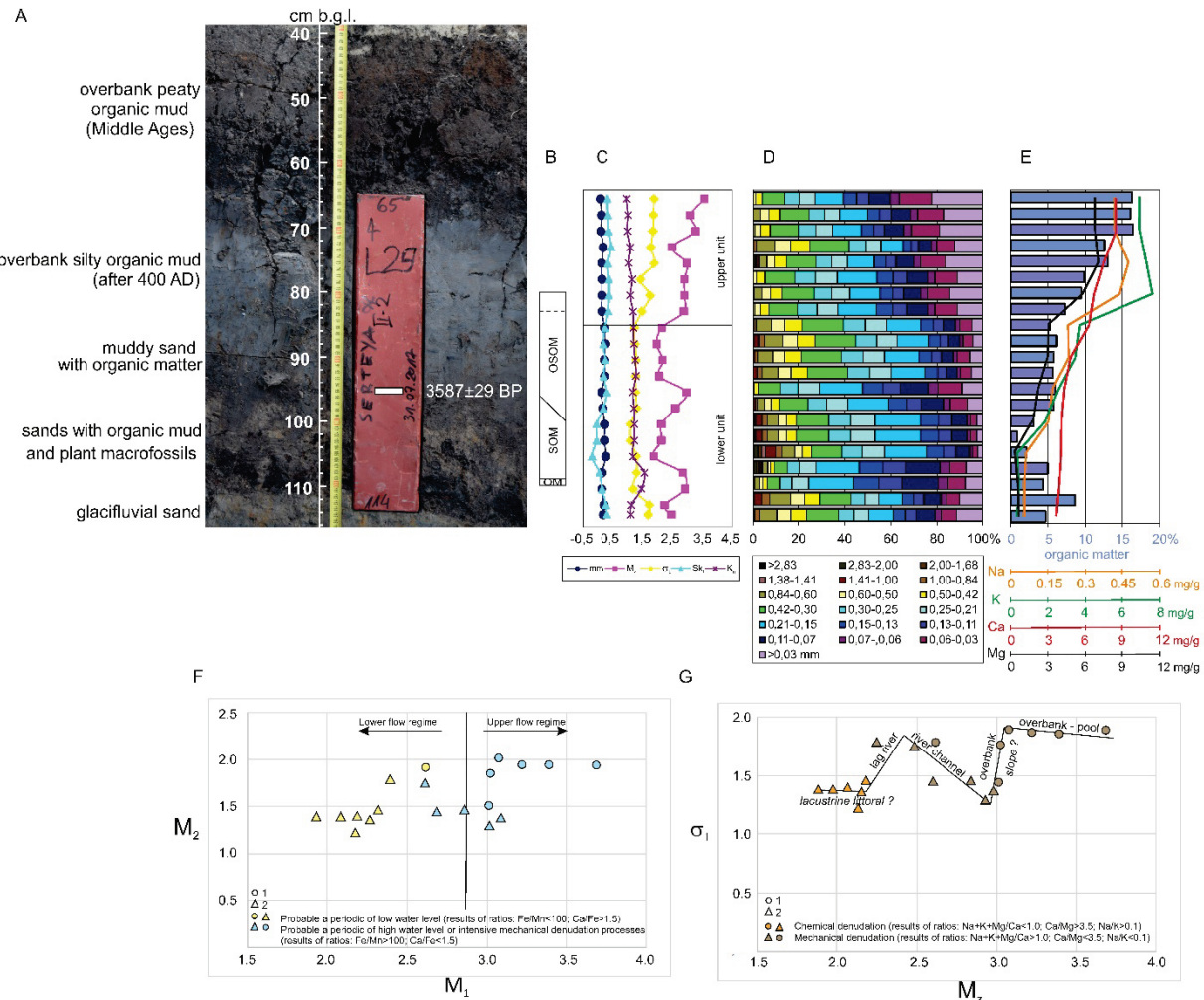


Fig. 2. Lithology, sedimentological and geochemical traits of STII L29 core deposits

A. Lithologic profile

B. Micromorphological units

C. Folk and Ward coefficients

mm – mean grain size [mm], M_z – mean grain size [ϕ], σ_1 – sorting index, Sk_1 – skewness, K_g – kurtosis

D. Grain-size distribution

E. Content of organic matter and Na, K, Ca, Mg elements

F. Lithodynamic interpretation of sediments after Sly *et al.* (1983) (analysis by J. Szmańda) against water levels reconstructed based on geochemical indicators: Fe/Mn, Cu/Zn and Ca/Fe (analysis by D. Okupny)

1 – sediments of upper unit U1; 2 – sediments of lower unit U2

G. Lithogenetic interpretation of sediments after Mycielska-Dowgiałło, Ludwikowska-Kędzia (2011) modified (analysis by J. Szmańda) against type of denudation processes reconstructed based on geochemical indicators: Na/K and Ca/Mg (analysis by D. Okupny)

1 – sediments of upper unit U1; 2 – sediments of lower unit U2

Plant macrofossil analysis was carried out for 21 samples (15–20 cm³ each) from the L29 profile. The samples were boiled with KOH to reduce the amount of sediment and remove humic matter, and then the material was examined with a stereo microscope. The conservation of the plant remains was done with a standard mixture of alcohol, water and glycerin in proportion 1:1:1, with the addition of thymol. Then, the fragments of the plants were dried with 50% ethyl alcohol and identified with the use of plant keys, atlases (e.g. Berggren 1969; Cappers *et al.* 2006; Velichkevich, Zastawniak 2006, 2008), other scientific descriptions and publications, a reference collection of contemporary seeds, fruits and wood, and a collection of fossil floras in the Palaeobotanical Museum of the W. Szafer Institute of Botany, Polish Academy of Sciences in Kraków. Qualitative and quantitative results were presented in diagrams, and drawn using the POLPAL software (Nalepka, Walanus 2003).

The samples for subfossil Cladocera analysis were processed according to Frey (1986). Microscopic identification (200× and 400× magnification) was based on a key by Szeroczyńska and Sarmaja-Korjonen (2007). Qualitative analysis was based on Bjerring *et al.* (2009). The samples for subfossil Chironomidae analysis were processed with standard methods described by Brooks *et al.* (2007) using a 90-µm sieve. Head capsules were separated from the sediment under binoculars (4×10 magnification) and identified under a microscope (mainly 10×40 magnification). The identification and ecological analysis follow mostly Brooks *et al.* (2007) and Andersen *et al.* (2013). The weight of the samples ranged from 15.48 to 32.48 g. Zonation of both Cladocera and Chironomidae analyses' results was done using CONISS software (Grimm 1987) and the stratigraphic diagram was prepared with Tilia software (Grimm 2016).

In this study, three more lithological cores were also taken into consideration. The first one, called STII M25, was located *ca* 8 m to the east of L29 (Figs 1, 3) and has been described in detail by Kittel *et al.* (2020). Two more profiles were situated at the Serteya II layer α site, on the kame surface, *ca* 25 m to the west of the L29 core. They were collected from the wall of an archaeological trench in square G/15 and in square B/15 (Fig. 1). A number of geoarchaeological soil methods were used to characterise the natural and anthropogenic formation processes of deposits, cultural layers and soils at the Serteya II layer α site. The G/15 profile was sampled for palaeopedological,

textural, geochemical and charcoal analyses. For the B/15 profile, only palaeopedological and geochemical analyses were conducted. Particle-size distribution using sieve analysis (Rühle 1973) was determined for seven sediment samples from the G/15 profile. The textural features, using Folk and Ward (1957) coefficients, the type of relationship between mean grain size (M_Z) and sorting (σ_1) after Mycielska-Dowgiałło and Ludwikowska-Kędzia (2011) and the C-M pattern after Passegå and Byramjee (Passegå 1964; Passegå, Byramjee 1969) were evaluated for inferences about the origin and deposition conditions of sediments. The organic matter content was measured by routine methods: Loss-On-Ignition (LOI) for the G/15 profile and the Tyurin method (wet combustion, similar to the Walkley-Black method) for the B/15 profile. Soil pH was specified with a potentiometer in the water soil suspension and the total P₂O₅ content by the Ginzburg method (Ginzburg 1981; Bengtsson, Enell 1986).

Six samples of charcoal were subjected to anthracological analysis. The charcoal particles were selected manually from the G/15 profile, from the depths of 50–60, 60–65 and 65–70 cm b.g.l and from the fill of a Neolithic pit. The samples contained from one to several charred wood fragments of length between 0.6 and 2.8 cm. In total, the taxonomic attribution of 21 fragments of charcoal was determined. The charcoal fragments were analysed in reflected light, under a Nikon Eclipse ME600P metallurgical microscope. To verify the taxonomical determinations, a reference wood collection of the W. Szafer Institute of Botany, Polish Academy of Science was used, as well as atlases of wood anatomy (Schweingruber 1978; Benkova, Schweingruber 2004).

Results

L29 core

Macroscopic description and chronology

The bottommost sediments of the studied L29 depositional sequence are sands with organic mud and plant macrofossils (depth from 114 to *ca* 100 cm b.g.l.). Above, at a depth between *ca* 100 and 83 cm b.g.l. muddy sand with organic matter was identified, which passes gradually upward into silty organic mud (*ca* 83 – *ca* 70 cm b.g.l.). The uppermost part of the profile is formed by peaty organic mud (Fig. 2). The bottommost sands with organic mud correspond to sediments of similar traits in the STII M25 core situated *ca* 8 m to the

east and chronologically correlated with the Early Holocene up to *ca* 4300 BC (Kittel et al. 2020). For the layer of muddy sand with organic matter, a ^{14}C date was obtained for macrofossils from a depth of 95 cm b.g.l. (i.e. *Pinus sylvestris* – 1 scale, *Urtica dioica* – 2 fruits, *Cristatella mucedo* – 7 statoblasts, charcoal – 3 fragments): 3587 ± 29 BP (MKL-A4888), i.e. 1971–1896 cal. BC (prob. 68.2%). The silty organic mud was deposited after *ca* 400 AD, as demonstrated by the ^{14}C date of a cow's mandible in square O27 and plant macrofossils from the STII M25 core (Kittel et al. 2020).

Geochemistry and sedimentology

From the sedimentological point of view, the studied mineral deposits of the L29 core can be divided into two main units: (1) the lower (115–85 cm b.g.l.) and (2) the upper (85–65 cm) (Fig. 2C). The lower unit consists of sands and silt sands with a mean grain size of 1.94–3.02 phi (0.26–0.12 mm), average organic matter content below 5% and low concentration of K (0.3–1.8 mg/g), Na (0.05–0.22 mg/g), Mg (0.3–2.95 mg/g) and Ca (3.5–6.2 mg/g). The upper unit consists of silty sands with mean grain size 3.02–3.68 phi (0.13–0.08 mm), average organic matter content of 12%, K of 7.16 mg/g, Na of 0.43 mg/g and Mg of 6.55 mg/g (Fig. 2E). Both analysed units are poorly sorted and have a massive structure, but the structure of the deposits between *ca* 100 and 110/115 cm b.g.l. is deformed (Fig. 3).

In both units (i.e. sands and silty sands), the fraction of fine or medium sands with modes in the range from 1.37 phi (0.39 mm) to 2.37 phi (0.2 mm) dominates (Fig. 2D). The content of medium sand fraction is at a maximum of 35% (at a depth of 85 cm) and the fine sand fraction – 38% (at a depth of 100–103 cm). In the silty sand, the accessory fraction is coarse silt – 6 phi (0.014 mm), and its content reaches 8% (at a depth of 70 cm). The particle-size distribution of deposits is positively skewed, which means that the modal fraction values are greater than the median.

The lower unit is underlain by glaciofluvial moderately sorted sands with gravel admixtures – the mean grain size ranges from 2.23 to 2.73 phi (0.21–0.15 mm).

Micromorphology

Table 1 summarises the results of micromorphological observations. The development of microstructure is visible in the studied sequence: starting from a single grain type (mostly quartz

grains) with a network of simple packing voids and relatively high porosity (OM: up to 50%), characteristic for the OM and the SOM (109–100 cm b.g.l.); through dominant bridged and pellicular grain types with compound packing voids, few channels and planar voids and lower porosity (*ca* 30%) in the SOM/OSOM and OSOM (100–90 cm); to channel and platy microstructure types, which are exclusive in the least porous (15–20%) uppermost part of the OSOM (83–80 cm), formed by silty organic mud (Figs 2B, 4). In terms of the related distribution of the coarse and fine mineral fraction (C:F limit at 2 μm), this corresponds with a shift from the monic (OM and SOM) to the porphyric type, where mineral grains are embedded in a “dusty” clay (clay with organic punctuations and detritus) matrix (OSOM: 83–80 cm). Gefuric/chitonic types are found in between (especially at 100–90 cm). The b-fabric manifests itself as grano- and porostriated in the OSOM horizon. A *ca* 1-cm-thick “intercalation” of medium and coarse sand in the SOM (*ca* 105 cm) and occasional “dusty” clay “crusts” capping mineral grains in the OSOM (96–90 cm) were identified; elsewhere, the well-to-moderately sorted mineral material is randomly oriented and distributed (no bedding or laminations).

The highest number of well preserved, brownish in colour, terrestrial plant remains (foliage twigs and leaves, seeds, other tissue fragments – bark?, sphagnum moss?), mostly horizontally aligned, were recorded in the OM (50–70%). They are frequent (15–30%), including in the SOM (apart from “mixed” areas), but seem more fragmented (detritus). In the overlying SOM/OSOM and OSOM the amount of plant remains decreases (OSOM, depth 83–80 cm: <5%) and they become increasingly mineralised – carbonised, humified (rarely) or pseudomorphosised by Fe/Mn replacement (Fe/Mn ratio exceeds 273, as shown by geochemical results). On the other hand, the uppermost part of the OSOM (83–80 cm) has the highest percentage (*ca* 5%) of punctuations and amorphous forms (rare), which are absent or rare (<5%-single) in the OM and SOM, respectively. The fine organic matter (e.g. punctuations) is found embedded in the clay matrix. A similar pattern pertains to the phytolith assemblage, which is most abundant (<5%, <5%-single) in the topmost section of the sampled profile (OSOM, 90–80 cm), where also single diatoms and sponge spicules were discovered; siliceous particles occur within the (dusty) clay matrix.

L29



Fig. 3. Relation of L29 and M25 cores after Kittel et al. (2020)

M25



Table 1

Serteya STII L29 monolith: micromorphological features

Horizon	Depth from surface (cm)	Microstructure	Porosity	Organic matter	Phytoliths	Anthropogenic inclusions	Pedofeatures										
							C:F related distribution (2 µm) total (%)	b-fabric pores	diatoms	sponge spicules	charcoal	bone fragments	translocated dusty clay (coatings, bridges)	clay crusts / clay-trich soil fragments	hypocoatings crusts / coatings / nodules	infiltrations mite excre- ments	Fe/Mn
OSOM	80-83	ch, pl	ch-pl	15-20	po	gst, pst	+ (m)	(++)	i	+	s	+	-	-	+	+	-
OSOM	83-90	ch, pl, pg	ch-pl, cdp	20-25	po-ch	gst, pst	(++) (m)	+	i, a (1?)	(+)	s	(+)	(b)	-	+	(+)	++
OSOM	90-96	pg, ch	cdp, ch-pl	20-30	ch-po (l)	gst, pst	++ (m), (p)	+	i	s	-	-	(+)	(b)	-	(+)	-
SOM / OSOM	96-100	bg-pg, ch	cdp, ch	30-35	g-ch	gst	++ (p), (m)	+	i	s	-	-	(+)	+	1	(+)	-
SOM	100-109	sg, bg (l)	p	25-40	m, g (l)	-	+++ / (++) (p), (m)	(+)/ -	i	s / -	-	s	s	-	(+)/ -	/ (++) (r) (+) / -	-
OM	109-110	sg	p	35-50	m	-	+++++ (p)	-	-	-	-	s	-	-	-	-	s / -

Description: microstructure: sg – single grain, bg – bridged grain, pg – pellicular grain, ch – channel, pl – channel, p – platy; pores: p – platy; voids: cdp – compound packing voids, ch – channels, pl – planar voids; C:F relate distribution: m – monic, g – granostriated, po – porostriated, bst – distribution pattern: i – isolated, a – articulated Frequency – pedofeatures (in brackets the frequencies for other groundmass components): s – single, (+) – <5% single (<5%), (++) – <2% single (<5%), (++) – <2.2% (<5%), (++) – <2.5% (5-15%), +++ – 5-10% (5-30%), +++++ – 10-20% (30-50%), ++++++ – >20% (50-70%).

Other: (l) – only local occurrence, (p) – well preserved, (m) – mineralized, (b) – bunt, (r) – redeposited

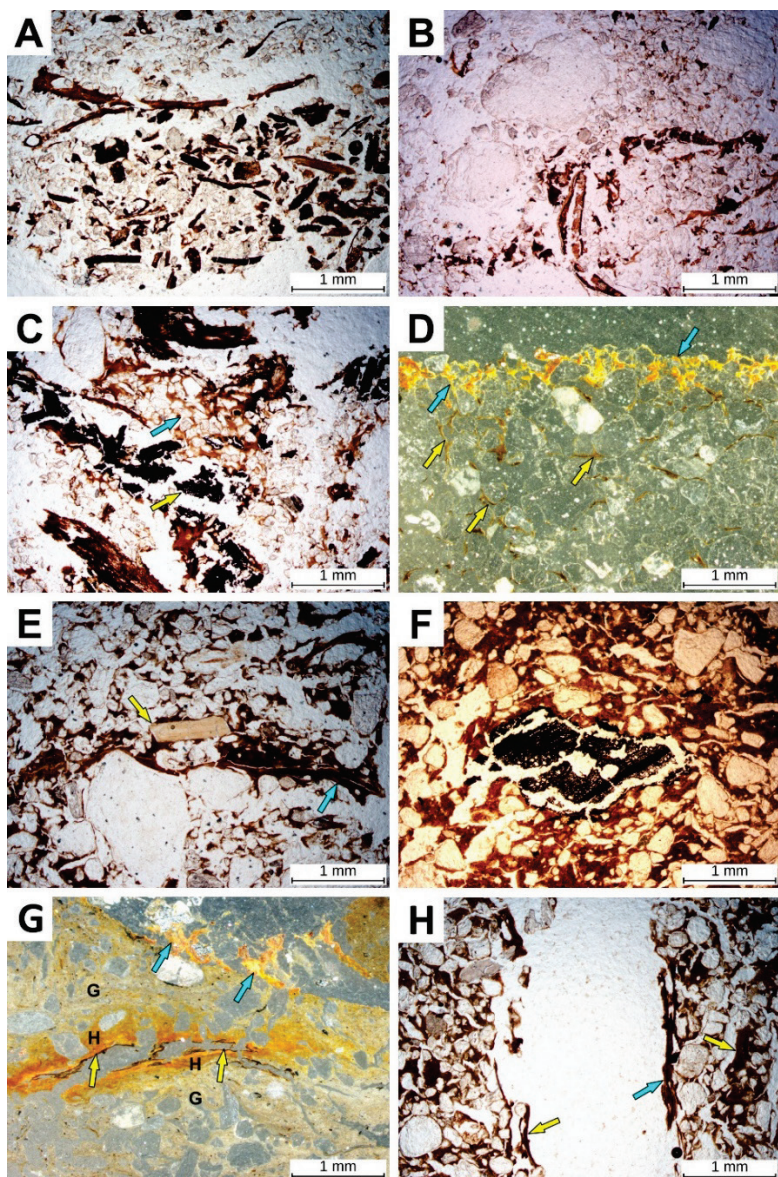


Fig. 4. Selected micromorphological features of STII L29 core deposits (analysis by M. Krupski)

- A. Well-preserved plant remains and sand (OM, lower half of photo) and SOM (upper half). PPL
- B. Boundary between undisturbed microfabric of SOM (right half of photo) and “mixed” zone. PPL
- C. Redeposited (?) elements of “mixed” zone microfabric: charcoal (yellow arrow) and clay-rich soil fragment (blue arrow). PPL
- D. Iron oxide precipitation around sand grains (blue arrows) in uppermost part of SOM. Clay coatings/bridges around and between sand grains (yellow arrows). OIL
- E. Moderately sorted sand grains of the OSOM bridged and coated/capped by organic-rich clay with Fe/Mn staining (blue arrow). Note horizontally aligned fragment of bone (yellow arrow). PPL
- F. Charcoal (middle) and moderately sorted sand grains embedded in a matrix of clay containing organic particles (dusty clay), in uppermost studied part of OSOM. PPL
- G. Redoximorphic features in uppermost part of OSOM: depletion (G) and precipitation of Fe/Mn: hypocoatings (H) and coatings (yellow arrows) along a pore, Fe-pseudomorphosised plant remains in a channel (blue arrows). OIL
- H. Vertical soil fauna channel with dusty clay coatings (yellow arrows) and Fe/Mn-pseudomorphosised plant remains (blue arrow). PPL

type of light: PPL – plane polarised light, OIL – oblique incident light

The muddy sand with organic matter (OSOM) seems to be relatively enriched in anthropogenic inclusions – charcoal, bone fragments (<2 mm in size, some of them apparently burnt) and a single flint fragment (100–96 cm), while in the underlying SOM and OM only single charcoal and bone fragments were identified, mostly within the “mixed” zone of the SOM.

Clay translocation features (dusty clay coatings and bridges) are characteristic for the profile, being very rare in the uppermost part of the SOM (bridges, <2%-single) and best pronounced in the OSOM (96–83 cm). Clay crusts (dusty clay) – most likely of a sedimentary nature – that cap mineral grains were found *in situ* in the OSOM – they also occur in redeposited, randomly oriented form (angular clay-rich soil fragments) in the “mixed” zone in the SOM or as channel infilling material in the OSOM (90–83 cm). Redoximorphic features are prominent in the sequence: they appear at the interface of the SOM and OSOM (*ca* 100 cm) and above, and take the form of nodules, hypocoatings along channel walls, and coatings. Concentrations of redox features (organic matter pseudomorphosis, coatings) locally also form horizontal “iron-

pans”/“crusts” – the continuity of one of which seems to be cut in the SOM by the edge of the “mixed” zone. Soil fauna activity is evidenced by void infillings in the OSOM and mite excrements recognised on single plant remains in the OM and SOM.

Plant macrofossils

Phase I (Se-1 L MAZ, 114–106 cm b.g.l.) (Fig. 5). In this phase, the remains of aquatic shallow standing water plants such as *Nuphar lutea*, *Potamogeton pusillus* or *Potamogeton gramineus* are present. The yellow water lily prefers eutrophic lakes, while the aforementioned Potamogeton species grow in cool waters with different trophic ranges from meso- to eutrophic. In this phase of the lake’s existence, rush vegetation (probably of the type *Magnocaricion* with *Carex pseudocyperus*, *Lycopus europaeus*, *Schoenoplectus lacustris* and *Mentha aquatica*) also grew on its shores. Moist, nitrophilous and periodically flooded banks were occupied by the type of riparian forests of *Alnus glutinosa* and *Urtica dioica*. Meanwhile, spruce grew in drier places.

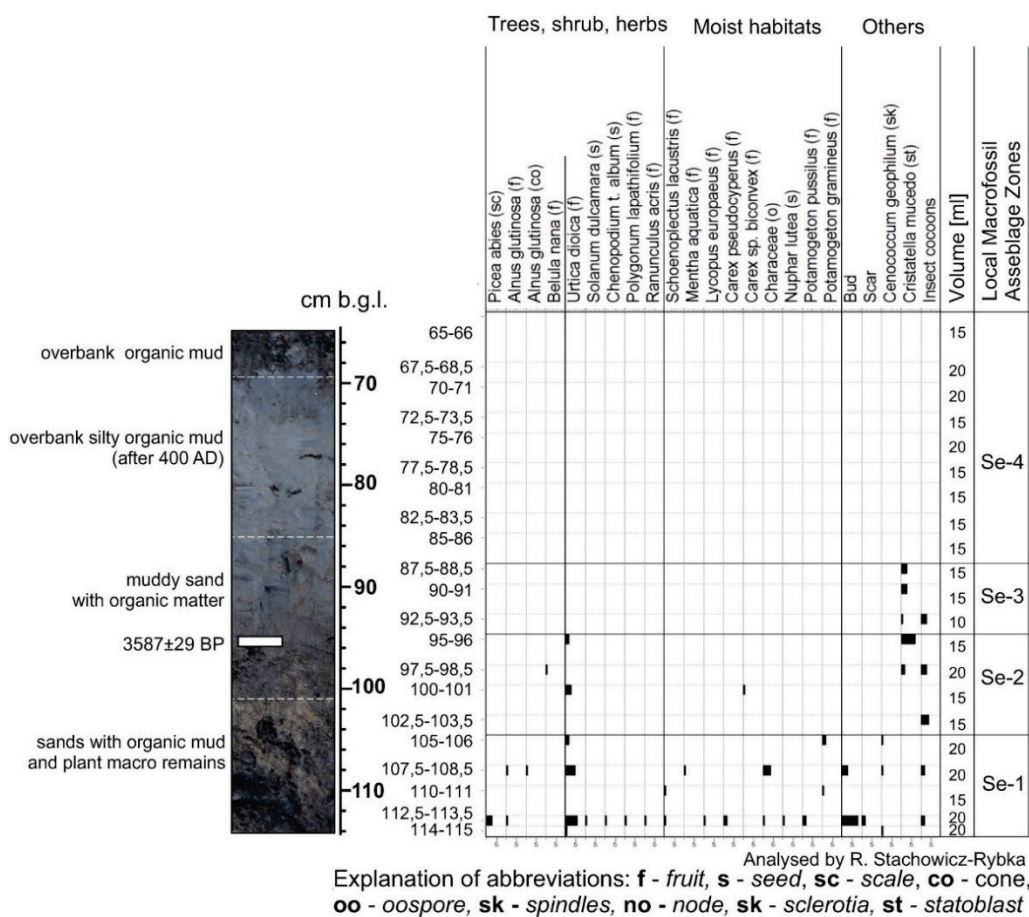


Fig. 5. Plant and other macrofossil diagram for STII L29 core deposits (analysis by R. Stachowicz-Rybka)

Phase II (Se-2 L MAZ, 106–96 cm) at this level the share of plant remains decreased, and the water macrophytes in particular disappeared. Among the plant macrofossils representing the aquatic environment, there were only the bryozoans *Cristatella mucedo*, which now most often occur in cool and clear waters with a temperature of usually around +16 °C (Økland, Økland 2000). *Carex* sp. biconvex and *Urtica dioica* continued to grow in moist, high-trophy habitats. Moreover, *Betula nana*, a species characteristic of the cool, boreal climate, appeared. Nevertheless, at present it occurs in a relict form in NE Russia – in the Novgorod Oblast and the Tver Oblast, i.e. regions adjacent to the Smolensk Oblast. (<https://www.discoverlife.org/mp/20q?search=Betula+nana&guide>). On the other hand, it is also possible that *Betula nana* nuts were redeposited from the Late Vistulian (Valdai) deposits.

Phase III (Se-3 L MAZ, 96–87.5 cm) contains very few plant remains, among which only *Cristatella mucedo* statoblasts were determined. This indicates that water conditions were still maintained. Insect remains are also present.

Phase IV (Se-4 L MAZ, 87.5–63 cm), the lack of plant macrofossils may suggest a quick flow of clastic material and processes of decomposition of organic remains.

Palaeozoological fossils

Cladocera

Phase I (wet stage: 114–100 cm b.g.l.) (Fig. 6). This is the phase with the highest Cladocera abundance. Pelagic species such as *Bosmina longispina* and *Bosmina coregoni* occur in this phase. The sediment-associated taxa represent *Monospilus dispar*, eutrophic *Alona guttata* and *Leydigia leydigii*. Warm littoral species such as *Graptoleberis testudinaria*, *Chydorus* sp. and *Kurzia lattissima* occur as well. At a depth of 102.5 cm there appears *Alona quadrangularis*, which inhabits the littoral zone of stagnant waters. It is an open-water phase, with rapid shallowing at its final stage.

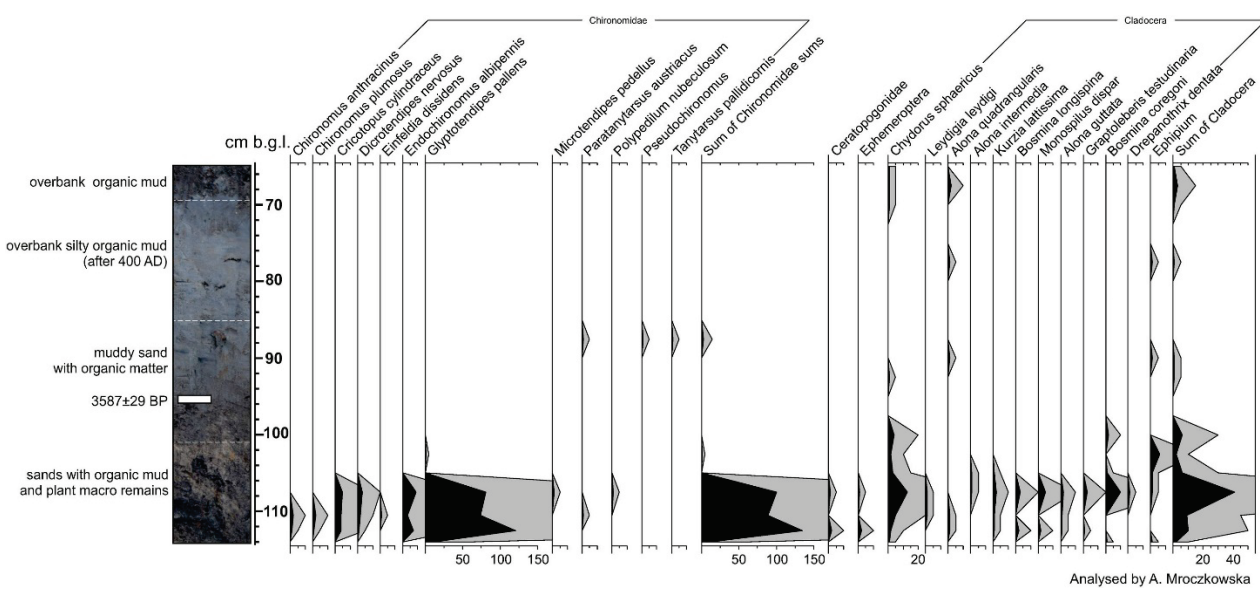


Fig. 6. Sum of subfossil Chironomidae and Cladocera remains for STII L29 core deposits (analysis by A. Mroczkowska)

Phase II (drought with episodic water level increase: 97.5–72.5 cm). During this phase, only single *Chydorus* sp. and *Alona quadrangularis* appear. The first species is a ubiquitous taxon with a large tolerance range. The temporary lack of Cladocera points towards episodes with an increased inflow of sediment to the periodic water bodies, which demonstrates shallowing and terrestrialisation processes (Pawlowski et al. 2013).

Phase III (wetter condition: 72.5–65 cm). *Alona quadrangularis* and *Chydorus* sp. indicate the presence of an at least semi-permanent water body.

Chironomidae

Phase I (wet phase: 114–107.5 cm b.g.l.). In the first phase, the *Glyptotendipes* type *pallens* is abundant. This species is associated with decaying

coarse organic matter at the lake littoral bottom and with macrophytes. Its larvae have a relatively high resistance to freezing. *Endochironomus* type *albibennis* and *Dicrotendipes* type *nervosus* are secondary taxa in the communities. They also inhabit the littoral of meso-eutrophic lakes and are sometimes reported from plant microhabitats. The other recorded taxon – *Cricotopus* type *cylindraceus* – is found in eutrophic lakes and meso-saprobic flowing waters. Ceratopogonidae are found in great numbers on aquatic plants occupying a wide range of ecological niches. Besides midges, Ephemeroptera larvae subfossils were discovered. Many mayflies are abundant in running waters (Brooks *et al.* 2007).

Phase II (dry phase: 107.5–65 cm). In this phase Chironomidae nearly completely disappear. The main factors that might cause the lack of Chironomidae communities are large inflows of sediments (river inflow, flooding or flushing, or slope wash processes), shallowing of the pond and/or the presence of cyanobacteria blooms (Nolte 1989; Jeppesen *et al.* 2001). At the core depth of 87.5 cm there are a few specimens of the *Paratanytarsus* type *austriacus*, *Pseudochironomus prasinatus* and *Tanytarsus* type *pallidicornis*. These morphospecies occur in the littoral zone of lakes, often on sandy bottoms (Pinder 1983), as well as in colder climatic conditions (like *Paratanytarsus* type *austriacus*, which is associated with macrophytes) (Buskens 1987; Brooks *et al.* 2007). *T. pallidicornis* type and *P. austriacus* type have been recorded in European stagnant and flowing waters, whereas *Pseudochironomus* type inhabits only stagnant waters. The *P. austriacus* reveal one spring generation in cold-temperate climate, whereas in warm-temperate regions of Eastern Europe it can reveal also a second, summer generation. *T. pallidicornis* type is a multivoltine species. *Pseudochironomus* type has one long generation that emerges in late summer. In Western Europe, *Pseudochironomus prasinatus* overwinter in second, third and fourth instar. The above indicates that all three species' third and fourth instar larvae could be found in winter and spring (until April) in the Serteyka River–lake backwaters (Gilka 1999, 2011; Moller Pillot 2009). The third and fourth instars larvae head capsules mostly accumulate in sediments (Brooks *et al.* 2007), and those instars were collected from the 87.5 cm layer in the L29 II zone.

Serteya II layer α profiles

Soils of the settlement Serteya II layer α partly represent the nature of Mid-Holocene pedogenesis (Aleksandrovsky, Aleksandrovskaya 2005). The studied profiles were located in the lower part of a gentle slope of the present day Serteyka River, in squares G/15 and B/15 (Fig. 1). The cultural horizons of the Early Middle Ages, Bronze Age and Neolithic were recorded in the G/15 profile, buried by slope deposits of the most recent centuries and a modern dump. The investigated profile was located between two Neolithic pits filled with dark, almost black, soil material. Here, due to the supply of fine particles along the slope and additional humidification, more eutrophic conditions were created and the intensity of soil degradation processes decreased. The thickness of the dark horizon of the buried soil is low (up to 10 cm), due to erosion and to removal of material from elevated ground to the pits, where it was mixed with other horizons. The increased dampness in the pits contributed to the preservation of organic matter, resulting in the formation of a thick, dark-coloured horizon in the pit infills. The upper part of the pits is less humidified and therefore the relict organic matter here degraded and became lighter. This was promoted by the processes of podzolisation typical of the Late Holocene (Aleksandrovsky, Aleksandrovskaya 2005).

The G/15 consists of seven main pedological units (Fig. 7, Table 2):

100–80 cm b.g.l. – glaciofluvial silty variegated sand with gravel with iron precipitation (B horizon);

80–70 cm – brown silty sand with humic admixtures (B horizon with Early Neolithic cultural layer);

70–65 cm – light grey silty sand with krotovinas (AB horizon with Middle and Late Neolithic cultural layer);

65–60 cm – whitish-grey silty sand with krotovinas (AB horizon with Bronze Age cultural layer);

60–50 cm – dark grey to black humic silty sand (Ah – humic horizon of buried soil with Early Middle Ages cultural layer);

50–40 cm – layered clayey and silty sand with humic admixtures (Middle Ages slope deposits);

40–0 cm – humic muddy sand (tillage diamicton and dump).

The bottommost samples of the studied G/15 profile represent substratum deposits of the Weichselian (Valdai) kame. These glaciofluvial deposits consist mostly of vari-grained sands – the fraction between 1.32 and 2.32 phi (0.4–0.2 mm) ranges between 30 and 36%. The percentage of coarse-grained sand and gravel (i.e. <1 phi, >0.5 mm) reaches up to 17.5% and of mud (i.e. >3.32 phi, <0.1 mm) – from 19 to 24%. The grain-size distribution of these deposits is bimodal with three peaks: two sandy at 2 or 2.32 (0.25 or 0.2 mm) and

one silty 3.99 phi (0.063 mm). This demonstrates a short period of clastic material transportation and partial preservation of earlier traits of source deposits (probably of glacial origin). Glaciofluvial deposits are characterised by mean grain size of 2.13–2.33 phi (i.e. 0.20–0.23 mm), sorting of 1.18–1.19 (i.e. poorly sorted) and symmetrical skewness. In the C-M diagram after Passegå and Byramjee, these sediments are placed within Class I, which shows that they were transported by rolling and saltation (Passegå, Byramjee 1969).

Table 2

Sertey II layer α: soil and sediment analyses: results of B/15 and G/15 profiles

Description of horizons	Depth [cm b.g.l.]	pH H ₂ O	Organic Matter [%]	P ₂ O ₅ [%]
Sq. B/15				
A	15–27	5.9	0.90	0.14
AB – slope deposits, Early Middle Ages pottery and remains of dwelling in bottom	27–42	6.2	0.76	0.11
Ah – Bronze Age pottery	42–48	6.25	2.52	0.45
Ah – Late Neolithic pottery dominates	48–65	6.4	1.83	0.53
AB – Late and Middle Neolithic pottery in upper part, Early Neolithic pottery in lower part	65–90	6.3	0.54	0.33
B – glaciofluvial deposits	90–120	6.45	0.22	0.20
Sq. G/15				
AB – slope deposits	30–40		4.09	0.18
AB – slope deposits, Middle Ages pottery	40–50		2.87	
Ah – Early Middle Ages pottery	50–60		3.59	0.50
AB – Bronze Ages pottery	60–65		1.35	0.15
AB – Late and Middle Neolithic pottery	65–70		1.48	0.18
Ah – Neolithic pit	100			0.32
B – glaciofluvial deposits	80–100		0.80 0.62	

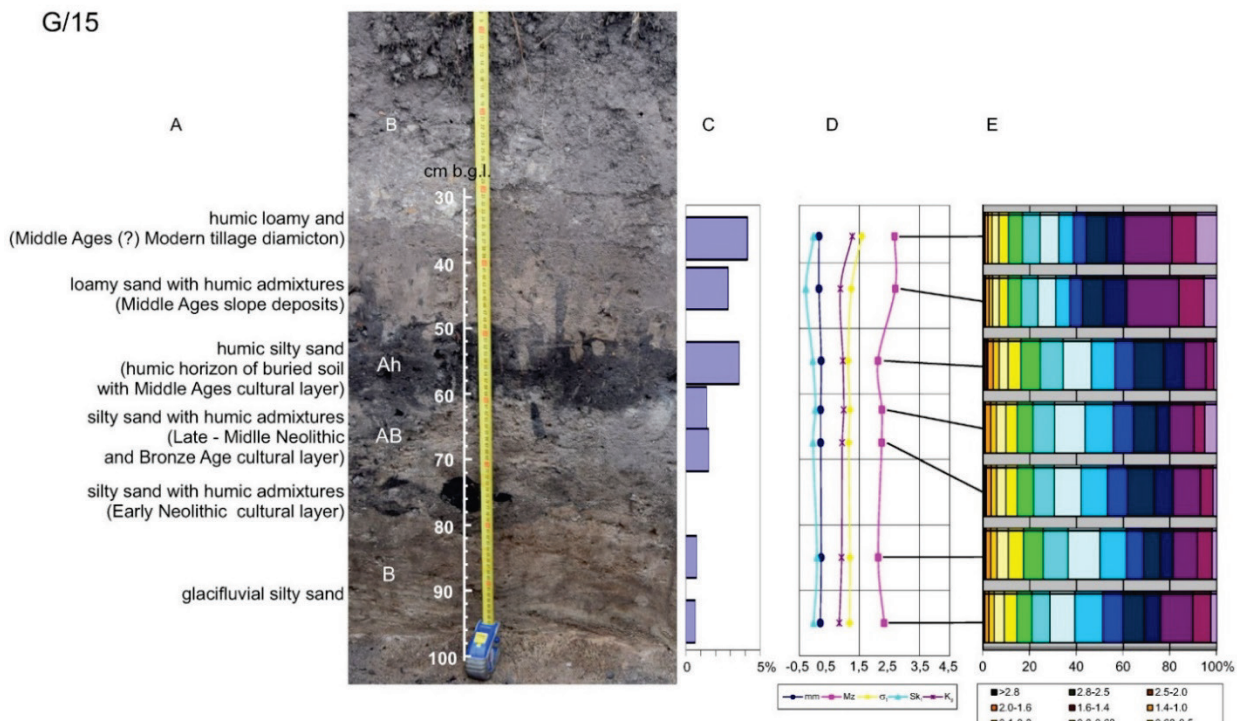
Traits similar to the substratum of glaciofluvial deposits can also be seen in the sedimentological characteristic of cultural layers. The mean grain size of deposits with cultural layers ranges from 2.12 to 2.25 phi (0.21–0.23 mm), sorting is 1.13–1.19 and the skewness remains symmetrical. However, the grain-size distribution of these deposits is trimodal with a further peak at 3 phi (i.e. 0.125 mm). This demonstrates the growing role of a new depositional factor – most probably slope processes at the site – in the period of formation of the Neolithic and Bronze Age cultural layer. Subsequently, in the upper part of these deposits a soil humic horizon (Ah) developed up to the Early Middle Ages.

The textural traits of slope deposits that cover the medieval buried soil differ substantially from the characteristics of underlying deposits. This stratum is marked by a distinct increase in the mud fraction (<0.1 mm) admixture – 38–40%, along with LOI (3–4%). The deposits are composed mostly of silt (3.82–3.32 phi, 0.1–0.071 mm) ranging 20.5–22.4%. The mean grain size is 2.7 phi (i.e. 0.16 mm), sorting – from 1.23 to 1.58 (poorly sorted) and the skewness ranges from -0.28 to -0.02 (coarse skewed to symmetrical). The described deposits can be recognised as “soil deluvium” according to Stochlak (1996) – i.e. slope wash deposits accumulated after the deforestation of an area, as a result of soil humic horizon erosion. In the very top part they pass into

unstructured (massive) tillage diamicton after Sinkiewicz (1995, 1998) or “agricultural deluvia” after Stochlak (1978, 1996). These deposits could also (at least partly) originate from an artificial

earthwork, meaning that they were accumulated as a result of intentional and direct human activity. This could explain the clear difference in textural traits, in comparison with underlying sediments.

G/15



B/15

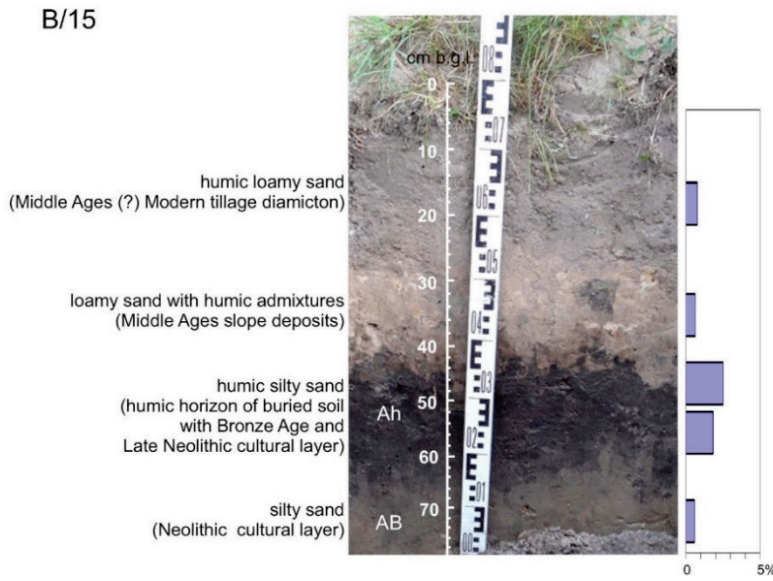


Fig. 7. Lithology of deposits of Serteya II layer α profile

- A. Lithologic profile
- B. Pedological horizons
- C. Content of organic matter
- D. Folk and Ward coefficients

mm – mean grain size [mm], M_z – mean grain size [phi], σ₁ – sorting index, Sk₁ – skewness, K_g – kurtosis

- E. Grain-size distribution

Anthracological studies showed the presence of five taxa of trees and shrubs within deposits of the G/15 profile: *Corylus avellana* L. hazel (eleven fragments), *Alnus sp.* alder (five fragments), *Acer platanoides* maple (three fragments) and one fragment each of *Juniperus communis* common juniper and *Abies sp.* fir. The taxonomic composition of the charcoals in individual samples is presented in Table 3. Both the number of fragments and taxonomic differentiation were very low. In the samples dated to the Middle and Late Neolithic

(samples 9, 11, 16) only charcoals of hazel and alder were identified. In the Bronze Age layer (no. 7) single fragments of fir and juniper were found, and in the Early Medieval samples (no. 2, 3) remains of hazel, maple and alder were discovered. Charcoals obtained from samples 3 and 16 were characterised by a smooth surface and rounded edges. In the case of a few fragments, in samples 3 and 7, numerous radial cracks, local wood tissue burnout and traces of vitrification were found. In sample 16 the remains of branch wood occurred.

Table 3

Serteya II layer α : taxonomic spectrum of charcoals from G/15 profile

Sample No.	Depth [cm b.g.l.]	Soil horizons	Number of charcoal fragments					Sum
			<i>Abies sp.</i>	<i>Acer platanoides</i>	<i>Alnus sp.</i>	<i>Corylus avellana</i>	<i>Juniperus communis</i>	
2	50–60	Ah			2	6		8
3				3				3
7	60–65	AB	1				1	2
9	65–70	AB			2	1		3
11					1			1
16	100	Neolithic pit				4		4

The presence of hazel and alder charcoals in Neolithic sediments reflects the widespread occurrence of these taxa in the upper Western Dvina River region during this period, as documented by pollen studies of Dolukhanov *et al.* (1989) and Tarasov *et al.* (2019). The importance of hazel shrubs for the economy of Neolithic communities at the Serteya II site has also been confirmed by previous research, which showed the use of hazelnuts as a food resource, and *Corylus* wood as material for the production of certain elements of pile-dwelling constructions (Mazurkevich *et al.* 2010). Wood charcoal fragments from the Neolithic pit were strongly smoothed and rounded, which in turn may suggest their displacement. According to Scott (2010), macroscopic charcoals may be transported over long distances, especially by slope wash processes.

The finding of *Abies* remnants in the sample attributed to the Bronze Age (no. 7) is a controversial discovery. The Serteya region is outside the modern range of the *Abies* genus. The closest to the studied region, but about 700 km from the site, is the north-eastern limit of the modern range of *Abies alba* in central Poland (Danielewicz 2012). According to Środoń (1983), there is no reliable palaeobotanical evidence that would indicate a wider, north-eastern range of the common

fir tree, including in earlier climatic periods. The most northerly range limit is that of *A. sibirica*, but it occurs only in the eastern part of Russia (Bugala 1991; Podbielkowski 2002; Johnson 2014), over 1,500 km from the Serteya site. Due to the lack of other confirmed palaeobotanical reports on the appearance of *Abies* macroremains in the forest communities of the East European Plain, contamination of sample 7 by younger material may be suspected. Xylological data indicate that *Abies alba* wood was an item of intensive long-distance trade in early historical periods (e.g. Pukienė 2008; Cywa 2018 with further literature). The single fragment of juniper charcoal was determined in sample 7. As the site is located within the contemporary range of *Juniperus communis* (Benkowa, Schweingruber 2004; Hantemirova *et al.* 2012), the local provenience of its wood is probable, though pollen grains of juniper have not been recorded in local palynological diagrams (Dolukhanov *et al.* 1989, 2004; Tarasov *et al.* 2019; Kittel *et al.* 2020). The structure of both fragments from sample 7 is characterised by numerous radial cracks and local vitrification of tissues. Such fusions and fissures can be caused by rapid combustion at high temperatures (Marguerie, Hunot 2007; Barnett 2012).

The B/15 consists of five units (Fig. 7, Table 2):
120–90 cm b.g.l. – glaciofluvial silty sand with iron precipitation (B horizon);

90–65 cm – greyish brown silty sand with krotovinas (AB horizon with Late and Middle Neolithic cultural layer and Early Neolithic cultural layer in the bottom);

65–42 cm – dark grey to black humic silty sand (Ah – humic horizon of buried soil with Late Neolithic and Bronze Age cultural layer);

42–27 cm – light brown clayey-silty sand with humic admixtures (Middle Ages slope deposits);

27–15 cm – grey and brown humic clayey-silty sand (tillage diamicton).

In section B/15, the cultural layer was found in the buried soil (Ah) with a thick (20–25 cm thick) dark-coloured humic horizon. A transition horizon AB (25 cm) was recognised below, with a large number of krotovinas. It overlies a brown coloured B horizon, in which krotovinas were also identified. The total thickness of the humus-rich part of the soil profile reaches 45–50 cm. The development of this profile is associated with a long meadow stage, probably of anthropogenic character. The high content of charcoal, including dispersed particles, obviously results from human activity. Probably, it also led to a darkening of the colour of the cultural layer.

A dark humic (carbon-rich) Ah horizon is well represented here and covered only by slope deposits as well as a modern drainage dump from the reclamation canal. The process of podzolisation has changed only the upper part of the humic horizon. The lower part of the Ah horizon, containing archaeological material, and the lower AB horizon, typical of soils of unforested areas (grassland and meadow black earth) are well preserved; noteworthy is the large number of krotovinas. The silty composition of this buried soil contributes to the preservation of organic matter. The considered stage of soil formation can be correlated with a wide period (Atlantic – middle Subboreal) on the basis of archaeological finds.

Phosphate analysis was applied in studies of the cultural layers in profiles G/15 and B/15 (Table 2). Phosphorus is distinguished by its stability in soils and remains in the cultural layer for a long time (Velleste 1952; Hamond 1983). Much depends on the form in which phosphorus is present. When applying phosphorus fertiliser, it is quickly washed away. But the settlements may have stable forms, primarily apatite (calcium phosphate), which forms the basis of bone. It is stable in muddy soils and is quickly washed out of sandy soils.

The stability of phosphorus in the studied soils differs. In the section in square B/15, more phosphorus was preserved in a thick buried soil layer, where the content of clay is higher. In the eroded soil (section G/15) it is preserved only in the early-medieval buried soil, while in the Bronze Age and Neolithic Age layers its content is similar to that of substratum deposits.

Discussion: sedimentological and post-depositional processes in the shore zone

The sediments of the lower unit (115–85 cm b.g.l.) – fine- and medium-grained sands with silt sands – were accumulated under various sedimentation conditions. Based on the distribution of samples on the mean grain size (M_1) and standard deviation (M_2) diagram (Fig. 2F), referring to the opinion of Sly *et al.* (1983), it can be concluded that they were deposited in upper flow regime conditions. Settlement velocity flow was on average 20 cm/s and ranged from 13 cm/s to 25 cm/s. The shear velocities of flow necessary for transport of the thickest grains were about 90 cm/s. Moreover, referring to the views of Mycielska-Dowgiałło and Ludwikowska-Kędzia (2011) and based on distribution of samples on the mean grain size (M_z) versus sorting (σ_1) diagram (Fig. 2G), they are river channel and bed lag alluvia, or glaciofluvial sediments. Having in mind the aforementioned considerations, and due to the relatively high content of organic matter (at the level of 4.85%) and low content of lithophilic elements (Na often below 0.1 mg/g, K often below 0.5 mg/g and Mg often below 1 mg/g) in these sediments, the deposits of the lower unit can be considered to be channel alluvia. Since the structure of the sediments of the lower sedimentation unit is deformed (Fig. 3), and they are located at the foot of the kame slope, it can be assumed that the sediments of this series were subsequently displaced as a result of slope wash processes. It must be stressed that slope wash processes were confirmed also for the G/15 profile in the Middle and Late Neolithic.

The results of palaeoecological analyses (both palaeobotanical and palaeozoological) demonstrate that the sediments from the depth between 115 and 106 cm b.g.l. in the L29 core contain species characteristic for shallow standing water, which indicates the nearby presence of a lake, as well as its possible episodic transgressions into the shore zone during periodic or seasonal increases in water level. After that, a rapid

shallowing of the reservoir is observed together with an increase in clastic material inflow. The sharp border of the Fe/Mn (from 273 to 137) and Cu/Zn (from 0.52 to 0.4) ratios also proves the sudden change in deposition environment. These sediments are enriched in lithophilic elements (Na, K and Mg), whereas the content of Ca is constant (*ca* 4.5 mg/g). The conclusion of the STII M25 core study, too, shows that a steady decrease in shallow water cover could have occurred in the studied area up to *ca* 4150 BC. The Early Neolithic communities existed at the Serteya II layer α site as well as on the lake shore before 4150 BC. During this time, cultural layers were destroyed – probably by slope processes and lake water transgressions. The most significant increase in water level was defined for the period between 4150 and 3600 BC (Kittel et al. 2020). However, it did not reach the area of the L29 core (Fig. 3). Evidence of intense settlement activity in the lake shore zone (Sertya II-2 site) was recorded for the period *ca* 4150–3250 BC and denudation processes were active even until *ca* 2500 BC (Kittel et al. 2020).

The micromorphological study of the stratigraphic sequence of the L29 monolith allows for more detailed assumptions regarding formation processes of the deposits in the palaeolake shore zone. The horizon described as organic mud (OM, 109–110 cm b.g.l.) consists mostly of terrestrial plant remains, many horizontally aligned, and detritus (Fig. 4A), with single fine charcoal fragments. It may represent the natural accumulation of organic material in the transition zone between the lake and land, but anthropogenic settlement activities, too, should be taken into account as a primary forming factor, as in the case of similar contexts (albeit with more numerous and differentiated anthropogenic inclusions) investigated at Lake Luokesa (Lithuania) and several Swiss lakeshore sites (Ismail-Meyer et al. 2013; Ismail-Meyer 2014). The relatively good state of preservation of the plant remains and only limited presence of soil fauna excrements (mites) indicate a considerably high accumulation rate, rapid burial and generally waterlogged conditions (Fe/Mn ratio above 280 and Ca/Fe ratio above 1.5) of the deposit at the depth 109–110 cm b.g.l. of the L29 core sequence.

The SOM layer (96/100–109 cm) is composed of moderately-well sorted sand, plant remains (many horizontally aligned, Fig. 4B), detritus and single charcoal and bone fragments. It also includes a poorly-moderately sorted “mixed” zone, juxtaposed with the original, undisturbed

microfabric; the majority of anthropogenic inclusions are found within this zone, along with occasional angular clay-rich soil fragments (Fig. 4B, C), similar to material building the OSOM (see below). A combination of inland and littoral factors may have been responsible for the formation of the SOM: erosion of the upper sandy slopes of the kame and the resulting sedimentation of runoff downslope have to be considered (Ismail-Meyer et al. 2013; Ismail-Meyer 2014). Also, the possibility that both the OM and SOM may have been (re)worked by episodic increases in the lake water level should be acknowledged, although no diatoms and only single sponge spicules were discovered. On the one hand, this would include the input of fine sand and detrital material, and, on the other hand, the possibility of the removal (truncation) of certain parts of the OM-SOM sequence (Karkanas et al. 2011; Ismail-Meyer et al. 2013). The coarser (medium, coarse) sand horizon at *ca* 105 cm b.g.l. is potentially a sign of an erosion surface in the lake shore zone.

Neither the OM nor SOM unit was formed in a subaqueous environment, as no laminations or bedding of silt and sand were observed (see: Karkanas et al. 2011; Stahlschmidt et al. 2015), but they remained largely waterlogged, which ensured good preservation of plant remains. At least periodic drying of the uppermost part of the SOM, at its microscopically gradual interface with the overlying OSOM horizon, is indicated by the presence at this depth of redoximorphic features (Vepraskas et al. 2018). The highest concentrations of Fe (above 12 mg/g) are double the values from the lower part of the profile, and moreover, they correlate with catchment erosion index (Na+K+Mg/Ca from 3.2 to 4.3). Among them is a horizontal Fe/Mn-rich “crust” (Fig. 4D) formed at *ca* 100 cm b.g.l., the continuity of which appears to be vertically cut by the edge of the “mixed” zone. In thin section, the mixed zone has a defined, (sub)angular shape, with vertical and oblique boundaries. Apart from single anthropogenic materials, the “mixed microfabric” includes randomly oriented and distributed mineral grains (also coarse and medium), few plant remains, detritus and occasional angular fragments of clay-rich crusts/soil, of the kind found *in-situ* in the overlying OSOM (Fig. 4B, C, E, F). The issue of whether these signs of reworking (mixing) are related to natural causes (e.g. bioturbation, deformation) or anthropogenic activity (e.g. digging) (Deák et al. 2017; Krupski et al. 2017), remains unclear at the moment. A similar feature was identified by Karkanas et al. (2018) and inter-

preted as oxidised surface crust disturbed possibly by trampling.

Again, a significant increase in the palaeolake water level took place *ca* 2300–2200 BC and later regression occurred (Kittel *et al.* 2020). The coarse detritus gyttja layer in the STII M25 core that accumulated in that time is interlaminated in the L29 core (at 100–83 cm b.g.l.) with muddy sand with organic matter, characterised by an enrichment in Fe and lithophilic elements in relation to Ca content (Fig. 2). The deposition of muddy sand with organic matter unit started shortly before 2000–1900 BC, as confirmed by the ^{14}C date of plant macrofossils from the depth of 95 cm b.g.l. This demonstrates that the lacustrine environment could periodically (e.g. during spring floodings) reach the L29 area *ca* 2300–2200 BC, as suggested by the palaeoecological proxies, mostly subfossil Cladoceran remains. In the later period, regression occurred again. From 2100 BC onwards, only short seasonal (spring) floodings with eutrophic water cover *ca* 2000–1900 BC were recorded in the STII M25 core (Kittel *et al.* 2020). In that period, a few chironomid head capsules representing three taxa (*Paratanytarsus austriacus*-type, *Pseudochironomus*-type and *Tanytarsus pallidicornis*-type) were recorded in the L29 (only at a depth of 87.5 cm) that are typical of stagnant and flowing waters in the European lowlands (Giłka 1999, 2011). At the same depth, the presence of *Cristatella mucedo*, usually found in lakes with a constant water level, confirms these observations (Økland, Økland 2000). The presence of midge subfossils in the layer of muddy sand with organic matter, coincides with incidental chironomids and bryozoan occurrence in nearby M25 (Kittel *et al.* 2020). Because the concentration of subfossils is very low (Fig. 6), it does not indicate the presence of a permanent water body. Such episodic aquatic midge records reveal periodic (seasonal) inundation of area L29. The local palaeogeographical situation, along with recorded chironomids' taxa phenology (Giłka 1999, 2011), suggests that L29 inundation took place during the spring season, when the water level of Serteya River increased due to snow thawing and fed the palaeolake in the Serteya II site area. Simultaneously, melting snow waters encouraged slope wash processes.

The clayey and silty sand with organic matter sequence recognised from 100/96 to 80 cm b.g.l. (OSOM unit) is characterised by more developed types of microstructure as compared to the OM and SOM. The moderately sorted mineral grains are bridged and coated/capped by the fine fraction

($<2\ \mu\text{m}$) (Fig. 4E) or embedded in a dusty clay matrix (in the uppermost 3 cm) (Fig. 4F). The plant remains are less numerous and more poorly preserved, but there are more punctuations and silt-sized detritus (within the clay), phytoliths, diatoms, and sponge spicules, as well as anthropogenic inclusions such as charcoal and bone fragments (also burnt). Considering the location of the L29 profile, these traits are consistent with a gradual build-up of deposits in a series of events that involved sedimentation of suspended material. Clay and organic matter laminae/crusts recognised locally may indicate surfaces created by individual flooding episodes. Some of these features include anthropogenic inclusions (Fig. 4E), which suggests that at least some of the artefacts within the OSOM may have been “brought” by the waters, as a result of flooding and/or slope wash processes.

The inflow of clastic material into the nearby lake reservoir is indicated by palaeoecological proxies. The vertical fluctuations of the $\text{Na}+\text{K}^+$ + Mg/Ca ratio, too, suggest periodic input of mineral matter from the catchment. Apart from short-term variations, a general increase in the catchment erosion indicator (to a value of 8.86) indicates a gradual increase in mechanical denudation near the reservoir. From a sedimentological point of view, the origin of sediments in the roof of lower sedimentation unit (*ca* 100–85 cm b.g.l.) can be interpreted as having accumulated in the littoral zone of the lake. According to Teisseyre (1988), these sediments are similar in texture to flood alluvia deposited in sub-aquatic conditions. Moreover, some of the clayey silty sands of deformed structure located at this depth can be considered to be deluvium deposited in a lake shore zone. The period of higher mechanical denudation corresponds with a decrease in the Ca/Fe ratio. The described geochemical stratification may be the result of a wetter climate phase and nutrient delivery due to wildfires in the catchment (Pleskot *et al.* 2018).

During the phases of inundation (flooding episodes) the reduction in Fe/Mn caused local gleying (Fig. 4G); the dispersion (deflocculation) of surface material also occurred, enabling downward movement of clay with organic matter particles (Fig. 4H) and silt after the waters had disappeared (Macphail *et al.* 2010; Vepraskas *et al.* 2018). This process was enhanced upon desiccation of the sediments, which resulted in the formation of cracks and “opening” of the deposits’ structure (Kühn *et al.* 2018). Further alterations indicate aerial exposure of the mudflats and their

subsequent drying – well visible are redoximorphic features, among them the replacement (pseudomorphosis) of organic matter (redeposited plant remains, roots *in situ*, detritus within clay laminae) with iron/manganese oxides (Fig. 4E, G, H), as well as signs of soil fauna activity (Fig. 4H) and plant growth (Macphail *et al.* 2010; Ismail-Meyer *et al.* 2013; Karkanas *et al.* 2018).

The period after *ca* 1700 BC is characterised by the process of natural succession of the lake towards a wetland in the STII M25 core. An intensification of slope processes occurred between *ca* 1850 BC and *ca* 1600 BC (Kittel *et al.* 2020), as a result of activity of the Bronze Age Textile Ceramics Culture communities in the first half of the 2nd mill. BC, on the kame surface at the Serteya II layer α site. The slope wash processes were documented in the G/15 profile for the Late Neolithic and Bronze Age and the intense inflow of clastic material is recorded in palaeo-ecological proxies in the L29 core.

Well-developed krotovinas indicate the genetic similarity of the buried soil recognised in both the G/15 and the B/15 profiles. Probably, erosion essentially affected the soil profile, and it is possible that the cultural layer was not only partially washed away, but also partly redeposited. As a result, the Bronze Age and Neolithic cultural layers are thin in the B/15 profile, *ca* 5 cm each, as is the overlying dark humic horizon of the Late Neolithic and Bronze Age buried soil. The results of a palaeopedological study of the B/15 profile led to the conclusion that the Serteya II layer α site area could have been used for agriculture in the Late Neolithic and Bronze Age, as evidenced by Tarasov *et al.* (2019; cf. however, Kittel *et al.* 2020). Due to the light sandy composition, these soils could have been cultivated easily in that period, while the adjacent areas, located on higher surfaces composed of moraine, were difficult for cultivation using the tools available at the time. Deforestation (confirmed also by palaeobotanical results) and extensive agriculture (traced by Tarasov *et al.* 2019) resulted in the creation of conditions suitable for slope wash processes on the slightly inclined silty sand surface.

In the top of the Bronze Age deluvium, a soil humic horizon formed until the Early Middle Ages in the G/15 profile. In the L29 core, the deposits of the upper sedimentation unit, i.e. silty sands with organic matter (85–65 cm b.g.l.), were accumulated under the conditions of a lower flow regime (Fig. 2), with an average settlement velocity of water flow of about 13 cm/s. Referring to the views of Mycielska-Dowgialło and Ludwi-

kowska-Kędzia (2011), based on the distribution of samples on the mean grain size (M_z) versus sorting (σ_1) diagram (Fig. 2G), it can be considered that they are overbank alluvia. The ^{14}C date set demonstrates that a fluvial system finally replaced the lacustrine system in the site area, and overbank deposition started between 300 and 1300 AD (Kittel *et al.* 2020). The terrestrialisation process and only semi-permanent water body occurrence are confirmed in our palaeozoological record, mostly recorded in Cladoceran remains. The intense inflow of clastic material suggests landscape openness of the site environment. From the Early Medieval layer in the G/15 profile, 11 fragments of well-preserved charcoals of alder, maple and ash were obtained, but only *Acer platanoides* charcoals had burnout traces and a few radial cracks. The intense human impact in Early Middle Ages Serteya II site area is evidenced by Tarasov *et al.* (2019) and also by new results by A. Hrynowiecka (pers. comm.).

Conclusions

Detailed analysis of lithological profiles and the archaeological context allowed for an understanding of Mid- and Late Holocene natural landscape evolution and human–environment relationships in a palaeolake shore zone of a recently glaciated area in the East European Plain. The geomorphological processes were highly influenced by lacustrine, slope and fluvial systems along with episodic human impact. All the changes that occurred are of natural, mostly climatic origin, but human impact on formation processes of deposits in the palaeolake shore zone is clearly visible and resulted in anthropogenic deposition and an acceleration of slope processes. The main phases of land relief formation in the Serteya II site shore zone (close to the STII L29 core) can be summarised as follows:

1. Mesolithic, Early- to Mid-Neolithic (from *ca* 9500 BC to 2300 BC) – natural accumulation of minerogenic and organic material in the transition zone between the lake and land, fluctuations in lake water level (inflow of minerogenic material, wave erosion), periodic drying; possible anthropogenic settlement activities; signs of slope processes from the Mid-Neolithic;

2. *Ca* 2300 BC – desiccation after the deposition of sediments at 115–100 cm in the L29 core;

3. Late Neolithic (*ca* 2300–2200 BC) – palaeolake water level increase; beginning of clayey silty sands with organic matter deposition;
4. Late Neolithic, Bronze Age (*ca* 2200–1500 BC) – successive deposition of muddy sands with organic matter (and anthropogenic inclusions) in the shore zone, during seasonal (spring-thaw) floods; stagnation of flood waters in shallow basins, subsequent drying-up of sediments followed by floral and faunal activity; possible slope wash processes resulting from snow melting in the area transformed by human activity;
5. Between *ca* 1500 BC and *ca* 400 AD – palaeolake regression, wetland development;
6. Middle Ages (after 400 AD) – overbank deposition; intense human impact;
7. A small area with fertile and open lands was located near the Neolithic–Middle Age settlement, which was possibly used for agricultural/cattle-breeding activities. Such anthropogenic influence may also be indicated by strong deforestation, which intensified slope processes.

Summarising, we want to stress that our results are the outcome of a geoarchaeological study, undertaken in strict cooperation with archaeological research already at the fieldwork stage. The reconstruction of complex conditions leading to the deposition of sediments in the palaeolake shore zone was possible only with the use of comprehensive palaeoenvironmental analyses of biotic remains and geochemical and sedimentological traits, as well as a pedological study with a very important role played by micromorphological analysis of deposits in the L29 core.

Acknowledgments

The palaeoecological research at Serteya II site is financed by grants from the “National Science Centre, Poland” based on the decision No. 2017/25/B/HS3/00274. Archaeological research was supported by a grant of the Russian Science Foundation (project “Lacustrine sites of the 4th–3rd mill. BC – the origins and development of pile-dwelling settlements phenomenon in NW Russia” №19-78-00009). The palaeobotanical analysis was supported by the W. Szafer Institute of Botany, Polish Academy of Sciences, from its statutory funds. The soil micromorphological observations were carried out at the Institute of Soil Science and Environmental Protection, Wrocław University of Environmental and Life Sciences, by kind permission of Prof. C. Kabała. We are indebted to J. Tomkowiak for help with geochemical sample processing. We also thank Ph.D. M.

Płociennik for his discussion and comments on our results.

References

- Aleksandrovsky A.L., Aleksandrovskaya E.I. 2005. *Evolyutsiya pochv i geograficheskaya sreda*. Nauka, Moskva.
- Andersen T., Cranston P., Epler J. 2013. Chironomidae of the Holarctic Region: Keys and Diagnoses. Part 1. Larvae. Insect Syst. Evol. Suppl. 66, Scandinavian Entomology Ltd., Lund.
- Barnett C. 2012. Additional specialist report “Environmental Wood charcoal” to the publication Suburban Life in Roman Durnovaria: Excavations at the Former County Hospital Site, Dorchester 2000–2001 by Mike Trevarthen, Wessex Archaeology; http://www.wessexarch.co.uk/files/projects/dorchester_county_hospital/02_Charcoal.pdf [available at 25.02.2012].
- Bengtsson L., Enell M. 1986. Chemical analysis. In: B.E. Berglund (ed.) *Handbook of Holocene Palaeoecology and Palaeohydrology*. John Wiley and Sons Ltd., Chichester: 423–451.
- Benkova V.E., Schweingruber F.H. 2004. Anatomy of Russian Woods. Haupt Verlag, Wien.
- Brooks S.J., Heiri O., Langdon P.G. 2007. The identification and use of palaeartic chironomidae larvae in palaeoecology. Quaternary Research Association, London.
- Berggren G. 1969. Atlas of seeds and small fruits of Northwest-European plant species with morphological descriptions. Part 2. Cyperaceae. Swedish Nat. Sci. Res. Council, Stockholm.
- Bjerring R., Becares E., Declerck S., Gross E.M., Hansson L.A., Kairesalo T., Nykänen M., Halkiewicz A., Kornijów R., Conde-Porcuna J.M., Seferlis M., Nõges T., Moss B., Amsinck S.L., Odgaard B.V., Jeppesen E. 2009. Subfossil Cladocera in relation to contemporary environmental variables in 54 Pan-European lakes. *Freshwater Biology* 54: 2401–2417.
- Bugała W. 1991. Drzewa i krzewy dla terenów zieleni. Państwowe Wydawnictwo Rolnicze i Leśne, Warszawa.
- Bullock P., Fedoroff N., Jongerius A., Stoops G., Tursina T. 1985. Handbook for soil thin section description. Waine Research, Wolverhampton.
- Buskens R. 1987. The chironomid assemblages in shallow lentic waters differing in acidity, buffering capacity and trophic level in the Netherlands. *Entomologica Scandinavica*, Suppl. 29: 217–224.
- Cappers R.T.J., Bekker R.M., Jans J.E.A. 2006. Digital seed atlas of the Netherlands. Barkhuis/Groningen University Library, Groningen.
- Courty M., Goldberg P., Macphail R. 1989. Soils and Micromorphology in Archaeology. Cambridge University Press, Cambridge.

- Cywa K. 2018. Uwarunkowania doboru surowca drzewnego w polskich grodach i ośrodkach wczesnomiejskich w średniowieczu – analiza ksylogiczna przedmiotów użytkowych. (Unpublished doctoral dissertation). Instytut Botaniki im. Władysława Szafera Polskiej Akademii Nauk, Kraków.
- Danielewicz W. 2012. Drzewa leśne Polski. In: W. Matuszkiewicz, P. Sikorski, W. Szwed, M. Wierzba (eds) *Zbiorowiska roślinne Polski. Lasy i zarośla. Ilustrowany przewodnik*. Wydawnictwo Naukowe PWN, Warszawa: 21-62.
- Deák J., Gebhardt A., Lewis H., Usai M.R., Lee H. 2017. Soils disturbed by vegetation clearance and tillage. In: C. Nicosia, G. Stoops (eds) *Archaeological Soil and Sediment Micromorphology*. Wiley-Blackwell: 233-264.
- Dolukhanov P.M., Gey N.A., Miklyayev A.M., Mazurkevich A.N. 1989. Rudnya-Sertseyska, A stratified dwelling-site in the upper Duna basin (a multidisciplinary research). *Fennoscandia Archaeologica* 6: 23-27.
- Dolukhanov P., Shukurov K., Arslanov A.N., Mazurkevich L.A., Savel'eva E.N., Dzinoridze M.A., Kulkova M., Zaitseva G.I. 2004. The Holocene Environment and Transition to Agriculture in Boreal Russia (Serteya Valley Case Study). *Internet Archaeology* 17, <http://intarch.ac.uk/journal/issue17>
- Frey D.G. 1986. Cladocera analysis. John Wiley & Sons Ltd.
- Folk R.L., Ward W. 1957. Brazos River bar: A study in the significance of grain size parameters. *Journal of Sedimentary Petrology* 27: 3-26.
- Gińska W. 1999. Sezonowa dynamika pojawiwybranych gatunków ochockowatych z plemienia Tanytarsini Pojezierza Kaszubskiego (Diptera: Chironomidae). *Acta Entomologica Silesiana* 7/8: 31-42.
- Gińska W. 2011. Analiza różnorodności faunistycznej ochockowatych z plemienia Tanytarsini w Europie (Diptera: Chironomidae). *DIPTERON*, 27: 11-31.
- Ginzburg K.E. 1981. Fozfor osnovnykh tipov pochv SSSR. Nauka, Moskva.
- Goldberg P., Macphail R. 2006. Practical and Theoretical Geoarchaeology. Wiley-Blackwell.
- Grimm E.C. 1987. CONISS: a FORTRAN 77 program for stratigraphically constrained cluster analysis by the method of incremental sum of squares. *Computers & Geosciences* 13: 13-35.
- Grimm E.C. 2016. *TiliaIT*. Available at <https://www.tiliait.com/>
- Hamond F.W. 1983. Phosphate analysis of archaeological sediments. In: *Landscape Archeology in Ireland*. Oxford. BAR British Series. Vol. 116: 47-80.
- Hantemirova E.V., Berkutenko A.N., Semerikov V.L. 2012. Systematics and gene geography of Juniperus communis inferred from isoenzyme data. *Russian Journal of Genetics* 48(9): 920-926.
- Ismail-Meyer K. 2014. The potential of micromorphology for interpreting sedimentation processes in wetland sites: a case study of a Late Bronze–early Iron Age lakeshore settlement at Lake Luokesa (Lithuania). *Vegetation History and Archaeobotany* 23: 367-382.
- Ismail-Meyer K., Rentzel P., Wiemann P. 2013. Neolithic Lakeshore Settlements in Switzerland: New Insights on Site Formation Processes from Micromorphology. *Geoarchaeology: An International Journal* 28: 317-339.
- Jeppesen E., Christoffersen K., Landkildehus F., Lauridsen T., Amsinck S. L., Riget F., Søndergaard M. 2001. Fish and crustaceans in northeast Greenland lakes with special emphasis on interactions between Arctic charr (*Salvelinus alpinus*), *Lepidurus arcticus* and benthic chydroids. *Hydrobiologia* 442: 329-337.
- Johnson O. 2014. Przewodnik Collinsa Drzewa. Multico Oficyna Wydawnicza, Warszawa.
- Karkanas P., Pavlopoulos K., Kouli K., Ntinou M., Tsartsidou G., Facorellis Y., Tsourou T. 2011. Palaeoenvironments and Site Formation Processes at the Neolithic Lakeside Settlement of Dispilio, Kastoria, Northern Greece. *Geoarchaeology: An International Journal* 26: 83-117.
- Karkanas P., Tourloukis V., Thompson N., Giusti D., Panagopoulou E., Harvati K. 2018. Sedimentology and micromorphology of the Lower Palaeolithic lakeshore site Marathousa 1, Megalopolis basin, Greece. *Quaternary International* 497: 123-136.
- Kittel P., Mazurkevich A., Dolbunova E., Kazakov E., Mroczkowska A., Pavlovskaja E., Piech W., Płociennik M., Sikora J., Teltevskaya Y., Wieckowska-Lüth M. 2018. Palaeoenvironmental reconstructions for the Neolithic pile-dwelling Serteya II site case study, Western Russia. *Acta Geographica Lodziensia* 107: 191-213.
- Kittel P., Mazurkevich A., Wieckowska-Lüth M., Pawłowski D., Dolbunova E., Gauthier E., Krapiec M., Maigrot Y., Danger M., Mroczkowska A., Okupny D., Płociennik M., Szmańda J., Thiebaut E., Słowiński M. 2020 (in press.) On the border between land and water: the environmental conditions of the Neolithic occupation from 4.3 until 1.6 ka BC at Serteya, Western Russia. *Geoarchaeology an Interdisciplinary Journal*.
- Koster E.H. 1978. Transverse rib: their characteristics, origin and paleohydrologic significance. In: A.D. Miall (ed.) *Fluvial sedimentology*. Canadian Society of Petroleum Geologists Memoir 5: 161-186.
- Krupski M., Kabala C., Sady A., Gliński R., Wojciechszak J. 2017. Double- and triple-depth digging and Anthrosol formation in a medieval and

- modern-era city (Wrocław, SW Poland). Geo-archaeological research on past horticultural practices. *Catena* 153: 9-20.
- Kühn P., Aguilar J., Miedema R., Bronnikova M. 2018. Textural Pedofeatures and Related Horizons. In: G. Stoops, V. Marcelino, F. Mees (eds) *Interpretation of micromorphological features of soils and regoliths*. Elsevier: 377-423.
- Macphail R.I., Allen M.J., Crowther J., Cruise G.M., Whittaker J.E. 2010. Marine inundation: Effects on archaeological features, materials, sediments and soils. *Quaternary International* 214: 44-55.
- Marguerie D., Hunot J.Y. 2007. Charcoal analysis and dendrology: data from archaeological sites in north-western France. *Journal of Archaeological Science* 34: 1417-1433.
- Mazurkevich A.N., Dolbunova E.V., Maigrot Y., Hook D. 2010. Results of underwater excavations of Serteya II and research of pile-dwellings in Northwest Russia. *Archaeologia Baltica* 14: 47-64.
- Mazurkevich A., Dolbunova E., Kittel P., Fassbender J., Maigrot Y., Mroczkowska A., Płociennik M., Sikora J., Słowiński M., Sablin M., Shirobokov I. 2017. Multi-disciplinary research on the Neolithic pile-dwelling Serteya II site (Western Russia) and the landscape reconstruction. In: A. Marciniak-Kajzer, A. Andrzejewski, A. Golański, S. Rzepecki (eds) *Nie tylko krzemienie. Not only flints*. Instytut Archeologii Uniwersytetu Łódzkiego, Łódzka Fundacja Badań Naukowych, Stowarzyszenie Naukowe Archeologów Polskich Oddział w Łodzi, Łódź: 103-128.
- Mazurkevich A., Kittel P., Maigrot Y., Dolbunova E., Mroczkowska A., Wieckowska-Lüth M., Piech W. 2020. Natural and anthropogenic impact on the formation of archaeological layers in a lake shore area: case study from the Serteya II site, Western Russia. *Acta Geographica Lodzienia* 110: 81-102.
- Moller Pillot H.K.M. 2009. Chironomidae larvae. Biology and Ecology of the Chironomini. KNNV Publishing, Zeist.
- Mycielska-Dowgiałło E., Ludwikowska-Kędzia M. 2011. Alternative interpretations of grain-size data from Quaternary deposits. *Geologos* 17,4: 189-203.
- Nalepka D., Walanus A. 2003. Data processing in pollen analysis. *Acta Palaeobotanica* 43: 125-134.
- Nicosia C., Stoops G. (eds) 2017. Archaeological Soil and Sediment Micromorphology. John Wiley & Sons, Oxford.
- Nolte U. 1989. Observations on neotropical rainpools (Bolivia) with emphasis on Chironomidae (Diptera). *Studies on Neotropical Fauna and Environment* 24: 105-120.
- Økland K.A., Økland J. 2000. Freshwater bryozoans (Bryozoa) of Norway: Distribution and ecology of Cristatella mucedo and Paludicella articulata. *Hydrobiologia* 421(1-3): 1-24.
- Passega R. 1964. Grain size representation by CM patterns as a geological tool. *Journal of Sedimentary Petrology* 34: 830-847.
- Passega R., Byramjee R. 1969. Grain size image of clastic deposits. *Sedimentology* 13: 830-847.
- Pawłowski D., Gruszka B., Gallas H., Petera-Zganiacz J. 2013. Changes in the biota and sediments of glacial Lake Koźmin, Poland, during the late Saalian (Illinoian). *Journal of Paleolimnology* 49: 679-696.
- Pawłowski D., Borówka R.K., Kowalewski G.A., Luoto T.P., Milecka K., Nevalainen L., Okupny D., Zieliński T., Tomkowiak J. 2016. Late Weichselian and Holocene record of the paleoenvironmental changes in a small river valley in Central Poland. *Quaternary Science Review* 135: 24-40.
- Pinder L.C.V. 1983. The larvae of Chironominae (Diptera: Chironomidae) of the Holarctic region—Keys and diagnoses. *Chironomidae of the Holarctic Region. Keys and Diagnoses, 1. Larvae, Entomol. Scand. Suppl.* 19: 149-294.
- Pleskot K., Tjallingii R., Makohonienko M., Nowaczuk N., Szczuciński W. 2018. Holocene paleohydrological reconstruction of Lake Strzeszyńskie (western Poland) and its implications for the central European climatic transition zone. *Journal of Paleolimnology* 59: 443-459.
- Podbielkowski Z. 2002. Fitogeografia części świata, Europa, Azja, Afryka, tom 1. Wydawnictwo Naukowe PWN, Warszawa.
- Pukienė R. 2008. Vilniaus Žemutinės pilys XIII – XVI a radinių medienos rūšys. *Lietuvos pilys* 4: 95-111.
- Rühle E. (ed.) 1973. Metodyka badań osadów czwartorzędowych. Wydawnictwo Geologiczne, Warszawa.
- Schweingruber F.H. 1978. Mikroskopische Holzanalyse. Zürcher AG, Zug.
- Scott A.C. 2010. Charcoal recognition, taphonomy and uses in palaeoenvironmental analysis. *Palaeogeography, Palaeoclimatology, Palaeoecology* 291: 11-39.
- Sinkiewicz M. 1995. Przeobrażenia rzeźby terenu i gleb w okolicy Biskupina wskutek denudacji antropogenicznej. In: W. Niewiarowski (ed.) *Zarys zmian środowiska geograficznego okolic Biskupina pod wpływem czynników naturalnych i antropogenicznych w późnym glaciale i holocenie*. Oficyna Wydawnicza "Turpress", Toruń: 281-290.
- Sinkiewicz M. 1998. Rozwój denudacji antropogenicznej w środkowej części Polski północnej. Uniwersytet Mikołaja Kopernika, Toruń.

- Sly P.G., Thomas R.L., Pelletier B.R. 1983. Interpretation of moment measures derived from water-lain sediments. *Sedimentology* 30: 219-233.
- Stahlschmidt M.C., Miller C.E., Ligouis B., Goldberg P., Berna F., Urban B., Conard N.J. 2015. The depositional environments of Schöningen 13 II-4 and their archaeological implications. *Journal of Human Evolution* 89: 71-91.
- Stochlak J. 1978. Struktury i tekstury młodoplejstoceńskich osadów deluwialnych. *Biuletyn Instytutu Geologicznego* 306: 115-174.
- Stochlak J. 1996. Osady deluwialne nieodłączny efekt procesu spłukiwania i propozycja ich podziału. In: A. Józefciuk (ed.) *Ochrona agroekosystemów zagrożonych erozją: ogólnopolskie sympozjum naukowe*. Puławy - Lublin - Zwierzyniec, 11-13 września 1996 r., Prace Naukowe, Część 2, Puławy: 111-132.
- Stoops G. 2003. Guidelines for Analysis and Description of Soil and Regolith Thin Sections. Soil Science Society of America, Madison.
- Sundborg A. 1967. Some Aspects on Fluvial Sediments and Fluvial Morphology I. General Views and Graphic Methods. Landscape and Processes: Essays in Geomorphology. *Geografiska Annaler* 49(2-4): 333-343.
- Szeroczyńska K., Sarmaja-Korjonen K. 2007. Atlas of subfossil Cladocera from Central and Northern Europe. Friends of the Lower Vistula Society.
- Środoń A. 1983. Jodła pospolita w historii naszych lasów. In: S. Białobok (ed.) *Jodła pospolita Abies alba Mill.* Nasze Drzewa Leśne 4. Instytut Dendrologii, Polska Akademia Nauk, Państwowe Wydawnictwo Naukowe, Warszawa-Poznań: 9-39.
- Tarasov P.E., Savelieva L.A., Long T., Leipe C. 2019. Postglacial vegetation and climate history and traces of early human impact and agriculture in the present-day cool mixed forest zone of European Russia. *Quaternary International* 516: 21-41.
- Teisseyre A.K. 1988. Mady dolin sudeckich. Cz. III: Suborealnie i subakwalnie deponowane osady pozakorytowe w świetle eksperymentu terenowego (1977-1979). *Geologia Sudetica* 23,2: 1-55.
- Velichkevich F.Yu., Zastawniak E. 2006. Atlas of the Pleistocene vascular plant macrofossils of Central and Eastern Europe. Part 1 – Pteridophytes and monocotyledons. W. Szafer Institute of Botany, Polish Academy of Sciences, Kraków.
- Velichkevich F.Yu., Zastawniak E. 2008. Atlas of the Pleistocene vascular plant macrofossils of Central and Eastern Europe. Part 2 – Herbaceous dicotyledons. W. Szafer Institute of Botany, Polish Academy of Sciences, Kraków.
- Velleste L. 1952. Analiz fosfatnykh soyedineniy pochvy dlya ustanoveniya mest drevnikh poseleniy. *Kratkiye Soobshcheniya Instituta Istorii Material'noy Kul'tury AN SSSR* 42: 135-140.
- Vepraskas M.J., Lindbo D.L., Stolt M.H. 2018. Redoximorphic Features. In: G. Stoops, V. Marcelino, F. Mees (eds) *Interpretation of micromorphological features of soils and regoliths*. Elsevier: 425-445.
- Vrydaghs L., Ball T., Devos Y. 2016. Beyond redundancy and multiplicity. Integrating phytolith analysis and micromorphology to the study of Brussels Dark Earth. *Journal of Archaeological Science* 68: 79-88.